Acta Ichthyologica et Piscatoria 53, 2023, 1–18 | DOI 10.3897/aiep.53.97702

PENSOFT.

ACTA
ICHTHYOLOGICA
ET PISCATORIA

A treatise about reliability in dating events of evolutionary history of brown trout *Salmo* cf. *trutta* (Actinopterygii) at Western Balkans: Impassable barriers, isolation of populations and assistance of geological timeframe

Ana MARIĆ[1], Danica SREĆKOVIĆ BATOĆANIN[2], Dubravka ŠKRABA JURLINA[1],
Miloš BRKUŠANIN[1], Jelena KARANOVIĆ[1], Tamara KANJUH[1],
Vera NIKOLIĆ[1], Danilo MRDAK[3], Predrag SIMONOVIĆ[1,4]

1 *Faculty of Biology, University of Belgrade, Belgrade, Serbia*
2 *Faculty of Mining and Geology, University of Belgrade, Belgrade, Serbia*
3 *Faculty of Sciences and Mathematics, University of Montenegro, Podgorica, Montenegro*
4 *Institute for Biological Research "Siniša Stanković", University of Belgrade, Belgrade, Serbia*

https://zoobank.org/BE5CFA72-0876-4D39-B639-FB89BF87F8FA

Corresponding author: Predrag Simonović (pedja@bio.bg.ac.rs)

Academic editor: Jan Kotusz ♦ **Received** 17 November 2022 ♦ **Accepted** 23 January 2023 ♦ **Published** 27 February 2023

Citation: Marić A, Srećković Batoćanin D, Škraba Jurlina D, Brkušanin M, Karanović J, Kanjuh T, Nikolić V, Mrdak D, Simonović P (2023) A treatise about reliability in dating events of evolutionary history of brown trout *Salmo* cf. *trutta* (Actinopterygii) at Western Balkans: Impassable barriers, isolation of populations and assistance of geological timeframe. Acta Ichthyologica et Piscatoria 53: 1–18. https://doi.org/10.3897/aiep.53.97702

Abstract

A pool of data already existing about D-loop, i.e., the Control Region (CR) haplotypes of the mitochondrial DNA (mtDNA) of brown trout, *Salmo trutta* Linnaeus, 1758, tentative Adriatic trout *Salmo farioides* Karaman, 1938, and tentative Macedonian trout, *Salmo macedonicus* (Karaman, 1924), and their reconstructed phylogeography makes a good starting point for resolving their evolutionary history. That includes the dating of particular events in it. The events have hitherto been dated using the method of a molecular clock. Various calibrations were applied for the mutation rate, owing to the incongruence between the time of divergence that various authors notified and general knowledge about events in geological history and the periods in which they occurred in the Mediterranean region. Since geological history events were mandatory for setting the scene for the evolutionary history of brown trout, the incongruence between them has questioned the molecular clock calibration's validity. From results about both the phylogeography and phylogenetic relations between native haplotypes (both partial and whole CR sequences) and the population genetics that characterized particular populations, we calculated the time of divergence between haplotypes in the regions of the western part of the Balkans: Iron Gate broader area in eastern Serbia, continental Montenegro and south-eastern Serbia. The distinct status of adjacent populations was verified by frequencies of microsatellites' alleles and the STRUCTURE analysis that examined the significance of differences between them. In particular, we examined the populations that were clearly separated either by physical barriers, such as a waterfall in eastern Serbia (e.g., the upper and lower River Rečka supplemented by nearby rivers Vratna and Zamna), or by underground drops in Montenegro (e.g., upper and lower River Zeta, and rivers Nožica and lower River Mrtvica as isolated counterparts). We used the so far most common substitution rate of 1% in a million years' (MY) period. The divergence times we obtained were compared to the events known for the region from available geological history data. There was a fairly good congruence between the dating obtained by the molecular clock method and that by geological history where the advanced, i.e., modern haplotypes, were concerned. In contrast, the congruence was worse for dating of divergence when more ancient haplotypes were in question, being much better if the mutational rate would be decreased to lower rates. That supported results both from the Rate Correlation Test about the independence of evolutionary rates in different lineages of brown trout, and from the Molecular

---

Clock Test, which revealed that the evolutionary rate throughout the phylogenetic tree is not equal. That implies a difference in the speed of evolution in them, which was likely slower and faster, in the ancient, pre-Pleistocene haplotypes and the advanced, Pleistocene ones, respectively. The setting of the variable, or non-linear (i.e., logarithmic) speed of evolving seems helpful, since the early cladogenesis with the dominance of mutations was most likely combined afterwards with the acting of other evolutionary mechanisms, especially of genetic drift in populations that passed through the bottleneck episodes of the abrupt decrease in population size during the unfavourable periods of their evolutionary history.

Keywords

brown trout, evolutionary history, geological history, tentative Adriatic trout, tentative Macedonian trout, molecular clock

Introduction

Brown trout, *Salmo trutta* Linnaeus, 1758, is natively dispersed across a wide geographic area in the Northern Hemisphere and its overall variability is striking. Apart from the variability inherent in its geographic distribution, brown trout's plasticity in life history traits in many local and often isolated populations resulted in particular ecological forms, i.e., the *morphae* that additionally complicated their taxonomy and nomenclature. Owing to that, by following the classification approach relying on the previously widely adopted typological species concept and employing predominantly external morphological features as taxonomic characters, more than 29 tentative taxa at both species and subspecies levels were assigned in time. Although new species concepts have been introduced since then, e.g., biological (Mayr 1969; Mayr and Ashlock 1991) and phylogenetic (Cracraft 1989), the proliferation of new locally dispersed brown trout taxa has not even slowed recently (Kottelat 1997; Kottelat and Freyhof 2007), increasing the current classification ambiguity.

Crête-Lafrenière et al. (2012) situated the origin of the genus *Salmo* at Oligocene, 26–29 million years (MY) ago and differentiation of the Atlantic salmon, *Salmo salar* Linnaeus, 1758, and the brown trout, *Salmo* cf. *trutta* Linnaeus, 1758, at mid-Miocene, 10–14 million years (MY) ago. Vladimirov (1948) and Osinov and Lebedev (2004) reported about the *Salmo* spp. fossil remnants occurring also in the Miocene layers (15 MY ago). There is another record of a fossil remain of *Salmo immigratus*† (Kramberger, 1891) at the vicinity of Samobor (Croatia) that makes an ancestry of *Salmo* spp. traceable in the western part of the Balkans down to 13 million years (MY), in the mid-Miocene strata (Anđelković 1989). Artamonova et al. (2021), however, considered that fossil remnant identification inaccurate, owing to its poor preservation. The intensive cladogenesis of *Salmo* cf. *trutta* that Crête-Lafrenière et al. (2012) reported after the fossil remnants found in the layers at the Caucasus dated at 2.5–5.0 MY ago (Pliocene).

Brown trout have a wide geographical dispersal area, with many isolated populations. The explanation for their wide geographical distribution and intense biogeographical differentiation could be geological processes, primarily of orogenic nature, that led either to geographical separation of aquatic realms, or the birth of a new palaeogeographical area. For example, the ascent of the Alpine chain led to a partition of the Tethyan Ocean on two different biogeographical entities, the Mediterranean and the Paratethys Seas, yet around the Eocene/Oligocene boundary (Piller and Harzhauser 2005). These basins were further subjected to internal differentiation and changes in the paleoenvironment (sea-level and salinity fluctuations, connections, isolation of water bodies, etc.).

In contrast to evolutionary dating suggested by the fossil records of ancient brown trout, there is great variability in the dating by method of molecular clock that uses different average mutational rates. Using the molecular clock method relying on the average mutational rate of 1% at each 1 MY in the mitochondrial DNA (mtDNA), Bernatchez (2001) estimated that recent brown trout speciation started 0.5–2.0 MY ago and passed the differentiation during the Pleistocene glaciations that lasted about 0.7 MY. On sharing the same common base pairs at particular places in the structure of their mtDNA's D-loop (i.e., the Control Region, CR) as synapomorphic characters, he defined initially five main clades that represent phylogeographic lineages - the haplogroups of brown trout, assigning the Danube (DA) haplogroup ancestral for all other haplogroups: Adriatic (AD), Mediterranean (ME), Atlantic (AT) and marmoratus (MA) (Bernatchez et al. 1992). Subsequently, two more haplogroups, the Duero (DU) (Suárez et al. 2001) and Tigris (TI) (Sušnik et al. 2005; Bardakçi et al. 2006), were introduced. The ancestral character of the DA clade of brown trout was concluded from their origin, estimated to 0.15–0.3 MY, and from their wide dispersal in southwestern Europe and adjacent regions. Using the Relaxed Bayesian molecular clock model on the nuclear loci, Pustovrh et al. (2014) estimated the emergence of the common brown trout clade's ancestor to be around 1.4 MY ago (Pleistocene), the divergence of AT and DU haplogroups from DA haplogroup to 1.2 MY ago, while the divergence of AD and ME haplogroups from the DA haplogroup was estimated to 0.82 MY ago, i.e., to the mid-Pleistocene period. They reconstructed the sister-group relation between the AT-DU clade on the one and DA-AD-ME clade of brown trout on the other hand. The molecular diversity in each of the clades is ascertained by reconstruction of relations between CR sequences of brown trout in local populations defined as haplotypes on the autapomorphies featuring them. Using exclusively the complete CR haplotypes' sequences in her analysis, Sanz (2018) inferred that the AD lineage is ancestral for all other brown trout lineages. She considered it reasonable to suggest that a large proportion of the ancient brown trout diversity, including the differentiation of the AD lineage, originated in the Balkans, with the alternative hypothesis of a pre-Pleistocene isolation of brown trout in the Asia Minor and diversification of DA, AD and TI lineages in its central part, Anatolia (Bardakçi et al. 2006).

Artamonova et al. (2021) shares the same opinion that many aquatic species originated in East or Central Asia and spread to Europe through the Paratethys, which was the migration corridor and a centre of origin of new aquatic species and genera since the Miocene. These processes were facilitated by the Late Oligocene desalination of the Paratethys (Popov et al. 2009). The Paratethys (Laskarev 1924), a vast intracontinental sea, began to form in the Late Eocene, about 37 MY ago, and was finally shaped during the Oligo-Miocene (Marović et al. 2002). Within it, distinct basins that experienced a complex pattern of changing seaways and land bridges were included, as well as those connecting them to the Mediterranean Sea and the western Indo–Pacific Ocean (e.g., Rögl 1998, 1999). The drainage area of the present River Rečka, that has recently evolved into the backcountry of the Iron Gate Gorge was within the Dacian basin of the Paratethys (Fig. 1), the smallest water body that roughly comprised the recent lowlands in southern Romania and northern Bulgaria, as well as northeastern Serbia (Jipa and Olariu 2009). The gradual infilling of the Dacian basin with the sediments derived by Carpathian Basin led to its disappearance and transformation into the accumulation area and a place of fluvial transport. That occurred during the Romanian era in Pliocene, 4.7–1.7 MY ago (Jipa 2015). According to Vasiliev et al. (2005), the transition of the Dacian Basin from brackish marine to continental domain was completed during a period about 700.000 years ago. It has been along with the whole former Paratethys subjected to vertical and a significant horizontal mobility and clockwise rotation, locally up to the Pleistocene. The established clockwise rotation for the Dacian basin was 5–20° (Marović et al. 2002).

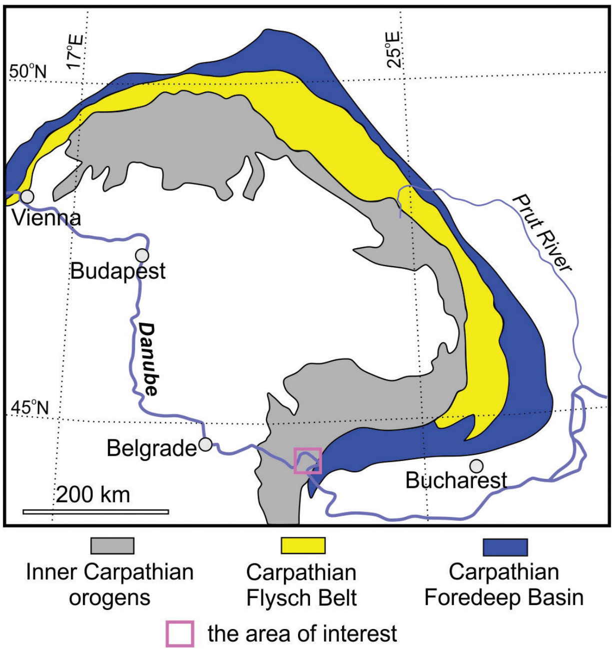

Figure 1. The broader area of the River Rečka (square outline) within the former Dacian Basin (roughly corresponding to the Carpathian Foredeep Basin, Flisch Belt and area south of it), with the Inner Carpathian Orogens a source of sediments for filling the Dacian Basin.

Earlier reconstructions of phylogeny between brown trout haplotypes were accomplished on their partial CR sequences (Bernatchez et al. 1992; Bernatchez 2001; Bardakçi et al. 2006; Marić et al. 2006). Marić et al. (2006) and Simonović et al. (2017) worked out a reconstruction of phylogeny from partial CR sequences seizing to the poly-T block in brown trout from DA and AD haplogroups in streams at the peninsular divide between the Aegean and Black Seas in SE Serbia. The basal position and ancient, i.e., plesiomorphic character of particular novel haplotypes, e.g., Da*Vr (GenBank Accession Number #DQ318125), Da*Dž (#DQ318124) and Ad*Bož (#DQ318128) they reported was strongly supported. The Da-s6 (# MW589188) (Kanjuh et al. 2021) is of the same ancient character. In addition to molecular markers (Marić et al. 2006; Simonović et al. 2017; Škraba Jurlina et al. 2020; Kanjuh et al. 2020, 2021), the external morphology (Simonović et al. 2007) also indicated the importance of the Balkans in recent brown trout lineages' delimitation. The presence of predominantly land-locked, resident form of brown trout, but also of the other trout (*Salmo* spp.) taxa originally occurring in the western part of the Balkans, is probably due to the warm climate and regression of Paratethys, as well as due to drying out of the Mediterranean in the upper Tertiary–Neogene, i.e., Late Miocene–Early Pliocene (i.e., the Messinian period), 5–6 MY ago. At the end of the Miocene, 5.5 MY ago, the Mediterranean Sea closed and almost dried ('Messinian Salinity Crisis') and then it was refilled with freshwater from the Paratethys Sea. This event may have facilitated the dispersal of freshwater organisms around the Mediterranean (Bianco 1990). Only a few tentative trout taxa, e.g., the lake-dwelling tentative Adriatic trout, *Salmo farioides* Karaman, 1938, in Lake Skadar system in Montenegro (Mrdak et al. 2006; Snoj et al. 2010; Škraba Jurlina et al. 2018, 2020), and marble trout, *Salmo marmoratus* Cuvier, 1829, in the Hutovo Blato marshland of the River Neretva system in Herzegovina (Snoj et al. 2010; Škraba Jurlina et al. 2020) recalled the potamodromy in their life history. Recent studies have shown that the present Lake Skadar is young and formed from initial marshland not earlier than 1200 years ago (Mazzini et al. 2015). However, the Skadar basin, with its system of sublacustrine springs, is ancient and dates back at least to the Pliocene, ca. 3 MY ago (Grabowski et al. 2018). Bošković et al. (2004) acknowledged the belief of the Italian botanist Baldacci (1929) that the permanent Lake Skadar has evolved from an ancient and very large sea bay into a marshland, due to significant supply of the alluvial sediments by the rivers Morača, Drim and Bojana, together with minor tributaries. The River Bojana cut its riverbed into the lake sediments (Bošković et al. 2004), whereas the initial rift structure of the majority of Balkan rivers, including the River Morača, which is the main inflow of Lake Skadar, as well as the rivers Struma (Strymon), Vardar (Axios) and Neretva, was formed along large faults in the mid–Late Miocene (e.g., Tzankov et al. 1996; Mulić et al. 2006).

During the Pleistocene glaciations, the stream-dwelling brown trout in the River Danube's drainage area passed through a very dynamic evolutionary history. Recent secondary connections between the River Danube's tributaries during the Pleistocene (Razpet et al. 2007) can partially explain the recent distribution of haplotypes in the Balkan Peninsula. Simonović et al. (2017) and Kanjuh et al. (2021) hypothesized that the occurrence of unique and vicariant brown trout haplotypes in particular river systems in the River Danube drainage area at the Western Balkans reflects different periods and areas of their emergence and diversification, when they had opportunities to spread, prior to the subsequent reduction to their recent, narrower dispersal areas. On one source, the Dacian basin of the Parathetys Sea, which would include the area of the recent eastern Serbia where the River Rečka is situated, communicated with the western, Pannonian basin over three straits until the Late Miocene (Badenian). Then the Wallachian uplift of a part of Carpathians caused the Iron Gate (*Porto ferre*) to retain as their only connection (Stevanović 1990). The other sources claim that the connection between the western, Pannonian and eastern, Dacian–Euxinic–Caspian basins of the Parathetys Sea diminished in the Late Miocene–Early Pliocene (i.e., Pontian–Messinian) (Anđelković 1970; Almaca 1990). Matoshko et al. (2019) estimated the final establishment of the Danube at 1.9–1.8 MY ago.

The most common native haplotypes in Serbia are of DA haplogroup, with AT and AD haplogroups detected as well (Marić et al. 2006; Tošić et al. 2016; Simonović et al. 2015, 2017). The most common DA haplotype in the brown trout populations throughout the River Danube drainage area in the western part of the Balkans is Da1, with recently even newly discovered sub-haplotypes (Kanjuh et al. 2021). However, the common haplotype from the River Crni Timok system and from the broader Iron Gate region is the modern and derived Da23c (#KC630984) (Tošić et al. 2014, 2016). It is indigenous for this area, since it occurs only in this region in the Iron Gate Gorge and the River Crni Timok system, and nowhere else. It is the most frequent haplotype there, recently occurring in 67% of brown trout. In addition to it, in the upper section of the northern fork of the River Rečka upstream of the Bledaria Waterfall, we detected only the otherwise widespread, but here vicariant, very limited and completely isolated Da1a haplotype (Tošić et al. 2016). In the western fork of the River Rečka, both Da23c and Da1 haplotypes were recorded (Marić et al. 2006). Tošić et al. (2016) and Simonović et al. (2017) reconstructed the Da1 haplotype as ancestral and the Da23c as the most derived in the modern, derived group of haplotypes of brown trout in the Western Balkans' streams. The Da2 haplotype in streams of the River Crni Timok system that we recorded is considered non-native, i.e., stocked (Tošić et al. 2016).

Observing the novel results obtained in Montenegro, it is necessary to emphasize that the whole area of Montenegro itself displays complex geological and tectonic evolution and significant differences in the distribution and abundance of water resources ranging from arid karst areas to areas rich in both surface and groundwater. The domination of carbonate rocks in geological composition of the mountains in Montenegro enabled the development of karst process and karst relief (Bešić 1969) that have had a great influence on the subsequent glaciation leading to specific glaciers' behaviour.

Water from the territory of Montenegro drains into two basins: the Adriatic Sea and the Black Sea, whose watersheds are separated by Triassic dolomites (Drobne et al. 1979).

Škraba Jurlina et al. (2018) reported an occurrence of the Adcs11 (#AY836340), Ad-M1 (#DQ381566) and Ad+Prz (#DQ318129) in the lower River Mrtvica, the right tributary of the River Morača in the Adriatic Sea basin of southern Montenegro. The occurrence of three native AD haplotypes there also testifies to the dynamic evolutionary history and multiple colonization events in that area. However, only the Adcs11 haplotype was detected in the resident, stream-dwelling tentative Adriatic trout from the upper River Mrtvica, supporting its ancestral character in relation to the other two AD haplotypes. The distinct character of two populations from the upper and lower River Mrtvica was explained by the partial migratory character of tentative Adriatic trout in the lower River Mrtvica, where the lake-dwelling tentative Adriatic trout ascend from Lake Skadar each year to the spawning grounds in the lower River Mrtvica (Škraba Jurlina et al. 2020). Further detailed research of brown trout in the lost streams at the Adriatic Sea basin, the River Nožica and in the upper River Zeta and in its tributary, the River Gračanica upstream (i.e., above) of their underground drops to the River Mala and lower River Zeta valley, respectively also revealed the occurrence of the Da1a haplotype (Simonović et al. 2017).

A broad karst massif, consisting of thick and permeable fluvioglacial sediments of the Würm glaciation stage, is situated between the River Morača Canyon and the lower River Zeta Plain, which considers tectonic depression formed at the Miocene/Pliocene boundary (Cvijić 1926). Groundwater from it enters either into the River Mrtvica, or into the lower River Zeta valley, as the surrounding

Upper Cretaceous flysch sediments represent a physical barrier to water, particularly for streams coming from the west. Similar behaviour is displayed by the Permian–Triassic clastites in the River Gračanica valley of the upper River Zeta system. Cvijić (1926) also has pointed out the importance of faults in the catchment area of the River Zeta that allowed either the uplift of the northern block or subsidence of the southern block. He attributed tectonic movements of lower intensity within the downstream region of the River Morača to stabilizing of the Skadar depression as has been inferred from the up to 88 m reduced height between the neighbouring terraces and a thick fluvioglacial deposit.

This study aims to clarify and support the evolutionary history of brown trout populations belonging to either the different haplogroups (e.g., in the Adriatic Sea basin), or different haplotypes of the same haplogroup (e.g., in the broader Iron Gate region of the River Danube drainage area) in the Western Balkans, including the results from use of microsatellites' loci as molecular markers. The records that we have gathered about the adjacent brown trout populations which remained entirely isolated, and phylogenetic relations between them that we reconstructed, illustrate the dispersal of brown trout of particular haplogroups and haplotypes as evolutionary units in various time periods over the western part of the Balkans. That is related to the facts from the geological history known in the region and their timing, in order to check the estimation of the timing of the events dated using the molecular clock technique. Calibration of the molecular clock using calibration points from externally derived dates, such as biogeographical and geological events, can be used for interpolation of divergence times (i.e., the event to be estimated falls within the calibration points or within the calibration point and the tip of the branch), their extrapolation (i.e., the event to be estimated falls beyond the calibration points), or combination of both (Wilke at al. 2009; Ho and Duchéne 2014). As for an application of the molecular clock in estimation of divergence time in salmonids, Osinov and Bernatchez (1996) stated the need for its re-calibration and proposed the substitution (i.e., the mutation) rate 0.8% per one million of year (MY^{-1}). Rambaut and Bronham (1998) already stated that molecular clock estimates of dating of evolutionary history events should be interpreted with caution owing to secondary contacts and isolation episodes between brown trout lineages. In addition, Apostolidis et al. (1997) stated that CR appears to evolve at a lower rate compared to other regions in *Salmo* spp. and used the substitution rate of 0.5%–0.9% MY^{-1} of Martin and Pallumbi (1993), estimating the divergence time between main mtDNA lineages (AT, DA, ME, AD and MA) in the time period of 2.5–6.0 MY ago (Late Miocene, i.e., Messinian–Early Pliocene). Discrepancies that occurred in estimations of divergences in various papers and possibility of the CR's lower rate of evolving urged Sanz (2018) to calibrate the molecular clock to its lower edge of the range commonly used for this fish group, at 0.75% MY^{-1}, as proposed by Shedlock et al. (1992). This resulted in estimations concordant with those obtained before, setting the linages' differentiation at the Pliocene–Pleistocene boundary at 2 MY ago. The greatest modifying of the molecular clock 0.31% MY^{-1} was proposed by Crête-Lafrenière et al. (2012). If applied, it would set the events far back in the past, to the Miocene–Pliocene boundary. Hence, we aimed here to examine few actual cases of distinctness in a very close range in the western part of the Balkans by comparing the dating of divergence between them using the phylogeography, i.e., the evolutionary history data and molecular clock with the dating of events using the geological history data.

Since a majority of haplotypes in both areas of interest was inferred as modern, i.e., derived (Simonović et al. 2017; Škraba Jurlina et al. 2018), we added to this calibration analysis the more ancient ones from southeastern Serbia belonging to both DA and AD haplogroups (Marić et al. 2006; Simonović et al. 2017), in order to provide material for calibration in the earlier period of brown trout evolutionary history in the region.

The microsatellites' analyses served to reveal the distinct population status of brown trout populations of the native haplogroups and haplotypes in streams in the Adriatic Sea basin in Montenegro and in the broader Iron Gate region, respectively.

Materials and methods

In this study, three populations of brown trout from streams in Serbia and Montenegro with impassable barriers were analysed (Fig. 2). Data from River Zeta (upper and lower River Zeta) and River Nožica are novel results, while data about the genetic structure of brown trout from River Mrtvica and River Rečka (Marić et al. 2006; Tošić et al. 2014; Škraba Jurlina et al. 2018, 2020) are taken from previous studies. The upper River Zeta flows southward through the high karst plateau, the Nikšić Karst Field. At the rim of the plateau, it drops several hundred meters in elevation through crevices and caves, to emerge as the lower River Zeta. It merges with the River Morača from the Pleistocene.

The River Nožica is situated also at the high karst plateau in southern Montenegro, in the drainage area of the River Morača, the main tributary of Lake Skadar in Montenegro. At the western rim of the plateau, it drops through the subterranean crevice, to emerge as the short River Mala that joins the River Morača. The River Rečka from eastern Serbia is situated at the Mt. Miroč in the broader Iron Gate Gorge area. It joins the River Danube under the name River Reka. In the headwaters' section, it is formed by the confluence of the two forks, northern and western ones. The northern fork in its most upstream part flows through the high and narrow mountain valley built by impermeable Cretaceous clastic rocks that enable a surface stream. At its end, it drops down from

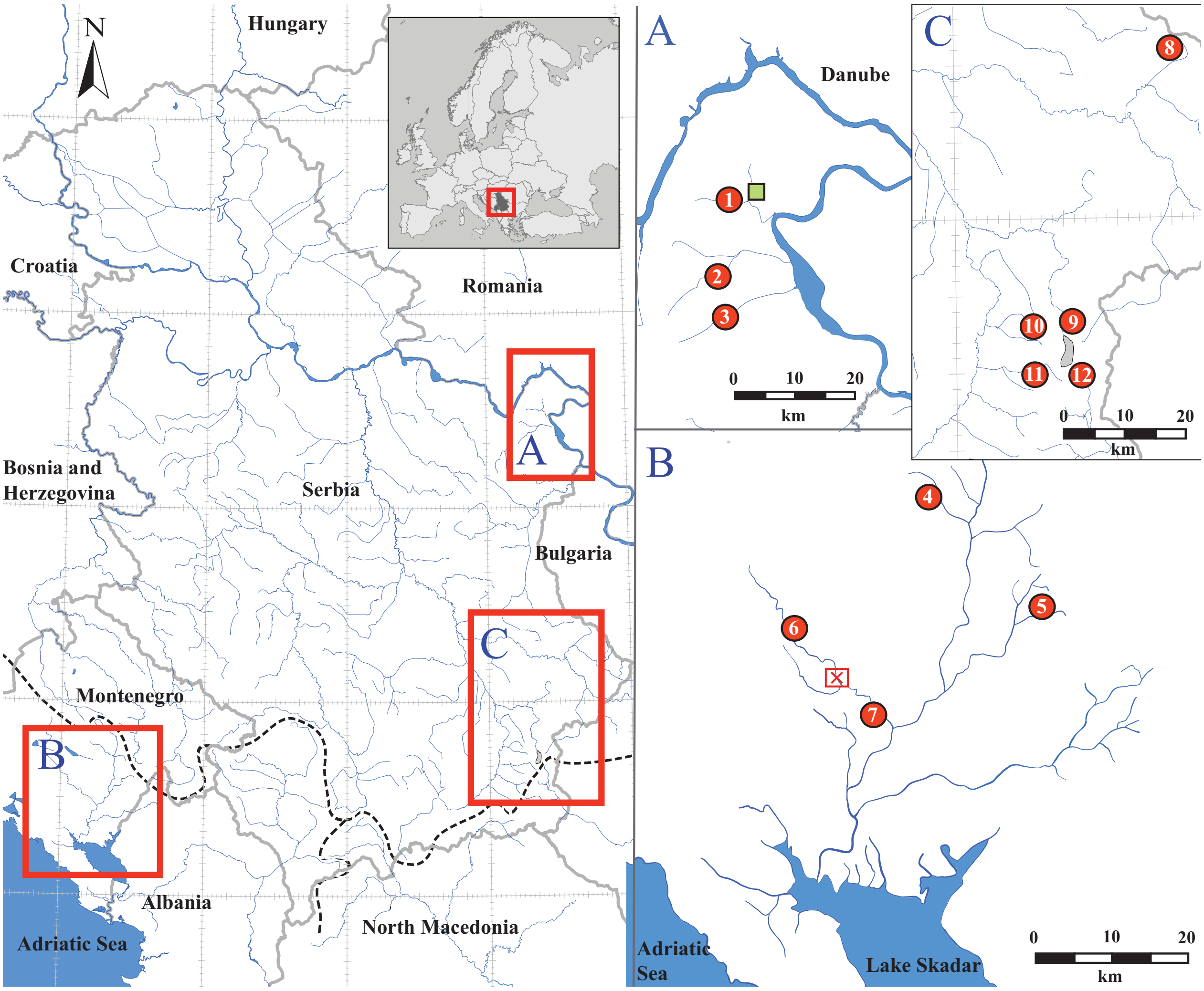

Figure 2. Regions in Serbia and Montenegro with the broader Iron Gate Gorge area (**A**), Adriatic Sea basin of Montenegro (**B**) and southwestern Serbia (**C**), where the populations of brown and tentative Adriatic and Macedonian trout were sampled (1, River Rečka; green quadrate denotes the Bledaria waterfall; 2, River Vratna; 3, River Zamna; 4, River Mrtvica; 5, River Nožica; 6, upper River Zeta; 7, lower River Zeta, red rectangle marks the subterranean drop; 8, River Studenačka; 9, River Vlasina; 10, River Džepska; 11, River Vrla; 12, River Božica). The dashed line denotes the peninsular divide between Adriatic, Black and Aegean Seas.

the (about) 12 meters high Bledaria Waterfall that is impassable for fish from the downstream section, where tufa is precipitating even today. The western fork is free of barriers upstream, all along to the karstic spring in a deep forest. The drainage area is in the southernmost part of the so-called Dževrin Greda, formed along a fault of the same name, which extends from the Tekija in the North–South direction about 18 km. Evolving as the vertical one, the fault has brought Cretaceous and the Upper Jurassic rocks over the younger, Pliocene units. However, such movements came to an end and the fault started to act until recently as a strike-slip or lateral right fault (Grubić 1992). Such activity resulted in migration of the eastern block to the south and the western block to the north, allowing the displacement of riverbeds. In the broader Iron Gate area, rivers Vratna and Zamna are closest to the River Rečka, making those populations adequate for this genetic analysis, since the microsatellite data for brown trout in the western fork of the River Rečka are lacking.

Sampling of materials for phylogeographic and genetic researches was accomplished during the period from 2004 to 2015. Brown trout anal fin clips (approximately 16 mm^2) were collected by electrofishing using AquaTech device IG200/1 (input 12 V per maximum 15A DC, output 500 V, and frequency 65 P s^{-1}) in Serbia and Suzuki-Bosch (220V DC, Imax = 6A) in Montenegro and stored in 96% ethanol. All sampled fish from analysed streams were released alive immediately after the sampling.

Sequences of haplotypes from southeastern Serbia were already published in Marić et al. (2006) and Simonović et al. (2017), and those from eastern Serbia (the broader Iron Gate area) and continental Montenegro were published in Škraba Jurlina et al. (2018, 2020). In total, 144 samples were analysed for CR mtDNA haplotype, 18 samples from the former region, whereas from the latter two regions 126 samples were analysed for CR mtDNA haplotype using a partial sequence until poly-T block and 100 were analysed for eight microsatellites' loci (Table 1). Total DNA was extracted from the tis-

Table 1. Number of samples in analysed rivers in Serbia with recorded mtDNA CR haplotypes analysed using eight microsatellite loci.

Locality	Haplogroups with detected haplotypes													Micro-satellites
	DA							AD					AT	
	Da1a	Da2	Da23c	Da*Dž	Da*Vr	Da-Vl	Da-s6	Adcs11	Ad*Prz	Ad-M1	Adcs1	Ad*Bož	Atcs1	
Džepska				1										
Vrla					2						1			
Vlasina						2								
Studenička							3							
Jerma											4			
Božica												7		
Upper Zeta	27	1											2	32
Lower Zeta								11	6					17
Nožica	18													12
Lower Mrtvica								9	3	1				12
Rečka (N fork)	11													11
Rečka (W fork)	2		1											—
Vratna	10		7										3	10
Zamna	6		6											6
Total	74	1	14	1	2	2	3	20	9	1	5	7	5	100

N fork = northern fork, W fork = western fork.

sue samples using the High-Salt Extraction technique of Miller et al. (1988) and Quick-gDNATM MiniPrep extraction kit following the manufacturer's instructions (Zymo Research Corporation, Irvine, CA). The CR of mtDNA was amplified using the forward primer Trutta_mt_F (5′-TGAATGAACCTGCCCTAGTAGC-3′, designed by M. Brkušanin), and the reverse primer HN20 (Bernatchez and Danzmann 1993), under the following conditions: initial denaturation (95°C, 5 min) followed by 30 cycles of strand denaturation (94°C, 45 s), primer annealing (52°C, 45 s) and DNA extension (72°C, 2 min) in the programmable Applied Byosistems thermal cycler. Each PCR reaction in volume of 30 µL contained 10 µM of each primer (ThermoScientific), 10 mM dNTP, 10× PCR buffer with MgCl2 (Kapa Biosystems), 1 U of *Taq* polymerase (Kapa Biosystems) and 100 ng (i.e., 1 µL) of genomic DNA. Amplified DNA fragments were run on a 1.5% agarose gel using Applichem SYBR Green for visualization. PCR products were purified and sequenced at Macrogen Europe. Sequencing reactions were performed in a DNA Engine Tetrad 2 Peltier Thermal Cycler (BIO-RAD) using the ABI BigDye Terminator v3.1 Cycle Sequencing Kit (Applied Biosystems), following the protocols supplied by the manufacturer by single-pass sequencing on each template using the forward (Trutta_mt_F) primer.

Haplotypes' sequences were aligned and edited using the Mega X (Kumar et al. 2018) software, and used for assessment of difference between them in positions, using either the whole CR (aligned to 993 bp in length), or its partial sequence up to the poly-T block (561 bp). The calculation of the time of divergence (t_D, in years) between particular haplotypes analysed here was based on the branching topology of phylogenetic tree (Wilke et al. 2009) inferred using the partial sequences of 561 bp of 13 haplotypes and applying the Maximum Likelihood (ML) method in the Mega X software package (Stecher et al. 2020). The branch length information, i.e., the time of divergence was estimated using the node depth (d_N, in number of substitutions per site), together with the substitution (i.e., the molecular clock) rate (λ, in number of substitutions per site and year):

$$t_D = \frac{d_N}{\lambda}$$

The calculation of divergence times between haplotypes followed the calibration of Bernatchez (2001) for mitochondrial DNA (mtDNA) at an average mutational rate λ_1 of 1% MY^{-1} and that of Crête-Lafrenière et al. (2012) at an average mutational rate λ_2 of 0.31% MY^{-1}. They served as an initial referent time of divergence for matching with the geological history events (Ho and Duchéne 2014) and for comparison with the time tree inferred using the RelTime method that does not require assumptions for linear rate variations to the supplied ML phylogenetic tree, with the Atcs1 haplotype as an outgroup, using the Mega XI software (Tamura et al. 2021). The calibration of nodes and distribution mode of the molecular clock together with the confidence interval (CI, a percentage of times expected to get close to the same estimate under the same experiment conditions) and offset (λ, distribution to the oldest fossil) were determined following Drummond et al. (2006). The testing of evolutionary rates in all brown trout lineages (i.e., haplogroups) was accomplished on 13 nucleotide sequences of haplotypes, using the Test of Molecular Clock. The test was performed comparing the ML value for the given tree topology with and without the molecular clock constraints under Kimura (1980) 2-parameter model (Kimura 1980). The independence of evolutionary rates in particular lineages was analysed using the Rate Correlation Test (Tao et al. 2019) for 13 haplotypes with the phylogeny given in phylogenetic tree reconstructed using the ML method and the best-fitting nucleotide substitution model with the Bayesian information criterion (BIC) that was determined using the jModelTest 2.1.7 software package (Darriba et al. 2012), with the 1000 bootstrap replications.

Eight microsatellite loci [SsoSL438 (Slettan et al. 1995), Ssa85 (O'Reilly et al. 1996), Str73INRA (Estoup et al. 1998, SSsp2216 (Paterson et al. 2004), Ssa410U-os (Cairney et al. 2000), SsaD190, SsaD71 (King et al. 2005), OMM1064 (Rexroad et al. 2002)] were combined in four duplex reactions with forward primer labelled with fluorescent dye. The final concentrations of PCR components were: 1× PCR buffer (Invitrogen), 0.2 mM dNTPs, appropriate concentration of primers, 1.5 mM MgCl$_2$, 0.5 U of *Taq* polymerase (Invitrogen), and ~100 ng of DNA. PCR programs were as follows: initial denaturation for 3 min on 94°C, followed by 30 cycles (35 for the 4th duplex) of denaturation for 45 s on 94°C, annealing for 1 min on 60°C (57°C for the 4th duplex) and elongation for 30 s on 72°C, and final elongation for 1 h on 72°C. Fragment analysis was performed using GeneScan 500 LIZ Size Standard (Applied Biosystems, USA) on an ABI-3130 Genetic Analyzer (Applied Biosystems, USA). Analysis was done using GeneMapper ID v3.2.1 software (Applied Biosystems, USA).

Alleles' frequencies, number of alleles per locus, expected (H_{exp}), and observed (H_{obs}) heterozygosities, as well as F_{st} values representing a measure of differentiation between populations and gene flow (N_m) calculated (following Wright 1969) as

$$(1 - F_{\mathrm{st}})(4F_{\mathrm{st}})^{-1}$$

were obtained using GENETIX 4.05 (Belkhir et al. 2004), as well as factorial correspondence analysis (FCA). FSTAT 2.9.3.2 software (Goudet 2002) was used to calculate allelic richness expressed as the mean number of alleles per locus ($\bar{A}_n$) and values for Fisher's F statistics per locus (F_{IS}, F_{IT}, F_{ST}). Allelic richness (A_r) and private allelic richness (P_{ar}) expressed as a number of alleles in a population and as a number of unique, i.e., private alleles that are present only in one population, respectively were calculated using programme HP Rare (Kalinowski 2005). To detect recent bottlenecks in populations we used Wilcoxon sign-rank test and mode shift test in program BOTTLENECK 1.2.02 (Cornuet and Luikart 1996; Piry et al. 1999). Wilcoxon sign-rank test was used under stepwise mutation model (SMM) and the two-phase model (TPM) with 95% for proportion of single-step mutations and variance mutation size set to 12 (Luikart et al. 1998) for significance estimation with 10 000 iterations.

Population structure was analysed using the STRUCTURE 2.3.4 program (Pritchard et al. 2000), using the admixture model with proposed number of clusters, K = 10. Length of burn in periods was set to 50 000 with the number of Markov Chain Monte Carlo (MCMC) repeats of 7 for each K depending on convergence after burning set to 500 000. Structure Harvester software (Earl and von Holdt 2012) was applied to estimate most probable K according to Evanno et al. (2005).

Results

Several mtDNA haplotypes were detected in analysed regions: seven of DA haplogroup, five of AD and one of AT haplogroup (Table 1). The upper Zeta carried haplotypes of DA haplogroup (93.33%) with two samples (6.67%) of AT haplogroup, while in the lower Zeta all samples carried haplotypes of AD haplogroup. All brown trout sampled from River Nožica had Da1 haplotype and the majority of samples (69.2%) from the lower River Mrtvica had Adcs11 haplotype, 23.1% had Ad*Prz and 7.7% had Ad-M haplotypes. Samples from the Northern fork of the River Rečka upstream of the impassable barrier (Bledaria Waterfall) possessed Da1a haplotype, and from the western fork haplotypes were Da1a and Da23c (Table 1).

The ML tree reconstructed (Fig. 3A) revealed the two main clades: that of the DA haplogroup and the second one comprising two sister subclades of the AT and AD haplogroups. The Test of Molecular Clock rejected the null hypothesis of equal evolutionary rate throughout the tree at a 5% significance level (with the molecular clock: $+G = -35114.352$, $+I = 13$; without the molecular clock: $+G = -943.416$, $+I = 24$; $P < 0.05$). The Rate Correlation Test for 13 haplotypes revealed independence (the score of $3.49 * 10^{-7}$, $P > 0.05$) of evolutionary rates in particular brown trout lineages. The best-fitting nucleotide substitution model that jModelTest software found by lowest BIC values and $\Delta = 0$ was Hasegawa–Kishino–Yano with Invariable sites (HKY + I). Calibration of nodes was accomplished using the exponential clock distribution ($\lambda = 0.31$, with the confidence interval CI = 1 – 12.9 and offset = 1).

Estimation of the time of divergence between brown trout that have the ancestral haplotypes using the partial CR haplotypes' sequences and under the $\lambda_1 = 1\%$ and $\lambda_2 = 0.31\%$ (Table 2) revealed that a divergence between AD (Ad*Bož) and DA (Da*Vr) lineages occurred at 1.972 MY and 3.450 MY ago, respectively and that a differentiation in tentative Adriatic trout within the AD haplogroup (Ad*Bož and Ad-M1) occurred at 0.535 and 1.725 MY ago, respectively, with the most derived haplotype Ad-M1 who diverged from Adcs11 at 0.357 and 1.150 MY ago, respectively.

Calculation of divergence times by TimeTree of Mega XI software using the substitution rate $\lambda = 0.31\%$ (Fig. 3B) revealed that the time of divergence between AD (Ad*Bož) and DA (Da*Vr) lineages occurred at 4.740 MY ago and that a differentiation in tentative Adriatic trout within the AD haplogroup (Ad*Bož and Ad-M1) occurred at 1.698 MY ago, with the most derived haplotype Ad-M1 who diverged from Adcs11 at 0.378 MY ago.

As for the analysis of their microsatellite loci, in brown trout from the Adriatic Sea basin, the highest expected heterozygosity (H_{exp}) was detected in the lower Mrtvica (0.63) and the lowest one in the lower section of the River Rečka (0.20). The highest observed heterozygosity (H_{obs}) was in the lower River Zeta (0.64), as well, and the lowest (0.24) in the River Rečka. Generally, the majority of localities had slightly lower values for observed heterozygosity except the lower Zeta, Vratna and Rečka (Table 3)

Table 2. Time of divergence (t_D) between brown trout of the native CR mtDNA haplotypes (in million years, MY) assessed using both only the first part of the CR to the poly T block (561 bp, above the diagonal) that was the only one available for particular haplotypes, and the maximal available common length (993 bp, below the diagonal) for haplotypes, whose complete CR sequences (as declared in the NCBI base) were available (d_N, number of substitutions per site; λ_1, substitution rate of 1%; λ_2, substitution rate of 0.31%).

MY		Da1a	Da23c	Da2	Da-Vl	Da-Dž	Da-s6	Da-Vr	Ad*Prz	Adcs11	Ad-M1	Adcs1	Ad*Bož	Atcs1
Da1a	d_N	—	1	1	2	4	1	5	9	9	11	9	9	9
	λ_1		0.178	0.178	0.357	0.713	0.178	0.891	1.604	1.604	1.961	1.604	1.604	1.604
	λ_2		0.575	0.575	1.150	2.300	0.575	2.875	5.175	5.175	6.325	5.175	5.175	5.175
Da23c	d_N	1	—	2	3	3	2	5	10	11	12	9	10	8
	λ_1	0.101		0.357	0.535	0.535	0.357	0.891	1.783	1.961	2.139	1.604	1.783	1.783
	λ_2	0.325		1.150	1.725	1.725	1.150	2.875	5.750	6.325	6.900	5.175	5.750	5.750
Da2	d_N	1	3	—	1	4	2	5	10	11	12	9	8	10
	λ_1	0.101	0.302		0.178	0.713	0.357	0.891	1.783	1.961	2.139	1.604	1.426	1.604
	λ_2	0.325	0.975		0.575	2.300	1.150	2.875	5.750	6.325	6.900	5.175	4.600	5.175
Da-Vl	d_N				—	5	3	6	11	10	11	8	10	7
	λ_1					0.891	0.535	1.070	1.961	1.783	1.961	1.426	1.783	1.248
	λ_2					2.875	1.725	3.450	6.325	5.750	6.325	4.600	5.750	4.025
Da-Dž	d_N					—	4	3	8	7	7	6	7	6
	λ_1						0.713	0.535	1.426	1.248	1.248	1.070	1.248	1.070
	λ_2						2.300	1.725	4.600	4.025	4.025	3.450	4.025	3.450
Da-s6	d_N	1	3	3			—	4	9	8	8	8	8	6
	λ_1	0.101	0.302	0.302				0.713	1.783	1.426	1.426	1.426	1.426	1.070
	λ_2	0.325	0.975	0.975				2.300	5.750	4.600	4.600	4.600	4.600	3.450
Da-Vr	d_N							—	7	7	8	6	6	6
	λ_1								1.248	1.248	1.426	1.070	1.070	1.070
	λ_2								4.025	4.025	4.600	3.450	3.450	3.450
Ad*Prz	d_N	10	11	11			11		—	3	3	2	5	6
	λ_1	1.007	1.108	1.108			1.108			0.535	0.535	1.070	0.891	1.070
	λ_2	3.249	3.573	3.573			3.573			1.725	1.725	3.450	2.875	3.450
Adcs11	d_N	10	12	12			10		3	—	1	6	2	6
	λ_1	1.007	1.208	1.208			1.007		0.302		0.178	1.070	0.357	1.070
	λ_2	3.249	3.898	3.898			3.249		0.975		0.575	3.450	1.150	3.450
Ad-M1	d_N	14	17	15			14		4	2	—	2	3	7
	λ_1	1.309	1.712	1.511			1.410		0.403	0.201		0.357	0.535	1.248
	λ_2	4.223	5.523	4.873			4.548		1.299	0.650		1.150	1.725	4.025
Adcs1	d_N	9		9			9		2	1	3	—	1	5
	λ_1	0.906	0.906	0.906			0.906		0.201	0.101	0.302		0.178	0.891
	λ_2	2.924	2.924	2.924			2.924		0.650	0.325	0.975		0.575	2.875
Ad*Bož	d_N			—									—	4
	λ_1													0.713
	λ_2			—										2.300
Atcs1	d_N	10	12	11			13		7	7	7	6		—
	λ_1	1.007	1.208	1.108			1.309		0.705	0.705	0.705	0.604		
	λ_2	3.249	3.898	3.573			4.223		2.274	2.274	2.274	1.949		

Table 3. Expected ($H_{\mathrm{exp.}}$) and observed ($H_{\mathrm{obs.}}$) heterozygosities in analysed populations with their standard deviations and P values (with the P = 0.99 as a significance criterion), and the mean allele number ($\bar{A}_n$).

	NZ	UZ	LZ	LM	VR	ZM	RE
H_{exp}	0.51 ± 0.23	0.53 ± 0.25	0.60 ± 0.32	0.63 ± 0.28	0.49 ± 0.29	0.37 ± 0.32	0.20 ± 0.26
H_{obs}	0.49 ± 0.29	0.45 ± 0.22	0.64 ± 0.36	0.54 ± 0.27	0.54 ± 0.32	0.30 ± 0.35	0.24 ± 0.34
P	0.88	1	1	1	0.88	0.63	0.50
$\bar{A}_n$	4.25	8.25	5.57	8.00	4.13	2.63	1.63

NZ = Nožica, UZ = upper Zeta, LZ = lower Zeta, LM = lower Mrtvica, VR = Vratna, ZM = Zamna, RE = Rečka.

Populations from upper and lower Zeta rivers had a greater number of alleles per locus than populations from rivers Nožica and Mrtvica (Table 3). Tentative Adriatic trout from the lower River Zeta had eight private alleles on SsaD71 and one on SsaD190. Single private alleles were identified at four loci for brown trout from the upper River Zeta (Str73INRA, Ssa410Uos, SSap2216, OM1064), three loci for tentative Adriatic trout from River Mrtvica (Ssa410Uos, SSap2216, OM1064), and one locus for brown trout from River Nožica (Ssa410Uos). The high number of private alleles indicates isolation of those populations that are confirmed by relatively small estimated gene flow (N_m) and relatively high F_{st} values between those populations (Table 4).

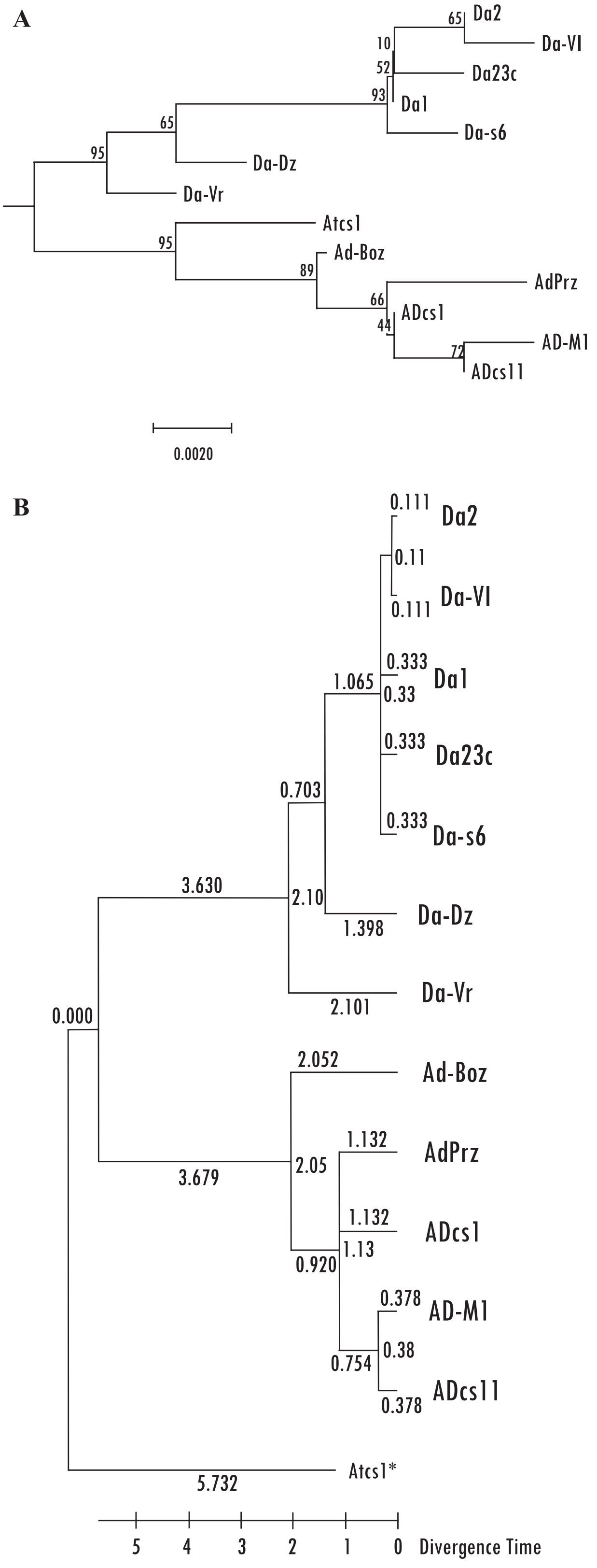

Figure 3. (**A**) Phyogenetic tree reconstructed from 13 CR mtDNA haplotypes' sequences of brown trout using maximum likelihood (ML) method from three (DA, AD and AT) phylogenetic lineages in the western part of the Balkans (numbers at each clade denote bootstrap probabilities); (**B**) Timetree inferred by applying the RelTime method to the phylogenetic tree shown in a) and the Hasegawa–Kishino–Yano substitution model, with the branch lengths below each of them and time of divergence to the right of each node.

Allelic richness in the population of brown trout from northern fork of the upper River Rečka above the Bledaria Waterfall was the lowest in Iron Gate region (1.75), as well as the observed heterozygosity (H_{obs} = 0.24), but still higher than expected heterozygosity (H_{exp} = 0.20). The presence of genetic bottleneck was not detected in this stream, but the deviation from L-shape allele frequency distribution under mode-shift test was present. This test does not show statistical significance, but the shape of the curve indicates deviation from Hardy–Weinberg equilibrium (HWE) in this river. In the previous studies (Tošić et al. 2016), the population from the northern fork of the River Rečka above the Bledaria Waterfall was clearly separated from other Iron Gate populations by Factorial Correspondence (FCA), cluster and STRUCTURE analyses. Small number of alleles per locus (Table 5) and one private allele (locus Ssa410UOS) indicated long-term isolation, as well.

The STRUCTURE analysis included the novel tentative Adriatic trout samples from the upper and lower River Zeta and novel brown trout sample from the River Nožica, whose microsatellites were analysed here for the first time, and the tentative Adriatic trout samples from the lower River Mrtvica and brown trout samples from the rivers Zamna and Vratna in the Đerdap (Iron Gate) Gorge area we have already reported about (Škraba Jurlina et al. 2020), and re-analysed here together with the novel samples. Results from that comprehensive sample structuring revealed the highest Delta K value of 119.6168 for K = 5 (Supplement 1), i.e., for the five clearly distinct populations (from the rivers Nožica, upper Zeta, western fork of Rečka and two genetic clusters: lower Mrtvica with lower Zeta and Zamna with Vratna) (Fig. 4). These results clearly show grouping of brown trout populations together, as well as putative Adriatic trout.

Discussion

Comparison of dating that various authors gave for particular events in the evolutionary history of genus *Salmo* (Vladimirov 1948; Anđelković 1989; Osinov and Lebedev 2004; Crête-Lafrenière et al. 2012) using both molecular and paleontological data has raised incongruence several times. Crête-Lafrenière et al. (2012) estimated the age of the family to 59.1 MY with the Confidence Interval of 63.2–58.1 MY on 63 species they analysed and the average mitochondrial rate of molecular divergence to about 0.31% MY^{-1} (with the Confidence Interval of 0.27%–0.36% MY^{-1}). That estimation and geological dating suggest that the values for times of divergence we calculated using the mutation rate of 1% MY^{-1} (Table 2) should be enlarged about threefold, to seize back to about 6 MY ago for divergence between the most ancestral haplotypes of the AD and DA lineages in the area in concern. That value roughly corresponds to those reported using the geological dating, although one should always have in mind that the rate of evolution in early cladogenesis might not necessarily correspond to that occurring

Table 4. Gene flow N_m (above the diagonal), and F_{st} values (below the diagonal) values between populations.

N_m / F_{st}	Nožica	Upper Zeta	Lower Zeta	Lower Mrtvica	Vratna	Zamna	Rečka
Nožica	—	0.83	0.52	0.58	0.79	0.65	0.28
Upper Zeta	0.22612	—	0.43	0.46	1.13	1.02	0.4
Lower Zeta	0.32416	0.36774	—	4	0.47	0.44	0.26
Lower Mrtvica	0.29924	0.34928	0.05983	—	0.49	0.47	0.26
Vratna	0.22336	0.17963	0.34985	0.33697	—	2	0.36
Zamna	0.26494	0.19405	0.36175	0.34527	0.10744	—	0.21
Rečka	0.45111	0.42333	0.48952	0.48348	0.42415	0.54356	—

Table 5. Eight microsatellite loci with the number of alleles per locus detected in analysed streams, with the calculated allelic richness (A_r) and private allelic richness (P_{ar}) in each of them (in an absence of data for microsatellites for brown trout in the River Rečka western fork, data for rivers Vratna and Zamna closest to it were used).

Locus	Locality (haplogroup/haplotype)						
	Upper Zeta (DA)	Lower Zeta (AD)	Nožica (DA)	Lower Mrtvica (AD)	Rečka (N fork) (Da1)	Vratna (Da23c)	Zamna (Da23c)
Str73INRA	5	3	2	3	1	1	1
Ssa85	4	2	4	2	1	2	1
SsaD71	8	13	6	7	3	3	4
Ssa410UOS	11	10	7	5	2	7	3
SSsp2216	13	3	7	5	2	5	5
SsaD190	4	5	2	5	1	3	2
OMM1064	15	3	5	3	2	4	4
SsoSL438	8	—	2	3	2	3	2
A_r	4.0	6.3	3.4	3.6	1.7	3.5	2.7
P_{ar}	1.4	1.5	1.1	1.2	0.7	1.5	1.0

N fork = northern fork.

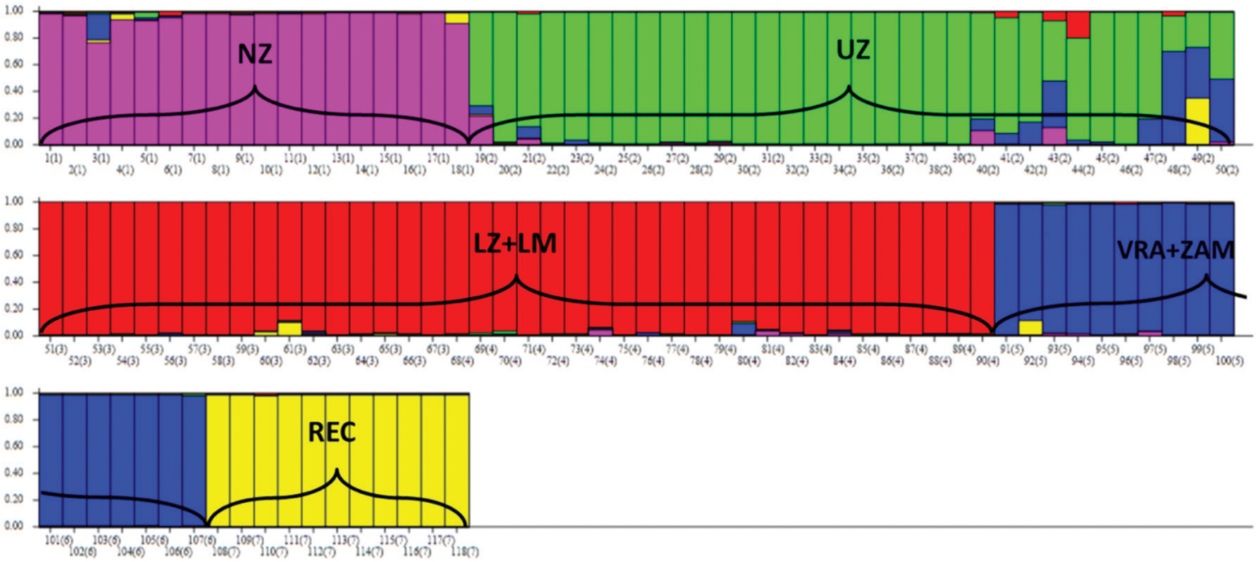

Figure 4. The STRUCTURE analysis reveals the distinct population status (represented by distinct colour) of particular brown trout populations (NZ, River Nožica; UZ, upper River Zeta; REC, River Rečka with one genetic cluster; VRA + ZAM, rivers Vratna and Zamna; LM + LZ, lower River Mrtvica and lower River Zeta as one genetic cluster in putative Adriatic trout) . *Y*-axis presents the participation of alleles from all populations (expressed as a fraction of individual genome ranging from 0–1) in the genome of each individual in all populations, while bars in the *x*-axis represent individuals and colour-assigned obtained genetic clusters i.e., populations.

later. Analyzing both more plesiomorphic (e.g., Da*Vr, Da*Dž and Da-s6) and derived haplotypes (e.g., Da1, Da2, Da22, Da23c, etc.) in the DA haplogroup of brown trout from the River Danube basin of the Western Balkans, Simonović et al. (2017) found the uniform rate of evolution in their D-loop sequences. On the contrary, this analysis revealed both that the evolutionary rate throughout the phylogenetic tree is not equal and that evolutionary rates in particular haplogroups are independent. It seems that it is not possible to assess the difference in rate of mutation between more ancient and closer periods of brown trout diversification for certain using the mtDNA molecular clock approach, though our results testify to the slower evolutionary rate in ancient, pre-Pleistocene haplotypes and faster evolutionary rate in more derived, the ones from Pleistocene. That is in line with the findings of Crête-Lafrenière et al. (2012), who stated that the evolutionary rate is dependent upon the timing of divergence, with the faster rates more applicable to recent speciation events.

Another difficulty in calibrating the molecular clock lies in the weight, *sensu* Mayr (1969) and Mayr and Ashlock (1991), of the character used for that, either regarding the type of the molecule, part of the sequence of the same molecule type employed, or in the length of the sequence (i.e., a 100%) from which the time of divergence is to be estimated (Osinov and Bernatchez 1996). Values for divergence between haplotypes (Table 2) reveal remarkable difference between the ones assessed using the partial sequences (up to the poly-T block) and the whole D-loop sequences (Table 2). That difference originates from the obvious difference in variability between the two D-loop parts noticeable in comparing haplogroups AD and DA and haplotypes within each of haplogroups. While using only the part of D-loop, for example, divergence times between AD and DA haplotypes are greater than if the whole D-loop sequence is used. In contrast, that time is greater for two AD halotypes (Adcs11 and Ad-M1) when the whole D-loop sequence is used.

Earlier phylogeographic studies in eastern Serbia revealed the presence of few CR mtDNA haplotypes (Tošić et al. 2014, 2016). Nuclear markers used in this study examined matching of population genetics to earlier results. Moderate-to-high values of observed heterozygosity for trout fish were also reported by Mrdak et al. (2012). Allelic richness in almost all brown trout populations in eastern Serbia indicates high genetic variability, regardless of their small population size caused by occasionally harsh environmental conditions. The lowest genetic variability was detected in the population from headwaters of the River Rečka northern fork upstream of the Bledarija waterfall. This population was distinctive in many ways compared to other analysed populations. In addition to the exclusive presence of the private Da1 haplotype (Tošić et al. 2016), the brown trout population from that fork of the River Rečka featured a low number of microsatellite alleles (Table 3), who were all private (Škraba Jurlina et al. 2020), which determined its uniqueness in the group of populations from the Iron Gate Gorge region (Fig. 3). The occurrence of private haplotype and alleles, as well as the loss of genetic variability in that brown trout population (Table 3) testifies to its long-term isolation and its native character. Its haplotype was reconstructed as ancestral in relation to brown trout that hold more derived Da23c haplotype (Tošić et al. 2014; Simonović et al. 2017). A waterfall more than 12 m in height maintained unsurmountable isolation from brown trout in the downstream section. This obstacle has prevented introgression into the ancestral population situated upstream of the waterfall. The greatest genetic differentiation revealed by Watterson's estimator (θ) and the lowest gene flow rate (N_m) values detected between distant brown trout populations from the River Rečka and other streams in the Iron Gate area (Table 4), as well as in River Crni Timok system (Škraba Jurlina et al. 2020) supported the very high differentiation of brown trout in the upstream section from the ones in the rivers Vratna and Zamna and most likely from those below the Bledaria waterfall. The STRUCTURE analysis for upstream situated brown trout revealed a very high level of differentiation both in this research and in Škraba Jurlina et al. (2020). The long-term isolation of the River Rečka population in the northern fork has likely favoured inbreeding and acting of the genetic drift as the most prominent evolutionary mechanisms acting there. Wilcoxon test revealed no significance for the bottleneck effect in this population (Table 3), but the deviation from the L-shaped distribution of allelic frequencies (the *mode-shift* test that has no statistical support) indicates its recent occurrence (Škraba Jurlina et al. 2020).

Indeed, the undertaken investigations on speleothem in the cave carved into the Barremian (Lower Cretaceous) reef limestones on the opposite, Romanian side of the Danube, showed that it was precipitated between ~75 ka and ~2 ka with at least two hiatuses (Constantin, unpublished[*]). The obtained dating is the age when the stream bed has already been incised. Horvatinčić et al. (2003) found that speleothem growth started several thousand years earlier than tufa and that the majority of tufa deposits in Europe formed within the last ca. 7000 years. It should be noted that the dating of karst areas in Serbia based on correlation of heights of speleological objects with the alluvial terraces, should be taken with caution and that precise data, such as those obtained by radiocarbon dating are missing. For example, alluvial terrace of sandy clays strata next to the confluence of the River Reka (the lower section of the River Rečka) to the Danube are considered equivalents of Mindel (0.337–0.374 MY ago) and Mindel–Riss (0.3–0.337 MY ago) interglacial stages (i.e., Mid-Pleistocene) (Dimitrijević et al. 1997). That dating seems roughly comparable to the dating of divergence of the Da23c haplotype from the Da1a to at least 0.101–0.178 MY ago and at most 0.325–0.575 MY ago (Table 2), using the partial and whole CR sequences and two mutation rates, respectively.

The dating of tectonic formation of the lower River Zeta valley and River Morača to Miocene–Pliocene boundary (Cvijić 1926) provides the support for immigration of brown trout of the AD molecular lineage there. That is in agreement with the hypothesizing of the scenario that happened in the high karst plateau of the Adriatic slope of the divide much later, during the Pleistocene glaciations, when brown trout of the DA haplogroup

---

[*] Constantin S. 2003. Evolutii paleoclimatice in Cuaternar pe baza speleotemelor din carstul Muntilor Banatului si Mehedinti Unpublished PhD thesis, Department of Geology, Bukarest University, Romania.

colonized the River Nožica. During the Pleistocene period, marked by alternating largescale glaciations interfered by short warm intervals, the highest mountains in Montenegro were covered by glaciers. Most of them advanced towards the River Morača incising channels into bedrock. Nevertheless, the glacier at Širokar, situated in the present headwaters' area of the River Tara, has been split by the so-called glacial bifurcation on two parts that have taken two different directions. The southern part has moved towards Lake Bukumir (Adriatic basin) and the northeastern part towards the River Vjeruša, a fork of the River Tara, i.e., into the Black Sea basin (Cvijić 1921; Đokić et al. 1976; Petrović 2007). Glacial bifurcation occurred as the consequence of karst relief instead of a fluvial one beneath a glacial cover, and was additionally supported by the gradual descent of the ice boundary allowing, albeit a minor part of the glacier, to reach Lake Bukumir, i.e., the Adriatic basin (Petrović 2007). Currently, this Pleistocene glacier bifurcating is the best available explanation for an occurrence (i.e., a transfer) of brown trout of the otherwise widespread Da1a haplotype in the River Nožica in the Adriatic Sea Basin, which was most likely initially devoid of any trout species. The native absence of any tentative brown trout taxon in particular streams of the Adriatic Sea Basin was already inferred, e.g., the River Vrijeka in Herzegovina and River Gacka in the high Lika Karst Field in Croatia (Simonović et al. 2017). The glaciers covering the highest mountains in Montenegro were exposed to melting during interglacial stages. Glaciations generally gave rise to erosional features in the highlands and depositional features on lowlands. Hence many of the large rivers in both seas' basins in Montenegro (e.g., rivers Tara, Mrtvica, Morača) along with some of the greatest recent canyons (e.g., the Canyon Platije of the River Morača) owe their origin to meltwater rivers at the beginning of Holocene (Đurović and Petrović 2007). The disappearance of glaciers and the release of snow and ice weight have led to postglacial uplifting of the mountainous area in Montenegro (determined recent upthrows of 2–4 and more millimetres per year), whereas parts around Lake Skadar basin and along the Adriatic Sea coastline subsided (Ivanović 1991). A divergence of the most recent haplotypes of the AD haplogroup in the region, Ad-M1 and Adcs11, was estimated to 0.178–0.575 MY and 0.302–0.975 MY ago, respectively (Table 2) as well as to 0.378 MY ago (Fig. 3B). That fits well into the Pleistocene period. It suggests also that those haplotypes occurred before the melting of glaciers in Holocene in the former River Morača system occurring there. The physical barriers of glaciers and uplifting of mountains could explain an occurrence of only ancestral Adcs11 haplotype and the absence of the other more derived Ad-M1 haplotype in the upper River Mrtvica at high altitudes (Škraba Jurlina et al. 2018). However, the ancient occurrence of the whole recent Skadar basin with its system of sublacustrine springs that dates back at least to the Pliocene, ca. 3 MY ago (Grabowski et al. 2018) suggests the possible dating of appearance of the Ad-Prz haplotype of tentative Adriatic trout, the most plesiomorphic in the AD lineage there. That dating is congruent with the one of 1.725 MY and 0.403–1.299 MY we obtained using the molecular clock method at two rates and two CR sequence lengths, respectively (Table 2), as well as with the 2.052 MY using the TimeTree option (Fig. 3B), providing the scene for their occurrence there.

On the (1) high levels of diversity at the haplogroups' level; (2) independent evolutionary histories and prominent endemism in tentative Adriatic and Macedonian, *Salmo macedonicus* (Karaman, 1924), trout at the Adriatic and Aegean Seas' basins, respectively reported from results of molecular studies, as well as (3) ancestral character reconstructed in particular Balkans populations (Marić et al. 2006; Apostolidis et al. 2011), this region was considered important for evolving of the AD lineage. The other region that Bardakci et al. (2006) and Arslan and Bardakci (2010) suggested is the Asia Minor, positioning the start of diversification there before the Pleistocene (i.e, in the Pliocene, more than 2 MY ago), while geological history events' dating reached the Miocene/Pliocene boundary (Cvijić 1926). Apostolidis et al. (1997) stated that the high level of endemism in AD lineage could be a consequence of ancient isolation and independent evolving of allopatric populations with limited natural contact between them. For example, the vicariant Adcs1 haplotype that Sušnik et al. (2007) have considered ancestral for the AD haplogroup was questioned by finding of the Ad*Bož haplotype of the very limited dispersal in tentative Macedonian trout living in sympatry with their conspecifics with the Adcs1 haplotype in few headwaters at the slopes of the Vlasina Plateau of the SE Serbia, which join the River Struma (Strymon) (Marić et al. 2006).

The contours of the whole Balkan area were finally shaped by geodynamic events during the Neoalpine history and the interaction of three geodynamic processes: Pannonian collapse, continuous epeirogeny upward movement and the Aegean collapse (Marović et al. 2007). The former, which started in the Ottnangian–Karpatian (18.1–17.2 MY ago), less in Badenian and Sarmatian led to development of subsidential structures, such as the River Morava Graben (e.g., Marović 1990; Marović et al. 2002). The strong epeirogenic uplifting of 500 to 1500 m proper to southwest and west attained the epeirogeny uplifting over 1500 meters in the Vlasina Plateau. Opposite it, the subsidence declined successively from south to north through the Pannonian into the Pontian, but might be renewed in some areas during the Pliocene/Quaternary and even the Upper Quaternary, as the consequence of the Aegean orogen collapse.

The course of the River Struma/Strymon is mainly controlled by the NNW–SSE trending Struma Lineament, a large tectonic structure that represents the tectonic boundary of the Serbo–Macedonian and the Rhodope massifs (Zagorchev 2007). The onset of the River Struma basin is attributed to collisional processes that have taken place from Late Oligocene to Middle–Late Miocene between the Apulia and Eurasia plates (Tranos et al. 2007; Tranos 2011). At the last glacial maximum (21 500 years BP), when the sea level was 120 m lower than today, the rivers Mesta/Nestos and Struma/Strymon formed a joint delta and found their way to the sea, as well as the Vardar/Axios (Perissoratis and Conispoliatis 2003).

In the inferred phylogeny, the ancient Ad*Bož haplotype was a sister clade of all others in the AD haplogroup (Marić et al. 2006). There was only one difference between the Adcs1 and Ad*Bož, and there were five and two different base pairs between each of them, respectively and Ad*Prz that is considered closely related, and six base pairs between each of them, respectively and the Da*Vr haplotype (Table 2), the most basal in the DA haplogroup (Fig. 3A). Cortey et al. (2004) estimated the differentiation of southern trout haplogroups using the molecular clock method at the Pliocene–Pleistocene climate cooling that occurred at 1 MY ago, with the strongest diversification in the AD haplogroup occurring at 0.2–0.15 MY ago, which is much sooner than our estimations of 2.139–6.900 MY ago between the Ad-M1 and Da23c (Table 2) and 5.730 MY ago (Fig. 3B), that is at the Pleistocene to the late Pliocene) for differentiation of southern brown trout haplogroups, and of 0.357–1.150 MY ago and 0.302–0.975 MY ago (Table 2), as well as of 0.378–2.052 MY ago for diversification in the AD haplogroup (Fig. 3B) in the Pliocene–Pleistocene boundary and in Pleistocene made using molecular clock at the mutation rates of 1% MY^{-1} and 0.31% MY^{-1} and using partial and whole CR sequences and TimeTree inferring, respectively. The dating of geological history events gives the scene for, i.e., supporting the ancient and ancestral character of both Da*Vr and Da*Dž on one, and Ad*Bož on the other side of the peninsular divide in the DA and AD haplogroups in the Vlasina Plateau area, respectively.

In conclusion, it seems that in addition to places of its occurrence, the dating of recent *Salmo* spp. evolutionary history remains vague. In addition to the phylogeography of brown trout, the reconstructed phylogenetic relations determining the ancestry and descendancy of particular evolutionary units (here referring to haplotypes) should be accounted in considering the dynamics of their evolving. The matters we again have posed here, e.g., (1) the speed of evolving in more recent, i.e., advanced and older, i.e., ancestral periods and evolutionary units (here referring to haplotypes), and (2) levels and the variability of parts of the D-loop, their usefulness in calibration of the molecular clock and their validation with the dating known from geological history, still need more research to get us closer to a more reliable estimation of dating of the divergence between brown trout lineages throughout their dispersal areas. While some dating of the more recent events of evolutionary history seems to correspond well to those of geological history and at local scale, others need more consideration in reaching that aim. It is certain that the ancient scene for evolving of ancestral brown trout haplotypes has been created from geological events either at a wider, continental geographical scale, e.g., gradual succession of the Parathetis Sea, or at the more regional scale, e.g., the formation of the river system in the Skadar Plane and during the Rhodopi Mountains uplifting at the Miocene–Pliocene boundary and mid-to-Late Miocene, respectively. The evolution and spread of the more recent haplotypes, on the other hand, has occurred on that scene in the circumstances of the Late Pliocene and Pleistocene cooling and glaciations, when glacial interconnections (e.g., at the Nikšić high karst plateau and that of the Širokar glacier bifurcating at the watershed divide between the River Vjeruša, i.e., the River Tara's fork, and River Nožica) played a significant role in dispersal of more advanced haplotypes. It might be hypothesized that those two "acts" of brown trout evolution lasted differently, i.e., unrolled at a different speed and that the distinct molecular clock (i.e., substitution-mutational) rates should be established for them, or the polled, i.e., the logarithmic rate instead of the current uniform, linear one should be set. That period of advanced brown trout and related tentative trout taxa evolving during the Pleistocene glaciations most likely included the acting of evolutionary mechanisms other than mutations (e.g., genetic drift), when they likely used to decrease in population size and pass through the bottleneck episodes. However, the evolving of their CR, their phylogeography and phylogenetic relations give us an opportunity to trace their evolutionary history in the scene that geological history has set to them.

Acknowledgements

Work was granted by the Ministry of Education, Science and Technological Development of the Republic of Serbia (Contracts No. 451-03-68/2022-14/200178, No. 451-03-68/2022-14/200007 and No. 451-03-68/2022-14/200126 for the University of Belgrade, Faculty of Biology, Institute for Biological Research "Siniša Stanković" and Faculty of the Mining and Geology, respectively).

References

Almaca C (1990) Neogene circum-Mediterranean paleogeography and Euro-Mediterranean *Barbus* biogeography. Arquivos do Museu Bocage, Nov. Série 1: 585–611.

Anđelković SJ (1970). Tercijerne ribe Srbije. Geološki anali Balkanskog poluostrva 35: 281–366.

Anđelković SJ (1989) Tertiary fish of Yugoslavia: A stratigraphic–paleonthological–paleoecological study. Paleontologia Jugoslavica 38: 1–121.

Apostolidis AP, Triantaphyllidis C, Kouvatsi A, Economidis PS (1997) Mitochondrial DNA sequence variation and phylogeography among

Salmo trutta L. (Greek brown trout) populations. Molecular Ecology 6(6): 531–542. https://doi.org/10.1046/j.1365-294X.1997.d01-176.x

Apostolidis AP, Stoumboudi MT, Kalogianni E, Cote G, Bernatchez L (2011) Genetic divergence among native trout *Salmo trutta* populations from southern Balkans based on mitochondrial DNA and microsatellite variation. Journal of Fish Biology 79(7): 1950–1960. https://doi.org/10.1111/j.1095-8649.2011.03136.x

Arslan S, Bardakci F (2010) Genetic structure of brown trout (*Salmo trutta*) populations from Turkey based on microsatellite data. Biochemical Genetics 48(11–12): 995–1014. https://doi.org/10.1007/s10528-010-9388-2

Artamonova VS, Bolotov IN, Vinarski MV, Makhrov AA (2021) Fresh- and brackish-water cold-tolerant species of southern Europe: Migrants from the Paratethys that colonized the Arctic. Water 13: e1161. https://doi.org/10.3390/w13091161

Baldacci A (1929) L'Albania. Istituto per l'Europa Orientale, Roma, 463 pp.

Bardakçi F, Degerli N, Ozdemir O, Basibuyuk HH (2006) Phylogeography of the Turkish brown trout *Salmo trutta* L.: mitochondrial DNA PCR-RFLP variation. Journal of Fish Biology 68(A): 36–55. https://doi.org/10.1111/j.0022-1112.2006.00948.x

Belkhir KP, Borsa P, Chikhi L, Raufaste N, Bonhomme F, Belkhir K (2004) GENETIX 4.05, logiciel sous Windows TM pour la génétique des populations. Laboratoire Génome, Populations, Interactions. Université de Montpellier II, Montpellier.

Bernatchez L (2001) The evolutionary history of brown trout (*Salmo trutta* L.) inferred from phylogeographic, nested clade, and mismatch analyses of mitochondrial DNA variation. Evolution 55(2): 351–379. https://doi.org/10.1111/j.0014-3820.2001.tb01300.x

Bernatchez L, Danzmann RG (1993) Congruence in control-region sequence and restriction-site variation in mitochondrial DNA of brook charr (*Salvelinus fontinalis* Mitchill). Molecular Biology and Evolution 10: 1002–1014. https://doi.org/10.1093/oxfordjournals.molbev.a040062

Bernatchez L, Guyomard R, Bonhomme F (1992) DNA sequence variation of the mitochondrial control region among geographically and morphologically remote European brown trout *Salmo trutta* populations. Molecular Ecology 1(3): 161–173. https://doi.org/10.1111/j.1365-294X.1992.tb00172.x

Bešić Z (1969) Geologija Crne Gore–Karst Crne Gore, no. 2, Zavod za geološka istraživanja Crne Gore, Titograd, 304 pp.

Bianco PG (1990) Potential role of the paleohistory of the Mediterranean and Paratethys basin on the early dispersal of Euro-Mediterranean freshwater fishes. Ichthyological Exploration of Freshwaters 1: 167–184.

Bošković M, Popović M, Alilović N (2004) Supplement to Skadar lake geogenesis, its inflow and outlet components and background on its regulation activities. Pp. 1–9. In: BALWOIS Conference Proceedings, Ohrid, Macedonia 25–29 May 2004.

Cairney M, Taggart JB, Høyheim B (2000) Characterization of microsatellite and minisatellite loci in Atlantic salmon (*Salmo salar* L.) and cross-species amplification in other salmonids. Molecular Ecology 9(12): 2155–2234. https://doi.org/10.1046/j.1365-294X.2000.105312.x

Cornuet JM, Luikart G (1996) Description and power analysis of two tests for detecting recent population bottlenecks from allele frequency data. Genetics 144(4): 2001–2014. https://doi.org/10.1093/genetics/144.4.2001

Cortey M, Garcia-Marin JL (2002) Evidence for phylogeographically informative sequence variation in the mitochondrial control region of Atlantic brown trout. Journal of Fish Biology 60(4): 1058–1063. https://doi.org/10.1111/j.1095-8649.2002.tb02429.x

Cortey M, Pla C, Garcia-Marin JL (2004) Historical biogeography of Mediterranean trout. Molecular Phylogenetics and Evolution 33(3): 831–844. https://doi.org/10.1016/j.ympev.2004.08.012

Cracraft J (1989) Speciation and its ontology: The empirical consequences of alternative species concept for understanding pattern and processes of differentiation. Pp. 28–59. In: Otte D (Ed.) Speciation and its Consequences, Sinauer, Sunderland, MA, USA.

Crête-Lafrenière A, Weir LK, Bernatchez L (2012) Framing the Salmonidae family phylogenetic portrait: A more complete picture from increased taxon sampling. PLoS One 7(10): e46662. https://doi.org/10.1371/journal.pone.0046662

Cvijić J (1921) Ledeno doba u Prokletijama. Glasnik Srpske Kraljevske Akademije, Beograd, Vol. 93, 191 pp.

Cvijić J (1926) Geomorfologija, knj. II, Državna štamparija Kraljevine Jugoslavije, Beograd, 506 pp.

Darriba D, Taboada GL, Doallo R, Posada D (2012) jModelTest 2: More models, new heuristics and high-performance computing. Nature Methods 9(8): 772. https://doi.org/10.1038/nmeth.2109

Dimitrijević MD, Mijović-Pilić D, Mijović-Pilić D (1997) Geology of Yugoslavia. Geoinstitute, Belgrade, 187 pp.

Drobne F, Božovič M, Žlebnik Lj, Premru V (1979) Osnutek tolmača k hidrogeološki karti Slovenije, M=1:500000. FSD Geološkog zavoda, Ljubljana.

Drummond AJ, Ho SYW, Phillips MJ, Rambaut A (2006) Relaxed phylogenetics and dating with confidence. PLoS Biology 4(5): e88. https://doi.org/10.1371/journal.pbio.0040088

Đurović P, Petrović A (2007) Large canyons in Dinaric and Prokletije mountains region in Montenegro. Geographica Pannonica 11(11): 14–18. https://doi.org/10.5937/GeoPan0711014D

Earl DA, Vonholdt BA (2012) STRUCTURE HARVESTER: A website and program for visualizing STRUCTURE output and implementing the Evanno method. Conservation Genetics Resources 4(2): 359–361. https://doi.org/10.1007/s12686-011-9548-7

Estoup A, Rousset F, Michalakis Y, Cornuet J-M, Adriamanga M, Guyomard R (1998) Comparative analysis of microsatellite and allozyme markers: A case study investigating microgeographic differentiation in brown trout (*Salmo trutta*). Molecular Ecology 7(3): 339–353. https://doi.org/10.1046/j.1365-294X.1998.00362.x

Evanno G, Regnaut S, Goudet J (2005) Detecting the number of clusters of individuals using the software STRUCTURE: A simulation study. Molecular Ecology 14(8): 2611–2620. https://doi.org/10.1111/j.1365-294X.2005.02553.x

Goudet J (2002) FSTAT version 2.9.3.2, a program to estimate and test gene diversities and fixation indices. Institute of Ecology, Lausanne. [Accessed on 20 August 2012] http://www2.unil.ch/popgen/softwares/fstat.htm

Grabowski M, Jabłońska A, Wysocka A, Pešić V (2018) The obscure history of the Lake Skadar and its biota: A perspective for future research. Pp. 47–62. In: Pešić V, Karaman G, Kostianoy AG (Eds) The Skadar/Shkodra Lake environment. Vol. 80 of The handbook of environmental chemistry. Springer, Cham, Switzerland. https://doi.org/10.1007/698_2018_349

Grubić A (1992) Geological section of Džervin Hill in NE Serbia. Annales Géologiques de la Péninsule Balkanique 55(1): 17–35.

Ho SYW, Duchéne S (2014) Molecular-clock methods for estimating evolutionary rates and timescales. Molecular Ecology 23(24): 5947–5965. https://doi.org/10.1111/mec.12953

Horvatinčić N, Krajcar Bronić I, Obelić B (2003) Differences in the ^{14}C age, δ^{13}C and δ^{18}O of Holocene tufa and speleothems in the Dinaric Karst. Palaeogeography, Palaeoclimatology, Palaeoecology 193(1): 139–157. https://doi.org/10.1016/S0031-0182(03)00224-4

Ivanović S (1991) Zemljotresi–fenomeni prirode. Crnogorska akademija nauka i umjetnosti, Građevinski fakultet Univerzita "Veljko Vlahović", Titograd, 207 pp.

Jipa CD (2015) The identity of a Paratethys Basin. Dacian Basin configuration—outcome of the Carpathian Foredeep along-arc migration. Geo-Eco-Marina 21: 159–166.

Jipa CD, Olariu C (2009) Dacian Basin. Depositional architecture and sedimentary history of a Parathetis Sea. Geo-Eco-Marina, Bucharest, Special publication No. 3, 268 pp.

Kalinowski ST (2005) HP-Rare: A computer program for performing rarefaction on measures of allelic diversity. Molecular Ecology Notes 5(1): 187–189. https://doi.org/10.1111/j.1471-8286.2004.00845.x

Kanjuh T, Marić A, Piria M, Špelić I, Maguire I, Simonović P (2020) Diversity of brown trout, *Salmo trutta* (Actinopterygii: Salmoniformes: Salmonidae), in the Danube River basin of Croatia revealed by mitochondrial DNA. Acta Ichthyologica et Piscatoria 50(3): 291–300. https://doi.org/10.3750/AIEP/02939

Kanjuh T, Tomić S, Marić A, Škraba Jurlina D, Nikolić V, Simonović P (2021) Trout *Salmo* spp. (Salmoniformes: Salmonidae) molecular diversity in streams on the southern slopes of the Stara Planina Mts. in Serbia. Acta Zoologica Bulgarica 73(3): 425–429.

Kimura M (1980) A simple method for estimating evolutionary rate of base substitutions through comparative studies of nucleotide sequences. Journal of Molecular Evolution 16(2): 111–120. https://doi.org/10.1007/BF01731581

King TL, Eackles MS, Letcher BH (2005) Microsatellite DNA markers for the study of Atlantic salmon (*Salmo salar*) kinship, population structure, and mixed-fishery analyses. Molecular Ecology Notes 5(1): 130–132. https://doi.org/10.1111/j.1471-8286.2005.00860.x

Kottelat M (1997) European freshwater fishes. An heuristic checklist of the freshwater fishes of Europe (exclusive of former USSR), with an introduction for non-systematics and comments on nomenclature and conservation. Biologia (suppl. 5): 1–271.

Kottelat M, Freyhof J (2007) Handbook of European freshwater fishes. Kottelat and Freyhof, Cornol–Berlin, 646 pp.

Kumar S, Stecher G, Li M, Knyaz C, Tamura K (2018) MEGA X: Molecular Evolutionary Genetics Analysis across computing platforms. Molecular Biology and Evolution 35(6): 1547–1549. https://doi.org/10.1093/molbev/msy096

Laskarev V (1924) Sur les équivalents du Sarmatien supérieur en Serbie. Recueil de traveaux offert à M. Jovan Cvijič par ses amis et collaborateurs. 73–85. Državna Štamparija, Beograd.

Luikart G, Cornuet J-M, Allendorf FW, Sherwin WB (1998) Distortion of allele frequency distributions provide a test for recent population bottlenecks. Journal of Heredity 89(3): 238–247. https://doi.org/10.1093/jhered/89.3.238

Marić S, Sušnik S, Simonovic P, Snoj A (2006) Phylogeographic study of brown trout from Serbia, based on mitochondrial DNA control region analysis. Genetics, Selection, Evolution 38(4): 411–430. https://doi.org/10.1186/1297-9686-38-4-411

Marović M (1990) Block feature and vertical neotectonic displacements in eastern Serbia as per morphostructural data. Annales Géologiques de la Péninsule Balkanique 54: 107–120.

Marović M, Đoković I, Milićević V, Toljić M, Gerzina N (2002) Paleomagnetism of the Late Paleogene and Neogene rocks of the Serbian Carpatho–Balkanides: Tectonic implications. Annales Géologiques de la Péninsule Balkanique 64(64): 1–12. https://doi.org/10.2298/GABP0264001M

Marović M, Toljić M, Rundić Lj, Milivojević J (2007) Neoalpine Tectonics of Serbia. Serbian Geological Society Monographie, Belgrade, 98.

Martin AP, Pallumbi SR (1993) Body size, metabolic rate, generation time, and the molecular clock. Proceedings of the National Academy of Sciences of the United States of America 90(9): 4087–4091. https://doi.org/10.1073/pnas.90.9.4087

Matoshko A, Matoshko A, de Leeuw A (2019) The Plio–Pleistocene demise of the east Carpathians foreland fluvial system and arrival of the Paleo–Danube to the Black Sea. Geologica Carpathica 70(2): 91–112. https://doi.org/10.2478/geoca-2019-0006

Mayr E (1969) Principles of systematic zoology, 1st edn. McGraw-Hill, New York, 428 pp.

Mayr E, Ashlock PD (1991) Principles of systematic zoology (2nd ed.). McGraw-Hill, New York, 475 pp.

Mazzini I, Gliozzi E, Koci R, Soulie-Morsche I, Zanchetta G, Baneschi I, Sadori L, Giardini M, van Weldeni A, Bushati S (2015) Historical evolution and Middle to Late Holocene environmental changes in lake Shkodra (Albania): New evidences from micropaleontological analysis. Palaeogeography, Palaeoclimatology, Palaeoecology 419: 47–59. https://doi.org/10.1016/j.palaeo.2014.08.012

Miller SA, Dykes DD, Polesky HF (1988) A simple salting out procedure from human nucleated cells. Nucleic Acids Research 16(3): 1215. https://doi.org/10.1093/nar/16.3.1215

Mrdak D, Simonović P, Sušnik S, Snoj A (2006) The existence of "strun"—*Salmo dentex* (Heckel 1851) as distinct species from *Salmo trutta fario* (Linnaeus, 1758), in Adriatic rivers of Montenegro. Pp. 137–142. In: II International Symposium of Ecologists of Montenegro – Proceedings of the Symposium.

Mrdak D, Nikolić V, Tošić A, Simonović P (2012) Molecular and ecological features of the soft-muzzled trout *Salmo obtusirostris* (Heckel, 1852) in the Zeta River, Montenegro. Biologia 67(1): 222–233. https://doi.org/10.2478/s11756-011-0150-y

Mulić M, Bašagić M, Čičić S (2006) Geodynamic investigations in Bosnia and Herzegovina. Pp. 195–207. In: Pinter N, Gyula G, Weber J, Stein S, Medak D (Eds) The Adria Microplate: GPS geodesy, tectonics and hazards. Nato Science Series 4: Earth and Environmental Sciences, Vol. 61. Springer, Dordrecht, the Netherlands. https://doi.org/10.1007/1-4020-4235-3_13

O'Reilly PT, Hamilton LC, McConnell SK, Wright JM (1996) Rapid analysis of genetic variation in Atlantic salmon (*Salmo salar*) by PCR multiplexing of dinucleotide and tetranucleotide microsatellites. Canadian Journal of Fisheries and Aquatic Sciences 53(10): 2292–2298. https://doi.org/10.1139/f96-192

Osinov AG, Bernatchez L (1996) "Atlantic" and "Danubian" phylogenetic groupings of brown trout *Salmo trutta* complex: Genetic divergence, evolution and conservation. Journal of Ichthyology 36(6): 723–746.

Osinov AG, Lebedev VS (2004) Salmonid fishes (Salmonidae, Salmoniformes): The systematic position in the superorder Protacanthopterygii, the main stages of evolution, and molecular dating. Journal of Ichthyology 44(9): 690–715.

Paterson S, Piertney Samova B, Knox D, Gilbey J, Verspoor E (2004) Characterization and PCR multiplexing of novel highly variable tetranucleotide Atlantic salmon (*Salmo salar* L.) microsatellites. Molecular Ecology Notes 4(2): 160–162. https://doi.org/10.1111/j.1471-8286.2004.00598.x

Perissoratis C, Conispoliatis N (2003) The impacts of sea-level changes during latest Pleistocene and Holocene times on the morphology of the Ionian and Aegean seas (SE Alpine Europe). Marine Geology 196(3): 145–156. https://doi.org/10.1016/S0025-3227(03)00047-1

Petrović A (2007) Pleistocena glacijacija gornjeg toka Veruše. Zbornik radova (Univerzitet u Beogradu-Geografski fakultet) 15: 13–22.

Piller EW, Harzhauser M (2005) The myth of the brackish Sarmatian Sea. Terra Nova 17(5): 450–455. https://doi.org/10.1111/j.1365-3121.2005.00632.x

Piry S, Luikart G, Cornuet JM (1999) BOTTLENECK: A program for detecting recent effective population size reductions from allele data frequencies. Journal of Heredity 90: 502–503. https://doi.org/10.1093/jhered/90.4.502

Popov SV, Ahmet′ev MA, Lopatin AV, Bugrova ÈM, Cyčevskaâ EK, Šerba IG, Andreeva-Grigorovič AS, Zaporožec NI, Nikolaeva IA, Kopp ML (2009) Paleogeografiâ i biogeografiâ bassejnov Paratetisa. Čast′ 1. Pozdnij èocen – rannyj miocen. Naučnyj mir, Moskva, Russia, 194 pp.

Pritchard JK, Stephens M, Donnelly P (2000) Inference of population structure using multilocus genotype data. Genetics 155(2): 945–959. https://doi.org/10.1093/genetics/155.2.945

Pustovrh G, Snoj A, Sušnik Bajec S (2014) Molecular phylogeny of *Salmo* of the western Balkans, based upon multiple nuclear loci. Genetics, Selection, Evolution 46(7): 7. https://doi.org/10.1186/1297-9686-46-7

Rambaut A, Bronham L (1998) Estimating divergence dates from molecular sequences. Molecular Biology and Evolution 15(4): 442–448. https://doi.org/10.1093/oxfordjournals.molbev.a025940

Razpet A, Marić S, Parapot T, Nikolić V, Simonović P (2007) Re-evaluation of *Salmo* data by Gridelli (1936)—description of stocking, hybridization and repopulation in the River Soča basin. Italian Journal of Zoology 74(1): 63–70. https://doi.org/10.1080/11250000601090081

Rexroad CE III, Coleman RL, Hershberger WK, Killefer J (2002) Rapid communication: Thirty-eight polymorphic microsatellite markers for mapping in rainbow trout. Journal of Animal Science 80(2): 541–542. https://doi.org/10.2527/2002.802541x

Rögl F (1998) Palaeogeographic considerations for Mediterranean and Paratethys Seaways (Oligocene to Miocene). Annalen des Naturhistorischen Museums in Wien 99A: 279–310.

Rögl F (1999) Mediterranean and Paratethys. Facts and hypotheses of an Oligocene to Miocene paleogeography (short overview). Geologica Carpathica 50: 339–349. https://doi.org/10.1017/CBO9780511542329.002

Sanz N (2018) [2] Phylogeographic structure of brown trout. Pp. 17–63. In: Lobon-Cervia J, Sanz N (Eds) Brown trout: Biology, ecology and management. John Wiley and Sons, Chichester, UK. https://doi.org/10.1002/9781119268352.ch2

Shedlock AM, Parker JD, Crispin DA, Pietsch TW, Burmer GC (1992) Evolution of the mitochondrial control region. Molecular Phylogenetics and Evolution 1(3): 179–192. https://doi.org/10.1016/1055-7903(92)90014-8

Simonović P, Marić S, Nikolić V (2007) Trout *Salmo* spp. complex in Serbia and adjacent regions of western Balkans: Reconstruction of evolutionary history from external morphology. Journal of Fish Biology 70C(sc): 359–380. https://doi.org/10.1111/j.1095-8649.2007.01516.x

Simonović P, Vidović Z, Tošić A, Škraba D, Čanak-Atlagić J, Nikolić V (2015) Risks to stocks of native trout of the genus S*almo* (Actinopterygii: Salmoniformes: Salmonidae) of Serbia and management for their recovery. Acta Ichthyologica et Piscatoria 45(2): 161–173. https://doi.org/10.3750/AIP2015.45.2.06

Simonović P, Tošić A, Škraba D, Nikolić V, Piria M, Tomljanović T, Šprem N, Mrdak D, Milošević D, Bećiraj A, Dekić R, Povž M (2017) Diversity of Brown trout *Salmo* cf. *trutta* (L.) in the River Danube basin of Western Balkans as assessed from the structure of their mitochondrial control region haplotypes. Journal of Ichthyology 57(4): 603–616. https://doi.org/10.1134/S0032945217040154

Škraba Jurlina D, Marić A, Karanović J, Nikolić V, Brkušanin M, Kanjuh T, Mrdak D, Simonović P (2018) Effect of the introgression of Atlantic brown trout, *Salmo trutta*, into Adriatic trout, *Salmo farioides* in a stream at the drainage area of the Adriatic Sea basin of Montenegro. Acta Ichthyologica et Piscatoria 48(4): 363–372. https://doi.org/10.3750/AIEP/02491

Škraba Jurlina D, Marić A, Mrdak D, Kanjuh T, Špelić I, Nikolić V, Piria M, Simonović P (2020) Alternative life-history in native trout (*Salmo* spp.) suppresses invasive effect of alien trout strains introduced into streams at the western part of the Balkans. Frontiers in Ecology and Evolution 8: 188. https://doi.org/10.3389/fevo.2020.00188

Slettan A, Olsaker I, Lie Ø (1995) Atlantic salmon, *Salmo salar*, microsatellites at the SSOSL25, SSOSL85, SSOSL311, SSOSL417 loci. Animal Genetics 26(4): 281–282. https://doi.org/10.1111/j.1365-2052.1995.tb03262.x

Snoj A, Glamuzina B, Razpet A, Zablocki J, Bogut I, Lerceteau-Köhler E, Pojskić N, Sušnik S (2010) Resolving taxonomic uncertainties using molecular systematics: *Salmo dentex* and the Balkan trout community. Hydrobiologia 651(1): 199–212. https://doi.org/10.1007/s10750-010-0297-5

Stecher G, Tamura K, Kumar S (2020) Molecular Evolutionary Genetics Analysis (MEGA) for macOS. Molecular Biology and Evolution 37(4): 1237–1239. https://doi.org/10.1093/molbev/msz312

Stevanović P (1990) Faciostratotipen in Bosnien, Serbien und Syrmien. Pp. 439–457. In: Malez M, Stevanović P (Eds) Chronostratigraphie und Neostratotypen, Neogen der Westlichen (“Zentral”) Paratethys 8, Pl1, Pontien. Jugoslawischen Akademie der Wissenschaften und Künste und der Serbichen Akademie der Wissenschaften und Künste, Zagreb–Beograd.

Suárez J, Bautista JM, Almodóvar A, Machordom A (2001) Evolution of mitochondrial control region in Palaeartic brown trout (*Salmo trutta*) populations: The biogeographical role of the Iberian Peninsula. Heredity 87(2): 198–206. https://doi.org/10.1046/j.1365-2540.2001.00905.x

Sušnik S, Schoffmann J, Weiss S (2005) Genetic verification of native brown trout from the Persian Gulf (Catak Cay River, Tigris basin). Journal of Fish Biology 67(3): 879–884. https://doi.org/10.1111/j.0022-1112.2005.00780.x

Sušnik S, Snoj A, Wilson IF, Mrdak D, Weiss S (2007) Historical demography of brown trout (*Salmo trutta*) in the Adriatic drainage including the putative *S. letnica* endemic to Lake Ohrid. Molecular Phylogenetics and Evolution 44(1): 63–76. https://doi.org/10.1016/j.ympev.2006.08.021

Tamura K, Stecher G, Kumar S (2021) Mega11: Molecular Evolution Analysis Genetics version 11. Molecular Biology and Evolution 38(7): 3033–3027. https://doi.org/10.1093/molbev/msab120

Tao Q, Tamura K, Battistuzzi FU, Kumar S (2019) A machine learning method for detecting autocorrelation of evolutionary rates in large phylogenies. Molecular Biology and Evolution 36(4): 811–824. https://doi.org/10.1093/molbev/msz014

Tošić A, Škraba D, Nikolić V, Mrdak D, Simonović P (2014) New mitochondrial DNA haplotype of brown trout *Salmo trutta* L. from Crni Timok drainage area in Serbia. Turkish Journal of Fisheries and Aquatic Sciences 14(1): 37–42. https://doi.org/10.4194/1303-2712-v14_1_05

Tošić A, Škraba D, Nikolić V, Čanak-Atlagić J, Mrdak D, Simonović P (2016) Haplotype diversity of brown trout in the broader Iron Gate area. Turkish Journal of Zoology 40: 655–662. https://doi.org/10.3906/zoo-1510-54

Tranos DM (2011) Strymon and Strymonikos Gulf basins (northern Greece): Implications on their formation and evolution from faulting. Journal of Geodynamics 51(4): 285–305. https://doi.org/10.1016/j.jog.2010.10.002

Tranos MD, Kachev VN, Mountrakis DM (2007) Transtensional origin of the NE–SW Simitli basin along the Strouma (Strymon) Lineament, SW Bulgaria. Journal of the Geological Society 165(2): 499–510. https://doi.org/10.1144/0016-76492007-089

Tzankov T, Angelova D, Nakov R, Burchfiel BC, Royden LH (1996) The Sub-Balkan graben system of central Bulgaria. Basin Research 8(2): 125–142. https://doi.org/10.1046/j.1365-2117.1996.01452.x

Vasiliev I, Krijgsman W, Stoica M, Langereis CG (2005) Mio-Pliocene magnetostratigraphy in the southern Carpathian foredeep and Mediterranean–Paratethys correlations. Terra Nova 17(4): 376–384. https://doi.org/10.1111/j.1365-3121.2005.00624.x

Vladimirov VI (1948) Ruč′evaâ forel′ Armenii i ee otnošenie k drugim predstavitelâm roda *Salmo*. Trudy Sevanskoj gidrobiologičeskoj stancii 10: 87–178.

Wilke T, Schultheis R, Albrecht C (2009) As time goes by: A simple fool's guide to molecular clock approaches in invertebrates. American Malacological Bulletin 27(1–2): 25–45. https://doi.org/10.4003/006.027.0203

Wright S (1969) Evolution and the genetics of populations, Volume 2: Theory of gene frequencies. University of Chicago Press, Chicago, 520 pp.

Zagorchev I (2007) Late Cenozoic development of the Strouma and Mesta fluviolacustrine systems, SW Bulgaria and northern Greece. Quaternary Science Reviews 26(22–24): 2783–2800. https://doi.org/10.1016/j.quascirev.2007.07.017

Acta Ichthyologica et Piscatoria 53, 2023, 19–26 | DOI 10.3897/aiep.53.99042

PENSOFT

ACTA
ICHTHYOLOGICA
ET PISCATORIA

Current status and length–weight relation of the European mudminnow, *Umbra krameri* (Actinopterygii: Esociformes: Umbridae), from Jieț River, Dolj County, southwestern Romania

Călin LAȚIU[1], Mihnea Florian MORARU[1], Paul UIUIU[1], Radu CONSTANTINESCU[1], Alexandru-Sabin NICULA[2,3], Tudor PAPUC[1], Vioara MIREȘAN[1], Daniel COCAN[1]

1 *Faculty of Animal Science and Biotechnologies, University of Agricultural Sciences and Veterinary Medicine Cluj-Napoca, Cluj-Napoca, Romania*
2 *Centre for Research on Settlements and Urbanism, Faculty of Geography, Babeș-Bolyai University, Cluj-Napoca, Romania*
3 *Centre of Mountain Economy of the National Institute for Economic Research "Costin C. Kirițescu", Romanian Academy, Bucharest, Romania*

https://zoobank.org/4AA3804F-2291-49EC-8316-6250903DCDD8

Corresponding authors: Daniel Cocan (daniel.cocan@usamvcluj.ro); Tudor Papuc (tudor.papuc@usamvcluj.ro)

Academic editor: Predrag Simonović ♦ **Received** 20 December 2022 ♦ **Accepted** 30 January 2023 ♦ **Published** 28 February 2023

Citation: Lațiu C, Moraru MF, Uiuiu P, Constantinescu R, Nicula A-S, Papuc T, Mireșan V, Cocan D (2023) Current status and length–weight relation of the European mudminnow, *Umbra krameri* (Actinopterygii: Esociformes: Umbridae), from Jieț River, Dolj County, southwestern Romania. Acta Ichthyologica et Piscatoria 53: 19–26. https://doi.org/10.3897/aiep.53.99042

Abstract

The habitat of the European mudminnow, *Umbra krameri* Walbaum, 1792, is continuously decreasing due to human intervention. The species has a "vulnerable" status according to the IUCN Red List. Thus, new information about the species is needed for conservation efforts. Minnow traps were used for capturing *Umbra krameri* and other small fishes in the Jieț River, Dolj County, southwestern Romania. Captured specimens of *U. krameri* were measured and weighed. Length–weight relations and relative condition factor were determined for the captured *U. krameri* specimens. A total of 94 fishes were captured using the minnow traps. They represented 7 species: European bitterling, *Rhodeus amarus* (Bloch, 1782), roach, *Rutilus rutilus* (Linnaeus, 1758), rudd, *Scardinius erythrophthalmus* (Linnaeus, 1758), Danubian spined loach, *Cobitis elongatoides* Băcescu et Mayer, 1969, weatherfish, *Misgurnus fossilis* (Linnaeus, 1758), tubenose goby, *Proterorhinus marmoratus* (Pallas, 1814), and *U. krameri*. The specimens of *Umbra krameri* represented 44% (41 specimens) of the total catch. The wet body weight (BW) of *U. krameri* ranged from 0.8 to 5.1 g, having a mean value of 2.102 g. The mean total length (TL) was 5.782 cm, ranging from 4.59 to 7.87 cm. According to the length–weight relation (LWR), the growth type of *U. krameri* was positive allometric based on the determined equation: $BW = 0.0068TL^{3.277}$. The mean value determined for the relative condition factor (K_n) was 1.0056486. The growth condition of 46% of the specimens was poor ($K_n < 1$; $n = 19$), while the other 54% were in good condition ($K_n \geq 1$; $n = 22$). The presently reported study provides information about the presence of *U. krameri* in the Jieț River (Dolj County, Romania), a location where the species has not been previously reported. The LWRs show an allometric positive growth. The relative condition factor shows that 46% of the specimens had poor growth, while the rest were in good condition. Minnow traps were an efficient tool for small fish capture.

Keywords

allometry, condition factor, Danube basin, vulnerable species, freshwater fish

Introduction

The European mudminnow, *Umbra krameri* Walbaum, 1792, is a small, stagnophilic fish from the order Esociformes, family Umbridae, being the only native umbrid of Europe. The species has the status "vulnerable" according to the IUCN Red List, with a decreasing population trend (IUCN 2023). The fish usually reaches 5 cm, with a maximum recorded length of 17 cm (Povž 1995). *Umbra krameri* has a laterally compressed head and caudal peduncle, a convex dorsal profile, rounded pectoral fins, and large cycloid scales (Bănărescu 1964). It has 33–35 scales on the mid-lateral line and presents dark spots on the body and head (Kottelat and Freyhof 2007). It has a distinguishable light color line on the flank (Bănărescu 1964).

Umbra krameri is mainly distributed in the Danube River catchment, but also in the Dniester catchment (Froese and Pauly 2022). Its presence was reported in Neusiedler and Balaton lakes (Lelek 1987; Bíró and Paulovits 1995), in the rivers Morava, Pek, Tisza, Er, Ier, Sava, Drava, and Mura (Ristić 1977; Wilhelm 1984, 1987, 2003; Mrakovčić and Kerovec 1990; Povž 1990; Delić et al. 1997; Sekulić et al. 1998; Mrakovčić et al. 2006; Govedič 2010; Petronić et al. 2010; Zanella unpublished[*]) and in Sibnica Canal (Cakić and Hristić 1987), and other places. The European mudminnow is mainly present in Austria, Slovakia, Hungary, Slovenia, Croatia, Serbia, Romania, Moldova, and Ukraine (Pekárik et al. 2014). Other authors mention the presence of the species in Bosnia, Bulgaria, and the Czech Republic (Bănărescu 1994).

In Romania, the fish is present in some ponds and marshes of Satu Mare, Bihor, Ilfov, Giurgiu, and Călărași counties, in the Danube, its delta, and the Prut River (Oțel 2007; Wilhelm and Ardelean 2009; Telcean et al. 2014). An unclear situation exists in some regions where the fish has been found only sporadically (Imecs and Nagy 2013; Năstase and Oțel 2016). It was also reported in Banat and Oltenia regions, southwestern Romania (Covaciu-Marcov et al. 2018).

The spawning of *U. krameri* usually occurs in March–April, when the temperature of the water ranges between 12 and 16°C. The female initiates the spawning, and two or more males participate. The fish needs a sandy substrate for spawning. The number of eggs is low, with peaks of 2700–2800 eggs reported, but usually between 200 and 1600 eggs (Müller et al. 2015). Not all eggs are laid, some are being resorbed. However, they have a higher chance of survival, as the female is a protective parent, chasing predators and removing nonviable eggs. At a temperature of 13°C, the eggs need 10 to 13 days to hatch (Müller et al. 2011).

Umbra krameri is highly dependent on some habitat conditions. It needs stagnant bodies of water or a very low water flow, low levels of turbidity, and dense macrophytes, preferring marshes, canals, and ponds (Wiesinger 1956; Bănărescu 1964; Wanzenböck 1995). The fish is well adapted to waters with low levels of dissolved oxygen. Its swim bladder is highly vascularized, enabling the fish to use atmospheric air as an oxygen source (Wilhelm 1998). One of the main reasons for the population decline is the loss of habitat due to anthropogenic activities (Keresztessy 1995). For example, Janković (1995) reported the species in the Negotinsko Blato floodplain, which later disappeared after infrastructure development in the area that destroyed its habitat. Bănărescu (1964) reported the species in Iasi County, Romania, but recent samplings in the area did not mention the species. Because of its specific demands for habitat conditions, The Habitat Directive of the European Union (92/43/EEC) includes the species in Annex II (species whose conservation requires the designation of Special Conservation Areas). Other authors also suggest the need for protective measures regarding this species (Takács et al. 2015; Marić et al. 2019), some even managing successful reproduction in captivity (Müller et al. 2015).

It is difficult to determine the exact area of distribution of *U. krameri*, as the species is losing habitat at a fast pace, being forced sometimes to migrate to new habitats. Other reasons for inconsistencies in reporting are the low number of studies regarding this species in areas where it might be present and the difficulty in capturing it using electrofishing when the fish remains in the mud or entangles itself in vegetation. Invasive species also pose a problem for the conservation of *U. krameri* populations. Müller et al. (2015) note that there are 3 species that threaten the *U. krameri* population: the Chinese sleeper, *Perccottus glenii* Dybowski, 1877, the eastern mudminnow, *Umbra pygmaea* (DeKay, 1842), and the Prussian carp, *Carassius gibelio* (Bloch, 1782), all three being considered invasive species in native areas of the European mudminnow.

Considering all the aforementioned aspects, this study aims to provide information on the presence, length–weight relation (LWR), and condition factor of the *U. krameri* population from one of its few existing habitats, namely the Jieț River, Dolj County, Romania. The information can supplement existing data regarding the species and may be used in conservation efforts.

Materials and methods

The Jieț River is a former tributary of the Jiu River, flowing from north to south and discharging in the Danube at Bechet. The general landscape is characterized by forest steppe and floodplains, being greatly affected by drought (Vijulie et al. 2017). The meandered course of the entire river is bordered by agricultural land. Fish sampling was performed from 26 to 27 March 2021 on the Jieț River, near the localities Tâmburești (44.0277457, 23.9221236), Murta (43.9913192, 23.9317484), and Sadova (43.9125837, 23.9133019), Dolj County (Figs. 1–2).

---

[*] Zanella D (1997) Rasprostranjenost i zaštita vrste Umbra krameri Walbaum, Pisces. BSc thesis, University of Zagreb, Zagreb, Croatia.

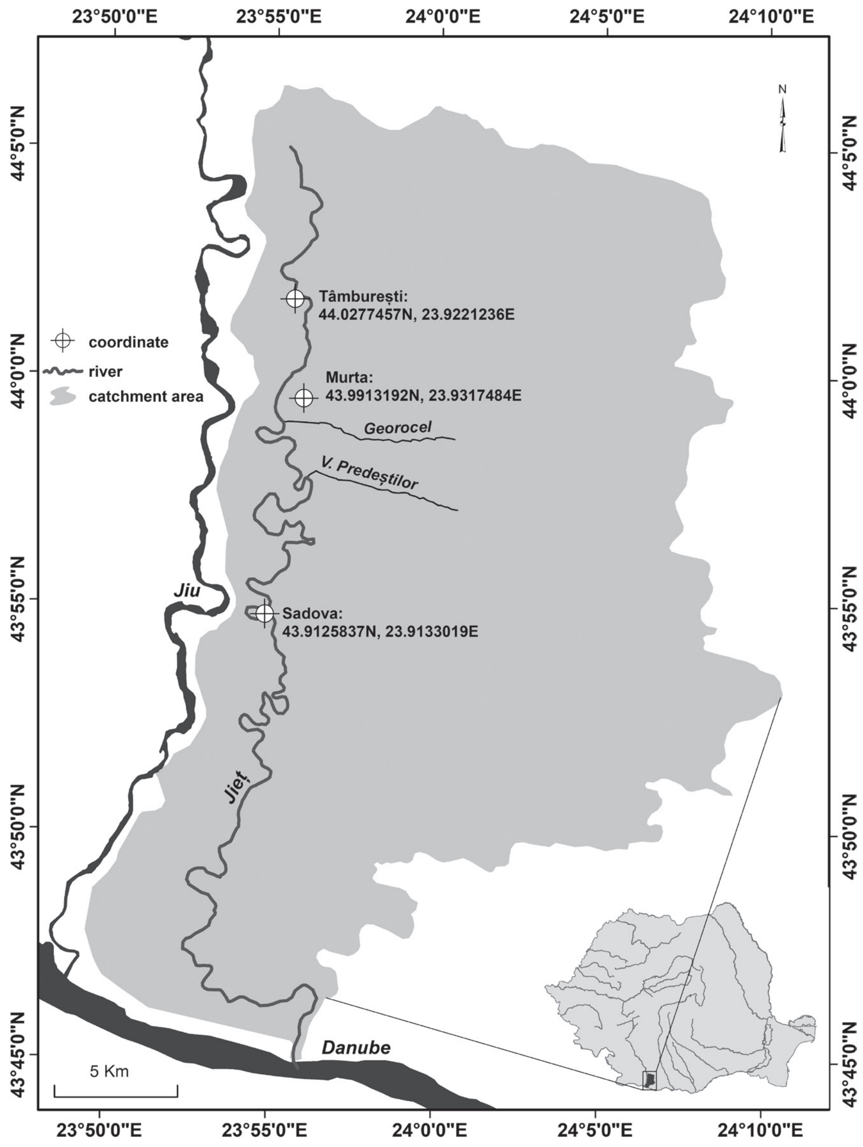

Figure 1. Location of sampling points on the Jieț River, Romania.

Figure 2. Natural landscape and habitat of *Umbra krameri* (Tâmburești, Murta and Sadova localities, Dolj County, Romania). Photo: M. Moraru, 2021.

Sampling sites were chosen for investigation based on local information and specialty literature (Bănărescu et al. 1995; Covaciu-Marcov et al. 2018).

Fish sampling was performed using 15 baitfish/minnow traps (umbrella type), a highly effective fishing gear, especially for small fish species (Portt et al. 2006; Arifianto et al. 2021). To increase the efficiency of the traps, 100 g of mixed sinking carp feed and trout pelleted feed (3 and 6 mm, respectively) were introduced into the trap's bait pocket. Fishing time for each trap was 12 h (from 20:00 to 08:00 h). Water temperature varied from 12.3 to 11.9°C. All the sampled specimens were released into their natural habitat after the body measurements were performed.

Body measurements, such as total length (TL), standard length (SL), maximum body height (H) , minimum body height (h), head length (HL), and eye diameter (ED) were performed using a caliper. The fish's wet body weight (BW) was determined using an Adam Dune DCT 2000 portable digital scale (to the nearest 0.1 g). In addition to TL and BW, which were used to determine LWR, the other measurements were determined for exploratory purposes and to supplement the specific literature devoted to *Umbra krameri*. We opted for a small number of performed body measurements for each individual based on unfavorable field conditions and to keep a minimal exposure of specimens to atmospheric air, as the species has a decreasing population trend and its conservation status is vulnerable (VU vulnerable according to IUCN). The TL was also used for age estimation, according to previous studies on the species (Wanzenböck 1995; Povž 1995; Wilhelm 2003). Descriptive statistics consisting of mean values, maximum values, minimum values, range, standard deviation, standard error of the mean, coefficient of variation, and LWR were determined in Microsoft Excel for Windows, MS Excel 2016, version 16.0.4266.1001.

The LWR was determined by applying the formula

$$\mathrm{BW} = a\mathrm{TL}^{b}$$

where a and b are the coefficients of the regression between BW and TL (Le Cren 1951). The values of coefficients a and b were determined by the least-square linear regression from the log-transformed values of TL and BW, using the formula

$$\mathrm{BW} = \log a + b \log \mathrm{TL}$$

(Morey et al. 2003; Sangun et al. 2007; Yosuva et al. 2018). To determine the type of growth for the sampled *U. krameri* specimens, values of b exponent were analyzed as follows: positive allometric growth, if $b > 3$; negative allometric growth, if $b < 3$; and isometric growth, if $b = 3$ (Froese 2006). Confidence intervals (CI) at 95% were determined to establish if the b value obtained from the linear regression was significantly different from the isometric value ($b = 3$). In addition, the t-test was used to determine if the obtained b value was significantly different from the isometric value and establish the growth type. The null hypothesis of isometric growth (H_0: $b = 3$) was also tested by t-test for $\alpha = 0.05$ (Mehanna and Farouk 2021). The relative condition factor (K_n) of each individual was determined by the following equation –

$$K_n = W_o W_e^{-1}$$

where W_o is the observed weight and W_e is the expected weight determined from the LWR (Jisr et al. 2018). The fish condition can be evaluated as follows: $K_n \geq 1$, when the fish growth condition is good, and $K_n < 1$, when the fish growth condition is poor (Le Cren 1951). Body measurements, calculations, and regression were performed on the combined sexes.

Results

A total of 94 fishes were captured using the minnow traps. They represented 7 species: European bitterling, *Rhodeus amarus* (Bloch, 1782), roach, *Rutilus rutilus* (Linnaeus, 1758), rudd, *Scardinius erythrophthalmus* (Linnaeus, 1758), Danubian spined loach, *Cobitis elongatoides* Băcescu et Mayer, 1969, weatherfish, *Misgurnus fossilis* (Linnaeus, 1758), tubenose goby, *Proterorhinus marmoratus* (Pallas, 1814), and *U. krameri* (Table 1).

The BW of the studied specimens of *U. krameri* ranged from 0.8 to 5.1 g, having a mean value of 2.102 g. The mean TL was 5.782 cm, ranging from 4.59 to 7.87 cm. The mean SL was 4.852 cm, ranging from 3.72 to 6.65 cm. The determined mean value of H was 1.245 cm, while the mean h was 0.6688 cm. HL ranged from 0.98 to 1.96 cm, with a determined mean value of 1.322 cm. ED ranged from 0.18 to 0.4 cm, and the mean value was 0.2805 cm. In terms of body measurement variation, BW recorded the highest coefficient (49.83%), while the lowest variation was observed in the case of TL (14.29%) (Table 2).

The growth type of *U. krameri* according to our determinations of LWR was allometric positive ($b = 3.227$), rejecting the null hypothesis (H_0: $b = 3$) (Table 3). The determined LWR equation for the studied species is $\mathrm{BW} = 0.0068\mathrm{TL}^{3.277}$.

The mean value determined for the relative condition factor (K_n) was 1.0056486, showing a general good condition ($K_n \geq 1$) (Fig. 3). When analyzing the minimum ($K_n = 0.788$), maximum ($K_n = 1.228$) and standard deviation (0.1425) values of K_n, it can be observed that the data is not grouped around the mean value. To provide a more accurate trend of the population, the data was divided into two categories as follows: group $K_n \geq 1$, and group $K_n < 1$. It was noted that 46% of the specimens were in a poor growth condition (group $K_n < 1$; $n = 19$) and 54% of the specimens were in good condition (group $K_n \geq 1$; $n = 22$).

Table 1. Fish species captured in the Jieț River using fish traps.

Order	Family	Species	No. of specimens
Cypriniformes	Acheilognathidae	*Rhodeus amarus* (Bloch, 1782)	2
	Leuciscidae	*Rutilus rutilus* (Linnaeus, 1758)	6
		Scardinius erythrophthalmus (Linnaeus, 1758)	1
	Cobitidae	*Cobitis elongatoides* Băcescu et Mayer, 1969	12
		Misgurnus fossilis (Linnaeus, 1758)	11
Esociformes	Umbridae	*Umbra krameri* Walbaum, 1792	41
Gobiiformes	Gobiidae	*Proterorhinus marmoratus* (Pallas, 1814)	21

Table 2. Descriptive statistics for the determined body measurements of *Umbra krameri* from the Jieț River, Romania.

Character	Descriptive statistics						
	n	Min	Max	Range	Mean ± SD	SEM	CV%
BW [g]	41	0.8	5.1	4.3	2.102 ± 1.0480	0.1636	49.83%
TL [cm]	41	4.59	7.87	3.28	5.782 ± 0.8264	0.1291	14.29%
SL [cm]	41	3.72	6.65	2.93	4.852 ± 0.7021	0.1096	14.47%
H [cm]	41	0.88	1.76	0.88	1.245 ± 0.2315	0.03616	18.59%
h [cm]	41	0.49	0.94	0.45	0.6688 ± 0.1189	0.01857	17.78%
HL [cm]	41	0.98	1.96	0.98	1.322 ± 0.2168	0.03386	16.39%
ED [cm]	41	0.18	0.4	0.22	0.2805 ± 0.0471	0.007358	16.80%

n = number of specimens, Min = minimum, Max = maximum, SD = standard deviation, SEM = standard error of mean, CV% = coefficient of variation; BW = wet body weight, TL = total length, SL = standard length, *H* = maximum height, *h* = minimum height, HL = head length, ED = eye diameter.

Table 3. The length–weight relation (LWR) determined for *Umbra krameri* from the Jieț River, Romania; equation BW = $0.0068\mathrm{TL}^{3.277}$.

LWR parameter					Growth type
a	*b*	*a* CI95%	*b* CI95%	R^2	
0.0068	3.227	0.0040–0.0115	2.876–3.567	0.9011	*b* > 3 (allometric positive)

a = intercept, *b* = the slope of the LWR regression, CI = confidence interval, R^2 = coefficient of determination of length–weight relation, BW = wet body weight, TL = total length.

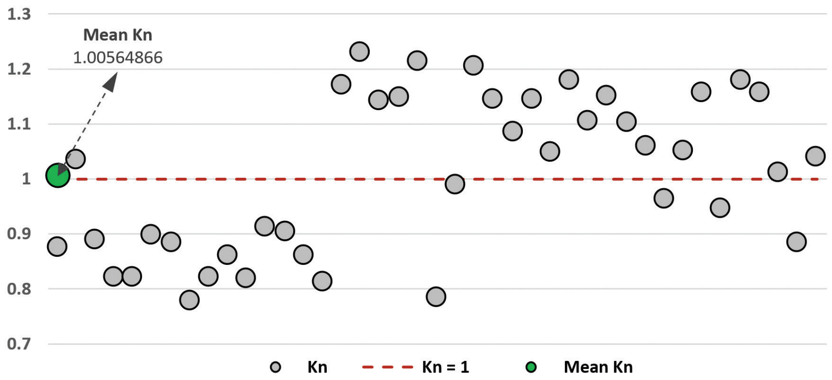

Figure 3. The relative condition factor: grey marker-individual values; green marker-mean value of the sample; red dotted line represents $K_n = 1$.

Discussion

The specimens of *Umbra krameri* represented 44% (41 specimens) of the total catch. According to the determinations of Wanzenböck (1995), Povž (1995), and Wilhelm (2003), the mean TL of *U. krameri* in different age groups were as follows 48.3 mm (0+ fish), 55.4 mm (1+), 63 mm (2+), 70.4 mm (3+), 82 mm (4+), = 91.5 mm (5+), and 105.5 mm (6+ fish). By comparing the above information to the observations from this study (Table 2), we estimated that the age of analyzed specimens from the Jieț River ranged from 0+ to 3+ years.

The LWR determined in the presently reported study was similar to that of other studies (Sekulić 2013; Bíró and Paulovits 1995; Wilhelm 2003), showing positive allometric growth. Other populations studied by Bíró and Paulovits (1995) and Sehr (2014) showed negative allometric growth. Based on the analyzed similar studies, comparable LWRs were also observed for the other two species of the genus *Umbra*: *Umbra pygmaea* and *Umbra limi* (Kirtland, 1840) (see Dederen et al. 1986; Verreycken et al. 2010; Robinson et al. 2010; Panek and Weis 2012). The LWRs obtained in other studies for members of the genus *Umbra* are presented in Table 4.

Table 4. Length–weight relations of *Umbra* species from analyzed specialty literature and presently reported study.

Species	Country/Area	Equation	*b*	*n*	Growth type	Sex	Reference
Umbra krameri	Serbia	$BW = 0.000001TL^{3.63}$	3.63	21	ALLO+	♀ + ♂	Sekulić 2013
	Serbia	$BW = 0.000001TL^{3.59}$	3.59	13	ALLO+	♂	Sekulić 2013
	Serbia	$BW = 0.0000005TL^{3.68}$	3.68	8	ALLO+	♀	Sekulić 2013
	Bosnia and Herzegovina	$BW = 0.000002TL^{3.46}$	3.46	32	ALLO+	♀ + ♂	Sekulić 2013
	Bosnia and Herzegovina	$BW = 0.000002TL^{3.44}$	3.44	11	ALLO+	♂	Sekulić 2013
	Bosnia and Herzegovina	$BW = 0.000004TL^{3.25}$	3.25	16	ALLO+	♀	Sekulić 2013
	Hungary	$BW = 0.000003TL^{3.5189}$	3.5189	479	ALLO+	♀ + ♂	Bíró and Paulovits 1995
	Hungary	$BW = 0.00076TL^{2.1771}$	2.1771	133	ALLO–	♀ + ♂	Bíró and Paulovits 1995
	Hungary	$BW = 0.00001TL^{3.1904}$	3.1904	133	ALLO+	♀ + ♂	Bíró and Paulovits 1995
	Austria	$BW = 0.00003TL^{2.7349}$	2.7349	261	ALLO–	♀ + ♂	Sehr 2014
	Romania	$BW = 0.0023TL^{3.3429}$	3.3429	252	ALLO+	♀ + ♂	Wilhelm 2003
	Romania	$BW = 0.0068TL^{3.277}$	3.277	41	ALLO+	♀ + ♂	Presently reported study
Umbra pygmaea	Flanders Belgium	$BW = 0.0075TL^{3.243}$	3.243	803	ALLO+	♀ + ♂	Verreycken et al. 2010
	North America	$BW = 0.00001TL^{3.182}$	3.182	97	ALLO+	♂	Panek and Weiss 2012
	North America	$BW = 0.00001TL^{3.032}$	3.032	84	ALLO+	♀	Panek and Weiss 2012
	Netherlands	$BW = 0.0034TL^{3.55}$	3.55	547	ALLO+	♀ + ♂	Dederen et al. 1986
Umbra limi	North America	$BW = 0.0069TL^{3.175}$	3.175	133	ALLO+	♀ + ♂	Robinson et al., 2010

b = the slope of the LWR regression, *n* = number of analyzed specimens; BW = wet body weight, TL = total length; ALLO+ = allometric positive growth; ALLO– = allometric negative growth.

The positive allometric growth determined for *U. krameri* (both sexes combined) from the Jieț River might have been affected by the sampling period (March 2021), which coincides with the spawning period of the species. In general, during the spawning period, fish of both sexes cease to feed and their sexual dimorphism becomes more pronounced. In terms of sexual dimorphism, Wanzenböck (1995) mentioned that males appear "more slender" than females and sexual differentiation should be viewed with caution. This may explain the determined differences in K_n.

According to Dederen et al. (1986), *U. pygmaea* and *U. limi* may play the role of top predators in their natural ecosystems, an aspect that may be observed in the presently reported case with *U. krameri*, especially as common predators as the northern pike *Esox lucius* and perch *Perca fluviatilis* were absent. Another similarity with the study of Dederen et al. (1986) is in terms of species structure, the presence of *R. rutilus* and *S. erythrophthalmus* being noticed in both instances.

Conclusion

The presently reported study provides basic information on the presence of *Umbra krameri* in the Jieț River (Dolj County, Romania) as well as the LWR and relative condition factor of the sampled specimens. The results from this study may prove useful to conservation programs needed for *U. krameri* and its habitat. In terms of fish sampling, the minnow traps were an efficient tool for small fish capture.

References

Arifianto A, Mufti E, Pramana A, Marhendra W, Kurniawan N (2021) Minnow trap color effectiveness test using cat food bait as aquatic sampling gear on diurnal fish in Gajah Mungkur Reservoir, Cental Java, Indonesia. Journal of Experimental Life Science 11(1): 15–20. https://doi.org/10.21776/ub.jels.2021.011.01.04

Bănărescu P (1964) Fauna Republicii Populare Romîne. Pisces – Osteichthyes. Vol. 13. Academia Republicii Populare Romîne, Bucharest, 964 pp.

Bănărescu P (1994) The present-day conservation status of the freshwater fish fauna of Romania. Ocrotirea Naturii şi a Mediului Înconjurător 38: 5–20.

Bănărescu P, Oțel V, Wilhelm A (1995) The present status of *Umbra krameri* Walbaum in Romania (Pisces, Umbridae). Annalen des Naturhistorischen Museums in Wien. Serie B, für Botanik und Zoologie 97: 496–501.

Bíró P, Paulovits G (1995) Distribution and status of *Umbra krameri* Walbaum, 1792, in the drainage of Lake Balaton, Hungary (Pisces: Umbridae). Annalen des Naturhistorischen Museums in Wien. Serie B, für Botanik und Zoologie 97B: 470–477.

Cakić P, Hristić D (1987) Ihtiofauna Panćevaćkog rita sa posebnim osvrtom na alohtone vrste riba. Glasnik Prirodnjačkog muzeja u Beogradu B42: 103–118.

Covaciu-Marcov SD, Cupșa D, Telcean IC, Sas-Kovacs I, Ferenți S (2018) Two new populations of the European mudminnow, *Umbra krameri* (Actinopterygii: Esociformes: Umbridae), in south-western Romania with the first record in the Banat region. Acta Ichthyologica et Piscatoria 48(3): 251–255. https://doi.org/10.3750/AIEP/02405

Dederen LHT, Leuven RSEW, Wendelaar SE, Oyen FGF (1986) Biology of the acid-tolerant fish species *Umbra pygmaea* (De Kay, 1842). Journal of Fish Biology 28(3): 307–326. https://doi.org/10.1111/j.1095-8649.1986.tb05168.x

Delić A, Grlica ID, Razlog-Grlica J (1997) Nova nalazista crnke (*Umbra krameri* Walbaum, 1792) u Hrvatskoj. Ribarstvo 55(3): 93–98.

Freyhof J (2011) *Umbra krameri*. The IUCN Red List of Threatened Species 2011: e.T22730A9380477. https://doi.org/10.2305/IUCN.UK.2008.RLTS.T22730A9380477.en [Accessed on 12 February 2023]

Froese R (2006) Cube law, condition factor and weight–length relationships: History, meta-analysis and recommendations. Journal of Applied Ichthyology 22(4): 241–253. https://doi.org/10.1111/j.1439-0426.2006.00805.x

Froese R, Pauly D (Eds) (2022) FishBase. [Version 08/2022] http://www.fishbase.org

Govedič M (2010) Ribe reke Drave med Mariborom in Hrvasko mejo 35 let po izgradnji hidroelektrarn. Pp. 22–23. In: Zajc P, Colnarič N, Vres B (Eds) International Conference on the Drava River Life in the river basin. Dravograd (Slovenia), September–October 2010. Jovan Hadži Institute of Biology Scientific Research Centre SASA, Dravograd.

Imecs I, Nagy AA (2013) Data concerning the fish fauna of the ROSCI0224 Scroviștea Natura 2000 site (Romania) and management measure proposals. Romanian Journal of Biology - Zoology 58(2): 101–114.

Janković D (1995) Ihtiofauna Djerdapske akumulacije pre i posle izgradnje HEPS Djerdap. Pp. 135–146. In: Brun G (Ed.) Proceedings of the Conference "Povratak zivota rekama". Belgrade, Serbia.

Jisr N, Younes G, Sukhn C, El-Dakdouki MH (2018) Length–weight relationships and relative condition factor of fish inhabiting the marine area of the Eastern Mediterranean city, Tripoli-Lebanon. Egyptian Journal of Aquatic Research 44(4): 299–305. https://doi.org/10.1016/j.ejar.2018.11.004

Keresztessy K (1995) Recent fish faunistical investigations in Hungary with special reference to *Umbra krameri* Walbaum, 1792. Annalen des Naturhistorischen Museums in Wien. Serie B, für Botanik und Zoologie 97B: 458–465.

Kottelat M, Freyhof J (2007) Handbook of European freshwater fishes. Publications Kottelat, Cornol, 660 pp.

Le Cren ED (1951) The length–weight relationship and seasonal cycle in gonad weight and condition in the perch (*Perca fluviatilis*). Journal of Animal Ecology 20(2): 201–219. https://doi.org/10.2307/1540

Lelek A (1987) The freshwater fishes of Europe. Vol. 9. Threatened fishes of Europe. Aula-Verlag, Wiesbaden, Germany, 343 pp.

Marić S, Stanković D, Šanda R, Ćaleta M, Čolić S, Šukalo G, Snoj A (2019) Genetic characterization of European mudminnow (*Umbra krameri*) populations from the Sava River system. Knowledge and Management of Aquatic Ecosystems 420(420): 46. https://doi.org/10.1051/kmae/2019035

Mehanna SF, Farouk AE (2021) Length–weight relationship of 60 fish species from the Eastern Mediterranean Sea, Egypt (GFCM-GSA 26). Frontiers in Marine Science 8: 625422. https://doi.org/10.3389/fmars.2021.625422

Morey G, Moranta J, Massutí E, Grau A, Linde M, Riera F, Morales-Nin B (2003) Weight–length relationships of littoral to lower slope fishes from the Western Mediterranean. Fisheries Research 62(1): 89–96. https://doi.org/10.1016/S0165-7836(02)00250-3

Mrakovčić M, Kerovec M (1990) *Umbra krameri*. Ekološki Glasnik 5/6: 68–69.

Mrakovčić M, Brigić A, Buj I, Ćaleta M, Mustafić P, Zanella D (2006) Red book of freshwater fishes in Croatia. Ministry of Culture of the Republic of Croatia, State Institute for Nature Protection, Zagreb, 253 pp.

Müller T, Balovan P, Tatar S, Müllerne TM, Urbanyi B, Demeny F (2011) A lapi poc (*Umbra krameri*) szaporitasa es nevelese a termeszetesvizi allomanyoc fenntartasa es megorzese erdekeben. Pisces Hungarici 5: 15–20.

Müller T, Wilhelm S, Imecs I (2015) Conservarea și reproducerea artificială a unor specii de pești de mlaștină periclitate: țigănuș, caracudă și țipar. Editura Green Steps, Brașov, 232 pp.

Năstase A, Oțel V (2016) Researches on the fish fauna in some SCIs Natura 2000 from Romania. Aquaculture, Aquarium, Conservation and Legislation 9(3): 327–340.

Oțel V (2007) Atlasul peștilor din Rezervația Biosferei Delta Dunării. Centrul de Informare Tehnologică Delta Dunării, Tulcea, 481 pp.

Panek FM, Weis JS (2012) Age, growth, and reproduction of the eastern mudminnow (*Umbra pygmaea*) at the Great Swamp National Wildlife Refuge, New Jersey. Northeastern Naturalist 19(2): 217–228. https://doi.org/10.1656/045.019.0206

Pekárik L, Hajdú J, Košo J (2014) Identifying the key habitat characteristics of threatened European mudminnow (*Umbra krameri*, Walbaum 1792). Fundamental and Applied Limnology 184(2): 151–159. https://doi.org/10.1127/1863-9135/2014/0477

Petronić S, Panić G, Radosević D, Travar J (2010) Rijetke i ugrožene biljne i životinjske vrste u posebnom rezervatu prirode "Gromiželj". Pp. 199–206. In: Šiljegović S (Ed.) 5th Conference on integrative protection, Republic Institute for Protection of Cultural, Historical and Nature Heritage of Republic of Srpska. Banja Luka,Bosnia and Herzegovina.

Portt CB, Coker GA, Ming DL, Randall RG (2006) A review of fish sampling methods commonly used in Canadian freshwater habitats. Canadian Technical Report of Fisheries and Aquatic Sciences 2604, 58 pp.

Povž M (1990) Velika senčica (*Umbra krameri* Walbaum, 1792) nova vrsta ribe Sloveniji. Varstvo Narave 16: 45–48.

Povž M (1995) Threatened fishes of the world: *Umbra krameri* Walbaum, 1792 (Umbridae). Environmental Biology of Fishes 43(3): 232. https://doi.org/10.1007/BF00005854

Ristić M (1977) Ribe i ribolov u slatkim vodama. Nolit, Beograd, Serbia, 61 pp.

Robinson JM, Jirka KJ, Chiotti JA (2010) Age and growth analysis of the central mudminnow, *Umbra limi* (Kirtland, 1840). Journal of Applied Ichthyology 26(1): 89–94. https://doi.org/10.1111/j.1439-0426.2009.01357.x

Sangun L, Akamca E, Akar M (2007) Weight–length relationships for 39 fish species from the north-eastern Mediterranean coast of Turkey. Turkish Journal of Fisheries and Aquatic Sciences 7: 37–40.

Sehr M (2014) Fish species assemblage, abundance and biodiversity in an old, modified Danube side arm. A description of the habitat relations of *Umbra krameri* Walbaum, 1792. Master Thesis, University of Vienna, Vienna, Austria. https://utheses.univie.ac.at/detail/33516

Sekulić NK (2013) Ecological characteristics and morphological-genetic differentiation in populations of European mudminnow (*Umbra krameri* Walbaum, 1792) from Bačka, Mačva and Semberija. PhD Thesis, University of Belgrade, Belgrade, Serbia. https://nardus.mpn.gov.rs/bitstream/handle/123456789/2109/Disertacija.pdf

Sekulić N, Budakov LI, Branković D (1998) Distribution of the European mudminnow *Umbra krameri* (Umbridae) in Serbia. Italian Journal of Zoology 65(sup1): 381–382. https://doi.org/10.1080/11250009809386851

Takács P, Erős T, Specziár A, Sály P, Vitál Z, Ferincz Á, Molnár T, Szabolcsi Z, Bíró P, Csoma E (2015) Population genetic patterns of threatened European mudminnow (*Umbra krameri* Walbaum, 1792) in a fragmented landscape: Implications for conservation management. PLoS One 10(9): e0138640. https://doi.org/10.1371/journal.pone.0138640

Telcean IC, Cupșa D, Sas-Kovacs I, Cicort-Lucaciu AS, Covaciu-Markov SD (2014) Some data upon the fish sauna from Carei plain natural protected area obtained with herpetological methods. North-Western Journal of Zoology 10: S135–S140.

Verreycken H, Geeraerts C, Duvivier C, Belpaire C (2010) Present status of the North American *Umbra pygmaea* (DeKay, 1842) (eastern mudminnow) in Flanders (Belgium) and in Europe. Aquatic Invasions 5(1): 83–96. https://doi.org/10.3391/ai.2010.5.1.10

Vijulie I, Matei E, Manea G, Tîrlă L, Cuculici R (2017) Land use reconversion in the drought-and aridity-affected areas in SW Romania (Bechet, Dolj County). Analale Universitatii Bucuresti. Seria Geografie, 69–81.

Wanzenböck J (1995) Current knowledge on the European mudminnow, *Umbra krameri* Walbaum, 1792 (Pisces: Umbridae). Annalen des Naturhistorischen Museums in Wien. Serie B, für Botanik und Zoologie 97B: 439–449.

Wiesinger M (1956) A lapi poc (*Umbra krameri* Walbaum). Akvarium es Terrarium 1(2): 37–40.

Wilhelm A (1984) Date privind creșterea țigănușului (*Umbra krameri* Walbaum) din bazinul Ierului. Buletinul de Cercetări Piscicole 1–2: 61–72.

Wilhelm A (1987) Ţigănuşul (*Umbra krameri* Walbaum) în Valea Ierului. Crisia, Oradea 17: 651–654.

Wilhelm S (1998) Halak onckes alatt. Studium Konyvkiado, Cluj-Napoca, 160 pp.

Wilhelm A (2003) Growth of the mudminnow (*Umbra krameri* Walbaum) in river Ér. Tiscia 34: 57–60.

Wilhelm S, Ardelean G (2009) Ţigănuşul (*Umbra krameri*) studiu monografic. Editura Daya, Satu-Mare, 131 pp.

Yosuva M, Jeyapragash D, Manigandan V, Machendiranathan M, Saravanakumar A (2018) Length–weight relationship and relative condition factor of yellowfin tuna (*Thunnus albacares*) from Parangipettai coast, southeast coast of India. Zoology and Ecology 28(2): 94–99. https://doi.org/10.1080/21658005.2018.1455319

Acta Ichthyologica et Piscatoria 53, 2023, 27–35 | DOI 10.3897/aiep.53.96788

PENSOFT.

ACTA ICHTHYOLOGICA ET PISCATORIA

The dominance of non-indigenous species in the catch composition of small-scale fisheries: A case study from the Kaş–Kekova Special Environmental Protection Area, Türkiye, Eastern Mediterranean

Fikret ÖNDES[1], Vahdet ÜNAL[2]

1 *Faculty of Fisheries, İzmir Katip Çelebi University, Balatçık, Izmir, Türkiye*
2 *Faculty of Fisheries, Ege University, Bornova, Izmir, Türkiye*

https://zoobank.org/A61CBEEC-D7B8-416E-9EE3-D4764FCF77FE

Corresponding author: Fikret Öndes (fikret.ondes@ikcu.edu.tr)

Academic editor: Sanja Matić-Skoko ♦ **Received** 27 October 2022 ♦ **Accepted** 11 January 2023 ♦ **Published** 8 March 2023

Citation: Öndes F, Ünal V (2023) The dominance of non-indigenous species in the catch composition of small-scale fisheries: A case study from the Kaş–Kekova Special Environmental Protection Area, Türkiye, Eastern Mediterranean. Acta Ichthyologica et Piscatoria 53: 27–35. https://doi.org/10.3897/aiep.53.96788

Abstract

This study aimed to determine the catch composition and compare the catch per unit effort (CPUE) of indigenous and non-indigenous species in longline and trammel net fisheries in the Mediterranean coasts of Türkiye. The data were collected weekly from May 2020 to September 2021 by commercial fishing vessels (n = 62 days for trammel nets, n = 75 days for longlines). The results of the study indicated that more than 90% of the catch composition consisted of non-indigenous species in trammel net fishery and *Pterois miles* (Bennett, 1828), *Siganus rivulatus* Forsskål et Niebuhr, 1775, *Siganus luridus* (Rüppell, 1829), and *Scarus ghobban* Forsskål, 1775 were the most commonly caught species. Although indigenous species were more common in longlines compared with trammel nets, non-indigenous species *Lagocephalus sceleratus* (Gmelin, 1789) and *Lagocephalus suezensis* Clark et Gohar, 1953 were represented by relatively high catch ratios. The results also revealed that the CPUE of non-indigenous species exhibited seasonal differences. Although some non-indigenous species caught within this study have a market value, some other highly invasive species do not. Therefore, it is critically important to develop effective management tools to control bio-invasion. This study provides the first comprehensive research by utilizing basic data with relatively long-term surveys in the small-scale fishery on the Mediterranean coasts of Türkiye. The outcomes of this study can provide guidance to decision-makers.

Keywords

fisheries management, invasive species, *Lagocephalus sceleratus*, marine invasion, *Pterois miles*, *Siganus luridus*, *Siganus rivulatus*, small-scale fisheries

Introduction

The Mediterranean basin has a high human population density and is considered a hotspot for climate change consequences (Macias et al. 2015). Numerous studies have also underlined that this ecosystem has been facing an increased threat of pollution and overfishing which have caused certain changes over the last several decades (Danovaro 2003; Tsikliras et al. 2013; Compa et al. 2019). Furthermore, some other anthropogenic factors like the opening and enlargement of the Suez Canal directly affected marine ecosystems and fisheries, mostly SSF (small-scale fisheries) (Galil et al. 2015; Penca et al. 2021). The impacts of these aforementioned factors have resulted in significant ecological changes. For instance, collapsed and decreased stocks, mass mortality in sessile organisms, increased numbers of threatened and endangered species, and altered prey–predator relations are commonly observed and decreased stocks have also caused economic changes such as a decrease in vessel numbers in SSF (Maynou et al. 2013; Tsikliras et al. 2015; Stergiou et al. 2016; Garrabou et al. 2019; Moullec et al. 2019; Birkan and Öndes 2020; Ramírez et al. 2021; IUCN 2022; OECD 2022). Another important indicator of the changes occurring in the Mediterranean ecosystem is the increased abundance and diversity of non-indigenous species (NIS) whose effects are starting to be better understood (Kletou et al. 2016; Çınar et al. 2021; Ulman et al. 2021; Zenetos et al. 2022). Similarly, Öztürk (2021) reported that the biota of the Mediterranean and the Black Sea has started to change significantly over the last few decades due to the introduction of NIS.

There is no doubt that in recent years some Lessepsian species are a major threat to biodiversity and ecosystem functioning, as well as causing an economic loss in some fisheries and are also causing a negative influence on human welfare (Ünal et al. 2015; Ünal and Göncüoğlu Bodur 2017; Öndes et al. 2018; Öndes and Gökçe 2021; Kourantidou et al. 2021). As in the aforementioned studies, researchers generally focused on the negative impacts of NIS, whilst their potential or realized benefits were scarcely discussed in the literature (Gozlan 2008; Oficialdegui et al. 2020; Vimercati et al. 2020; Kourantidou et al. 2022). Indeed, NIS comprise between 50%–90% of the total fish biomass in some areas of the Eastern Mediterranean Sea (Goren and Galil 2005; Edelist et al. 2011; Bronstein et al. 2017). A more recently published study (Çınar et al. 2021) highlighted that a total of 539 marine NIS were recorded in Türkiye until the end of 2020 and among them, 413 species were reported from the Levantine coasts of Türkiye. Çınar et al. (2021) also stated that 58% of NIS migrated from the Red Sea. Previous studies apparently indicated that the number of NIS increased over the last several decades in the Mediterranean ecosystem (Zenetos et al. 2012; Zenetos et al. 2022). Even though the literature included many studies on the occurrence, distribution patterns, and biological characteristics of Lessepsians (e.g., Golani 1998; Mavruk and Avsar 2008; Arndt and Schembri 2015; Iglésias and Frotté 2015), information on their catch characteristics in artisanal fisheries is very limited (e.g., Carpentieri et al. 2009), and there is also a big gap related to their seasonal catch per unit of effort (CPUE). Furthermore, in contrast to indigenous species, government statistics do not include regular information on the catch, effort, and prices of NIS (TURKSTAT 2022). Hence, only scientific studies provide that kind of data on the catch characteristics of these species at present. Therefore, in the presently reported study, we aimed to fill the existing gap to some extent. Thus, we assessed the catch composition, and also analyzed and compared the CPUE of indigenous and NIS in the SSF using trammel nets and longlines based on weekly onboard observations in the Mediterranean coasts of Türkiye between May 2020 and September 2021.

Materials and methods

This study was carried out in Kalkan, Kaş, and the Kaş–Kekova Special Environmental Protection Area (SEPA) located on the southern Mediterranean coasts of Türkiye (Fig. 1). This area is known as one of the most important locations for SSF for many years and the main target species of the longline fishery are *Lichia amia* (Linnaeus, 1758), *Epinephelus costae* (Steindachner, 1878), and *Pagrus pagrus* (Linnaeus, 1758), whereas the main target species in trammel net fishery are *Siganus luridus* (Rüppell, 1829), *Siganus rivulatus* Forsskål et Niebuhr, 1775, and *Epinephelus costae*. The Kekova SEPA was created in 1990 and became the Kaş–Kekova SEPA in 2006. The overall area covers 258 km^2 and the marine area covers 166 km^2 (Mangos and Claudot 2013). A total of 51 active fishers fished in the Kaş–Kekova SEPA (including Kalkan) and the mean number of days at sea for fishers was estimated as 141 days (Ünal unpublsished[*]). Regarding the habitat structure of the Kaş–Kekova SEPA, Akçalı et al. (2019) reported a total of 10 habitat types and it was determined that the broadest area was covered by *Halophila stipulacea*, *Posidonia oceanica*, and Corallinales gen. spp.

The data were collected weekly from May 2020 to September 2021 by commercial fishing vessels which included trammel nets and longlines. Each month, both trammel net and bottom set longline surveys were attempted four times. However, the data were limited (n = 62 days for trammel nets and n = 75 days for longlines) due to adverse weather conditions in some months, and the commercial landings of the fleet were also negatively affected by these weather conditions at certain times of the year. Regarding the trammel net surveys, the mesh sizes of used gear were 28 and 36 mm and the length of the daily used net ranged between 1000 and 2600 m. On the other hand, concerning the longline surveys, the number of hooks deployed was 10 and pilchard, *Sardina pilchardus* (Walbaum, 1792), was used as bait, which is most commonly used by commercial fishers. The hook number of longlines ranged between 250 and 550 during the survey. The longline surveys were carried out between 20 and 150 m at depth (mainly higher than 50 m), whereas the depth of trammel net surveys varied between 15 and 100 m (mainly lower than 50 m). During the onboard observation, details relating to fishing operations (hook number, net length, soak time) and habitat structure were recorded. The catch composition in terms of wet weight was recorded onboard by observers. The total length (TL) of all specimens of species was measured using calipers and the wet weight of these specimens was recorded using

---

[*] Ünal V (2021) Socio-economic status of small-scale fisheries in Fethiye–Göcek and Kaş–Kekova SEPAs: Cooperation, perception, satisfaction and continuity of profession. Mediterranean Conservation Society (AKD), Final report, 96 pp.

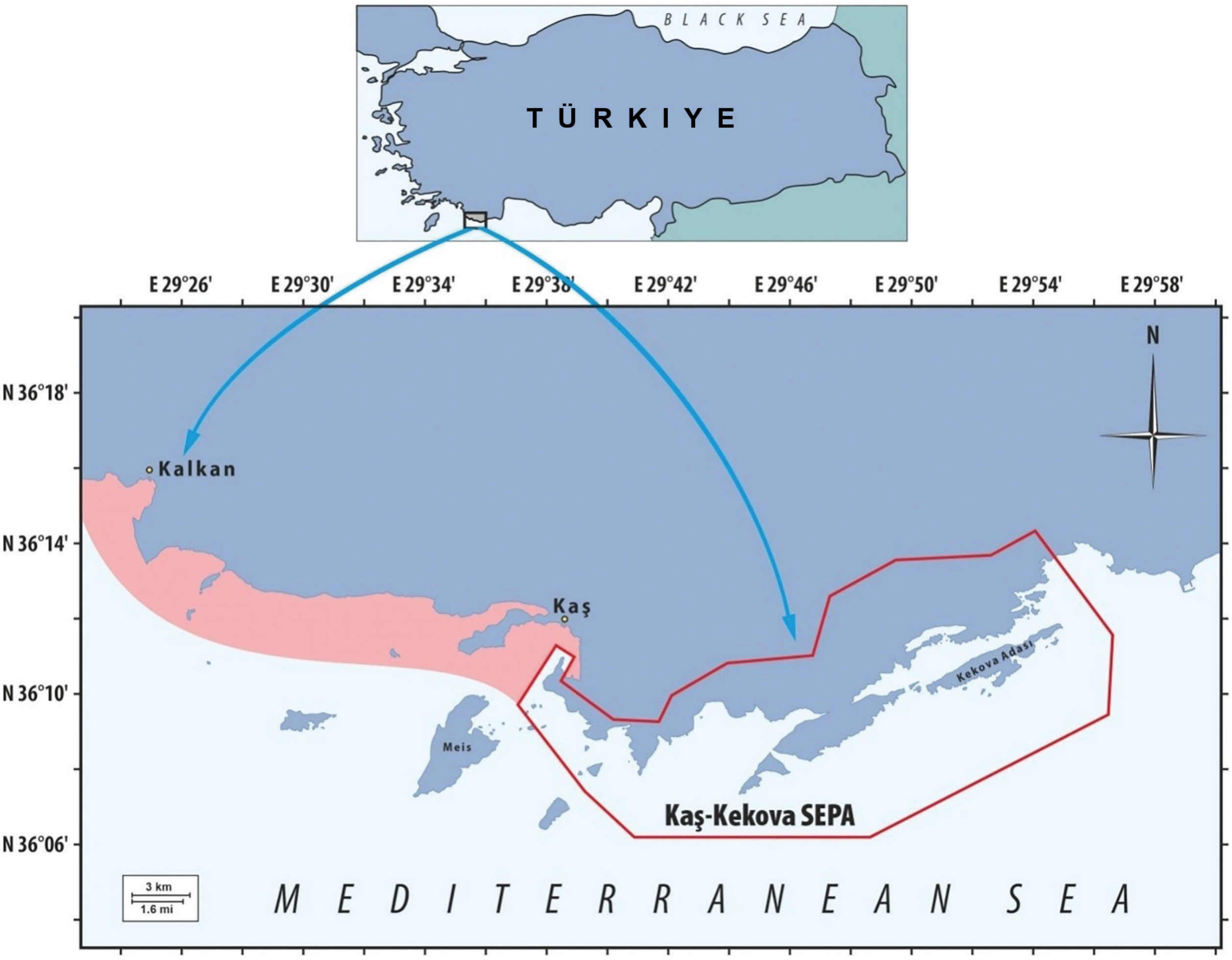

Figure 1. Map of the study area.

electronic balances. The CPUE values were calculated by standardization of the used net length and hook number; the zero catches were also taken into account in CPUE calculation. For longline surveys, the CPUE estimation was standardized for 1000 hooks (Güçlüsoy et al. 2020), while concerning the trammel net surveys, the standardized net length was 1000 m. The Kruskal–Wallis test was used to analyze whether CPUE of indigenous species and NIS shows significant differences depending on sampling seasons. SPSS software (Version 20) was used in this study.

Results

The results indicated that the mean CPUE of indigenous species was markedly high compared to NIS in longlines (Fig. 2A). The mean CPUE of indigenous species was 18 ± 2 kg, whilst the mean CPUE of NIS was calculated as 3 ± 1 kg. On the contrary, the mean CPUE values of indigenous species were low in trammel nets (Fig. 2B, 2C). The mean CPUE of indigenous species and NIS was reported as 0.3 ± 0.2 kg and 3.9 ± 0.7 kg, respectively in a trammel net with 28 mm mesh size, whereas the mean CPUE of indigenous species and NIS was reported as 0.1 ± 0.1 kg and 3 ± 0.4 kg, respectively in trammel net with 36 mm mesh size. There was a marginally significant difference in the CPUE of indigenous species among the different sampling seasons, with the CPUE highest in autumn (Kruskal–Wallis test, $\chi^2 = 19.89$, $P < 0.001$), while the CPUE of NIS did not change seasonally in the longline surveys and the highest mean value was found in winter (Kruskal–Wallis test, $\chi^2 = 2.99$, $P = 0.394$) (Fig. 2D). Concerning the trammel net with 28 mm mesh size, there was no significant difference in the CPUE of indigenous species in different seasons (Kruskal–Wallis test, $\chi^2 = 1.48$, $P = 0.477$). Similarly, for the same fishing gear, the CPUE of NIS did not significantly change by season (Kruskal–Wallis test, $\chi^2 = 4.59$, $P = 0.101$). The highest mean CPUE of indigenous species and NIS was found in summer and spring respectively (Fig. 2E). According to the trammel net survey data regarding mesh size 36 mm, the CPUE of both indigenous species and NIS showed significant differences across all seasons (indigenous species: Kruskal–Wallis test, $\chi^2 = 17.77$, $P < 0.001$, NIS: $\chi^2 = 18.16$, $P < 0.001$) and the highest mean values were recorded in summer for both groups (Fig. 2F).

Regarding the catch composition, 32 species were observed throughout the longline surveys and the percentage of indigenous species was 74% (Table 1). *Lichia amia*, *Pagrus pagrus*, and *Muraena helena* Linnaeus,

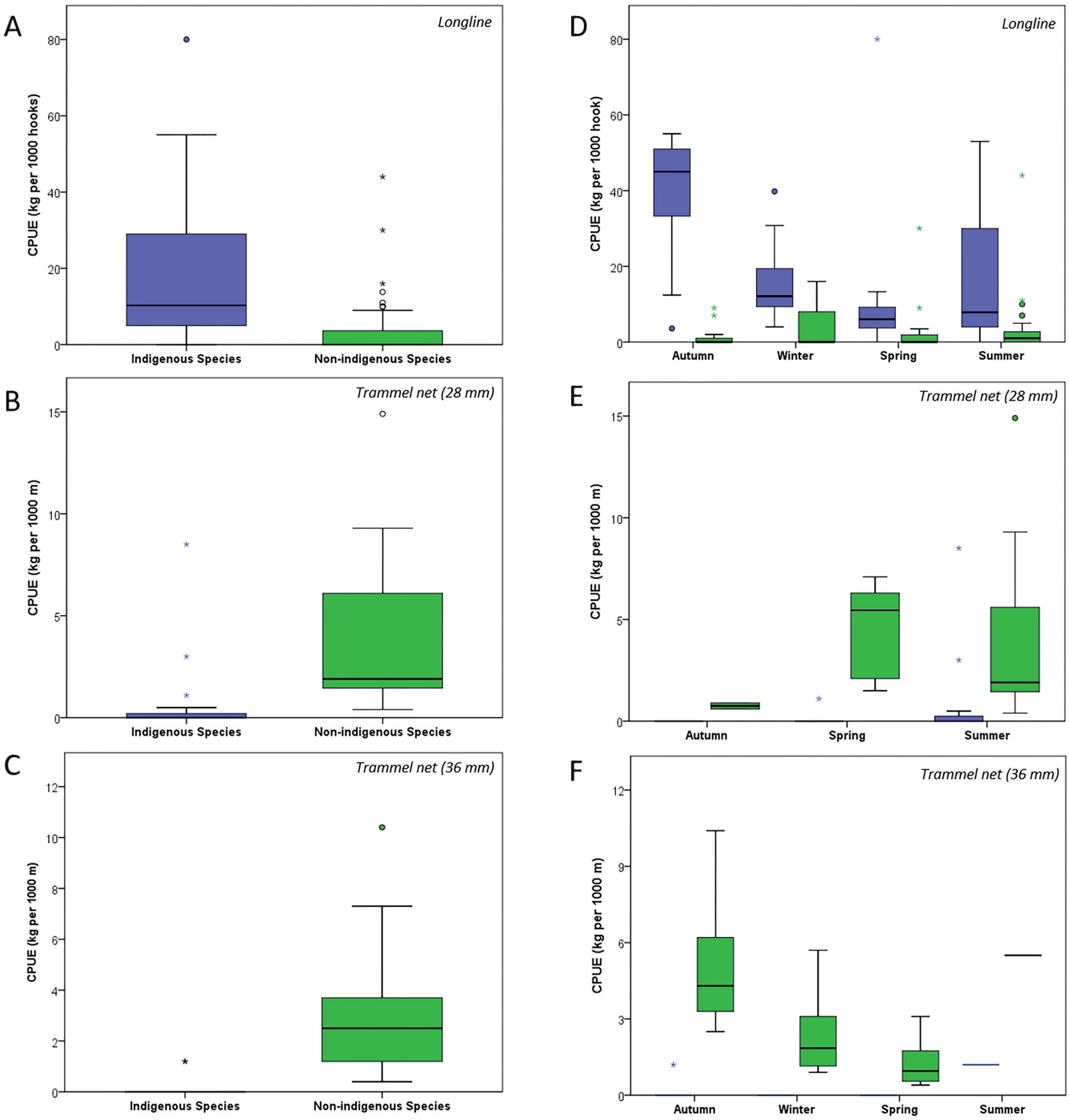

Figure 2. The CPUE values of indigenous and non-indigenous species: **A**) longline, **B**) trammel net (28 mm mesh size), **C**) trammel net (36 mm mesh size), seasonal CPUE values of indigenous and non-indigenous species: **D**) longline, **E**) trammel net (28 mm mesh size), **F**) trammel net (36 mm mesh size). The blue and green box-plots indicate indigenous species and non-indigenous species, respectively.

1758 were the common indigenous species, whereas the highest catches of NIS were represented by *Lagocephalus sceleratus* (Gmelin, 1789), *Lagocephalus suezensis* Clark et Gohar, 1953, and *Pterois miles* (Bennett, 1828) (Fig. 3A). In addition, NIS were common in trammel nets (mesh size 28) and they accounted for 94%. Nine NIS were observed in the nets; *Siganus luridus*, *Siganus rivulatus*, *Pterois miles*, *Scarus ghobban* Forsskål, 1775, *Lagocephalus sceleratus*, *Sargocentron rubrum* (Forsskål, 1775), *Saurida lessepsianus* Russell, Golani et Tikochinski, 2015, *Upeneus moluccensis* (Bleeker, 1855), and *Parupeneus forsskali* (Fourmanoir et Guézé, 1976) (Fig. 3B). Similarly, the composition of trammel nets with a larger mesh size (36 mm) mainly consisted of NIS (98%). The most prevalent, among the species caught in the above-mentioned gear was lionfish *Pterois miles*, followed by *Siganus luridus*, *Scarus ghobban*, *Siganus rivulatus*, *Sargocentron rubrum*, *Lagocephalus sceleratus*, *Fistularia commersonii* Rüppell, 1838, *Upeneus pori* Ben-Tuvia et Golani, 1989, *Lagocephalus suezensis*, *Upeneus moluccensis*, and *Saurida lessepsianus* (Fig. 3C). The results also showed that ecologically important fish species including *Pagellus erythrinus* (Linnaeus, 1758), *Conger conger* (Linnaeus, 1758),

Table 1. Catch composition (finfish and shellfish), percentage, and biomass information of bottom set longline and trammel nets 28 and 36 mm for 75, 27, and 35 fishing days, respectively.

Catch composition of longline	Percentage [%]	Biomass [kg]	Catch composition of trammel net (28 mm)	Percentage [%]	Biomass [kg]	Catch composition of trammel net (36 mm)	Percentage [%]	Biomass [kg]
Lichia amia	18.85	101.2	*Siganus luridus*	25.66	48.7	*Pterois miles*	34.62	63
Pagrus pagrus	13.38	71.85	*Siganus rivulatus*	25.5	48.4	*Siganus luridus*	23.08	42
Muraena helena	12.24	65.7	*Pterois miles*	22.13	42	*Scarus ghobban*	16.98	30.9
Epinephelus costae	10.47	56.2	*Scarus ghobban*	7.38	14	*Siganus rivulatus*	8.96	16.3
Pagellus erythrinus	9.04	48.5	*Lagocephalus sceleratus*	6.43	12.2	*Sargocentron rubrum*	6.26	11.4
Lagocephalus sceleratus	8.63	46.3	*Sargocentron rubrum*	5.22	9.9	*Lagocephalus sceleratus*	4.18	7.6
Conger conger	5.10	27.4	*Sparisoma cretense*	2.11	4	*Fistularia commersonii*	2.03	3.7
Lagocephalus suezensis	4.30	23.1	*Pagellus erythrinus*	1.48	2.8	*Lichia amia*	1.15	2.1
Xiphias gladius	3.37	18.1	*Epinephelus costae*	1.21	2.3	*Upeneus pori*	1.04	1.9
Dentex macrophthalmus	2.85	15.3	*Torpedo marmorata*	0.58	1.1	*Lagocephalus suezensis*	0.55	1
Pagrus caeruleostictus	2.44	13.1	*Saurida lessepsianus*	0.53	1	*Epinephelus costae*	0.55	1
Epinephelus aeneus	2.12	11.4	*Scorpaena porcus*	0.42	0.8	*Upeneus moluccensis*	0.38	0.7
Phycis blennoides	0.78	4.2	*Sepia officinalis*	0.37	0.7	*Saurida lessepsianus*	0.11	0.2
Pterois miles	0.75	4	*Upeneus moluccensis*	0.34	0.7	*Scorpaena porcus*	0.11	0.2
Homarus gammarus	0.75	4	*Parupeneus forsskali*	0.32	0.6			
Sargocentron rubrum	0.63	3.4	*Diplodus vulgaris*	0.21	0.4			
Saurida lessepsianus	0.63	3.4	*Spicara smaris*	0.11	0.2			
Loligo vulgaris	0.56	3						
Scarus ghobban	0.52	2.8						
Dentex dentex	0.43	2.3						
Nemipterus randalli	0.37	2						
Diplodus sargus	0.34	1.8						
Torpedo marmorata	0.30	1.6						
Raja sp.	0.24	1.3						
Oblada melanurus	0.20	1.1						
Parupeneus forsskali	0.17	0.9						
Diplodus vulgaris	0.15	0.8						
Pagellus acarne	0.11	0.6						
Serranus cabrilla	0.10	0.55						
Siganus luridus	0.09	0.5						
Serranus scriba	0.04	0.2						
Sparisoma cretense	0.04	0.2						

Dentex macrophthalmus (Bloch, 1791), *Phycis blennoides* (Brünnich, 1768), *Diplodus sargus* (Linnaeus, 1758), *Pagellus acarne* (Risso, 1827), *Serranus scriba* (Linnaeus, 1758), *Sparisoma cretense* (Linnaeus, 1758) and invertebrate species *Homarus gammarus* (Linnaeus, 1758) and *Loligo vulgaris* Lamarck, 1798 were observed in longline catch composition (Table 1). Similarly, *Scorpaena porcus* Linnaeus, 1758 and *Spicara smaris* (Linnaeus, 1758) were caught by trammel net (Table 1).

Discussion

This study provided evidence of a predominance of NIS in trammel net catches, while the same were less prevalent in the longlines in Kalkan, Kaş, and the Kaş–Kekova SEPA, Eastern Mediterranean. Traditionally, trammel net fishery is generally performed in shallow waters compared with the longline fishery in the Kaş–Kekova SEPA and Kalkan, and it is well-known that some Lessepsian species prefer to live in shallow waters (Corsini et al. 2005; Öndes et al. 2018). Therefore, this can be considered an important factor resulting in the differences in Lessepsian catches by trammel nets and longlines. Likewise, the relation between changes in the behaviors of fishers and the CPUE of Lessepsians was discussed by Van Rijn et al. (2020). The study noted that fishers preferred to fish in shallower waters where Lessepsians were common; thus, their CPUE values showed an increase. Today it is well-known that the stocks of many indigenous species which could be potential predators or competitors of NIS in the Mediterranean have been markedly reduced by overfishing (Vasilakopoulos et al. 2014; Piroddi et al. 2017). Moreover, according to TURKSTAT's data, the total landings of many indigenous species in the Mediterranean (Levantine) coasts of Türkiye showed a marked decrease over the periods of 2001–2010 and 2011–2020. For instance, the decline percentages of some commonly fished species in the SSF were as follows: *Dentex dentex* (Linnaeus, 1758) (77%), *Pagrus caeruleostictus* (Valenciennes, 1830) (76%), *Pagrus pagrus* (75%), *Oblada melanurus* (Linnaeus, 1758) (72%), *Zeus faber* Linnaeus, 1758 (65%), *Lichia amia* (53%), *Diplodus vulgaris* (Geoffroy Saint-Hilaire, 1817) (52%), and *Xiphias gladius* Linnaeus, 1758 (29%) (TURKSTAT 2022). On the other hand, the total landings of some species, such as *Sarda sarda* (Bloch, 1793) and *Scomber colias* Gmelin, 1789, showed an increase for the same period (TURKSTAT 2022).

In the presently reported study, the most common two species in the trammel nets with 28 mm mesh size were *Siganus luridus* and *Siganus rivulatus*, and these

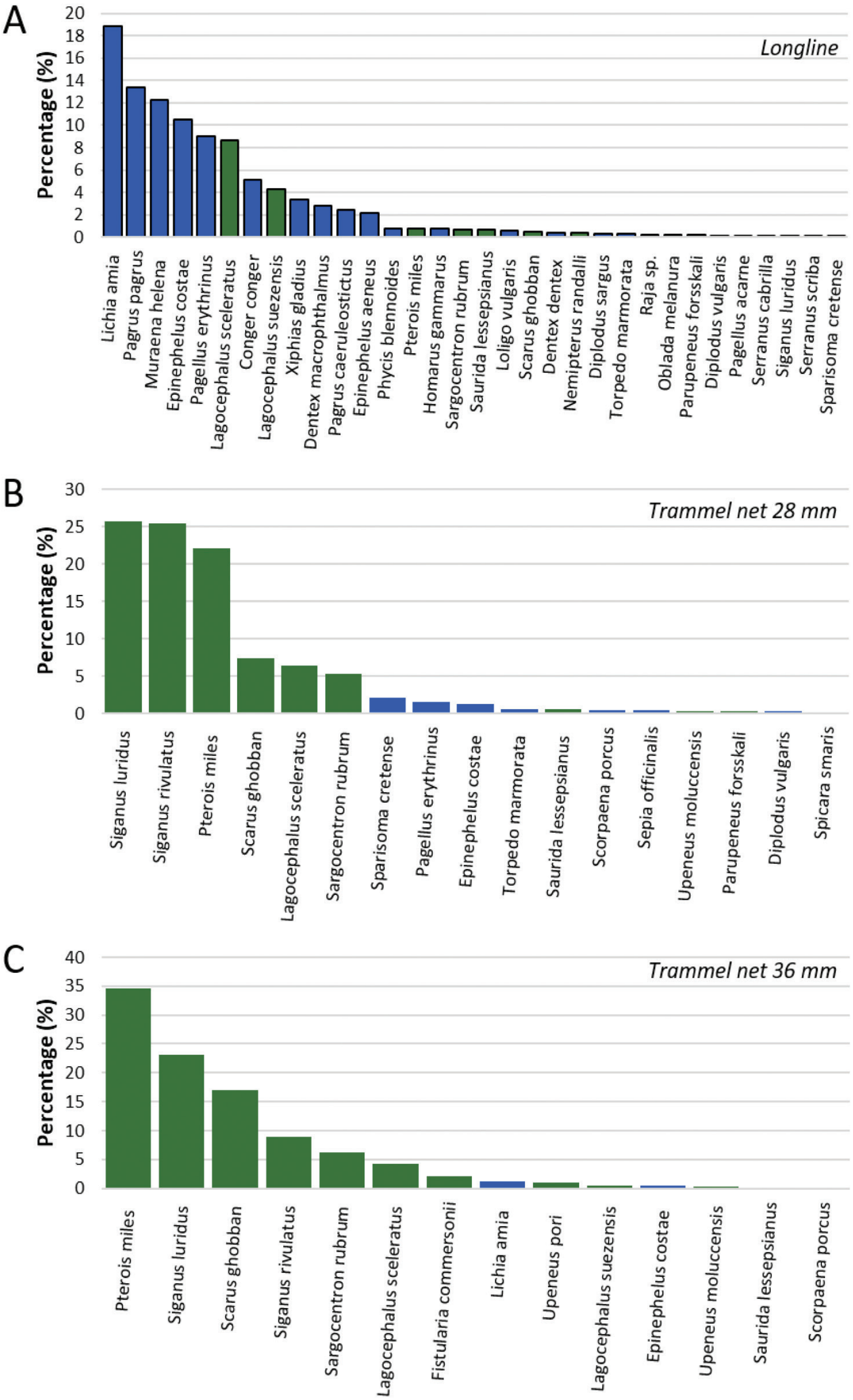

Figure 3. Catch composition (with percentages) of **A**) longline, **B**) trammel net (28 mm), **C**) trammel net (36 mm) in the Levantine coasts of Türkiye. The blue and green bars indicate indigenous species and non-indigenous species, respectively.

consisted of more than half of the total catch. These species also represented significant amounts in the catch of trammel net with a 36 mm mesh size. Akyol et al. (2022) reported that *Siganus rivulatus* and *Siganus luridus* were commonly caught in the gillnet fishery in the southern Aegean Sea. Similarly, Bakhoum (2018) evaluated the catch composition of trammel nets from December 2011 to May 2014 off the Egyptian Mediterranean coast of Alexandria and noticed that Lessepsian fish *Siganus rivulatus* was the most dominant species with an index of the relative dominance of 54.47%. Lessepsian species also started to be an important part of the catch composition of Mediterranean trawl fishery. For example, Mavruk et al. (2017) collected data on the catch composition of trawl fishery from 2004 to 2015 in the Gulf of Iskenderun, in the northeastern Mediterranean, and reported that Lessepsians represented 27%, 62%, and 85% of the total teleost fishes in the number of species, biomass, and abundance, respectively. They also highlighted that the dominance of Lessepsian fishes showed an increase with an annual rate of 2.77 (LW-% (biomass)) per year throughout their study period. Furthermore, Yemisken et al. (2014) investigated the catch composition of trawl fishery in the Gulf of Iskenderun and noted that 27 Lessepsian species were found, and 9 of them began to be target species for trawlers.

The presently reported study demonstrated that the highest CPUE of NIS in trammel nets with 28 mm mesh size was found in the spring and summer months. Similarly, Öndes et al. (2018) reported that the highest bycatch of pufferfish species was observed in the summer months on the Levantine coasts of Türkiye. Furthermore, Akyol et al. (2022) found lower CPUE values for NIS compared with the presently reported study. This situation may be related to the difference in sampling sites; Akyol et al. (2022) collected data further north from our study area where the population structure of NIS were different. Concerning the seasonal difference of CPUE in trammel nets with 36 mm mesh size, the highest values were recorded in autumn in the presently reported study. Similarly, Akyol et al. (2022) reported that the highest CPUE values of NIS were found in autumn.

Our study reports a total of 12 and 9 non-indigenous species in trammel nets and longline surveys, respectively. Among them, 8 species including *Siganus luridus*, *Siganus rivulatus*, *Upeneus pori*, *Upeneus moluccensis*, *Sargocentron rubrum*, *Nemipterus randalli* Russell, 1986, *Pterois miles*, and *Saurida lessepsianus* have been sold at local markets. Undoubtedly, having the market value and demand for these species is desirable for both fishers and ecosystem health. There are some factors that may persuade consumers to consume these new species more. For example, the prices of these species are generally more affordable compared to many native species that show decreased populations due to overfishing. Other reasons may be related to the flavor of these species and people's gastronomic curiosity. Moreover, awareness studies and projects are carried out by some NGOs (e.g., Mediterranean Conservation Society) and their enterprises encouraging the consumption of these species in the region (Pers. comm., Funda Kök). On the other hand, some studies (Ünal et al. 2015; Ünal and Göncüoğlu Bodur 2017) suggested the application of a bounty system, which has been in practice in Northern Cyprus since 2012, (Anonymous 2012) in order to combat species such as pufferfish, which do not have a market value yet. Decision makers would seem to be amenable to implementing these suggestions in Türkiye as well. For this purpose, a communiqué (a notification) was published in the official gazette, and a regulation was made to pay the fishers for each puffer fish tail they provided (Anonymous 2021). In fact, in terms of catch amount and value, the rate of NIS in the SSF should not be disregarded. Ünal (unpublished[*]) reported that the proportion of NIS within the total catch in the Kaş–Kekova SEPA was 40% and two of the five most important species in terms of total catch amount and value were NIS.

Conclusions

In conclusion, the presently reported study shows that indigenous species are dominant in bottom set longline fishery, while NIS are represented with higher CPUE in trammel net fishery in Kalkan, Kaş, and the Kaş–Kekova SEPA, Eastern Mediterranean. Furthermore, in general, the dominance of indigenous species has shown a dramatic decrease over recent decades. Although there have been measures taken by decision-makers to cope with this situation, they are insufficient. In addition to management measures and practices, it is observed that related scientific studies are also insufficient. Therefore, we suggest further research focusing on the catch composition of both trammel and gill nets that have smaller mesh sizes used by the fleet.

Acknowledgments

This study was supported by Akdeniz Koruma Derneği (Mediterranean Conservation Society) (AKD) through several grants under the "management of invasive alien species" program in partnership with Fauna Flora International (FFI). Therefore, we would like to express our sincere thanks to AKD and FFI for their support. We are also grateful to local fishers for their positive approach to sharing information with us during the data collection.

---

[*] Ünal V (2021) Socio-economic status of small-scale fisheries in Fethiye–Göcek and Kaş–Kekova SEPAs: Cooperation, perception, satisfaction and continuity of profession. Mediterranean Conservation Society (AKD), Final report, 96 pp.

References

Akçalı B, Kaboğlu G, Bizsel KC, Kavcioğlu R, Savaş Y, Bengil F, Özaydinli M, Kayaalp J, Sönmez Flitman R, Ergün G, Güçlüsoy H (2019) Habitat mapping in marine protected areas: contributions to management plans in Foça and Kaş–Kekova Special Environmental Protection Areas. Pp. 23–28. In: Langar H, Ouerghi A (Eds) Proceedings of the 6th Mediterranean Symposium on Marine Vegetation, 14–15 January 2019, Antalya, Turkey.

Akyol O, Ceyhan T, Düzbastılar FO, Ertosluk O (2022) The exotic species and their catch per unit effort (CPUE) from gillnet fisheries in the southern Aegean coasts (Türkiye). COMU Journal of Marine Sciences and Fisheries 5(1): 87–93. https://doi.org/10.46384/jmsf.1122273 [In Turkish]

Anonymous (2012) Balon baliklarinin toplatilmasi. Karar no: 1621/2012, Önerge no: K(II) 1697–2012. [Withdrawal of the puffer fish species from the fishermen. Motion. No: 1621/2012, Resolution number: K(II) 1697–2012.] Ministry of Agriculture and Natural Resources, Turkish Republic of Northern Cyprus. [In Turkish]

Anonymous (2021) Balon baliği avciliğinin desteklenmesine iliskin teblig (Teblig no: 2021/20, Sayi: 31524). [Notification for the promotion of pufferfish fishing. Notification no: 2021/20, issue: 31524] Ministry of Agriculture and Forestry, Republic of Türkiye. [In Turkish]

Arndt E, Schembri PJ (2015) Common traits associated with establishment and spread of Lessepsian fishes in the Mediterranean Sea. Marine Biology 162(10): 2141–2153. https://doi.org/10.1007/s00227-015-2744-3

Bakhoum S (2018) Fish assemblages in surf zone of the Egyptian Mediterranean coast off Alexandria. Turkish Journal of Fisheries and Aquatic Sciences 19(4): 351–362.

Birkan R, Öndes F (2020) Socio-economic characteristics of small-scale fisheries in the Aegean Sea, Turkey (eastern Mediterranean). Acta Ichthyologica et Piscatoria 50(3): 257–268. https://doi.org/10.3750/AIEP/02840

Bronstein O, Georgopoulou E, Kroh A (2017) On the distribution of the invasive long-spined echinoid *Diadema setosum* and its expansion in the Mediterranean Sea. Marine Ecology Progress Series 583: 163–178. https://doi.org/10.3354/meps12348

Carpentieri P, Lelli S, Colloca F, Mohanna C, Bartolino V, Moubayed S, Ardizzone GD (2009) Incidence of Lessepsian migrants on landings of the artisanal fishery of south Lebanon. Marine Biodiversity Records 2: e71. https://doi.org/10.1017/S1755267209000645

Çınar ME, Bilecenoğlu M, Yokeş MB, Öztürk B, Taşkin E, Bakir K, Doğan A, Açik Ş (2021) Current status (as of end of 2020) of marine alien species in Turkey. PLoS One 16(5): e0251086. https://doi.org/10.1371/journal.pone.0251086

Compa M, Alomar C, Wilcox C, van Sebille E, Lebreton L, Hardesty BD, Deudero S (2019) Risk assessment of plastic pollution on marine diversity in the Mediterranean Sea. Science of the Total Environment 678: 188–196. https://doi.org/10.1016/j.scitotenv.2019.04.355

Corsini M, Margies P, Kondilatos G, Economidis PS (2005) Lessepsian migration of fishes to the Aegean Sea: First record of *Tylerius spinosissimus* (Tetraodontidae) from the Mediterranean, and six more fish records from Rhodes. Cybium 29(4): 347–354.

Danovaro R (2003) Pollution threats in the Mediterranean Sea: An overview. Chemistry and Ecology 19(1): 15–32. https://doi.org/10.1080/0275754031000081467

Edelist D, Sonin O, Golani D, Rilov G, Spanier E (2011) Spatiotemporal patterns of catch and discards of the Israeli Mediterranean trawl fishery in the early 1990s: Ecological and conservation perspectives. Scientia Marina 75(4): 641–652. https://doi.org/10.3989/scimar.2011.75n4641

Galil BS, Boero F, Campbell ML, Carlton JT, Cook E, Fraschetti S, Gollasch S, Hewitt CL, Jelmert A, Macpherson E, Marchini A, McKenzie C, Minchin D, Occhipinti-Ambrogi A, Ojaveer H, Olenin S, Piraino S, Ruiz GM (2015) ‘Double trouble’: The expansion of the Suez Canal and marine bioinvasions in the Mediterranean Sea. Biological Invasions 17(4): 973–976. https://doi.org/10.1007/s10530-014-0778-y

Garrabou J, Gómez-Gras D, Ledoux JB, Linares C, Bensoussan N, López-Sendino P, Bazairi H, Espinosa F, Ramdani M, Grimes S, Benabdi M, Souissi JB, Soufi E, Khamassi F, Ghanem R, Ocaña O, Ramos-Esplà A, Izquierdo A, Anton I, Rubio-Portillo E, Barbera C, Cebrian E, Marbà N, Hendriks IE, Duarte CM, Deudero S, Díaz D, Vázquez-Luis M, Alvarez E, Hereu B, Kersting DK, Gori A, Viladrich N, Sartoretto S, Pairaud I, Ruitton S, Pergent G, Pergent-Martini C, Rouanet E, Teixidó N, Gattuso J-P, Fraschetti S, Rivetti I, Azzurro E, Cerrano C, Ponti M, Turicchia E, Bavestrello G, Cattaneo-Vietti R, Bo M, Bertolino M, Montefalcone M, Chimienti G, Grech D, Rilov G, Tuney Kizilkaya I, Kizilkaya Z, Eda Topçu N, Gerovasileiou V, Sini M, Bakran-Petricioli T, Kipson S, Harmelin JG (2019) Collaborative database to track mass mortality events in the Mediterranean Sea. Frontiers in Marine Science 6: e707. https://doi.org/10.3389/fmars.2019.00707

Golani D (1998) Distribution of Lessepsian migrant fish in the Mediterranean. Italian Journal of Zoology 65(S1): 95–99. https://doi.org/10.1080/11250009809386801

Goren M, Galil BS (2005) A review of changes in the fish assemblages of Levantine inland and marine ecosystems following the introduction of non-native fishes. Journal of Applied Ichthyology 21(4): 364–370. https://doi.org/10.1111/j.1439-0426.2005.00674.x

Gozlan RE (2008) Introduction of non-native freshwater fish: Is it all bad? Fish and Fisheries 9(1): 106–115. https://doi.org/10.1111/j.1467-2979.2007.00267.x

Güçlüsoy H, Öndes F, Tosunoğlu Z (2020) The catch characteristics of a set longline fishery in the Foça Special Environmental Protection Area, Turkey. Acta Ichthyologica et Piscatoria 50(3): 247–255. https://doi.org/10.3750/AIEP/02809

Iglésias S, Frotté L (2015) Alien marine fishes in Cyprus: Update and new records. Aquatic Invasions 10(4): 425–438. https://doi.org/10.3391/ai.2015.10.4.06

IUCN (2022) Summary statistics. IUCN. https://www.iucnredlist.org/resources/summary-statistics#Summary%20Tables

Kletou D, Hall-Spencer JM, Kleitou P (2016) A lionfish (*Pterois miles*) invasion has begun in the Mediterranean Sea. Marine Biodiversity Records 9(1): e46. https://doi.org/10.1186/s41200-016-0065-y

Kourantidou M, Cuthbert R, Haubrock P, Novoa A, Taylor N, Leroy B, Capinha C, Renault D, Angulo E, Diagne C, Courchamp F (2021) Economic costs of invasive alien species in the Mediterranean basin. NeoBiota 67: 427–458. https://doi.org/10.3897/neobiota.67.58926

Kourantidou M, Haubrock PJ, Cuthbert RN, Bodey TW, Lenzner B, Gozlan RE, Nuñez MA, Salles J-M, Diagne C, Courchamp F (2022) Invasive alien species as simultaneous benefits and burdens: Trends, stakeholder perceptions and management. Biological Invasions 24(7): 1–22. https://doi.org/10.1007/s10530-021-02727-w

Macias DM, Garcia-Gorriz E, Stips A (2015) Productivity changes in the Mediterranean Sea for the twenty-first century in response to changes in the regional atmospheric forcing. Frontiers in Marine Science 2: 79. https://doi.org/10.3389/fmars.2015.00079

Mangos A, Claudot MA (2013) Economic study of the impacts of marine and coastal protected areas in the Mediterranean. Plan Bleu Papers 13, Plan Bleu, Valbonne, France.

Mavruk S, Avsar D (2008) Non-native fishes in the Mediterranean from the Red Sea, by way of the Suez Canal. Reviews in Fish Biology and Fisheries 18(3): 251–262. https://doi.org/10.1007/s11160-007-9073-7

Mavruk S, Bengil F, Yeldan H, Manasirli M, Avsar D (2017) The trend of Lessepsian fish populations with an emphasis on temperature variations in Iskenderun Bay, the northeastern Mediterranean. Fisheries Oceanography 26(5): 542–554. https://doi.org/10.1111/fog.12215

Maynou F, Morales-Nin B, Cabanellas-Reboredo M, Palmer M, García E, Grau AM (2013) Small-scale fishery in the Balearic Islands (W Mediterranean): A socio-economic approach. Fisheries Research 139: 11–17. https://doi.org/10.1016/j.fishres.2012.11.006

Moullec F, Barrier N, Drira S, Guilhaumon F, Marsaleix P, Somot S, Ulses C, Velez L, Shin Y-J (2019) An end-to-end model reveals losers and winners in a warming Mediterranean Sea. Frontiers in Marine Science 6: 345. https://doi.org/10.3389/fmars.2019.00345

OECD (2022) The number of endangered animal and plant species is increasing. OECD. https://www.oecd.org/coronavirus/en/themes/the-number-of-endangered-animal-and-plant-species-is-increasing

Oficialdegui FJ, Sánchez MI, Clavero M (2020) One century away from home: How the red swamp crayfish took over the world. Reviews in Fish Biology and Fisheries 30(1): 121–135. https://doi.org/10.1007/s11160-020-09594-z

Öndes F, Gökçe G (2021) Distribution and fishery of the invasive blue crab (*Callinectes sapidus*) in Turkey based on local ecological knowledge of fishers. Journal of Anatolian Environmental and Animal Sciences 6(3): 325–332. https://doi.org/10.35229/jaes.891379

Öndes F, Ünal V, Özbilgin Y, Deval M, Turan C (2018) By-catch and monetary loss of pufferfish in Turkey, the Eastern Mediterranean. Su Ürünleri Dergisi 35(4): 361–372. https://doi.org/10.12714/egejfas.2018.35.4.01

Öztürk B (2021) Non-indigenous species in the Mediterranean and the Black Sea. Studies and Reviews No. 87. General Fisheries Commission for the Mediterranean, FAO, Rome.

Penca J, Said A, Cavallé M, Pita C, Libralato S (2021) Sustainable small-scale fisheries markets in the Mediterranean: Weaknesses and opportunities. Maritime Studies 20(2): 141–155. https://doi.org/10.1007/s40152-021-00222-5

Piroddi C, Coll M, Liquete C, Macias D, Greer K, Buszowski J, Christensen V (2017) Historical changes of the Mediterranean Sea ecosystem: Modelling the role and impact of primary productivity and fisheries changes over time. Scientific Reports 7(1): e44491. https://doi.org/10.1038/srep44491

Ramírez F, Pennino MG, Albo-Puigserver M, Steenbeek J, Bellido JM, Coll M (2021) SOS small pelagics: A safe operating space for small pelagic fish in the western Mediterranean Sea. Science of the Total Environment 756: e144002. https://doi.org/10.1016/j.scitotenv.2020.144002

Stergiou KI, Somarakis S, Triantafyllou G, Tsiaras KP, Giannoulakia M, Petihakis G, et al. (2016) Trends in productivity and biomass yields in the Mediterranean Sea Large Marine Ecosystem during climate change. Environmental Development 17: 27–74. https://doi.org/10.1016/j.envdev.2015.09.001

Tsikliras AC, Dinouli A, Tsalkou E (2013) Exploitation trends of the Mediterranean and Black Sea fisheries. Acta Adriatica 54(2): 273–282.

Tsikliras AC, Dinouli A, Tsiros VZ, Tsalkou E (2015) The Mediterranean and Black Sea fisheries at risk from overexploitation. PLoS One 10(3): e0121188. https://doi.org/10.1371/journal.pone.0121188

TURKSTAT (2022) Su Ürünleri İstatistikleri. Turkstat. [In Turkish] https://biruni.tuik.gov.tr/medas/?kn=97&locale=tr

Ulman A, Yıldız T, Demirel N, Çanak Ö, Yemişken E, Pauly D (2021) The biology and ecology of the invasive silver-cheeked toadfish (*Lagocephalus sceleratus*), with emphasis on the Eastern Mediterranean. NeoBiota 68: 145–175. https://doi.org/10.3897/neobiota.68.71767

Ünal V, Göncüoğlu Bodur H (2017) The socio-economic impacts of the silver-cheeked toadfish on small-scale fishers: A comparative study from the Turkish coast. Su Ürünleri Dergisi 34(2): 119–127. https://doi.org/10.12714/egejfas.2017.34.2.01

Ünal V, Göncüoğlu H, Durgun D, Tosunoğlu Z, Deval C, Turan C (2015) Silver-cheeked toadfish, *Lagocephalus sceleratus* (Actinopterygii: Tetraodontiformes: Tetraodontidae), causes a substantial economic losses in Turkish Mediterranean coast:a call for decision makers. Acta Ichthyologica et Piscatoria 45(3): 231–237. https://doi.org/10.3750/AIP2015.45.3.02

Van Rijn I, Kiflawi M, Belmaker J (2020) Alien species stabilize local fisheries catch in a highly invaded ecosystem. Canadian Journal of Fisheries and Aquatic Sciences 77(4): 752–761. https://doi.org/10.1139/cjfas-2019-0065

Vasilakopoulos P, Maravelias CD, Tserpes G (2014) The alarming decline of Mediterranean fish stocks. Current Biology 24(14): 1643–1648. https://doi.org/10.1016/j.cub.2014.05.070

Vimercati G, Kumschick S, Probert AF, Volery L, Bacher S (2020) The importance of assessing positive and beneficial impacts of alien species. NeoBiota 62: 525–545. https://doi.org/10.3897/neobiota.62.52793

Yemisken E, Dalyan C, Eryilmaz L (2014) Catch and discard fish species of trawl fisheries in the Iskenderun Bay (northeastern Mediterranean) with emphasis on Lessepsian and chondricthyan species. Mediterranean Marine Science 15(2): 380–389. https://doi.org/10.12681/mms.538

Zenetos A, Gofas S, Morri C, Rosso A, Violanti D, Raso JG, et al. (2012) Alien species in the Mediterranean Sea by 2012. A contribution to the application of European Union's Marine Strategy Framework Directive (MSFD). Part 2. Introduction trends and pathways. Mediterranean Marine Science 13(2): 328–352. https://doi.org/10.12681/mms.327

Zenetos A, Albano PG, Lopez Garcia E, Stern N, Tsıamis K, Galanidi M (2022) Established non-indigenous species increased by 40% in 11 years in the Mediterranean Sea. Mediterranean Marine Science 23(1): 196–212. https://doi.org/10.12681/mms.29106

Acta Ichthyologica et Piscatoria 53, 2023, 37–43 | DOI 10.3897/aiep.53.100933

PENSOFT

ACTA ICHTHYOLOGICA ET PISCATORIA

Reproductive biology of largescaled mullet, *Parachelon grandisquamis* (Actinopterygii: Mugiliformes: Mugilidae), in the Marine Protected Area of Niamone–Kalounayes (Casamance estuary, Senegal)

Patrick DIEDHIOU[1], Alassane SARR[1], Ousseynou SAMBA[1], Modou SENE[1],
Alexandre Langlais BOURASSA[2], Waly NDIAYE[1]

1 *Cheikh Anta Diop, University of Dakar, University Institute of Fisheries and Aquaculture (UCAD/IUPA), Dakar, Senegal*
2 *AECOM Consultants Inc., Montreal, Quebec, Canada*

https://zoobank.org/11E149EC-7CCB-4394-9DF5-FDC4743268B5

Corresponding author: Patrick Diedhiou (patrickdiedhiou76@yahoo.com)

Academic editor: Sanja Matić-Skoko ♦ **Received** 23 January 2023 ♦ **Accepted** 11 March 2023 ♦ **Published** 20 April 2023

Citation: Diedhiou P, Sarr A, Samba O, Sene M, Bourassa AL, Ndiaye W (2023) Reproductive biology of largescaled mullet, *Parachelon grandisquamis* (Actinopterygii: Mugiliformes: Mugilidae), in the Marine Protected Area of Niamone–Kalounayes (Casamance estuary, Senegal). Acta Ichthyologica et Piscatoria 53: 37–43. https://doi.org/10.3897/aiep.53.100933

Abstract

In Senegal, studies on the family Mugilidae are rare and little data is available on their reproductive biology. This study, carried out in the MPA of Niamone–Kalounayes (Casamance River estuary, Senegal) aims to enhance our knowledge of the reproductive biology of the largescale mullet, *Parachelon grandisquamis* (Valenciennes, 1836), a species highly prized by the local population as a food source. To better understand its reproductive biology, a series of monthly samplings over twelve (12) months from July 2021 to June 2022 was carried out. Experimental fisheries were carried out at six (6) stations located in secondary channels lined with mangroves, using a seine net (250 m long and 25 mm mesh side). A total of 361 individuals were sampled, including 321 female specimens and 40 male specimens. The calculated sex ratio was in favor of females (1:8), with a significant difference between the calculated sex ratio and the theoretical 1:1 sex ratio ($\chi^2 = 218.73$; P-value < 0.05). In the MPA of Niamone–Kalounayes, the breeding period of *P. grandisquamis* extends from March to July, from the end of the dry season up to the beginning of the wet season. The sizes at first sexual maturity were 17 cm in males and 18 cm in females, showing that in the MPA of Niamone–Kalounayes, males and females of *P. grandisquamis* reach sexual maturity at very close sizes ($\chi^2 = 0.02$; $P > 0.05$). As this species is subject to the intense fishery by many actors in the area, these findings may be proven useful in the process of developing a management plan for this particular species.

Keywords

Casamance estuary, experimental fisheries, marine protected area, *Parachelon grandisquamis*, reproductive biology, Senegal

Introduction

Studies on fish reproduction are inherently biological and ecological in essence (Albaret and Legendre 1985). Mugilidae, a family of fish commonly known as mullets, are permanent residents and often abundant fish in marine environments and brackish water ecosystems such as estuaries, lagoons, and small creeks around mangroves (Harrison 2008). Represented by two genera present in West Africa, *Chelon* and *Mugil*, the Mugilidae is one of the most abundant taxa in the estuaries of Senegal (Albaret 1984).

In the Casamance region, these species are highly prized by the local population as an important food source and are often the subject of specialized fisheries. These taxa are also widely distributed in West African estuaries (Albaret 2003; Diedhiou unpublished[*]; Dieme unpublished[**]) and constitute along with the Cichlidae one of the most abundant families. The abundance of mullets in estuarine and coastal areas is linked to the permanent presence of food in the area, but also to their feeding habits (Diouf 1996). They occupy a relatively low position in the food web (Wright 1988). However, studies on the fisheries and biology of Mugilidae, and more precisely on the largescaled mullet, *Parachelon grandisquamis* (Valenciennes, 1836), in Senegal, are rare. This study, carried out in the Marine Protected Area (MPA) of Niamone–Kalounayes, located in the Casamance River estuary, aims to deepen our knowledge on the reproductive biology of *P. grandisquamis*, but also help the development of a management plan for this species in the different areas of the MPA where fishing is authorized and regulated. Specifically, the goal of this study is to better describe the reproductive biology of this species, using biological parameters such as the sex ratio, the period and duration of reproduction, the gonadosomatic index, and the size at the first sexual maturity.

Methods

Presentation of the study area. Located right in the Ziguinchor region of the Casamance River basin, the MPA of Niamone–Kalounayes covers the maritime, estuarine, and freshwater portions of the Casamance River and covers an area of 63 894 ha. It is formed by a complex and diffuse system of channels commonly called *bolongs* and is bordered by mangroves that are characteristic of intertropical brackish wetlands. This MPA is delimited in the north by the classified forest of Kalounayes, in the east by the Soungrougrou River, in the west by the backwater of Bignona to the Affiniam Dam, and in the south by the south shore of the Casamance River (Fig. 1). The main objectives of the creation of this MPA were the restoration of habitats and natural resources, the improvement of living conditions of animal populations and the establishment of an adapted governance system (DAMPC unpublished[***]).

Sampling method. Data collection was conducted following a monthly sampling series, from July 2021 to June 2022. The experimental fisheries were carried out in secondary channels bordered by mangroves, using a 250 m long beach seine (25 mm mesh). Captured individuals of *Parachelon grandisquamis* were identified using fish identification keys (FAO 1992; Paugy et al. 2003; Seret and Opic 2011). At each site, every individual's total length (TL; cm), total weight (TW; g), eviscerated weight (EVW; g), and gonad weight (GW; g) were recorded. The fish were measured using a 1 mm precision ichthyometer and weighed with a digital electronic scale of precision 0.1 g and a maximum reach of 3000 g. The sex and the stage of sexual maturity of each individual were determined after gonad examination and the size of the oocytes, based on the work of Fontana (1969) (Table 1).

Sex ratio (SR) expresses the relative abundance of males and females in a given population. This ratio is necessary for the evaluation of the reproductive potential of fish and can also be used for estimating the size of stocks. For this study, the SR was calculated according to the formula from Kahn and al. (2021)

$$\mathrm{SR} = \frac{N_\mathrm{M}}{N_\mathrm{F}}$$

where N_M is the number of males and N_F is the number of females.

Gonadosomatic index and reproductive period. The gonadosomatic index (GSI) is used to determine spawning periods during the sexual cycle of a given species. The GSI is determined from the individual data of each fish and is calculated according to the following formula (Analbery unpublished[****])

$$\mathrm{GSI} = \frac{W_\mathrm{G}}{W_\mathrm{EV}} \times 100$$

where W_G is the gonads' weight [g] and W_EV is the eviscerated weight [g].

Size at first sexual maturity. The size of the first sexual maturity (L_m) corresponds to the length for which 50% of the captured individuals are mature during the breeding season. It is used to monitor the degree of sexual maturity according to the size of the individuals (Amenzoui et al. 2004–2005). The percentage per size class of females or males having reached stage 3 and above was calculated in relation to the total number of sexually mature females or males. A logistic function relating the percentages of mature fish to length (Ghorbel et al. 1996) was used:

$$M_\% = \frac{100}{1 + e^{-\alpha(\mathrm{TL} - L_\mathrm{m})}}$$

where $M_\%$ is the percentage of individuals that have attained sexual maturity, e is a constant, TL is the total length of the fish, and L_m is the length where 50% of the sampled individuals are mature, and α is the relation parameter.

---

[*] Diedhiou P (2019) Contribution à l'étude des peuplements de poissons de l'aire marine protégée de Niamone–Kalounayes (Casamance). Mémoire Masteur Ecologie et Gestion des Ecosystèmes Aquatique, IUPA, UCAD, Dakar, 32 pp.

[**] Dieme S (2021) La diversité des Mugilidae dans les aires marines protégées Niamone–Kalounayes et Kassa–Balantacunda. Mémoire Masteur Aménagement et Gestion durable des Ecosystèmes forestiers et Agroforestiers (AGDEFA), UFR (ST), UASZ, Sénégal, 43 pp.

[***] DAMPC (2015) Plan de gestion de l'AMP de Niamone–Kalounayes 2016–2020. Dakar, 92 pp.

[****] Analbery M (2004) Biologie, écologie et pêche de *Hemiramphus brasiliensis*. Thèse de doctorat, Université de Bretagne, France.

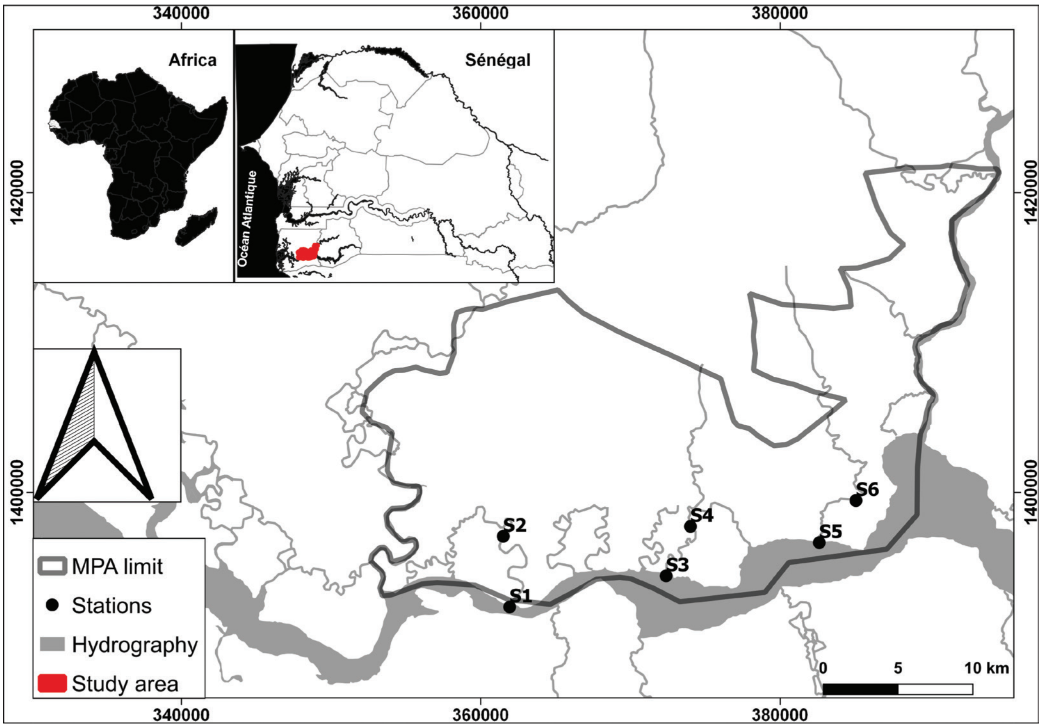

Figure 1. Map of the Marine Protected Area of Niamone–Kalounayes (Senegal) and sampling stations.

Table 1. Representation of the different stages of sexual maturity according to Fontana (1969).

Stage	External macroscopic features of gonads	
	Female	Male
I **(immature)**	Firm, small size, transparent, or light pink; oocytes invisible	White or slightly translucent, very thin and resembling knife blade
II **(sexual rest)**	Substantially identical to stage I	Substantially identical to stage I
III **(ripening)**	Firm and colored (pale pink to light orange), some oocytes visible through ovarian membrane	Firm and whitish; no liquid flowing if an incision is made
IV **(advanced ripening)**	Larger and less firm, usually light orange; oocytes visible through ovarian membrane; surface of ovary granular	Softer and whiter; whitish fluid flowing as soon as an incision is made
V **(ripe individual)**	Very large occupying entire abdominal cavity; ovarian membrane very thin; hyalin and large eggs perfectly visible and are expelled at slightest pressure exerted on abdomen	Large and soft; semen flows at the slightest pressure on the abdomen
VI **(post-spawning)**	Very vascularized and flaccid; color varying from salmon pink to red; oocytes not visible through ovarian membrane; multiple hyaline spaces	Flaccid and delicately vascularized, particularly in posterior part
VII **(spent)**	Completely collapsed and very flaccid; red color due to very strong vascularization; characteristic appearance of empty sack	Very flaccid, exhausted, and highly vascularized

Statistical analyzes. A chi-square test (χ^2) was used to compare the sex ratio with the theoretical sex ratio (1:1) for each sampled month. An analysis of variance (ANOVA) was used to compare the change in mean gonadosomatic index (mean GSI) between months for the same sex. Differences were considered significant at $P < 0.05$. All statistical analyses were performed within the R software (version 3.6.0) (R Core Team 2018).

Results

Sex ratio (SR). Among the 361 individuals of *Parachelon grandisquamis* sampled in the MPA of Niamone–Kalounayes, 40 were males and 321 were females (1:8). This unbalanced overall SR found in the presently reported study was significantly different from the theoretical sex ratio of 1:1 ($\chi^2 = 218.73$; $P < 0.05$) (Table 2). Very significant monthly variations ($P < 0.05$) in SR in favor of females were also encountered during all sampling months (Table 2). It seems that during the time of this study, female individuals of *P. grandisquamis* were highly dominant in the MPA.

Sexual maturity. The monthly variation of the sexual maturity stages in both sexes showed a variation over the whole year with variable proportions from one month to another (Fig. 2). Indeed, in males, immature individuals of sexual maturity stages (I and II) were encountered throughout the year, except for May and June. The highest percentages were recorded in August (100%), December (100%), November (80%), and January (80%). In female individuals, however, they were present throughout the year. The maximum number of individuals were observed in October (89%), August (84%), and January (82%).

Table 2. Monthly changes in the sex ratio of *Parachelon grandisquamis* in the Marine Protected Area of Niamone–Kalounayes (Senegal) from July 2021 to June 2022.

Months	Males	Females	Total	Sex ratio (M:F)	χ^2	*P*-value	Significance
January	5	29	34	1:5.8	16.94	3.86e–05	$P < 0.001$
February	1	29	30	1:29.0	26.13	3.19e–07	$P < 0.001$
March	2	28	30	1:14.0	22.53	2.06e–06	$P < 0.001$
April	1	32	33	1:32.0	29.12	6.80e–08	$P < 0.001$
May	3	28	31	1:9.3	20.16	7.12e–06	$P < 0.001$
June	2	34	36	1:17.0	28.44	9.64e–08	$P < 0.001$
July	4	26	30	1:6.5	16.13	5.90e–05	$P < 0.001$
August	5	19	24	1:3.8	8.16	0.004	$P < 0.001$
September	9	21	30	1:2.3	4.80	0.02	$P < 0.05$
October	2	27	29	1:13.5	21.55	3.44e–06	$P < 0.001$
November	5	19	24	1:3.8	8.16	0.004	$P < 0.001$
December	1	29	30	1:29.0	26.13	3.19e–07	$P < 0.001$
Total	**40**	**321**	**361**	**1:8.0**	**218.73**	< 2.20e–16	$P < 0.001$

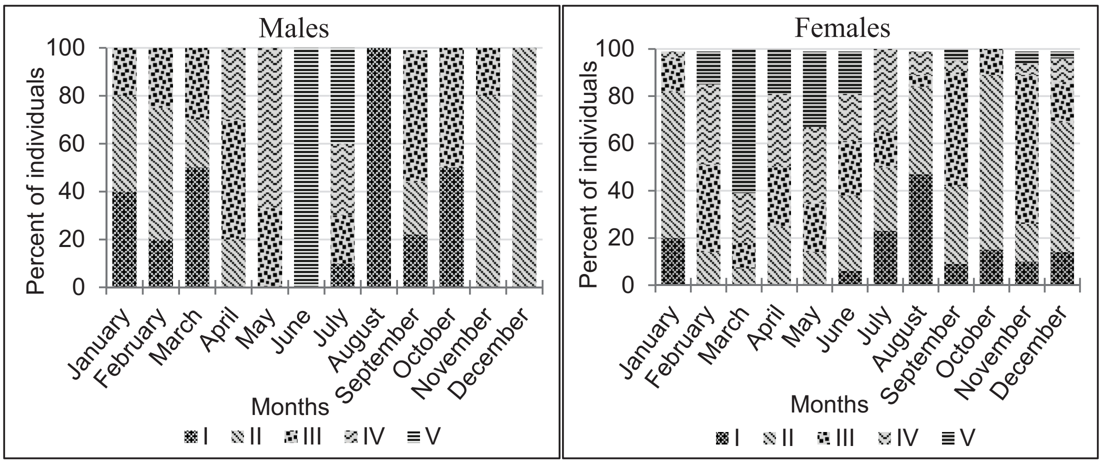

Figure 2. Monthly evolution of the sexual maturity stages of males and females of *Parachelon grandisquamis* in the Marine Protected Area of Niamone–Kalounayes (Senegal), from July 2021 to June 2022.

Mature individuals of sexual maturity stages (III, IV, and V) were present every month of the year for both sexes outside the month of December for males, reaching a maximum in the months of May (100%), June (100%), and July (90%) in males, and March (93%), May (85%), and February (85%) in females. No individual at the post-laying stage (stage VI) had been reported in the samples.

These results show that *Parachelon grandisquamis* exhibits continuous breeding throughout the year in the MPA of Niamone–Kalounayes, with a peak in sexual maturity from May to July in males and from March to June in females.

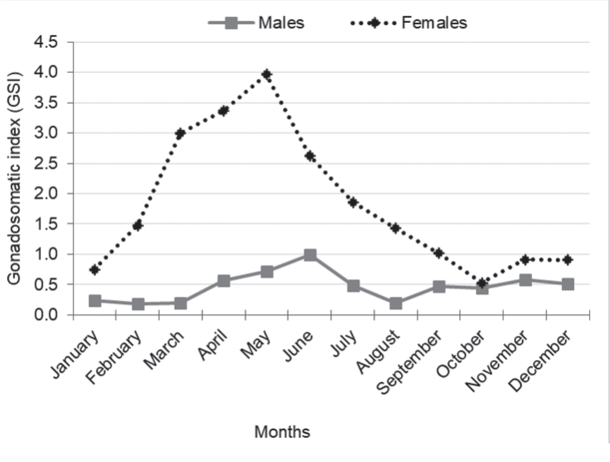

Figure 3. Monthly evolution of the GSI of *Parachelon grandisquamis* in the Marine Protected Area of Niamone–Kalounayes (Senegal), between July 2021 and June 2022.

Gonadosomatic index and reproductive period. During the entire study, the calculated mean GSI was overall higher in females than in males. In females, higher GSI values were found from March to June, with a peak in May (3.96). The lowest values were observed in October and January (0.53 and 0.75, respectively). Females also seem to reach sexual maturity a bit earlier than males (May and June). For male individuals, the highest GSI values were recorded from April to July, with a peak observed in June (0.99). From January to March and from August to December, the GSI values are relatively low (Fig. 3). These results show that individuals of *Parachelon grandisquamis* roaming the MPA probably have a single breeding period that spread over five months, from March to July (ANOVA, $P < 0.05$). These findings show that this species prefers to spawn between the end of the dry season and the beginning of the wet season.

Size at first sexual maturity. In males, the smallest total length recorded is 15 cm and the largest is 24 cm (mean 19.55cm ± 1.98). In female individuals, the smallest total length is 14 cm and the largest is 27 cm (mean 21.36 cm ± 2.04). The size at first sexual maturity (L_m) observed is 17 cm for males and 18 cm for females (Fig. 4). Female *Parachelon grandisquamis* in the MPA reached sexual maturity at a size very close to that of males. The observed difference in mean sexual maturity length (L_m) between the two sexes was not significant ($\chi^2 = 0.02$; $P > 0.05$).

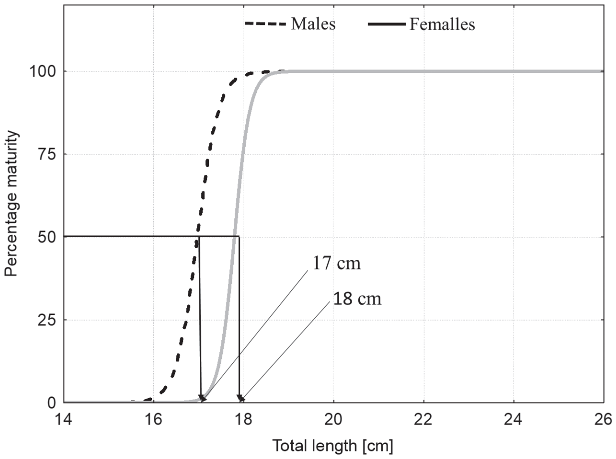

Figure 4. Size determination curve at first sexual maturity (L_m) for males and females of *Parachelon grandisquamis* in the Marine Protected Area of Niamone–Kalounayes (Senegal).

Discussion

This study was conducted with the aim of providing basic elements allowing the curator and the management committee of the MPA of Niamone–Kalounayes to have strong and up-to-date scientific information for better management of this species in view of its importance for the local population.

The sex ratio observed in this study highly favored females (1:8). These results are different from those obtained in other similar studies conducted in Côte d'Ivoire, where a higher proportion of males in the *Parachelon grandisquamis* population was observed (Diaby et al. 2012; Alla and Adepo-Gourene 2020). The imbalance in the sex ratio is a relatively common natural phenomenon in many fish species (Atsé et al. 2009). Generally, the majority of mullets have an unbalanced sex ratio that can be either in favor of females (Albaret and Legendre 1985; Ergene 2000; Ameur et al. 2003; Abou-Seedo and Dadzie 2004) or in a few instances, of males (Fehri Bedoui et al. 2002; Katselis et al. 2002). Several hypotheses have been put forward to explain this imbalance in the sex ratio (Buslé and Bruslé 1977): (1) segregation of the sexes according to the seasons, the fish moving in separate schools; (2) differential distribution by height and age; (3) selective natural mortality; (4) a different migratory activity; (5) selectivity of fishing gear, which would catch one group more than another. The difference observed in the sex ratio of *P. grandisquamis* could also be explained by the influence of physicochemical parameters of the species' living environment but also by reproduction (Yao et al. 2017). The variation in the sex ratio observed also depends on the physiological state of the fish studied (Aka et al. 2004). Furthermore, among teleosts generally, males are more abundant during the reproductive period, whereas during the period of sexual rest, females are most often predominant in experimental fisheries (Djadji et al. 2013). During the breeding season, males regroup around females, which would explain the considerable increase in the number of males compared to females (Koné et al. 2014). In addition, among the Mugilidae, there is segregation by sex and age group during their movement (Vall unpublished*). Therefore, the most accessible school for fishing gear would show a predominance of one of the sexes in catches. This was not the case in this study, as the abundance of males was relatively constant and low during all sampling months.

Another factor that can also explain this difference in the sex ratio is the size of the sample. Since this study was carried out in the Marine Protected Area, and not on the entire Casamance River estuary, these results might only be an artifact of the limited sampling size and effort that could be made during this study. Apart from the post-spawning and spent stages (VI and VII), all other stages of sexual maturity were observed in this study, with different percentages from month to month. Changes in the percentage of maturity showed that mature individuals in stages IV and V remained dominant during the period from March to July for both sexes, with a greater proportion in May for females and in June for males. These peaks in maturity are coinciding accordingly with peaks in GSI found for the presently reported study. Just as observed in the MPA of Niamone–Kalounayes, a breeding period ranging from the mid-dry to early wet season has also been reported in *P. grandisquamis* in Côte d'Ivoire (Alla and Adepo-Gourene 2020). Other studies have shown that gonadal maturation can begin in the dry season and end in the wet season in the majority of Mugilidae, corroborating results from this study (Albaret 1984; Albaret and Legendre 1985; Djadji et al. 2018). At this time of year, environmental and trophic conditions are therefore more favorable to ensure larval development and survival of fry (Pagès and Citeau 1990).

Based on the results of the presently reported study, *Parachelon grandisquamis* males reach sexual maturity at a slightly smaller size (17 cm) than females (18 cm) in

---

* Vall MOV (2004) Etude de la dynamique des systèmes d'exploitation et de l'écobiologie de la reproduction de trois Mugilidés: *Mugil cephalus* (Linnaeus, 1758), *Liza aurata* (Perguria, 1892) et *Mugil capurrii* (Risso, 1810). Analyse de leurs Stratégies d'Occupations des secteurs littoraux Mauritaniens et de leurs possibilités d'Amenagement. Thèse de Doctorat, Université de Nice-Sophia Antipolis, France.

the MPA. This result could be related to early sexual maturity of males or faster growth of females as observed in the majority of teleosts (Toguyemi et al. 1997; Poulet unpublished*). A smaller length at first sexual maturity for males has been observed in other Mugilidae populations elsewhere in West Africa (Albaret and Legendre 1985; Diaby unpublished**; Djadji unpublished***), and more recently for the same species (Alla and Adepo-Gourene 2020). According to some authors, this difference observed in sizes at first sexual maturity could be related to environmental conditions (availability of food, temperature, salinity, the quantity of dissolved oxygen, etc.) that would favor faster growth of females to the detriment of males. It could also simply be due to genetic properties which will make males more precocious and reach the first sexual maturity before females (Yao et al. 2017).

Conclusion

Reproductive parameters such as sex ratio (SR), gonadosomatic index (GSI), and size at first maturity (L_m) for *Parachelon grandisquamis* were determined for the first time in the MPA of Niamone–Kalounayes. Results from this study could be used as a reference for better fishing regulations practices, but also in future work on the biology of the species or other Mugilidae at the MPA level. Overall, 361 individuals were sampled, including 321 females and 40 males. The sex ratio was in favor of females (1:8). Males reach sexual maturity (17 cm) at a size very close to that of females (18 cm). *Parachelon grandisquamis* spawned in the MPA, with a breeding period ranging from the end of the dry season in March to the beginning of the wet season in July. The timing of this reproductive activity is clearly shown in this study by a higher proportion of individuals in advanced stages of maturation (stages III, IV, and V) during this period. From the results of this study, it is clearly shown that *P. grandisquamis* is spawning in the MPA during a single spawning event between March and July and that the sex ratio is greatly imbalanced in favor of females, even though the sizes at first sexual maturity for both sexes are very similar. These results, obtained after twelve months of sampling, provide information on the reproduction of *P. grandisquamis* that can help in decision-making for better management of the resource.

From a sustainable management perspective of this species, it would be beneficial to add the size at first sexual maturity (L_m) as a management measure. Values of L_m could be calculated and used as a threshold to code for the selectivity of fishing gear (e.g., appropriate mesh size). In that sense, the minimum catch size should be variable depending on the season. The minimum catch size should be adjusted to be bigger than the size at first sexual maturity, so that it would allow this species to reproduce at least once before being caught. Finally, the exploitation of this species should be limited during the main breeding season (March–July), to encourage higher levels of reproductive activity and consequently, better recruitment each and every year.

Acknowledgments

The authors would like to thank Professor Alassane Sarr, the Director of the University Institute of Fisheries and Aquaculture, for his supervision and guidance in carrying out this study. We would like to thank all the fishermen of the MPA management committee for their support during the experimental fisheries. Our thanks to Captain Sarany Diedhiou, curator of the MPA, and all the staff for their assistance and support in carrying out this study.

References

Abou-Seedo F, Dadzie S (2004) Reproductive cycle in the male and female grey mullet, *Liza klunzingeri* in the Kuwaiti waters of the Arabian Gulf. Cybium 28(2): 97–104. https://doi.org/10.26028/cybium/2004-282-002

Aka Z, Koç HT, Turan C (2004) A study on growth of the anchovy *Engraulis encrasicolus*, Linnaeus (1758) in Turkish Seas, Turkey. Pakistan Journal of Biological Sciences 7(7): 1121–1126. https://doi.org/10.3923/pjbs.2004.1121.1126

Albaret JJ (1984) Premières observations sur la faune ichtyologique de la Casamance. Archives du Centre de Recherches Océanographiques de Dakar-Thiaroye, 22 pp.

Albaret JJ (2003) Caractérisation de l'état de référence des peuplements de poissons d'une aire protégée en zone de mangrove: le bolon de Bamboung (Sine Saloum, Sénégal). Rapport de convention Narou Heuleuk/ AFD/ IRD, Dakar, décembre, 50 pp.

---

[*] Poulet N (2004) Le sandre (*Sander lucioperca*): Biologie, comportement et dynamique des populations en Carmargue (Bouches du Rhône, France). Thèse de Doctorat, Université Toulouse III-Paul Sabatier, France.

[**] Diaby M (2014) Distribution spatio-temporelle, pêche et dynamique de la population des Mugilidae (poissons, téléostéens) de la lagune de Grand-Lahou (Côte d'Ivoire). Thèse de Doctorat, Université Nangui Abrogoua, Côte d'Ivoire.

[***] Djadji ELG (2015) Etude des traits biologiques et du régime alimentaire de deux espèces de Mugilidae, *Liza falcipinnis* (Valenciennes, 1836) et *Mugil cephalus* (Linnaeus, 1758) dans les complexes lagunaires Ebrié et Grand-Lahou, Côte d'Ivoire. Thèse de Doctorat, Université de Cocody, Côte d'Ivoire.

Albaret J-J, Legendre M (1985) Biologie et écologie des Mugilidae en lagune Ebrié (Côte d`Ivoire) Intérêt potentiel pour l`aquaculture lagunaire. Revue d’Hydrobiologie Tropicale 18(4): 281–303.

Alla EYGH, Adepo-Gourene AB (2020) Stratégies de reproduction de trois espèces de Mugilidae, *Liza dumerili* (Steindachner, 1870), *L. grandisquamis* (Valenciennes, 1836) et *L. falcipinnis* (Valenciennes, 1836) dans la lagune Ebrié, Sud, Côte d`Ivoire. Afrique Science 16(1): 279–299.

Amenzoui K, Ferhan-Tachinante F, Yahyaoui A, Mesfioui HA, Kifani S (2004–2005) Etude de quelques aspects de la reproduction de *Sardina pilchardus* (Walbaum, 1792) de la région de Laâyoune (Maroc). Bulletin de l’Institut Scientifique, Rabat, section Sciences de la Vie 26–27: 43–50.

Ameur B, Bayed A, Benazzou T (2003) Rôle de la communication de la lagune de Merja Zerga (Gharb, Maroc) avec l’océan Atlantique dans la reproduction d’une population de *Mugil cephalus* (Poisson Mugilidae). Bulletin de l’Institut Scientifique, Rabat, section Sciences de la Vie 17: 77–82.

Atsé BC, Konan KJ, Kouassi NJ (2009) Biologie de la reproduction du Cichlidae *Tylochromis jentinki* dans la lagune Ébrié (Côte d`Ivoire). Cybium 33(1): 11–19. https://doi.org/10.26028/cybium/2009-331-002

Bruslé J, Bruslé S (1977) Les muges de Tunisie: pêche lagunaire et biologie de la reproduction de trois espèces (*Mugil capito*, *Mugil cephalus* et *Mugil chelo*) des lacs d’Ichkeul et de Tunis. Rapports et procés-verbaux des réunions Commission internationale pour l’exploration scientifique de la Mer Méditerranée 24(5): 101–130.

Diaby M, N’da K, Akadje CM (2012) Distribution spatio-temporelle des poissons Mugilidae dans la lagune de Grand-lahou (Côte d`Ivoire). International Journal of Biological and Chemical Sciences 6(4): 1608–1623. https://doi.org/10.4314/ijbcs.v6i4.20

Diouf PS (1996) Les peuplements de poissons des milieux estuariens de l’Afrique de l’Ouest: l’exemple de l’estuaire hyperhalin du Sine–Saloum. Thèse de Doctorat 3e cycle, Université de Montpellier II, France.

Djadji ELG, Atse BC, Sylla S, Konan JK, Kouassi JN (2013) Reproduction du Mugilidae *Mugil cephalus* Linné, 1758 dans deux complexes lagunaires (lagunes Ébrié et de Grand-Lahou) de la Côte d`Ivoire. International Journal of Biological and Chemical Sciences 7(4): 1701–1716. https://doi.org/10.4314/ijbcs.v7i4.25

Djadji ELG, Sylla S, Zan-bi TT, Atse BC (2018) Reproductive biology of the mullet *Liza falcipinnis* (Valenciennes, 1836) in two African complexs lagoons (Ebrié and Grand-Lahou) (Côte d`Ivoire). International Journal of Research—Granthaalayah 6(5): 114–127. https://doi.org/10.29121/granthaalayah.v6.i5.2018.1433

Ergene S (2000) Reproduction characteristics of thinlip grey mullet, *Liza ramata* (Risso, 1826) inhabiting Akgöl–Paradeniz lagoons (Göksü Delta). Turkish Journal of Zoology 24(2): 159–164.

FAO (1992) Guide de terrain des ressources marines commerciales du golf de Guinée. FAO, Rome, 268 pp.

Fehri Bedoui R, Gharbi H, El Abed A (2002) Période de reproduction et maturité sexuelle de *Liza aurata* (Poisson, Mugilidae) des côtes Est et Sud tunisiennes. Bulletin de l’Institut National des Sciences et Technique de la Mer, Salammbô 29: 11–15.

Fontana A (1969) Etude de la maturité sexuelle des sardinelles *Sardinella eba* (Val) et *Sardinella aurita* C. et V. de la région de Pointe-Noire. Cahiers ORSTOM, Serie oceanographie 7(2): 101–114.

Ghorbel M, Jarboui O, Bradai MN, Bouain A (1996) Détermination de la taille de première maturité sexuelle par une fonction logistique chez *Limanda limanda*, *Pagellus erythrinus* et *Scorpaena porcus*. Bulletin de l’Institut National des Sciences et Technique de la Mer, Salammbô Num. Spéc. 3: 24–27.

Harrison IJ (2008) Mugilidae. Pp. 450–471. In: Stiassny MLJ, Teugels GG, Hopkins CD (Eds) Poissons d’Eaux Douces et Saumâtres de Basse Guinée, Ouest de l’Afrique Centrale (vol. 2). IRD Editions, Paris, France.

Kahn JE, Watterson JC, Hager CH, Mathies N, Hartman KJ (2021) Calculating adult sex ratios from observed breeding sex ratios for wide-ramping, intermittently breeding species. Ecosphere 12(5): 1–11. https://doi.org/10.1002/ecs2.3504

Katselis G, Koutsikopoulos C, Kaspiris P (2002) Age determination and growth of leaping mullet, (*Liza saliens*, R. 1810) from the Messolonghi Etoliko lagoon (western Greece). Mediterranean Marine Science 3(2): 147–158. https://doi.org/10.12681/mms.253

Koné A, N’da K, Kouassi SK, Agnissan JPA (2014) Dynamique de la population exploitée de deux requins: *Sphyrna zygeana* (Linnaeus, 1758) et *Isurus oxyrinchus* (Rafinesque, 1809) des côtes ivoiriennes. International Journal of Biological and Chemical Sciences 8(4): 1633–1643. https://doi.org/10.4314/ijbcs.v8i4.25

Pagès J, Citeau J (1990) Rainfall and salinity of a sahelian estuary between 1927 and 1987. Journal of Hydrology 113(1–4): 325–341. https://doi.org/10.1016/0022-1694(90)90182-W

Paugy D, Lévêque C, Teugels DD (2003) The fresh and brackish water fishes of West Africa. Muséum national d’Histoire naturelle, Paris, France, 1272 pp.

R Core Team (2018) A language and environment for statistical computing. R Foundation for Statistical Computing, Vienna, Austria. https://www.R-project.org/

Seret B, Opic P (2011) Poissons de mer de l’Ouest africain tropical, IRD, Marseille, France 450 pp.

Toguyemi A, Fauconneau B, Boujard T, Fostier A, Kuhn ER, Mol KA, Baroiller JF (1997) Feeding behaviour and food utilisation in tilapia, *Oreochromis niloticus*: Effect of sex ratio and relationship with the endocrine status. Physiology and Behavior 62(2): 273–279. https://doi.org/10.1016/S0031-9384(97)00114-5

Wright JM (1988) Seasonal and spatial differences in the fish assemblage of the non-estuarine Sulaibikhat Bay, Kuwait. Marine Biology 100(1): 13–20. https://doi.org/10.1007/BF00392950

Yao N, Diaha N’guessan C, Monin Amande J, Angui Kouame JP, Abekan E, N’dri Assan F, N’da Konan (2017) Sex-ratio, stades de maturité, taille de première maturité et facteur de condition de *Canthidermis maculata* capturé dans l’océan Atlantique Est. Sex ratio, maturity stages, first maturity size and condition factor of *Canthidermis maculata* caught in the eastern Atlantic Ocean. International Journal of Biological and Chemical Sciences 11(6): 2876–2886. https://doi.org/10.4314/ijbcs.v11i6.25

Acta Ichthyologica et Piscatoria 53, 2023, 45–49 | DOI 10.3897/aiep.53.101350

PENSOFT.

ACTA
ICHTHYOLOGICA
ET PISCATORIA

Records of malformed sea catfishes (*Ariopsis seemanni* and *Ariopsis guatemalensis*) (Actinopterygii: Siluriformes: Ariidae) off San Blas (Mexican Pacific)

Felipe GUZMÁN-MORALES[1], Angélica Yomira RAMOS-ÁVILA[1],
Mariana DÍAZ-SANTANA-ITURRIOS[2], Esperanza GRANADOS-AMORES[3],
Jasmín GRANADOS-AMORES[4]

1 *Programa de Maestría en Ciencias Biológico Agropecuarias, Universidad Autónoma de Nayarit, Xalisco, Nayarit, Mexico*
2 *Marine Conservation Medicine and Ecosystem Health, Centinela del Mar A.C., La Paz, Baja California Sur, Mexico*
3 *Programa de Doctorado en Ciencias Biológico Agropecuarias, Universidad Autónoma de Nayarit, Xalisco, Nayarit, Mexico*
4 *Escuela Nacional de Ingeniería Pesquera (ENIP-UAN), San Blas, Nayarit, Mexico*

https://zoobank.org/73AA157C-7258-4C69-A568-5A02ED13E2C7

Corresponding author: Jasmín Granados-Amores (j.granados@uan.edu.mx)

Academic editor: Adnan Tokaç ♦ **Received** 1 February 2023 ♦ **Accepted** 4 April 2023 ♦ **Published** 20 April 2023

Citation: Guzmán-Morales F, Ramos-Ávila AY, Díaz-Santana-Iturrios M, Granados-Amores E, Granados-Amores J (2023) Records of malformed sea catfishes (*Ariopsis seemanni* and *Ariopsis guatemalensis*) (Actinopterygii: Siluriformes: Ariidae) off San Blas (Mexican Pacific). Acta Ichthyologica et Piscatoria 53: 45–49. https://doi.org/10.3897/aiep.53.101350

Abstract

Fish malformations can be an important hint for assessing the well-being of their populations and the quality of their habitats. Malformations have been observed in species of the order Siluriformes, including the family Ariidae. In this study, we report malformations in the blue sea catfish, *Ariopsis guatemalensis* (Günther, 1864), and the tete sea catfish, *Ariopsis seemanni* (Günther, 1864), collected in San Blas, Mexico. The malformations include missing eye, cleft lip, and malformed barbels. Such malformations could be blamed on substantial levels of pesticides in the environment, genetic factors, and/or a pathogenic effect of some parasites specific to the studied fish species.

Keywords

abnormality, Ariidae, deformity, estuarine system, ichthyology, Siluriformes, Mexican Pacific

Introduction

Fish malformations are visible internal or external changes or abnormalities caused by environmental stresses, parasitic infections, genetic mutations, nutrient deficiencies, and exposure to chemicals (Yokoyama et al. 2004; Kelly et al. 2010). The physiological functioning of fish can worsen through the presence of such malformations and their effects include deficient buoyancy, feeding, and reproductive difficulties, as well as problems in avoiding predators (Eissa et al. 2009). Therefore, recording malformations is an important task to properly monitor the well-being of fish populations and water quality.

Malformations have been reported for several families in the order Siluriformes (see Wakida-Kusunoki and Amador del Ángel 2017). The siluriform fish family Ariidae comprises about 150 species, popularly known as sea catfishes, 13 of which have been recorded in the Mexican Pacific (Rodríguez-Romero et al. 2012; Robertson and Allen 2015; Palacios-Salgado et al. 2018). The main characteristics distinguishing sea catfishes are their long barbels located in the buccal area and their large-sized lapilli otoliths (Acero and Betancur-R 2002; Marceniuk and Menezes 2007; Bogan and Agnolin 2011). Other important anatomical features include bony plates on the head and near the dorsal fin, and a leading spine in both pectoral and dorsal fins, present in some species (Ribeiro et al. 2012).

Albinism has been the most frequently reported abnormality in several species of the family Ariidae (i.e., Gupta and Bhowmik 1958; Rajapandian and Sundaram 1967; Baragi et al. 1976; Krishna Pillai and Somvanshi 1979; Das et al. 2006; Chavan et al. 2008; Leal et al. 2013; and Wakida-Kusunoki and Amador del Ángel 2017), although there are some studies describing morphological malformations found in these fish. For instance, a specimen of *Carlarius latiscutatus* (Günther, 1864) showed severely deformed fin rays and spines, possibly caused by water pollution (Ugbomeh et al. 2022). For the Mexican coasts in particular, Chávez and Saucedo Barrón (1988) reported conjoined twins of *Ariopsis felis* (Linnaeus, 1766) in Celestun, Yucatan. For the same species (*Ariopsis felis*) collected off the coast of Tabasco, Wakida-Kusunoki and Amador del Ángel (2017) described vertebral malformations. Maldonado-Coyac et al. (2015) reported an ocular malformation in *Bagre panamensis* (Gill, 1863) collected in Mazatlan, Sinaloa. More recently, Tirado León (2019) found vertebral malformations in seven sea catfish species belonging to four genera: *Bagre panamensis*; *Bagre pinnimaculatus* (Steindachner, 1876); *Cathorops liropus* (Bristol, 1897); *Cathorops raredonae* Marceniuk, Betancur-R et Acero, 2009; *Occidentarius platypogon* (Günther, 1864); *Ariopsis guatemalensis* (Günther, 1864); and *Ariopsis seemanni* (Günther, 1864). To increase the current knowledge concerning malformations in species of the family Ariidae, the aim of this study was to record such features detected in sea catfishes caught during fishing activities in San Blas, Nayarit, Mexican Pacific.

Methods

Over a one-year period (September 2015 through September 2016), we advertised the purchase of malformed fishes at the port of San Blas, Nayarit, Mexico. Fishermen who captured "deformed" fishes and were willing to help us delivered the material collected to the facilities of Escuela Nacional de Ingenieria Pesquera of Universidad Autonoma de Nayarit in exchange for the promised reward. Six specimens of sea catfishes were collected as bycatch in an estuarine zone 0.5–1.0 km away from the port of San Blas. In this area, fishing is conducted in brackish shallow (<3 m) water, where fishermen (usually 2 per vessel) arrive in boats and deploy seine nets (9–10 cm mesh size) to catch the fish. The specimens were preserved in ice and transported to the Laboratory of Genetics and Geometric Morphometrics of the Escuela Nacional de Ingenieria Pesquera of Universidad Autonoma de Nayarit. Each sea catfish was identified at the species level following Kaliola and Bussing (1995) and Robertson and Allen (2015). Specimens were labeled and deposited in the Collection of Malformed Fish located in the laboratory mentioned above (Voucher numbers: CPMIP 8, CPMIP 10, CPMIP 13, CPMIP 15, CPMIP 18, and CPMIP 21). The standard length (SL) of the specimens was recorded using a vernier caliper. A normal (in terms of its diagnostic features) individual of each species was used as a control/comparison. Malformed and control specimens were photographed using a 20.2-megapixel Canon EOS70D digital camera

Results

The six collected sea catfishes were identified as *Ariopsis guatemalensis* (*n* = 3) and *A. seemanni* (*n* = 3). Four of these specimens (*Ariopsis guatemalensis* (CPMIP 13 and CPMIP 21) and *A. seemanni* (CPMIP 15 and CPMIP 18)) showed morphological malformations such as missing eye, cleft lip, malformed barbels, comparatively small eye, and abnormal tooth plate. The two remaining sea catfishes (CPMIP 10 and CPMIP 8) were the control specimens (normal) representing each respective species. The specific characteristics of the normal and malformed specimens are described in the following sections.

Diagnostic features. Defined following Kaliola and Bussing (1995) and Robertson and Allen (2015). *Ariopsis guatemalensis*: eye small, 25% of distance between eyes; palate teeth arranged in four patches, medial patches narrowly separated at midline and continuous with outer patches; four tooth patches similar size; 3 pairs of barbels (on chin and both jaws) (see specimen CPMIP 10, Fig. 1B, 1F, 1H). *Ariopsis seemanni*: eye large, 36%–63% of distance between eyes; thin lower tooth plate and divided in two sections (see specimen CPMIP 8, Fig. 1J, 1L).

Descriptions of the abnormal features. *Ariopsis guatemalensis*: specimen CPMIP 13 lacked the right eye opening and the eyeball (Fig. 1A). Specimen CPMIP 21 featured a small (41.7% of right eye size, Fig. 1D) and undeveloped left eye (Fig. 1C). In addition, this fish had a cleft lip, thus, malformed upper tooth plate and barbels (Fig. 1E and 1G). *Ariopsis seemanni*: specimen CPMIP 15 showed a comparatively small right eye (43% of left eye size, Fig. 1J) (Fig. 1I). Specimen CPMIP 18 had a malformed lip and lower plates (Fig. 1K).

Discussion

Studies reporting fish malformations have attributed their presence to biotic and abiotic factors affecting the fish during their life cycle (Overstreet and Edwards 1976; Pragatheeswaran et al. 1987; Kelly et al. 2010; Tirado León 2019). However, while it is not possible to detect a true correlation between such factors and malformations from specimens caught in the wild—as experiments

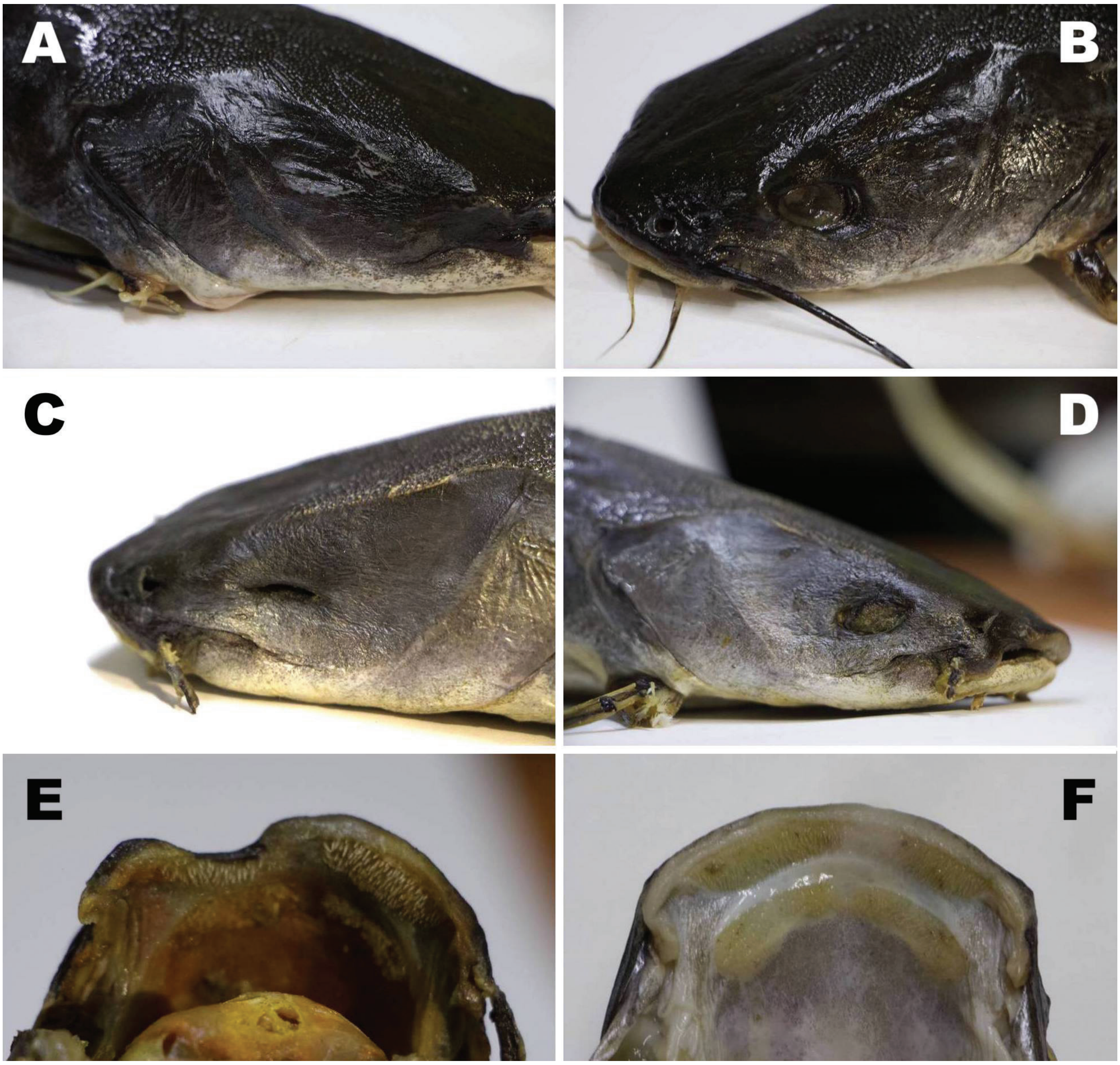

Figure 1. Malformations of *Ariopsis guatemalensis* and *Ariopsis seemanni* collected off San Blas (Mexican Pacific). **A**) specimen of *A. guatemalensis* lacking right eye (CPMIP 13); **B**) normal left eye of a specimen of *A. guatemalensis* (CPMIP 10); **C**) specimen of *A. guatemalensis* with small undeveloped eye (CPMIP 21); **D**) normal right eye of a specimen of *A. guatemalensis* (CPMIP 21); **E**) malformed upper tooth plate and cleft lip of a specimen of *A. guatemalensis* (CPMIP 21); **F**) specimen of *A. guatemalensis* with normal lip and tooth plate (CPMIP 10). **[Figure continues on next page]**

under controlled conditions would be required—knowing the biology and ecology of the species under study can shed light on the causes that could be triggering the development of these malformations. For instance, Chávez and Saucedo Barrón (1988) suggested that oxygen deficiencies, either due to high egg density or to aerial exposure in low tide during egg incubation, could have caused the formation of conjoined twins in *Ariopsis felis*. In addition, for this species (*Ariopsis felis*), the vertebral malformations detected by Wakida-Kusunoki and Amador del Ángel (2017) were attributed to several factors including exposure to pesticides, poor immunologic response, injuries at a certain stage of the fish life cycle, or fluctuations in the water quality of the coast of Tabasco. Moreover, Maldonado-Coyac et al. (2015) reported that the ocular malformation found in *Bagre panamensis* could have been triggered both by anthropogenic activities in Mazatlan, Sinaloa and the genetic configuration of the specimen. Finally, Tirado León (2019), who found vertebral malformations in several sea catfish species including the two species in the presently reported study (*Ariopsis guatemalensis* and *A. seemanni*), obtained the malformed fish from different locations on the coast of Nayarit, counting our sampling site (San Blas), and suggested that parasitic infections and the chronic exposure to pollutants such as pesticides and heavy metals were the two main factors causing such malformations. Indeed, the coast of Nayarit is subjected to the constant

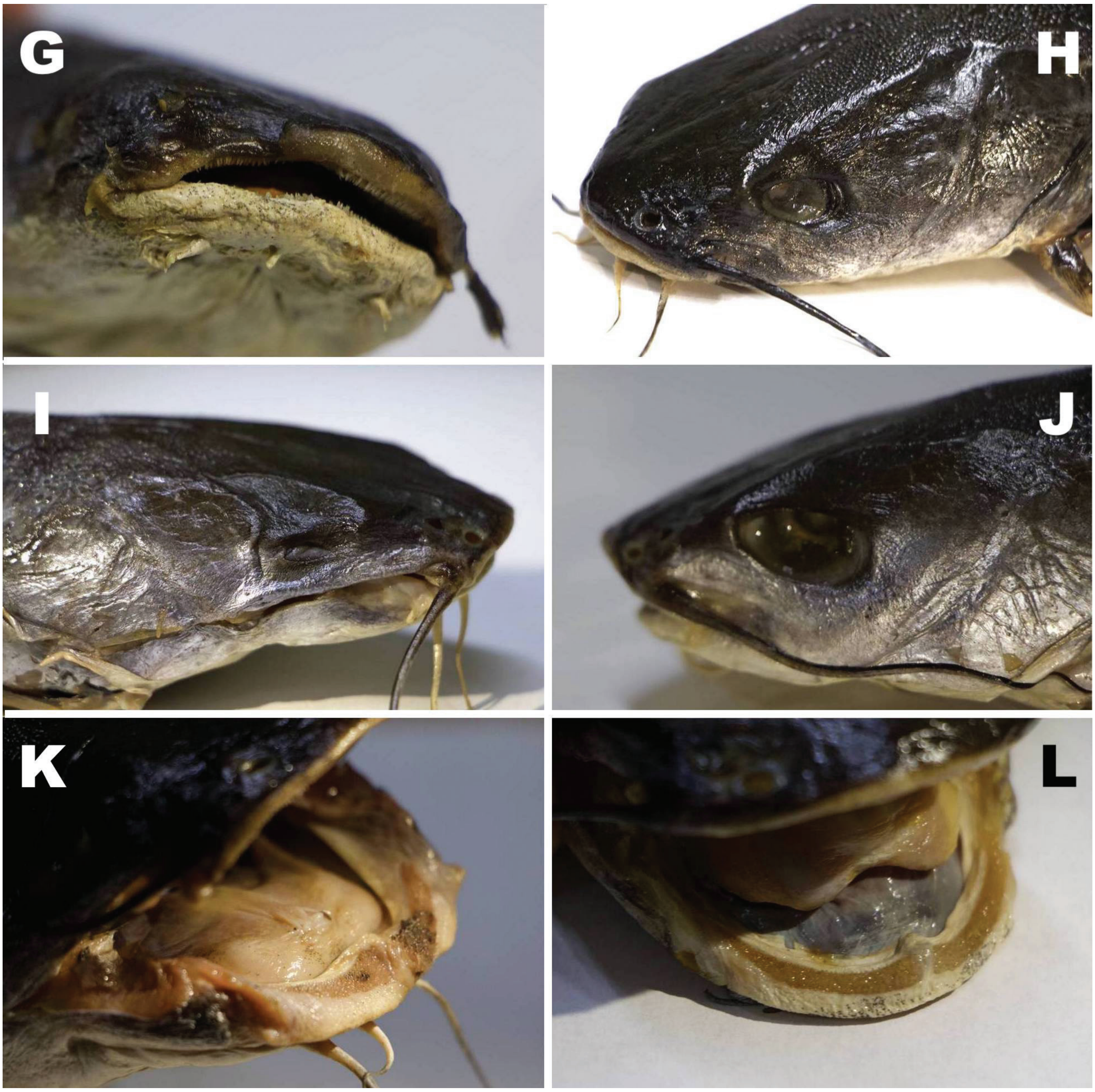

Figure 1 (Continuation). Malformations of *Ariopsis guatemalensis* and *Ariopsis seemanni* collected off San Blas (Mexican Pacific). **G**) malformed barbels of a specimen of *A. guatemalensis* (CPMIP 21); **H**) normal barbels specimen of a specimen of *A. guatemalensis* (CPMIP 10); **I**) specimen of *A. seemanni* with small right eye (CPMIP 15); **J**) normal left eye of a specimen of *A. seemanni* (CPMIP 8); **K**) specimen of *A. seemanni* with malformed lower tooth plate (CPMIP 18); **L**) normal lower tooth plate of *A. seemanni* (CPMIP 8).

input of pesticides and concomitant heavy metals that are washed from agricultural fields of the state or carried from very distant locations by many rivers such as the Colorado, Sonora, Yaqui, Mayo, Fuerte, Sinaloa, Culiacan, San Lorenzo, Acaponeta, San Pedro, Lerma-Santiago, Armeria, Coahuayana, Balsas, Papagayo, Verde, Tehuantepec, and Suchiate (Espinosa-Carreon et al. 2004). In addition, the presence of parasites has been reported in the fishery resources of the study area (Cunningham et al. 2005; Álvarez-Guerrero and Alba-Hurtado 2007; Kelly et al. 2010). Although we concur with the possible causes of malformations discussed by Tirado León (2019) for the two species treated in our study, we are aware that more environmental monitoring studies are needed on the Pacific Mexican coasts. We suggest that sea catfishes could thus be used as bioindicators of an environmental stress.

Acknowledgments

The authors thank the fishermen who carried out artisanal fisheries in the port of San Blas, Nayarit, Mexico. This work was translated into English by SciLangTranslation.

References

Acero PA, Betancur-R R (2002) Description of *Arius neogranatensis*, a new species of sea catfish from Colombia, with an identification key for Caribbean ariid fishes. Aqua 6: 5–10.

Álvarez-Guerrero C, Alba-Hurtado F (2007) Estuarine fish and turtles as intermediate and paratenic hosts of *Gnathostoma binucleatum* in Nayarit, México. Parasitology Research 102(1): 117–122. https://doi.org/10.1007/s00436-007-0738-x

Baragi VM, Yaragal RB, James PSBR (1976) On an albino of the marine cat fish, *Tachysurus tenuispinis* (Day). Matsya 2: 82.

Bogan S, Agnolin FL (2011) Descripción de una nueva especie de bagre marino fósil (Teleostei, Siluriformes, Ariidae) del Mioceno de la provincia de Río Negro, Argentina. Papéis Avulsos de Zoologia 51(25): 373–382. https://doi.org/10.1590/S0031-10492011002500001

Chavan BB, Sundaram S, Sawant AD, Das T (2008) Record of complete albinism in marine catfish, *Osteogeneiosus militaris* (Linnaeus, 1758), landed at Mumbai. Marine Fisheries Information Service, Technical and Extension Series 197: 15–17.

Chávez H, Saucedo Barrón CJ (1988) Colecta de ejemplares siameses del bagre *Arius felis* (Linnaeus) en Yucatán, México (Pisces: Ariidae). Annales de la Escuela Nacional de Ciencias Biológicas 32: 117–121.

Cunningham ME, Markle DF, Watral VG, Kent ML, Curtis LR (2005) Patterns of fish deformities and their association with trematode cysts in the Willamette River, Oregon. Environmental Biology of Fishes 73(1): 9–19. https://doi.org/10.1007/s10641-004-3153-5

Das T, Chavan BB, Sundaram S (2006) A rare record of albino catfish, *Arius caelatus* landed at Mumbai. Marine Fisheries Information Service, Technical and Extension Series 188: 21–22.

Eissa AE, Mustapha M, El-Husseiny IN, Saeid S, Saleh O, Borhan T (2009) Identification of some skeletal deformities in freshwater teleosts raised in Egyptian aquaculture. Chemosphere 77(3): 419–425. https://doi.org/10.1016/j.chemosphere.2009.06.050

Espinosa-Carreon TL, Strub PT, Beier E, Ocampo-Torres F, Gaxiola-Castro G (2004) Seasonal and interannual variability of satellite-derived chlorophyll pigment, surface height, and temperature off Baja California. Journal of Geophysical Research 109(C3): C03039. https://doi.org/10.1029/2003JC002105

Gupta PD, Bhowmik RM (1958) A case of albinism in *Arius jella* Day from India. Science and Culture 24(6): 283.

Kaliola PJ, Bussing WA (1995) Ariidae. Bagres marinos. Pp. 860–886. In: Fischer W, Krupp F, Schneider W, Sommer C, Carpenter KE, Niem V (Eds) Guía FAO para identificación de especies para los fines de la pesca. Pacífico Centro-Oriental. 3 Vols. FAO, Rome.

Kelly DW, Thomas H, Thieltges DW, Poulin R, Tompkins DM (2010) Trematode infection causes malformations and population effects in a declining New Zealand fish. Journal of Animal Ecology 79(2): 445–452. https://doi.org/10.1111/j.1365-2656.2009.01636.x

Krishna Pillai S, Somvanshi VS (1979) A case of complete albinism in marine cat fish *Arius caelatus* (Valenciennes). Indian Journal of Fisheries 26(1/2): 240–241.

Leal ME, Schulz UH, Albornoz PL, Machado R, Ott PH (2013) First record of partial albinism in two catfish species of *Genidens* (Siluriformes: Ariidae) in an estuary of southern Brazil. Brazilian Archives of Biology and Technology 56(2): 237–240. https://doi.org/10.1590/S1516-89132013000200008

Maldonado-Coyac JA, Escobar-Sánchez O, Ramírez-Pérez JS, Moreno-Sánchez XG, Palacios-Salgado DS (2015) First case of abnormality in the chihuil sea catfish (*Bagre panamensis*) from Mexican waters. Fish California and Game 101(3): 188–192.

Marceniuk AP, Menezes NA (2007) Systematics of the family Ariidae (Ostariophysi, Siluriformes), with a redefinition of the genera. Zootaxa 1416(1): 1–126. https://doi.org/10.11646/zootaxa.1416.1.1

Overstreet RM, Edwards RH (1976) Mesenchymal tumors of some estuarine fishes of the northern gulf of México. II. Subcutaneous fibromas in the southern flounder, *Paralichthys lethostlgma*, and the sea catfish, *Arius felis*. Bulletin of Marine Science 26: 41–40.

Palacios-Salgado DS, Flores-Ortega JR, Zavala-Leal OI, Granados-Amores J, Nieto-Navarro JT, Tapia-Varela R, Ruiz-Velazco JMJ, Moreno-Sánchez XG, Cadena-Roa MA (2018) Length–weight relationship for sea catfishes (Siluriformes: Ariidae) from the southeastern Gulf of California with new records on maximum length. Journal of Applied Ichthyology 34(3): 700–702. https://doi.org/10.1111/jai.13511

Pragatheeswaran V, Loganathan B, Natarajan R, Venugopalan VK (1987) Cadmium induced vertebral deformities in an estuarine fish, *Ambassis commersoni* Cuvier. Proceedings of the Indian Academy of Science 96(4): 389–393. https://doi.org/10.1007/BF03179592

Rajapandian ME, Sundaram KS (1967) A case of complete albinism in the marine cat-fish *Tachysurus dussumieri* (Cuvier and Valenciennes). Journal of the Marine Biological Association of India 9(1): 194–195.

Ribeiro EB, Almeida ZS, Carvalho-Neta RNF (2012) Hábito alimentar do bagre *Sciades herzbergii* (Siluriformes, Ariidae) da Ilha dos Caranguejos. Maranhão, Brasil. Arquivo Brasileiro de Medicina Veterinaria e Zootecnia 64(6): 1761–1765. https://doi.org/10.1590/S0102-09352012000600048

Robertson DR, Allen GR (2015) Peces Costeros del Pacífico Oriental Tropical: sistema de Información en línea. Versión 2.0 Instituto Smithsonian de Investigaciones Tropicales, Balboa, República de Panamá. http://biogeodb.stri.si.edu/sftep/es/pages

Rodríguez-Romero J, López-Martínez J, Herrera-Valdivia E, Hernández-Vázquez S, Acevedo-Cervántes A (2012) Elenco taxonómico de los peces acompañantes de la captura de camarón en la porción oriental del Golfo de California. Pp. 71–91. In: López Martínez J, Morales-Bojórquez E (Eds) Efectos de la pesca de arrastre en el Golfo de California. Centro de Investigaciones Biológicas del Noroeste, S.C. y Fundación Produce Sonora, México.

Tirado León DE (2019) Caracterización de malformaciones vertebrales en bagres (Siluriformes: Ariidae) del litoral de Nayarit, México. Tesis de Maestría. Universidad Autónoma De Nayarit.

Ugbomeh AP, Jawad LA, Frank JJ, Akani GC (2022) Report on the incidences of skeletal anomalies in three fish species from Bonny tributary (Niger delta), Nigeria. Proceedings of the Zoological Institute RAS 326(1): 14–22. https://doi.org/10.31610/trudyzin/2022.326.1.14

Wakida-Kusunoki AT, Amador del Ángel LE (2017) Vertebral deformities in hardhead catfish *Ariopsis felis* (Siluriformes: Ariidae) in the southeastern Mexico. Revista de Biología Marina y Oceanografía 52(1): 159–162. https://doi.org/10.4067/S0718-19572017000100013

Yokoyama H, Freeman MA, Yoshinaga T, Ogawa K (2004) *Myxobolus buri*, the myxosporean parasite causing scoliosis of yellowtail, is synonymous with *Myxobolus acanthogobii* infecting the brain of the yellowfin goby. Fisheries Science 70(6): 1036–1042. https://doi.org/10.1111/j.1444-2906.2004.00903.x

Acta Ichthyologica et Piscatoria 53, 2023, 51–57 | DOI 10.3897/aiep.53.103579

PENSOFT.

ACTA
ICHTHYOLOGICA
ET PISCATORIA

A new record of *Squalus montalbani* (Chondrichthyes: Squaliformes: Squalidae) from the Nansha (Spratly) Islands, South China Sea

Mengyi ZHANG[1], Binbin SHAN[2,3], Yan LIU[2,3], Liangming WANG[2],
Changping YANG[2], Manting LIU[2], Qijian XIE[2], Dianrong SUN[2]

1 *College of Aquaculture, Zhejiang Ocean University, Zhejiang, China*
2 *Tropical Aquaculture Research and Development Center, South China Sea Fisheries Research Institute, Chinese Academy of Fishery Sciences, Sanya, China*
3 *Key Laboratory of Marine Ranching, Ministry of Agriculture and Rural Affairs, Guangzhou, China*

https://zoobank.org/57D84DA2-6CB5-416A-A5E0-9F36AC1EC287

Corresponding author: Dianrong Sun (sundianrong@yeah.net)

Academic editor: Ronald Fricke ♦ **Received** 16 March 2023 ♦ **Accepted** 19 April 2023 ♦ **Published** 9 May 2023

Citation: Zhang M, Shan B, Liu Y, Wang L, Yang C, Liu M, Xie Q, Sun D (2023) A new record of *Squalus montalbani* (Chondrichthyes: Squaliformes: Squalidae) from the Nansha (Spratly) Islands, South China Sea. Acta Ichthyologica et Piscatoria 53: 51–57. https://doi.org/10.3897/aiep.53.103579

Abstract

The Indonesian greeneye spurdog (or a dogfish shark), *Squalus montalbani* Whitley, 1931, is widely distributed in the warm temperate to tropical waters of Indonesia, Philippines, the island of Taiwan, and Australia. Previous studies suggested that the distribution of dogfish shark species in the South China Sea is composed of two species, *Squalus mitsukurii* Jordan et Snyder, 1903 and *Squalus brevirostris* Tanaka, 1917. In March 2020 a dogfish shark specimen was collected from the Nansha (Spratly) Islands, South China Sea. We identified it as *S. montalbani* based on morphology and mitochondrial DNA barcoding. Our results confirmed the presence of *S. montalbani* in the South China Sea, leading us to conclude that it represents a new species record of the genus *Squalus* in the region. Furthermore, our findings demonstrate that the combined approach is highly effective in identifying *Squalus* species that share similar morphological characteristics.

Keywords

fish taxonomy, mitochondrial DNA barcoding, new record, South China Sea, *Squalus montalbani*

Introduction

The family Squalidae includes 2 genera, 39 species. Among these species, 36 species represents dogfish sharks (genus *Squalus*) (Ziadi-Künzli et al. 2020; Ariza et al. 2022; WoRMS Editorial Board 2023). Due to difficulties in morphological characteristics between different dogfish sharks, species in *Squalus* have a high taxonomic complexity (Viana et al. 2016). Thus, studies related to the taxonomy, evolution, and new species records are especially meaningful. Species of the genus *Squalus* are mainly distributed in the continental shelf waters, upper slope waters, and underwater cracks of the Atlantic, Pacific, and Indian oceans (Viana et al. 2016).

It has been reported that there were 9 species of *Squalus* genus distributed in China, including *Squalus acanthias* Linnaeus, 1758; *Squalus mitsukurii* Jordan et Snyder, 1903; *Squalus brevirostris* Tanaka, 1917; *Squalus blainville* (Risso, 1827); *Squalus formosus* White et Iglésias, 2011; *Squalus japonicus* Ishikawa, 1908; *Squalus megalops* (MacLeay, 1881); *Squalus montalbani* Whitley, 1931; and *Squalus suckleyi* (Girard, 1855) (see Zhu et al.

1963, 1984; Cheng and Zheng 1987; Shao 2023; Zhang 1960; Zhu 1960; White and Iglesias 2011; Straube et al. 2013). Among these species, *S. montalbani* has been found off the island of Taiwan, Australia, Philippines, Indonesia, in eastern Indian Ocean and Western Central Pacific regions (Graham 2019). Previous reports suggested that the distribution of dogfish shark species in the South China Sea is limited to only two species, namely *S. mitsukurii* and *S. brevirostris* (see Zhu 1962, 1979, 1984; Zhang et al. 2018).

A single dogfish shark specimen, at our disposal, collected in the middle of the South China Sea prompted us to identify it using morphological methods and DNA barcoding technique. The specimen could potentially represent a new record of a dogfish species for the studied area.

Material and methods

A single dogfish shark specimen was collected by Jianwei Zhou, at the Dianjian Fishing Harbour Marina, Beihai (mainland China), on March 2020. The fish originated from in the Nansha Archipelago (known also as the Spratly Islands), South China Sea (09°47′57″N, 114°5′35″E). The specimen was identified based on morphological characteristics used by Last et al. (2007).

A piece of muscle tissue was cut from the specimen, stored in 95% ethanol, and DNA was extracted with a DNA Extraction Kit of Tiangen, then PCR amplification. 5′-TCGACTAATCATAAAGATATCGGCAC-3′ and 5′-ACTTCAGGGTGACCGAAGAATCAGAA-3′ were used as primer sequences for cytochrome oxidase I (COI) amplification (Ivanova et al. 2007). PCR amplifications were performed in 25 μL volume including 1 μL of forward primer (F, 10 uM · L^{-1}), 1 μL of reverse primer (R, 10 uM · L^{-1}), 2 μL of dNTPs (2.5 mM · L^{-1} each), 0.15 μL of EasyTaq DNA Polymerase (5 U · $\mu\mathrm{L}^{-1}$), 2.5 μL of 10 × PCR buffer (25 uM · L^{-1}), 1 μL of DNA template (50 ng · uL^{-1}). The PCR conditions consisted of use of 95°C for 5 min for initial denaturation, 35 cycles of 94°C for 35 s, annealing at 54°C for 35 s, and extension at 72°C for 35 s, with a final extension at 72°C for 10 min. The above reactions were conducted through Biometra thermal cycler (Gottingen, Germany). Finally, the PCR products were stored in 4°C environment. Agarose gel was used for electrophoresis and was sequenced. Subsequently, the COI gene sequence of this specimen was obtained and revised through DNASTAR software (DNASTAR Inc., Madison, WI, USA).

Thirteen COI sequences of the genus *Squalus* were downloaded from NCBI for phylogenetic study, *Somniosus rostratus* (Risso, 1827) (KJ083255) was selected as the outgroup to root the tree (Table 1). The genetic relation between COI sequences was analyzed by the maximum likelihood method (ML, Felsenstein 1981). Phylogenetic tree construction first used JModeltest (Posada 2008) based on AIC (Akaike 1973) to filter the best alternative model as TPM2uf+I+G, then use RAxML-NG (Kozlov et al. 2019) to construct the ML phylogenetic tree based on Bootstrap method (Felsenstein 1985). The number of Bootstraps is set to 1000 times, and finally, the online tool ITOL (Letunic and Bork 2007) was used to view and adjust the phylogenetic tree (https://itol.embl.de/). The genetic distances of species were calculated in pairs using MEGA7 (Kumar et al. 2016), and thermodynamic maps of genetic distances were constructed using the R software (Ihaka and Gentleman 1996) combination package (Wei et al. 2017).

Table 1. Species and the GenBank accession numbers of the COI sequences used in phylogenetic tree construction.

Species	GenBank accession number	Reference
Squalus montalbani	KF590396	Sembiring et al. 2015
Squalus mitsukurii	MT123865	Ziadi-Künzli et al. 2020
Squalus brevirostris	EF539300	Ward et al. 2007
Squalus acanthias	KJ205210	Knebelsberger et al. 2014
Squalus blainville	KU198594	Kousteni et al. 2016
Squalus megalops	GU130698	Straube et al. 2010
Squalus hemipinnis	KF590514	Sembiring et al. 2015
Squalus nasutus	JN313288	Daly-Engel et al. 2018
Squalus chloroculus	EF539301	Ward et al. 2007
Squalus grahami	EU399028	Ward et al. 2008
Squalus crassispinus	DQ108248	Ward et al. 2005
Squalus formosus	MT123847	Ziadi-Künzli et al. 2020
Squalus cubensis	MG792175	Pfleger et al. 2018
Somniosus rostratus	KJ083255	Moura et al. 2015

Results

Morphological characteristics of the studied specimen of *Squalus montalbani* were shown in Fig. 1. The detailed measurements (in absolute values) were included in Table 2. Those absolute values yielded the relative values presented below.

Diagnosis. Body elongate to robust; trunk depth 12.2% TL; pre-first dorsal length 29.0% TL; pre-second dorsal length 61.2% TL; interdorsal space 25.4% TL; low raked dorsal fins; prepectoral length 22.5% TL; pelvic-caudal space 26% TL; dark spots on upper caudal lobe showing saddle-like extension toward upper caudal lobe margin.

The above morphological characteristics basically conform to the description of the Indonesian greeneye spurdog (dogfish shark), *Squalus montalbani*, in the literature (Last et al. 2007). In addition, based on observations of the morphological characteristics of the sample teeth, dermal denticles tricuspidate and rhomboid were found, in agreement with those described by Viana and De-Carvalho (2018).

The COI gene (655 bp) was sequenced from our sample. The accession number for the sequence submitted to GenBank is OQ826088. The phylogenetic tree was constructed through the downloaded sequences, as shown in Fig. 2. Sample_SM belongs to the genus *Squalus*. *Squalus acanthias*, *Squalus cubensis* Howell Rivero, 1936, *S. brevirostris*, and *S. blainville* are clustered in one group. As an outgroup of phylogenetic tree, *Somniosus rostratus* is a branch alone. Sample_SM and the rest of the species clustered in another group.

The genetic distance thermodynamic diagram shows (Fig. 3) that the genetic distance of COI sequence be-

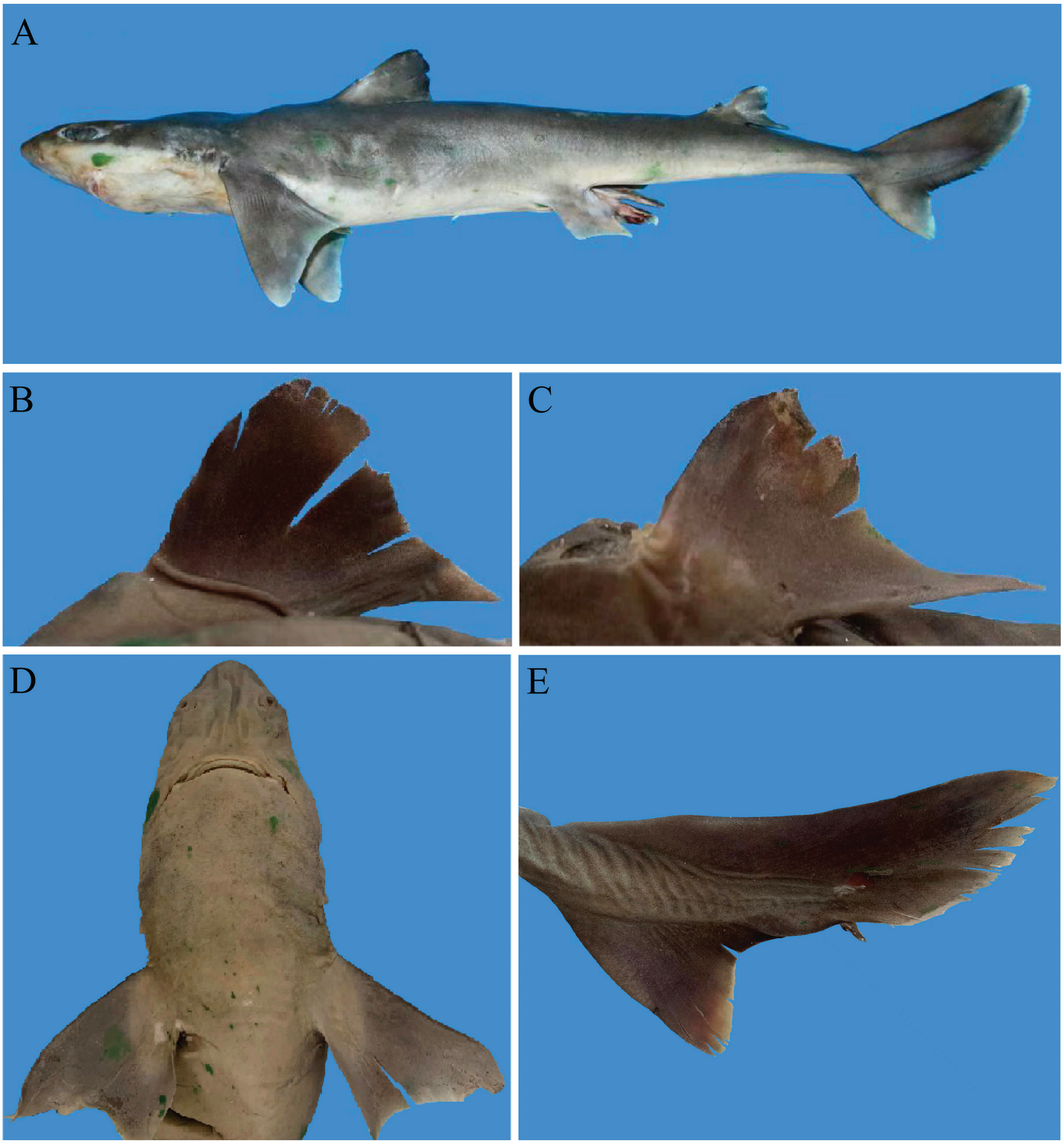

Figure 1. *Squalus montalbani* (sample_SM; length 550 mm TL); (**A**) Left lateral view; (**B**) Lateral view of the first dorsal fin; (**C**) Lateral view of the second dorsal fin; (**D**) Ventral view of the head; (**E**) Coloration of the caudal fin.

tween different species, the intraspecific genetic distance of *Squalus* genus is 0.01–0.09. The genetic distance between sample_SM and *S. montalbani* is 0, and that between sample_SM and *Squalus chloroculus* Last, White et Motomura, 2007 is 0.01, which further proves that sample_SM and *S. montalbani* are the same species having a close relation with *S. chloroculus*. Thus, both the morphological and genetic analysis strongly supports our identification of the newly found dogfish shark specimen as *S. montalbani*. Therefore, the presently studied specimen constitutes a new record of *Squalus montalbani* from the Nansha (Spratly) Archipelago, South China Sea.

Discussion

Due to the unique growth characteristics of the genus *Squalus*, its species have highly similar morphological characters that are difficult to identify, thus hindering taxonomic studies of the genus (Geraci et al. 2017), just as *Squalus montalbani* was once considered by Compagno (1984) to be a junior synonym of *S. mitsukurii*. Over the years, scholars have used ambiguous morphological diagnostic characters to distinguish between different species of the genus *Squalus* and have not achieved uniformity in diagnostic methods for the same species, leading to extensive taxonomic confusion and synonymization in the

Table 2. External measurements of *Squalus montalbani* (based on a single specimen).

Abbr.	Character	Absolute value [cm]
TL	Total length	55.0
PCL	Precaudal length	43.0
PD2	Pre-second dorsal length	33.0
PD1	Pre-first dorsal length	16.0
SVL	Pre-vent length	27.5
PP2	Prepelvic length	27.7
PP1	Prepectoral length	12.4
HDL	Head length	10.8
PG1	Prebranchial length	12.6
PSP	Prespiracular length	6.9
POB	Preorbital length	4.1
PRN	Prenarial length	3.2
POR	Preoral length	5.0
INLF	Inner nostril-labial furrow space	2.6
MOW	Mouth width	4.8
ULA	Labial furrow length	1.5
INW	Internarial space	3.2
INO	Interorbital space	4.5
EYL	Eye length	1.8
EYH	Eye height	1.0
SPL	Spiracle length	0.8
GS1	First gill-slit height	0.8
GS5	Fifth gill-slit height	1.1
IDS	Interdorsal space	14
DCS	Dorsal-caudal space	6.5
PPS	Pectoral-pelvic space	13.0
PCA	Pelvic-caudal space	14.3
D1L	First dorsal length	7.1
D1A	First dorsal anterior margin	5.4
D1B	First dorsal base length	3.8
D1H	First dorsal height	3.2
D1I	First dorsal inner margin	3.0
D1P	First dorsal posterior margin	4.3
P1A	Pectoral anterior margin	7.6
P1I	Pectoral inner margin	4.5
P1B	Pectoral base length	2.7
P1P	Pectoral posterior margin	5.9
P2L	Pelvic length	5.5
P2H	Pelvic height	3.8
P2I	Pelvic inner margin	1.8
CDM	Dorsal caudal margin	11.0
CPV	Preventral caudal margin	5.5
CPU	Upper postventral caudal margin	8.5
CPL	Lower postventral caudal margin	2.4
CFW	Caudal fork width	3.9
CFL	Caudal fork length	4.6
HANW	Head width at nostrils	4.0
HAMW	Head width at mouth	6.0
HDW	Head width	7.0
TRW	Trunk width	6.7
ABW	Abdomen width	5.8
TAW	Tail width	3.7
CPW	Caudal peduncle width	1.8
HDH	Head height	4.2
TRH	Trunk height	5.0
ABH	Abdomen height	5.5
TAH	Tail height	2.6
CPH	Caudal peduncle height	2.0
CLO	Clasper outer length	2.7
CLI	Clasper inner length	3.9
CLB	Clasper base width	1.0

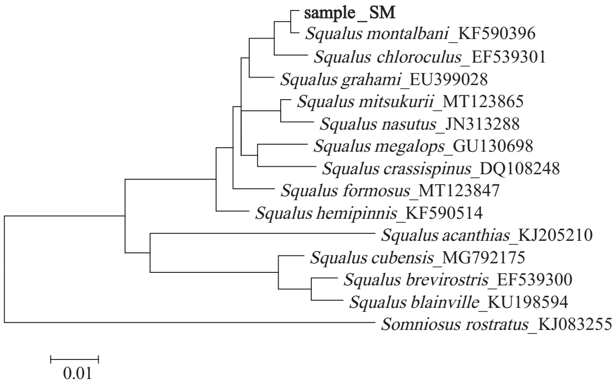

Figure 2. Maximum likelihood phylogenetic tree based on the COI sequence. *Somniosus rostratus* (KJ083255) was chosen as the outgroup to root the tree.

past (Veríssimo et al. 2017). The lack of well-preserved holotypes for many shark species, misidentifications in databases and in the literature, and challenges in retrieving representative series of specimens for comparison are top-down impediments to the proper taxonomic identification and the potential revision of genera (Veríssimo et al. 2014).

On the other hand, the slow growth, low reproductive capacity (Cortés 2000), and ease of capture by trawling and longlining, with a high proportion of bycatch, are the main reasons for the dramatic decline in the population of the genus *Squalus* (see Dulvy et al. 2014). Therefore, the majority of the species of the genus *Squalus* have been included in the IUCN Red List, and they have been classified in five categories according to their threatened level: Data Deficient, Least Concern, Near Threatened, Vulnerable, and Endangered (IUCN 2020). And the majority of the of the species of the genus *Squalus* in the Red List are currently classified as Data Deficient, Least Concern, Near Threatened, while eight species are classified as Vulnerable and Endangered, namely, *S. acanthias*, *S. chloroculus*, *S. brevirostris*, *S. mitsukurii*, *S. japonicus*, *S. montalbani*, *Squalus hemipinnis* White, Last et Yearsley, 2007, *S. formosus* (IUCN 2020). *Squalus montalbani* in Australia most of its range with light or absent fishing pressure, and the deeper parts of its depth range may provide refuge from fishing. Therefore, it is assessed as Vulnerable species (Graham 2019).

The genus *Squalus* has a low evolutionary rate (Hara et al. 2018) and its morphology is very similar, so species identification is often carried out by subtle morphological differences. Currently, morphological identification of the genus *Squalus* is based on the color and morphological characteristics of the caudal fin, the morphological characteristics of the head and trunk, and various morphological measurement parameters (Last et al. 2007). Last et al. (2007) have stated that *S. montalbani* and *S. chloroculus* have been confused, and our results show that they are genetically very close to each other; the genetic differentiation between *S. montalbani* and *S. chloroculus* is minimal, so there is a reason for their confusion. Both share the same morphological characteristics: relatively large body size, dark tail, low dorsal fin spines, and small, sloping first dorsal fin. However, there are also

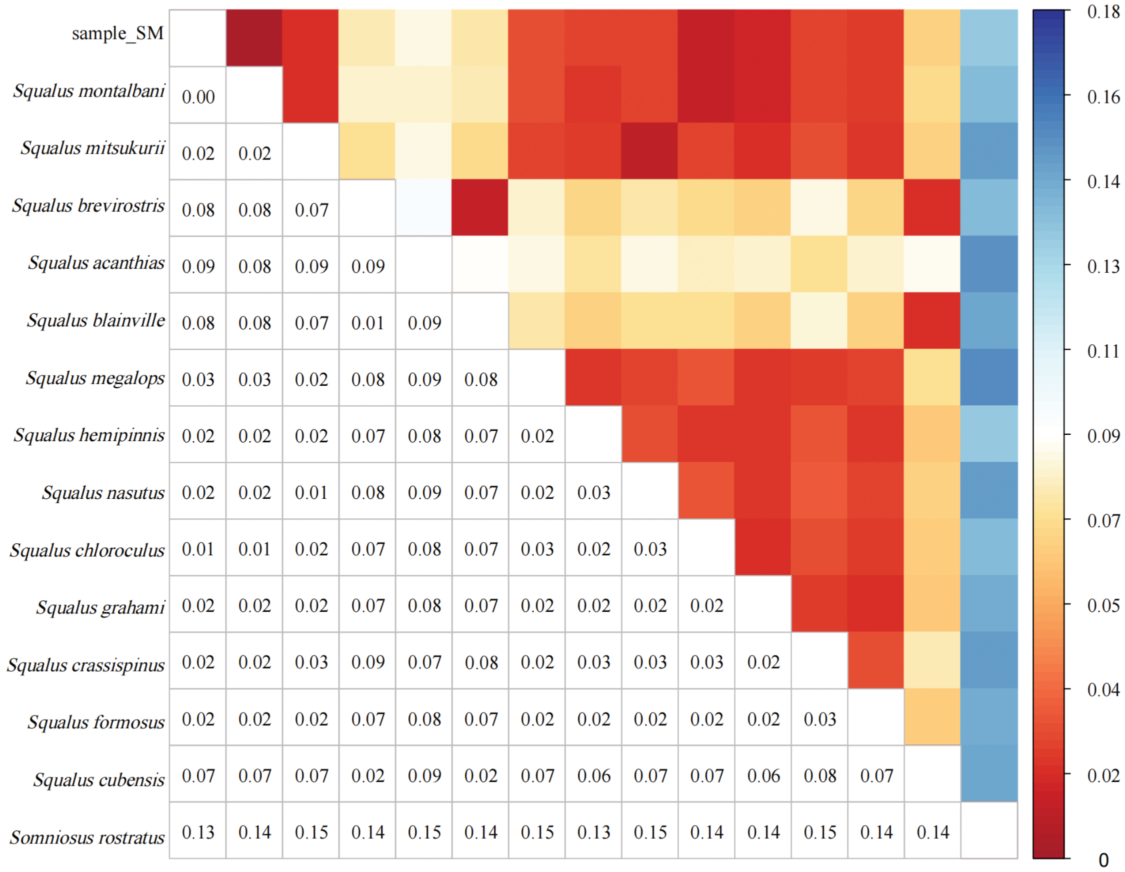

sample_SM															
Squalus montalbani	0.00														
Squalus mitsukurii	0.02	0.02													
Squalus brevirostris	0.08	0.08	0.07												
Squalus acanthias	0.09	0.08	0.09	0.09											
Squalus blainville	0.08	0.08	0.07	0.01	0.09										
Squalus megalops	0.03	0.03	0.02	0.08	0.09	0.08									
Squalus hemipinnis	0.02	0.02	0.02	0.07	0.08	0.07	0.02								
Squalus nasutus	0.02	0.02	0.01	0.08	0.09	0.07	0.02	0.03							
Squalus chloroculus	0.01	0.01	0.02	0.07	0.08	0.07	0.03	0.02	0.03						
Squalus grahami	0.02	0.02	0.02	0.07	0.08	0.07	0.02	0.02	0.02	0.02					
Squalus crassispinus	0.02	0.02	0.03	0.09	0.07	0.08	0.02	0.03	0.03	0.03	0.02				
Squalus formosus	0.02	0.02	0.02	0.07	0.08	0.07	0.02	0.02	0.02	0.02	0.02	0.03			
Squalus cubensis	0.07	0.07	0.07	0.02	0.09	0.02	0.07	0.06	0.07	0.07	0.06	0.08	0.07		
Somniosus rostratus	0.13	0.14	0.15	0.14	0.15	0.14	0.15	0.13	0.15	0.14	0.14	0.15	0.14	0.14	

Figure 3. Pairwise comparison of genetic differentiation between the sample in the presently reported study (sample_SM) and other 14 species of the Squaliformes based on COI gene sequence data. The genetic distance relation is expressed according to the color depth of the color block (above diagonal). The genetic distance value (below diagonal).

slight differences between the two, with the dorsal fin of *S. chloroculus* being smaller compared to *S. montalbani*, having a wider base of the fin spines, shorter adult claspers, and the upper postventral caudal margin is short relative to the lower postventral margin, having a marginally higher mean precaudal count (Last et al. 2007).

According to the data obtained in this study, the intraspecific genetic distances of the genus *Squalus* mainly ranged from 0.01 to 0.09, which indicates that the differentiation rate of the genus *Squalus* is very low, namely, the genetic expression is relatively conserved, resulting in a very similar morphology of the genus *Squalus*. Therefore, traditional taxonomic methods alone are not sufficient to identify species of the genus *Squalus*, and in recent years, molecular methods have begun to be used to supplement traditional taxonomic methods to make the identification of species of the genus more accurate, but molecular methods cannot completely replace traditional taxonomic methods at present (Schlick-Steiner et al. 2010). It is now customary to use a combination of traditional taxonomic methods and molecular methods of COI or NADH mitochondrial DNA labeling to identify the genus *Squalus*. This combined approach has proven to be very effective in identifying such species (Lim et al. 2022; Cerutti-Pereyra et al. 2012; Gabbanelli et al. 2018).

Funding

1. Hainan Provincial Natural Science Foundation of China (No. 320QN361).
2. National Natural Science Foundation of China (42206109).
3. Asia Cooperation Fund Project—Modern fishery cooperation between China and neighboring countries around the South China Sea.

References

Akaike H (1973) Maximum likelihood identification of Gaussian autoregressive moving average models. Biometrika 60(2): 255–265. https://doi.org/10.1093/biomet/60.2.255

Ariza AA, Adachi AM, Roque P, Hazin FH, Vianna M, Rotundo MM, Delpiani SM, Díaz de Astarloa JM, Delpiani G, Oliveira G, Foresti F, Cruz VP (2022) DNA barcoding and species delimitation for dogfish sharks belonging to the *Squalus* genus (Squaliformes: Squalidae). Diversity 14(7): e544. https://doi.org/10.3390/d14070544

Cerutti-Pereyra F, Meekan MG, Wei NW, O'Shea O, Bradshaw CJ, Austin CM (2012) Identification of rays through DNA barcoding:

An application for ecologists. PLoS One 7(6): e36479. https://doi.org/10.1371/journal.pone.0036479

Cheng QT, Zheng BS (1987) [A systematic search of Chinese fishes.] Science Press, Beijing, China. [In Chinese]

Compagno LJV (1984) Sharks of the world. An annotated and illustrated catalogue of shark species known to date. Part 1. Hexanchiformes to Lamniformes. FAO, Rome.

Cortés E (2000) Life history patterns and correlations in sharks. Reviews in Fisheries Science 8(4): 299–344. https://doi.org/10.1080/10408340308951115

Daly-Engel TS, Koch A, Anderson JM, Cotton CF, Rubbs RD (2018) Description of a new deep-water dogfish shark from Hawaii, with comments on the *Squalus mitsukurii* species complex in the West Pacific. ZooKeys 798: 135–157. https://doi.org/10.3897/zookeys.798.28375

Dulvy NK, Fowler SL, Musick JA, Cavanagh RD, Kyne PM, Harrison LR, Carlson JK, Davidson LN, Fordham SV, Francis MP, Pollock CM, Simpfendorfer CA, Burgess GH, Carpenter KE, Compagno LJ, Ebert DA, Gibson C, Heupel MR, Livingstone SR, Sanciangco JC, Stevens JD, Valenti S, White WT (2014) Extinction risk and conservation of the world's sharks and rays. eLife 3: e00590. https://doi.org/10.7554/eLife.00590

Felsenstein J (1981) Evolutionary trees from DNA sequences: A maximum likelihood approach. Journal of Molecular Evolution 17(6): 368–376. https://doi.org/10.1007/BF01734359

Felsenstein J (1985) Confidence limits on phylogenies: An approach using the bootstrap. Evolution International Journal of Organic Evolution 39(4): 783–791. https://doi.org/10.2307/2408678

Gabbanelli V, Diaz de Astarloa JM, Gonzalez-Castro M, Vazquez DM, Mabragana E (2018) Almost a century of oblivion: Integrative taxonomy allows the resurrection of the longnose skate *Zearaja brevicaudata* (Marini, 1933) (Rajiformes: Rajidae). Comptes Rendus Biologies 341(9–10): 454–470. https://doi.org/10.1016/j.crvi.2018.10.002

Geraci ML, Ragonese S, Norrito G, Scannella D, Falsone F, Vitale S (2017) [Chapter 2] A tale on the demersal and bottom dwelling Chondrichthyes in the south of Sicily through 20 years of scientific survey. Pp. 13–37. In: da Silva Rodrigues Filho LF, de Luna Sales JB (Eds.) Chondrichthyes—Multidisciplinary approach. IntechOpen, London, UK. https://doi.org/10.5772/intechopen.69333

Graham KJ (2019) *Squalus montalbani*. The IUCN Red List of Threatened Species 2019: e.T161404A68645208. [Accessed on 29 April 2023] https://doi.org/10.2305/IUCN.UK.2019-1.RLTS.T161404A68645208.en

Hara Y, Yamaguchi K, Onimaru K, Kadota M, Koyanagi M, Keeley SD, Tatsumi K, Tanaka K, Motone F, Kageyama Y, Nozu R, Adachi N, Nishimura O, Nakagawa R, Tanegashima C, Kiyatake I, Matsumoto R, Murakumo K, Nishida K, Terakita A, Kuratani S, Sato K, Hyodo S, Kuraku S (2018) Shark genomes provide insights into elasmobranch evolution and the origin of vertebrates. Nature Ecology and Evolution 2(11): 1761–1771. https://doi.org/10.1038/s41559-018-0673-5

Ihaka R, Gentleman R (1996) R: a language for data analysis and graphics. Journal of Computational and Graphical Statistics 5(3): 299–314. https://doi.org/10.1080/10618600.1996.10474713

IUCN (2020) The IUCN Red List of Threatened Species. Version 2020-1. IUCN, Gland, Switzerland.

Ivanova NV, Zemlak TS, Hanner RH, Hebert PD (2007) Universal primer cocktails for fish DNA barcoding. Molecular Ecology Notes 7(4): 544–548. https://doi.org/10.1111/j.1471-8286.2007.01748.x

Knebelsberger T, Landi M, Neumann H, Kloppmann M, Sell AF, Campbell PD, Laakmann S, Raupach MJ, Carvalho GR, Costa FO (2014) A reliable DNA barcode reference library for the identification of the north European shelf fish fauna. Molecular Ecology Resources 14(5): 1060–1071. https://doi.org/10.1111/1755-0998.12238

Kousteni V, Kasapidis P, Kotoulas G, Megalofonou P (2016) Evidence of high genetic connectivity for the longnose spurdog *Squalus blainville* in the Mediterranean Sea. Mediterranean Marine Science 17(2): 371–383. https://doi.org/10.12681/mms.1222

Kozlov AM, Darriba D, Flouri T, Morel B, Stamatakis A (2019) RAxML-NG: A fast, scalable and user-friendly tool for maximum likelihood phylogenetic inference. Bioinformatics 35(21): 4453–4455. https://doi.org/10.1093/bioinformatics/btz305

Kumar S, Stecher G, Tamura K (2016) MEGA7: Molecular evolutionary genetics analysis version 7.0 for bigger datasets. Molecular Biology and Evolution 33(7): 1870–1874. https://doi.org/10.1093/molbev/msw054

Last PR, White WT, Pogonoski JJ (2007) Descriptions of new dogfishes of the genus *Squalus* (Squaloidea: Squalidae). Hobart Tas. CSIRO Marine and Atmospheric Research c: 55–69.

Letunic I, Bork P (2007) Interactive Tree of Life (iTOL): An online tool for phylogenetic tree display and annotation. Bioinformatics 23(1): 127–128. https://doi.org/10.1093/bioinformatics/btl529

Lim KC, White WT, Then AY, Naylor GJ, Arunrugstichai S, Loh KH (2022) Integrated taxonomy revealed genetic differences in morphologically similar and non-sympatric *Scoliodon macrorhynchos* and *S. laticaudus*. Animals 12(6): 681. https://doi.org/10.3390/ani12060681

Moura T, Silva MC, Figueiredo I (2015) Barcoding deep-water chondrichthyans from mainland Portugal. Marine and Freshwater Research 66(6): 508–517. https://doi.org/10.1071/MF14095

Pfleger MO, Grubbs RD, Cotton CF, Daly-Engel TS (2018) *Squalus clarkae* sp. nov., a new dogfish shark from the Northwest Atlantic and Gulf of Mexico, with comments on the *Squalus mitsukurii* species complex. Zootaxa 4444(2): 101–119. https://doi.org/10.11646/zootaxa.4444.2.1

Posada D (2008) jModelTest: Phylogenetic model averaging. Molecular Biology and Evolution 25(7): 1253–1256. https://doi.org/10.1093/molbev/msn083

Schlick-Steiner BC, Steiner FM, Seifert B, Stauffer C, Christian E, Crozier RH (2010) Integrative taxonomy: A multisource approach to exploring biodiversity. Annual Review of Entomology 55(1): 421–438. https://doi.org/10.1146/annurev-ento-112408-085432

Sembiring A, Pertiwi NP, Mahardini A, Wulandari R, Kurniasih EM, Kuncoro AW, Cahyani NK, Anggoro AW, Ulfa M, Madduppa H, Carpenter KE, Barber PH, Mahardika GN (2015) DNA barcoding reveals targeted fisheries for endangered sharks in Indonesia. Fisheries Research 164: 130–134. https://doi.org/10.1016/j.fishres.2014.11.003

Shao KT (2023) Taiwan Fish Database. [Accessed 3 May 2023] http://fishdb.sinica.edu.tw

Straube N, Iglesias SP, Sellos DY, Kriwet J, Schliewen UK (2010) Molecular phylogeny and node time estimation of bioluminescent lantern sharks

(Elasmobranchii: Etmopteridae). Molecular Phylogenetics and Evolution 56(3): 905–917. https://doi.org/10.1016/j.ympev.2010.04.042

Straube N, White WT, Ho HC, Rochel E, Corrigan S, Li C, Naylor GJ (2013) A DNA sequence-based identification checklist for Taiwanese chondrichthyans. Zootaxa 3752(1): 256–278. https://doi.org/10.11646/zootaxa.3752.1.16

Veríssimo A, Cotton CF, Buch RH, Guallart J, Burgess GH (2014) Species diversity of the deep-water gulper sharks (Squaliformes: Centrophoridae: *Centrophorus*) in North Atlantic waters-current status and taxonomic issues. Zoological Journal of the Linnean Society 172(4): 803–830. https://doi.org/10.1111/zoj.12194

Veríssimo A, Zaera-Perez D, Leslie R, Iglésias SP, Séret B, Grigoriou P, Sterioti A, Gubili C, Barría C, Duffy C, Hernández S, Batjakas JE, Griffiths AM (2017) Molecular diversity and distribution of eastern Atlantic and Mediterranean dogfishes *Squalus* highlight taxonomic issues in the genus. Zoologica Scripta 46(4): 414–428. https://doi.org/10.1111/zsc.12224

Viana ST, Carvalho MD, Gomes UL (2016) Taxonomy and morphology of species of the genus *Squalus* Linnaeus, 1758 from the Southwestern Atlantic Ocean (Chondrichthyes: Squaliformes: Squalidae). Zootaxa 4133(1): 1–89. https://doi.org/10.11646/zootaxa.4133.1.1

Viana ST, De-Carvalho MR (2018) *Squalus rancureli* Fourmanoir, 1979, a new junior synonym of the blacktailed spurdog *S. melanurus* Fourmanoir, 1979, and updated diagnosis of *S. bucephalus* Last, Séret & Pogonoski, 2007 from New Caledonia (Squaliformes, Squalidae). Zoosystema 40(9): 159–177. https://doi.org/10.5252/zoosystema2018v40a9

Ward RD, Zemlak TS, Innes BH, Last PR, Hebert PD (2005) DNA barcoding Australia's fish species. Philosophical Transactions of the Royal Society of London. Series B, Biological Sciences 360(1462): 1847–1857. https://doi.org/10.1098/rstb.2005.1716

Ward RD, Holmes BH, Zemlak TS, Smith PJ (2007) DNA barcoding discriminates spurdogs of the genus *Squalus*. Pp. 117–130. In: Last PR, White WT, Pogonoski JJ (Eds) Descriptions of new dogfishes of the genus *Squalus* (Squaloidea: Squalidae). CSIRO Marine and Atmospheric Research Paper 014, Hobart, Australia.

Ward RD, Holmes BH, White WT, Last PR (2008) DNA barcoding Australasian chondrichthyans: Results and potential uses in conservation. Marine and Freshwater Research 59(1): 57–71. https://doi.org/10.1071/MF07148

Wei T, Simko V, Levy M, Xie Y, Jin Y, Zemla J (2017) Package 'corrplot'. Statistician 56(316): e24.

White WT, Iglesias SP (2011) *Squalus formosus*, a new species of spurdog shark (Squaliformes: Squalidae), from the western North Pacific Ocean. Journal of Fish Biology 79(4): 954–968. https://doi.org/10.1111/j.1095-8649.2011.03068.x

Whitley GP (1931) New names for Australian fishes. Australian Zoologist 6: 311–344.

WoRMS Editorial Board (2023) World Register of Marine Species. [Accessed 1 May 2023] https://www.marinespecies.org [at VLIZ. doi:10.14284/170]

Zhang CL (1960) [The survey report of the fishes of Bohai and Yellow Sea.] Science Press, Beijing, China. [In Chinese]

Zhang R, Lin LS, Li Y, Song PQ, Chen YJ, Zhang J (2018) [Species composition and quantity distribution of sharks in the southwestern sea of the Nansha Islands and mouth of the Beibu Bay.] Marine Fisheries (01): 27–37. [In Chinese]

Zhu YD (1960) [Chondrichthyes of China.] Science Press, Beijing, China, 225 pp. [In Chinese]

Zhu YD (1962) [Ichthyography of the South China Sea.] Science Press, Beijing, China. [In Chinese]

Zhu YD, Zhang CL, Cheng QT (1963) [Ichthyography of the East China Sea.] Science Press, Beijing, China. [In Chinese]

Zhu YD, Cheng QT, Meng QW (1979) [Ichthyography of the South China Sea Islands.] Science Press, Beijing, China. [In Chinese]

Zhu YD, Meng QW, Li S (1984) A new species of dogfish from China. Journal of Oceanology and Limnology 15(4): 283–286. [In Chinese]

Ziadi-Künzli F, Soliman T, Imai H, Sakurai M, Maeda K, Tachihara K (2020) Re-evaluation of deep-sea dogfishes (genus *Squalus*) in Japan using phylogenetic inference. Deep-sea Research. Part I, Oceanographic Research Papers 160: 103261. https://doi.org/10.1016/j.dsr.2020.103261

Acta Ichthyologica et Piscatoria 53, 2023, 59–64 | DOI 10.3897/aiep.53.101788

PENSOFT.

ACTA
ICHTHYOLOGICA
ET PISCATORIA

Length–weight relations of 39 continental-shelf and deep-water fishes (Actinopterygii) from northwestern Gulf of México

Ariel A. CHI-ESPÍNOLA[1], M. Eugenia VEGA-CENDEJAS[1],
J. Mirella HERNÁNDEZ DE SANTILLANA[1]

1 *Laboratorio de Taxonomía y Ecología de Peces, CINVESTAV-IPN, Mérida, Yucatán, Mexico*

https://zoobank.org/F6267C13-6D1A-4FAE-AD92-C16CDCC0601B

Corresponding author: M. Eugenia Vega-Cendejas (maruvega@cinvestav.mx)

Academic editor: Rodolfo Reyes ♦ **Received** 10 February 2023 ♦ **Accepted** 25 April 2023 ♦ **Published** 23 May 2023

Citation: Chi-Espínola AA, Vega-Cendejas ME, Hernández De Santillana JM (2023) Length–weight relations of 39 continental-shelf and deep-water fishes (Actinopterygii) from northwestern Gulf of México. Acta Ichthyologica et Piscatoria 53: 59–64. https://doi.org/10.3897/aiep.53.101788

Abstract

Fishes from the northwestern Gulf of Mexico were surveyed during four oceanographic campaigns (February and October 2016, June and September 2017) using a shrimp trawl net and benthic sled net in 20 locations at depths that ranged from 43 to 3608 m. Length–weight relations (LWR) were estimated for 39 fish species (in alphabetical order): *Bembrops gobioides* (Goode, 1880); *Centropristis philadelphica* (Linnaeus, 1758); *Chauliodus sloani* Bloch et Schneider, 1801; *Chlorophthalmus agassizi* Bonaparte, 1840; *Chloroscombrus chrysurus* (Linnaeus, 1766); *Citharichthys spilopterus* Günther, 1862; *Coelorinchus caelorhincus* (Risso, 1810); *Cyclopsetta chittendeni* Bean, 1895; *Cyclothone alba* Brauer, 1906; *Cyclothone braueri* Jespersen et Tåning, 1926; *Cyclothone pseudopallida* Mukhacheva, 1964; *Dibranchus atlanticus* Peters, 1876; *Epigonus pandionis* (Goode et Bean, 1881); *Fowlerichthys radiosus* (Garman, 1896); *Laemonema goodebeanorum* Meléndez et Markle, 1997; *Lagocephalus laevigatus* (Linnaeus, 1766); *Lepophidium brevibarbe* (Cuvier, 1829); *Lutjanus campechanus* (Poey, 1860); *Malacocephalus occidentalis* Goode et Bean, 1885; *Merluccius albidus* (Mitchill, 1818); *Micropogonias furnieri* (Desmarest, 1823); *Monolene sessilicauda* Goode, 1880; *Ogcocephalus declivirostris* Bradbury, 1980; *Peristedion greyae* Miller, 1967; *Porichthys plectrodon* Jordan et Gilbert, 1882; *Prionotus longispinosus* Teague, 1951; *Prionotus paralatus* Ginsburg, 1950; *Pristipomoides aquilonaris* (Goode et Bean, 1896); *Rhynchoconger flavus* (Goode et Bean, 1896); *Sardinella aurita* Valenciennes, 1847; *Saurida brasiliensis* Norman, 1935; *Sternoptyx diaphana* Hermann, 1781; *Symphurus diomedeanus* (Goode et Bean, 1885); *Synagrops bellus* (Goode et Bean, 1896); *Trachurus lathami* Nichols, 1920; *Trichiurus lepturus* Linnaeus, 1758; *Trichopsetta ventralis* (Goode et Bean, 1885); *Urophycis cirrata* (Goode et Bean, 1896); *Zalieutes mcgintyi* (Fowler, 1952). The fish species studied represented 28 families (in alphabetical order): Antennariidae, Batrachoididae, Bembropidae, Bothidae, Carangidae, Chlorophthalmidae, Congridae, Cyclopsettidae, Cynoglossidae, Dorosomatidae, Epigonidae, Gonostomatidae, Lutjanidae, Macrouridae, Merlucciidae, Moridae, Ogcocephalidae, Ophidiidae, Phycidae, Sciaenidae, Serranidae, Sternoptychidae, Stomiidae, Synagropidae, Synodontidae, Tetraodontidae Trichiuridae, Triglidae. A new maximum standard length (SL) was recorded for *Cyclothone alba*, *C. braueri*, *C. pseudopallida*, and *Lepophidium brevibarbe*. A positive allometric growth was reported in nine species, negative allometric growth in 16 species, and isometric growth in 14 species.

Keywords

bathyal, continental shelf, deep-water fish, Gulf of Mexico, length–weight relation

Introduction

Currently, demersal fishes in the northwestern Gulf of Mexico are under pressure from a growing industry focusing on oil exploration and extraction (Patiño-Ruiz et al. 2003). They are also affected by trawling, forming part of the discarded fauna from shrimp fishing in the area (Chávez-López and Morán-Silva 2019). One way to assess the scope and impact of these activities on biodiversity is by drawing up a list of the fish fauna in the area, as well as determining the affected life cycles, which are identified by studying the sizes of the fish specimens (Hernández-Padilla et al. 2020). For this process, length–weight relation (LWR) analyses are used, which commonly focus on identifying fish stocks, and the growth rate of a particular species, among others (Sandoval-Huerta et al. 2015). Therefore, the presently reported study was intended to determine the LWR of 39 dominant fish species from the northwestern region of the Gulf of Mexico in areas ranging from the continental shelf to the bathyal zone.

Materials and methods

Data collection was carried out during four oceanographic study surveys aboard the research vessel *RV JUSTO SIERRA*, each trip with an approximate duration of 10 days during the months of February and October 2016, and June and September 2017 (adequate weather conditions and project logistics). The activity was carried out at 20 sampling sites comprising depths between 43 and 3608 m. Two types of fishing gear were implemented, depending on the depth of each site, a shrimp trawl (18.29 m long and 4.57 cm mesh size) for depths between 50 and 500 m (9 sites) and a benthic sled net (32.4 m long and 2.5 cm mesh size) for depths between 500 and 3608 m (11 sites); both nets were hauled for one mile at a constant speed of 2.7 knots.

The collected fishes were labeled and immediately frozen at –20°C. They were subsequently transferred to the laboratory, where they were identified using specialized references (Carpenter 2002a, 2002b; McEachran and Fechhelm 2005). Individual weight and standard length (SL) were determined for all specimens and supplemented with the relevant site information, such as the coordinates, and depth. All specimens were measured and weighed fresh, fixed, and preserved in 80% ethyl alcohol. Some fish individuals were deposited in the ichthyological collection (CINV-NEC) of CINVESTAV-Merida in Mexico. The following 39 species, representing 28 families were investigated (Table 1), including *Rhynchoconger flavus* (Goode et Bean, 1896) [Congridae]; *Sardinella aurita* Valenciennes, 1847 [Dorosomatidae]; *Cyclothone alba* Brauer, 1906, *Cyclothone braueri* Jespersen et Tåning, 1926, *Cyclothone pseudopallida* Mukhacheva, 1964 [Gonostomatidae]; *Sternoptyx diaphana* Hermann, 1781 [Sternoptychidae]; *Chauliodus sloani* Bloch et Schneider, 1801 [Stomiidae]; *Saurida brasiliensis* Norman, 1935 [Synodontidae]; *Chlorophthalmus agassizi* Bonaparte, 1840 [Chlorophthalmidae]; *Coelorinchus caelorhincus* (Risso, 1810), *Malacocephalus occidentalis* Goode et Bean, 1885 [Macrouridae]; *Laemonema goodebeanorum* Meléndez et Markle, 1997 [Moridae]; *Merluccius albidus* (Mitchill, 1818) [Merlucciidae]; *Urophycis cirrata* (Goode et Bean, 1896) [Phycidae]; *Lepophidium brevibarbe* (Cuvier, 1829) [Ophidiidae]; *Porichthys plectrodon* Jordan et Gilbert, 1882 [Batrachoididae]; *Chloroscombrus chrysurus* (Linnaeus, 1766), *Trachurus lathami* Nichols, 1920 [Carangidae]; *Citharichthys spilopterus* Günther, 1862, *Cyclopsetta chittendeni* Bean, 1895 [Cyclopsettidae]; *Monolene sessilicauda* Goode, 1880, *Trichopsetta ventralis* (Goode et Bean, 1885) [Bothidae]; *Symphurus diomedeanus* (Goode et Bean, 1885) [Cynoglossidae]; *Trichiurus lepturus* Linnaeus, 1758 [Trichiuridae]; *Bembrops gobioides* (Goode, 1880) [Bembropidae]; *Synagrops bellus* (Goode et Bean, 1896) [Synagropidae]; *Epigonus pandionis* (Goode et Bean, 1881) [Epigonidae]; *Centropristis philadelphica* (Linnaeus, 1758) [Serranidae]; *Lutjanus campechanus* (Poey, 1860), *Pristipomoides aquilonaris* (Goode et Bean, 1896) [Lutjanidae]; *Prionotus longispinosus* Teague, 1951, *Prionotus paralatus* Ginsburg, 1950, *Peristedion greyae* Miller, 1967 [Triglidae]; *Micropogonias furnieri* (Desmarest, 1823) [Sciaenidae]; *Fowlerichthys radiosus* (Garman, 1896) [Antennariidae]; *Dibranchus atlanticus* Peters, 1876, *Ogcocephalus declivirostris* Bradbury, 1980, *Zalieutes mcgintyi* (Fowler, 1952) [Ogcocephalidae]; and *Lagocephalus laevigatus* (Linnaeus, 1766) [Tetraodontidae].

We calculated the length–weight relation using the allometric formula

$$W = aL^b$$

where W is the weight of the fish [g], L is the standard length [cm], a is the intercept and b is the allometric coefficient/slope. The values of a and b were calculated with Statgraphics software (Centurion XV, Version 15.1.02, Copyright 1982–2006 StatPoint, Inc.) with a linear least squares regression using a logarithmic scale. With the value of the slope (b), it was established if the fish species has negative growth ($b < 3$) or positive allometric growth ($b > 3$) and $b = 3$, indicating isometric growth (Froese et al. 2011). Outliers were removed using logarithmic plots, and limits for a and b were estimated by a Student's t-test with a 95% confidence (Froese 2006). For comparison, information on the maximum length (L_{max}) and the length at first maturity (L_m) is taken from FishBase and other references, with the respective length type being indexed (TL= total length, FL= Fork length). This study provides LWR that had not yet been reported for 11 species representing four different families. In some cases, when the number of specimens and/or the range of sizes was very narrow to estimate the a

Table 1. Length–weight relations for 39 fish species caught in northwestern Gulf of México.

Species	Depth [m]	*n*	SL [cm]	Weight [g]	*a*	95% CI *a*	*b*	95% CI *b*	Growt type	R^2	Reference data	
											L_m [cm]	L_{max} [cm]
Rhynchoconger flavus		35	14.2–42.7	4.4–133.0	0.0012	0.001–0.003	3.055	2.817–3.293	I	0.954	—	150.0_{TL}
Sardinella aurita		51	7.0–19.3	4.1–99.3	0.0124	0.007–0.022	3.024	2.831–3.216	I	0.953	12.0_{TL}	41.0_{TL}
Cyclothone alba	≥500	75	1.3–5.6	0.02–0.42	0.0076	0.007–0.009	2.309	2.168–2.449	–A	0.936	1.56_{SL2}	2.9_{SL}
Cyclothone braueri	≥500	22	1.4–4.6	0.02–0.23	0.0045	0.002–0.005	3.000	—	I	0.975	$2.0_{SL,2}$	3.8_{SL}
Cyclothone pseudopallida	≥500	71	1.5–4.8	0.02–0.51	0.0076	0.006–0.009	2.518	2.333–2.703	–A	0.914	$1.75_{SL,2}$	4.6_{SL}
Sternoptyx diaphana	≥500	26	1.2–4.5	0.09–4.21	0.0503	0.041–0.062	2.892	2.671–3.114	I	0.968	—	5.5_{SL}
Chauliodus sloani	≥500	25	4.5–19.2	0.09–17.03	0.0012	0.001–0.002	3.181	2.919–3.442	+A	0.965	$15.1_{SL,3}$	35.0_{SL}
Saurida brasiliensis		203	3.1–9.7	0.3–8.8	0.0171	0.015–0.020	2.708	2.632–2.783	–A	0.961	$8.0_{SL,1}$	25.0_{TL}
Chlorophthalmus agassizi	≥500	74	11.4–19.5	13.7–100.0	0.0038	0.002–0.006	3.401	3.222–3.579	+A	0.952	$11.5_{TL,4}$	40.0_{TL}
Coelorinchus caelorhincus	≥500	27	13.0–30.0	5.2–112.0	0.0006	0.0003–0.0013	3.509	3.271–3.749	+A	0.973	$17.2_{TL,5}$	48.0_{TL}
Malacocephalus occidentalis	≥500	15	27.0–38.5	49.3–162.8	0.0003	0.0002–0.0003	3.648	2.936–4.359	+A	0.904	—	45.0_{TL}
Laemonema goodebeanorum	≥500	15	7.5–27.3	2.4–191.5	0.0023	0.001–0.004	3.379	3.104–3.655	+A	0.982	—	30.3_{SL}
Merluccius albidus	≥500	40	27.3–40.9	212.8–699.7	0.0373	0.022–0.064	2.627	2.471–2.782	–A	0.968	$23.0_{SL,6}$	$70.0_{TL,6}$
Urophycis cirrata		23	20.4–43.5	86.4–770.7	0.0162	0.008–0.033	2.864	2.659–3.069	I	0.976	—	66.0_{TL}
Lepophidium brevibarbe		26	11.3–28.8	4.6–117.1	0.0017	0.001–0.003	3.313	3.151–3.475	+A	0.987	$10.1_{TL,7}$	27.3_{SL}
Porichthys plectrodon		217	4.2–18.3	1.2–93.3	0.0182	0.015–0.022	2.856	2.771–2.941	–A	0.953	$8.0_{FL,8}$	29.0_{TL}
Chloroscombrus chrysurus		40	11.6–16.3	31.5–68.4	0.0182	0.017–0.018	3.000	—	I	0.967	11.2_{FL}	65.0_{TL}
Trachurus lathami		32	10.4–17.9	18.8–77.6	0.0443	0.026–0.076	2.598	2.394–2.802	–A	0.957	11.4_{TL}	40.0_{TL}
Citharichthys spilopterus		70	6.4–11.9	5.2–27.8	0.0283	0.021–0.038	2.763	2.632–2.894	–A	0.963	$12.0_{SL,9}$	21.0_{TL}
Cyclopsetta chittendeni		231	4.5–28.8	1.2–371.3	0.0119	0.009–0.014	3.081	3.012–3.148	I	0.972	$14.5_{TL,9}$	$33.0_{TL,9}$
Monolene sessilicauda		36	4.9–11.8	1.1–9.6	0.0095	0.006–0.014	2.858	2.667–3.048	I	0.964	—	18.0_{TL}
Trichopsetta ventralis		873	3.6–18.0	0.5–59.6	0.0109	0.010–0.012	3.092	3.045–3.139	I	0.950	—	20.0_{TL}
Symphurus diomedeanus		21	5.0–14.7	0.9–31.0	0.0067	0.004–0.012	3.169	2.927–3.411	+A	0.975	—	22.0_{TL}
Trichiurus lepturus		17	7.4–65.3	0.1–103.3	0.0001	0.0001–0.0002	3.357	3.198–3.515	+A	0.993	30.0_{TL}	234.0_{TL}
Bembrops gobioides	≥500	21	8.8–23.4	3.9–82.6	0.0039	0.002–0.008	3.203	2.934–3.471	+A	0.970	—	30.0_{TL}
Synagrops bellus		20	6.3–20.7	4.6–166.6	0.0174	0.010–0.031	3.029	2.813–3.243	I	0.979	$13.0_{TL,13}$	$46.0_{TL,14}$
Epigonus pandionis	≥500	56	9.8–20.2	22.8–154.2	0.0358	0.022–0.058	2.809	2.633–2.984	–A	0.950	$11.2_{TL,15}$	23.5_{TL}
Centropristis philadelphica		42	9.7–23.5	23.2–289.3	0.0323	0.020–0.053	2.862	2.676–3.047	I	0.960	—	30.0_{TL}
Lutjanus campechanus		35	8.0–24.7	12.7–467.2	0.0237	0.013–0.042	3.032	2.806–3.258	I	0.958	$9.41_{FL,11}$	100.0_{TL}
Pristipomoides aquilonaris		477	3.3–20.0	1.0–197.2	0.0251	0.024–0.025	2.873	2.830–2.916	–A	0.973	—	56.0_{TL}
Prionotus longispinosus		183	3.9–24.7	1.3–307.6	0.0397	0.030–0.053	2.771	2.660–2.881	–A	0.931	$12.0_{TL,16}$	35.0_{TL}
Prionotus paralatus		180	7.8–17.5	7.5–85.2	0.0142	0.011–0.018	3.056	2.959–3.153	I	0.956	$10.0_{TL,16}$	$18.0_{SL,16}$
Peristedion greyae		123	12.8–18.4	11.9–33.4	0.0110	0.007–0.017	2.738	2.580–2.895	–A	0.907	—	23.9_{TL}
Micropogonias furnieri		26	12.0–20.2	40.4–155.5	0.0643	0.035–0.118	2.594	2.368–2.821	–A	0.959	24.3_{TL}	60.0_{SL}
Fowlerichthys radiosus		47	2.6–9.4	1.5–57.2	0.1357	0.105–0.176	2.578	2.411–2.744	–A	0.956	—	25.0_{TL10}
Dibranchus atlanticus		178	3.4–10.8	1.5–25.7	0.0696	0.059–0.083	2.434	2.351–2.517	–A	0.957	$10.9_{TL,17}$	39.4_{TL}
Ogcocephalus declivirostris		23	6.1–10.3	6.8–37.5	0.0304	0.019–0.048	3.027	2.805–3.248	I	0.975	—	16.5_{TL}
Zalieutes mcgintyi		17	3.3–7.3	1.4–10.5	0.0579	0.039–0.087	2.634	2.415–2.853	–A	0.978	—	10.0_{TL}
Lagocephalus laevigatus		30	3.9–36.0	4.2–1050.3	0.0601	0.040–0.090	2.672	2.512–2.833	–A	0.976	$24.5_{SL,12}$	100.0_{TL}

n = number of individuals, SL = standard length, TL = total length, *a* = intercept (equation parameter), *b* = slope (equation parameter), 95% CI = 95% confidence limits (for both equation parameters), R^2 = coefficient of determination. Species in bold denote new maximum length. I = isometric growth, –A = negative allometric growth, +A = positive allometric growth. Isometric growth is assumed in the species with low number of specimens and/or narrow range sizes (no value for 95% CI *b*) (Froese, 2006; Hay et al. 2020). Reference data = literature data, including information covered by FishBase, Subscript references: 1= McEachran and Fechhelm 1998, 2 = Harold 2015, 3 = Marks 2016, 4 = Onghia et al. 2006, 5 = Paramo et al. 2017a, 6 = McEachran et al. 2015a, 7 = Robins 2015, 8 = Vianna et al. 2000, 9 = Carpenter et al. 2015, 10 = McEachran et al. 2015b, 11 = Kulaw et al. 2017, 12 = Shao et al. 2014, 13 = Vaske et al. 2009, 14 = Singh-Renton et al. 2015, 15 = Paramo et al. 2017b, 16 = Collette et al. 2015, 17 = Rees 1963.

and *b* parameters of the LWR, we assumed an isometric relation (b = 3) (Froese 2006; Hay et al. 2020) and the value of the intercept (a) will be obtained with the following formula

$$a = \frac{\sum_{i=1}^{n} \frac{W}{L^3}}{n}$$

Results

The descriptive statistics and the estimated LWR parameters for 39 species are summarized in Table 1. All LWR estimates were statistically significant ($P < 0.05$), yielding $R^2 > 0.900$. New maximum lengths are reported for four species: *Cyclothone alba* (5.6 cm SL), *C. braueri* (4.6 cm SL), *C. pseudopallida* (4.8 cm SL), and *Lepophidium brevibarbe* (28.8 SL). All the values of "*a*" ranged between 0.0001 (*Trichiurus lepturus*) and 0.1357 (*Fowlerichthys radiosus*); and the "*b*" values oscillated between 2.309 (*Cyclothone alba*) and 3.648 (*Malacocephalus occidentalis*). Positive allometric growth was reported in nine species, negative allometric growth in 16 species, and isometric growth in 14 species.

The LWR of 11 species that correspond to 10 families have not been previously reported, so it is an important contribution to their knowledge. These families and species are Congridae: *Rhynchoconger flavus*, Gonostomatidae: *Cyclothone alba*, Moridae: *Laemonema goodebeanorum*, Cyclopsettidae: *Cyclopsetta chittendeni*, Bothidae: *Monolene sessilicauda*, Cynoglossidae: *Symphurus diomedeanus*, Bembropidae: *Bembrops gobioides*, Triglidae:

Prionotus paralatus, Antennariidae: *Fowlerichthys radiosus*, and Ogcocephalidae: *Ogcocephalus declivirostris*, *Zalieutes mcgintyi*.

Discussion

The abundance of fish species associated with depths greater than 500 m, is usually low and the available information on their populations and growth rates are scarce (Danovaro et al. 2017). Therefore, any new data on their biology is important. The deep-sea species reported in this study are carnivorous, occurring in the vertical gradients of the continental slope and the bathyal zone, and were exemplified by *Epigonus pandionis*, *Merluccius albidus*, *Chauliodus sloani*, *Chlorophthalmus agassizi* (see Ramírez et al. 2019). Furthermore, we highlight an amplitude in its maximum length reported by the literature corresponding to *Cyclothone alba* from 2.9 to 5.6 cm SL, *Cyclothone braueri* from 3.8 to 4.6 cm SL, *Cyclothone pseudopallida* from 4.6 to 4.8 cm SL (Harold 2015) and *Lepophidium brevibarbe* from 27.3 to 28.8 cm SL. In addition, we consider that these species are the ones that are possibly being most affected during oil extraction maneuvers and hydrocarbon leaks in the depths (Fisher et al. 2016). The genus *Cyclothone* corresponds to the most abundant resource in these deep zones (Olivar et al. 2017) and is perhaps the main food source that generates stability in populations, so its impact would generate a disparity in the deep marine ecosystem.

LWR studies in the northern Gulf of Mexico have been very scarce. In these studies, the species analyzed include *Chloroscombrus chrysurus* and *Citharichthys spilopterus* (see Dawson 1965; Galindo-Cortés et al. 2015) and a single deep-sea species *Urophycis cirrata* (see Matlock et al. 1988). The majority of the species mentioned in these investigations are associated with shallow coastal areas. In the presently reported study, LWR information is provided on ecologically important species found at depths greater than 500 m, including records of both juvenile and sexually matured organisms. With this information, the reports of these species in the area were completed, as well as the delivery of new biological information on the deep-sea ecosystem, which is a poorly studied region located in the north of the Gulf of Mexico, and where samples are difficult to obtain (Blomberg and Montagna 2014). Likewise, we recorded species of *Micropogonias furnieri* and *Citharichthys spilopterus* that did not reach sexual maturity and were captured by shrimp trawls of the same dimensions as the fishing boats, so it is possible that both species are showing a decrease in their populations.

The slope (b) that was estimated in this study was between the expected range of 2.5 to 3.5 (Froese 2006), except for *Cyclothone alba* (2.309) and *Dibranchus atlanticus* (2.434) that were found below this range of values, and for *Malacocephalus occidentalis* which is above those values (3.648). For *Cyclothone braueri* and *Chloroscombrus chrysurus* with a low number of specimens and/or with low range sizes (Carlander 1997), the LWR was calculated assuming $b = 3.0$, being the value of the intercept considered by the formula of Hay et al. (2020). These low values can be attributed also to the combination of one or more of the following factors: habitat, area/season effect, gonad maturity stages, sex, stomach fullness, health condition, population, and differences within species and preservation techniques (Tesch 1971; Froese 2006; Bautista-Romero et al. 2012). Finally, a total of nine and 16 species showed positive and negative allometric growth, respectively, while isometric growth was reported in 14 species.

Author contribution

(following Contributor Roles Taxonomy of CRediT https://credit.niso.org):

Ariel Adriano Chi Espinola: Conceptualization, Formal Analysis, Investigation, Methodology, Visualization, Writing—original draft preparation, Writing—review and editing.

María Eugenia Vega Cendejas: Conceptualization, Funding acquisition, Investigation, Project administration, Resources, Supervision, Validation, Visualization, Writing—original draft preparation, Writing—review and editing.

Jovita Mirella Hernández de Santillana: Conceptualization, Data curation, Formal analysis, Methodology, Visualization, Writing—original draft preparation.

Acknowledgments

This is a contribution from the Gulf of México Research Consortium (CIGOM). We are grateful to Alex Acosta, María Blanqueto, Sergio Zavala and Mariana Uribe for processing the samples. This research was funded by the Mexican National Council for Science and Technology - Mexican Ministry of Energy - Hydrocarbon Fund, project 201441.

References

Bautista-Romero S, González-Peláez S, Campos-Dávila L, Lluch-Cota DB (2012) Length–weight relationships of wild fish captured at the mouth of Río Verde, Oaxaca. Mexico and connected lagoons (Miniyua, El Espejo, Chacahua and Patoría). Journal of Applied Ichthyology 28: 269–271. https://doi.org/10.1111/j.1439-0426.2011.01914.x

Blomberg BN, Montagna PA (2014) Meta-analysis of Ecopath models reveals secondary productivity patterns across the Gulf of Mexico. Ocean and Coastal Management 100: 32–40. https://doi.org/10.1016/j.ocecoaman.2014.07.014

Carlander KD (1997) Handbook of freshwater fishery biology. Vol. 2. Life history data on centrarchid fishes of the United States and Canada. Iowa State University Press, Ames, IA, USA.

Carpenter KE (Ed.) (2002a) The living marine resources of the Western Central Atlantic. Volume 2: Bony fishes part 1 (Acipenseridae to

Grammatidae). FAO Species Identification Guide for Fishery Purposes and American Society of Ichthyologists and Herpetologists Special Publication No. 5. FAO, Rome, 601–1374.

Carpenter KE (Ed.) (2002b) The living marine resources of the Western Central Atlantic. Volume 3 Bony fishes part 2 (Opistognathidae to Molidae), sea turtles and marine mammals. FAO Species Identification Guide for Fishery Purposes and American Society of Ichthyologists and Herpetologists Special Publication No. 5. FAO, Rome, 1375–2127.

Carpenter KE, Munroe T, Robertson R (2015) *Citharichthys spilopterus*. The IUCN Red List of Threatened Species 2015: e.T16439236A16509962. https://doi.org/10.2305/IUCN.UK.2015-4.RLTS.T16439236A16509962.en

Chávez-López R, Morán-Silva A (2019) Revisión de la composición de especies de peces capturadas incidentalmente en la pesquería de camarón en el Golfo de México. Revista Ciencia Pesquera 27: 65–82.

Collette B, Grubbs D, Pezold F, Simons J, Caruso J, Carlson J, McEachran JD, Brenner J, Tornabene L, Chakrabarty P, Robertson R (2015) *Prionotus longispinosus*, *Prionotus paralatus.* The IUCN Red List of Threatened Species 2015: e.T196695A2474787. https://doi.org/10.2305/IUCN.UK.2015-4.RLTS.T196695A2474787.en

Danovaro J, Aguzzi J, Fanelli E, Billett D, Gjerde K, Jamieson A, Ramirez-Llodra A, Smith CR, Snelgrove PVR, Thomsen L, Van Dover CL (2017) An ecosystem-based deep-ocean strategy. Science 355: 452–454. https://doi.org/10.1126/science.aah7178

Dawson CE (1965) Length–weight relationships of some Gulf of Mexico fishes. Transactions of the American Fisheries Society 94: 279–280. https://doi.org/10.1577/1548-8659(1965)94[279:LROSGO]2.0.CO;2

Fisher CR, Montagna PA, Sutton TT (2016) How did the Deepwater Horizon oil spill impact deep-sea ecosystems? Oceanography 29: 182–195. https://doi.org/10.5670/oceanog.2016.82

Froese R (2006) Cube law, condition factor and weight–length relationships: History, meta-analysis and recommendations. Journal of Applied Ichthyology 22: 241–253. https://doi.org/10.1111/j.1439-0426.2006.00805.x

Froese R, Pauly D (2022) FishBase. [Accessed October 2022] https://www.fishbase.se

Froese R, Tsikliras AC, Stergiou KI (2011) Editorial note on weight–length relations of fishes. Acta Ichthyologica et Piscatoria 41: 261–263. https://doi.org/10.3750/AIP2011.41.4.01

Galindo-Cortés G, Meiners C, Jiménez-Badillo L (2015) Length–weight relationships for 30 fish species caught in coastal waters of Veracruz, western Gulf of Mexico. Revista de Biología Marina y Oceanografía 50: 141–147. https://doi.org/10.4067/S0718-19572015000100012

Harold A (2015) *Cyclothone braueri*. The IUCN Red List of Threatened Species 2015: e.T198757A42691694. https://doi.org/10.2305/IUCN.UK.2015-4.RLTS.T198757A42691694.en

Hay A, Xian W, Bailly N, Liang C, Pauly, D (2020) The why and how of determining length–weight relationships of fish from preserved museum specimens. Journal of Applied Ichthyology 36(3): 373–379. https://doi.org/10.1111/jai.14014

Hernández-Padilla JC, Capetillo-Piñar N, Aranceta-Garza F, Yee-Duarte JA, Vélez-Arellano N, Velázquez-Abunader I (2020) Length–weight relationships of 12 marine fish species from the Pacific coast of Guatemala associated with small-scale fisheries. Journal of Applied Ichthyology 14: 863–865. https://doi.org/10.1111/jai.14093

Kulaw DH, Cowan JH Jr, Jackson MW (2017) Temporal and spatial comparisons of the reproductive biology of northern Gulf of Mexico (USA) red snapper (*Lutjanus campechanus*) collected a decade apart. PLoS ONE 12: e0172360. https://doi.org/10.1371/journal.pone.0172360

Marks AD (2016) Reproductive ecology of dragonfishes (family: Stomiidae) in the Gulf of Mexico. Frontiers in Marine Science 7. https://doi.org/10.3389/fmars.2020.00101

Matlock GC, Nelson WR, Jones RS, Green AW (1988) Length–length and weight–length relationships of seven deep-water fishes in the Gulf of Mexico. Texas Parks and Wildlife Department, Coastal Fisheries Branch. Management Data Series Number 136/1988, Austin, TX, USA.

McEachran JD, Fechhelm JD (1998) Fishes of the Gulf of Mexico, Volume 1: Myxiniformes to Gasterosteiformes. University of Texas Press, Austin, TX, USA. https://doi.org/10.7560/752061

McEachran JD, Fechhelm JD (2005) Fishes of the Gulf of Mexico, Volume 2: Scorpaeniformes to Tetraodontiformes. University of Texas Press, Austin, TX, USA. https://doi.org/10.7560/706347

McEachran JD, Polanco-Fernandez A, Russell B (2015a) *Merluccius albidus*, *Fowlerichthys radiosus*. The IUCN Red List of Threatened Species 2015: e.T16466377A16509742. https://doi.org/10.2305/IUCN.UK.2015-4.RLTS.T16466377A16509742.en

McEachran JD, Polanco-Fernandez A, Russell B (2015b) *Fowlerichthys radiosus*. The IUCN Red List of Threatened Species 2015: e.T16467178A16510067. https://doi.org/10.2305/IUCN.UK.2015-4.RLTS.T16467178A16510067.en

Olivar MP, Hulley PA, Castellón A, Emelianov M, López C, Tuset VM, Contreras T, Molí B (2017) Mesopelagic fishes across the tropical and equatorial Atlantic: Biogeographical and vertical patterns. Progress in Oceanography 151: 116–137. https://doi.org/10.1016/j.pocean.2016.12.001

Onghia GD', Sion L, Maiorano P, Mytilineou Ch, Dalessandro S, Carlucci R, Desantis S (2006) Population biology and life strategies of *Chlorophthalmus agassizi* Bonaparte, 1840 (Pisces: Osteichthyes) in the Mediterranean Sea. Marine Biology 149: 435–446. https://doi.org/10.1007/s00227-005-0231-y

Paramo J, Motta J, De La Hoz J (2017a) Population structure of grenadier fish *Coelorinchus caelorhincu*s in deep waters of the Colombian Caribbean Coast. Boletín de Investigaciones Marinas y Costeras 46: 1–19. https://doi.org/10.25268/bimc.invemar.2017.46.1.720

Paramo J, Fuentes D, Wiff W (2017b) Population structure and distribution of deep-water cardinal fish *Epigonus occidentalis* (Epigonidae) and *Epigonus pandionis* (Epigonidae) in the Colombian Caribbean Sea. Journal of Ichthyology 57: 424–433. https://doi.org/10.1134/S0032945217030109

Patiño-Ruiz J, Rodríguez-Uribe MA, Hernández-Flores ER, Lara-Rodriguez J, Gómez-González AR (2003) El cinturón Plegado Perdido Mexicano. Estructura y Potencial Petrolero. Boletín de la Asociación Mexicana de Geólogos Petroleros 2003: 3–20.

Ramírez JM, Vázquez-Bader AR, Gracia A (2019) Ichthyofaunal list of the continental slope of the southern Gulf of Mexico. ZooKeys 846: 117–132. https://doi.org/10.3897/zookeys.846.31944

Rees EI (1963) The batfish, *Dibranchus atlanticus* Peters, on the Canadian Atlantic slopes. Journal of the Fisheries Research Board of Canada 20(6): 1513–1517. https://doi.org/10.1139/f63-103

Robins RH (2015) *Lepophidium brevibarbe*. The IUCN Red List of Threatened Species 2015: e.T16501868A16510077. https://doi.org/10.2305/IUCN.UK.2015-4.RLTS.T16501868A16510077.en

Sandoval-Huerta ER, Madrigal-Guridi X, Domínguez-Domínguez O, Ruiz-Campos G, González-Acosta AF (2015) Length–weight and length–length relations for 14 fish species from the central Mexican pacific coast. Acta Ichthyologica et Piscatoria 45: 199–201. https://doi.org/10.3750/AIP2015.45.2.10

Shao K, Liu M, Jing L, Hardy G, Leis JL, Matsuura K (2014) *Lagocephalus laevigatus*. The IUCN Red List of Threatened Species 2014, e.T190380A1950085. https://doi.org/10.2305/IUCN.UK.2014-3.RLTS.T190380A1950085.en

Singh-Renton S, Robertson R, Marechal J, Aiken KA, Dooley J, Collette BB, Oxenford H, Pina-Amargos F, Kishore R (2015) *Synagrops bellus*. The IUCN Red List of Threatened Species 2015: e.T13458323A13462780. https://doi.org/10.2305/IUCN.UK.2015-4.RLTS.T13458323A13462780.en

Tesch FW (1971) Age and growth. Pp. 93–123. In: Ricker WE (Ed.) Methods for assessment of fish production in fresh waters. 2nd edn. Blackwell Scientific Publications, Oxford, UK.

Vaske T, Freire AT, Bismarck OF (2009) Aspectos biológicos do peixe-olhudo-dentinho, *Synagrops bellus* (Actinopterygii: Acropomatidae), da plataforma externa e talude superior do estado de São Paulo, Brasil. Pan-American Journal of Aquatic Sciences 4: 179–187.

Vianna M, Acácio RG, Tomas I, Verani RR (2000) Aspects of the biology of the Atlantic Midshipman, *Porichthys porosissimus* (Teleostei, Batrachoididae): An important by-catch species of shrimp trawling off southern Brazil. Revista Brasileira de Oceanografia 48: 131–140. https://doi.org/10.1590/S1413-77392000000200004

Acta Ichthyologica et Piscatoria 53, 2023, 65–80 | DOI 10.3897/aiep.53.103358

PENSOFT.

ACTA
ICHTHYOLOGICA
ET PISCATORIA

Estimation of selectivity parameters for target and bycatch fishes of the trammel net fisheries in the northern Aegean Sea (eastern Mediterranean Sea)

Angeliki ADAMIDOU[1,2], Konstantinos TOULOUMIS[1],
Manos KOUTRAKIS[1], Athanassios C. TSIKLIRAS[2]

1 *Fisheries Research Institute, ELGO-DIMITRA, Nea Peramos, Kavala, Greece*
2 *Laboratory of Ichthyology, School of Biology, Aristotle University of Thessaloniki, Thessaloniki, Greece*

https://zoobank.org/25915C92-2A76-45FD-A210-0C60E6754B3C

Corresponding author: Angeliki Adamidou (adamidou@inale.gr)

Academic editor: Sanja Matić-Skoko ♦ **Received** 11 March 2023 ♦ **Accepted** 26 April 2023 ♦ **Published** 23 May 2023

Citation: Adamidou A, Touloumis K, Koutrakis M, Tsikliras AC (2023) Estimation of selectivity parameters for target and bycatch fishes of the trammel net fisheries in the northern Aegean Sea (eastern Mediterranean Sea). Acta Ichthyologica et Piscatoria 53: 65–80. https://doi.org/10.3897/aiep.53.103358

Abstract

The size selectivity of trammel nets was investigated in the northern Aegean Sea using 10 different inner-panel mesh sizes ranging from 16 to 70 mm nominal mesh size (bar length). Selectivity estimates were made for the eight most abundant target and bycatch fish species, namely black scorpionfish, *Scorpaena porcus* Linnaeus, 1758; annular seabream, *Diplodus annularis* (Linnaeus, 1758); red mullet, *Mullus barbatus* Linnaeus, 1758; surmullet, *Mullus surmuletus* Linnaeus, 1758; round sardinella, *Sardinella aurita* Valenciennes, 1847; European hake, *Merluccius merluccius* (Linnaeus, 1758); greater weever, *Trachinus draco* Linnaeus, 1758; and blotched picarel, *Spicara flexuosum* Rafinesque, 1810, which accounted for 51.5% by number and 42.7% by weight of the fish caught with trammel nets in the sea trials. The SELECT method was used to estimate the selectivity parameters. Five different selectivity functions (i.e., normal scale, normal location, gamma, log-normal, and bi-normal) were applied with the bi-normal function providing the best fit as it had the lowest deviance value for all species and the lowest values for the dispersion parameter (D/df). The mesh size of 16 mm in most of the cases retained specimens below the size at first maturity (L_m). The mesh size of 19 mm seems more appropriate for red mullet, surmullet, and blotched picarel, the mesh size of 22 mm for annular seabream and round sardinella, while for European hake and black scorpionfish, the mesh size larger than 26 mm would be more appropriate.

Keywords

bycatch, Mediterranean Sea, SELECT, size-selectivity, small-scale fisheries, trammel nets

Introduction

Over the past 40 years, population growth, economic and technological development, and dietary diversification have increased the demand for fish products, putting pressure on fish stocks (FAO 2022). Patterns of exploitation have expanded and a global trend towards overexploitation of fisheries resources has emerged. The proportion of global fisheries stocks within biologically sustainable levels was 64.6% in 2019 (FAO 2022), while in European waters, recent assessments show that 69% of stocks are subject to persistent overfishing and half of them are outside safe biological limits (Froese et al. 2018). In the Mediterranean and the Black Sea, 83% of assessed stocks were classified as overfished (Froese et al. 2018). It should be noted that the above figures do not take into account stocks of non-target species of low commercial value which are fished as bycatch and are often not assessed because their catch data are generally lacking (Tsikliras et al. 2021).

Although their effect is often overlooked, small-scale fisheries (SSF) contribute to the stock exploitation status, as they provide more than a quarter of the global marine fisheries catch and supply almost half of the landings intended for human consumption (FAO 2022). Nevertheless, the social, economic, and cultural importance of SSF to coastal communities is disproportionately higher than its impact on fish and invertebrate stocks (Jacquet and Pauly 2008; Palmer et al. 2017), since they employ 90% of the fisheries workforce globally, either directly on-board vessels or in parallel inshore activities. In the Mediterranean Sea, SSF mainly consist of small-sized vessels (usually < 12 m) that undertake short fishing trips (1–3 days), have a crew of 1–3 people, family-owned capital, and a small investment in vessel equipment and fishing gears (Gil et al. 2018; Liontakis et al. 2020). In Greece, SSF provide income and employment to the local communities in coastal areas and several remote islands, while being recognized as part of local cultural heritage and are closely linked to local traditions (Liontakis et al. 2020; Tzanatos et al. 2020).

The Mediterranean SSF are characterized by their multi-species and multi-gear nature (Stergiou et al. 2016). Different species are targeted seasonally and locally according to market demand, resource availability, and possible local restrictions, leading to the use of many different fishing gears and techniques (Maynou et al. 2011; Palmer et al. 2017). Among the variety of fishing gears used in Mediterranean SSF, set nets (trammel nets and gillnets) are the most popular (García-Rodríguez et al. 2006; Lucchetti et al. 2020). This is also true for Greek SSF as trammel nets and gillnets are used throughout the country and constitute the main component of the most common *métiers*, namely those targeting red mullets (*Mullus* spp.), cuttlefish (*Sepia officinalis*), common sole (*Solea solea* (Linnaeus, 1758)) and caramote prawn (*Penaeus kerathurus*) (Adamidou 2007).

Although the fishing gears employed in SSF (mostly passive gears) are considered to be more size and species selective, have a moderate to low discard rate (Kelleher 2005), and are less damaging to stocks and habitats than the towed gears used in large-scale fisheries (Huse et al. 2000; Stergiou et al. 2002), the total amount of discards they produce should not be ignored, considering a large number of vessels in the sector (Bellido et al. 2011; Sartor et al. 2018). Fish retained by fishing gear is usually an unknown proportion of the various size classes available in the exploited population. The probability of catching and retaining a given size of fish with a given mesh size (or hook) is defined as selectivity (Kitahara 1971) and is represented by a selectivity curve. The selectivity of a fishing gear describes the catching capacity and efficiency of the gear. It can be used to minimize the likelihood of catching non-targeted unwanted species or species of certain age groups by modifying the selective characteristics of fishing gears. Apart from that, it is also used to estimate population length frequency distribution, as well as length at age (Millar and Fryer 1999).

The most important aspect of gear selectivity is that it is directly associated with fisheries management since fishing regulations based on allowable mesh sizes require precise knowledge of gear selectivity. Up to now, the majority of fisheries in the Mediterranean Sea are managed by controlling the fishing effort and by technical measures (closed areas and seasons, minimum landing size, minimum mesh sizes) (Lucchetti et al. 2020). The latest reform of the Common Fisheries Policy (CFP) intends to reduce overfishing, enable the transition to low-impact fisheries and create strong incentives for fishers to move to more selective fishing practices by modifying their traditional fishing gears to improve their size and species selection (EU Regulation 1380/2013). Through that, the main goals are to restore and maintain populations of all commercial fish stocks above the biomass level that allows maximum sustainable yield (MSY) (Article 2, point 2 of EU Regulation 1380/2013), and to eliminate discards and reduce unwanted catches through the landing obligation of all catches of species subject to the minimum conservation reference size (MCRS), previously known as minimum landing size (Article 15 of EU Reg.1380/2013).

In the Mediterranean Sea, several studies have investigated the selectivity of fishing gears with the aim of reducing bycatch of undersized species, both commercial and non-commercial. The vast majority of the studies (>70%) concerned the bottom trawls targeting finfish (Sala and Lucchetti 2011; Özbilgin et al. 2012) or crustaceans (Guijarro and Massutí 2006; Kaykaç et al. 2009). Studies on the selectivity of SSF gears were mainly related to gillnets and investigated the effects of different mesh sizes (Petrakis and Stergiou 1995; Sbrana et al. 2007) and twine thickness/material (Ayaz et al. 2011). Few studies compared the selectivity of gillnets and trammel nets (Fabi et al. 2002; Karakulak and Erk 2008), while an overview of gill net and trammel net size selectivity in the Mediterranean has been published (Lucchetti et al. 2020). Regarding trammel nets, although they are the most important fishing gears of the Mediterranean small-scale fisheries (Lucchetti et al. 2020), there are very few studies that refer to their size selectivity and most assess the impact of selectivity on target species (Erzini et al. 2006; Kalaycı and Yeşilçiçek 2012; Bolat and Tan 2017); thus, information on bycatch remains scarce.

The objective of this study is to assess the impact of trammel net size selectivity on both target and bycatch species in SSF of the northern Aegean Sea. The selectivity parameters for the most abundant target and bycatch species were calculated and compared for different mesh sizes aiming to propose the most appropriate mesh size on a species basis that will ensure the sustainability of key *métiers* of SSF and minimize their negative effects on fish stocks.

Materials and methods

Experimental nets and fishing operation. The sea trials were conducted seasonally, from April 2016 to February 2017, for 5 successive days each season (20 sea trials in total), on board a chartered commercial SSF fleet vessel (8.5 m in length, 4.3 GT, 45 HP). The study area was Strymonikos Gulf in the western part of the northern Aegean Sea (Fig. 1).

The data were collected during a trammel net selectivity survey. The technical characteristics and the structure of trammel nets are described in the literature (He et al. 2021) as well as their dominant catching mechanism, the pocketing (Fabi et al. 2002), and the other ways in which a fish can be caught in a net, namely gilled, wedged, or entangled (Ricker 1975 and references therein).

Thirty bottom-set trammel nets were used, all newly made for the study. Ten different combinations of inner and outer panel mesh sizes were used as follows: 16/100 mm, 19/100 mm, 22/110 mm, 26/130 mm, 30/150 mm, 36/160 mm, 42/180 mm, 50/200 mm, 60/240 mm, 70/265 mm (bar length of inner/outer sheets of trammel nets). Mesh size increased following a geometric order, depending on the commercial availability. All nets were made with the same net type and twine diameter. Multifilament nylon (PA) twine, of 0.23 mm thickness was used for the inner sheets of the trammel nets, whereas for the outer sheets, the twine thickness ranged from 0.36 mm to 0.45 mm depending on mesh size. All nets had almost the same length (100 m stretched/50 m mounted) and depth (1.5 m stretched), therefore the fishing effort was considered the same for all mesh sizes. Also, the inner sheets of the trammel nets were of the same depth for all mesh sizes, greater than that of outer panels, in order to have the same slack with the outer panels (Holst et al. 1998) (see Suppl. material 1). The float lines were made of 5 mm diameter braided rope and were approximately 50 m long. Floats of expanded polystyrene were used giving a buoyancy of 34.3 g/m. The lead lines were made of 4 mm diameter braided rope, with leads inside weighing 80 g/m. The lead lines were about 1.15% longer than the float lines. The hanging ratio was 0.50 on the headline and 0.51 on the lead line.

The nets were rigged in 3 fleets of 10 nets each with different mesh sizes. The position of each net in the fleet was determined randomly and no net had the same

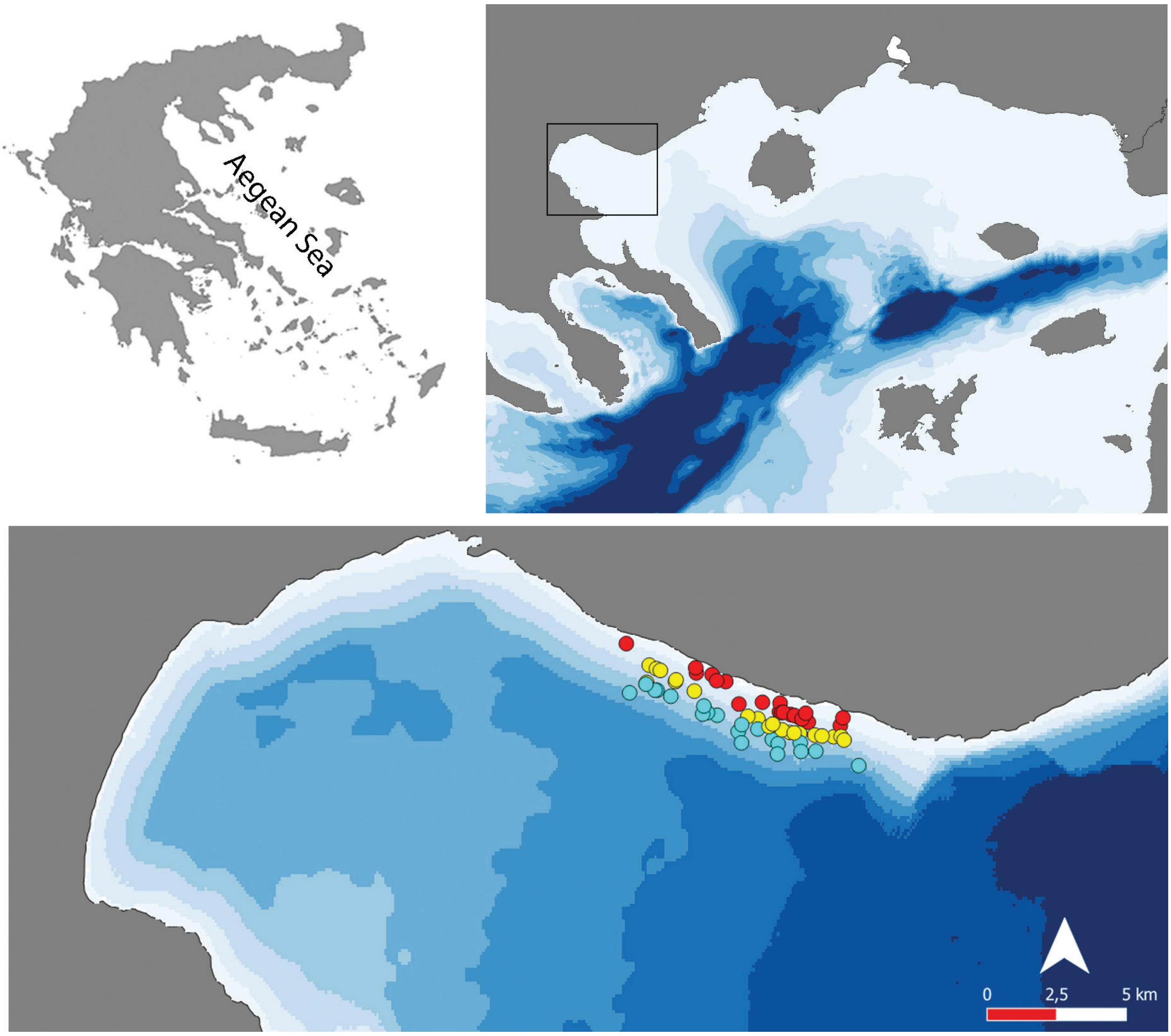

Figure 1. Map of the study area showing also the haul positions during the fishing trials. The different colors correspond to different depth zones (red: 0–20 m, yellow: 20–40 m, turquoise: 40–60 m).

position in the three fleets, to reduce possible interaction between nets of different efficiency (Millar 1992). Also, the end positions of the fleets were occupied by all types of different mesh sizes (as possible). There were escape areas of 1.5 m between the adjacent nets to avoid any guiding effect from one net to the next (Holst et al. 1998). The nets were deployed from the coastline to a depth of 60 m, as coastal fisheries in the area typically exploit these depths, in three depth zones (0–20 m, 20–40 m, and 40–60 m), one fleet in each depth zone, to investigate any possible effect of depth in net selectivity. The fleets were deployed simultaneously, set late in the afternoon (17:00–19:00), and hauled the following morning (05:00–07:00) according to commercial practices, with an average soaking time of 12 h.

Upon retrieval, the entire catch was sorted according to the fleet, net type, and mesh size, and marine organisms were classified to the species level. An additional sorting into target and bycatch fraction was done by the fisher, with no interference from researchers on board. The method of capture was recorded as far as it was possible. Given that several target and bycatch species were caught in the experimental sea trials, it was not practically possible to record the method of capture of each fish. In addition, some species (e.g., greater weever) were still very mobile even after capture, which caused the net to rotate around their body, making it difficult to determine the method of capture. For other species (e.g., black scorpionfish) which appeared to be gilled or enmeshed, the net was also collected in the spines and rays, so it was also difficult to determine the method of capture.

Total weight and number were recorded for the catch of each species per fleet, and mesh size while specific measurements for each individual were recorded in the laboratory. The total length (TL, cm) and body girth (G, cm) for fishes and dorsal mantle length (DML, cm) for cephalopods were measured to the nearest 0.1 cm and the carapace length (CL, cm) for crustaceans to the nearest 0.01 cm, the individual total weight (W, g) was measured to nearest 0.01 g. The taxonomy and nomenclature of the species are according to FishBase (Froese and Pauly 2022).

Data analysis. Due to the small sample per species, a temporal (by season) or spatial (by depth stratum) stratified selectivity analysis was not possible; thus, data from all sampling periods and depth strata were pooled together into a single dataset per species. Length frequency distributions (LFDs) were estimated for all species (1 cm size classes or 2 cm size classes for species with a wide length range) per mesh size. In order to use the proper parametric (ANOVA) or non-parametric test (Kruskal–Wallis) for the comparison of the mean/median TL among different mesh sizes the normality of the TL data per species was tested with a Shapiro–Wilk normality test. Based on the outcome either one-way analysis of variance (ANOVA) or the non-parametric Kruskal–Wallis test was applied. Additionally, paired Kolmogorov–Smirnov (K–S) test with a significance level of ±95% ($\alpha = 0.05$) was applied to compare the LFDs by different mesh sizes per species. The proportion of fish below the minimum conservation reference size (MCRS, according to EU regulation and the national legislation) and the length at first maturity (L_m) obtained from the literature, were also calculated for each species and mesh size. As mentioned above, fish are caught in trammel nets in four different ways. Two of them (gilling and wedging) are related to their body size, while the other two (entanglement and entrapment) are independent of it. When estimating selectivity, it is important to know whether fish were gilled/wedged or entangled/entrapped. Therefore, the ratio of gill (GG/MP) and maximum girth (MG/MP) to mesh perimeter were calculated for all species and mesh sizes to investigate the method of capture of each species at different mesh sizes and to confirm the observed method of capture.

Selectivity estimation. When the length distribution of the fished population is known, a direct estimation of the selectivity can be applied (Hamley 1975). This is possible for towed gears by collecting the individuals that escape from the codend to the codend cover. In passive gears (nets, longlines) it is impossible to collect escaping fish to estimate the actual size of the population on the fishing ground, and therefore an indirect estimation is most frequently used (Millar 1992; Madsen et al. 1999). This process usually involves deploying several nets/longlines, all of the same size, and different mesh/hook sizes in random order, fishing simultaneously on the same population with equal effort. The selectivity is then estimated by comparing the observed catch frequencies across the several meshes/hooks used (Millar 1992). This procedure was followed in the presently reported experimental survey.

The trammel net selectivity was estimated using the SELECT (Share Each Length's Catch Total) method, initially developed for trawling (Millar 1992) and then extended to set nets and hooks (Millar and Holst 1997), by which the expected catch proportions are fitted to the observed catch proportions using maximum likelihood which also allows the between-haul variability to be taken into account (Millar and Fryer 1999). SELECT method is described by the equation

$$n_{lj} \sim Po(p_j \cdot \lambda_l \cdot r_j\,(l)) \text{ and the log-likelihood of } n_{lj} \text{ is}$$

$$\textstyle\sum_l \cdot \sum_j \{n_l \, log_e \, [(p_j \cdot \lambda_l \cdot r_j\,(l)) - (p_j \cdot \lambda_l \cdot r_j\,(l))]\}$$

where n_{lj}: the number of fish of length l caught in mesh size j; λ_l the abundance of length l fish contacting the gear; p_j: the relative fishing intensity of the net of mesh size j; $r_j\,(l)$: the retention probability of length l fish in the mesh size j.

Five different patterns of selectivity were applied and tested to the data, corresponding to five functions, four unimodal: the normal location (modal length proportional to mesh size, spread fixed), normal scale, gamma and lognormal, and one bimodal (Bi-normal):

$$\text{Normal location } (k, \sigma) \ \exp\left(-\frac{(l - k{\cdot}m_j)^2}{2\sigma^2}\right)$$

$$\text{Normal scale } (k_1, k_2) \ \exp\left(-\frac{(l - k_1{\cdot}m_j)^2}{2k_2{\cdot}m_j^2}\right)$$

$$\text{Log normal } (\mu, \sigma)$$

$$\frac{1}{l}\exp\left(\mu_1 + \log\left(\frac{m_j}{m_1}\right) - \frac{\sigma^2}{2} \quad \frac{\left(\log(l) - \mu_1 - \log\left(\frac{m_j}{m_1}\right)\right)^2}{2\sigma^2}\right)$$

$$\text{Gamma } (\alpha, k) \left(\frac{l}{(\alpha - 1)k{\cdot}m_j}\right)^{\alpha - 1} \exp\left(\alpha - 1 - \frac{l}{k{\cdot}m_j}\right)$$

$$\text{Bi-normal } (k_1, k_2, k_3, k_4, c)$$

$$\exp\left(-\frac{(l - k_1{\cdot}m_j)^2}{2k_2^2{\cdot}m_j^2}\right) + c.\exp\left(-\frac{(l - k_3{\cdot}m_j)^2}{2k_4^2{\cdot}m_j^2}\right)$$

where m_j is the mesh size j, μ is the mean size (modal length) of fish caught, σ is the standard deviation of the size of fish (spread), and k, k_1, k_2, k_3, k_4, and c, are selection parameters or constants.

For the selectivity curves, it was assumed that the number of fish of length class l encountering the gear was Poisson distributed; each net was equally efficient at catching fish of optimum/modal length, and hence the selectivity curves are all of the same height; the selection curve follows Baranov's principle of geometrical similarity according to which modal length and spread (SD) of the fish caught increase proportionally to mesh size (Ricker 1975 and references therein). This assumption was not followed only when a normal location function, which assumes a fixed spread, was applied.

For the estimation of the selectivity curves, species with a sufficient number of individuals are needed. Therefore, species with a low number of captured specimens ($n \leq 70$) or low representation in mesh sizes (present in less than 3 different mesh sizes) were excluded from the analysis (Millar and Fryer 1999). For the validation of the goodness of fit, the model deviance (D) was calculated using all length classes with nonzero catch and the mesh sizes for which selectivity curves could be estimated ($n > 5$). The degrees of freedom (df) were also computed automatically. The best-fitting model was the one with the lowest value of deviance and dispersion parameter i.e., ratio $D/\text{df} \leq 1$ (Holst et al. 1998). Model fitting was also evaluated based on visual inspection of model diagnostics, such as the residual deviance plots. All estimations were performed within an R programming environment (R Core Team 2022) through the function "*select_Millar*" from TropFishR package (Mildenberger et al. 2017).

Results

Length frequency distributions. During the experimental trials, a total of 3233 specimens (235.9 kg) of 94 species (84 fishes, 4 crustaceans, and 6 cephalopods) were caught in trammel nets. Despite the large number of species caught, the catch was dominated by a few species whose numbers of individuals were sufficient for further statistical analysis and which also met the criteria for estimating the selectivity curves. Analyses were therefore carried out for the eight most abundant fish species, which accounted for 51.5% by number and 42.7% by weight of the fish caught with trammel nets. These fish species were the black scorpionfish, *Scorpaena porcus* Linnaeus, 1758; annular seabream, *Diplodus annularis* (Linnaeus, 1758); red mullet, *Mullus barbatus* Linnaeus, 1758; surmullet, *Mullus surmuletus* Linnaeus, 1758; round sardinella, *Sardinella aurita* Valenciennes, 1847; European hake, *Merluccius merluccius* (Linnaeus, 1758); greater weever, *Trachinus draco* Linnaeus, 1758; and blotched picarel, *Spicara flexuosum* Rafinesque, 1810.

Their relative abundance in number (N) and total weight (TW) were as follows: black scorpionfish (13.9% N, 8.8% TW); annular seabream (13.1% N, 7.8% TW); red mullet (6.7% N, 5% TW); surmullet (5.3% N, 5% TW); round sardinella (5.5% N, 4.8% TW); European hake (2.1% N, 6.4% TW); greater weever (2.8% N, 3.8% TW) and blotched picarel (2% N, 1.1% TW) (Table 1). Red mullet and surmullet are the main target species for the trammel net fishery and the rest are bycatch species.

The length frequency distributions (LFDs) of the eight species studied, by mesh size, and from data pooled across all mesh sizes, are shown in Fig. 2. The majority of LFDs were skewed to the right, the shape of the LFD curve from pooled data appears to be bimodal for annular seabream, red mullet, and blotched picarel, unimodal for surmullet, round sardinella and black scorpionfish while for European hake and greater weever, the variability in numbers per length class seems to have hidden the modality pattern. In all cases, the LFDs of the different mesh sizes were overlapping to a greater or lesser extent depending on the species. The Kolmogorov–Smirnov (K–S) test for the mesh size paired comparisons on the LFDs per species, showed that the distributions were significantly different ($P < 0.05$) for surmullet (100%), black scorpionfish (80%; 8 of 10 combinations), round sardinella and blotched picarel (66.7%; 2 of 3 combinations, for both species), annular seabream and red mullet (60%; 9 of 15 and 6 of 10 combinations respectively), while were not significantly different ($P > 0.05$) for European hake (73.3%; 11 of 15 combinations) and greater weever (93.3%; 13 of 14 combinations) (see Suppl. material 2).

For the majority of the species, the abundance in number decreased with increasing mesh size, hence, four smaller mesh sizes (i.e., 16, 19, 22, and 26 mm bar length) were the most efficient in abundance and biomass catch rates (Table 1). The mean and median length and the mean weight of fish increased with mesh size

Table 1. Descriptive statistics of total length and weight for the eight most abundant species fished with trammel nets from April 2016 to February 2017 in the northern Aegean Sea, proportion of fish below MCRS and L_m and ratios of gill (GG/MP) and maximum girth (MG/MP) to mesh perimeter.

Species	MS [mm]	*n*	RF%	TL [cm] mean ± SD	TL [cm] median	TL [cm] min–max	% <MCRS	% <L_m	TW [kg]	% TW	*W* [g] mean ± SD	GG/MP	MG/MP
Annular seabream, *Diplodus annularis*	16	120	28.3	12.6 ± 2.29	13.1	8.3–18.1	32	24	4.4	23.9	36.7 ± 20.6	1.32	1.54
	19	101	23.8	13.4 ± 1.54	13.4	9.1–16.7	20	1	4.2	22.7	41.4 ± 17.0	1.17	1.37
	22	100	23.6	13.5 ± 1.32	13.3	10.0–17.3	7	1	4.2	22.6	42.2 ± 16.4	1.00	1.18
	26	89	21.0	14.7 ± 0.88	14.5	13.2–18.0	0	0	4.8	25.8	53.6 ± 12.0	0.96	1.12
	30	7	1.7	16.0 ± 1.18	16.5	13.7–16.9	0	0	0.5	2.9	75.9 ± 16.4	0.91	1.07
	36	5	1.2	14.7 ± 1.72	13.8	13.1–17.1	0	0	0.3	1.5	54.8 ± 22.5	0.69	0.80
	42	2	0.5	14.7 ± 1.63	14.7	13.5–15.8	0	0	0.1	0.6	55.4 ± 22.4	0.60	0.69
European hake, *Merluccius merluccius*	16	21	30.0	28.6 ± 5.13	27.5	17.8–38.5	5	62	4.0	26.3	198.4 ± 100.0	1.81	1.92
	19	9	12.9	27.4 ± 4.46	26.8	21.3–33.2	0	67	1.5	9.7	162.6 ± 85.2	1.37	1.47
	22	11	15.7	28.4 ± 6.01	26.5	22.2–41.3	0	73	2.1	13.9	190.0 ± 152.7	1.27	1.35
	26	19	27.1	32.0 ± 3.10	32.0	26.7–39.0	0	37	4.7	31.4	248.6 ± 85.3	1.21	1.27
	30	5	7.1	34.6 ± 3.57	36.1	28.3–37.0	0	20	1.6	10.8	325.1 ± 80.5	1.09	1.19
	36	3	4.3	33.9 ± 4.63	34.5	29.0–38.2	0	33	0.9	6.2	309.3 ± 123.5	0.96	1.00
	42	1	1.4	26.0	26.0		0	100	0.1	0.8	116.0	0.55	0.57
	50	1	1.4	27.8	27.8		0	100	0.1	1.0	146.7	0.50	0.55
Red mullet, *Mullus barbatus*	16	139	63.5	15.8 ± 2.01	15.1	12.5–22.0	0	1	6.0	51.7	43.7 ± 20.9	1.19	1.30
	19	36	16.4	18.3 ± 1.66	18.5	15.3–23.9	0	0	2.5	21.1	70.3 ± 23.8	1.18	1.30
	22	31	14.2	18.1 ± 1.72	18.2	12.0–21.0	0	3	2.1	17.8	66.8 ± 16.5	1.02	1.10
	26	10	4.6	20.2 ± 2.64	20.8	14.6–22.7	0	0	0.9	7.9	91.9 ± 29.7	0.96	1.02
	30	3	1.4	16.9 ± 2.93	18.1	13.6–19.1	0	0	0.2	1.5	58.0 ± 24.5	0.69	0.75
Surmullet, *Mullus surmuletus*	16	82	47.7	16.9 ± 2.34	17.2	11.7–22.5	0	31	4.8	41.5	59.0 ± 26.4	1.33	1.43
	19	45	26.2	17.7 ± 1.61	17.8	15.2–22.0	0	4	3.0	26.1	67.5 ± 21.7	1.15	1.27
	22	38	22.1	18.8 ± 1.68	18.6	16.2–22.5	0	0	3.1	26.2	82.4 ± 23.6	1.08	1.18
	26	5	2.9	21.4 ± 0.65	21.6	20.4–22.0	0	0	0.6	5.2	122.3 ± 15.9	1.03	1.14
	30	1	0.6	17.1	17.1		0	0	0.1	0.5	63.1	0.75	0.84
	36	1	0.6	15.8	15.8		0	0	0.0	0.4	49.7	0.58	0.63
Round sardinella, *Sardinella aurita*	16	63	35.6	19.9 ± 1.25	20.0	16.9–22.4	0	0	3.6	32.4	58.1 ± 12.3	1.22	1.36
	19	58	32.8	20.3 ± 0.96	20.2	18.8–23.1	0	0	3.4	30.7	59.9 ± 8.5	1.04	1.13
	22	56	31.6	21.5 ± 0.96	21.4	19.5–23.8	0	0	4.1	36.9	75.9 ± 8.7	0.95	1.09
Black scorpionfish, *Scorpaena porcus*	16	112	24.8	12.6 ± 1.55	12.5	8.5–16.5	0	96	4.3	20.8	38.9 ± 14.5	1.36	1.47
	19	148	32.8	12.7 ± 1.54	12.5	9.9–18.6	0	95	5.9	28.8	40.0 ± 16.1	1.13	1.23
	22	139	30.8	13.6 ± 1.52	13.4	9.3–10.7	0	90	6.7	32.6	48.3 ± 20.4	1.04	1.13
	26	40	8.9	15.1 ± 1.82	14.7	12.1–20.0	0	70	2.6	12.8	67.6 ± 28.2	1.00	1.07
	30	10	2.2	15.6 ± 3.40	16.4	10.4–20.1	0	30	0.8	3.8	77.3 ± 41.4	0.91	0.97
	42	2	0.4	18.6 ± 4.60	18.6	21.8–37.1	0	0	0.3	1.3	136.5 ± 102.9	0.77	0.83
Blotched picarel, *Spicara flexuosum*	16	43	61.4	14.7 ± 1.55	15.0	11.5–17.8	0	0	1.4	55.4	32.5 ± 10.2	1.07	1.23
	19	23	32.9	16.2 ± 0.77	15.9	14.6–17.8	0	0	0.9	37.0	42.5 ± 5.6	1.00	1.13
	22	4	5.7	16.8 ± 0.45	16.9	16.1–17.1	0	0	0.2	7.6	47.8 ± 4.0	0.95	1.05
Greater weever, *Trachinus draco*	16	9	9.8	21.6 ± 3.87	20.5	15.5–27.8	0	11	0.7	7.6	78.1 ± 37.7	1.29	1.45
	19	46	50.0	23.5 ± 3.88	23.6	15.3–31.4	0	11	4.4	57.2	95.3 ± 48.4	1.17	1.29
	22	8	8.7	23.8 ± 3.07	23.1	19.7–28.7	0	0	0.8	8.4	97.5 ± 35.9	1.01	1.11
	26	8	8.7	27.2 ± 3.29	27.8	23.2–31.5	0	0	1.2	12.6	146.6 ± 65.0	0.98	1.07
	30	8	8.7	23.7 ± 7.27	26.0	14.5–32.7	0	38	1.0	11.1	129.1 ± 99.2	0.76	0.87
	36	9	9.8	21.9 ± 5.07	20.4	13.4–30.0	0	11	0.7	7.6	78.4 ± 54.4	0.57	0.63
	42	1	1.1	26.2	26.2		0	0	0.1	1.3	123.3	0.60	0.62
	50	1	1.1	19.5	19.5		0	0	0.0	0.4	41.3	0.36	0.37
	60	2	2.2	28.2 ± 0.71	28.2	27.7–28.7	0	0	0.4	3.8	175.2 ± 50.1	0.47	0.54

MS = mesh size (bar length), *n* = number of fish, RF% = relative frequency, TL = total length, SD = standard deviation, MCRS = minimum conservation reference size, L_m = length at maturity, TW = total weight, *W* = individual weight, GG = gill girth, MG = maximum girth; MP = mesh perimeter).

for round sardinella, black scorpionfish, and blotched picarel and with slight variations for annular seabream, red mullet, and surmullet (Table 1). For European hake, a wide range of sizes was caught with few individuals per length class for each mesh size; the mean length of hake tended to increase with increasing mesh size, however, there was no clear relation between mesh size and fish length (Table 1). For greater weever, the larger proportion of catch was collected in one mesh size (19 mm) while similar proportions were caught in the remaining mesh sizes with no clear relation between mesh size and fish size. The mean length tended to increase with increasing mesh size only for the four smaller mesh sizes (Table 1). A statistically significant difference among the mean fish length of the different mesh sizes was observed for European hake (ANOVA: $F = 2.58$, $P = 0.02$), surmullet (ANOVA: $F = 8.83$, $P = 0.00$), round sardinella (ANOVA: $F = 37.78$, $P = 0.00$) and among the median fish length for annular seabream (Kruskal–Wallis: $H = 85.38$, $P = 0.00$), red mullet

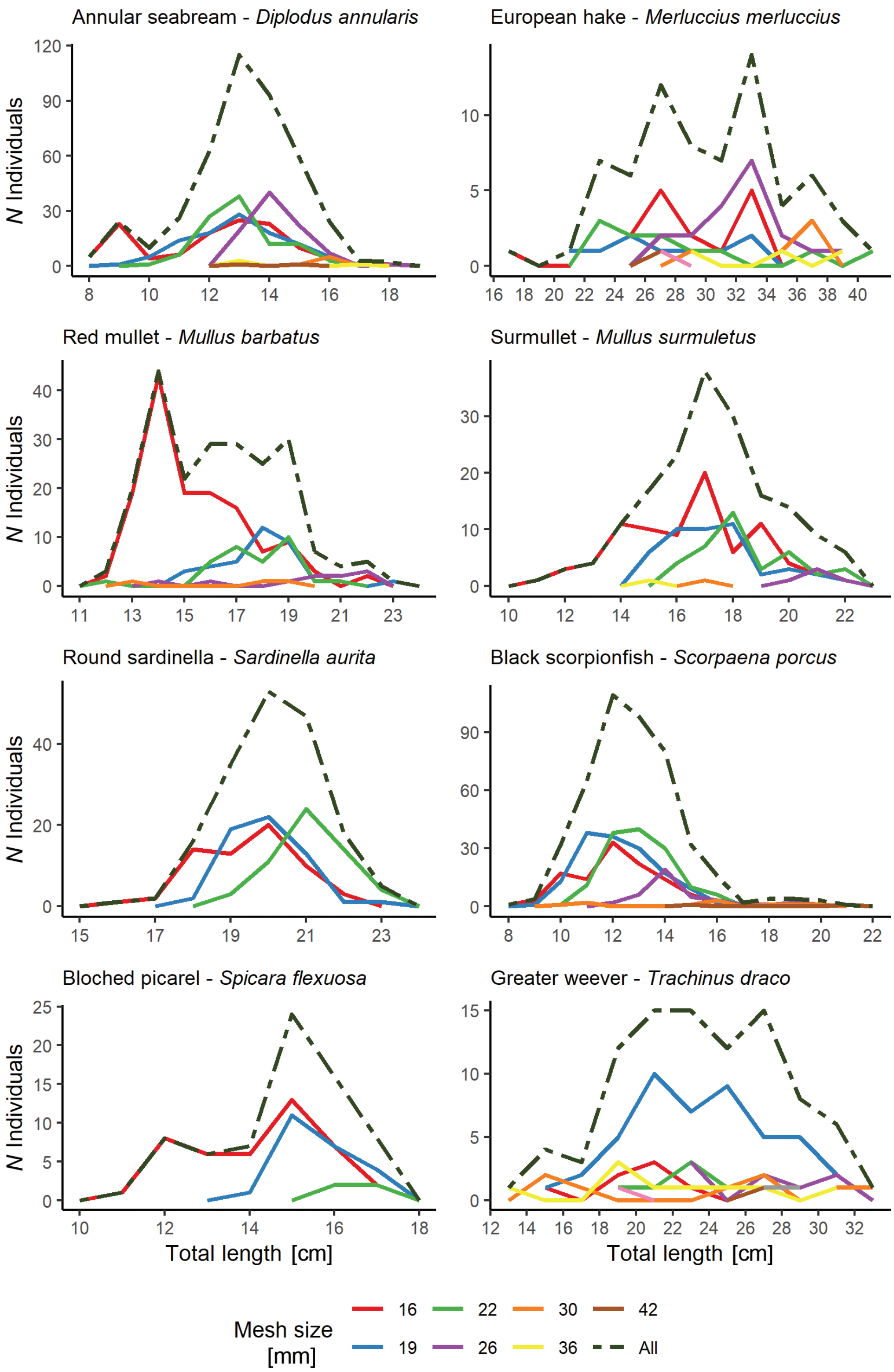

Figure 2. Length frequency distributions per mesh size and from pooled data across all mesh sizes for the eight most abundant species fished in trammel nets from April 2016 to February 2017 in the northern Aegean Sea (eastern Mediterranean Sea).

(Kruskal–Wallis: $H = 68.63$, $P = 0.00$), black scorpionfish (Kruskal–Wallis: $H = 83.18$, $P = 0.00$), blotched picarel (Kruskal–Wallis: $H = 21.35$, $P = 0.00$). No statistically significant difference was observed for greater weever (ANOVA: $F = 1.58$, $P = 0.14$).

The GG/MP and MG/MP ratios indicated that in some cases fishes were caught in mesh sizes larger than expected (e.g., annular seabream in 36 and 42 mm mesh sizes, red mullet in 30 mm mesh, and surmullet in 30 and 36 mm mesh sizes) or smaller than expected (e.g., annular seabream, red mullet, surmullet, in 16 and 19 mm mesh sizes and round sardinella, black scorpionfish in 16 mm mesh size) (Table 1), which indicate that a certain number of individuals of these species were caught entangled by maxillaries and teeth or entrapped/pocketed. For European hake and greater weever, the GG/MP and MG/MP ratios indicate that both fishes were caught in mesh sizes larger than expected (European hake in 42 and

50 mm mesh size and greater weever in 30, 36, 42, 50, 60 mm mesh sizes) and smaller than expected (European hake in 16 and 19 mm mesh size and greater weever in 16 mm mesh size) (Table 1) confirming capture in nets other than gilled or wedged.

Only some individuals of annular seabream (30%, 20%, and 7% at mesh sizes 16, 19, and 22 mm respectively) and to a lesser extent European hake (5% at mesh size 16 mm) were recorded below the minimum conservation reference size (MCRS) (Table 1). However, when examining the fish size in relation to size at first maturity (L_m), the entire catch was above L_m only for round sardinella and blotched picarel and most of the catch for red mullet. For European hake and black scorpionfish, most of the catch was below the L_m, for annular seabream and surmullet a considerable part of the catch was below the L_m at the smaller mesh size, and for greater weever different proportions were below the L_m at different mesh sizes (Table 1).

Estimation of the selectivity parameters. The selectivity parameters were estimated per species for each of the tested selectivity functions (Table 2). The bimodal function provided the best fit having the lowest deviance value for all species and the lowest values for dispersion parameter (D/df) for all species except greater weever. Over-dispersion was observed for red mullet, round sardinella, and greater weever. The fitted selectivity curves and the corresponding deviance residuals are shown in Fig. 3. The first mode of the selectivity curves corresponds to fish that were gilled or wedged, while the second mode describes the selectivity associated with fish that are entangled or entrapped/pocketed. The residual plots reveal that for annular seabream the fishing power of the mesh size 36 mm was greater (positive residuals) while that of the mesh size 30 mm was lower (negative residuals) than modeled. For red mullet the fishing power of mesh sizes 22 mm (for the smaller length classes) and 26 mm (for the larger length classes) were great-

Table 2. Selectivity parameters estimates resulting from the use of four uni-modal and one bi-modal models, with the corresponding deviances, degrees of freedom, and the mesh sizes whose catch was used in estimating the selectivity parameters for the eight most abundant species fished with trammel nets from April 2016 to February 2017 in the northern Aegean Sea (eastern Mediterranean Sea).

Species	Model	Parameters	Deviance	df	*D*/df	Mesh sizes
Annular seabream, *Diplodus annularis*	Normal location	$(k, \sigma) = (0.686, 3.366)$	166.41	53	3.14	16, 19, 22, 26, 30, 36
	Normal scale	$(k_1, k_2) = (0.743, 0.022)$	206.62	53	3.90	
	Log normal	$(\mu, \sigma) = (2.476, 0.211)$	162.87	53	3.07	
	Gamma	$(\alpha, k) = (22.533, 0.033)$	174.83	53	3.30	
	Bi-modal	$(k_1, k_2, k_3, k_4, c) = (0.582, 0.035, 0.861, 0.167, 0.601)$	**60.82**	50	1.22	
European hake, *Merluccius merluccius*	Normal location	$(k, \sigma) = (1.463, 9.173)$	51.11	46	1.24	16, 19, 22, 26, 30
	Normal scale	$(k_1, k_2) = (1.668, 0.261)$	62.85	46	1.37	
	Log normal	$(\mu, \sigma) = (3.302, 0.313)$	52.15	46	1.26	
	Gamma	$(\alpha, k) = (10.889, 0.158)$	59.67	46	1.30	
	Bi-modal	$(k_1, k_2, k_3, k_4, c) = (1.219, 0.123, 2.017, 0.395, 0.521)$	**46.25**	43	1.08	
Red mullet, *Mullus barbatus*	Normal location	$(k, \sigma) = (1.053, 3.446)$	105.51	34	3.10	16, 19, 22, 26
	Normal scale	$(k_1, k_2) = (1.079, 0.024)$	90.30	34	2.66	
	Log normal	$(\mu, \sigma) = (2.873, 0.174)$	87.19	34	2.56	
	Gamma	$(\alpha, k) = (38.979, 0.028)$	87.26	34	2.57	
	Bi-modal	$(k_1, k_2, k_3, k_4, c) = (0.965, 0.092, 1.412, 0.262, 0.448)$	**75.10**	31	2.42	
Surmullet, *Mullus surmuletus*	Normal location	$(k, \sigma) = (1.036, 3.465)$	50.33	34	1.48	16, 19, 22, 26
	Normal scale	$(k_1, k_2) = (1.080, 0.030)$	59.69	34	1.76	
	Log normal	$(\mu, \sigma) = (2.857, 0.178)$	49.52	34	1.46	
	Gamma	$(\alpha, k) = (34.738, 0.032)$	52.43	34	1.54	
	Bi-modal	$(k_1, k_2, k_3, k_4, c) = (0.833, 0.066, 1.193, 0.151, 0.425)$	**31.63**	31	1.02	
Round sardinella, *Sardinella aurita*	Normal location	$(k, \sigma) = (1.093, 2.816)$	40.10	14	2.86	16, 19, 22
	Normal scale	$(k_1, k_2) = (1.127, 0.025)$	44.12	14	3.15	
	Log normal	$(\mu, \sigma) = (2.896, 0.138)$	40.33	14	2.88	
	Gamma	$(\alpha, k) = (53.227, 0.021)$	41.54	14	2.97	
	Bi-modal	$(k_1, k_2, k_3, k_4, c) = (1.027, 0.037, 1.252, 0.105, 0.598)$	**26.94**	11	2.45	
Black scorpionfish, *Scorpaena porcus*	Normal location	$(k, \sigma) = (0.692, 2.807)$	83.19	54	1.54	16, 19, 22, 26, 30
	Normal scale	$(k_1, k_2) = (0.726, 0.017)$	120.32	54	2.23	
	Log normal	$(\mu, \sigma) = (2.453, 0.193)$	94.78	54	1.76	
	Gamma	$(\alpha, k) = (29.045, 0.025)$	101.13	54	1.87	
	Bi-modal	$(k_1, k_2, k_3, k_4, c) = (0.608, 0.047, 0.814, 0.142, 0.539)$	**46.85**	47	1.00	
Blotched picarel, *Spicara flexuosum*	Normal location	$(k, \sigma) = (0.919, 1.760)$	5.36	12	0.45	16, 19, 22
	Normal scale	$(k_1, k_2) = (0.934, 0.009)$	6.83	12	0.57	
	Log normal	$(\mu, \sigma) = (2.706, 0.106)$	4.65	12	0.39	
	Gamma	$(\alpha, k) = (94.074, 0.010)$	5.27	12	0.44	
	Bi-modal	$(k_1, k_2, k_3, k_4, c) = (0.829, 0.041, 0.980, 0.082, 0.406)$	**1.58**	9	0.18	
Greater weever, *Trachinus draco*	Normal location	$(k, \sigma) = (1.270, 2.574)$	55.07	31	1.78	16, 19, 22, 26
	Normal scale	$(k_1, k_2) = (3.305, 0.068)$	56.75	31	1.83	
	Log normal	$(\mu, \sigma) = (3.050, 0.221)$	55.98	31	1.81	
	Gamma	$(\alpha, k) = (22.746, 0.059)$	56.05	31	1.81	
	Bi-modal	$(k_1, k_2, k_3, k_4, c) = (1.222, 0.207, 1.604, 0.081, 0.569)$	**54.10**	22	2.46	

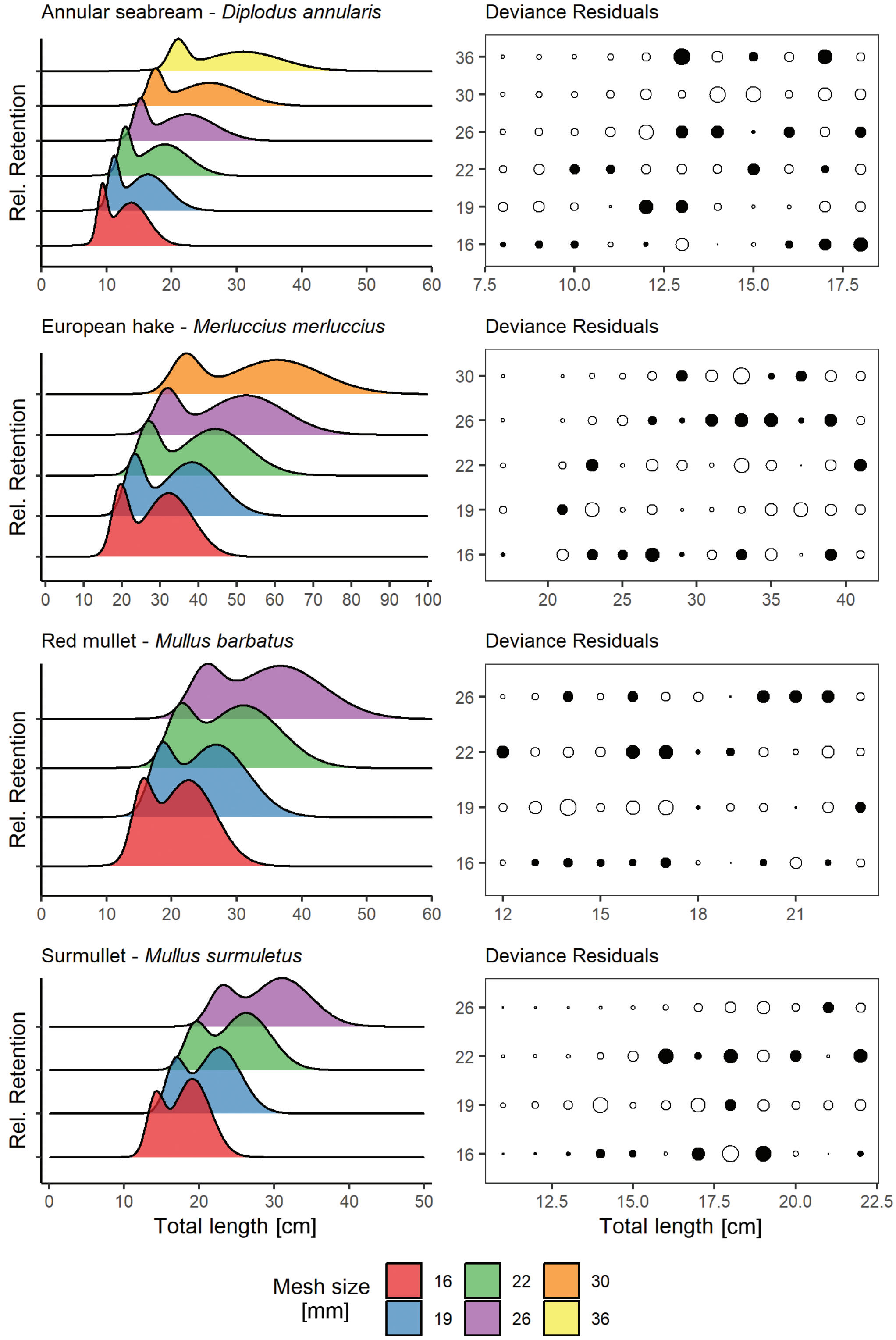

Figure 3. Selectivity curves for the eight most abundant species fished from April 2016 to February 2017 in trammel nets in the northern Aegean Sea (eastern Mediterranean Sea), and the respective deviance residual plots. Full circle indicates a positive residual and open circle a negative residual. Bubble size proportional to the residual value. [Figure continues on next page.]

er than expected (positive residuals), while that of the mesh size 19 mm (for the smaller length classes) lower than expected (negative residuals). For round sardinella the fishing power of the mesh size 19 mm was lower than modeled (negative residuals). For greater weever, the residuals had a non-random pattern, especially for mesh size 19 mm. The estimated modal lengths and spreads of the eight species studied, by mesh size, for the best-fit model are shown in Table 3. Modal length increased with mesh size as well as spread, following Baranov’s principle (Ricker 1975) of geometrical similarity, but varied by species.

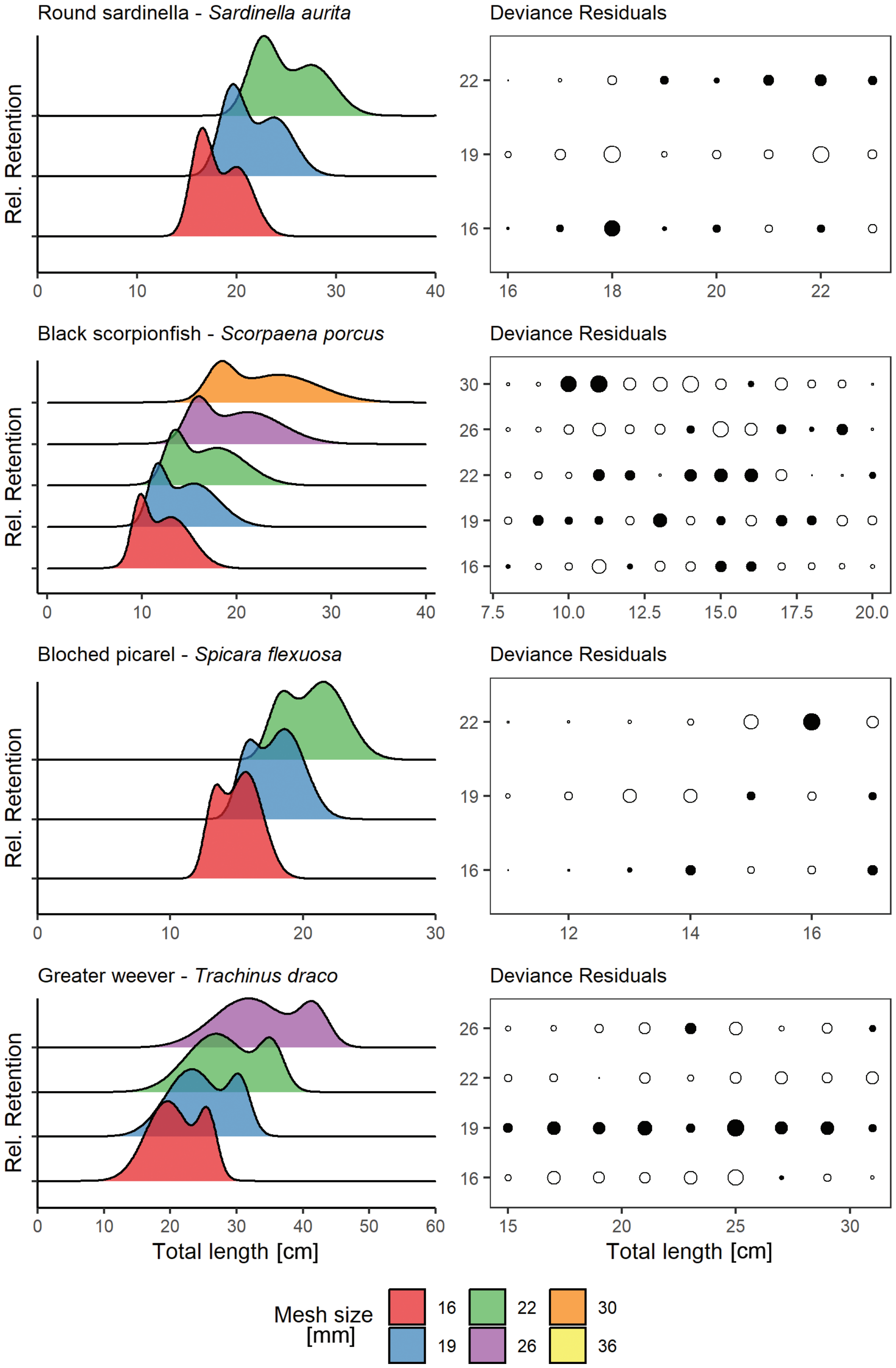

Figure 3 (Continuation). Selectivity curves for the eight most abundant species fished from April 2016 to February 2017 in trammel nets in the northern Aegean Sea (eastern Mediterranean Sea), and the respective deviance residual plots. Full circle indicates a positive residual and open circle a negative residual. Bubble size proportional to the residual value.

Discussion

The presently reported study analyzed the catch rates, length frequency distributions, and size selectivity of the eight most abundant fish species caught with trammel nets in the northern Aegean Sea (black scorpionfish, *Scorpaena porcus*; annular seabream, *Diplodus annularis*; red mullet, *Mullus barbatus*; surmullet, *Mullus surmuletus*; round sardinella, *Sardinella aurita*; European hake, *Merluccius merluccius*; greater weever, *Trachinus draco*; and blotched picarel, *Spicara flexuosum*). An attempt was made to match the technical characteristics

Table 3. Modal length and spread values, by mesh size, for the best-fit model for each of the eight most abundant species fished from April 2016 to February 2017 with trammel nets in the northern Aegean Sea (eastern Mediterranean Sea).

Species	Model	Mesh size (bar length) [mm]	Modal length	Spread
Annular seabream, *Diplodus annularis*	Bi-modal	16	9.31	0.56
		19	11.06	0.67
		22	12.80	0.77
		26	15.13	0.91
		30	17.46	1.05
		36	20.95	1.26
European hake, *Merluccius merluccius*	Bi-modal	16	19.50	1.96
		19	23.16	2.33
		22	26.81	2.70
		26	31.69	3.19
		30	36.56	3.68
Red mullet, *Mullus barbatus*	Bi-modal	16	15.44	1.47
		19	18.33	1.74
		22	21.22	2.02
		26	25.08	2.38
Surmullet, *Mullus surmuletus*	Bi-modal	16	14.14	1.05
		19	16.79	1.25
		22	19.44	1.44
		26	22.97	1.71
Round sardinella, *Sardinella aurita*	Bi-modal	16	16.43	1.07
		19	19.51	1.27
		22	22.59	1.47
Black scorpionfish, *Scorpaena porcus*	Bi-modal	16	9.73	0.75
		19	11.55	0.88
		22	13.37	1.02
		26	15.81	1.21
		30	18.24	1.40
Blotched picarel, *Spicara flexuosum*	Bi-modal	16	13.27	0.66
		19	15.76	0.78
		22	18.24	0.90
Greater weever, *Trachinus draco*	Bi-modal	16	19.56	3.32
		19	23.22	3.94
		22	26.89	4.56
		26	31.78	5.39

of the experimental nets as closely as possible to those used in Greek commercial fisheries in order to achieve compatibility with commercial practice. Therefore, different mesh sizes of the outer panel were used, with the ratio of the mesh sizes of the inner and outer panels corresponding to the local construction of the nets. Previous studies on trammel nets have shown that the mesh size of the outer panel generally had no significant effect on the size selectivity and catch rates of experimental trammel nets (Erzini et al. 2006; Stergiou et al. 2006), which were also considered. For all species except European hake and greater weever, the number of specimens caught decreased with increasing mesh size (Table 1), which can be attributed to intra- and interspecific decreases in abundance and biomass with fish size (Stergiou et al. 2006).

All species appear to have been caught in nets in more than two ways. Apart from gilling and wedging, a certain number of specimens were entangled and entrapped, but in different proportions depending on the species, as indicated by the ratios GG/MP, MG/MP (Table 1). This was also reflected in the shapes of the LFDs (Fig. 2) which were skewed to the right or were bi- or multi-modal, and on the selectivity models as the bi-normal curve gave the best fit for all species (Fig. 3). For red mullet, round sardinella, and greater weever, overdispersion was observed which has little effect on parameter estimates (Millar and Holst 1997), but signifying either a lack of fit of the model or a violation of the Poisson distribution assumption (Millar and Fryer 1999). From visual inspection of the residual deviance plots, it appears that the residuals for red mullet and round sardinella, were randomly distributed without following a pattern, indicative of a good fit. The overdispersion therefore suggests that the species may not have behaved independently, due to the schooling behavior of the fish, which violates the Poisson distribution assumption. For greater weever, where the residuals seem to follow a pattern, we assume a lack of fit of the model and the results should be treated with caution.

The selectivity of the fishing gears should be evaluated in relation to species-specific biological parameters, such as length at first maturity (L_m) and fecundity, to ensure the stock is exploited sustainably (Tsikliras and Stergiou 2014). For that reason, the modal length estimates from the bi-normal function for each species and mesh size were compared with the minimum conservation reference size (MCRS) and the size at first maturity (L_m) of each species. The efficiency of each mesh size during the experimental trials was also taken into account to suggest the most appropriate mesh size for each species for an economically viable fishery (Bellido et al. 2011). The mesh size of the inner panels was only used to estimate size selectivity, as the mesh size of the outer panel generally had no significant effect on the size selectivity and catch rates of the experimental trammel nets (Erzini et al. 2006; Stergiou et al. 2006). The results of the presently reported study were compared with those of previous studies on the selectivity of trammel nets in the Mediterranean and adjacent seas, for the species for which information was available (Table 4). As the methods used to estimate selectivity parameters differed among studies, it was not always easy to distinguish between actual differences in selectivity and different results due to the method used (Fonseca et al. 2005).

The two target species, red mullet and surmullet, constitute one of the more widespread *métiers* in trammel net fishery in Greece. The same nets are used in the commercial fishery for both species (“barbounodicta”), deployed however in different seasons. For red mullet, the mesh size of 16 mm was the most efficient in abundance and biomass catch rates, with no specimen below the MCRS (11 mm for red mullet) and very few below the median L_m of 12.9 mm (ranges between 10.5 and 15.5 mm) in the Mediterranean Sea (Tsikliras and Stergiou 2014 and references therein) (Table 1). The modal length estimates are very similar to those previously reported in the Black Sea for all mesh sizes and nearly coincide for the mesh sizes 16 and 22 mm (Table 4). The operational condition (mesh size range) and the modeling (bi-normal model of SELECT method) were also in agreement (Kalaycı and Yeşilçiçek 2012). Lower values of modal length were re-

Table 4. Comparison of the results of the presently reported study with previous selectivity studies that deal with the same species in Mediterranean and adjacent Seas.

Species	Area	*n*	Length [cm]	Selectivity	Model	MS	Modal	Spread	Reference
Annular seabream, *Diplodus annularis*	N. Aegean Sea (Turkey)	190	7.7–16.8	SELECT	BiM	16	8.82	0.53	Karakulak and Erk 2008
						18	9.93	0.6	
						20	11.03	0.66	
						22	12.13	0.73	
	Adriatic Sea	180	5.5–22.0	Sechin	UniM	22.5	12.1	NA	Fabi et al. 2002
	Ligurian Sea	269	6.5–19.0	Sechin	UniM	22.5	12.1	NA	Fabi et al. 2002
	Cyclades		6.0–18.0	SELECT	BiM	20	11.0	NA	Erzini et al. 2006
						24	12.5	NA	
						28	15.0	NA	
Red mullet, *Mullus barbatus*	Antalya Bay	247	10.8–22.3	SELECT	BiM	20	17.0	1.14	Olguner and Deval 2013
		166	10.8–22.3			22	18.7	1.25	
	E. Black Sea (Turkey)	541	7.4–22.6	SELECT	BiM	16	15.49	2.06	Kalaycı and Yeşilçiçek 2012
						17	16.46	2.18	
						18	17.42	2.31	
						20	19.36	2.57	
						22	21.3	2.83	
	Finike Bay (Turkey)	420	12.1–26.3	HOLT	UniM	22	18.58	NA	Bolat and Tan 2017
						24	20.27	NA	
						26	21.96	NA	
	Adriatic Sea	131	9.0–19.5	Sechin	UniM	22.5	16.7	NA	Fabi et al. 2002
	Ligurian Sea	722	8.5–21.0	Sechin	UniM	22.5	16.7	NA	Fabi et al. 2002
Surmullet, *Mullus surmuletus*	N. Aegean Sea (Turkey)	411	11.3–27.7	SELECT	BiM	16	14.7	1.47	Karakulak and Erk 2008
						18	16.54	1.65	
						20	18.38	1.84	
						22	20.22	2.02	
	Cyclades		8.0–36.0	SELECT	BiM	20	17.5	NA	Erzini et al. 2006
						24	21.5	NA	
						28	25.0	NA	
Black scorpionfish, *Scorpaena porcus*	E. Black Sea (Turkey)	942	8.4–27.9	SELECT	BiM	16	9.17	2.82	Kalaycı and Yeşilçiçek 2012
						17	9.74	3.00	
						18	10.31	3.18	
						20	11.46	3.52	
						22	12.61	3.88	
	Cyclades		8.0–46.0	SELECT	BiM	20	13.0	NA	Erzini et al. 2006
						24	15.0	NA	
						28	17.5	NA	

n = number of fish, MS = mesh size, BiM = Bimodal, UniM =Unimodal.

ported in Antalya Bay, Levantine Sea (Olguner and Deval 2013) in Finike Bay, Levantine Sea (Bolat and Tan 2017), and in the Adriatic and the Ligurian Sea (Fabi et al. 2002) but the difference could be attributed to the different methodology among the studies (Table 4).

For surmullet, the higher yield was observed also at a mesh size of 16 mm with one-third of the catch being below L_m (median 15.5 mm, ranges between 11.9 mm and 17.8 mm in the Mediterranean Sea according to Tsikliras and Stergiou 2014 and references therein). At the next larger mesh size of 19 mm, all individuals were above MCRS and only 4% were below L_m (Table 1). The modal length estimates are similar for all mesh sizes to those previously reported in the northern Aegean (Karakulak and Erk 2008), using the SELECT method (Table 4). Similar selection curves and similar modal lengths were observed in the Cyclades, central Aegean (Erzini et al. 2006).

According to modal length estimates, the 19 mm mesh size is clearly the more suitable trammel net mesh size for surmullet, while for red mullet the largest amount of catch was recorded at a mesh size of 16 mm. However, larger red mullet individuals of almost double the weight, and therefore of greater commercial value, were caught in the larger mesh size (19 mm), which appears to be more profitable for fishers. Given the heavy exploitation of red mullet by the bottom-trawling fleet and the high number of undersized individuals caught by trawlers, a 19 mm mesh trammel net would be considered a more sustainable *métier*. A minimum mesh size of 18 mm in the red mullet trammel net fishery has been previously proposed in the eastern Mediterranean Sea to promote sustainable fisheries that will ensure profits for the fishers and catch for the future (Karakulak and Erk 2008, Kalaycı and Yeşilçiçek 2012).

Concerning bycatch, annular seabream is a species with a low commercial value for small individuals and slightly higher value for larger individuals that are usually sold mixed with other sparids. The higher catch rates were obtained in mesh sizes from 16 to 26 mm while the rest of the mesh sizes had negligible catch. Mesh size 16 mm was most efficient in terms of catch in numbers and 26 mm in terms of biomass. The modal length estimates are in close agreement with those previously reported in the northern Aegean Sea (Karakulak and Erk 2008), the Cyclades (central Aegean) (Erzini et al. 2006), and the Adriatic and Ligurian seas (Fabi et al. 2002). From a fisheries management perspective, the catch of mesh sizes 22 and 26 mm was above MCRS (12 mm) and L_m (12.2 mm: Koc et al. 2002), and the most appropriate mesh size that will ensure the sustainable exploitation of the species seems to be between these two mesh sizes. Indeed, a mesh size of 22.5 mm has been previously proposed in Italy (Fabi et al. 2002) while an even larger mesh size of 27 mm has been suggested in Turkey (Karakulak and Erk 2008).

One of the main target species in gillnet, longline, and bottom-trawl fisheries (Deniz et al. 2020), European hake is a very valuable bycatch in trammel net fisheries. Most of the catch of the species was fished in mesh sizes from 16 to 26 mm, with mesh sizes 16 and 26 mm being most efficient in terms of abundance and 26 mm in terms of biomass. Nearly no individuals were below MCRS (20 cm), which is considered very low for a large-sized fish such as hake that matures well after 20 cm (Tsikliras and Stergiou 2014). For that reason, a considerable number of individuals (>60%) per mesh size were below L_m (30.5 cm, ranges between 21.5 and 42.5 cm; Tsikliras and Stergiou 2014 and references therein) for mesh sizes 16, 19, 22 mm, and a significant proportion (37%) for mesh size 26 mm (Table 1). Considering the length at first maturity of hake and its heavy exploitation by many gears in the Mediterranean (Cardinale et al. 2017), a mesh size larger than 26 mm would be most adequate for the sustainable exploitation of the species.

Round sardinella and blotched picarel are both bycatch species with low commercial value. They were fished by 16, 19, and 22 mm mesh sizes and all individuals caught were above MCRS (10 cm for round sardinella, 8 cm for blotched picarel according to national legislation) and above L_m (14.7mm ranging from 11.5 to 16.8 cm for round sardinella; 10.1 cm ranging between 9.5 and 10.7 cm for blotched picarel; Tsikliras and Stergiou 2014 and references therein). The mesh size of 22 mm was more efficient in terms of biomass for round sardinella, while for blotched picarel the largest catch was recorded at 16 mm mesh size. However, the higher individual weight of blotched picarel individuals were caught by the 19 mm mesh size which results in a higher commercial value of the catch because of the positive relation between fish size and its market price (Tsikliras and Polymeros 2014).

The most common bycatch species in trammel nets, black scorpionfish is a low commercial value species with only the bigger individuals (>15 cm) being marketed while the smaller ones are discarded (Tsikliras et al. 2021). Most of the catch of the species was fished in three mesh sizes 16, 19, and 22 mm (Table 1), with nearly all individuals being below L_m (15.3 cm ranging from 13.8 to 17.5 cm according to Tsikliras and Stergiou, 2014 and references therein). The results of our study are in agreement with those reported in the Black Sea (Kalaycı and Yeşilçiçek 2012) and in the Cyclades, central Aegean (Erzini et al. 2006). Considering the length at first maturity a mesh size larger than 26 mm seems to be better for the sustainable exploitation of the species.

Greater weever is also a bycatch species in trammel net fisheries, with no commercial value for small sizes and low commercial value for ones larger than 25 cm (Tsikliras et al. 2021). Greater weever was caught by nearly all mesh sizes, with half of the catch obtained with 19 mm mesh. No differences were found between mesh sizes in either LFDs or mean length. All individuals were above the MLS (8 cm, according to national legislation), while, as there is no clear relation between mesh size and fish size, a number of specimens below L_m (18.5 cm, ranging from 12 to 25 cm: Ak and Genç 2013) were recorded in several mesh sizes (Table 1). Because of the lack of fit of the model as shown by the residuals plot, the estimates of the selectivity parameters should be considered with caution and no prediction of the appropriate mesh size was made.

Conclusions

Overall, the higher yield for nearly all species was observed in the smaller mesh size of 16 mm. However, this mesh size retained specimens below size at first maturity (L_m) in most of the cases and below MCRS for some species (Table 1). Biomass rather than abundance is a better indicator of the more appropriate mesh size because small individuals of the species have lower economic value than large ones, which are sold at higher prices and provide greater economic profit to fishers (Colloca et al. 2013; Tsikliras and Polymeros 2014). The mesh size of 19 mm seems to be more efficient for the main target species, red mullet, and surmullet. Regarding bycatch species, since most of them have a low commercial value, the aim was not to determine the mesh sizes that will provide the higher abundance but to determine the mesh sizes that will retain large specimens in order to obtain the highest possible market value (Tsikliras and Polymeros 2014), while allowing the smaller specimens to escape. With this perspective, for the bycatch species, a mesh size of 19 mm is more appropriate for blotched picarel, a mesh size of 22 mm for round sardinella, and annular seabream, while for European hake and black scorpionfish a mesh size over 26 mm would be more appropriate.

Modifying the size selectivity of fishing gears, and thus their capture efficiency, has been widely proposed to mitigate unwanted bycatch and discards (Bellido et al. 2011), to reduce the catch of immature individuals so they can survive to spawn (Vassilakopoulos et al. 2011), and to limit the capture of larger individuals in order to protect the most productive spawners (Hixon et al. 2014). Therefore, a thorough knowledge of fishing gear selection properties is crucial for sustainable fisheries management (Froese et al. 2018). Management actions could leverage this selectivity information to reduce catches of species of concern by modifying minimum and maximum mesh sizes (Sbrana et al. 2007). The length at first maturity (L_m)is a crucial population parameter for maintaining stock biomass; therefore, it should be considered the basis for setting MCRS of exploited stocks and proposing the appropriate mesh sizes (Tsikliras and Stergiou 2014). However, the results of the presently reported study also highlight the difficulties of managing multispecies fisheries based only on mesh size, since the optimal mesh varies considerably among species.

Acknowledgments

The authors would like to thank Antonis Anatolitis for his help during the experimental trials and the editor and reviewers for their useful comments that improved this work.

References

Adamidou A (2007) Commercial fishing gears and methods used in Hellas. Pp. 118–131. In: Papaconstantinou C, Zenetos A, Vassilopoulou C, Tserpes G (Eds) State of Hellenic fisheries. Hellenic Centre for Marine Research, Athens, Greece.

Ak O, Genç Y (2013) Growth and reproduction of the greater weever (*Trachinus draco* L., 1758) along the eastern coast of the Black Sea. Journal of the Black Sea/Mediterranean Environment 19(1): 95–110.

Ayaz A, Altinagac U, Özekinci U, Özen O, Altin A, Ismen A (2011) Effect of twine thickness on selectivity of gillnets for bogue, *Boops boops*, in Turkish waters. Mediterranean Marine Science 12(2): 358–368. https://doi.org/10.12681/mms.37

Bellido JM, Santos MB, Pennino MG, Valeiras X, Pierce GJ (2011) Fishery discards and bycatch: Solutions for an ecosystem approach to fisheries management? Hydrobiologia 670(1): 317–333. https://doi.org/10.1007/s10750-011-0721-5

Bolat Y, Tan D (2017) Selectivity of multifilament trammel nets of different mesh sizes on the red mullet (*Mullus barbatus* L, 1758) in Western Mediterranean, Turkey. Iranian Journal of Fisheries Science 16(1): 127–137.

Cardinale M, Osio GC, Scarcella G (2017) Mediterranean Sea: A failure of the European fisheries management system. Frontiers in Marine Science 4: 72. https://doi.org/10.3389/fmars.2017.00072

Colloca F, Cardinale M, Maynou F, Giannoulaki M, Scarcella G, Jenko K, Bellido JM, Fiorentino F (2013) Rebuilding Mediterranean fisheries: A new paradigm for ecological sustainability. Fish and Fisheries 14(1): 89–109. https://doi.org/10.1111/j.1467-2979.2011.00453.x

Deniz T, Göktürk D, Ateş C (2020) Selectivity parameters of European hake gillnets for target and by-catch species with a perspective on small-scale fisheries management in the Sea of Marmara, Turkey. Regional Studies in Marine Science 33: 100934. https://doi.org/10.1016/j.rsma.2019.100934

Erzini K, Gonçalves JMS, Bentes L, Moutopoulos DK, Casal JAH, Soriguer MC, Puente E, Errazkin LA, Stergiou KI (2006) Size selectivity of trammel nets in southern European small-scale fisheries. Fisheries Research 79(1–2): 183–201. https://doi.org/10.1016/j.fishres.2006.03.004

Fabi G, Sbrana M, Biagi F, Grati F, Leonori I, Sartor P (2002) Trammel net and GNS selectivity for *Lithognathus mormyrus* (L., 1758), *Diplodus annularis* (L., 1758) and *Mullus barbatus* (L., 1758) in the Adriatic and Ligurian seas. Fisheries Research 54(3): 375–388. https://doi.org/10.1016/S0165-7836(01)00270-3

FAO (2022) The state of world fisheries and aquaculture 2022. Towards blue transformation. FAO, Rome. https://doi.org/10.4060/cc0461en

Fonseca P, Martins R, Campos A, Sobral P (2005) Gillnet selectivity off the Portuguese western coast. Fisheries Research 73(3): 323–339. https://doi.org/10.1016/j.fishres.2005.01.015

Froese R, Pauly D (Eds) (2022) FishBase. [Version 08/2022]. http://www.fishbase.org

Froese R, Winker H, Coro G, Demirel N, Tsikliras AC, Dimarchopoulou D, Scarcella G, Quaas M, Matz-Lück N (2018) Status and rebuilding of European fisheries. Marine Policy 93: 159–170. https://doi.org/10.1016/j.marpol.2018.04.018

García-Rodríguez M, Fernández AM, Esteban A (2006) Characterisation, analysis and catch rates of the small-scale fisheries of the Alicante Gulf (SE Spain) over a 10 years' time series. Fisheries Research 77(2): 226–238. https://doi.org/10.1016/j.fishres.2005.09.002

Gil MM, Catanese G, Palmer M, Hinz H, Pastor E, Mira A, Grau A, Koleva E, Grau AM, Morales-Nin B (2018) Commercial catches and discards of a Mediterranean small-scale cuttlefish fishery: implications of the new EU discard policy. Scientia Marina 82S1: 155–164. https://doi.org/10.3989/scimar.04735.03B

Guijarro B, Massutí E (2006) Selectivity of diamond- and square-mesh codends in the deepwater crustacean trawl fishery off the Balearic Islands (western Mediterranean). ICES Journal of Marine Science 63(1): 52–67. https://doi.org/10.1016/j.icesjms.2005.08.011

Hamley JM (1975) Review of gillnet selectivity. Journal of the Fisheries Research Board of Canada 32(11): 1943–1969. https://doi.org/10.1139/f75-233

He P, Chopin F, Suuronen P, Ferro RST, Lansley J (2021) Classification and illustrated definition of fishing gears. FAO Fisheries and Aquaculture Technical Paper 672, Rome. https://doi.org/10.4060/cb4966en

Hixon MA, Johnson DW, Sogard SM (2014) BOFFFFs on the importance of conserving old-growth age structure in fishery populations. ICES Journal of Marine Science 71(8): 2171–2185. https://doi.org/10.1093/icesjms/fst200

Holst R, Madsen N, Fonseca P, Moth-Poulsen T, Campos A (1998) Manual for gillnet selectivity. [Subsidized by the European Commission and available on the Internet], 43 pp.

Huse I, Løkkeborg S, Soldal AV (2000) Relative selectivity in trawl, longline and gillnet fisheries for cod and haddock. ICES Journal of Marine Science 57(4): 1271–1282. https://doi.org/10.1006/jmsc.2000.0813

Jacquet J, Pauly D (2008) Funding priorities: Big barriers to small-scale fisheries. Conservation Biology 22(4): 832–835. https://doi.org/10.1111/j.1523-1739.2008.00978.x

Kalaycı F, Yeşilçiçek T (2012) Investigation of the selectivity of trammel nets used in red mullet (*Mullus barbatus*) fishery in the eastern Black Sea, Turkey. Turkish Journal of Fisheries and Aquatic Sciences 12(4): 937–945. https://doi.org/10.4194/1303-2712-v12_4_21

Karakulak FS, Erk H (2008) Gillnets and trammel net selectivity in the northern Aegean Sea, Turkey. Scientia Marina 72(3): 527–540.

Kaykaç H, Özbilgin H, Tokaç A (2009) Effects of mesh configuration on the selectivity of demersal trawl codends for *Nephrops norvegicus* (Linnaeus, 1758) (Decapoda, Nephrophidae). Crustaceana 82(12): 1569–1578. https://doi.org/10.1163/001121609X12487811051705

Kelleher K (2005) Discards in the world's marine fisheries. An update. Fisheries and Aquaculture Technical Paper 470, FAO, Rome.

Kitahara T (1971) On selectivity curve of gillnet. Nippon Suisan Gakkaishi 37(4): 289–296. https://doi.org/10.2331/suisan.37.289

Koc HT, Cakir D, Aka Z (2002) Age, growth, sex-ratio, spawning season and mortality of Annular Bream, *Diplodus annularis* Linnaeus (1758) (Pisces: Sparidae) in Edremit Gulf (Aegean Sea). Pakistan Journal of Biological Sciences 5(10): 1126–1130. https://doi.org/10.3923/pjbs.2002.1126.1130

Liontakis A, Tzouramani I, Mantziaris S, Sintori A (2020) Unravelling the role of gender in fisheries' socio-economic performance: The case of Greek small-scale fisheries. Sustainability 12(13): 5304. https://doi.org/10.3390/su12135304

Lucchetti A, Virgili M, Petetta A, Sartor P (2020) An overview of gill net and trammel net size selectivity in the Mediterranean Sea. Fisheries Research 230: 105677. https://doi.org/10.1016/j.fishres.2020.105677

Madsen N, Holst R, Wileman D, Moth-Poulsen T (1999) Size selectivity of sole gillnets fished in the North Sea. Fisheries Research 44(1): 59–73. https://doi.org/10.1016/S0165-7836(99)00048-X

Maynou F, Recasens L, Lombarte A (2011) Fishing tactics dynamics of a Mediterranean small-scale coastal fishery. Aquatic Living Resources 24(2): 149–159. https://doi.org/10.1051/alr/2011131

Mildenberger TK, Taylor MH, Wolff M (2017) TropFishR: an R package for fisheries analysis with length-frequency data. Methods in Ecology and Evolution 8(11): 1520–1527. https://doi.org/10.1111/2041-210X.12791

Millar RB (1992) Estimating the size selectivity of fishing gear by conditioning on the total catch. Journal of the American Statistical Association 87(420): 962–968. https://doi.org/10.1080/01621459.1992.10476250

Millar RB, Fryer RJ (1999) Estimating the size-selection curves of towed gears, traps, nets and hooks. Reviews in Fish Biology and Fisheries 9(1): 89–116. https://doi.org/10.1023/A:1008838220001

Millar RB, Holst R (1997) Estimation of gillnet and hook selectivity using Log-Linear Models. ICES Journal of Marine Science 54(3): 471–477. https://doi.org/10.1006/jmsc.1996.0196

Olguner MT, Deval MC (2013) Catch and selectivity of 40 and 44 mm trammel nets in small-scale fisheries in the Antalya Bay, Eastern Mediterranean. Su Ürünleri Dergisi 30(4): 167–173. https://doi.org/10.12714/egejfas.2013.30.4.04

Özbilgin H, Metin G, Tosunoğlu Z, Tokaç A, Kaykaç H, Aydin C (2012) Seasonal variation in the trawl codend selectivity of common pandora (*Pagellus erythrinus*). Journal of Applied Ichthyology 28(2): 194–199. https://doi.org/10.1111/j.1439-0426.2011.01920.x

Palmer M, Tolosa B, Grau AM, Gil MM, Obregón C, Morales-Nin B (2017) Combining sale records of landings and fishers knowledge for predicting metiers in a small-scale, multi-gear, multispecies fishery. Fisheries Research 195: 59–70. https://doi.org/10.1016/j.fishres.2017.07.001

Petrakis G, Stergiou KI (1995) Gillnet selectivity for *Diplodus annularis* and *Mullus barbatus* in Greek waters. Fisheries Research 21(3–4): 455–464. https://doi.org/10.1016/0165-7836(94)00293-6

R Core Team (2022) RStudio Team (2022). RStudio: Integrated Development for R. RStudio, PBC, Boston, MA. http://www.rstudio.com/

Ricker WE (1975) Computation and interpretation of biological statistics of fish populations. Bulletin of the Fisheries Research Board of Canada, No. 191.

Sala A, Lucchetti A (2011) The effect of mesh size and codend circumference on selectivity in the Mediterranean demersal trawl fisheries. Fisheries Research 111(2): 252–258. https://doi.org/10.1016/j.fishres.2011.04.012

Sartor P, Li Veli D, De Carlo F, Ligas A, Massaro A, Musumeci C, Sartini M, Rossetti I, Sbrana M, Viva C (2018) Reducing unwanted catches of trammel nets: experimental results of the "guarding net" in the caramote prawn, *Penaeus kerathurus*, small-scale fishery of the Ligurian Sea (western Mediterranean). Scientia Marina 82(S1): 131–140. https://doi.org/10.3989/scimar.04765.15B

Sbrana M, Belcari P, de Ranieri S, Sartor P, Viva C (2007) Comparison of the catches of European hake (*Merluccius merluccius*, L. 1758) taken with experimental gillnets of different mesh sizes in the northern Tyrrhenian Sea (western Mediterranean). Scientia Marina 71(1): 47–56. https://doi.org/10.3989/scimar.2007.71n147

Stergiou KI, Moutopoulos DK, Erzini K (2002) Gill net and longlines fisheries in Cyclades waters (Aegean Sea): Species composition and gear competition. Fisheries Research 57(1): 25–37. https://doi.org/10.1016/S0165-7836(01)00334-4

Stergiou KI, Moutopoulos DK, Soriguer MC, Puente E, Lino PG, Zabala C, Monteiro P, Errazkin LU, Erzini K (2006) Trammel net catch species composition, catch rates and métiers in southern European waters: A multivariate approach. Fisheries Research 79(1–2): 170–182. https://doi.org/10.1016/j.fishres.2006.03.003

Stergiou KI, Somarakis S, Triantafyllou G, Tsiaras KP, Giannoulaki M, Petihakis G, Machias A, Tsikliras AC (2016) Trends in productivity and biomass yields in the Mediterranean Sea Large Marine Ecosystem during climate change. Environmental Development 17: 57–74. https://doi.org/10.1016/j.envdev.2015.09.001

Tsikliras AC, Polymeros K (2014) Fish market prices drive overfishing of the 'big ones'. PeerJ 2: e638. https://doi.org/10.7717/peerj.638

Tsikliras AC, Stergiou KI (2014) Size at maturity of Mediterranean marine fishes. Reviews in Fish Biology and Fisheries 24(1): 219–268. https://doi.org/10.1007/s11160-013-9330-x

Tsikliras AC, Touloumis K, Pardalou A, Adamidou A, Keramidas I, Orfanidis G, Dimarchopoulou D, Koutrakis M (2021) Status and exploitation of 74 un-assessed demersal fish and invertebrate stocks in the Aegean Sea (Greece) using abundance and resilience. Frontiers in Marine Science 7: 578601. https://doi.org/10.3389/fmars.2020.578601

Tzanatos E, Georgiadis M, Peristeraki P (2020) Small-Scale Fisheries in Greece: Status, Problems, and Management. In: Small-Scale Fisheries in Europe: Status, Resilience and Governance. Springer, Dordrecht, the Netherlands, 125 pp. https://doi.org/10.1007/978-3-030-37371-9_7

Vassilakopoulos P, O'Neill FG, Marsal T (2011) Misspent youth: Does catching immature fish affect fisheries sustainability? ICES Journal of Marine Science 68(7): 1525–1534. https://doi.org/10.1093/icesjms/fsr075

Supplementary material 1

Technical parameters for the experimental trammel nets

Authors: Angeliki Adamidou, Konstantinos Touloumis, Manos Koutrakis, Athanassios C. Tsikliras

Data type: table (Excel spreadsheet)

Link: https://doi.org/10.3897/aiep.53.103358.suppl1

Supplementary material 2

Results of the Kolmogorov–Smirnov test used to compare the LFDs of paired mesh sizes at the 95,0% confidence level

Authors: Angeliki Adamidou, Konstantinos Touloumis, Manos Koutrakis, Athanassios C. Tsikliras

Data type: Statistics (Excel spreadsheet)

Link: https://doi.org/10.3897/aiep.53.103358.suppl2

Acta Ichthyologica et Piscatoria 53, 2023, 81–88 | DOI 10.3897/aiep.53.102643

PENSOFT.

ACTA
ICHTHYOLOGICA
ET PISCATORIA

Microfibers in the gut of invasive armored catfish (*Pterygoplichthys* spp.) (Actinopterygii: Siluriformes: Loricariidae) in an urban lake in the floodplain of the Grijalva River basin, Mexico

Gabriela ANGULO-OLMOS[1], Nicolás ÁLVAREZ-PLIEGO[2], Alberto J. SÁNCHEZ[2], Rosa FLORIDO[2], Miguel Ángel SALCEDO[2], Arturo GARRIDO-MORA[2], Allan K. CRUZ-RÁMIREZ[2]

1 *Programa de Maestría en Ciencias Ambientales, División Académica de Ciencias Biológicas, Universidad Juárez Autónoma de Tabasco, Villahermosa, Tabasco, Mexico*

2 *Diagnóstico y Manejo de Humedales Tropicales, División Académica de Ciencias Biológicas, Universidad Juárez Autónoma de Tabasco, Villahermosa, Tabasco, Mexico*

https://zoobank.org/46F7A015-FC29-47AF-96B7-3E90CC2041D6

Corresponding author: Gabriela Angulo-Olmos (gabygao225@gmail.com)

Academic editor: Predrag Simonović ♦ **Received** 24 February 2023 ♦ **Accepted** 24 April 2023 ♦ **Published** 26 May 2023

Citation: Angulo-Olmos G, Alvarez-Pliego N, Sánchez AJ, Florido R, Salcedo MÁ, Garrido-Mora A, Cruz-Rámirez AK (2023) Microfibers in the gut of invasive armored catfish (*Pterygoplichthys* spp.) (Actinopterygii: Siluriformes: Loricariidae) in an urban lake in the floodplain of the Grijalva River basin, Mexico. Acta Ichthyologica et Piscatoria 53: 81–88. https://doi.org/10.3897/aiep.53.102643

Abstract

The intake of microplastics by freshwater fishes has been scarcely studied, and it is not yet clear whether the amount of particles these vertebrates ingest is associated with their feeding strategies. Hence, this study is focused on the suckermouth armored catfish (*Pterygoplichthys* spp.) under the hypothesis that, due to its detritivorous habits and demersal distribution, it may show evidence of the presence of microplastics in the sediments of a lake located in the Metropolitan Area of Villahermosa. A total of 21 organisms contained plastic microfibers throughout their digestive systems. These were treated with three solutions (hydrogen peroxide, potassium hydroxide, and sodium hypochlorite) to separate the microplastics. A total of 147 plastic particles of two categories were collected: microfibers (92%) and fragments (8%). Considering these results, as well as evidence in the literature, these species may constitute a global indicator of the incorporation into the trophic chain of microfibers deposited in the sediments of freshwater ecosystems.

Keywords

cosmopolitan, demersal, detritivorous, freshwater, invasive, Loricariidae, microfibers, non-native

Introduction

Plastics constitute the largest group of pollutants that enter freshwater ecosystems, mainly as discarded solid wastes and via wastewater treatment plant discharges, runoff, rain, and even air (Dris et al. 2016; Li et al. 2018; Zhang et al. 2019). Microplastics' (MP) particles (<5 mm), have been scarcely documented for limnetic environments, and according to Lambert and Wagner (2018), less than 4% of publications on MP focus on this type of aquatic systems, and even fewer on lakes (Free et al. 2014; Yuan et al. 2019; Adeogun et al. 2020; Hurt et al. 2020). MP in freshwater environments are present in at least four forms: fibers, fragments, films, and pellets

(Free et al. 2014; Dris et al. 2018; Li et al. 2018; Vidal et al. 2021), and their origin may be determined depending on their form. For example, pellets come from personal care products (Fendall and Sewell 2009), while microfibers result from the decomposition of larger plastic objects like bags, clothing, and at present, personal protection articles that have been increasingly used in response to COVID-19 (Fadare and Okoffo 2020; Wu et al. 2020; Shruti et al. 2021; Yang et al. 2021). Microfibers have thus become the dominant form due to their numerical abundance in the digestive systems of fish and in freshwater ecosystem sediments (Wu et al. 2020; Vidal et al. 2021; Yang et al. 2021).

It has been suggested that the distribution of MP in these aquatic ecosystems is markedly heterogeneous and is mixed with other natural particles (Klein et al. 2018). Their distribution in the water column or in sediments is related to their density with respect to that of the water (Cole et al. 2011; Li et al. 2020). Due to their distribution in the water column and in sediments, MP may be easily ingested as prey, or incidentally by pelagic and demersal fish that employ different feeding strategies (Campbell et al. 2017; Lusher et al. 2017a; Abbasi et al. 2018; Parker et al. 2020). In addition, the association between MP and microbial organisms, and their adsorption of organic matter, favor their deposition and accumulation processes on lentic ecosystem substrates (Galgani et al. 2019; Parker et al. 2020; Yang et al. 2021) which, in turn, could increase their presence in the digestive system of detritivorous demersal fish.

Mostly, MP in the digestive system of freshwater fishes have been reported in bottom-feeding carnivores, since they account for 49% of the species studied (Sanchez et al. 2014; Peters and Bratton 2016; Jabeen et al. 2017; McNeish et al. 2018; dos Santos et al. 2020; Kuśmierek and Popiołek 2020; Vidal et al. 2021). In contrast, only 13% of registered species were detritivores (Silva-Cavalcanti et al. 2016; McNeish et al. 2018; Adeogun et al. 2020; Vidal et al. 2021). Among these detritivore fishes, stood out the demersal Siluriformes. For example, the armored catfish, *Hoplosternum littorale* (Hancock, 1828) had an intake of 83% and 3.6 MP particles per individual (N_{MP}/ind) in the Pajeú River, Brazil (Silva-Cavalcanti et al. 2016), and another two species, *Otocinclus arnoldi* Regan, 1909 and *Hypostomus commersoni* Valenciennes, 1836 with MP ingestion from 80% to 100% and 1.4 to 2.5 N_{MP}/ind in Uruguayan streams of the Plata River basin (Vidal et al. 2021).

In the northern region of Middle America, non-native invasive species of the armored catfish *Pterygoplichthys* spp. have been recorded as demersal detritivores and are numerically dominant in the urban and suburban aquatic ecosystems of the floodplain of the Grijalva River (Sánchez et al. 2019). Due to its cosmopolitan distribution (Orfinger and Goodding 2018), feeding, and morphology, it is expected that this catfish frequently swallows microplastics deposited in limnetic sediment. If tested, the armored catfish can be proposed as a global bioindicator to quantify the uptake into the trophic chain of microfibers accumulated in the sediments of lentic ecosystems or low hydraulic energy areas in rivers (meanders), such as the low-lying areas or lakes associated with rivers on coastal plains where environmental conditions have negatively affected aquatic fauna (Sánchez et al. 2012; Torres-Martínez et al. 2017). In order to prove the hypothesis, the aim of this study was to quantify the microfibers ingested by armored catfish after having been deposited and fragmented on the substrate of a low-lying area or a riparian lake with environmental disturbance conditions similar to those recorded for other urban ecosystems (Yuan et al. 2019; Adeogun et al. 2020).

Methods

The catfish were caught in La Pólvora Lake, which is located (17°58′56″N, 092°55′30″W and 17°58′45″N, 092°55′31″W) in the Metropolitan Area of Villahermosa (MAV) in the Grijalva River basin (Fig. 1). It has an area of 40 650 m^2. It is a riparian depression that has been hydrologically isolated from the Grijalva River by urban infrastructure and has no marginal vegetation due to its rehabilitation as an urban park since 1985. For this reason, its volume is maintained by runoff and extreme or extraordinary flood events (Sánchez et al. 2012). The lake is surrounded by governmental and commercial buildings, schools, and houses. It is subject to strong pressure from activities that take place in the area, which have resulted in hypereutrophic conditions due to high concentrations of phosphorus ($0.116–0.126\ \mathrm{mg} \cdot \mathrm{L}^{-1}$) and chlorophyll *a* ($69–101\ \mu\mathrm{g} \cdot \mathrm{L}^{-1}$) and pollution due to high values of fecal coliforms (7900–240 000 MPN/100 mL) and a low number of aquatic species (Sánchez et al. 2012; Torres-Martínez et al. 2017; SEIACC 2021).

On 23 March 2015, 21 specimens of 280 to 370 mm total length (TL) were collected with a set gillnet (50 m long, 2 m depth, 6.5 cm mesh size) and a cast net (1 cm mesh size). The specimens were preserved in a 10% formalin solution for 15 days, after which they were rinsed in running water to eliminate the formaldehyde and kept in 70% alcohol. The identification included 13 females with gonads in stages III and IV of maturation (in accordance with Núñez and Duponchelle 2008), and eight males for which it was not possible to determine the maturation stage since the gonads were affected by the preservation in formaldehyde and alcohol. Regarding the ventral pigmentation pattern, eight specimens presented spots, seven vermiculations, and six mixed pigmentation (spots and vermiculations) (Table 1). In view of this, it was decided to keep the identification of the specimens at the genus level (*Pterygoplichthys* spp.) following the keys of Armbruster and Page (2006) as, due to the history of management and cultivation of these organisms and the limited of genetic studies in the Grijalva River basin (Vargas-Rivas et al. 2023), it has been suggested that the pigmentation patterns and the morphological characteristics are insufficient to identify species (Wu et al. 2011; Nico et al. 2012; Álvarez-Pliego et al. 2015).

We determined the total length (TL) [mm] and total weight (*W*) [g] of each organism. Individual MP particles were extracted from the digestive tract through a

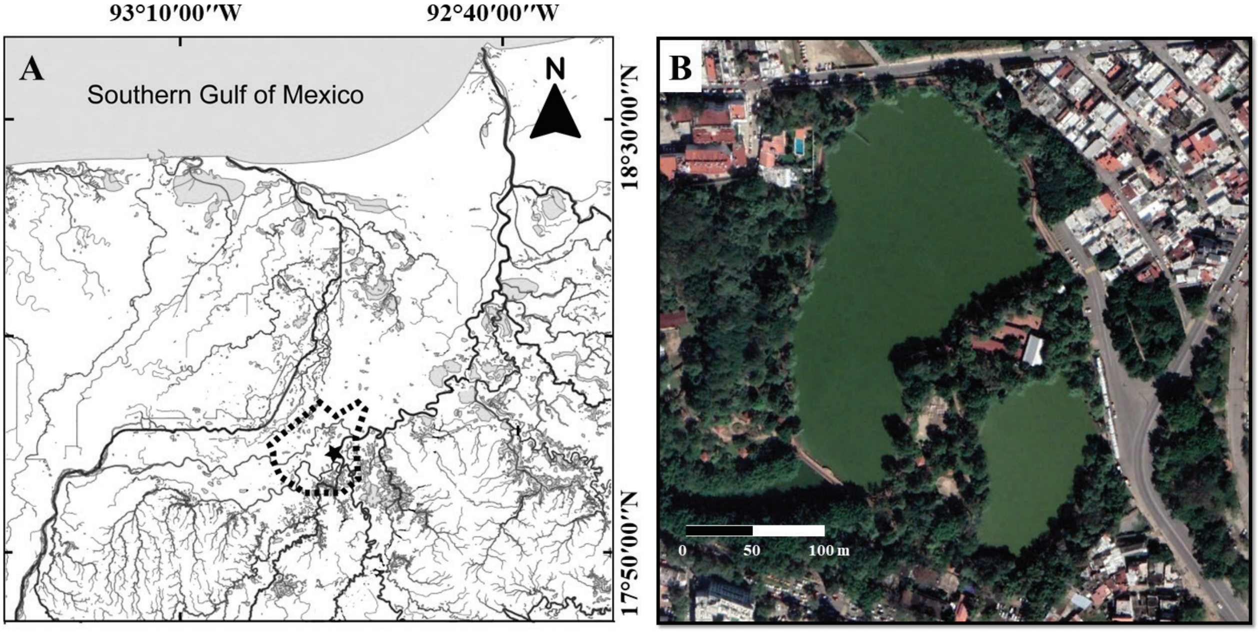

Figure 1. **A**) Study area; Metropolitan Area of Villahermosa. Map modified from INEGI (2021). **B**) La Pólvora lake (Satélite Airbus 2023).

dissection in the visceral cavity, by making two cuts in the ventral area of the fish from the anus to the origin of the right pectoral fin and repeating the process towards the left pectoral fin. The weight of the digestive tract (gut) (W_G) was determined [g] and it was placed in glass vessels of 110 mL and submerged in solutions of 30 mL of 35% hydrogen peroxide (H_2O_2) for 48 h and 30 mL of 4% potassium hydroxide (KOH) for 120 h at room temperature (Campbell et al. 2017; Abbasi et al. 2018) in order to dissolve tissues and organic matter without damaging or altering the forms, colors, and sizes of the MP. A solution of 4% sodium hypochlorite (NaClO) was later added for an additional week to the samples in which organic matter persisted (Collard et al. 2015). Once the organic matter had dissolved, the sample was washed with distilled water through a 10 µm mesh sieve to separate and obtain the MP. The remainder was observed with a 10× lens on an OLYMPUS BX41 microscope to identify and classify the MP following the categories proposed by Free et al. (2014): 1) granule or particle (irregularly shaped cube with smooth to jagged edges and no smooth plane), 2) fiber (thin thread-shaped structure), 3) fragment (irregularly shaped cube with at least one smooth plane) and 4) film (transparent with two smooth planes).

The number of MP (N_{MP}) was counted per specimen and for all the organisms studied in order to obtain a mean number of MP per individual (N_{MP}/ind) following the protocol of Vidal et al. (2021). The relation between the number of MP and the gut weight (N_{MP}/W_G) was obtained using body measurements data. These results were compared with data recorded in previous publications where the MP in the stomach contents of freshwater detritivorous fish in urban aquatic environments, for which a search was carried out through Scopus and Web of Science, using as keywords: freshwater, fish, microplastic, detritivore, and urban.

Table 1. Individuals of suckermouth catfishes (*Pterygoplichthys* spp.) collected in La Pólvora Lake, Mexico.

TL [mm]	W [g]	W_G [g]	Sex	Pigmentation pattern	N_{MP}		N_{MP}/W_G
					Fiber	Fragment	
280	261	19	M	SV	9	–	0.47
280	264	23	M	SV	2	–	0.09
290	200	19	F	S	4	–	0.21
293	239	12	M	S	5	1	0.50
300	238	9	F	S	6	–	0.67
300	297	21	M	V	15	–	0.71
305	342	25	F	V	2	–	0.08
305	296	12	M	V	6	–	0.50
308	264	20	F	V	11	–	0.55
310	294	6	M	SV	3	–	0.50
310	254	10	F	S	2	–	0.20
310	244	22	M	SV	8	7	0.68
315	370	31	F	SV	2	–	0.06
320	458	31	F	V	4	–	0.13
320	556	43	F	V	6	–	0.14
320	260	18	F	V	10	2	0.67
330	351	27	F	S	6	–	0.22
335	425	40	F	S	12	1	0.33
352	290	20	F	SV	12	1	0.65
355	502	32	M	S	7	–	0.22
370	482	70	F	S	3	–	0.04

TL = total length, W = total fish weight, W_G = gut weight, F = female, M = male, S = spots, V = vermiculations, SV = spots with vermiculations, N_{MP} = number of microplastics per gut weight.

Results

MP were found in the 21 analyzed specimens, varying from two to up to 15 pieces in two animals (Table 1). A total of 147 particles of two categories were counted: microfibers (92%) and fragments (8%) (Fig. 2, Table 1). The mean number of MP per individual (N_{MP}/ind) was 7 ± 4.5. Also observed in some of the processed samples were remains of plant matter, microcrustaceans (harpacticoid copepods), and detritus (Fig. 2). It was also possible to see that some fibers were tied up among filaments of aquatic vegetation.

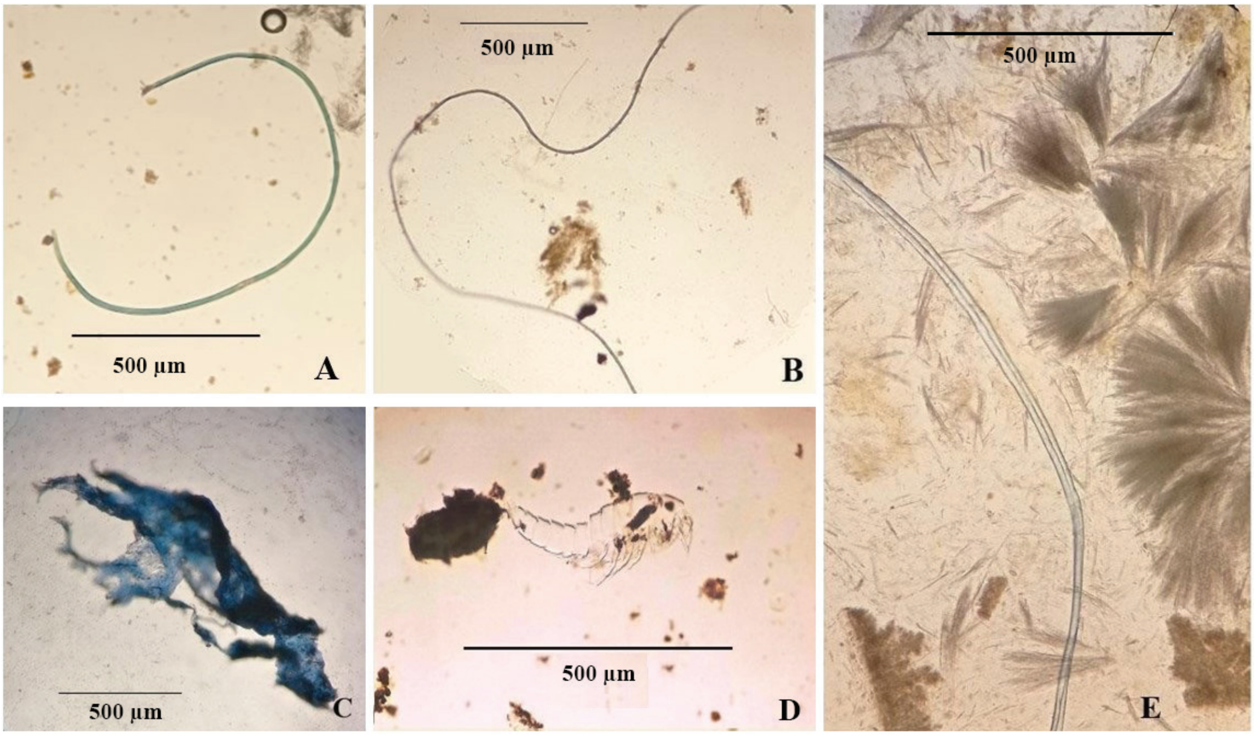

Figure 2. Microplastics found in the digestive tract of armed catfish (*Pterygoplichthys* spp.) and other elements detected. **A** and **B**) Fiber, **C**) Fragment, **D**) Copepod, **E**) Remains of vegetation and organic matter.

Discussion

The high percentage of microfibers (92%) in all plastic fragments identified in the stomach contents of the armored catfish is consistent with the predominance of this category of MP in freshwater demersal detritivore fish (Silva-Cavalcanti et al. 2016; McNeish et al. 2018; Kuśmierek and Popiołek 2020; Li et al. 2020; Vidal et al. 2021; Yang et al. 2021; Blankson et al. 2022), and in turn explains that one of the main sources of microfibers in La Pólvora Lake is the decomposition of larger materials that are transported by different means (Allen et al. 2017; Dris et al. 2018; Li et al. 2018; Zhang et al. 2019). Related to the high environmental pressure caused by human activities, the hydrological isolation of lakes around the world has generated hypereutrophic conditions, low biological diversity, damage to organisms, and the presence of dominant invasive species (Li et al. 2018; Escalera-Vázquez et al. 2020; Jiang et al. 2022), where runoff and rainfall remained as the main contributions of water inputs as a result of the hydraulic isolation and the microtopography (D'Arcy and Carignan 2011). These conditions of hydraulic isolation are more marked during the dry season when runoff and rainfall are scarce and the volume and level of the water decrease, allowing the retention of materials and their settlement on the sediments (Jeppesen et al. 2015; Cruz-Ramírez et al. 2019; Yang et al. 2021). This condition has been frequently reported in urban and suburban lakes located on the coastal plain of the Grijalva River basin (Sánchez et al. 2012, 2019; Salcedo et al. 2018; Cruz-Ramírez et al. 2019).

In the case of La Pólvora Lake, hypereutrophic conditions (Sánchez et al. 2012), fecal coliforms above the allowed for public recreational use limits regarding services to the public (SEIACC 2021), a decrease in biodiversity that includes the absence of macrocrustaceans and the presence of non-native species like the armored catfish (Sánchez et al. 2012, 2019), have been recorded. Also, histopathological alterations such as testicular degeneration in the threadfin shad *Dorosoma petenense* (Günther, 1867) and melanomacrophage centers in the ovaries of *D. petenense* and *Thorichthys meeki* Brind, 1918 (see Torres-Martínez et al. 2017) have been detected. Although the reason for these types of lesions has not been investigated in La Pólvora Lake, background studies have reported that changes in the liver tissue of Japanese rice fish, *Oryzias latipes* (Temminck et Schlegel, 1846) (see Rochman et al. 2013) are tied to the plastic chemical compounds being bioaccumulated and affecting fish metabolism (Kuśmierek and Popiołek 2020; Parker et al. 2020).

The previously mentioned disturbance conditions are supplemented with the results of the presently reported study which show that the amount of microfibers recorded in the digestive systems of the armored catfish specimens is very similar to that recorded for other species of aquatic environments adjacent to urban centers (McNeish et al. 2018; Vidal et al. 2021). This proves the frequency of contributions of this type of particles that result from the decomposition of larger plastics (bags, clothing, consumer products) discarded by people that then enter La Pólvora Lake. This, together with the topographical characteristics and the above-stated human impacts, increases the concentration of MP in these aquatic ecosystems (Free et al. 2014; Peters and Bratton 2016). Likewise, some demersal freshwater fish species with similar feeding strategies to those of suckermouth armored catfish have registered high concentrations of MP, dominated by microfibers. For instance, in urban lakes of 7.63 N_{MP}/ind (Yuan et al. 2019), in urban rivers of 3.6–6.4 N_{MP}/ind (Silva-Cavalcanti et al. 2016; McNeish et al. 2018), and in suburban streams of 0.63–21.4 N_{MP}/ind (Vidal et al. 2021) (Table 2).

At present, the geographical comparison of the quantification and description of MP in the digestive systems of fish is still inaccurate since the results have been reported through only three procedures: 1) the mean number of particles and the categories determined in all the individuals reviewed (Silva-Cavalcanti et al. 2016; McNeish et al. 2018; Yuan et al. 2019; Vidal et al. 2021); 2) the range of MP observed (Silva-Cavalcanti et al. 2016; Yuan et al. 2019; Adeogun et al. 2020); and 3) the use of fluorescence techniques to count MP (Adeogun et al. 2020). However, the available information makes it possible to see that the intake of these pollutants by bottom-dwelling detritivorous fish in lentic environments is greater than that taken by fish in river environments where detritivorous fish recorded values <6.4 N_{MP}/ind, while mean values were >7 N_{MP}/ind in the first case, including those reported in this study (Table 2).

The presence of MP in freshwater fishes has been documented since 2014, and since then the number of studies related to these freshwater vertebrates has increased. However, more research is needed to better determine whether the type of feeding of each species is related to the amount and type of MP found in their guts. The presently reported study documents the presence of microfibers in an invasive, bottom-feeding detritivorous loricariid fish that may be used as a global fish indicator of MP accumulated in sediments and their possible transfer to the trophic chain, as was observed in this study and in others that studied this type of species (Silva-Cavalcanti et al. 2016; McNeish et al. 2018; Vidal et al. 2021).

The microfibers detected in the stomach contents of the *Pterygoplichthys* spp. specimens appear to have not been affected by the use of reagents (10% formaldehyde and 70% alcohol) in the preservation process, considering the high number of detected particles (147). However, Lusher et al. (2017b) indicated that synthetic polyamides such as nylon may be damaged by concentrations of 10% formaldehyde and suggested that other preservation techniques like drying or freezing be used in studies of MP in fish. In the case of not being able to preserve fish as is suggested, an alternative could be the dissection of the digestive tract and its preservation in 4% diluted formalin and a saturated solution of sodium borate to reduce acidity and maintain a neutral pH.

Table 2. Freshwater detritivorous fishes with microplastics (MP) recorded in the digestive tract (gut).

Reference	Species	Family	Hab.	N	N_{MP}/Ind	N_{MP}	Fibers [%]	Env.
Silva-Cavalcanti et al. 2016	*Hoplosternum littorale* (Hancock, 1828)	Callichthyidae	Dem	48	3.6	1–24	46.6	UR
McNeish et al. 2018	*Catostomus commersonii* (Lacepède, 1803)	Catostomidae	Dem	16	6.4		97	SR
Jabeen et al. 2017	*Carassius auratus* (Linnaeus, 1758)	Cyprinidae	BenPel	11	7.63	1–18	46.8	UL
Blankson et al. 2022	*Sarotherodon melanotheron* Rüppell, 1852	Cichlidae	Dem	19	–	1–34	–	UL
Blankson et al. 2022	*Chrysichthys nigrodigitatus* (Lacepède, 1803)	Caroteidae	Dem	3	–	1–3	–	UL
Vidal et al. 2021	[Total value for 6 species listed below]						85	
Vidal et al. 2021	*Ancistrus taunayi* Ribeiro, 1918	Loricariidae	Dem	2	1	–		SS
Vidal et al. 2021	*Otocinclus arnoldi* Regan, 1909	Loricariidae	Dem	7	1.43	–		SS
Vidal et al. 2021	*Hypostomus commersoni* Valenciennes, 1836	Loricariidae	Dem	5	2.4	–		SS
Vidal et al. 2021	*Rineloricaria* sp.	Loricariidae	Dem	14	1.07	–		SS
Vidal et al. 2021	*Steindachnerina biornata* (Braga et Azpelicueta, 1987)	Curimatidae	BenPel	8	0.63	–		SS
Vidal et al. 2021	*Hisonotus nigricauda* (Boulenger, 1891)	Loricariidae	BenPel	3	0.67	–		SS
Presently reported study	*Pterygoplichthys* spp.	Loricariidae	Dem	21	7	1–15	92	UL

Hab. = habitat, Dem = demersal, BenPel = benthopelagic, N = number of fish specimens examined, N_{MP} = number of microplastics, N_{MP}/Ind = number of microplastics per individual studied, Fibers = the percentage of fibers among microplastic fragments found; Env. = environment, UR = urban river, SR = suburban river, UL = urban lagoon, SS = suburban stream.

Conclusion

The proposal to use the armored catfish as an indicator of the dominant microfibers present in urban aquatic environment sediments is very feasible considering the results obtained in this study. Its use may also serve a dual purpose: 1) to detect these pollutants in an urban lake due to its high tolerance and dominance in altered environments, and 2) as an invasive species in several regions of the five continents, its scientific use may constitute a method to regulate the populations of these non-native fish without affecting autochthonous species.

In addition, the predominance of microfibers found in the stomach contents of armored catfish and other bottom-feeding species in urban aquatic environments suggests that the main source of pollutants is the weathering or fragmentation of plastic products of urban use. Related to this, the activation of sanitary measures (since 2019) in response to COVID-19 produced an exponential consumption of medical articles of personal use including facemasks, gloves, masks, and sanitizing towels, several of them a main source of plastic microfibers (Fadare and Okoffo 2020; Wu et al. 2020; Shruti et al. 2021), which in turn increased their presence in the solid urban wastes. In this context, a further and acute increase of MP in aquatic organisms and ecosystems may be expected, mainly in urban lakes where the suckermouth armored catfish is a dominant species.

Acknowledgments

We would like to thank Andrea Raz-Guzman, PhD., UNAM, for editorial services and the translation into English. The first author received a master's degree scholarship (741723) from the Consejo Nacional de Ciencia y Tecnología (CONACyT) granted for the period of 2019–2021.

References

Abbasi S, Soltani N, Keshavarzi B, Moore F, Turner A, Hassanaghaei M (2018) Microplastics in different tissues of fish and prawn from the Musa Estuary, Persian Gulf. Chemosphere 205: 80–87. https://doi.org/10.1016/j.chemosphere.2018.04.076

Adeogun AO, Ibor OR, Khan EA, Chukwuka AV, Omogbemi ED, Arukwe A (2020) Detection and occurrence of microplastics in the stomach of commercial fish species from a municipal water supply lake in southwestern Nigeria. Environmental Science and Pollution Research International 27(25): 31035–31045. https://doi.org/10.1007/s11356-020-09031-5

Allen D, Arthur S, Haynes H, Olive V (2017) Multiple rainfall event pollution transport by sustainable drainage systems: The fate of fine sediment pollution. International Journal of Environmental Science and Technology 14(3): 639–652. https://doi.org/10.1007/s13762-016-1177-y

Álvarez-Pliego N, Sánchez AJ, Forido R, Salcedo MA (2015) First record of South American suckermouth armored catfishes (Loricariidae, *Pterygoplichthys* spp.) in the Chumpan River system, southeast Mexico. BioInvasions Records 4(4): 309–314. https://doi.org/10.3391/bir.2015.4.4.14

Armbruster JW, Page LM (2006) Redescription of *Pterygoplichthys punctatus* and description of a new species of *Pterygoplichthys* (Siluriformes: Loricariidae). Neotropical Ichthyology 4(4): 401–409. https://doi.org/10.1590/S1679-62252006000400003

Blankson ER, Tetteh PN, Oppong P, Gbogbo F (2022) Microplastics prevalence in water, sediment and two economically important species of fish in an urban riverine system in Ghana. PLoS ONE 17(2): e0263196. https://doi.org/10.1371/journal.pone.0263196

Campbell SH, Williamson PR, Hall BD (2017) Microplastics in the gastrointestinal tracts of fish and the water from an urban prairie creek. Facets 2(1): 395–09. https://doi.org/10.1139/facets-2017-0008

Cole M, Lindeque P, Halsband C, Galloway TS (2011) Microplastics as contaminants in the marine environment: A review. Marine Pollution Bulletin 62(12): 2588–2597. https://doi.org/10.1016/j.marpolbul.2011.09.025

Collard F, Gilbert B, Eppe G, Parmentier E, Das K (2015) Detection of anthropogenic particles in fish stomachs: An isolation method adapted to identification by Raman spectroscopy. Archives of Environmental Contamination and Toxicology 69(3): 331–339. https://doi.org/10.1007/s00244-015-0221-0

Cruz-Ramírez AK, Salcedo MA, Sánchez AJ, Mendoza JD, Barba E, Álvarez-Pliego N, Florido R (2019) Intra-annual variation of Chlorophyll-a and nutrients in a hydraulically perturbed wetland in the floodplain of the Grijalva river basin. Hidrobiológica 29(3): 163–170. https://doi.org/10.24275/uam/izt/dcbs/hidro/2020v29n3/Cruz

D'Arcy P, Carignan R (2011) Influence of catchment topography on water chemistry in southeastern Quebec Shield Lakes. Canadian Journal of Fisheries and Aquatic Sciences 54(10): 2215–2227. https://doi.org/10.1139/f97-129

dos Santos T, Bastian R, Felden J, Rauber AM, Reynalte-Tataje DA, Teixeira de Mello F (2020) First record of microplastics in two freshwater fish species (*Iheringhthys labrosus* and *Astyanax lacustris*) from the middle section of the Uruguay River, Brazil. Acta Limnologica Brasiliensia 32: e26. https://doi.org/10.1590/s2179-975x3020

Dris R, Gasperi J, Saad M, Mirande C, Tassin B (2016) Synthetic fibers in atmospheric fallout: A source of microplastics in the environment. Marine Pollution Bulletin 104(1–2652): 290–293. https://doi.org/10.1016/j.marpolbul.2016.01.006

Dris R, Gasperi J, Tassin B (2018) Sources and fate of microplastics in urban areas: A focus on Paris megacity. In: Wagner M, Lambert S (Eds) Freshwater microplastics, Emerging environmental contaminants. Vol. 269 in The handbook of Environmental Chemistry Springer, Cham, Switzerland, 69–83. https://doi.org/10.1007/978-3-319-61615-5_4

Escalera-Vázquez LH, García-López JE, Sosa-López A, Calderón-Cortés N, Hinojosa-Garro D (2020) Impact of the non-native locariid fish *Pterygoplichthys pardalis* in native fish community on a seasonal tropical floodplain in Mexico. Aquatic Ecosystem Health and Management 22(4): 462–472. https://doi.org/10.1080/14634988.2019.1700343

Fadare OO, Okoffo ED (2020) Covid-19 face masks: A potential source of microplastic fibers in the environment. Science of the Total Environment 737: 140279. https://doi.org/10.1016/j.scitotenv.2020.140279

Fendall LS, Sewell MA (2009) Contributing to marine pollution by washing your face: Microplastics in facial cleansers. Marine Pollution Bulletin 58(8): 1225–1228. https://doi.org/10.1016/j.marpolbul.2009.04.025

Free CM, Jensen OP, Mason SA, Eriksen M, Williamson NJ, Boldgiv B (2014) High-levels of microplastic pollution in a large, remote, mountain lake. Marine Pollution Bulletin 85(1): 156–163. https://doi.org/10.1016/j.marpolbul.2014.06.001

Galgani L, Tsapakis M, Pitta P, Tsiola A, Tzempelikou E, Kalantzi I, Esposito C, Loiselle A, Tsotskou A, Zivanovic S, Dafnomili E, Diliberto S, Mylona K, Magiopoulos I, Zeri C, Pitta E, Loiselle S (2019) Microplastics increase the marine production of particulate forms of organic matter. Environmental Research Letters 14(124085): 124085. https://doi.org/10.1088/1748-9326/ab59ca

Hurt R, O'Reilly CM, Perry WL (2020) Microplastic prevalence in two fish species in two U.S. reservoirs. Limnology and Oceanography Letters 5(1): 147–153. https://doi.org/10.1002/lol2.10140

INEGI (2021) Simulador de Flujos de Agua de Cuencas Hidrográficas Versión 4.0. 2021. Instituto Nacional de Estadística y Geografía. [Accessed 12 April 2023] https://antares.inegi.org.mx/analisis/red_hidro/siatl

Jabeen K, Su L, Li J, Yang D, Tong C, Mu J, Shi H (2017) Microplastics and mesoplastics in fish from coastal and fresh waters of China. Environmental Pollution 221: 141–149. https://doi.org/10.1016/j.envpol.2016.11.055

Jeppesen E, Brucet S, Naselli-Flores L, Papastergiadou E, Stefanidis K, Nõges T, Nõges P, Attayde JL, Zohary T, Coppens J, Bucak T, Fernandes Menezes R, Sousa Freitas FR, Kernan M, Søndergaard M, Beklioğlu M (2015) Ecological impacts of global warming and water abstraction on lakes and reservoirs due to changes in water level and related changes in salinity. Hydrobiologia 750(1): 201–227. https://doi.org/10.1007/s10750-014-2169-x

Jiang X, Li Z, Shu F, Chen J (2022) Effects of river–lake disconnection and eutrophication on freshwater mollusc assemblages in floodplain lakes: Loss of congeneric species leads to changes in both assemblage composition and taxonomic relatedness. Environmental Pollution 292(A): e118330. https://doi.org/10.1016/j.envpol.2021.118330.

Klein S, Dimzon IK, Eubeler J, Knepper TP (2018) Analysis, occurrence, and degradation of microplastics in the aqueous environment. In: Wagner M, Lambert S (Eds) Freshwater microplastics, Emerging environmental contaminants. Vol. 269 in The handbook of Environmental Chemistry Springer, Cham, Switzerland, 51–67. https://doi.org/10.1007/978-3-319-61615-5_3

Kuśmierek N, Popiołek M (2020) Microplastics in freshwater fish from central European lowland river (Widawa R, SW Poland). Environmental Science and Pollution Research International 27(10): 11438–11442. https://doi.org/10.1007/s11356-020-08031-9

Lambert S, Wagner M (2018) Microplastics Are Contaminants of Emerging Concern in Freshwater Environments: An Overview. In: Wagner M, Lambert S (Eds) Freshwater microplastics, Emerging environmental contaminants. Vol. 269 in The handbook of Environmental Chemistry Springer, Cham, Switzerland, 1–23. https://doi.org/10.1007/978-3-319-61615-5_1

Li J, Liu H, Chen P (2018) Microplastics in freshwater systems: A review on occurrence, environmental effects, and methods for microplastics detection. Water Research 137: 362–374. https://doi.org/10.1016/j.watres.2017.12.056

Li C, Busquets R, Campos LC (2020) Assessment of microplastics in freshwater systems: A review. Science of the Total Environment 707: 135578. https://doi.org/10.1016/j.scitotenv.2019.135578

Lusher AL, Hollman PCH, Mendoza-Hill JJ (2017a) Microplastics in fisheries and aquaculture: status of knowledge on their occurrence and implications for aquatic organisms and food safety. Fisheries and Aquaculture Technical No. 615. FAO, Rome, 126 pp.

Lusher A, Welden N, Sobral P, Cole M (2017b) Sampling, isolating and identifying microplastics ingested by fish and invertebrates. Analytical Methods 9(9): 1346–1360. https://doi.org/10.1039/C6AY02415G

McNeish RE, Kim LH, Barret HA, Mason SA, Kelly JJ, Hoellein TJ (2018) Microplastic in riverine fish is connected to species traits. Scientific Reports 8(1): 1–12. https://doi.org/10.1038/s41598-018-29980-9

Nico LG, Butt PL, Johnston GR, Jelks HL, Kail M, Walsh SJ (2012) Discovery of South American suckermouth armored catfishes (Loricariidae, *Pterygoplichthys* spp.) in the Santa Fe River drainage, Suwannee River basin, USA. BioInvasions Records 1(3): 179–200. https://doi.org/10.3391/bir.2012.1.3.04

Núñez J, Duponchelle F (2008) Towards a universal scale to assess sexual maturation and related life history traits in oviparous teleost fishes. Fish Physiology and Biochemistry 35(1): 167–180. https://doi.org/10.1007/s10695-008-9241-2

Orfinger AB, Goodding D (2018) The global invasion of the suckermouth armored catfish genus *Pterygoplichthys* (Siluriformes: Loricariidae): Annotated list of species, distributional summary, and assessment of impacts. Zoological Studies 57: 1–16. https://doi.org/10.6620/ZS.2018.57-07

Parker B, Andreou D, Green ID, Britto JR (2020) Microplastics in freshwater fishes: Occurrence, impacts and future perspectives. Fish and Fisheries 22(3): 467–488. https://doi.org/10.1111/faf.12528

Peters CA, Bratton SP (2016) Urbanization is a major influence on microplastic ingestion by sunfish in the Brazos River basin, central Texas, USA. Environmental Pollution 210: 380–387. https://doi.org/10.1016/j.envpol.2016.01.018

Rochman CM, Hoh E, Kurobe T, Teh SJ (2013) Ingested plastic transfers hazardous chemicals to fish and induces hepatic stress. Scientific Reports 3(1): 3263. https://doi.org/10.1038/srep03263

Salcedo MA, Sánchez AJ, Cruz-Ramírez A, Álvarez-Pliego N, Florido R, Ruíz-Carrera V, Garrido A, Alejo-Díaz R (2018) Aplicación del índice de calidad del agua (wqi-nsf) en lagunas metropolitanas y rurales. Agro Productividad 11(7): 81–86.

Sánchez AJ, Salcedo MA, Macossay-Cortéz AA, Feria-Díaz Y, Vázquez L, Ovando N, Rosado L (2012) Calidad ambiental de la laguna urbana La Pólvora en la cuenca del río Grijalva. IMTA-TC 3: 143–152.

Sánchez AJ, Álvarez-Pliego N, Espinosa-Pérez H, Florido R, Macossay-Cortez A, Barba E, Salcedo MÁ, Garrido-Mora A (2019) Species richness of urban and rural fish assemblages in the Grijalva basin floodplain, southern Gulf of Mexico. Cybium 43(3): 213–293. https://doi.org/10.26028/cybium/2019-433-005

Sanchez W, Bender C, Porcher J-M (2014) Wild gudgeons (*Gobio gobio*) from French rivers are contaminated by microplastics: Preliminary study and first evidence. Environmental Research 128: 98–100. https://doi.org/10.1016/j.envres.2013.11.004

Satélite Airbus (2023) Parque Público: La Pólvora [Imagen Satelital] Google Earth. https://earth.google.com/web/@17.98061586,-92.92612815,7.97313418a,697.41433558d,35y,359.74749997h,0t,0r?utm_source=earth7&utm_campaign=vine&hl=es-419

SEIACC (2021) Monitoreo de Calidad del Agua en lagunas del municipio Centro, Departamento de Monitoreo Ambiental de la Subsecretaría de Sustentabilidad y Cambio Climático, Gobierno de Tabasco, Villahermosa. [Accessed 25 Sept. 2021] https://tabasco.gob.mx/boletines-pmca-lagunas

Shruti VC, Pérez-Guevara F, Kutralam-Muniasamy G (2021) Wet wipes contribution to microfiber contamination under COVID-19 era: An important but overlooked problem. Environmental Challenges 5: 100267. https://doi.org/10.1016/j.envc.2021.100267

Silva-Cavalcanti JS, Silva JDB, de Franca EJ, Araújo MCB, Gusmão F (2016) Microplastics ingestion by a common tropical freshwater fishing resource. Environmental Pollution 221: 218–226. https://doi.org/10.1016/j.envpol.2016.11.068

Torres-Martínez AA, Sánchez AJ, Álvarez-Pliego N, Hernández-Franyutti A, López- Hernández JC, Bautista-Regil J ((2017) Gonadal histopathology of fish from La Pólvora urban lagoon in the Grijalva basin. Revista Internacional de Contaminación Ambiental 33(4): 713–717. https://doi.org/10.20937/RICA.2017.33.04.14

Vargas-Rivas AG, Barba-Macias E, Sánchez AJ, Castellanos Morales G (2023) Lack of mtDNA genetic diversity despite phenotypic variation and environmental heterogeneity in the exotic suckermouth armored catfish (*Pterygoplichthys pardalis*). Biological Invasions 25(4): 1035–1056. https://doi.org/10.1007/s10530-022-02961-w

Vidal C, Lozoya JP, Tesitore G, Goyenola G, Teixeira-de-Mello F (2021) Incidence of watershed land use on the consumption of meso and microplastics by fish communities in Uruguayan lowland streams. Water 13(11): 1575. https://doi.org/10.3390/w13111575

Wu LW, Liu CC, Lin SM (2011) Identification of exotic sailfin catfish species (*Pterygoplichthys*, Loricariidae) in Taiwan based on morphology and mtDNA sequences. Zoological Studies 50(2): 235–246.

Wu M, Yang C, Du C, Liu H (2020) Microplastics in waters and soils: Occurrence, analytical methods and ecotoxicological effects. Ecotoxicology and Environmental Safety 202: 110910. https://doi.org/10.1016/j.ecoenv.2020.110910

Yang L, Zhang Y, Kang S, Wang Z, Wu C (2021) Microplastics in freshwater sediment: A review on methods, occurrence, and sources. Science of the Total Environment 754: 141948. https://doi.org/10.1016/j.scitotenv.2020.141948

Yuan W, Liu X, Wang W, Di M, Wang J (2019) Microplastic abundance, distribution and composition in water, sediments, and wild fish from Poyang Lake, China. Ecotoxicology and Environmental Safety 170: 180–187. https://doi.org/10.1016/j.ecoenv.2018.11.126

Zhang Y, Gao T, Kang S, Sillanpää M (2019) Importance of atmospheric transport for microplastics deposited in remote areas. Environmental Pollution 254 (Part A): 112953. https://doi.org/10.1016/j.envpol.2019.07.121

Acta Ichthyologica et Piscatoria 53, 2023, 89–94 | DOI 10.3897/aiep.53.103531

PENSOFT.

ACTA
ICHTHYOLOGICA
ET PISCATORIA

New record of *Chromis weberi* (Actinopterygii: Ovalentaria: Pomacentridae) from Jeju Island, southern Korea

Se Hun MYOUNG[1], Jung-Goo MYOUNG[2], Min-Su WOO[3], Maeng Jin KIM[4], Min Gu KANG[5], Joo Myun PARK[5]

1 *Fisheries Resources Research Center, National Institute of Fisheries Science, Tongyeong, South Korea*
2 *Marine Bio-Resources Research Unit, Korea Institute of Ocean Science and Technology, Busan, South Korea*
3 *Ulleungdo-Dokdo Ocean Science Station, Korea Institute of Ocean Science and Technology, Ulleung, South Korea*
4 *West Sea Fisheries Research Institute, National Institute of Fisheries Science, Incheon, South Korea*
5 *Dokdo Research Center, Korea Institute of Ocean Science and Technology, Uljin, South Korea*

https://zoobank.org/0829E904-D9F3-4ABF-8F8F-6D2D59663627

Corresponding author: Joo Myun Park (joomyun.park@kiost.ac.kr)

Academic editor: Ronald Fricke ♦ **Received** 15 March 2023 ♦ **Accepted** 2 May 2023 ♦ **Published** 6 June 2023

Citation: Myoung SH, Myoung J-G, Woo M-S, Kim MJ, Kang MG, Park JM (2023) New record of *Chromis weberi* (Actinopterygii: Ovalentaria: Pomacentridae) from Jeju Island, southern Korea. Acta Ichthyologica et Piscatoria 53: 89–94. https://doi.org/10.3897/aiep.53.103531

Abstract

Discovering tropical marine species outside of their distribution limits is important for evaluating the impact of climate change on marine ecosystems. One specimen (31.6 mm standard length) of a tropical fish, *Chromis weberi* Fowler et Bean, 1928, representing the family Pomacentridae, was first recorded from Jeju Island, Korea, on 8 December 2021. It was characterized by black posterior margins of the preopercle and opercle and black upper and lower lobes of the caudal fin. A specimen of this species collected from Munseom was distinguished from *Chromis xanthura* (Bleeker, 1854) based on distinct differences in the tips of the upper and lower caudal fin lobes, which are not black in *C. xanthura*. In addition, *C. weberi* was easily distinguished from the other four species in the genus *Chromis*, by the mitochondrial DNA cytochrome *c* oxidase subunit I gene sequence (345 bp), with genetic distances ranging from 0.130 to 0.252. This study documents the first record of *C. weberi* in temperate Korean waters, implying a poleward range expansion for this species. The Korean name 'geom-eun-jeom-ggo-ri-ja-ri-dom' has been proposed for *C. weberi*.

Keywords

Chromis species, mt DNA-COI, northernmost record, Northwest Pacific, Weber's chromis

Introduction

Damselfishes (Pomacentridae) are usually distributed in the tropical Indo–Pacific region and occasionally in warm temperate seas (Allen 1991; Nelson et al. 2016). The family Pomacentridae comprises 348 species belonging to 28 genera worldwide, of which 105 species from 17 genera are distributed in Japan and adjacent sea areas (Aonuma et al. 2013). However, only 20 species from seven genera have hitherto been recorded in Korean waters (Marine Biodiversity Institute of Korea 2022). Damselfishes are morphologically deep and laterally compressed, with a relatively small body and mouth. They often have incomplete lateral line scales, and display color variation among individuals of the same species and locality (Froese and Pauly 2022). In addition, they lay elliptical demersal eggs guarded by males (Carpenter and Niem 2001; Froese and Pauly 2022).

Chromis weberi Fowler et Bean, 1928 is a tropical marine fish species widely distributed in warm Indo–

Pacific seas from the Red Sea and eastern Africa to southern New Caledonia between the latitudes 34°05′54″N and 33°11′18″S (Froese and Pauly 2022; GBIF 2023). *Chromis weberi* was described as a new species in 1928. Several studies have reported it in taxonomic checklists providing its basic biological information (Randall et al. 1998; Carpenter and Niem 2001; Nakabo 2013). Despite this and its widespread distribution, there is a lack of information regarding its biology and ecology.

Poleward range extension has increased the incursion of species of tropical origin into temperate seas due to recent climate change (Gervais et al. 2021). For example, increasing ocean temperatures allow tropical fishes, especially juveniles, to survive winter in temperate waters, which may facilitate a poleward range shift of the fishes (Figueira and Booth 2010). Considering the occurrence of warm-water species in temperate seas and their rate of introduction to these areas, the regional biodiversity and ecological processes may be impacted by such non-native species in invaded areas (Dragičević et al. 2021). Therefore, climate-driven changes in species distributions and consequent ecosystem restructuring are expected to have critical ecological, social, and economic implications (Wernberg et al. 2016).

In this study, we report a new northernmost record of *C. weberi* in Korean waters based on a specimen collected from Munseom, Jeju Island using a scoop net while SCUBA diving. Species identification was based on morphological characteristics and mitochondrial cytochrome *c* oxidase subunit I (mt-COI) sequences. The results of the presently reported study will contribute to understanding their distribution range and the management of local ecosystems experiencing the incursion of non-native marine species.

Materials and methods

One specimen of *Chromis weberi* was collected from Munseom (33°13′39.05″N, 126°33′48.79″E) along the southern coast of Jeju Island (Fig. 1). Sampling via SCUBA diving was performed during the day for approximately 20 m in sandy and rocky bottoms on 8 December 2021. The water temperature was 19°C at the time of sampling. Immediately after capture, the specimen was transported live to the laboratory, where an image of the specimen was taken after immobilizing it. Then, meristic counts and body morphometrics were recorded following Hubbs and Lagler’s (1958) method. The body morphometric characters were determined to the nearest 0.1 mm using digital vernier calipers and a stereo microscope. The specimen was then preserved in 5% formalin for 12 h and transferred to 70% ethanol for deposition at the Korea Institute of Ocean Science and Technology (KIOST).

Total genomic DNA was extracted from the muscle tissue using 10% Chelex resin (Bio-Rad, Hercules, CA, USA) to compare the molecular data. A portion of the mt-COI gene was amplified using specific primers (Radchenko et al. 2010). A polymerase chain reaction (PCR) was performed in a 30 µL reaction tube containing 3 µL genomic DNA, 5 µL 10× PCR buffer, 4 µL 2.5 mM deoxynucleoside triphosphate, 1 µL of each primer, 0.3 µL Ex-Taq DNA polymerase, and 15.7 µL sterile distilled H_2O, using a thermal cycler (MJ mini PTC-1148, Bio-Rad, USA). The PCR profile consisted of initial denaturation at 95°C for 5 min, followed by 34 cycles of denaturation at 95°C for 1 min, annealing at 50°C, extension at 72°C for 1 min, and a final extension at 72°C for 5 min. The PCR products were purified using ExoSAP-IT (United States Biochemical Corporation USA) and sequenced using an ABI PRISM BigDye Terminator v.3.1 Ready Reaction Cycle Sequencing Kit (Applied Biosystems, Inc. USA) using an ABI 3730xl DNA analyzer (Applied Biosystems Inc.). We compared our molecular data with mt-COI DNA sequences from other Pomacentridae fishes (*Chromis albicauda* Allen et Erdmann, 2009; *Chromis analis* (Cuvier, 1830); *Chromis notata* (Temminck et Schlegel, 1843); *Chromis fumea* (Tanaka, 1917); and *Chromis mirationis* Tanaka, 1917) and one outgroup (*Sillago japonica* Temminck et Schlegel, 1843) obtained from GenBank (https://www.ncbi.nlm.nih.gov/nucleotide). The sequences were aligned using ClustalW (Thompson et al. 1994) in BioEdit version 7 (Hall 1999). Genetic divergence was calculated using the Kimura 2-parameter (K2P) model (Kimura 1980) and MEGA 6 (Tamura et al. 2013). Phylogenetic trees were constructed using the neighbor-joining method (Saitou and Nei 1987) in MEGA 6 (Tamura et al. 2013), with confidence assessed based on 10 000 bootstrap replications.

In addition, the presently reported record of *C. weberi* on Juju Island was compared with previous global records based on the biological databases of the Global Biodiversity Information Facility (GBIF 2023).

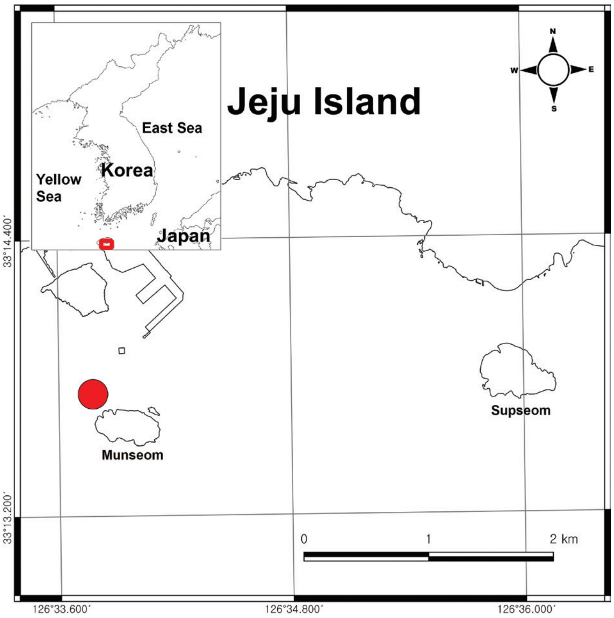

Figure 1. Map showing where the *Chromis weberi* specimen was collected off Munseom, Jeju Island, Korea Strait.

Results

Family Pomacentridae Bonaparte, 1831
Genus *Chromis* Cuvier, 1814

Chromis weberi Fowler et Bean, 1928

English vernacular name: Weber's chromis

Note. (Fig. 2) Body counts, measurements, and proportions of body parts expressed as the percentage of the standard length (SL) are shown in Table 1.

Material examined. KIOST 00001, 1 specimen, 31.6 mm SL, Munseom, Jeju Island, Korea (33°13′39.05″N, 126°33′48.79″E).

Description. Body deep and laterally compressed (Fig. 2); mouth small and terminal, with conical teeth in both jaws; single dorsal fin with deeply notched fin membrane originating vertically above pelvic fin; lateral line tubular and incomplete below dorsal soft rays. Head brown, and dorsal surface of head dark brown and iridescent under eyes and anterior tip (Fig. 2). Dorsal side of body dark brown; ventral side light brown. Posterior margins of preopercles and opercles black. Spiny rays and anterior soft rays of dorsal fin, anterior part of anal fins, and tips of upper and lower lobes of caudal fin black. Base of pelvic fins slightly black and becoming transparent toward tip. Posterior soft rays of dorsal fin and anal fin and central part of caudal fin transparent.

Table 1. Comparison of counts and measurements of *Chromis weberi*.

Morphological characters	Presently reported specimen	Masuda et al. 1984	Nakabo 2013
Counts			
Dorsal rays	XIII, 11	XIII, 11	XIII, 11
Anal rays	II, 11	II, 11	II, 11–12
Pectoral rays	18	18–20	18–20
LL_P	17	17–19	17–19
GR	8–9 + 19–22	8–9 + 19–22	8–9 + 19–22
Standard length (SL) [mm]	31.61	—	—
Measurements [%SL]			
Total length	135.1	—	—
Body depth	44.6	—	—
Head length	30.6	—	—
Snout length	6.1	—	—
Orbit diameter	12.7	—	—
Upper jaw length	10.1	—	—
Pre-dorsal length	41.3	—	—
Pre-anal length	71.7	—	—
Length of dorsal fin base	49.1	—	—
Length of anal fin base	18.4	—	—
Depth of caudal peduncle	15.7	—	—
Length of caudal peduncle	18.4	—	—

Genetics. Analysis of the mt-COI gene sequence (345 bp) showed that the specimen differed from other *Chromis* species recorded in the region with a genetic distance values of 0.130–0.252 (Fig. 3).

Figure 2. *Chromis weberi*, fresh, 31.6 mm SL, off Munseom, Jeju Island, South Korea.

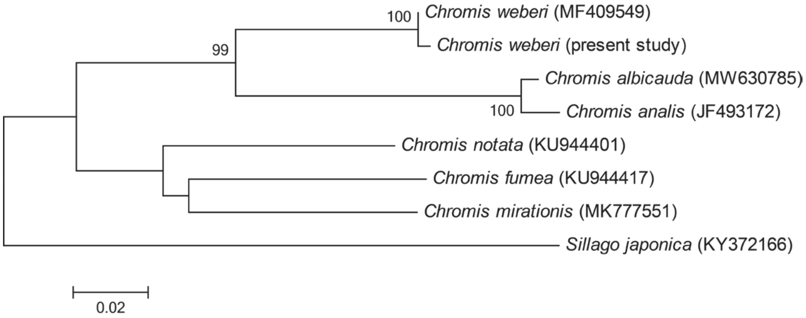

Figure 3. Neighbor-joining tree showing the relation between *Chromis weberi* (presently reported study; MF409549) and other *Chromis* spp., with one outgroup (*Sillago japonica*) using mt-COI DNA sequences. Numbers at branches indicate bootstrap probabilities in 1000 bootstrap replications. Bar indicates a genetic distance of 0.02.

Discussion

The body morphometrics of the specimen matched well the original description of *Chromis weberi* (see Fowler and Bean 1928), with black posterior margins of the preopercles and opercles and black upper and lower lobes of the caudal fin (Aonuma et al. 2013). The body morphology of *C. weberi* is similar to that of *Chromis xanthura* (Bleeker, 1854) with the only distinct difference being the tips of the upper and lower caudal fin lobes, which are not black in *C. xanthura* (see Aonuma et al. 2013). The mt-COI DNA sequence also confirmed genetic differences from other damselfishes from Korea. Therefore, this study documents the first record of *C. weberi* in Korean waters and we suggest the new Korean name of 'geom-eun-jeom-ggo-ri-ja-ri-dom'* for this species.

Chromis weberi is a typical subtropical fish species distributed mainly between 32°N and 23°S (Froese and Pauly 2022). According to the GBIF database (Fig. 4), the northernmost distribution of *C. weberi* was recorded at 34°05′54″N in 1975 on the eastern Pacific coast of Japan affected by the Kuroshio warm current (GBIF 2023). Except for this one record, the northern distribution limit of the species is 30°N, whereas the southern distribution limit is approximately 35°S (GBIF 2023). Therefore, this study reports a new and additional northernmost record of *C. weberi*, implying a poleward expansion of the species distribution.

Several studies have reported a worldwide poleward expansion in marine fish distributions in relation to climate change (Sunday et al. 2015; Park et al. 2017; Gervais et al. 2021; Azzola et al. 2022; Imamura et al. 2022). For example, on the eastern coast of Australia, a number of tropical Pomacentrids have dispersed to the southern temperate waters as a result of ocean warming (Figueira and Booth 2010; Fowler et al. 2018). In addition, several tropical marine fishes have been newly detected in Korean waters, especially around Jeju Island (Choi et al. 2013; Kim and Song 2014; Lee and Kim 2021), and these reports of such new records have gradually increased in recent years. The mechanisms of poleward range extensions of tropical marine fishes are generally based on a tendency of larval dispersal into temperate areas from natal tropical reefs, strength poleward inflow of warm current for advection of tropical larvae, recruitment to temperate reefs, and then the existence of sub-tropical breeding populations (Fowler et al. 2018). Although no data had been previously available on the occurrence of *C. weberi* larvae in Korean seas, some Pomacentrids larvae have been recorded in these regions, implying poleward extension of distribution through larval dispersal and subsequent colonization (Huh et al. 2013; Song et al. 2014).

The occurrence of these species in temperate Korean seas is attributed chiefly to the gradual increase in sea surface temperature and the northward trend of the Tsushima Warm Current as a result of global climate change (Jung et al. 2014; Son et al. 2020). Interannual trends in water temperature indicate that the marine ecosystem in Jeju Island is gradually changing into a subtropical sea (Suh et al. 2011; Seo and Park 2021). Therefore, we can expect a progressive increase in reporting of tropical and subtropical marine species to be recorded in the southern Korea Strait.

The discovery of a specimen of *C. weberi* along the southern coast of Jeju Island implies a poleward range extension of species distribution that can be attributed to the effects of climate change. Efforts to discover unrecorded species will help evaluate the influence of climate change on temperate marine ecosystems. In addition, this study

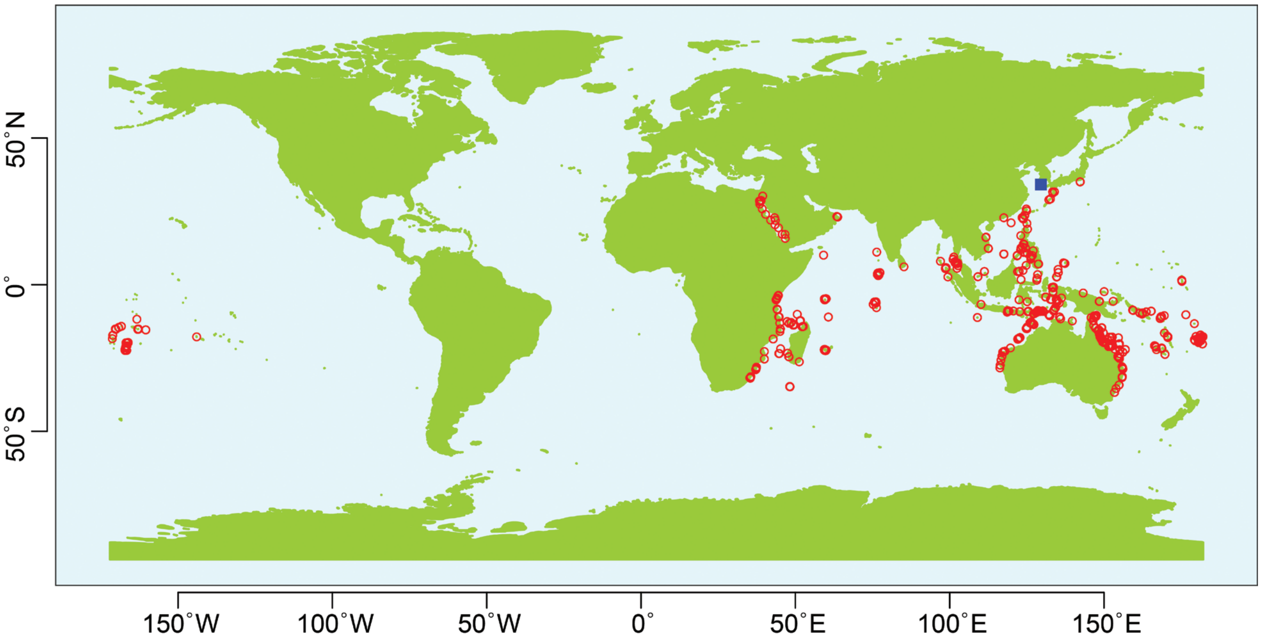

Figure 4. Distribution records of *Chromis weberi*, showing historical records (red circles) from the Global Biodiversity Information Facility (GBIF 2023) and the new record (blue square) off Jeju Island, South Korea.

---

* 검은점꼬리자리돔.

provides essential data for a better understanding of the current status of the marine ecosystem on Jeju Island and planning for future management in terms of biodiversity of local marine ecosystems in places of impending biodiversity crisis due to the introduction of tropical and/or subtropical marine species.

Acknowledgments

This research was funded by the Korea Institute of Ocean Science and Technology (grant number PEA0111) and supported by a grant from the National Institute of Fisheries Sciences (grant number R2023009).

References

Allen GR (1991) Damselfishes of the world. Mergus Publishers, Melle, Germany, 271 pp.

Aonuma Y, Yoshino T, Yagishita N (2013) Pomacentridae. Pp. 1029–1066. In: Nakabo T (Ed.) [Fishes of Japan with pictorial keys to the species.] 3rd ed. Tokai University Press, Tokyo, Japan. [In Japanese]

Azzola A, Furfaro G, Trainito E, Doneddu M, Montefalcone M (2022) Seawater warming favours the northward range expansion of Lessepsian species in the Mediterranean Sea: The cephalaspidean *Lamprohaminoea ovalis*. Journal of the Marine Biological Association of the United Kingdom 102(3–4): 167–173. https://doi.org/10.1017/S0025315422000339

Carpenter KE, Niem VH (Eds.) (2001) The living marine resources of the Western Central Pacific. Volume 6. Bony fishes part 4 (Labridae to Latimeriidae), estuarine crocodiles, sea turtles, sea snakes and marine mammals. FAO species identification guide for fishery purposes), FAO, Rome, 3381–4218.

Choi Y, Kim B, Lee H-H (2013) [The fish fauna of little Munsom in Jeju-do, Korea.] Hangug Hwangyeong Saengmul Haghoeji—Korean Journal of Environmental Biology 31(1): 45–52. [In Korean] https://doi.org/10.11626/KJEB.2013.31.1.045

Dragičević B, Ugarković P, Krželj M, Zurub D, Dulčić J (2021) New record of *Pterois* cf. *miles* (Actinopterygii: Scorpaeniformes: Scorpaenidae) from the eastern middle Adriatic Sea (Croatian waters): Northward expansion. Acta Ichthyologica et Piscatoria 51(4): 379–383. https://doi.org/10.3897/aiep.51.75811

Figueira WF, Booth DJ (2010) Increasing ocean temperatures allow tropical fishes to survive overwinter in temperate waters. Global Change Biology 16(2): 506–516. https://doi.org/10.1111/j.1365-2486.2009.01934.x

Fowler HW, Bean BA (1928) The fishes of the families Pomacentridae, Labridae, and Callyodontidae, collected by the United States Bureau of Fisheries steamer “Albatross,” chiefly in Philippine seas and adjacent waters. Volume 7 in Contributions to the biology of the Philippine Archipelago and adjacent regions. Smithsonian Institution, United States National Museum Bulletin 100.

Fowler AM, Parkinson K, Booth DJ (2018) New poleward observations of 30 tropical reef fishes in temperate southeastern Australia. Marine Biodiversity 48(4): 2249–2254. https://doi.org/10.1007/s12526-017-0748-6

Froese R, Pauly D (Eds.) (2022) FishBase. [Version 08/2022] https://www.fishbase.org

GBIF (2023) Global Biodiversity Information Facility. https://www.gbif.org

Gervais CR, Champion C, Pecl GT (2021) Species on the move around the Australian coastline: A continental-scale review of climate-driven species redistribution in marine systems. Global Change Biology 27(14): 3200–3217. https://doi.org/10.1111/gcb.15634

Hall TA (1999) BioEdit: A user-friendly biological sequence alignment editor and analysis program for Windows 95/98/NT. Nucleic Acids Symposium Series 41: 95–98.

Hubbs CL, Lagler KF (1958) Fishes of the Great Lakes Region. Bulletin of Cranbrook Institution of Science 26: 1–213.

Huh SH, Choi HC, Baeck GW, Kim HW, Park JM (2013) [Seasonal distribution of larval fishes in the central and southern surface waters of the East Sea.] Hangug Susan Haghoi Ji—Korean Journal of Fisheries and Aquatic Sciences 46(2): 216–222. [In Korean] https://doi.org/10.5657/KFAS.2013.0216

Imamura H, Koeda K, Ho HC (2022) A northward range extension of *Thysanophrys papillaris* (Actinopterygii: Scorpaeniformes: Platycephalidae) to Taiwan. Acta Ichthyologica et Piscatoria 52(4): 267–271. https://doi.org/10.3897/aiep.52.91098

Jung S, Pang IC, Lee JH, Choi I, Cha HK (2014) Latitudinal shifts in the distribution of exploited fishes in Korean waters during the last 30 years: A consequence of climate change. Reviews in Fish Biology and Fisheries 24(2): 443–462. https://doi.org/10.1007/s11160-013-9310-1

Kim MJ, Song CB (2014) New record of the white trevally, *Pseudocaranx dentex* (Carangidae, Perciformes) from Korea. Korean Journal of Ichthyology 26: 340–344.

Kimura M (1980) A simple method for estimating evolutionary rate of base substitution through comparative studies of nucleotide sequences. Journal of Molecular Evolution 16(2): 111–120. https://doi.org/10.1007/BF01731581

Lee YJ, Kim JK (2021) First record of *Chaetodon vagabundus* Linnaeus, 1758 (Pisces, Chaetodontidae) collected from Jeju Island, Korea. Journal of the Korean Society of Fisheries and Ocean Technology 57(2): 127–133. https://doi.org/10.3796/KSFOT.2021.57.2.127

Marine Biodiversity Institute of Korea (2022) [National list of marine species.] Namu Press, Seocheon. [In Korean]

Nakabo T (Ed.) (2013) [Fishes of Japan with pictorial keys to the species I, II and III.] Tokai University Press, Hadano, Japan. [In Japanese]

Nelson JS, Grande TC, Wilson VH (2016) Fishes of the world. 5th edn. John Wiley and Sons, Hoboken NJ, USA, 386 pp. https://doi.org/10.1002/9781119174844

Park JM, Huh SH, Choi HC, Kwak SN (2017) Larval distribution of the common dolphinfish *Coryphaena hippurus* Linnaeus 1758 (Coryphaenidae) in the East Sea/Sea of Japan. Journal of Applied Ichthyology 33(4): 815–818. https://doi.org/10.1111/jai.13387

Radchenko O, Chereshnev I, Petrovskaya A (2010) Relationships and position of the genus *Neozoarces* of the subfamily Neozoarcinae in the system of the suborder Zoarcoidei (Pisces, Perciformes) by molecular-genetic data. Journal of Ichthyology 50(3): 246–251. https://doi.org/10.1134/S0032945210030045

Randall JE, Allen GR, Steene RC (1998) Fishes of the Great Barrier Reef and Coral Sea. University of Hawaii Press. Honolulu, HI, USA, 594 pp.

Saitou N, Nei M (1987) The neighbor-joining method: A new method for reconstructing phylogenetic trees. Molecular Biology and Evolution 4: 406–425. https://doi.org/10.1093/oxfordjournals.molbev.a040454

Seo S, Park YG (2021) Tracking a coastal wave buoy, lost from the southern coast of Jeju Island, using Lagrangian particle modeling. Journal of Marine Science and Engineering 9(8): 795. https://doi.org/10.3390/jmse9080795

Son MH, Lee CI, Park JM, Kim HJ, Riedel R, Hwang I, Kim Y-N, Jung HK (2020) The northward habitat expansion of the Korean top shell *Turbo sazae* (Gastropoda: Vetigastropoda: Turbinidae) in the Korean Peninsula: Effects of increasing water temperature. Journal of Marine Science and Engineering 8(10): 782. https://doi.org/10.3390/jmse8100782

Song YS, Kwun HJ, Kim JK, Senou H (2014) A new record of juvenile *Chromis mirationis* (Perciformes: Pomacentridae) from Korea, revealed by molecular analysis, with a comparison to juvenile Chromis notata. Fisheries and Aquatic Sciences 17(2): 263–267. https://doi.org/10.5657/FAS.2014.0263

Suh YS, Hwang JD, Pang IC, Han IS, Jo JD, Lee NK (2011) [Long-term variations of sea surface temperature in inshore and offshore waters of Jeju Island.] Korean Journal of Nature Conservation 5: 135–140. [In Korean]

Sunday JM, Pecl GT, Frusher S, Hobday AJ, Hill N, Holbrook NJ, Edgar GJ, Stuart-Smith R, Barrett N, Wernberg T, Watson RA, Smale DA, Fulton EA, Slawinski D, Feng M, Radford DT, Thompson PA, Bates AE (2015) Species traits and climate velocity explain geographic range shifts in an ocean-warming hotspot. Ecology Letters 18(9): 944–953. https://doi.org/10.1111/ele.12474

Tamura K, Stecher G, Peterson D, Filipski A, Kumar S (2013) MEGA6: Molecular Evolutionary Genetics Analysis, version 6.0. Molecular Biology and Evolution 30(12): 2725–2729. https://doi.org/10.1093/molbev/mst197

Thompson JD, Higgins DG, Gibson TJ (1994) CLUSTAL W: Improving the sensitivity of progressive multiple sequence alignment through sequence weighting, position-specific gap penalties and weight matrix choice. Nucleic Acids Research 22(22): 4673–4680. https://doi.org/10.1093/nar/22.22.4673

Wernberg T, Bennett S, Babcock RC, De Bettignies T, Cure K, Depczynski M, Dufois F, Fromont J, Fulton CJ, Hovey RK, Harvey ES, Holmes TH, Kendrick GA, Radfor B, Santana-Garcon J, Saunders BJ, Smale DA, Thomsen MS, Tuckett CA, Tuya F, Vanderklift MA, Wilson S (2016) Climate-driven regime shift of a temperate marine ecosystem. Science 353(6295): 169–172. https://doi.org/10.1126/science.aad8745

Acta Ichthyologica et Piscatoria 53, 2023, 95–105 | DOI 10.3897/aiep.53.103246

PENSOFT.

ACTA
ICHTHYOLOGICA
ET PISCATORIA

Parasites as biological tags of divergence of black-striped pipefish, *Syngnathus abaster* (Actinopterygii: Syngnathiformes: Syngnathidae), populations in their natural and acquired range

Volodymyr YURYSHYNETS[1], Yuriy KVACH[2,3], Iryna SYNIAVSKA[4],
Oleksandra SHEVCHENKO[5], Yuliia KUTSOKON[4]

1 *Institute of Hydrobiology, National Academy of Science of Ukraine, Kyiv, Ukraine*
2 *Institute of Marine Biology, National Academy of Science of Ukraine, Odesa, Ukraine*
3 *Odesa I. I. Mechnikov National University, Odesa, Ukraine*
4 *Schmalhausen Institute of Zoology, National Academy of Science of Ukraine, Kyiv, Ukraine*
5 *Institute for Problems of Cryobiology and Cryomedicine of the National Academy of Sciences of Ukraine, Kharkiv, Ukraine*

https://zoobank.org/87ACE162-DBD5-4631-8A68-D37ADDEE506B

Corresponding author: Yuriy Kvach (yuruy.kvach@gmail.com)

Academic editor: Wojciech Piasecki ♦ **Received** 10 March 2023 ♦ **Accepted** 4 May 2023 ♦ **Published** 12 June 2023

Citation: Yuryshynets V, Kvach Y, Syniavska I, Shevchenko O, Kutsokon Y (2023) Parasites as biological tags of divergence of black-striped pipefish, *Syngnathus abaster* (Actinopterygii: Syngnathiformes: Syngnathidae), populations in their natural and acquired range. Acta Ichthyologica et Piscatoria 53: 95–105. https://doi.org/10.3897/aiep.53.103246

Abstract

The presently reported study was intended to describe the current range of an Atlanto–Mediterranean fish, the black-striped pipefish, *Syngnathus abaster* Risso, 1827, in Ukrainian waters and to analyze biological tags (size parameters and parasites) of its different populations. The parasitological survey was carried at five different localities, including one marine site, two deltaic zones, and two localities in the middle Dnipro basin. The study provides comprehensive new data on parasites of the black-striped pipefish in Ukraine, with supporting data on its newly acquired freshwater range. A total of 21 parasite species (taxa) were revealed. Several parasite species were recorded for the first time on this host, i.e., *Trichodinella epizootica* (Raabe, 1950); *Trypanosoma* sp.; *Bothriocephalus scorpii* (Müller, 1776); *Progrillotia dasyatidis* Beveridge, Neifar et Euzet, 2004; *Ophiotaenia europaea* Odening, 1963; *Cryptocotyle jejuna* (Nicoll, 1907); *Metorchis xanthosomus* (Creplin, 1846); *Tylodelphys clavata* (von Nordmann, 1832); *Holostephanus luehei* Szidat, 1936; *Contracaecum rudolphii* Hartwich, 1964; *Mothocya epimerica* Costa in Hope, 1851; and Unionidae gen. sp. Formation of the species' parasite component community depends entirely on environmental factors, with local parasite community features forming due to 1) presence of "marine" unicellular parasite species (ciliates) in marine localities (10‰–17‰ salinity) only, the community forming as a refraction of relative stenohalinity (*Trichodina rectuncinata* Raabe, 1958), findings of "marine" ciliate species in freshwater locations representing examples of successful osmoconformation (*Trichodina partidisci* Lom, 1962); or 2) presence of multicellular parasites in localities with abiotic/biotic conditions that allow completion of complex life cycles, such as those of trematodes (freshwater/marine mollusks as obligate first hosts) or cestodes (freshwater/marine invertebrates as intermediate hosts or marine/freshwater vertebrates as definitive hosts).

Keywords

brackish water, freshwater, Mediterranean species, neolimnetics, range extension, Ukraine

Introduction

Species range extension is a natural process stretched over time and it ultimately contributes to the formation of biodiversity (Alexandrov et al. 2007; Polačik et al. 2008). However, over recent decades, human activity has caused natural range borders to change significantly, spreading many species, including fishes (Bij de Vaate et al. 2002; García-Berthou et al. 2005; Hirsch et al. 2016). As a result, non-native (or alien) species are now having adverse effects (e.g., Ponto–Caspian gobiids in the Rhine River basin and the North-American Great Lakes, rainbow trout in European mountain locations, etc.) in many recipient ecosystems and, as such, they represent one of the biggest challenges for global biodiversity today (Leppäkoski et al. 2002; Hirsch et al. 2016).

Ukraine is located at a major crossing of transport corridors (land, freshwater, and marine), representing important routes for the spread of alien aquatic species (Alexandrov et al. 2007; Semenchenko et al. 2016). At least two crucial aquatic biological invasion routes pass through Ukraine's aquatic ecosystems, the so-called Southern and Central Corridors (Panov et al. 2009), and many Ponto–Caspian and Mediterranean species have now increased their ranges along these corridors (Tutman et al. 2012; Semenchenko et al. 2016; Marenkov 2018; Dobrzycka-Krahel et al. 2023). One such group is the "neolimnetics", which have a marine/brackish water origin but have spread into freshwater habitats in Ukraine and other European countries. These include species such as the Ponto–Caspian gobiids, the Ukrainian stickleback, *Pungitius platygaster* (Kessler, 1859); the black-striped pipefish, *Syngnathus abaster* Risso, 1827; and the big-scale sand smelt, *Atherina boyeri* Risso, 1810 (see Kvach and Kutsokon 2017).

The black-striped pipefish is an Atlanto–Mediterranean fish species with a natural range from the southern Gulf of Biscay in the north to Gibraltar in the south, the Mediterranean and Black Seas, and the estuarine zones of their rivers (Dawson 1986). It has a maximum body length of 21.5 cm (more commonly 16.0 cm) and a maximum weight of 3.0 g (age unknown). It lives along the coastal zone, mainly in shallow waters, and is tolerant of waters with different salinities (e.g., it is found along the coast of Crimea and in the Dnipro River near Kyiv), though it is far more common and numerous in estuaries and desalinated coasts than in open sea areas. The species matures at 2–3 years of age with a body length of ca. 7.0 cm and spawns from April to September, laying up to 200 eggs (usually ca. 100). The male accepts eggs from several females and carries them around in a brood sac. The species feeds on plankton and benthic organisms, tiny and medium-sized crustaceans, insect larvae, fish roe, and occasionally algae.

While the species has a brackish water origin, its high tolerance to freshwater has allowed it to spread up all large rivers in the Black Sea basin, i.e., the Danube, Dniester, Southern Buh, and Dnipro (Slastenenko 1956). It has been recorded in the Ros River (Dnipro basin) since the beginning of the 20th century and is now present in all reservoirs and the rivers Prypyat and Desna, though it is presently only found in small tributaries in the lower part of the basin (Beling 1923; Zimbalevskaya et al. 1989; Movchan 2012; Movchan and Roman 2014). In the Danube, the species has been recorded as far as Serbia and Bosnia and Herzegovina (Sekulić et al. 1999; Tutman et al. 2012).

Parasites are commonly used as biological tags of their host populations (Moser 1991; Mackenzie 2002). Fish parasite communities can be used to discriminate fish stocks and populations and, as such, a process known as "biological tagging" (Catalano et al. 2014; Poulin and Kamiya 2015; Kvach et al. 2017; Kutsokon et al. 2022) and the same biological tag can be used as a marker to clarify the possible origin of invasive populations (Hohenadler et al. 2018a, 2018b; Ondračková et al. 2012b; 2019; 2021). A total of 18 parasite species have been recorded for populations of the Black Sea basin black-striped pipefish (Gaevskaya et al. 1975). However, data for parasites in its acquired range are primarily related to the Danubian population in Bulgaria, where nine species were recorded (Ondračková et al. 2012a), and the Dnipro population in Ukraine, where just two ciliate species were recorded (*Trichodina partidisci* Lom, 1962 and *Trichodina acuta* Lom, 1961; see Yurishinets 2010). Consequently, very little is known about parasites acquired in the species' non-native freshwater habitats.

Therefore, the presently reported study aimed to describe the current range of black-striped pipefish in Ukrainian waters and obtain biological tag data (parasites) for the populations.

Materials and methods

The fish were sampled using the 10 × 1 m dipnet and a 1 × 0.5 m diameter hand net (0.5 cm mesh). In total, 107 fish were sampled from five different localities during the warm seasons of 2020–2021 (Table 1; Fig. 1). These included one marine locality (Gulf of Odesa), two deltaic zones (Danube and Dniester deltas), and two localities in the middle Dnipro basin (Lake Vyazky and the Stuhna River). In the Danube Delta, fish were sampled from three different sites (Fig. 1), considered the same locali-

Table 1. Number (*n*) and standard length (SL) of *Syngnathus abaster* from different localities in Ukraine.

Locality		Geographic coordinates	*n*	Standard length	
				Mean ± SD	Min–max
Black Sea (Gulf of Odesa)		46.443020; 30.772734	37	114.9 ± 22.8	65–203
Danube Delta		45.408702; 29.583393	20	107.5 ± 18.3	78–145
Dniester Delta		46.466634; 30.197059	17	104.1 ± 29.0	58–166
Dnipro basin	Lake Vyazky	50.368624; 30.653934	15	111.5 ± 16.2	79–140
	Stuhna River	50.149168; 30.731980	16	102.9 ± 24.0	51–143

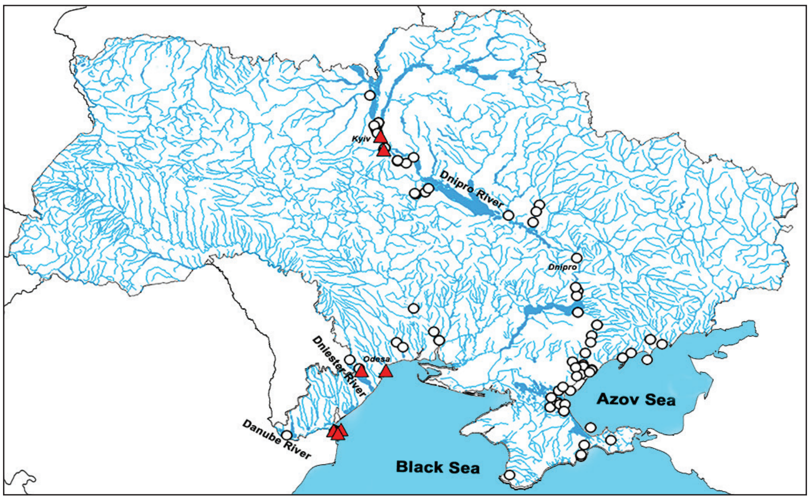

Figure 1. Map of Ukraine indicating the sampling localities with current sampling sites (2020–2021) marked with triangles.

ty for further analysis. The salinity of the Gulf of Odesa is 10‰–17‰ depending on the season (Zaitsev 1992). Once caught, the fish were transported alive to the laboratory in aerated cans filled with water from the sampling site, where they were placed in aerated aquaria containing water from the place of capture for no more than two days (Kvach et al. 2016) before being examined for parasites.

Findings of black-striped pipefish from other sites were registered (without removing the fish) and used to evaluate the range of the species (Fig. 1). In addition, a literature search was undertaken (Movchan 2012; Movchan and Roman 2014; Demchenko 2017; Kutsokon and Kvach 2021; Kutsokon and Roman 2021; Kutsokon et al. 2021a, 2021b) to obtain the latest information on the species' present-day range.

Prior to dissection, the standard length (SL, mm) and sex was determined for each fish (Table 1). After humanely sacrificing the fish, smears of gill and fins mucosa were taken, dried, and stained according to Klein (1958) to identify ciliates. Likewise, blood smears were dried and stained in hematoxylin (Giemsa 1904) to identify other unicellular organisms. Fresh smears from muscle and the gall and uterine bladders were examined for myxozoans and any living spores mounted onto gelatin gel as semi-permanent preparations for further identification. Monogeneans were placed onto glass slides and mounted in glycerin-ammonium-picrate for morphological study (Malmberg 1957). Cestodes, digeneans, and nematodes were fixed with hot 4% formalin (Cribb and Bray 2010), and glochidia and crustaceans in cold 4% formalin. Acanthocephalans and nematodes were mounted in glycerin as temporary slides for further species identification, while cestodes and digeneans were stained in iron acetocarmine and mounted onto Canada balsam slides (Georgiev et al. 1986). All parasites were identified to the lowest possible taxa, with parasite taxonomy presented following the World Register of Marine Species (WoRMS 2022). Parasitological terminology and principal indices, such as prevalence, intensity, mean intensity, and abundance, were used in accordance with Bush et al. (1997):

Prevalence (P)

$$P = \frac{n}{N} \times 100\%$$

where n is the number of infected fish and N is the number of fish examined.

Intensity (of infection) (I) is the number of individuals of a particular parasite species in a single infected host (individual fish) usually presented as the intensity range (I_R) (minimum–maximum).

Mean intensity (of infection) (I_M)

$$I_M = \frac{N_{TP}}{N_{inf}}$$

where N_{TP} is the total number of individuals of a particular parasite species found in all fish examined and N_{inf} is the number of infected fish.

Abundance (A)

$$A = \frac{N_T}{N}$$

where N_T is the total number of individuals of a particular parasite species found in all fish examined and N is the number of fish examined.

For microparasites (unicellular and myxozoans), only the prevalence was calculated, with the intensity of infection evaluated by the presence of microparasites in the microscope's field of view (Mierzejewska et al. 2012) as:

- Sporadic (S), from 1 to < 10 individuals in the material examined;
- Not numerous (NN), < 10 individuals in < 10% of field of view;
- Numerous (N), up to 20 individuals in > 50% of field of view;
- Very numerous (VN), > 20 individuals in > 50% of field of view;
- Mass (M), dozens of individuals in each field of view.

The Czekanowski–Sørensen index (CSI) was calculated (Sørensen 1948) to analyze differences in parasite fauna at different localities, with differences considered high in cases where index parameters were < 50%.

Statistical differences in length were evaluated using *t*-tests and *F*-tests for comparing two samples in Statistica for Windows 10 (StatSoft). Standard deviation values (SD) were calculated for mean parameters in each case. Visualization of fish size data was carried out in PAST v.4.03 (Paleontological Statistics Software system), using the search statistics methods (box and whisker), comparative analysis, and cluster analysis (Hammer et al. 2001). Discriminant analysis was then performed to evaluate differences in the respective parasite communities.

Results

We observed no significant difference in the length of black-striped pipefish from marine (Gulf of Odesa), estuarine (Danube and Dniester deltas), or freshwater (Lake Vyazky and Stuhna River) localities (Fig. 2).

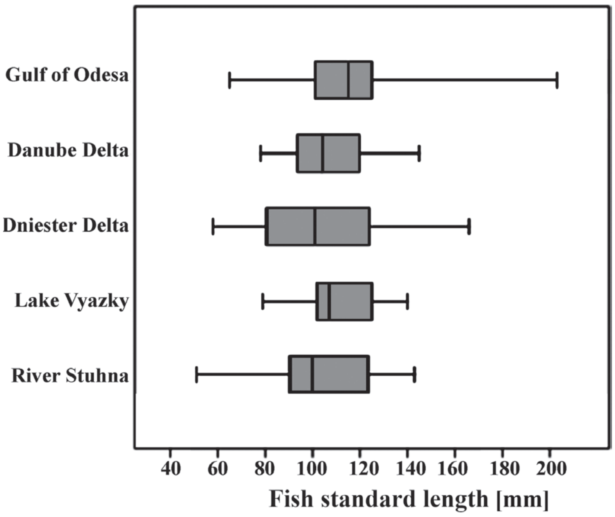

Figure 2. Box (median, 50% sample size) and whisker (min, max) plot for size (SL, mm) of *Syngnathus abaster* populations from different localities in Ukraine.

Based on published literature and databases, we consider the modern range of black-striped pipefish in Ukraine to include both brackish and freshwaters of the Black Sea basin (Fig. 1). In rivers where the populations have been established since the middle of the 20th century, the species is still to be found mainly in the lower reaches, though it has spread as far as the Belarus border in the Dnipro Reservoir cascade (Fig. 1), and into many of the lower first-order tributaries of the Dnipro River, regardless of size (i.e., medium rivers such as the Ros and Desna, and small rivers such as the Leglych and Mokra Moskovka). Despite much long-term research in the area, the black-striped pipefish has not been found in upper-flow tributaries to date. While the highest recorded finding was in the middle flow of the Ros River in 1923 (Beling 1923), all later records of the species have been from the lower reaches of the river (Kutsokon 2010). The species is also found in the lower reaches of the Dniester, Danube (along the entire stretch within the borders of Ukraine), Tyligul, Southern Buh, and rivers of the Crimean and Northern Azov coasts (Demchenko 2017; Kutsokon and Kvach 2021; Kutsokon and Roman 2021; Kutsokon et al. 2021b).

The parasite fauna of Ukrainian black-striped pipefish consisted of 21 parasite species (taxa), including five unicellular taxa, four cestodes, nine digeneans, one nematode, one isopod, and unidentified glochidia: *Trichodina* spp., *Trichodina partidisci* Lom, 1962, *Trichodina rectuncinata* Raabe, 1958, *Trichodinella epizootica* (Raabe, 1950) [CILIOPHORA]; *Trypanosoma* sp. [KINETOPLASTEA]; *Proteocephalus* sp., *Bothriocephalus scorpii* (Müller, 1776), *Progrillotia dasyatidis* Beveridge, Neifar et Euzet, 2004, *Ophiotaenia europaea* Odening, 1963 [CESTODA]; *Orientocreadium pseudobagri* Yamaguti, 1934, *Nicolla skrjabini* (Iwanitzky, 1928), *Cryptocotyle concava* (Creplin, 1825), *Cryptocotyle jejuna* (Nicoll, 1907), *Timoniella imbutiformis* (Molin, 1859), *Metorchis xanthosomus* (Creplin, 1846), *Diplostomum* spp., *Tylodelphys clavata* (von Nordmann, 1832), *Holostephanus luehei* Szidat, 1936 [DIGENEA]; *Contracaecum rudolphii* Hartwich, 1964 [NEMATODA]; *Mothocya epimerica* Costa in Hope, 1851 [CRUSTACEA]; Unionidae gen. sp. [BIVALVIA] (Table 2). Parasite richness varied from 2–3 species in the Dnipro basin and up to eight species in the Black Sea. The majority of parasites were represented by larval stages, with just two digeneans—*Orientocreadium pseudobagri*, *Nicolla skrjabini*—and an isopod *Mothocya epimerica* found as adults.

The most numerous species were ciliates of *Trichodina* spp., with the prevalence varying from 5.9% to 100% and intensity of infection of up to several thousand cells (Table 2). Among the ciliates, we identified at least three species, most represented by *Trichodina partidisci*, found in both freshwater (except the isolated Lake Vyazky) and marine/brackish sites. This is a small-sized species (23.7–31.5 µm; 27.6 ± 2.9), with a denticle ring diameter of 10.4–16.1 µm (13.5 ± 2.0) and a denticle number of 18–24 (22). It can be recognized by the broadly rounded distal surface of its denticle blade and the (usually) few, irregular unstained granules in the central part of its adhesive disc (Fig. 3). *Trichodina rectuncinata*, a species common on marine fish, was only found in the Gulf of Odesa. Again, this is a small-sized species (23.0–30.5 µm, 28.8 ± 1.7) with a denticle ring diameter of 12.3–15.2 µm (13.6 ± 1.2) and a denticle number of 22–25 (24), recognized by a triangular blade with a cavity in the center (Fig. 3). *Trichodinella epizootica*, a small mobilid typical of freshwaters, was registered in just one fish from the Danube Delta.

Ukrainian pipefish populations differed with the abundance values for *Nicolla skrjabini* and *Diplostomum* spp.

Table 2. Parasite communities of *Syngnathus abaster* from various localities in Ukraine (as determined in the presently reported study).

Parasite species **Developmental stage** **Location on host**	**Index**	**Black Sea (Gulf of Odesa)**	**Danube Delta**	**Dniester Delta**	**Dnipro basin**	
					Lake Vyazky	**Stuhna River**
Trichodina spp. [*Trichodina partidisci* Lom, 1962, *Trichodina rectuncinata* Raabe, 1958, *Trichodina* sp., *Trichodinella epizootica* (Raabe, 1950)]	P [%]	64.1	68.2	5.9		22.2
trophont	I_R	S–M	S–M	NN		VN
gills, skin, fins						
Trypanosoma sp.	P [%]			5.9		
trypomastigote	I_R			NN		
blood						
Proteocephalus sp.	P [%]		4.5			
plerocercoid	I_M ± SD		1.0			
gut	I_R		1			
	A		0.05			
Bothriocephalus scorpii	P [%]	7.7				
plerocercoid	I_M ± SD	2.7 ± 2.1				
gut	I_R	1–5				
	A	0.5				
Progrillotia dasyatidis	P [%]	5.1				
plerocercoid	I_M ± SD	4.5 ± 0.7				
gut	I_R	4–5				
	A	0.5				
Ophiotaenia europaea	P [%]			5.9		
plerocercoid	I_M ± SD			1.0		
mesentery	I_R			1		
	A			0.1		
Orientocreadium pseudobagri	P [%]		13.6	5.9		
marita	I_M ± SD		5.3 ± 5.9	1.0		
gut	I_R		1–12	1		
	A		0.7	0.1		
Nicolla skrjabini	P [%]			11.8		
marita	I_M ± SD			1.5 ± 0.7		
gut	I_R			1–2		
	A			0.2		
Cryptocotyle concava	P [%]	10.3				
metacercariae	I_M ± SD	4.5 ± 3.9				
mesentery, fins	I_R	1–10				
	A	1.1				
Cryptocotyle jejuna	P [%]	7.7				
metacercariae	I_M ± SD	4.7 ± 4.7				
mesentery, fins	I_R	1–10				
	A	0.8				
Timoniella imbutiformis	P [%]	2.6				
metacercariae	I_M ± SD	1.0				
muscles	I_R	1				
	A	0.1				
Metorchis xanthosomus	P [%]		4.5			
metacercariae	I_M ± SD		1.0			
mesentery	I_R		1			
	A		0.05			
Diplostomum spp.	P [%]				26.7	16.7
metacercariae	I_M ± SD				1.25 ± 0.5	1.3 ± 0.6
eyes	I_R				1–2	1–2
	A				0.3	0.2
Tylodelphys clavata	P [%]			5.9		
metacercariae	I_M ± SD			1.0		
eyes	I_R			1		
	A			0.1		
Holostephanus luehei	P [%]		9.1			
metacercariae	I_M ± SD		1.0			
mesentery	I_R		1			
	A		0.1			

Parasite species Developmental stage Location on host	Index	Black Sea (Gulf of Odesa)	Danube Delta	Dniester Delta	Dnipro basin	
					Lake Vyazky	Stuhna River
Contracaecum rudolphii	P [%]	2.6	4.5			
larvae	$I_M \pm$ SD	4.0	2			
mesentery	I_R	4	2			
	A	0.2	0.1			
Mothocya epimerica	P [%]	2.6				
adult	$I_M \pm$ SD	1.0				
gills	I_R	1				
	A	0.1				
Unionidae gen. sp.	P [%]			5.9	6.7	5.6
glochidia	$I_M \pm$ SD			5.0	2	5
gills	I_R			5	2	5
	A			0.3	0.1	0.3

P = prevalence, I_M = mean intensity, I_R = intensity range (min–max); A = abundance; SD = standard deviation; values of microparasites intensity (range) according to Mierzejewska et al. (2012) as: S = sporadic, NN = not numerous, N = numerous, VN = very numerous, M = mass.

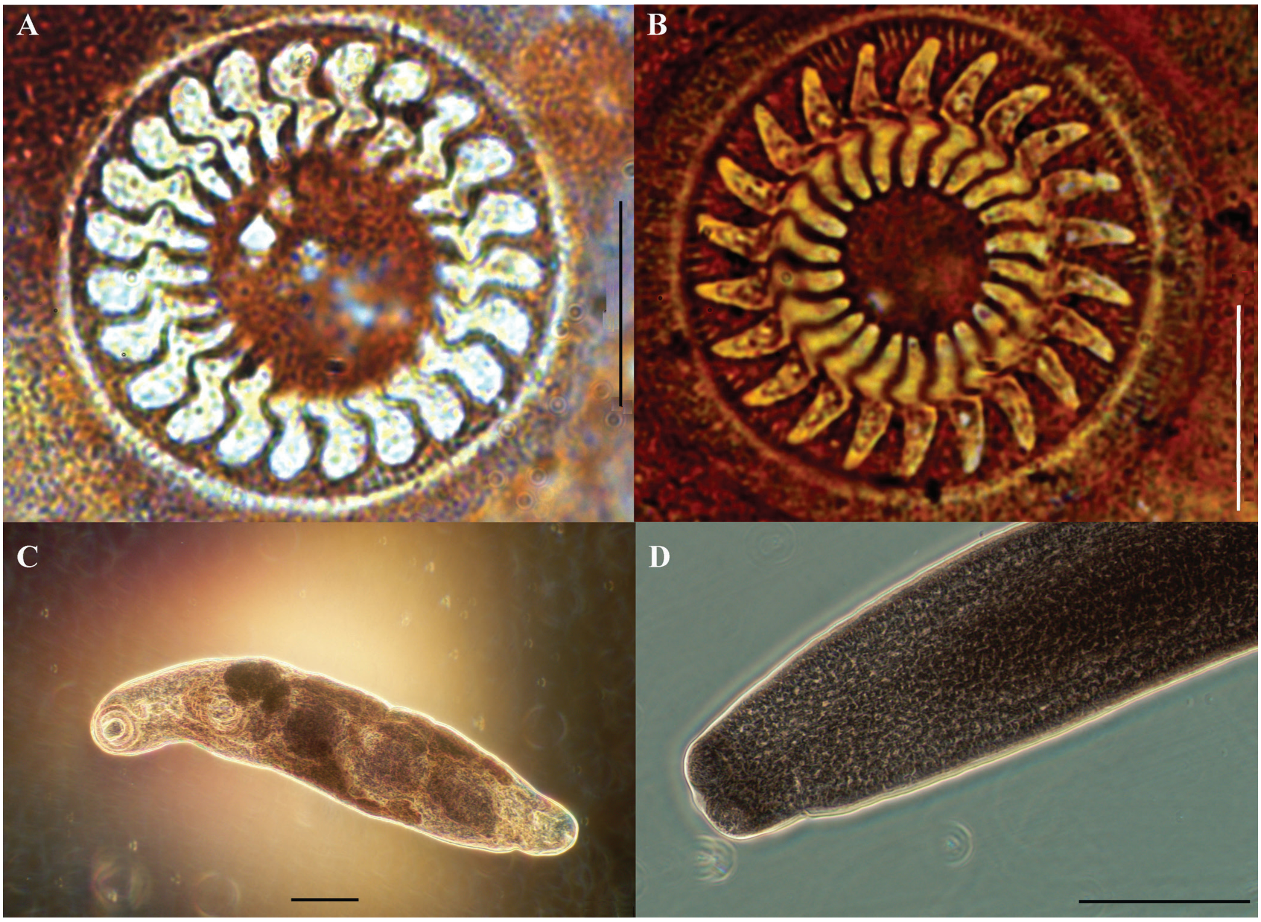

Figure 3. Typical parasites of *Syngnathus abaster* from different localities in Ukraine. **A**) *Trichodina partidisci* (Danube Delta); **B**) *Trichodina rectuncinata* (Black Sea, Gulf of Odesa); **C**) *Orientocreadium pseudobagri* (Danube Delta); **D**) *Proteocephalus* sp. (Danube Delta). Scale bars: 10 µm (A, B), 300 µm (C, D).

(Table 3), with a comparative analysis of parasite communities using the Czekanowski–Sørensen index (CSI) distinguished marine populations from freshwater/brackish populations (Fig. 4). CSI, Mahalanobis distance, and the Fischer criterium all showed significant differences between the Gulf of Odesa and the Danube and Dniester deltas (Table 4), with CSI parameters showing the largest differences between all localities.

Discussion

This study provides comprehensive new data on the parasites of black-striped pipefish in Ukraine, along with supporting data on its acquired range in Ukrainian freshwaters. Our new data confirm that the species is now found in the coastal zones of the Black Sea and the Sea of Azov and the deltaic zones of rivers and reservoirs of

Table 3. Discriminant function analysis of parasite communities of *Syngnathus abaster* from different localities in Ukraine.

Parasite species	Wilks' Lambda	Partial Lambda	*F*-remove (4,89)	*P*-value	Toler.	1-Toler. (R^2)
Trichodina spp.	0.42	0.91	2.08	0.09	0.59	0.41
Trypanosoma sp.	0.41	0.93	1.60	0.18	0.98	0.02
Bothriocephalus scorpii	0.41	0.95	1.15	0.34	0.98	0.02
Ophiotaenia europaea	0.41	0.93	1.60	0.18	0.98	0.02
Proteocephalus sp.	0.40	0.95	1.06	0.38	0.99	0.01
Progrillotia dasyatidis	0.39	1.00	0.02	1.00	0.54	0.46
Nicolla skrjabini	**0.44**	**0.89**	**2.86**	**0.03**	**0.97**	**0.03**
Orientocreadium pseudobagri	0.42	0.91	2.16	0.08	0.06	0.94
Cryptocotyle concavum	0.39	1.00	0.10	0.98	0.03	0.97
Cryptocotyle jejuna	0.39	1.00	0.03	1.00	0.03	0.97
Timoniella imbutiformis	0.39	0.98	0.45	0.77	0.99	0.01
Diplostomum spp.	**0.45**	**0.87**	**3.39**	**0.01**	**0.98**	**0.02**
Tylodelphys clavata	0.41	0.93	1.60	0.18	0.98	0.02
Holostephanus luehei	0.42	0.92	1.98	0.11	0.84	0.16
Metorchis xanthosomum	0.41	0.94	1.31	0.27	0.06	0.94
Contracaecum rudolphii	0.39	0.99	0.28	0.89	0.54	0.46
Mothocya epimerica	0.39	1.00	0.01	1.00	0.25	0.75
Unionidae gen. sp.	0.40	0.96	0.89	0.48	0.92	0.08

Wilks' Lambda: approx. 0.38655; *F* (72.352) = 1.3380; $P < 0.05$); **Bold** font dentotes significant differences.

Table 4. Matrix of differences between parasite fauna/communities of pipefish from different localities.

Locality	Index	Black Sea (Gulf of Odesa)	Danube Delta	Dniester Delta	Lake Vyazky
Danube Delta	ICS	**28.57**	100.00		
	MD	**2.72**	0.00		
	F	**1.78**			
Dniester Delta	ICS	**13.33**	**30.77**	100.00	
	MD	**4.21**	**4.27**	0.00	
	F	**2.33**	**1.91**		
Lake Vyazky	ICS	**0.00**	**0.00**	**22.22**	100.00
	MD	2.42	2.78	3.92	0.00
	F	1.22	1.16	1.46	
Stuhna River	ICS	**18.18**	**22.22**	**40.00**	**40.00**
	MD	1.72	2.31	3.12	0.21
	F	0.99	1.07	1.27	0.08

CSI = Czekanowski–Sørensen index, MD = squared Mahalanobis distances, F = Fischer criterium. Significant differences ($P < 0.05$) are marked in **bold.**

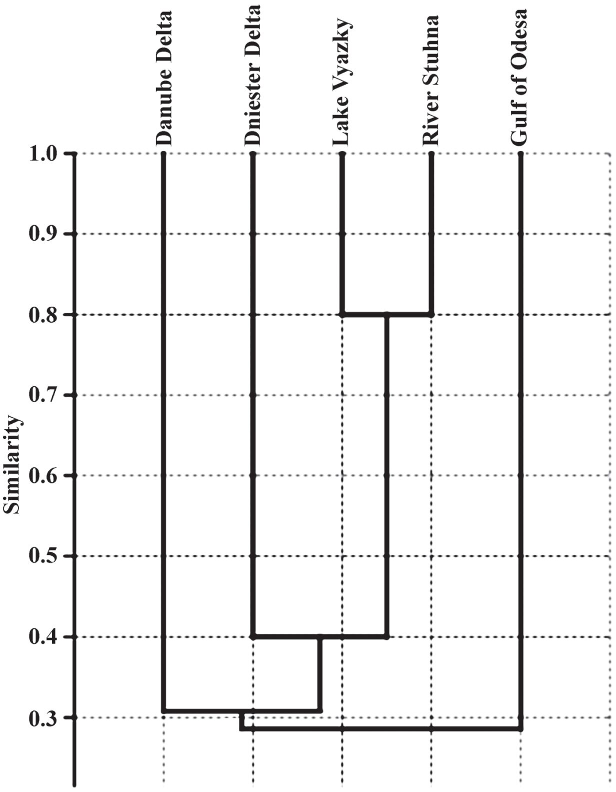

Figure 4. Dendrogram of similarity expressed by Czekanowski–Sørensen index for parasites component communities of *Syngnathus abaster* at different localities in Ukraine.

the Dnipro basin (Movchan 2011; Snigirov et al. 2020). However, the only new findings we recorded were inside the species' established range in the Lower Dnipro basin, suggesting that its Ukrainian range has probably now stabilized since it started spreading in the middle of the 20th century.

Several parasite species were registered on this host for the first time, i.e., *Trichodinella epizootica*, *Trypanosoma* sp., *Bothriocephalus scorpii*, *Progrillotia dasyatidis*, *Ophiotaenia europaea*, *Cryptocotyle jejuna*, *Metorchis xanthosomus*, *Tylodelphys clavata*, *Holostephanus luehei*, *Contracaecum rudolphii*, *Mothocya epimerica*; and Unionidae gen. sp. (Table 2). In addition, we confirmed the presence of several species previously recorded on the black-striped pipefish, including several ciliate species. While these are common on a wide spectrum of freshwater and brackish water hosts (Kostenko 1981; Grupcheva et al. 1989; Yurishinets 2010), no specific ciliates were previously known for black-striped pipefish. The most common species found was *Trichodina partidisci*, a parasite of mugilid fish in the Black Sea (Lom 1962) that has a wide spectrum of hosts (Grupcheva et al. 1989; Lom and Dyková 1992). In Ukrainian freshwaters, it is known from pipefish in the middle Dnieper basin (Yurishinets 2010). A second species, *Trichodina rectuncinata*, a widespread marine fish parasite, has previously been recorded in different areas of the Atlantic and Pacific oceans (Xu et al. 2001; Islas-Ortega et al. 2020; Öztürk and Güven 2022).

All four cestode species on black-striped pipefish were only registered at the plerocercoid stage. Two of the cestodes, *Bothriocephalus scorpii* and *Progrillotia dasyatidis* were marine species reported in the Gulf of Odesa. *Bothriocephalus scorpii* has been known as a parasite of turbot, *Scophthalmus maximus* (Linnaeus, 1758), scorpionfish (Scorpaenidae), mullet (Mugilidae), mackerel (Scombridae), and rays (Batoidea); *Progrillotia dasyatidis* is a parasite of a stingray, *Dasyatis pastinaca* (Linnaeus, 1758) (see Beveridge et al. 2004; Kuchta et al. 2008). While *Progrillotia dasyatidis* is common in fishes from the Gulf of Odesa (Kvach et al. 2022), *Bothriocephalus scorpii* has only been registered in adjacent water bodies (Kvach 2010). *Proteocephalus* sp. (see Fig. 3b), recorded in pipefish from the Danube, is a common parasite of Danubian freshwater fishes (Bauer 1985) and has previously been reported in pipefish from the middle Danube (Ondračková et al. 2012a). Finally, *Ophiotaenia europaea* is a parasite of grass snakes that uses fishes as its paratenic hosts (Sharpilo and Monchenko 1971). While it has previously been registered in fish from the Danube Delta (Kvach et al. 2020), this is the first time it has been registered in the Dniester River.

While the freshwater digeneans, *Orientocreadium pseudobagri* and *Nicolla skrjabini*, were recorded as adults in the gut of pipefish from the Danube and Dniester deltas (Table 2; Fig. 3), other digeneans were only represented by metacercariae, with either marine fish as their definitive hosts (*Timoniella imbutiformis*) or fish-eating birds (*Cryptocotyle concava*, *Cryptocotyle jejuna*, *Metorchis xanthosomus*, *Diplostomum* sp., *Tylodelphys clavata*). Moreover, we have not recorded those metacercariae with a wide spectrum of hosts, e.g., Cyathocotylidae fam. spp., *Echinochasmus perfoliatus* (Ratz, 1908), and *Metagonimus* sp., despite these having previously been reported in pipefish from the middle Danube basin (Ondračková et al. 2012a).

In the Gulf of Odesa and the Danube Delta, sporadic cases of parasitism by *Contracaecum rudolphii* nematode larvae were noted, the adult worms being common parasites of pelicans, herons, mergansers, and cormorants (Sreedevi et al. 2017). Previous authors (e.g., Gaevskaya et al. 1975) have also noted the presence of another species of this genus, *Contracaecum microcephalum* (Rudolphi, 1809), along with larvae of *Agamonema* sp. nematode in the parasitefauna of marine pipefish.

The isopod *Mothocya epimerica*, a parasite of the branchial and oral cavities of sand-smelts (*Atherina* spp.), was only noted at a marine location with few indications of invasion (Bruce 1986; Leonardos and Trilles 2004). The parasitic copepods *Ergasilus lizae* Krøyer, 1863 and *Ergasilus ponticus* Markevich, 1940 have also previously been reported from marine populations of the black-striped pipefish (Gaevskaya et al. 1975).

Parasitism on the gills of unionid bivalve larvae (Unionidae) was noted for three of four freshwater localities, though with relatively low invasion rates (P = 5%–7%, I_R = 2–5 ind.).

The acanthocephalans *Paracanthocephaloides incrassatus* (Molin, 1858) (see Gaevskaya et al. 1975) and *Acanthocephaloides irregularis* Amin, Oğuz, Heckman, Tepe & Kvach, 2011 (see Amin et al. 2011) have both been recorded in pipefish populations from Black Sea localities, while the acquisition of *Pomphorhynchus laevis* (Zoega in Müller, 1776) has been confirmed from the middle Danube (Ondračková et al. 2012a). We have not found, however, the above-mentioned parasite species during the presently reported study.

The black-striped pipefish is now widespread in Ukrainian bodies of water, particularly in coastal brackish and freshwaters of the Black Sea and the Sea of Azov basins. In Ukraine, it is found along all shores of the Black and Azov Seas and in the estuaries, near-estuary and estuarine zones of their rivers, from where it has entered reservoirs and rivers connected to the sea (below the Danube, Dniester, and Southern Buh). It is also found in all reservoirs along the Dnipro and the Siversky Donets River (Movchan 2011). Previous studies have confirmed differences in biotope preferences between marine pipefish, which prefer plant thickets, and those in freshwaters, which prefer muddy biotopes (Ondračková et al. 2012a; middle Danube).

Ondračková et al. (2012a) noted the absence of any parasites specific to this fish species, suggesting that the formation of the species' parasite component communities depends entirely on the environmental factors affecting each population. In such cases, the local features of the parasite communities will depend on the following:

- The presence of "marine" species of unicellular parasites (ciliophores) in marine localities (10‰–17‰ salinity) only as a refraction of relative stenohalinity (*Trichodina rectuncinata*), or findings of "marine" ciliate species in freshwater locations, as an example of successful osmoconformation (*Trichodina partidisci*).
- The presence of multicellular parasites in localities with abiotic/biotic conditions that allow completion of complex life cycles, i.e., trematodes (freshwater/marine mollusks as obligate first hosts) or cestodes (freshwater/marine invertebrates as intermediate hosts or marine/freshwater vertebrates as definitive hosts).

Overall, the parasite fauna of neolimnetic black-striped pipefish exhibits two main parasite community formation strategies in their acquired ecosystems:

- Parasite release (very poor communities in freshwater).
- Acquisition of local parasite species, which have overcome the filters of encounter and adaptation (Combes 1995).

Our findings confirm that analyzing changes in the structure of neolimnetic fish parasitic communities that overcome geographical and ecological barriers is a convenient model for establishing the patterns and features of hydrobiont distribution beyond the boundaries of natural habitats.

Acknowledgments

This study was partly carried out under the framework of the project "Development of scientific backgrounds of comprehensive monitoring and threats of distribution of invasive fish species by riverine systems and transitional waters of Ukraine (based on the parasite, population, and genetic markers)" (#2020.02/0171; National Research Foundation of Ukraine). We want to thank Mykola Prychepa and Yulia Kovalenko for kindly providing the sample from Lake Vyazky and for their help with basic laboratory processing. In addition, we thank Dr Kevin Roche for help with English proofreading.

References

Alexandrov B, Boltachev A, Kharchenko T, Lyashenko A, Son M, Tsarenko P, Zhukinsky V (2007) Trends of aquatic alien species invasions in Ukraine. Aquatic Invasions 2(3): 215–242. https://doi.org/10.3391/ai.2007.2.3.8

Amin OM, Oğuz MC, Heckmann RA, Tepe Y, Kvach Y (2011) *Acanthocephaloides irregularis* n. sp. (Acanthocephala: Arhythmacanthidae) from marine fishes off the Ukrainian Black Sea coast. Systematic Parasitology 80(2): 125–135. https://doi.org/10.1007/s11230-011-9312-0

Bauer ON (1985) Opredelitelʹ parazitov presnovodnyh ryb fauny SSSR, Tom 2, Parazitičeskie mnogokletočnye (Pervaâ častʹ). Izdatelʹstvo Nauka, Leningrad, USSR, 425 pp. [In Russian]

Beling DE (1923) Zametki po ihtiofaune Ukrainy. 1. Morskaâ igla – *Syngnathus nigrolineatus* Eischw. v bassejne Dnepra. Russkij gibrobiologičeskij žurnal 2(3–4): 71–73. [In Russian]

Beveridge I, Neifar L, Euzet L (2004) Review of the genus *Progrillotia* Dollfus, 1946 (Cestoda: Trypanorhyncha), with a redescription of *Progrillotia pastinacae* Dollfus, 1946 and description of *Progrillotia dasyatidis* sp. n. Folia Parasitologica 51(1): 33–44. https://doi.org/10.14411/fp.2004.005

Bij de Vaate A, Jażdżewski K, Ketelaars HAM, Gollasch S, Van der Velde G (2002) Geographical patterns in range extension of Ponto–Caspian macroinvertebrate species in Europe. Canadian Journal of Fisheries and Aquatic Sciences 59(7): 1159–1174. https://doi.org/10.1139/f02-098

Bruce NL (1986) Revision of the isopod crustacean genus *Mothocya* Costa, in Hope, 1851 (Cymothoidae: Flabellifera), parasitic on marine fishes. Journal of Natural History 20(5): 1089–1192. https://doi.org/10.1080/00222938600770781

Bush AO, Lafferty KD, Lotz JM, Shostak AW (1997) Parasitology meets ecology on its own terms: Margolis et al. revisited. Journal of Parasitology 83(4): 575–583. https://doi.org/10.2307/3284227

Catalano SR, Whittington ID, Donnellan SC, Gillanders BM (2014) Parasites as biological tags to assess host population structure: Guidelines, recent genetic advances, and comments on a holistic approach. International Journal for Parasitology, Parasites and Wildlife 3(2): 220–226. https://doi.org/10.1016/j.ijppaw.2013.11.001

Combes C (1995) Interactions durables. Ecologie et évolution du parasitisme. Masson, coll. Ecologie, n° 26, Paris, France, 524 pp.

Cribb TH, Bray RA (2010) Gut wash, body soak, blender and heat-fixation: Approaches to the effective collection, fixation, and preservation of trematodes of fishes. Systematic Parasitology 76(1): 1–7. https://doi.org/10.1007/s11230-010-9229-z

Dawson CE (1986) Syngnathidae. Pp. 628–639. In: Whitehead PJP, Bauchot M-L, Hureau J-C, Nielsen J, Tortonese E (Eds) Fishes of the North-eastern Atlantic and the Mediterranean, Volume 2. UNESCO, Paris.

Demchenko V (2017) Fishes of Ukraine. Ukrainian Biodiversity Information Network. http://ukrbin.com/literature.php?sort=id&action=reltaxa&id=3978

Dobrzycka-Krahel A, Stepien CA, Nuc Z (2023) Growing neocosmopolitan distributions of invertebrate aquatic invasive species due to euryhaline geographic history and human-mediated dispersal: Origins from the Ponto–Caspian versus other regions. Ecological Processes 12: 2. https://doi.org/10.1186/s13717-022-00412-x

Gaevskaya AV, Gusev AV, Delyamure SL, Donets ZS, Iskova NI, Kornyushin VV, Kovaleva AA, Margaritov NM, Markevich AP, Mordvinova TN, Naidenova NN, Nikolaeva VM, Parukhin AM, Pogoreltseva TP, Smogorzhevskaya LA, Solonchenko AI, Shtein GA, Shulman SS (1975) Opredelitelʹ parazitov pozvonočnyh Černogo i Azovskogo morej. Naukova Dumka, Kiev, USSR, 552 pp. [In Russian]

García-Berthou E, Alcaraz C, Pou-Rovira Q, Zamora L, Coenders G, Feo C (2005) Introduction pathways and establishment rates of invasive aquatic species in Europe. Canadian Journal of Fisheries and Aquatic Sciences 62(2): 453–463. https://doi.org/10.1139/f05-017

Georgiev B, Biserkov V, Genov T (1986) *In toto* staining method for cestodes with iron acetocarmine. Helminthologia 23: 279–281.

Giemsa G (1904) Eine Vereinfachung und Vervollkommnung meiner Methylenazur-Methylenblau-Eosin-Färbemethode zur Erzielungder Romanowsky-Nacht'schen Chromatin-Färbung. Centralblatt für Bakteriologie. Parasitenkunde und Infektionskrankheiten 37: 308–311.

Grupcheva G, Lom J, Dyková I (1989) Trichodinids (Ciliata: Urceolariidae) from gills of some marine fishes with the description of *Trichodina zaikai* sp. n. Folia Parasitologica 36(3): 193–207.

Hammer Ø, Harper DAT, Ryan PD (2001) PAST: Paleontological statistics software package for education and data analysis. Palaeontologia Electronica 4: 9.

Hirsch PE, N'Guyen A, Adrian-Kalchhauser I, Burkhardt-Holm P (2016) What do we really know about the impacts of one of the 100 worst invaders in Europe? A reality check. Ambio 45(3): 267–279. https://doi.org/10.1007/s13280-015-0718-9

Hohenadler MAA, Honka KI, Emde S, Klimpel S, Sures B (2018a) First evidence for a possible invasional meltdown among invasive fish parasites. Scientific Reports 8(1): 15085. https://doi.org/10.1038/s41598-018-33445-4

Hohenadler MAA, Nachev M, Thielen F, Taraschewski H, Grabner D, Sures B (2018b) *Pomphorhynchus laevis*: An invasive species in the river Rhine? Biological Invasions 20(1): 707–217. https://doi.org/10.1007/s10530-017-1527-9

Islas-Ortega AG, Basson L, Marcotegui P, Ruiz-Campos G, de Jager GP, Rivas G, Aguilar-Aguilar R (2020) Trichodinids (Ciliophora: Trichodinidae) on rocky-tidal fishes from the Baja California peninsula, Mexico. Journal of Parasitology 106(5): 689–698. https://doi.org/10.1645/20-80

Klein BM (1958) The dry silver method and its proper use. Journal of Protozoology 5(2): 99–103. https://doi.org/10.1111/j.1550-7408.1958.tb02535.x

Kostenko SM (1981) Fauna Ukraïny , tom 36, vypusk 4, Urtseoliariidy (peritrihi, mobîlîî). Naukova Dumka, Kyiv, URSR, 146 pp. [In Ukrainian]

Kuchta R, Scholz T, Bray RA (2008) Revision of the order Bothriocephalidea Kuchta, Scholz, Brabec et Bray, 2008 (Eucestoda) with amended generic diagnoses and keys to families and genera. Systematic Parasitology 71(2): 81–136. https://doi.org/10.1007/s11230-008-9153-7

Kutsokon YK (2010) Sučasnij vidovij sklad ribnoho naselennâ basejnu rîčki Ros'. Materîali mîžnarodnoï naukovoï konferencîï. Problemi vivčennâ î ohoroni tvarinnoho svîtu u prirodnih î antropogennih ekosistemah. (Chernivtsi, 2010). DrukArt, Chernivtsi, 37–39. [In Ukrainian with English summary]

Kutsokon Y, Kvach Y (2021) Invasive, neolimnetic and aboriginal fish species in Dnipro, Danube and Southern Buh basins (Ukraine, 2021). Version 1.7. Ukrainian Nature Conservation Group (NGO). Occurrence dataset accessed via GBIF.org on 2022-11-14. https://doi.org/10.15468/pwtyfq

Kutsokon Y, Roman A (2021) The own findings of fish of Ukraine during 2001–2021. Version 1.6. Ukrainian Nature Conservation Group (NGO). Occurrence dataset accessed via GBIF.org on 2022-11-14. https://doi.org/10.15468/zdqq8t

Kutsokon Y, Didenko O, Shcherbatiuk M, Gurbyk O, Buzevych O, Marushchak O (2021a) Fishes of water bodies of Rzhyshchiv city amalgamated territorial community (CATC). Version 1.5. Ukrainian Nature Conservation Group (NGO). Occurrence dataset accessed via GBIF.org on 2022-11-14. https://doi.org/10.15468/ftwx4e

Kutsokon Y, Roman A, Kvach Y, Shcherbatiuk M (2021b) Fish communities in three rivers of the South Podolia, Black Sea basin, Ukraine. Acta Zoologica Bulgarica 73(3): 385–391.

Kutsokon YK, Yuryshynets VI, Shcherbatiuk MM, Marushchak OY, Zaichenko NV, Dupak VS (2022) Alien fish species and their parasites of the Zdvyzh River: General characteristics, marker indicators, the monitoring scheme. Hydrobiological Journal 58(6): 28–45. https://doi.org/10.1615/HydrobJ.v58.i6.20

Kvach Y (2010) Helminths of the marbled goby (*Pomatoschistus marmoratus*), a Mediterranean immigrant in the Black Sea fauna. Vestnik Zoologii 44(6): 509–518. https://doi.org/10.2478/v10058-010-0034-6

Kvach Y, Kutsokon Y (2017) The non-indigenous fishes in the fauna of Ukraine: A potentia ad actum. BioInvasions Records 6(3): 269–279. https://doi.org/10.3391/bir.2017.6.3.13

Kvach Y, Ondračková M, Janáč M, Jurajda P (2016) Methodological issues affecting the study of fish parasites. I. Duration of live fish storage prior to dissection. Diseases of Aquatic Organisms 119(2): 107–115. https://doi.org/10.3354/dao02990

Kvach Y, Ondračková M, Bryjová A, Jurajda P (2017) Parasites as biological tags of divergence in Central European gudgeon populations (Actinopterygii: Cyprinidae: Gobioninae). Biologia 72(6): 671–679. https://doi.org/10.1515/biolog-2017-0073

Kvach Y, Kutsokon I, Roman A, Čeirāns A, Pupins M, Kirjušina M (2020) Parasite acquisition by the invasive Chinese sleeper (*Perccottus glenii* Dybowski, 1877) (Gobiiformes: Odontobutidae) in Latvia and Ukraine. Journal of Applied Ichthyology 36(6): 785–794. https://doi.org/10.1111/jai.14100

Kvach Y, Snigirov S, Leonchyk Y, Zamorov V (2022) The first data on parasite community of the black scorpionfish, *Scorpaena porcus* (Actinopterygii: Scorpaenidae), from the north-western Black Sea. Journal of Applied Ichthyology 38(2): 204–211. https://doi.org/10.1111/jai.14300

Leonardos I, Trilles J-P (2004) Reproduction of *Mothocya epimerica* (Crustacea: Isopoda: Cymothoidae), parasitic on the sand smelt *Atherina boyeri* (Osteichthyes: Atherinidae) in Greek lagoons. Diseases of Aquatic Organisms 62: 249–253. https://doi.org/10.3354/dao062249

Leppäkoski E, Gollasch S, Olenin S (2002) Invasive aquatic species of Europe. Distribution, impacts and management. Kluwer Academic Publishers, Dordrecht, 584 pp. https://doi.org/10.1007/978-94-015-9956-6

Lom J (1962) Trichodinid ciliates from fishes of the Rumanian Black Sea coast. Parasitology 52(1–2): 49–61. https://doi.org/10.1017/S0031182000023982

Lom J, Dyková I (1992) Protozoan parasites of fishes. Elsevier, New York, 315 pp.

Mackenzie K (2002) Parasites as biological tags in population studies of marine organisms: An update. Parasitology 124(7): 153–163. https://doi.org/10.1017/S0031182002001518

Malmberg G (1957) Om forekomsten av *Gyrodactylus* pa svenska fiskar. Skrifter Utgivna av Sodra Sveriges Fiskeriforening 1956: 19–76.

Marenkov ON (2018) Abundance and biomass estimation of this summer individuals of alien fish species in Zaporizke Reservoir. Ukrainian Journal of Ecology 8(1): 92–96. https://doi.org/10.15421/2018_192

Mierzejewska K, Kvach Y, Woźniak M, Kosowska A, Dziekońska-Rynko J (2012) Parasites of an Asian fish, the Chinese sleeper *Perccottus glenii*, in the Włocławek Reservoir on the Lower Vistula River, Poland: In search of the key species in the host expansion process. Comparative Parasitology 79(1): 23–29. https://doi.org/10.1654/4519.1

Moser M (1991) Parasites as biological tags. Parasitology Today 7(7): 182–185. https://doi.org/10.1016/0169-4758(91)90128-B

Movchan YV (2011) Ribi Ukraïni. [Fishes of Ukraine.] Zoloti Vorota, Kyiv, Ukraïna, 444 pp. [In Ukrainian]

Movchan YV (2012) Sučasnîj sklad îhtîofauni basejnu verhn'oho Dnipra (faunističnij oglâd). [Contemporary fish fauna of the Upper Dnipro basin (faunistic review).] Zbìrnik prac′ zoologìčnogo muzeû 43: 35–50. [In Ukrainian with English summary]

Movchan YV, Roman AM (2014) Sučasnîj sklad îhtîofauni basejnu seredn′oho Dnipra (faunističnij oglâd). [Modern fish fauna of middle Dnipro basin (faunistic review).] Zbìrnik prac′ zoologìčnogo muzeû 45: 25–45. [In Ukrainian with English summary]

Ondračková M, Slováčková I, Trichkova T, Polačik M, Jurajda P (2012a) Shoreline distribution and parasite infection of black-striped pipefish *Syngnathus abaster* Risso, 1827 in the lower River Danube. Journal of Applied Ichthyology 28(4): 590–596. https://doi.org/10.1111/j.1439-0426.2012.01967.x

Ondračková M, Šimková A, Civáňová K, Vyskočilová M, Jurajda P (2012b) Parasite diversity and microsatellite variability in native and introduced populations of four *Neogobius* species (Gobiidae). Parasitology 139(11): 1493–1505. https://doi.org/10.1017/S0031182012000844

Ondračková M, Kvach Y, Martens A, Jurajda P (2019) Limited parasite acquisition by non-native *Lepomis gibbosus* (Antinopterygii: Centrarchidae) in two ponds at the Upper Rhine in Germany. Journal of Helminthology 93(4): 453–460. https://doi.org/10.1017/S0022149X18000469

Ondračková M, Janáč M, Borcherding J, Grabowska J, Bartáková V, Jurajda P (2021) Non-native gobies share predominantly immature parasites with local fish hosts. Journal of Vertebrate Biology 70(4): 21050. https://doi.org/10.25225/jvb.21050

Öztürk T, Güven A (2022) Trichodinid ectoparasites (Ciliophora: Peritrichida) from gills of some marine fishes of Sinop coasts of the Black Sea, with the first report of *Trichodina rectuncinata*. Aquatic Research 5(4): 295–306. https://doi.org/10.3153/AR22029

Panov VE, Alexandrov B, Arbačiauskas K, Binimelis R, Copp GH, Grabowski M, Lucy F, Leuven RSEW, Nehring S, Paunović M, Semenchenko V, Son MO (2009) Assessing the risks of aquatic species invasions via European inland waterways: From concepts to environmental indicators. Integrated Environmental Assessment and Management 5(1): 110–126. https://doi.org/10.1897/IEAM_2008-034.1

Polačik M, Janáč M, Trichkova T, Vassilev M, Keckeis H, Jurajda P (2008) The distribution and abundance of the *Neogobius* fishes in their native range (Bulgaria) with notes on the non-native range in the Danube River. Fundamental and Applied Limnology 18(Suppl. 166): 193–208. https://doi.org/10.1127/lr/18/2008/193

Poulin R, Kamiya T (2015) Parasites as biological tags of fish stocks: A meta-analysis of their discriminatory power. Parasitology 142(1): 145–155. https://doi.org/10.1017/S0031182013001534

Sekulić N, Cakić P, Lenhardt M, Vučić D, Budakov LJ (1999) Short-snouted pipefish *Syngnathus abaster* (Acanthopterygii: Syngnathidae) in Yugoslav section of the Danube. Ichthyologia 3: 79–82.

Semenchenko V, Son MO, Novitski R, Kvach Y, Panov VE (2016) Checklist of non-native benthic macroinvertebrates and fish in the Dnieper River basin. BioInvasions Records 5(3): 185–187. https://doi.org/10.3391/bir.2016.5.3.10

Sharpilo VP, Monchenko VI (1971) On the life cycle of *Ophiotaenia europaea* Odening, 1963 (Cestoda, Ophiotaeniidae). Vestnik Zoologii 6: 90–92.

Slastenenko E (1956) Karadeniz havzası balıkları. E.B.K. Yayini, Istanbul, 711 pp.

Snigirov SM, Zamorov VV, Karavanskyi YV, Pitsyk VZ, Kurakin OP, Abakumov OM, Liumkis PV, Snigirov PM, Morozov YV, Kvach YV, Kutsokon YK (2020) Taksonomîčna ta ekologo-faunîstichna harakteristika sučasnoï îkhtîofauni Odeskoï zatoki, Dnîstrovskogo peredgirlovogo uzmorâ î priberežnih vod o. Zmîînyj. Visnyk Odeskoho natsionalnoho universytetu. Biolohiia 25(2): 113–139. https://doi.org/10.18524/2077-1746.2020.2(47).218060 [In Ukrainian with English summary]

Sørensen TA (1948) A new method of establishing groups of equal amplitude in plant sociology based on similarity of species content and its application to analysis of vegetation on Danish commons. Kongelige Danske Videnskabernes Selskabs, Biologiske Skrifter 5: 1–34.

Sreedevi C, Prasuna K, Lavanya K, Kanaka Swarna Latha K (2017) *Contracaecum rudolphii* Hartwich, 1964 (Nematoda: Anisakidae) in a wild spot-billed pelican (*Pelecanus philippensis*): a case report. Journal of Parasitic Diseases 41(4): 959–962. https://doi.org/10.1007/s12639-017-0918-2

Tutman P, Burić M, Skaramuca B (2012) First substantiated record of the black-striped pipefish, *Syngnathus abaster* (Actinopterygii: Syngnathiformes: Syngnathidae), in the freshwaters of Bosnia and Herzegovina. Acta Ichthyologica et Piscatoria 42(3): 259–262. https://doi.org/10.3750/AIP2011.42.3.11

WoRMS (2022) World Register of Marine Species. [Accessed 2022-10-27.] https://doi.org/10.14284/170

Xu K, Song W, Warren A, Choi JK (2001) Trichodinid ectoparasites (Ciliophora: Peritrichida) of some marine fishes from coastal regions of the Yellow Sea and Bohai Sea. Systematic Parasitology 50(1): 69–79. https://doi.org/10.1023/A:1011865124047

Yurishinets VI (2010) Symbiotic organisms of some alien species of freshwater fishes and mollusks of water bodies of the Danube River and Dnieper River basins. Russian Journal of Biological Invasions 1(2): 141–144. https://doi.org/10.1134/S207511171002013X

Zaitsev YP (1992) Ekologičeskoe sostojanie šelfovoj zony Černogo morâ u poberež'â Ukrainy (obzor). Gidrobiologičeskij žurnal 28(4): 3–18. [In Russian with English summary]

Zimbalevskaya LN, Sukhoivan PG, Chernogorenko MI (1989) Bespozvonočnye i ryby Dnepra i jego vodohranilišč. Naukova Dumka, Kiev, USSR, 242 pp. [In Russian]

Acta Ichthyologica et Piscatoria 53, 2023, 107–122 | DOI 10.3897/aiep.53.101239

PENSOFT.

ACTA
ICHTHYOLOGICA
ET PISCATORIA

New records of ray-finned fishes (Actinopterygii) from Puerto Morelos Reef National Park (Mexican Caribbean)

Francisco MARTÍNEZ-SERVÍN[1], Yareli Margarita LÓPEZ-ARROYO[1],
Aurora Lizeth MORENO-VÁZQUEZ[1], D. Ross ROBERTSON[2],
Alfrancis Teresa ARREDONDO-CHÁVEZ[1], Juan Antonio SÁNCHEZ-JIMÉNEZ[1],
Oscar Gabriel ÁVILA-MORALES[1], Xavier MADRIGAL-GURIDI[1],
José Adán CABALLERO-VÁZQUEZ[3], Juan J. SCHMITTER-SOTO[4],
Omar DOMÍNGUEZ-DOMÍNGUEZ[1], María Gloria SOLÍS-GUZMÁN[1]

1 *Laboratorio de Biología Acuática, Facultad de Biología, Universidad Michoacana de San Nicolás de Hidalgo, Ciudad Universitaria s/n, Morelia, Michoacán, Mexico*
2 *Smithsonian Tropical Research Institute, Balboa, Panama*
3 *Centro de Investigación Científica de Yucatán, A.C. Unidad de Ciencias del Agua, Laboratorio de Ecología y Biodiversidad de Organismos Acuáticos, Cancún, Quintana Roo, Mexico*
4 *Departamento de Sistemática y Ecología Acuática, El Colegio de la Frontera Sur, Chetumal, Quintana Roo, Mexico*

https://zoobank.org/AF9B5354-C55A-4142-8C65-9A4ED283B2BD

Corresponding author: María Gloria Solís-Guzmán (maria.solis@umich.mx)

Academic editor: Ronald Fricke ♦ **Received** 31 January 2023 ♦ **Accepted** 27 May 2023 ♦ **Published** 23 June 2023

Citation: Martínez-Servín F, López-Arroyo YM, Moreno-Vázquez AL, Robertson DR, Arredondo-Chávez AT, Sánchez-Jiménez JA, Ávila-Morales OG, Madrigal-Guridi X, Caballero-Vázquez JA, Schmitter-Soto JJ, Domínguez-Domínguez O, Solís-Guzmán MG (2023) New records of ray-finned fishes (Actinopterygii) from Puerto Morelos Reef National Park (Mexican Caribbean). Acta Ichthyologica et Piscatoria 53: 107–122. https://doi.org/10.3897/aiep.53.101239

Abstract

We documented the nearshore ray-finned fishes in Puerto Morelos Reef National Park (PMRNP) by sampling 57 localities, including rocky intertidal pools, sandy bottoms, *Thalassia* beds, coral reefs, artificial reefs, karstic-slab bottoms, demersal-pelagic areas, and sessile-*Sargassum* patches. We recorded seven species new to Caribbean Mexican waters and one hundred and six species new to the PMRNP, most of which are small cryptobenthic reef fish. The resultant checklist includes 349 species, and specimens of 285 of which (81.7%) have been deposited in an ichthyological museum collection. These include both voucher organisms and with tissue samples for genetic analysis. A comparison with inventories at other localities of the Greater Caribbean indicates that more targeted sampling for cryptobenthic and deep-reef fishes is needed to provide a complete inventory. We also comment on the local use of some species as fishery resources.

Keywords

cryptobenthic, marine fish, Mexican Caribbean, new records

Introduction

The Mexican Caribbean is part of the central province of the Greater Caribbean biogeographic region (Robertson and Cramer 2014), a large area that includes all of the Caribbean Sea, except the northern coast of South America. This area is a semi-closed sea with a long and complex geological history (Pindell and Kennan 2009) that produced an arc of islands, the Antilles, along its eastern boundary. It is an area of low productivity, with abundant coral reefs and large areas of ancillary habitats, including seagrass beds and mangroves closely associated with the reefs. The Greater Caribbean also has many endemic shore fishes, up to 700 species (Robertson et al. 2015). The Mexican Caribbean is part of Yucatan's karstic limestone rock peninsula extending northeast from Central America into the Gulf of Mexico. The Caribbean coast of Mexico, in the State of Quintana Roo, extends 400 km from Cabo Catoche in the north to Xcalak in the south (Schmitter-Soto et al. 2000; de la Lanza-Espino et al. 2013). It has a narrow continental shelf, no upwelling areas, low productivity, substantial amounts of freshwater entering the coastal fringe from subterranean aquifers, low input of suspended solids, and surface water temperatures consistently above 25°C (Robertson et al. 2015; Rioja-Nieto and Álvarez-Filip 2019). These conditions have facilitated the formation of the second largest coral reef barrier in the world, the Mesoamerican Barrier Reef System, which also includes substantial amounts of ancillary habitats used by reef fishes: mangroves, "karstic-slab" bottoms (sheets of limestone rock-forming low profile, low complexity rocky bottoms, loose coral rubble, and rockeries), seagrasses, macroalgal beds, and soft bottoms (gravel, sand, and mud). This habitat diversity along the Mexican Caribbean has promoted the development of a rich shore-fish fauna, with more than 577 species (Schmitter-Soto et al. 2000).

The fishes and reefs in the area support large amounts of tourist activity, primarily through sport diving, and the artisanal and sport fishing industry (Cinner and Pollnac 2004). Despite this high diversity and economic importance of the Mexican Caribbean reefs, community-level research on coastal fishes of that area is relatively scarce, and no in-depth studies have been carried out on reef fishes. Previous studies have covered mainly on the southern portion of that area focusing on fishes on coral patches (Caballero-Vázquez and Schmitter-Soto 2001), fishes in coastal lagoons (Avilés-Torres et al. 2001; Caballero-Vázquez et al. 2005), fish assemblages (Vásquez-Yeomans and González-Vera 1992; Lara and González 1998; Loreto et al. 2003; Núnez-Lara et al. 2005; Cobián-Rojas et al. 2018; Schmitter-Soto et al. 2018), fish diets (Valdez-Moreno et al. 2012), and on fishes in seagrass habitats (Álvarez-Guillén et al. 1986; Yeager and Arias-González 2008; Zarco-Perelló and Enríquez 2019). Schmitter-Soto et al. (2000) presented a general checklist of Mexican Caribbean marine fishes. In the northern Mexican Caribbean, Reséndez-Medina (1975) provided a list for the Nichupté Lagoon, Fenner (1991) analyzed the impact of hurricanes on the fishes of Cozumel Island and Loreto and Lazcano (2017) explored Arrowsmith Bank. However, the northern portion is the most populated area, experiencing rapid coastal development and increased tourism infrastructure. This includes Mexico's most important area for tourism, the Tulum–Cancun touristic corridor, which exerts high pressure on marine natural resources, including reef communities (COESPO 2017; Rioja-Nieto and Álvarez-Filip 2019).

Several natural protected areas have been established to reduce the impact of human activities in the Mexican Caribbean, including Puerto Morelos Reef National Park (PMRNP), established in 1988 (SEMARNAP 2000). The PMRNP Management Plan recorded 226 fish species (SEMARNAP 2000). However, very few research articles have been published listing the fish species found in the park (Álvarez-Guillén et al. 1986; Álvarez-Cadena et al. 2007; Zarco-Perelló and Enríquez 2019), and the recent new record of a reef blenny (*Hypsoblennius exstochilus* Böhlke, 1959) in the Mexican Caribbean, which was found in PMRNP (Sánchez-Jiménez et al. 2017), indicates that taxonomic inventories of the Mexican Caribbean are yet to be completed.

The main goal of presently reported study was to provide an updated checklist, including new records for the Mexican Caribbean and the PMRNP, of the ray-finned fish fauna from this park while incorporating information on local use by fishermen. We also compare the relative abundance of different shallow and deep reef-associated fishes in the Greater Caribbean Region (GCR) and at six sites. Because there have been few fish studies conducted in the northern Mexican Caribbean, and since all of them were focused on conspicuous reef fishes and relied on visual censuses, we expected a substantial increase of the known fish richness, mainly in cryptobenthic and non-coral reef species. This knowledge will increase understanding of regional fish diversity and could be useful for this protected area's conservation and management strategies.

Materials and methods

Puerto Morelos Reef National Park (PMRNP) covers 9066 ha, in a narrow strip along ~20 km of the coastline (Fig. 1). The center of the park is defined by a barrier reef that runs parallel to the coast, with its outer margin exposed to wave action throughout the year. Inshore from the barrier reef is a shallow, sheltered lagoon that varies between 60 and 3000 m in width and its maximum depth approximates 8 m. PMRNP is within an area of low tidal amplitude (Merino and Otero 1991); the dominant current flows to the north and is stronger than in more southern localities of the coast (Muhling et al. 2013). This park also encompasses other habitats used by fishes, including mangrove forests along the shoreline, *Thalassia* seagrass beds within the lagoon, sand bottoms, artificial reefs, gorgonian fields, rocky intertidal pools, karstic-slab bottoms (sheets of horizontal, low relief karstic limestone rock, sometimes with gorgonians, small, scattered coral growths, loose coral rubble, and rockeries), patch reefs, freshwater springs, and deep areas (>40 m) (SEMARNAP 2000). The park boundary extends only 1–3 km beyond the outer edge of the barrier reef into the northern approaches to the channel that separates Cozumel Island from the mainland. Almost all park area outside the barrier reef is shallower than 30–50 m. There is only one section of the park where water depths extends 50 m (see nautical chart SM922.3; SEMAR 2023). That section of the park, in its southeast corner, represents < 0.5% of the area of the PMRNP.

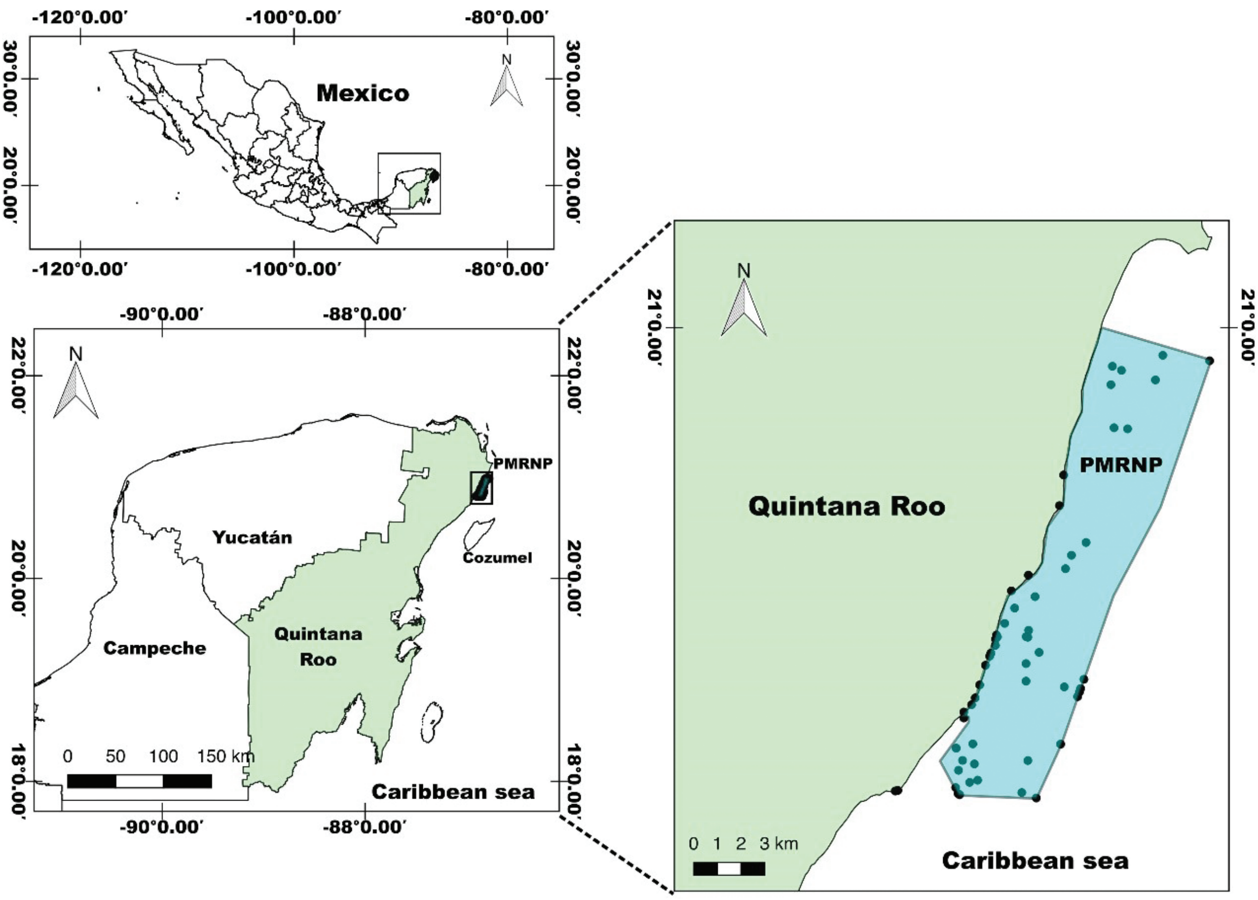

Figure 1. Sample locations in Puerto Morelos Reef National Park in Quintana Roo State, Mexico. Shadow blue represents the polygon of the National Park. Black points within the park indicate collecting sites.

Collection methods. This study covers the results from fish collections at 57 localities scattered throughout most of PMRNP (Table 1 and Fig. 1). We conducted field samplings from May 2014 to May 2015. Habitats sampled included karstic rock intertidal pools, sandy bottoms, *Thalassia* beds, coral reefs, artificial reefs, submerged karstic-slab bottoms, and patches of benthic *Sargassum* macroalgae attached to the sand and pelagic areas (mid- to surface waters in areas offshore from the barrier reef). Methods varied according to the habitat to be sampled. Collections at depths of 4 to 40 m were carried out by SCUBA diving. Non-cryptic fishes were speared using multi-pronged pole spears. Cryptobenthic fishes are species that live closely associated with or within benthic habitats, are visually cryptic in form and behavior, and often are small (Viesca-Lobatón et al. 2008; Brandl et al. 2018). Such species were collected using clove oil (eugenol) anesthetic at a ratio of 1:5 (eugenol:ethanol) for coral reefs, artificial reefs, and submerged karstic-slab bottoms, and 1:40 for collections at tide pools (see Table 1). We captured sedated fish with a slurp gun or hand net. For some sand-bottom sites, we use a seine net, 10 m long × 2 m high with a 1 cm open mesh. We cooperated with local artisanal fishermen to collect incidental and commercial species at the limits of the National Park. We caught those fishes with hook-an-line and gillnets of 7–12 cm mesh size at a maximum depth of 80 m. We also obtained information about the use of those species from those fishers. The habitat type from which each species was collected is also included in the checklist.

We took photographs of most freshly collected specimens soon after collection when we took tissue samples from the pectoral fin, which were placed at 96% analytical grade ethanol and stored at –80°C in the Tissue Collection of the Ichthyological Collection at Universidad Michoacana (CPUM, registration key: MICH.-PEC-227-07-09). Whole-fish specimens were then fixed in 5% or 10% formalin neutralized with sodium borate and subsequently preserved in 70% ethanol. Voucher specimens were deposited in the fish collection (CPUM). We identified fishes using the keys and descriptions from Humann and Deloach (2002), Carpenter (2002), and Robertson et al. (2015). Twenty species that were difficult to identify morphologically had their identity corroborated using mitochondrial DNA barcodes. For 16 species, we used the gene cytochrome c oxidase subunit (*cox1*); for the *Bathygobius* species, we used mitochondrial cytochrome b (*cytb*). We amplified the *cox1* gene with the primers Fish1F and Fish1R, following Ward et al. (2005), and for *cytb* we used the primers Glud-G and H16460 following Perdices et al. (2002). The sequences of the 16 species with *cox1* were deposited in Genbank under ascension numbers MZ720809–MZ720822 and MZ868935, and MZ870594. We corroborated the identity of species with the Boldsystem or Genbank sequences (Blast) to verify identification.

Table 1. Georeferenced and habitat type of the sampling sites in Puerto Morelos Reef National Park in Quintana Roo State, México.

Sampling site	Latitude, Longitude	Habitat type	Depth [m]
Ojo Norte	20.8863, –86.8572	S, R	5–9
Ojo de Agua	20.8499, –86.8732	S, R	3–7
Muelle Fiscal	20.8418, –86.8778	AR	5–10
La Bocana	20.8748, –86.8525	R, SB, S	2–10
Limones	20.9888, –86.7971	R	3–8
Boya Zona Norte	20.9788, –86.8001	S	15–20
Barco hundido	20.8544, –86.8371	AR	25–40
Jardín frontal	20.8313, –86.8741	R	6–10
La Pared	20.8246, –86.8783	R, SB	6–12
Pared frontal	20.8231, –86.8735	R, SB	4–10
Cueva de tiburón	20.8684, –86.8473	R, SB	15–20
Rordman	20.8745, –86.8518	TF	5–9
Fish market	20.8136, –86.8811	R, SB	10–18
Hoyanquita	20.8206, –86.8799	TF, R, S, SB	10–15
Cuevones	20.9129, –86.8282	TF, R, SB, S	6–12
Punta Caracol	20.8910, –86.8489	TF, SB, R, S	3–7
El volador	20.8111, –86.8801	S, R, SB	10–15
El Oasis	20.8107, –86.8795	S, TF, R, SB	8–15
Picudas	20.8773, –86.8515	R, SB	5–9
Bocana sur	20.8754, –86.8646	S, TF	1–3
Muelle UNAM	20.8681, –86.8668	AR	1–3
Punta Norte	20.9769, –86.8182	R	9–12
Mantarraya	20.8157, –86.8754	S, TF, SB	11–15
Los Abanicos	20.9078, –86.8342	S, TF, SB	8–11
Bonanza sur	20.9594, –86.8169	R, SB	3–9
Canal Limones	20.9827, –86.8139	S, R	4–9
El Rapidin	20.8115, –86.8543	S, SB	35–40
Frente al CID	20.8296, –86.8809	TF, S, SB	1–5
Manatí	20.9844, –86.8176	R	11–15
Muelle Desire	20.8631, –86.8690	AR	1–3
Red ball	20.8245, –86.8518	AR	8–12
Cazones	20.9023, –86.8366	R, SB	10–14
Límite del Parque Norte	20.9866, –86.7782	P	40
Mar Casa de Playa	20.8997, –86.8516	S, TF	1–4
Ojo Pargo	20.8801, –86.8612	S, R	7
La Herradura	20.8166, –86.8722	S, SB	8–14
Punta Brava	20.8124, –86.9045	RI	< 1
Muelle Puerto	20.8472, –86.8746	AR	1–3
Pelicanos	20.8442, –86.8778	S, TF, SB	1–3
Nichupte	20.8296, –86.8809	S	1–3
Punta Sur del Parque	20.8094, –86.8484	P	80
Muelle Los Gemelos	20.8737, –86.8650	AR	1–3
Lado Sur Punta Brava	20.8122, –86.9056	S	1–3
Royalton	20.9403, –86.8373	S, SP	1–3
Frente Muelle General	20.8312, –86.8386	S, TF	1–3
Restaurante Único	20.8552, –86.8714	S	1–3
Matón Viejo	20.9590, –86.8114	SP	2–5
Petempich	20.9279, –86.8390	S, TF	1–3
Silversam	20.8933, –86.8585	RI	< 1
Frente a la CONANP	20.8669, –86.8673	S	1–3
Hotel Excellent	20.8746, –86.8642	TF	1–3
Hotel Dreams	20.8712, –86.8650	S, TF	1–3
Pescadores Sitio 2	20.8567, –86.8526	P	50
Pescadores Sitio 3	20.8505, –86.8317	P	60
Pescadores Sitio 4	20.8537, –86.8304	P	30
Pescadores Sitio 5	20.8575, –86.8291	P	80
Pescadores Sitio 6	20.8522, –86.8310	P	50

Collection habitat: R = coral reef, TF = *Thalassia* bed, S = sandy bottom, P = pelagic, AR = artificial reef, SB = karstic-slab bottom, RI = intertidal pool, SP = *Sargassum* patch. **Bold** type denotes sites at which clove oil was used to collect cryptobenthic fish.

The species recorded in the management plan of PMRNP (SEMARNAP 2000) that were not collected in this study were also included in the list, except for a few species whose identification we considered uncertain. We also included records from FishNet, GBIF, and IDigBio of fish found in the PMRNP. Families, genera, and species in the resultant checklist (Table 2) are arranged alphabetically. The determination of fish names and their taxonomic validity was aided based on the online version of Eschmeyer's Catalog of Fishes (Fricke et al. 2023). It should be emphasized that this updated monthly Catalog is not a nomenclatural act.

We classified different types of shallow and deep reef fishes collected in PMRNP according to categories used in the most recent version of the list of "Reef-associated bony fishes of the Greater Caribbean" published by Robertson and Tornabene (2020). That database classified fishes as pelagic, demersal (use the bottom and water column), and benthic (restricted to the bottom, with cryptobenthic a subcategory of that group). It also divides species into shallow and deep forms, with the former including species found above 40 m, while deep forms are entirely or primarily restricted to depths below 40 m. Using this categorization, we compared variation in the taxonomic structure of shallow and deep components of the fauna of PMRNP to that of six well-studied sites scattered from Bermuda to the southern Caribbean (see Robertson et al. 2020, 2022).

Table 2. Checklist of shallow water ray-finned fishes known from Puerto Morelos Reefs National Park, México. [Abbreviations explained in the table's footnote.]

FAMILY and species	New records	Habitat	References and vouchers	USG	CRS
FAMILY ACANTHURIDAE					
Acanthurus chirurgus (Bloch, 1787)		R, TF, S, AR, SB	3, 5, CPUM		
Acanthurus coeruleus Bloch et Schneider, 1801		R, TF, S, AR, SB	3, CPUM		
Acanthurus tractus Poey, 1860		R, TF, S, AR	1, 3, 5, CPUM		
FAMILY ALBULIDAE					
Albula goreensis Valenciennes, 1847	G	TF	CPUM		
Albula vulpes (Linnaeus, 1758)		S, TF	3, 5, CPUM		
FAMILY ANTENNARIIDAE					
Histrio histrio (Linnaeus, 1758)		TF, SP	3, 5, CPUM		+
FAMILY APOGONIDAE					
Apogon aurolineatus (Mowbray, 1927)		"RA	5		+
Apogon binotatus (Poe, 1867)		"RA	5		+
***Apogon maculatus* (Poey, 1860)**	NP, GBIF	R	3, CPUM		+
Apogon planifrons Longley et Hildebrand, 1940		R	5, CPUM		+
Apogon quadrisquamatus Longley, 1934		"RA	3, 5		+
***Apogon robbyi* Gilbert** et **Tyler, 1997**	NM, GBIF	R	3, CPUM		+
***Apogon townsendi* (Breder, 1927)**	NP, GBIF	R	3, CPUM		+
Astrapogon puncticulatus (Poey, 1867)		R, S	3, 5, CPUM		+
***Phaeoptyx conklini* (Silvester, 1915)**	NP	R	CPUM		+
***Phaeoptyx pigmentaria* (Poey, 1860)**	NP, GBIF	R	3, CPUM		+
FAMILY ATHERINIDAE					
Atherina harringtonensis Goode, *1*877		P	5, CPUM		
Atherinomorus stipes (Muller et Troschel, 1848)		P	3, 5, CPUM		
FAMILY AULOSTOMIDAE					
Aulostomus maculatus Valenciennes, 1841		R, TF, AR	1, 3, 5, CPUM		
FAMILY BALISTIDAE					
Balistes capriscus Gmelin, 1789		R, TF, S, AR	3, 5, CPUM	SF	
Balistes vetula Linnaeus, 1758		R, AR, P	1, 3, 5, CPUM	SF	
Canthidermis sufflamen (Mitchill, 1815)		R, TF, S, AR, SB, P	1, 3, 5, CPUM		
Melichthys niger (Bloch, 1786)		"RA	5		
Xanthichthys ringens (Linnaeus, 1758)		R	3, CPUM		
FAMILY BATRACHOIDIDAE					
***Sanopus astrifer* (Robins et Starck, 1965)**	NP, GBIF	R	3, CPUM		+
FAMILY BELONIDAE					
Platybelone argalus (Lesueur, 1821)		P	3, 5, CPUM		
***Strongylura marina* (Walbaum, 1792)**	NP, GBIF	P	3, CPUM		
***Strongylura notata* (Poey, 1860)**	NP, GBIF	P	3, CPUM		
***Strongylura timucu* (Walbaum, 1792)**	NP, GBIF	P	3, CPUM		
***Tylosurus acus* (Lacepéde, 1803)**	GBIF	P	3, CPUM		
Tylosurus crocodilus (Péron et Lesueur, 1821)		P	3, 5, CPUM		
FAMILY BLENNIIDAE					
Entomacrodus nigricans Gill, 1859		RI	5, CPUM		+
Hypsoblennius exstochilus Böhlke, 1959		SB	CPUM		+
Ophioblennius macclurei (Silvester, 1915)		R	3, 5, CPUM		+
Scartella cristata (Linnaeus, 1758)		RI	3, 5, CPUM		+

FAMILY and species	New records	Habitat	References and vouchers	USG	CRS
FAMILY BOTHIDAE					
Bothus lunatus (Linnaeus, 1758)		R, S	3, 5, CPUM		+
***Bothus maculiferus* (Poey, 1860)**	NP, GBIF	S	3, CPUM		+
Bothus ocellatus (Agassiz, 1831)		S	3, 5, CPUM		+
FAMILY CALLIONYMIDAE					
***Callionymus bairdi* (Jordan, 1888)**	NP, GBIF	R	3, CPUM		+
FAMILY CARANGIDAE					
Alectis ciliaris (Bloc, 1787)		“BP	5		
Caranx bartholomaei (Cuvier, 1833)		TF, S	1, 3, 5, CPUM		
Caranx crysos (Mitchill, 1815)		TF, S	1, 3, 5, CPUM		
Caranx hippos (Linnaeus, 1766)		“BP	5		
Caranx latus Agassiz, 1831		P	3, 5, CPUM	LC	
Caranx ruber (Bloch, 1793)		R, TF, S, AR, SB, P	1, 3, 5, CPUM	LC	
***Chloroscombrus chrysurus* (Linnaeus, 1766)**	NP, GBIF	P	3, CPUM		
Decapterus macarellus (Cuvier, 1833)		S, TF, RI, AR	3, 5, CPUM	B	
***Decapterus punctatus* (Cuvier, 1829)**	NP, GBIF	P	3, CPUM		
Selar crumenophthalmus (Bloch, 1793)		S, TF	3, CPUM		
***Selene brownii* (Cuvier, 1816)**	NP, GBIF, G	R	3, CPUM		
***Selene setapinnis* (Mitchill, 1815)**	NP, GBIF	R	3, CPUM		
Selene vomer (Linnaeus, 1758)		R, TF, S	3, 5, CPUM		
***Seriola dumerili* (Risso, 1810)**	NP	TF	PR	CF	
Seriola rivoliana Valenciennes, 1833		TF	3, 5, CPUM	CF	
Trachinotus falcatus (Linnaeus, 1758)		TF	1, 3, 5, CPUM	LC	
Trachinotus goodei Jordan et Evermann, 1896		TF	3, 5, CPUM	LC	
FAMILY CARAPIDAE					
Carapus bermudensis (Jones, 1874)		“RA	5		+
FAMILY CENTROPOMIDAE					
Centropomus undecimalis (Bloch, 1792)		P	3, 5, CPUM	LC	
FAMILY CHAENOPSIDAE					
***Acanthemblemaria aspera* (Longley, 1927)**	NP, GBIF	R, SB, AR	3, CPUM		+
Acanthemblemaria greenfieldi Smith-Vaniz et Palacio, 1974		R, SB	3, 5, CPUM		+
***Acanthemblemaria maria* Böhlke, 1961**	NP, GBIF, G	R	3, CPUM		+
***Acanthemblemaria spinosa* Metzelaar, 1919**	NP, GBIF	R, SB	3, CPUM		+
Chaenopsis cf ***limbaughi* Robins** et **Randall, 1965**	NM, G	TF, S	CPUM		+
Chaenopsis ocellata Poey, 1865		TF	3, 5, CPUM		+
***Chaenopsis roseola* Hastings** et **Shipp, 1981**	NM, GBIF	S	3, CPUM		+
***Stathmonotus tekla* Nichols, 1910**	NP, GBIF	SB, RI	3, CPUM		+
FAMILY CHAETODONTIDAE					
Chaetodon capistratus Linnaeus, 1758		R, TF, S, AR	1, 3, 5, CPUM		
Chaetodon ocellatus Bloch, 1787		R, TF, S	3, 5, CPUM		
Chaetodon sedentarius Poey, 1860		“RA	5		
Chaetodon striatus Linnaeus, 1758		R, TF, S, AR, SB	1, 3, 5, CPUM		
***Prognathodes aculeatus* (Poey, 1860)**	NP	R	CPUM		
FAMILY CIRRHITIDAE					
***Amblycirrhitus pinos* (Mowbray, 1927)**	NP, GBIF	R	3, CPUM		+
FAMILY CLUPEIDAE					
***Harengula clupeola* (Cuvier, 1829)**	NP, GBIF	TF	CPUM	B	
Harengula humeralis (Cuvier, 1829)	G	S, TF	3, 5, CPUM	B	
Harengula jaguana Poey, 1865		P	3, 5, CPUM	B	
Jenkinsia lamprotaenia (Gosse, 1851)		“P	3	B	
Jenkinsia stolifera (Jordan et Gilbert, 1884)		“P	5	B	
Opisthonema oglinum (Lesueur, 1818)		“P	3, 5	B	
FAMILY CONGRIDAE					
***Heteroconger longissimus* Günther, 1870**	NP, GBIF	S	3, CPUM		
FAMILY CORYPHAENIDAE					
Coryphaena equiselis Linnaeus, 1758		“P	3		
Coryphaena hippurus Linnaeus, 1758		P	3, 5, PR	SF	
FAMILY DACTYLOPTERIDAE					
***Dactylopterus volitans* (Linnaeus, 1758)**	NP, GBIF	S	3, CPUM		+
FAMILY DACTYLOSCOPIDAE					
***Gillellus uranidea* Böhlke, 1968**	NP, GBIF	R, RI, SB	3, CPUM		+
FAMILY DIODONTIDAE					
Chilomycterus antillarum Jordan et Rutter, 1897		“RA	5		
Chilomycterus schoepfii (Walbaum, 1792)		“RA	5		

FAMILY and species	New records	Habitat	References and vouchers	USG	CRS
Diodon holocanthus Linnaeus, 1758		R, TF, S	1, 3, 5, CPUM		
Diodon hystrix Linnaeus, 1758		R	3, 5, CPUM		
FAMILY ECHENEIDAE					
***Echeneis naucrates* Linnaeus, 1758**	NP	P	CPUM		
Echeneis neucratoides Zuiew, 1786		“P	3		
***Remora osteochir* (Cuvier, 1829)**	NP, GBIF	P	3, CPUM		
Remora remora (Linnaeus, 1758)		“P	1		
FAMILY ELOPIDAE					
Elops saurus Linnaeus, 1766		P	3, 5, CPUM		
***Elops smithi* McBride, Rocha, Ruiz-Carus** et **Bowen 2010**	NP, GBIF	TF	3, CPUM		
FAMILY ENGRAULIDAE					
Anchoa cayorum (Fowler, 1906)		P	3, 5, CPUM		
Anchoa colonensis (Hildebrand, 1943)		P	5, CPUM		
Anchoa lamprotaenia Hildebrand, 1943	G	P	5, CPUM		
Anchoa parva (Meek et Hildebrand, 1923)		“P	5		
FAMILY EPHIPPIDAE					
***Chaetodipterus faber* (Broussonet, 1782)**	NP, GBIF	TF	3, CPUM		
FAMILY EXOCOETIDAE					
***Hirundichthys speculiger* (Valenciennes, 1847)**	NP, GBIF	P	3, CPUM		
FAMILY FISTULARIIDAE					
***Fistularia tabacaria* Linnaeus, 1758**	NP, GBIF	S, TF	3, CPUM		
FAMILY GEMPYLIDAE					
Diplospinus multistriatus Maul, 1948		“P, “B	3		
Gempylus serpens Cuvier, 1829		“P, “B	3		
Nesiarchus nasutus Johnson, 1862		“BP	3		
FAMILY GERREIDAE					
Eucinostomus argenteus Baird et Girard, 1855		R, TF, S, AR	3, 5, CPUM	LC	
Eucinostomus gula (Quoy et Gaimard, 1824)		TF, S, RI	3, 5, CPUM	B	
Eucinostomus jonesii (Günther, 1879)		TF	3, 5, CPUM	B	
***Eucinostomus lefroyi* (Goode, 1874)**	NP	TF, S, RI	CPUM	B	
Eucinostomus melanopterus (Bleeker, 1863)		TF	3, 5, CPUM	B	
Gerres cinereus (Walbaum, 1792)		TF	1, 2, 3, 5, CPUM	B	
FAMILY GOBIESOCIDAE					
Acyrtops beryllinus (Hildebrand et Ginsburg, 1927)		“D	5		+
Gobiesox punctulatus (Poey, 1876)		“RA	5		+
***Tomicodon cryptus* Williams et Tyler 2003**	NM, G	R, RI	CPUM		+
***Tomicodon lavettsmithi* Williams et Tyler 2003**	NM, G	R, RI	CPUM		+
FAMILY GOBIIDAE					
***Barbulifer antennatus* Böhlke et Robins, 1968**	NP, GBIF	SB	3, CPUM		+
***Barbulifer ceuthoecus* (Jordan et Gilbert, 1884)**	NP	RI	CPUM		+
***Bathygobius antilliensis* Tornabene, Baldwin et Pezold 2010**	NP, G*	RI	CPUM		+
Bathygobius curacao (Metzelaar, 1919)	G*	RI	5, CPUM		+
***Bathygobius lacertus* (Poey, 1860)**	NP, G*	RI	CPUM		+
Bathygobius soporator (Valenciennes, 1837)	G*	TF	5, CPUM		+
***Coryphopterus dicrus* Böhlke et Robins, 1960**	NP, GBIF	R, SB, AR	3, CPUM		+
***Coryphopterus eidolon* Böhlke et Robins, 1960**	NP, GBIF	R	3, CPUM		+
***Coryphopterus glaucofraenum* Gill, 1863**	NP, GBIF	R	3, CPUM		+
***Coryphopterus hyalinus* Böhlke et Robins, 1962**	NP	R	CPUM		
***Coryphopterus personatus* (Jordan et Thompson, 1905)**	NP, GBIF	R	3, CPUM		
***Coryphopterus tortugae* (Jordan, 1904)**	NP, GBIF, G	R	3, CPUM		+
***Ctenogobius saepepallens* (Gilbert et Randall, 1968)**	NP, GBIF	S	3, CPUM		+
***Elacatinus colini* Randall et Lobel 2009**	NM, G	R	CPUM		+
***Elacatinus prochilos* (Böhlke et Robins, 1968)**	NP	R, SB	CPUM		+
***Gnatholepis thompsoni* Jordan, 1904**	NP, GBIF	R, S, SB, AR	3, CPUM		+
***Lythrypnus nesiotes* Böhlke et Robins, 1960**	NP, GBIF	R	3, CPUM		+
***Lythrypnus okapia* Robins et Böhlke, 1964**	NM, GBIF	R	3, CPUM		+
***Microgobius carri* Fowler, 1945**	NP, GBIF	S	3, CPUM		+
***Priolepis hipoliti* (Metzelaar, 1922)**	NP, GBIF	R	3, CPUM		+
***Ptereleotris helenae* (Randall, 1968)**	NP, GBIF	S	3, CPUM		
***Risor ruber* (Rosen, 1911)**	NP, GBIF	R	3, CPUM		+
FAMILY GRAMMATIDAE					
Gramma loreto Poey, 1868		R	3, 5, CPUM		

FAMILY and species	New records	Habitat	References and vouchers	USG	CRS
FAMILY HAEMULIDAE					
Anisotremus surinamensis (Bloch, 1791)		TF	3, 5, CPUM		
Anisotremus virginicus (Linnaeus, 1758)		R, AR	3, 5, CPUM	LC	
Brachygenys chrysargyreum (Günther, 1859)		R	3, 5, CPUM		
***Emmelichthyops atlanticus* Schultz, 1945**	NP, GBIF	R	3, CPUM		
Haemulon album Cuvier, 1830		R, P	5, CPUM	CF	
Haemulon atlanticus Carvalho, Marceniuk, Oliveira et Wosiacki, 2020		"RA	5		
Haemulon aurolineatum Cuvier, 1830		R, TF, S, AR, RI	1, 3, 5, CPUM		
***Haemulon bonariense* Cuvier, 1830**	NP, GBIF	TF	3, CPUM		
Haemulon carbonarium Poey, 1860		R, S, RI	3, 5, CPUM		
Haemulon flavolineatum (Desmarest, 1823)		R, TF, S, AR	1, 3, 5, CPUM	LC	
Haemulon macrostomum Günther, 1859		R, TF	3, 5, CPUM		
Haemulon melanurum (Linnaeus, 1758)		R, S, P	1, 3, 5, CPUM	LC	
Haemulon parra (Desmarest, 1823)		R, TF, SB, AR, RI,	1, 3, 5, CPUM		
Haemulon plumierii (Lacepede, 1801)		R, TF, S, AR	1, 3, 5, CPUM	CF	
Haemulon sciurus (Shaw, 1803)		S	3, 5, CPUM	CF	
Haemulon striatum (Linnaeus, 1758)		R, TF, S, AR, SB, P	3, 5, CPUM		
***Haemulon vittatum* (Poey, 1860)**	NP, GBIF	AR	3, CPUM		
FAMILY HEMIRAMPHIDAE					
Hemiramphus brasiliensis (Linnaeus, 1758)		P	3, 5, CPUM		
Hyporhamphus unifasciatus (Ranzani, 1841)		P	3, 5, CPUM		
FAMILY HOLOCENTRIDAE					
Holocentrus adscensionis (Osbeck, 1765)		R, P	3, 5, CPUM		
Holocentrus rufus (Walbaum, 1792)		R, P, AR	3, 5, CPUM		
Myripristis jacobus (Cuvier, 1829)		R	3, 5, CPUM		
***Neoniphon coruscum* (Poey, 1860)**	NP, GBIF	R, S	3, CPUM		
***Neoniphon marianus* (Cuvier, 1829)**	NP, GBIF	R	3, CPUM		
***Neoniphon vexillarium* (Poey, 1860)**	NP, GBIF	R, S, TF	3, CPUM		
FAMILY ISTIOPHORIDAE					
***Makaira nigricans* (Lacepede, 1802)**	NP	P	PR	SF	
FAMILY KYPHOSIDAE					
Kyphosus sectatrix (Linnaeus, 1766)		R, TF, S, AR, RI	3, 5, CPUM		
Kyphosus vaigiensis (Quoy et Gaimard, 1825)		TF	3, 5, CPUM		
FAMILY LABRIDAE					
Subfamily Labrinae					
Bodianus rufus (Linnaeus, 1758)		R, AR	3, 5, CPUM		
***Clepticus parrae* (Bloch et Schneider, 1801)**	NP, GBIF	R, S	3, CPUM		
Doratonotus megalepis (Günther, 1862)		"RA	5		+
Halichoeres bivittatus (Bloch, 1791)		R, TF, S, AR, RI	1, 3, 5, CPUM		
Halichoeres garnoti (Valenciennes, 1839)		R, TF, S, AR	3, 5, CPUM		
Halichoeres maculipinna (Muller et Troschel, 1848)		R, TF, SB	1, 3, 5, CPUM		
Halichoeres pictus (Poey, 1860)		R, RI, SB	1, CPUM		
Halichoeres poeyi (Steindachner, 1867)		R, TF, SB	1, 3, 5, CPUM		
Halichoeres radiatus (Linnaeus, 1758)		R, AR	3, 5, CPUM	LC	
Lachnolaimus maximus (Walbaum, 1792)		R, TF	3, 5, CPUM	CF	
Thalassoma bifasciatum (Bloch, 1791)		TF, S, RI, SB, AR	1, 3, 4, 5, CPUM		
***Xyrichtys martinicensis* (Valenciennes, 1840)**	NP, GBIF	S	3, CPUM		
Xyrichtys novacula (Linnaeus, 1758)		S	1, 3, CPUM		
Xyrichtys splendens Castelnau, 1855	G	TF, S	1, 3, 5, CPUM		
Subfamily Scarinae					
Cryptotomus roseus (Cope, 1871)		SB	1, 3, 5, CPUM		
Nicholsina usta (Valenciennes, 1840)		R, TF, SB	3, 5, CPUM		
*Scarus coelestinus (*Valenciennes, 1840)		"RA	5		
Scarus coeruleus (Edwards, 1771)		"RA	5		
Scarus guacamaia (Cuvier, 1829)		"RA	5		
Scarus iseri (Bloch, 1789)		R, TF	1, 3, 5, CPUM		
Scarus taeniopterus (Lesson, 1829)		R, TF	3, 5, CPUM		
Scarus vetula (Bloch et Schneider, 1801)		"RA	3, 5		
Sparisoma atomarium (Poey, 1861)		R, TF, S, AR, SB	1, 3, 5, CPUM		
Sparisoma aurofrenatum (Valenciennes, 1840)		R, S	3, 5, CPUM		
Sparisoma chrysopterum (Bloch et Schneider, 1801)		R, TF, S	1, 3, 5, CPUM		
Sparisoma radians (Valenciennes, 1840)		R, TF, RI	1, 3, 5, CPUM		
Sparisoma rubripinne (Valenciennes, 1840)		R, TF	1, 3, 5, CPUM		
Sparisoma viride (Bonnaterre, 1788)		TF, S	1, 3, 5, CPUM		

FAMILY and species	New records	Habitat	References and vouchers	USG	CRS
FAMILY LABRISOMIDAE					
Gobioclinus bucciferus (Poey, 1868)		R, RI	3, 5, CPUM		+
Gobioclinus gobio (Valenciennes, 1836)	NP	R, SB	CPUM		+
Gobioclinus kalisherae (Jordan, 1904)	NP, GBIF	R, RI, SB	3, CPUM		+
Labrisomus nuchipinnis (Quoy et Gaimard, 1824)		R, TF, AR	3, 5, CPUM		+
Malacoctenus boehlkei (Springer, 1959)	NP, GBIF	R	3, CPUM		+
Malacoctenus erdmani (Smith, 1957)	NP, GBIF	R, SB	3, CPUM		+
Malacoctenus gilli (Steindachner, 1867)		R, RI	2, 3, 5, CPUM		+
Malacoctenus macropus (Poey, 1868)		R, TF, SB	3, 5, CPUM		+
Malacoctenus triangulatus (Springer, 1959)		R, SB	3, 5, CPUM		+
Malacoctenus versicolor (Poey, 1876)		RI	CPUM		+
Paraclinus cingulatus (Evermann et Marsh, 1899)		“RA	5		+
Paraclinus fasciatus (Steindachner, 1876)		R, RI, SB	3, 5, CPUM		+
Paraclinus nigripinnis (Steindachner, 1867)	NP, GBIF	R, RI, SB	3, CPUM		+
Starksia occidentalis (Greenfield, 1979)	NP, G	R, SB	CPUM		+
Starksia weigti (Baldwin et Castillo, 2011)		R	CPUM		+
FAMILY LOBOTIDAE					
Lobotes surinamensis (Bloch, 1790)	NP, GBIF	TF, RI	3, CPUM		
FAMILY LUTJANIDAE					
Lutjanus analis (Cuvier, 1828)		R, TF, S	1, 3, 5, CPUM	CF	
Lutjanus apodus (Walbaum, 1792)		R, TF, S, RI	3, 5, CPUM	CF	
Lutjanus buccanella (Cuvier, 1828)	NP	P	CPUM	CF	
Lutjanus campechanus (Poey, 1860)		“RA	5	CF	
Lutjanus griseus (Linnaeus, 1758)		R, TF, S, AR	3, 5, CPUM	CF	
Lutjanus jocu (Bloch et Schneider, 1801)		R, TF, S, SB	3, 5, CPUM	CF	
Lutjanus mahogoni (Cuvier, 1828)		R, TF, S, AR, RI	3, 5, CPUM		
Lutjanus synagris (Linnaeus, 1758)		R	3, 5, CPUM	CF	
Lutjanus vivanus (Cuvier, 1828)	NP	P	CPUM	CF	
Ocyurus chrysurus (Bloch, 1791)		R, TF, S, AR	1, 3, 5, CPUM	CF	
Rhomboplites aurorubens (Cuvier, 1829)	NP, GBIF	R, P, AR	3, CPUM	CF	
FAMILY MALACANTHIDAE					
Malacanthus plumieri (Bloch, 1786)		S	3, 5, CPUM	CF	
FAMILY MONACANTHIDAE					
Aluterus monoceros (Linnaeus, 1758)		“RA	1		
Aluterus scriptus (Osbeck, 1765)		R, TF, AR	3, 5, CPUM		
Cantherhines pullus (Ranzani, 1842)		R	3, 5, CPUM		
Monacanthus ciliatus (Mitchill, 1818)		TF	1, 3, 5, CPUM		
Monacanthus tuckeri (Bean, 1906)		R	1, 3, 5, CPUM		
Stephanolepis hispidus (Linnaeus, 1766)		TF, S	1, 3, 5, CPUM		
Stephanolepis setifer (Bennett, 1831)		TF, S, RI	3, 5, CPUM		
FAMILY MUGILIDAE					
Mugil cephalus (Linnaeus, 1758)		TF	5, CPUM		
Mugil curema (Valenciennes, 1836)		TF	3, CPUM		
Mugil liza (Valenciennes, 1836)	NP, GBIF	TF	3, CPUM		
FAMILY MULLIDAE					
Mulloidichthys martinicus (Cuvier, 1829)		R, TF, S, SB	5, CPUM		
Pseudupeneus maculatus (Bloch, 1793)		TF, S	1, 3, 5, CPUM		
FAMILY MURAENIDAE					
Echidna catenata (Bloch, 1795)	NP	RI	CPUM		+
Gymnothorax funebris (Ranzani, 1839)		R	3, 5, PR		+
Gymnothorax miliaris (Kaup, 1856)	NP, GBIF	R, TF	3, CPUM		+
Gymnothorax moringa (Cuvier, 1829)		R, TF, SB, AR	3, 5, CPUM		+
Gymnothorax vicinus (Castelnau, 1855)		R, TF	3, 5, CPUM		+
FAMILY OGCOCEPHALIDAE					
Ogcocephalus corniger (Bradbury, 1980)		“D	3		
Ogcocephalus nasutus (Cuvier, 1829)	G	S	5, CPUM		
FAMILY OPHICHTHIDAE					
Myrichthys breviceps (Richardson, 1848)		“RA	3, 5		+
Myrichthys ocellatus (Lesueur, 1825)		S	5, CPUM		+
Myrophis punctatus (Lütken, 1852)	NP	TF	CPUM		
Phaenomonas longissima (Cadenet et Marchal, 1963)		“D	3		
FAMILY OPISTOGNATHIDAE					
Opistognathus macrognathus (Poey, 1860)	NP, GBIF	S	3, CPUM		+
Opistognathus nothus (Smith-Vaniz, 1997)	NP, GBIF	S	3, CPUM		+
Opistognathus whitehursti (Longley, 1927)	NP, GBIF, G	S	3, CPUM		+

FAMILY and species	New records	Habitat	References and vouchers	USG	CRS
FAMILY OSTRACIIDAE					
Acanthostracion polygonius (Poey, 1876)		TF	1, 3, 5, CPUM		
Acanthostracion quadricornis (Linnaeus, 1758)		R	1, 3, 5, CPUM		
Lactophrys bicaudalis (Linnaeus, 1758)		R, TF, AR, SB	1, 3, 5, CPUM		
Lactophrys trigonus (Linnaeus, 1758)		R, TF, AR	1, 3, 5, CPUM		
Lactophrys triqueter (Linnaeus, 1758)		TF	1, 3, 5, CPUM		
FAMILY PEMPHERIDAE					
Pempheris schomburgkii (Müller et Troschel, 1848)		R, TF, AR	3, 5, CPUM		+
FAMILY POLYNEMIDAE					
***Polydactylus oligodon* (Günther, 1860)**	NP	TF, S	3, 5, CPUM		
Polydactylus virginicus (Linnaeus, 1758)		TF, S	3, 5, CPUM		
FAMILY POMACANTHIDAE					
Centropyge argi (Woods et Kanazawa, 1951)		“RA	3		
***Holacanthus bermudensis* (Goode, 1876)**	NP, GBIF	S	3, CPUM		
Holacanthus ciliaris (Linnaeus, 1758)		R, TF, AR, SB	3, 5, CPUM		
Holacanthus tricolor (Bloch, 1795)		R, TF, S, AR, SB	3, 5, CPUM		
Pomacanthus arcuatus (Linnaeus, 1758)		R, S	3, 5, CPUM		
Pomacanthus paru (Bloch, 1787)		R, TF	1, 3, 5, CPUM		
FAMILY POMACENTRIDAE					
Abudefduf saxatilis (Linnaeus, 1758)		R, S	3, 5, CPUM		
Abudefduf taurus (Muller et Troschel, 1848)		R	5, CPUM		
Chromis cyanea (Poey, 1860)		R, S	3, 5, CPUM		
Chromis insolata (Cuvier, 1830)		R, TF, S	3, 5, CPUM		
Chromis multilineata (Guichenot, 1853)		RI	3, 5, CPUM		
Microspathodon chrysurus (Cuvier, 1830)		R	3, 5, CPUM		
***Stegastes adustus* (Troschel, 1865)**	NP	R, TF, AR, RI	^3, CPUM		
Stegastes diencaeus (Jordan et Rutter, 1897)		R, RI, SB, AR	3, 5, CPUM		
Stegastes leucostictus (Muller et Troschel, 1848)		R, TF, RI, SB	1, 3, 5, CPUM		
Stegastes partitus (Poey, 1868)		R, TF, AR, SB	3, 5, CPUM		
Stegastes planifrons (Cuvier, 1830)		R, RI, SB, AR	3, 5, CPUM		
Stegastes xanthurus (Poey, 1860)		R, RI, AR	3, 5, CPUM		
FAMILY PRIACANTHIDAE					
Heteropriacanthus cruentatus (Lacepède, 1801)		R, P	3, 5, CPUM	CF	
FAMILY SCIAENIDAE					
Equetus punctatus (Bloch et Schneider, 1801)		“RA	5		
Odontoscion dentex (Cuvier, 1830)		R, TF	3, 5, CPUM		+
Pareques acuminatus (Bloch et Schneider, 1801)		R, TF, S, SB, AR	1, 3, 5, CPUM		
Pareques umbrosus (Jordan et Eigenmann, 1889)		“RA	5		
Umbrina coroides Cuvier, 1830		TF, S	3, 5, CPUM		
FAMILY SCOMBRIDAE					
Acanthocybium solandri (Cuvier, 1832)		P	3, 5, CPUM	SF	
Auxis rochei (Risso, 1810)		“P	3	SF	
***Euthynnus alletteratus* (Rafinesque, 1810)**	NP	P	PR	SF	
Katsuwonus pelamis (Linnaeus, 1758)		P	3, PR	SF	
Scomberomorus brasiliensis Collette, Russo et Zavala-Camin, 1978		“P	3		
Scomberomorus cavalla (Cuvier, 1829)		P	5, PR	SF	
Scomberomorus regalis (Bloch, 1793)	G	TF, P	1, 3, 5, CPUM	SF	
***Thunnus atlanticus* (Lesson, 1831)**	NP	P	PR	SF	
FAMILY SCORPAENIDAE					
Pterois volitans (Linnaeus, 1758)		R, TF, AR	3, 4, CPUM	CF	+
***Scorpaena bergii* Evermann et Marsh, 1900**	NP, GBIF	R, SB	3, CPUM		+
Scorpaena calcarata (Goode et Bean, 1882)		R	CPUM		+
Scorpaena grandicornis (Cuvier, 1829)		“RA	5		+
***Scorpaena inermis* (Cuvier, 1829)**	NP, GBIF	R	3, CPUM		+
Scorpaena plumieri (Bloch, 1789)		R, TF, AR, SB	3, 5, CPUM		+
***Scorpaenodes caribbaeus* (Meek et Hildebrand, 1928)**	NP	R	CPUM		+
FAMILY SERRANIDAE					
***Alphestes afer* (Bloch, 1793)**	NP, GBIF	R	3, CPUM		+
Cephalopholis cruentata (Lacepede, 1802)		R	3, 5, CPUM	CF	
Cephalopholis fulva (Linnaeus, 1758)		R	3, 5, CPUM	CF	
Epinephelus adscensionis (Osbeck, 1765)		“RA	5	CF	
Epinephelus guttatus (Linnaeus, 1758)		R	3, 5, CPUM	CF	
Epinephelus itajara (Lichtenstein, 1822)		R, S	5, PR	CF	
Epinephelus morio (Valenciennes, 1828)		R	5, CPUM	CF	

FAMILY and species	New records	Habitat	References and vouchers	USG	CRS
Epinephelus striatus (Bloch, 1792)		R, S	5, CPUM	CF	
Hypoplectrus guttavarius (Poey, 1852)	NP, GBIF	R, S	3, CPUM		
Hypoplectrus indigo (Poey, 1851)	NP, GBIF	R	3, CPUM		
Hypoplectrus nigricans (Poey, 1852)	NP, GBIF	R	3, CPUM		
Hypoplectrus puella (Cuvier, 1828)		R, P	3, 5, CPUM		
Hypoplectrus unicolor (Walbaum, 1792)	NP, GBIF	R	3, CPUM		
Hyporthodus nigritus (Holbrook, 1855)	NP	R, TF, P	PR	CF	
Mycteroperca bonaci (Poey, 1860)		P	3, 5, CPUM	CF	
Mycteroperca interstitialis (Poey, 1860)		R, TF	3, 5, CPUM		
Mycteroperca phenax (Jordan et Swain, 1884)		“RA	5	CF	
Mycteroperca tigris (Valenciennes, 1833)		“RA	5	CF	
Mycteroperca venenosa (Linnaeus, 1758)		TF	3, 5, CPUM	CF	
Rypticus saponaceus (Bloch et Schneider, 1801)		R	3, 5, CPUM		+
Rypticus subbifrenatus (Gill, 1861)	NP	R, RI, SB	CPUM		+
Serranus baldwini (Evermann et Marsh, 1899)		R, TF	5, CPUM		+
Serranus tabacarius (Cuvier, 1829)		“RA	5		
Serranus tigrinus (Bloch, 1790)		P	3, 5, CPUM		
Serranus tortugarum (Longley, 1935)		“RA	5		
FAMILY SPARIDAE					
Archosargus rhomboidalis (Linnaeus, 1758)	NP, GBIF	P	3, CPUM		
Calamus bajonado (Bloch et Schneider, 1801)		P	1, 3, 5, PR	CF	
Calamus calamus (Valenciennes, 1830)		TF, S, P	3, 5, CPUM	CF	
Calamus leucosteus (Jordan et Gilbert, 1885)	NP, GBIF	P	3, CPUM	CF	
Calamus penna (Valenciennes, 1830)		P	5, PR	CF	
Calamus proridens (Jordan et Gilbert, 1884)	NP, GBIF	P	3, CPUM	CF	
Lagodon rhomboides (Linnaeus, 1766)		P	3, 5, CPUM		
FAMILY SPHYRAENIDAE					
Sphyraena barracuda (Edwards, 1771)		R, TF	1, 3, 5, CPUM	CF, SF	
Sphyraena borealis (DeKay, 1842)		“P	1		
FAMILY SYNGNATHIDAE					
Anarchopterus tectus (Dawson, 1978)		“D	3		+
Bryx dunckeri (Metzelaar, 1919)		“D	3		+
Cosmocampus brachycephalus (Poey, 1868)	NP, GBIF	S	3, CPUM		+
Cosmocampus elucens (Poey, 1868)		“BP	3, 5		+
Hippocampus erectus (Perry, 1810)	NP, GBIF	TF	3, CPUM		+
Hippocampus reidi (Ginsburg, 1933)	NP, GBIF	TF	3, CPUM		+
Hippocampus zosterae (Jordan et Gilbert, 1882)	NP, GBIF	TF	3, CPUM		
Syngnathus caribbaeus (Dawson, 1979)		TF	5, CPUM		+
Syngnathus floridae (Jordan et Gilbert, 1882)	NP, GBIF	TF	3, CPUM		
Syngnathus pelagicus (Linnaeus, 1758)	NP, G	TF, SP	CPUM		
FAMILY SYNODONTIDAE					
Synodus intermedius (Agassiz, 1829)	NP, GBIF	AR	3, CPUM		+
Synodus saurus (Linnaeus, 1758)		“D	3, 5		+
Trachinocephalus myops (Forster, 1801)		“D	5		+
FAMILY TETRAODONTIDAE					
Canthigaster jamestyleri (Moura et Castro, 2002)		“RA	1		
Canthigaster rostrata (Bloch, 1786)		R	1, 3, 5, CPUM		
Lagocephalus laevigatus (Linnaeus, 1766)	NP, GBIF	R	3, CPUM		
Sphoeroides pachygaster (Muller et Troschel, 1848)	NP, GBIF	R, TF	3, CPUM		
Sphoeroides spengleri (Bloch, 1785)		TF	1, 3, 5, CPUM		
Sphoeroides testudineus (Linnaeus, 1758)		R, TF, S, AR, SB, P	1, 3, 5, CPUM		
FAMILY TRIPTERYGIIDAE					
Enneanectes altivelis (Rosenblatt, 1960)	NP	AR	CPUM		+
Enneanectes boehlkei (Rosenblatt, 1960)	NP	R	CPUM		+
Enneanectes jordani (Evermann et Marsh, 1899)	NP	R	CPUM		+

USG = usage; CRS = cryptic species; **New records:** NP = new for the PNAPM, NM = new for Mexico, GBIF = new records from this study hosted by GBIF (**all new records are in bold**), G = genetic corroboration with *cox1* gene, G* = genetic corroboration with *cytb* gene. **Habitats of collected specimens:** R = coral reefs, TF = *Thalassia* beds, S = sandy bottoms, P = pelagic, AR = artificial reefs, SB = karstic-slab bottoms, RI = rocky intertidal pools, SP = Sargasso patches. FishBase habitats of species other than those collected during this study: “D = demersal, “RA = reef associated, “P = pelagic, “BP = benthopelagic. **Sources of information:** 1) Zarco-Perelló and Enríquez (2019); 2 = FishNet2, 3 = GBIF, 4 = iDigBi, 5 = SEMARNAP (2000) park management plan; CPUM = specimens deposited in the Fish Collection of Universidad Michoacana de San Nicolás de Hidalgo, PR = photographic or observed records. **Usage:** B = bait, CF = commercial fishing, LC = local consumption, SF = sport fishing. **Cryptobenthic species:** Robertson and Tornabene (2020).

Results

We sampled 2987 individuals from 57 localities. Some localities were represented by more than one habitat type, with the number of habitat sites sampled as follows: two rocky tide pools, 27 sandy bottoms, 15 *Thalassia* beds, 21 coral reefs, seven artificial reefs, 19 karstic-slab bottoms, six pelagic areas, and two benthic *Sargassum* patches (Table 1).

The checklist of "bony fishes" (=ray-finned fishes) of PMRNP compiled from the different sources comprises 349 species belonging to 17 orders, 67 families, and 169 genera (Table 2). The families representing the greatest number of species were Labridae (28), Serranidae (25), Gobidae (22), Haemulidae (17), and Carangidae (17). The genera with the highest number of species were *Haemulon* Cuvier, 1829 (13), *Lutjanus* Bloch, 1790 (9), and *Apogon* Lacepède, 1801 (7) (Table 1).

Of the 349 species in the checklist, 82% (285) were collected and deposited at the CPUM. In addition, 12 species (3%) were observed or photographed but not caught (Table 2). Records of 15% (52 species) were obtained from literature or public repositories. Of the 297 species recorded during the fieldwork, 106 were new records for the PMRNP, and seven were new records for Mexico: *Apogon robbyi* Gilbert et Tyler, 1997; *Chaenopsis roseola* Hastings et Shipp, 1981; *Chaenopsis* cf *limbaughi* Robins et Randall, 1965; *Tomicodon cryptus* Williams et Tyler, 2003; *Tomicodon lavettsmithi* Williams et Tyler, 2003; *Elacatinus colini* Randall et Lobel, 2009; and *Lythrypnus okapia* Robins et Böhlke, 1964. The identification of 12 newly reported species and eight previously reported species were corroborated genetically (Table 2). All species showed > 99% statistically significant matches in comparing the target sequences with a sequence in public repositories, except *Chaenopsis* cf *limbaughi*, which showed a similarity of 94%.

Of the 297 collected and photographed species, 159 were recorded from a single habitat type, with 56 (19%) found only on coral reefs, 39 (13%) in the pelagic zone, 30 (10%) in *Thalassia* beds, 19 (6%) in sandy bottoms, 9 (3%) in rocky intertidal pools, three (1%) in karstic-slab bottoms and three (1%) in artificial reefs. In addition, 138 (47%) species were collected in more than one habitat type (Table 1 and Fig. 2).

The 349 species found in PMRNP correspond to 35% of all the reef-associated ichthyofauna reported for the Great Caribbean (992 species; see Robertson and Tornabene 2020). Of this, 15.7% represent pelagic species. Of the 84.3% non-pelagic species, 58.5% are demersal species, 39.1% are benthic, 38.4 cryptobenthic, and 26.8% are core reef species. Only one—*Lutjanus vivanus* (Cuvier, 1828)—is considered a deep-reef species (Tables 3, 4)

The fishery catches included 70 species, of which 12 are used as bait, 39 are captured for commercial sale, ten are used for local consumption, and ten species from sport fishers. Serranidae (12), Lutjanidae (10), and Scombridae (7) were the families with the highest number of species used in fisheries (Fig. 3 and Table 2).

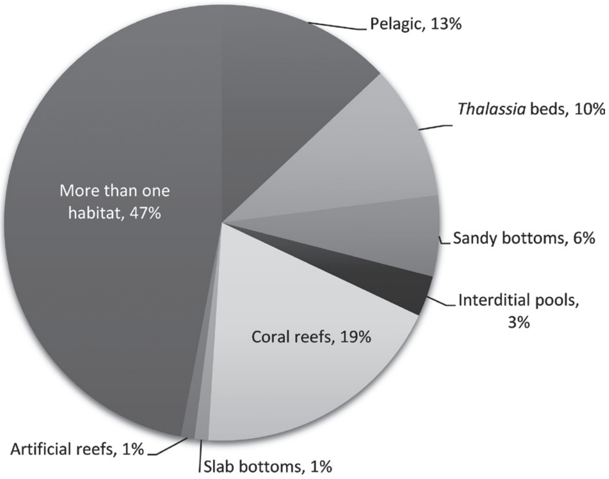

Figure 2. Percentage of habitat type from which the fish species were captured at Puerto Morelos Reef National Park in Quintana Roo State, Mexico.

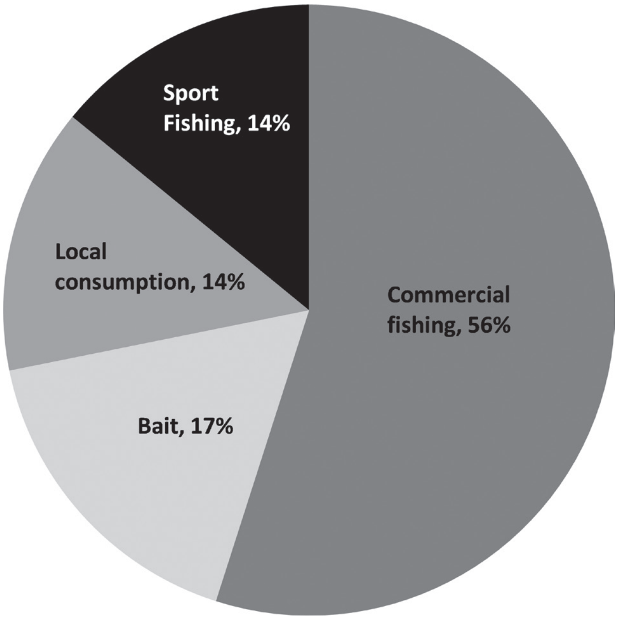

Figure 3. Percentage of human usage of the 70 species of fish caught in Puerto Morelos National Park in Quintana Roo State, Mexico, according to the Cooperative Society of Fisheries Production of Puerto Morelos.

Discussion

The present checklist represents the first comprehensive systematic list of fishes recorded from Puerto Morelos Reef National Park, with 349 species included, 285 of which are represented by voucher organisms that have been included in a registered ichthyological collection and from which tissue samples for genetic analyses also are in that collection (e.g., CPUM). Of the 297 captured or photographed species, 114 (39%) represent new records for PMRNP or for Mexico. Although 82 of those 114 new records can be found in the database of the aggregator GBIF, those records are for specimens collected as a part of presently reported study and deposited in the CPUM.

Table 3. Relative abundance of different types of shallow and deep reef-associated fishes in the Great Caribbean region (GCR), at Puerto Morelos Reef National Park (PMRNP), and at six sites scattered throughout the GCR.

Parameter	GCR	PMRNP	Alligator	Bermuda	St. Croix	Roatan	Statia	Curacao
Species (n)	992	349	482	353	493	481	341	529
Pelagics (n)	78	55	53	44	51	42	34	50
Pelagic species [% of fauna]	8.0	**15.7**	11.0	12.5	10.3	8.7	10.0	9.5
Non-pelagic species [% of fauna]	92.0	84.3	89.0	87.5	89.7	91.3	90.0	90.5
Demersal species [%]	34.6	**58.5**	49.2	54.7	45.0	44.0	56.4	44.7
Benthic [%]	65.4	39.1^{PL}	50.8	45.3	55.0	56.0	43.6	55.3
Cryptobenthic species [%]	64.6	38.4^{PL}	49.9	43.7	54.3	55.6	43.0	54.7
Core CRF species [%]	45.9	26.8^{PL}	27.7	19.1	35.7	39.0	30.0	35.7
Shallow non-pelagics (n)	772	293	407	284	424	393	266	401
Percent of fauna	84.6	99.6	94.9	91.9	95.9	89.6	86.7	83.7
Demersal species [%]	34.9	**58.7**	48.2	53.9	43.9	44.5	56.8	45.6
Benthic species [%]	65.1	39.2^{PL}	51.8	46.1	55.9	55.5	43.2	54.4
Cryptobenthic species [%]	64.0	38.5^{PL}	50.9	44.7	55.2	54.7	42.4	53.6
Core CRF species [%]	46.0	26.9	29.2	20.4	37.3	29.2	20.4	37.3
Deep non-pelagics (n)	141	1.0^{PL}	22	25	18	46	41	78
Deep non-pelagics [% of fauna]	14.2	0.3	4.6	7.1	3.7	9.6	12.0	14.7

n = number; **bold** numbers indicate percentage values substantially higher than the corresponding values for the region. ^{PL} indicate percentage values substantially lower than the corresponding values for the region.

Table 4. Comparison between pelagic and non-pelagic species in six well-studied GC and PMRNP sites.

Site	Shallow non-pelagics	Deep non-pelagics	Pelagics
PMRNP	293	1	55
Bermuda	284	25	44
Alligator	407	22	53
Roatan	393	46	42
St Croix	424	18	51
Statia	266	41	34
Curacao	401	78	50

The high proportion of new records is likely related to the lack of systematic inventory surveys made in this and other marine protected areas of the Mexican Caribbean (Álvarez-Cadena et al. 2007; Zarco-Perelló and Enríquez 2019). Also, the checklist presented in the management plan of PMRNP is based in one bibliographic record from all the Mexican ichthyofauna (Espinosa-Pérez et al. 1993), and one prospective study made in *Thalassia* beds (Álvarez-Guillén et al. 1986).

The seven new records for Mexico obtained are: *Apogon robbyi*, known from the western Caribbean and Florida; *Chaenopsis roseola*, known from the west Florida shelf; *Chaenopsis* cf *limbaughi*, reported from the Caribbean and Bahamas; *Tomicodon cryptus*, reported from some Antilles islands; *T. lavettsmithi*, previously known only from Belize; *Elacatinus colini*, reported from Belize and Honduras; and *Lythrypnus okapia*, reported from the northern Caribbean and Bahamas. Of these new records, the identifications of *Chaenopsis* cf *limbaughi*, *Tomicodon cryptus*, *T. lavettsmithi*, and *Elacatinus colini* were corroborated by comparison of their mtDNA sequences with those in GenBank using BLAST (http://www.ncbi.nlm.nih.gov/genbank) and by Boldsystems (http://www.boldsystems.org).

The most common habitat types in the national park are coral reefs, *Thalassia* beds, and soft bottoms (Fig. 4). While 169 of the 297 collected or photographed species were found in coral reefs (57%), *Thalassia* fields (119) and sandy bottoms (87) accounted for 40% and 29%, respectively. The seven new records for Mexico and 51 of the 106 (48%) new records to PMRNP are cryptobenthic species. The above mentioned 106 species represent 20.8% of the cryptobenthic reef fishes (588) known from the Great Caribbean (Robertson and Tornabene 2020). This is a relatively low percentage, considering that 59.2% of fishes in the Great Caribbean Region, between 43% and 54.3% in Dutch Caribbean islands, 55.6% in Roatan, and 49.9% in Alligator Reef, Florida, are cryptobenthic forms (Robertson et al. 2020, 2022). We also found that the percentage of benthic, cryptobenthic, and deep-reef species are underrepresented in PMRNP compared to other locations in the Great Caribbean (Tables 3, 4). This indicates that most of the existing inventory efforts in PMRNP have been aimed at conspicuous shallow, demersal coral reef fishes. In our comparison, we also found that the percentage of demersal and pelagic species in PMRNP is higher than in other sites. Including local fishery species in PMRNP inventory could contribute to that pattern. PMRNP has the highest absolute abundance of such species of any sites listed in Table 3.

Our results highlight the need for future inventory efforts to focus more intensely on the cryptic component. The increase in the diversity of cryptic species in PMRNP recorded during the presently reported study is strongly

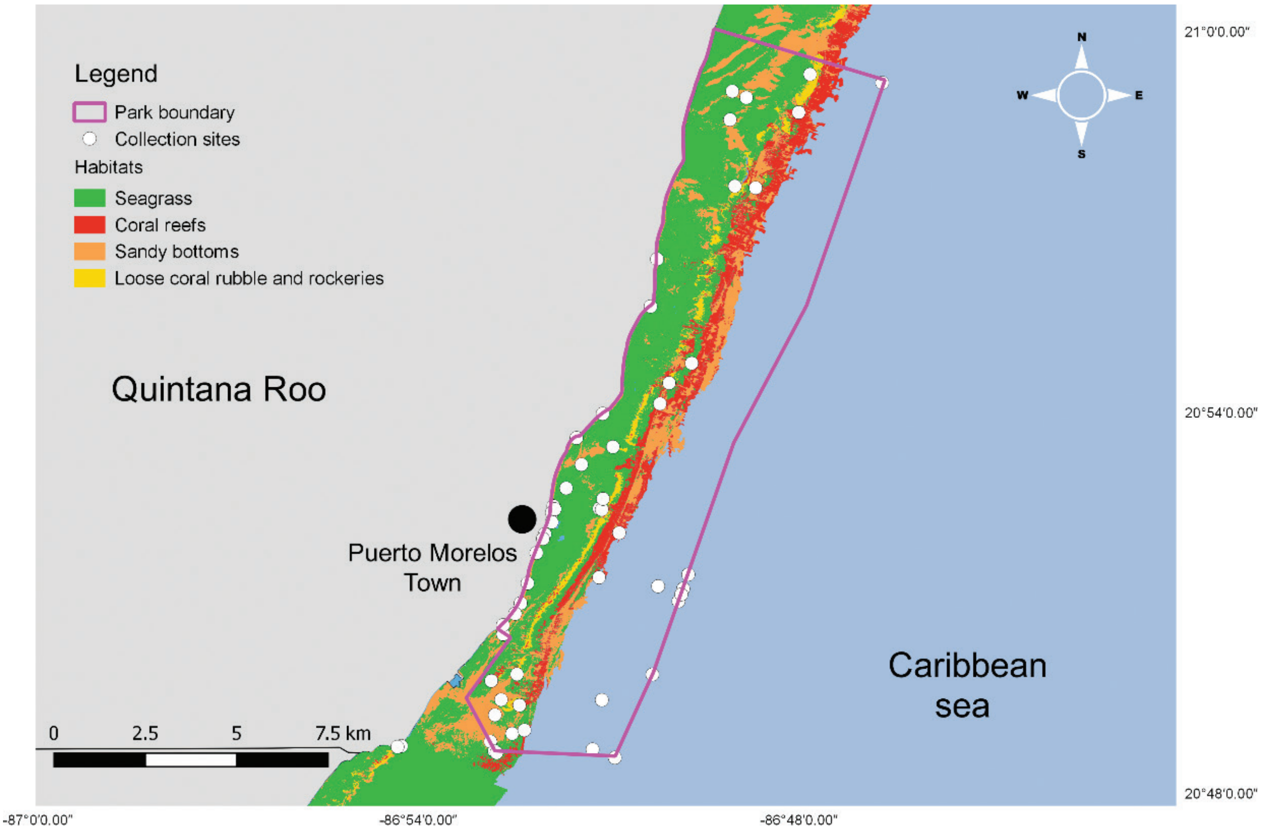

Figure 4. Distribution of four major habitat types within Puerto Morelos Reef National Park in Quintana Roo State, Mexico. White dots indicate the collection sites.

related to using anesthetic collections, often lacking in inventory studies (e.g., Robertson et al. 2020). Previous studies conducted in PMRNP were based on visual censuses, photo identification, and video transects (Arias-González et al. 2008; Zarco-Perelló and Enríquez 2019). However, collections are needed to provide reference organisms for taxonomic corroboration, biological or ecological studies. In addition, obtaining tissue samples for molecular work of voucher specimens can be used for future evolutionary or integrative systematic and taxonomic studies. Also, many small, nocturnal, or visually cryptic species are unlikely to be counted in a visual census, particularly in regions with large areas with highly complex habitat structures, as is the case with coral reefs in PMRNP (SEMARNAP 2000).

Currently, only one deep-reef species is known from the PMRNP, a meager number compared to other localities. However, although deep areas with benthic habitats occupy only a tiny percentage of the park, no sampling has been specifically directed at assessing what demersal and benthic fish species occur there. Even the few of hectares of deep habitat in the park's southeast corner could contain a substantial number of deep-reef species depending on what habitat types are present.

In artisanal fishing, the species local fishermen consider to have the highest economic value is the invasive red lionfish, *Pterois volitans* (Linnaeus, 1758), followed by the groupers and snappers (Serranidae and Lutjanidae), all top predators. In addition, large numbers of individuals of the family Clupeidae are caught to be used as bait (Table 2) in an unregulated fishery. Since those species are also an important food source to fish predators, the effects of this activity on the park ecosystem need to be examined. Finally, tourism is the most important commercial activity involving the PMRNP fish, including sport fishing and diving.

Our work reported 106 new species records for Puerto Morelos Reef National Park (PMRNP) and seven new species records for Mexico, this being a complete ray-finned fish fauna checklist previously available for the area by 48% (SEMARNAP 2000), highlighting the need for future inventory efforts in marine ichthyofauna in Mexican Caribbean, mainly focused in cryptobenthic and deep-reef species. Our results also should provide important input for decisions about the conservation and management of the coastal area of northern Quintana Roo, such as the conservation of less charismatic species and areas, such as cryptobenthic species or sites such as *Thalassia* seagrass fields or rocky intertidal areas.

Acknowledgments

This work was funded by the National Commission for the Knowledge and Use of Biodiversity (CONABIO) through project LH003 to ODD. The National Commission of Protected Natural Areas (CONANP) of Puerto Morelos supported fieldwork activities. We would like to thank especially the captains of the CONANP boats. The samplings were made under the PPF/DGOPA/2013 fishing permit.

References

Álvarez-Cadena JN, Ordóñez-López U, Amaral-Mendivil AR, Ornelas Roa M, Uicab-Sabido A (2007) Larvas de peces del litoral arrecifal del norte de Quintana Roo, Mar Caribe de México. Hidrobiológica 17(2): 139–150.

Álvarez-Guillén H, García-Abad MC, Tapia-García M, Villalobos Zapata GJ, Yánez-Arancibia A (1986) Prospección ictiológica en la zona de pastos marinos de la laguna arrecifal en Puerto Morelos, Quintana Roo, verano 1984. Anales del Instituto de Biología, Universidad Nacional Autónoma de México 13: 317–366.

Arias-González JE, Legendre P, Rodríguez-Zaragoza FA (2008) Scaling up beta diversity on Caribbean coral reefs. Journal of Experimental Marine Biology and Ecology 366(1–2): 28–36. https://doi.org/10.1016/j.jembe.2008.07.035

Avilés-Torres S, Schmitter-Soto JJ, Barrientos-Medina RC (2001) Patrones espaciales de la riqueza de peces en lagunas del sur de Quintana Roo, México. Hidrobiológica 11: 141–148.

Brandl SJ, Goatley CH, Bellwood DR, Tornabene L (2018) The hidden half: Ecology and evolution of cryptobenthic fishes on coral reefs. Biological Reviews of the Cambridge Philosophical Society 93(4): 1846–1873. https://doi.org/10.1111/brv.12423

Caballero-Vázquez JA, Schmitter-Soto JJ (2001) Diversity of fishes in small coral patches of the Mexican Caribbean. Bulletin of Marine Science 68(2): 337–342.

Caballero-Vázquez JA, Gamboa-Pérez HC, Schmitter-Soto JJ (2005) Composition and spatio-temporal variation of the fish community in the Chacmochuch Lagoon system, Quintana Roo, Mexico. Hidrobiológica 15: 215–225.

Carpenter KE (Ed.) (2002) The living marine resources of the Western Central Atlantic. Volume 3: Bony fishes part 2 (Opistognathidae to Molidae), sea turtles and marine mammals. FAO Species Identification Guide for Fishery Purposes and American Society of Ichthyologists and Herpetologists Special Publication No. 5. FAO, Rome, 1375–2127.

Cinner JE, Pollnac RB (2004) Poverty, perceptions and planning: Why socioeconomics matter in the management of Mexican reefs. Ocean and Coastal Management 47(9–10): 479–493. https://doi.org/10.1016/j.ocecoaman.2004.09.002

Cobián-Rojas D, Schmitter-Soto JJ, Aguilar-Perera A, Aguilar Betancourt CM, Ruiz-Zárate MÁ, González-Sansón G, Chevalier-Monteagudo PP, García-Rodríguez A, Herrera-Pavón RL, Perera-Valderrama S, Caballero-Aragón H, de la Guardia-Llansó E (2018) Diversidad de las comunidades de peces en dos áreas marinas protegidas del Caribe y su relación con el pez león. Revista de Biología Tropical 66(1): 189–203. https://doi.org/10.15517/rbt.v66i1.28197

COESPO (Consejo Estatal de Población) (2017) Anuario estadístico y geográfico de Quintana Roo. Instituto Nacional de Estadística y Geografía, Mexico City, Mexico, 405 pp.

De la Lanza Espino G, Pérez MAO, Pérez JLC (2013) Diferenciación hidrogeomorfológica de los ambientes costeros del Pacífico, del Golfo de México y del Mar Caribe. Investigaciones Geográficas. Boletín del Instituto de Geografía 2013(81): 33–50. https://doi.org/10.14350/rig.33375

Espinosa Pérez H, Dillanes MTG, Mata PF 1993. Listados faunísticos de México. III. Los peces dulceacuicolas Mexicanos. Universidad Nacional Autonoma de Mexico, Mexico, 98 pp.

Fenner DP (1991) Effects of hurricane Gilbert on coral reefs, fishes and sponges at Cozumel, Mexico. Bulletin of Marine Science 48(3): 719–730.

Fricke R, Eschmeyer WN, Van der Laan R (2023) Eschmeyer's catalog of fishes: Genera, species, references. California Academy of Sciences, San Francisco, CA, USA. [Accessed 20 May 2023] http://researcharchive.calacademy.org/research/ichthyology/catalog/fishcatmain.asp

Humann P, Deloach N (2002) Reef fishes identification, Florida, Caribbean, Bahamas. New World Publications Inc., Jacksonville, FL, USA, 481 pp.

Lara EN, González EA (1998) The relationship between reef fish community structure and environmental variables in the southern Mexican Caribbean. Journal of Fish Biology 53(sA): 209–221. https://doi.org/10.1111/j.1095-8649.1998.tb01028.x

Loreto RM, Lazcano MA (2017) Caracterización de Banco Arrowsmith, Quintana Roo, México. Amigos de Sian Ka'an Serie Documentos 7: 80–95.

Loreto RM, Lara M, Schmitter-Soto JJ (2003) Coral reef fish assemblages at Banco Chinchorro, Mexican Caribbean. Bulletin of Marine Science 73: 153–170.

Merino M, Otero L (1991) Atlas ambiental costero, Puerto Morelos, Quintana Roo. Centro de Investigaciones de Quintana Roo, Chetumal, 80 pp.

Muhling BA, Smith RH, Vásquez-Yeomans L, Lamkin JT, Johns EM, Carrillo L, Sosa-Cordero E, Malca E (2013) Larval fish assemblages and mesoscale oceanographic structure along the Mesoamerican Barrier Reef System. Fisheries Oceanography 22(5): 409–428. https://doi.org/10.1111/fog.12031

Núnez-Lara E, Arias-González JE, Legendre P (2005) Spatial patterns of Yucatan reef fish communities: Testing models using a multi-scale survey design. Journal of Experimental Marine Biology and Ecology 324(2): 157–169. https://doi.org/10.1016/j.jembe.2005.04.011

Perdices A, Bermingham E, Montilla A, Doadrio I (2002) Evolutionary history of the genus *Rhamdia* (Teleostei: Pimelodidae) in Central America. Molecular Phylogenetics and Evolution 25(1): 172–189. https://doi.org/10.1016/S1055-7903(02)00224-5

Pindell JL, Kennan L (2009) Tectonic evolution of the Gulf of Mexico, Caribbean and northern South America in the mantle reference frame: An update. Geological Society of London, Special Publications 328(1): 1–55. https://doi.org/10.1144/SP328.1

Reséndez-Medina A (1975) Lista preliminar de peces colectados en las lagunas de Nichupté y Bojórquez, Cancún, Quintana Roo, México. Anales del Instituto de Biología. Universidad Nacional Autónoma de México 46: 87–100.

Rioja-Nieto R, Álvarez-Filip L (2019) Coral reef systems of the Mexican Caribbean: Status, recent trends and conservation. Marine Pollution Bulletin 140: 616–625. https://doi.org/10.1016/j.marpolbul.2018.07.005

Robertson DR, Cramer KL (2014) Defining and dividing the greater Caribbean: Insights from the biogeography of shorefishes. PLoS One 9(7): e102918. https://doi.org/10.1371/journal.pone.0102918

Robertson DR, Tornabene L (2020) Reef-associated bony fishes of the Greater Caribbean: a checklist (Version 3). Zenodo. https://doi.org/10.5281/zenodo.4279301

Robertson DR, Peña EA, Posada JM, Claro R (2015) Peces: Gran Caribe una guía para peces costeros del Gran Caribe, sistema de información en línea. Instituto Smithsonian de Investigaciones Tropicales, Balboa, Panamá. http://biogeodb.stri.si.edu/caribbean

Robertson DR, Estapé CJ, Estapé AM, Peña E, Tornabene L, Baldwin CC (2020) The marine fishes of St Eustatius Island, northeastern Caribbean: An annotated, photographic catalog. ZooKeys 1007: 145–180. https://doi.org/10.3897/zookeys.1007.58515

Robertson DR, Tornabene L, Lardizabal CC, Baldwin CC (2022) Submersibles greatly enhance research on the diversity of deep-reef fishes in the Greater Caribbean. Frontiers in Marine Science 8: e2123. https://doi.org/10.3389/fmars.2021.800250

Sánchez-Jiménez JA, Arredondo-Chávez AT, López-Arroyo MY, Caballero-Vázquez JA, Domínguez-Domínguez O (2017) Nuevo registro de *Hypsoblennius exstochilus* (Actinopterygii: Blenniidae) en el Caribe mexicano. Revista Mexicana de Biodiversidad 88(1): 265–267. https://doi.org/10.1016/j.rmb.2017.01.012

Schmitter-Soto JJ, Vásquez-Yeomans L, Aguilar-Perera A, Curiel-Mondragón C, Caballero-Vázquez JA (2000) Lista de peces marinos del Caribe mexicano. Anales del Instituto de Biología Universidad Nacional Autónoma de México 71: 143–177.

Schmitter-Soto JJ, Aguilar-Perera A, Cruz-Martínez A, Herrera-Pavón RL, Morales-Aranda AA, Cobián-Rojas D (2018) Interdecadal trends in composition, density, size, and mean trophic level of fish species and guilds before and after coastal development in the Mexican Caribbean. Biodiversity and Conservation 27(2): 459–474. https://doi.org/10.1007/s10531-017-1446-1

SEMAR (2023) Venta de Cartas Náuticas. Secretaría de Marina, Gobierno de México. [Accessed 20 May 2023] https://digaohm.semar.gob.mx/hidrografia/VentaCartasPublicacionesNauticas.html

SEMARNAP (Secretaría de Medio Ambiente, Recursos Naturales y Pesca) (2000) Programa de Manejo del Parque Nacional Arrecife de Puerto Morelos. Instituto Nacional de Ecología, Mexico City, Mexico, 224 pp.

Valdez-Moreno MC, Quintal-Lizama C, Gómez-Lozano R, García-Rivas MC (2012) Monitoring an alien invasion: DNA barcoding and the identification of lionfish and their prey on coral reefs of the Mexican Caribbean. PLoS ONE 7(6): e36636. https://doi.org/10.1371/journal.pone.0036636

Vásquez-Yeomans L, González-Vera MA (1992) Peces marinos de las costas de Quintana Roo: un listado preliminar. Pp. 361–373. In: Navarro-López D, Suárez-Morales E (Eds) Diversidad biológica de la Reserva de la biosfera de Sian Ka'an, Quintana Roo, México. Centro de Investigaciones de Quintana Roo, Chetumal, Mexico.

Viesca-Lobatón C, Balart E, González-Cabello A, Mascareñas-Osorio I, Aburto-Oropeza O, Reyes-Bonilla H, Torreblanca E (2008) Peces arrecifales. Pp. 385–427. In: Danemann GD, Ezcurra E (Eds) Bahía de Los Ángeles: recursos naturales y comunidad. Línea base 2007. Pronatura Noroeste AC, Secretaría de Medio Ambiente y Recursos Naturales, Instituto Nacional de Ecología, San Diego Natural History Museum, Mexico City, Mexico.

Ward RD, Zemlak TS, Innes BH, Last PR, Hebert PDN (2005) DNA barcoding Australia's fish species. Philosophical Transactions of the Royal Society of London. Series B, Biological Sciences 360(1462): 1847–1857. https://doi.org/10.1098/rstb.2005.1716

Yeager LA, Arias-Gonzalez JE (2008) Preliminary survey of fish community composition in seagrass habitat in two back-reef lagoons of the southern Mexican Caribbean. Gulf and Caribbean Research 20(1): 41–47. https://doi.org/10.18785/gcr.2001.06

Zarco-Perelló S, Enríquez S (2019) Remote underwater video reveals higher fish diversity and abundance in seagrass meadows, and habitat differences in trophic interactions. Scientific Reports 9(1): 1–11. https://doi.org/10.1038/s41598-019-43037-5

Acta Ichthyologica et Piscatoria 53, 2023, 123–127 | DOI 10.3897/aiep.53.105318

PENSOFT.

ACTA
ICHTHYOLOGICA
ET PISCATORIA

First record of *Mastacembelus notophthalmus* (Actinopterygii: Synbranchiformes: Mastacembelidae) for Belitung Island, Indonesia

Veryl HASAN[1], Lucas O. VIEIRA[2], Josie SOUTH[3], Felipe P. OTTONI[2]

1 *Department of Aquaculture, Faculty of Fisheries and Marine, Airlangga University, Surabaya, Jawa Timur, Indonesia*
2 *Laboratory of Systematics and Ecology of Aquatic Organisms, Federal University of Maranhão, Chapadinha, Maranhão, Brazil*
3 *School of Biology, Faculty of Biological Sciences, University of Leeds, Leeds, UK*

https://zoobank.org/64BC7326-F255-40D4-A528-51DAD5A635F4

Corresponding author: Veryl Hasan (veryl.hasan@fpk.unair.ac.id)

Academic editor: Jan Kotusz ♦ **Received** 21 April 2023 ♦ **Accepted** 19 June 2023 ♦ **Published** 14 July 2023

Citation: Hasan V, Vieira LO, South J, Ottoni FP (2023) First record of *Mastacembelus notophthalmus* (Actinopterygii: Synbranchiformes: Mastacembelidae) for Belitung Island, Indonesia. Acta Ichthyologica et Piscatoria 53: 123–127. https://doi.org/10.3897/aiep.53.105318

Abstract

This study was conducted aiming to record for the first time the occurrence of *Mastacembelus notophthalmus* Roberts, 1989 in Belitung Island (Indonesia), and update the geographic distribution of this species. Although this species is categorized as LC according to the IUCN Red List, it is rarely reported in fish inventories, with few specimens sampled. Moreover, data on the geographic distribution, population size, and other population details of *M. notophthalmus* are scarce and insufficient to predict possible threats and propose appropriate conservation measures and policies. A single specimen of *Mastacembelus* was collected using a fish trap on 20 February 2023, in a swamp, located in the middle course of the Lenggang River, Belitung Island, Indonesia. This specimen was identified as *M. notophthalmus* and this finding constitutes the southernmost record for this species, expanding its geographic range. In addition, the new record site is about 700 km south-east of the nearest locality in Peninsular Malaysia, about 250 km south-east of the nearest locality in Bangka Island, about 600 km south-east of the nearest locality in Sumatra, and about 500 km south-west from the nearest locality in Borneo. Better ecological and biological data concerning distribution, habitat, and stressors is crucial to reassess the conservation status of *M. notophthalmus*, and possible future conservation measures and policies. Therefore, we emphasize here the urgency for more comprehensive and accurate data to facilitate conservation assessments and management in Indonesia.

Keywords

distribution extension, freshwaters, life below water, native species, spiny eel

Introduction

Mastacembelus notophthalmus Roberts, 1989 is a freshwater spiny eel species representing the family Mastacembelidae (see Kottelat 2013; Fricke et al. 2023). This species has an IUCN Red List (International Union for Conservation of Nature's Red List of Threatened Species) status of least concern (LC), usually occurring in large rivers, with clear or slightly turbid water and pebbles as substrate (Ahmad 2020). Like other species of the genus *Mastacembelus* Scopoli, 1777, it is consumed as food by local fishers, therefore overexploitation is the main conservation threat to *M. notophthalmus* (see Britz 2007; Brown et al. 2010; Day et al. 2017). There are currently no active conservation measures in place for this species as there are broad ecological data deficiencies regarding geographic distribution, potential threats, and population dynamics. Current knowledge regarding geographic distribution is likely to be underestimated as very few specimens of this species are collected during general fish surveys (Ahmad 2020).

Mastacembelus notophthalmus is known to occur in the western portion of Peninsular Malaysia (Malaysia) (Roberts 1989; Shafiq et al. 2014; Ahmad 2020; Fricke et al. 2023); in the northern and central portions of Sumatra (Indonesia) (Roberts 1989; Ng et al. 2019; Ahmad 2020; Ng and Tan 2020; Fricke et al. 2023); and in the western portion of Borneo (Indonesia) (Roberts 1989; Kottelat et al. 1993). And recently, Hasan et al. (2023a) reported the species for Bangka Island (Indonesia). In addition, Hasan et al. (2023a) argued that it is possible that *M. notophthalmus* occurs in other islands close to the West Malaysia mainland, Sumatra, and Borneo.

This work records for the first time the occurrence of *M. notophthalmus* in Belitung Island (Indonesia). This record represents the southernmost record for this species, extending its geographical distribution further south, and recording its occurrence on one additional island. In addition, we provide here a detailed and updated map of the geographic distribution of *M. notophthalmus*.

Methods

A single specimen of *Mastacembelus notophthalmus* (Fig. 1) was collected using a fish trap on 20 February 2023, in a swamp, located in the middle course of the Lenggang River, (02°57′14″S, 108°09′21″E), Lenggang Village, Gantung Sub-District, East Belitung District, Belitung Island, Indonesia (Figs. 2 and 3). The collection site is characterized by having slow water flow and abundant water plants on the river (Fig. 4). The specimen was preserved in formalin 10% (Hasan et al. 2019). It was deposited in the Ichthyological Collection of the Airlangga Natural History Museum (ANMH), Faculty of Fisheries and Marine Sciences, Universitas Airlangga, Surabaya, Indonesia.

The morphological inspection of the specimen followed Roberts (1989), complemented by photographs of the life specimen which were taken immediately after capture, aiming to document the coloration pattern in life.

Results

Family Mastacembelidae Swainson, 1839
Genus *Mastacembelus* Scopoli, 1777

Mastacembelus notophthalmus Roberts, 1989

(Fig. 1; Table 1)

New records. Belitung Island, East Belitung District, Indonesia; middle course of the Lenggang River; 02°57′14″S, 108°09′21″E; 20 February 2023; W. Kusumah leg.; caught with a fish trap; 1 ♂ (ANMH0007).

Identification. The specimen collected in the Lenggang River, Belitung Island (Indonesia), was identified as *Mastacembelus notophthalmus* (Fig. 1) based on characters proposed by Roberts (1989). The diagnostic features exhibited by the specimen include: (1) a dark vertical bar below eye; (2) dorsal region mostly dark brown with some yellowish irregular vermiculated marks; (3) ventral region yellowish with incomplete and inconspicuous dark brown horizontal stripe; and (4) caudal, dorsal, and anal fins yellowish with vertical dark brown bars (see Fig. 1).

Table 1. Meristic and morphometric characters of *Mastacembelus notophthalmus* from the Lenggang River, East Belitung District, Belitung Island (presently reported study; AMNH0007), and Malay Peninsula (Roberts 1989).

Meristic data	*Mastacembelus notophthalmus*	
	AMNH0007	Roberts 1989
Dorsal spines	37	37–39
Dorsal-fin rays	81	73–86
Anal-fin rays	82	69–85
Pectoral-fin rays	26	24–26
Caudal-fin rays	18	15–18
Morphometric data; absolute value		
Standard length, (SL) [mm]	410.5	248.0
Morphometric data; relative values (in percent of SL)		
Head length	1.48	—
Snout length	0.46	—
Predorsal length	6.69	—
Preanal length	6.57	—

Figure 1. Live specimen of *Mastacembelus notophthalmus* from the Lenggang River, East Belitung District, Belitung Island, Indonesia, 410.5 mm SL (AMNH0007) (photograph: W. Kusumah).

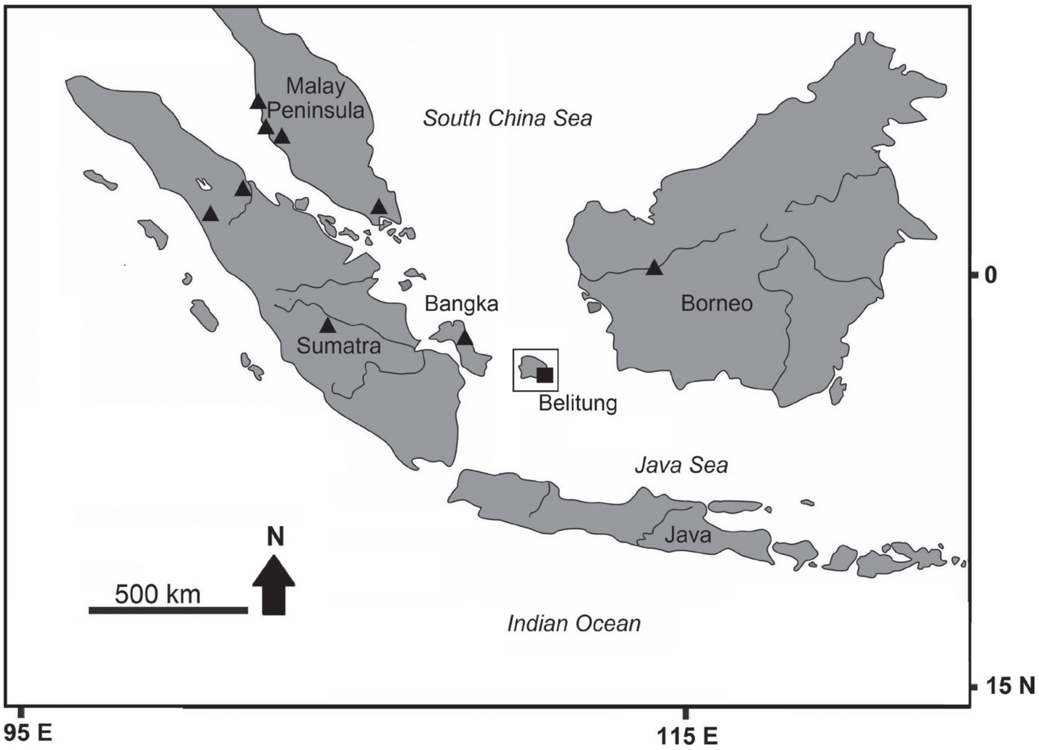

Figure 2. Map of the known distribution of *Mastacembelus notophthalmus*. The new record in Belitung Island, Indonesia (black square); published records (black triangles) are based on Roberts (1989), Kottelat et al. (1993), Ng et al. (2019); Ahmad (2020); Ng and Tan (2020), and Hasan et al. (2023a).

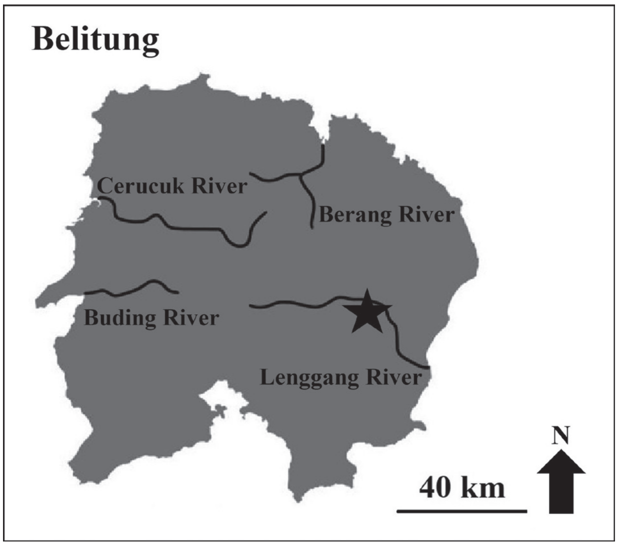

Figure 3. The presently reported collection site of *Mastacembelus notophthalmus* on the Lenggang River in East Belitung District, Bangka Island, Indonesia.

Figure 4. Collection site of the presently reported *Mastacembelus notophthalmus* (AMNH0007); slow water flow and abundant water plants on the river, Lenggang River, in East Belitung District, Belitung Island, Indonesia (photograph: W. Kusumah).

Meristic and morphometric characters of the *M. notophthalmus* specimen from Belitung Island are presented in Table 1. These meristic features also support the identification of the species as *M. notophthalmus*.

The specimen identified in the presently reported study as *M. notophthalmus* differs from other species of the genus *Mastacembelus* occurring in Indonesia and surroundings by the following features: the presence of a dark vertical bar below the eye (vs. absence in *Mastacembelus unicolor* Cuvier, 1832; *Mastacembelus erythrotaenia* Bleeker, 1850; and *Mastacembelus favus* Hora, 1923); number of dorsal spines (37) (vs. 34–35 in *M. unicolor*, 33–34 in *M. erythrotaenia*, and 33–35 in *M. favus*); number of dorsal-fin rays (81) (vs. 68–70 in *M. erythrotaenia*); number of anal-fin rays 82 (vs. 68–69 in *M. erythrotaenia*); number of pectoral-fin rays 26 (vs. 24–25 in *M. erythrotaenia*); and number of caudal-fin rays (18) (vs. 19–22 in *M. unicolor*, 14–15 in *M. erythrotaenia*, and 12–15 in *M. favus*).

Discussion

The new record of *Mastacembelus notophthalmus* provided here for Belitung Island, specifically for the Lenggang River, Lenggang Village, Gantung Sub-District, East Belitung District, Belitung Island, Indonesia, is the southernmost record for this species, expanding its geographic distribution. In addition, the new record site is about 700 km south-east of the nearest locality in Peninsular Malaysia, about 250 km south-east of the nearest locality in Bangka Island, about 600 km south-east of the nearest locality in Sumatra, and about 500 km south-west from the nearest locality in Borneo. New records of freshwater fishes are essential contributions to the natural sciences (Hasan et al. 2022). They are necessary to support appropriate conservation-related decisions and environmental impact assessments (Hasan et al. 2023b; Nurjirana et al. 2022; Hasan et al. 2021). Therefore, this new record fills an important gap in the geographic distribution of the species, as well as registering an additional island for the species (Fig. 3).

It is important to emphasize that, despite being categorized as least concern (LC) according to the IUCN Red List, this species is rarely reported in fish inventories, with few specimens sampled (Ahmad 2020). Moreover, according to Ahmad (2020), data on the geographic distribution, population size, and other population details of *M. notophthalmus* are scarce and insufficient to predict possible threats and propose appropriate conservation measures and policies. Better ecological and biological data concerning distribution, habitat, and stressors is crucial to reassess the conservation status of *M. notophthalmus*, and possible future conservation measures and policies. Therefore, we emphasize here the urgency of obtaining more comprehensive and accurate data to facilitate conservation assessments and management in Indonesia.

Given these needs, and the recent reports documenting a far broader distribution for *M. notophthalmus* than historically considered (Hasan et al. 2023a), we provide some implementation recommendations to increase knowledge in the region. Traditional fish sampling using seine nets, gill nets, dip nets, fyke nets, and fish traps evidently have a low detection probability for *Mastacembelus* spp., this is due to their thin, elongated body shapes allowing them to escape from nets, which utilize the most commonly used mesh sizes. If using traditional methods, we recommend using mesh sizes ranging from 20 to 50 mm or crayfish traps with fine mesh sizes to prevent escape (Çoban et al. 2021). Combining electro-fishing methods with molecular approaches, such as eDNA, and traditional net surveys would likely exponentially increase detection levels for uncommonly caught species. There is an active fishery for *Mastacembelus* spp. in Indonesia (Ahmad 2020), thus implementing a fisheries-dependent catch assessment survey would supplement fisheries independent data. This would serve a dual purpose as a biodiversity survey and generate vital information on the overall state of the fishery, allowing inference regarding population structure, size, and exploitation.

Author contributions

Data curation: VH. Investigation: VH, LOV, JS, FPO. Methodology: VH, FPO. Resources: VH. Writing – original draft: VH, LOV, JS, FPO. Writing – review and editing: VH, LOV, JS, FPO.

Acknowledgments

The authors thank Mr Wanda Kusumah, Mr Firman Yusnandar, and Mr Imam Wijaya as our guide, and the Universitas Airlangga, Indonesia, for funding our research (No. 254/UN3/2023). FPO thanks the Conselho Nacional de Desenvolvimento Científico e Tecnológico, Brazil (CNPq; grant 307974/2021–9 to FPO), and the Fundação de Amparo à Pesquisa e ao Desenvolvimento Científico e Tecnológico do Maranhão, Brazil (FAPEMA) for providing the financial and infrastructure support to carry out his scientific research. The authors thank two anonymous reviewers for their useful comments.

References

Ahmad AB (2020) *Mastacembelus notophthalmus*. The IUCN Red List of Threatened Species 2020: e.T181181A1707093. [Electronic version accessed on 21 March 2023] https://doi.org/10.2305/IUCN.UK.2020-2.RLTS.T181181A1707093.en

Britz R (2007) Two new species of *Mastacembelus* from Myanmar (Teleostei: Synbranchiformes: Mastacembelidae). Ichthyological Exploration of Freshwaters 18(3): 257–268.

Brown KJ, Rüber L, Bills R, Day JJ (2010) Mastacembelid eels support Lake Tanganyika as an evolutionary hotspot of diversification. BMC Evolutionary Biology 10(1): 1–11. https://doi.org/10.1186/1471-2148-10-188

Çoban MZ, Eroğlu M, Düşükcan M (2021) Some biological properties of spiny eel (*Mastacembelus mastacembelus*, Banks & Solander, 1794) living in the upper Euphrates River basin, Turkey. Scientific Reports 11(1): 11761. https://doi.org/10.1038/s41598-021-91223-1

Day JJ, Fages A, Brown KJ, Vreven EJ, Stiassny ML, Bills R, Friel JP, Rüber L (2017) Multiple independent colonizations into the Congo Basin during the continental radiation of African *Mastacembelus* spiny eels. Journal of Biogeography 44(10): 2308–2318. https://doi.org/10.1111/jbi.13037

Fricke R, Eschmeyer WN, Van Der Laan R (2023) Eschmeyer's catalog of fishes: Genera, species, references. California Academy of Sciences, San Francisco, CA, USA. [Electronic version accessed on 21 March 2023] http://researcharchive.calacademy.org/research/ichthyology/catalog/fishcatmain.asp

Hasan V, Pratama FS, Malonga WAM, Cahyanurani AB (2019) First record of the Mozambique tilapia, *Oreochromis mossambicus* Peters, 1852 (Perciformes, Cichlidae), on Kangean Island, Indonesia. Neotropical Biology and Conservation 14(2): 207–211. https://doi.org/10.3897/neotropical.14.e35601

Hasan V, Gausmann P, Ottoni FP (2021) First scientific observation of the threatened speartooth shark *Glyphis glyphis* (Müller & Henle, 1839) (Carcharhiniformes: Carcharhinidae) in Indonesia. Cybium 45(4): 321–324. https://doi.org/10.26028/cybium/2021-454-010

Hasan V, South J, Katz AM, Ottoni FP (2022) First record of the small-eyed loter *Prionobutis microps* (Weber, 1907) (Teleostei: Eleotridae: Butinae) in Java, Indonesia. Cybium 46(1): 49–51. https://doi.org/10.15560/19.1.51

Hasan V, Swarlanda Katz AM, South J, Ottoni FP, Nurjirana, Gani A (2023a) (in press) First record of the uncommon spiny eel *Mastacembelus notophthalmus* Roberts, 1989 (Synbranchiformes: Mastacembelidae) for Bangka Island, Indonesia. Cybium 47(2): 189–191. https://doi.org/10.26028/cybium/2023-008

Hasan V, Ottoni FP, South J (2023b) First record of the vulnerable freshwater fish *Lobocheilos falcifer* (Valenciennes, 1842) (Teleostei, Cyprinidae) in Sumatra, Indonesia. Check List 19(1): 1–5. https://doi.org/10.15560/19.1.51

Kottelat M (2013) The fishes of the inland waters of southeast Asia: A catalogue and core bibliography of the fishes known to occur in freshwaters, mangroves and estuaries. Raffles Bulletin of Zoology 27: 1–663.

Kottelat M, Whitten AJ, Kartikasari SN, Wirjoatmodjo S (1993) Freshwater fishes of western Indonesia and Sulawesi. Periplus Editions, Hong Kong, 221 pp.

Ng HH, Tan HH (2020) A new, uniquely patterned spiny eel (Teleostei: Mastacembelidae) from southern Borneo, Kalimantan Tengah, Indonesia. Zootaxa 4819(1): 170–178. https://doi.org/10.11646/zootaxa.4819.1.9

Ng CKC, Kim TY, Ahmad A, Khaironizam MDZ (2019) Provisional checklist of freshwater fish diversity and distribution in Perak, Malaysia, and some latest taxonomic concerns. Zootaxa 4567(3): 515–545. https://doi.org/10.11646/zootaxa.4567.3.5

Nurjirana B, Keith AI, Haris P, Moore A, Afrisal AM, Gani A, Hasan V, Wuniarto E, Bakri AA, Adriany DT (2022) Additional records of *Sicyopus discordipinnis* (Watson, 1995) (Oxudercidae: Sicydiinae) in Central Sulawesi, Indonesia. Cybium 46(1): 41–43. https://doi.org/10.26028/cybium/2022-461-006

Roberts TR (1989) The freshwater fishes of western Borneo (Kalimantan Barat, Indonesia). Memoirs of the California Academy of Sciences 14: i–xii + 1–210.

Shafiq ZM, Shah ASRM, Zarul HH, Syaiful MM, Khaironizam MZ, Khaled P, Hamzah Y (2014) An annotated checklist of fish fauna of Bukit Merah Reservoir and its catchment area, Perak, Malaysia. Check List 10(4): 822–828. https://doi.org/10.15560/10.4.822

Acta Ichthyologica et Piscatoria 53, 2023, 129–135 | DOI 10.3897/aiep.53.107199

PENSOFT

ACTA ICHTHYOLOGICA ET PISCATORIA

Length–weight relations for 19 freshwater fish species (Actinopterygii) from the lowland Elbe River, Germany

Janek SIMON[1], Wolf-Christian LEWIN[2], Erik FLADUNG[1]

1 *Potsdam Institute of Inland Fisheries, Potsdam, Germany*
2 *Thünen Institute of Baltic Sea Fisheries, Rostock, Germany*

https://zoobank.org/90E2F83A-6AEA-4F4A-8EFB-B59D906A43CB

Corresponding author: Janek Simon (janek.simon@ifb-potsdam.de)

Academic editor: Rodolfo Reyes ♦ **Received** 30 May 2023 ♦ **Accepted** 13 August 2023 ♦ **Published** 8 September 2023

Citation: Simon J, Lewin W-C, Fladung E (2023) Length–weight relations for 19 freshwater fish species (Actinopterygii) from the lowland Elbe River, Germany. Acta Ichthyologica et Piscatoria 53: 129–135. https://doi.org/10.3897/aiep.53.107199

Abstract

Monthly and mean length–weight relations (LWRs) were calculated for 19 freshwater fish species from the middle section of the lowland Elbe River (Germany): *Abramis brama* (Linnaeus, 1758); *Alburnus alburnus* (Linnaeus, 1758); *Anguilla anguilla* (Linnaeus, 1758); *Ballerus ballerus* (Linnaeus, 1758); *Blicca bjoerkna* (Linnaeus, 1758); *Cobitis taenia* Linnaeus, 1758; *Esox lucius* Linnaeus, 1758; *Gobio gobio* (Linnaeus, 1758); *Gymnocephalus cernua* (Linnaeus, 1758); *Leuciscus aspius* (Linnaeus, 1758); *Leuciscus idus* (Linnaeus, 1758); *Leuciscus leuciscus* (Linnaeus, 1758); *Lota lota* (Linnaeus, 1758); *Perca fluviatilis* Linnaeus, 1758; *Romanogobio albipinnatus* (Lukasch, 1933); *Rutilus rutilus* (Linnaeus, 1758); *Sander lucioperca* (Linnaeus, 1758); *Scardinius erythrophthalmus* (Linnaeus, 1758); and *Squalius cephalus* (Linnaeus, 1758). The values of the exponent b in the LWR $W = a\mathrm{TL}^b$ ranged from 2.882 (*Lota lota*) to 3.517 (*Cobitis taenia*) and the correlation coefficient (r^2) was greater than 0.96 for all species except for *Cobitis taenia* with 0.93. The relations allow for the accurate estimation of weight from length data with reduced handling times of fish in the field while enabling comparisons with other regions and future studies. The calculated LWRs together with species-specific abundance and catch data will be useful for fisheries modeling and estimating population status and related fish species protection, especially for the endangered species in the Elbe River.

Keywords

Elbe River, freshwater fish, Germany, length–weight relation, LWR

Introduction

Fish size is a key variable for several ecological and physiological processes such as sexual maturity, predation, mortality, and ontogenetic diet shifts (Erzini 1994; Wootton 1999; Froese and Binohlan 2000; Evans and Claiborne 2005; Byström et al. 2012) and has important implications for population dynamics (Erzini 1994). Length data are recorded in standard fish sampling programs and essential for studies on growth rates, age structure, and other aspects of fish population dynamics (Kolher et al. 1995). Weight data, in contrast, are collected less frequently in field studies due to the additional technical effort and time required to weigh fish in the field (Martin-Smith 1996; Koutrakis and Tsikliras 2003; Sinovčić et al. 2004). Length–weight relations (LWR) not only allow weight to be estimated from commonly collected length data (Beyer 1991), but also have various applications in fish biology, physiology, ecology, and fisheries assessment. These relations enable seasonal variations in fish growth to be identified and allow a rough assessment of the nutritional status through the calculation of condition indexes, e.g., the mean condition factor (Le Cren 1951; Ricker 1975; Bagenal and Tesch 1978; Richter et al. 2000; Froese 2006). LWRs are also useful to determine whether somatic growth is isometric (weight increases proportionally to length) or allometric (weight does not increase proportionally to length) (Le Cren 1951; Ricker 1975). Furthermore, they allow life history and morphological comparisons between different fish species, or between fish populations of the same species from different habitats and/or regions (Petrakis and Stergiou 1995; Gonçalves et al. 1997; Wootton 1999). Finally, LWRs are also often used in stock assessment models to estimate stock biomass from limited sample sizes, to estimate weight-at-age (Petrakis and Stergiou 1995; Koutrakis and Tsikliras 2003), and to convert growth-in-length to growth-in-weight (Pauly 1993).

LWRs have been estimated for a large number of species. However, since the variation within a species or population is large (Froese et al. 2014), local data and LWRs are likely to be more accurate. Nevertheless, LWRs for European populations of freshwater fish species are relatively rare (Verreycken et al. 2011) and mostly available for fish from lakes (Holubová et al. 2022). To the best of our knowledge, there is no published information on LWRs of fish species in the middle part of the Elbe River in Germany. The intent of this study was therefore to describe the LWRs for freshwater fish in the middle part of a large German river.

Material and methods

The Elbe River has the 4th largest catchment area in central Europe with 148 000 km^2, a mean discharge of 861 m^3 s^{-1} at its mouth, and a surface area of about 231 000 ha (Simon et al. 2005). The sampling took place in the middle part of the Elbe River at three sampling sites (stream kilometers 337–350 (52.209314°N, 11.713875°E–52.311094°N, 11.767025°E), 418–423 (52.803450°N, 12.025439°E–52.843850°N, 12.040528°E) and 452–453 (52.974142°N, 11.772764°E). Sampling was performed annually over a four-year period (1997–2000) with fishing campaigns in spring (April–May), summer (July), and early and late autumn (September and November, respectively). Fishes were caught by a combination of DC electrofishing (FEG 5000), seine netting, drift nets, and benthic multi-mesh gillnetting (mesh sizes 6–75 mm). All caught fishes were identified to species level, and total length (TL, to the nearest 0.5 cm) and wet weight (W, measurement accuracy for individuals < 5 g ± 0.1 g and for individuals > 5 g ± 1 g) were measured individually in the field.

The following species were measured and weighed individually: *Abramis brama* (Linnaeus, 1758); *Alburnus alburnus* (Linnaeus, 1758); *Anguilla anguilla* (Linnaeus, 1758); *Ballerus ballerus* (Linnaeus, 1758); *Blicca bjoerkna* (Linnaeus, 1758); *Cobitis taenia* Linnaeus, 1758; *Esox lucius* Linnaeus, 1758; *Gobio gobio* (Linnaeus, 1758); *Gymnocephalus cernua* (Linnaeus, 1758); *Leuciscus aspius* (Linnaeus, 1758); *Leuciscus idus* (Linnaeus, 1758); *Leuciscus leuciscus* (Linnaeus, 1758); *Lota lota* (Linnaeus, 1758); *Perca fluviatilis* Linnaeus, 1758; *Romanogobio albipinnatus* (Lukasch, 1933); *Rutilus rutilus* (Linnaeus, 1758); *Sander lucioperca* (Linnaeus, 1758); *Scardinius erythrophthalmus* (Linnaeus, 1758); and *Squalius cephalus* (Linnaeus, 1758). Fifteen other species were collected but were excluded from the analyses as they were represented by insufficient numbers.

For sex determination, subsamples of fishes from seven species (*Ballerus ballerus*, *Gobio gobio*, *Leuciscus aspius*, *Leuciscus idus*, *Leuciscus leuciscus*, *Squalius cephalus*, and *Lota lota*) were killed, frozen, and stored under vacuum at –22°C. Sex was determined visually after thawing, a binocular microscope (WILD M32 Typ S, Fa. Heerbrugg, Germany) was used for smaller fishes.

The collected data was subjected to quality control and defined selection criteria (Froese 2006; Froese et al. 2011; Verreycken et al. 2011). In the final dataset, species-specific LWRs were calculated for every sampled month of the year and all sampled months combined. In addition, for seven species LWRs were calculated separately for each sex. The LWRs were estimated from the formula, $W = a\mathrm{TL}^b$, with W being total body weight [g], TL the total length [cm], and a and b the coefficients of the regression.

The parameters a and b of LWRs were estimated by power regression analyses on the non-transformed data, and the association degree between variables (W and TL) was calculated by the coefficient of determination (r^2). The standard errors (SE) and 95% confidence intervals (CI) of a and b estimates and the statistical significance level of r^2 were also determined.

Linear regression analyses (least-squares method) on log-transformed TL and W data were used to test for the influence of sex on the relation between TL and W. The model fits were assessed by residual diagnostics including the visual inspection of quantile-quantile plots (QQ plots) and residuals vs. fitted plots, accompanied by tests for the residual distribution (Kolmogorov–Smirnov (KS) test), dispersion, and outliers (Hartig 2021). For all statistical hypotheses testing the significance level was set at $\alpha < 0.05$.

The statistical analyses were performed with R 4.0.5 (R Core Team 2021) and the additional packages “FSA” (Ogle et al. 2021), and “nlstools” (Baty et al. 2015). The package DHARMa (Hartig 2021) was used to assess the model fits of the regression.

Results

During this study, a total of 26 434 fish representing 19 species from seven families were examined. The sample size ranged from 153 for *Romanogobio albipinnatus*, to 4490 for *Abramis brama* (Table 1). Depending on the species, the smallest total lengths measured were between 3.5 and 13 cm. The maximum length values for approximately half of the species were close to the maximum lengths observed in Europe (Kottelat and Freyhof 2007; Verreycken et al. 2011; Froese and Pauly 2022).

Table 1. Descriptive statistics and estimated length–weight-relation parameters for 19 freshwater fish species of the lowland Elbe River, Germany between months.

Species	Endangered status		Month	*n*	TL_{min}	TL_{max}	FishBase TL_{max}	W_{min}	W_{max}	Length–weight relation parameters				
	FFH	RL BB/D								*a*	95% CI of *a*	*b*	95% CI of *b*	r^2
Anguilla anguilla		V/3	May	399	13.0	70.5		2	571	0.001	0.001–0.001	3.285	3.23–3.34	0.979
			July	481	13.5	76.5		3	820	0.001	0.001–0.001	3.211	3.17–3.25	0.976
			September	520	13.0	72.0		3	805	0.001	0.001–0.001	3.266	3.23–3.31	0.978
			November	134	16.5	65.0		7	498	0.001	0.001–0.002	3.102	3.03–3.17	0.983
			Total year	1547	13.0	76.5	133.0	2	820	0.0007	0.001–0.001	3.209	3.18–3.24	0.975
Cobitis taenia	II	2/2	July	46	6.0	11.5		1	12	0.0007	0.001–0.001	3.926	3.65–4.21	0.950
			September	68	6.0	12.0		0.8	10	0.002	0.001–0.004	3.341	3.14–3.55	0.949
			Total year	124	6.0	12.0	13.5	0.8	12	0.002	0.001–0.003	3.517	3.33–3.70	0.927
Esox lucius		DNE/3	May	82	5.3	78.0		1	3036	0.006	0.004–0.008	3.016	2.93–3.10	0.994
			July	244	9.0	75.5		4	2725	0.008	0.007–0.010	2.931	2.88–2.98	0.994
			September	170	16.0	75.5		20	2939	0.005	0.004–0.007	3.046	2.98–3.11	0.989
			November	126	17.5	82.5		30	3851	0.007	0.005–0.009	2.987	2.93–3.05	0.992
			Total year	652	5.3	82.5	137.0	1	3851	0.006	0.006–0.007	3.001	2.97–3.03	0.991
Gobio gobio		DNE/CNE	May	114	5.0	16.5		0.5	45	0.007	0.005–0.008	3.110	3.03–3.20	0.987
			July	127	3.2	16.0		0.2	42	0.004	0.003–0.005	3.285	3.19–3.38	0.982
			September	349	3.5	17.0		0.2	38	0.006	0.005–0.007	3.129	3.08–3.18	0.987
			November	335	4.2	18.0		0.5	47	0.004	0.003–0.004	3.275	3.23–3.32	0.990
			Total year	935	3.2	18.0	21.0	0.2	47	0.005	0.005–0.006	3.189	3.16–3.22	0.985
Romanogobio albipinnatus	II	G/2	September	70	4.0	11.5		0.3	11	0.003	0.002–0.004	3.364	3.23–3.49	0.975
			November	48	5.5	12.5		1	15	0.003	0.002–0.005	3.303	3.08–3.53	0.960
			Total year	153	4.0	12.5	13.0	0.3	15	0.004	0.003–0.005	3.234	3.12–3.34	0.964
Abramis brama		DNE/CNE	May	909	4.0	55.0		0.5	1641	0.011	0.009–0.012	2.985	2.95–3.02	0.985
			July	1434	3.8	56.5		0.5	1927	0.014	0.013–0.016	2.910	2.88–2.94	0.982
			September	1312	3.8	56.5		0.5	2282	0.01	0.008–0.011	3.010	2.98–3.04	0.979
			November	591	4.0	55.5		0.5	1694	0.01	0.008–0.013	2.990	2.94–3.04	0.977
			Total year	4490	3.8	56.5	82.0	0.5	2282	0.01	0.010–0.012	2.973	2.95–2.99	0.981
Alburnus alburnus		CNE/CNE	May	339	4.3	19.5		0.5	48	0.003	0.003–0.004	3.257	3.18–3.34	0.963
			July	451	3.5	19.5		0.2	46	0.003	0.003–0.004	3.258	3.18–3.32	0.964
			September	545	3.0	19.5		0.1	58	0.003	0.002–0.003	3.307	3.24–3.37	0.973
			November	232	3.5	18.5		0.2	48	0.003	0.002–0.004	3.313	3.21–3.42	0.976
			Total year	1670	3.0	19.5	25.0	0.1	58	0.003	0.003–0.003	3.288	3.25–3.32	0.969
Ballerus ballerus		3/3	May	189	8.3	45.5		3.5	86	0.002	0.002–0.003	3.355	3.29–3.42	0.989
			July	107	6.5	49.0		1	1085	0.004	0.003–0.006	3.200	3.10–3.30	0.989
			September	62	15.0	47.0		21	960	0.003	0.002–0.004	3.294	3.18–3.41	0.990
			Total year	397	6.5	49.0	40.0	1	1085	0.003	0.002–0.003	3.294	3.25–3.34	0.989
Blicca bjoerkna		DNE/CNE	May	744	3.5	36.0		0.4	604	0.006	0.005–0.006	3.237	3.20–3.27	0.987
			July	779	5.5	34.0		1	566	0.006	0.005–0.006	3.239	3.21–3.27	0.987
			September	706	5.5	33.0		1	462	0.006	0.006–0.007	3.188	3.16–3.22	0.983
			November	413	4.3	33.5		0.7	432	0.006	0.004–0.007	3.25	3.18–3.32	0.972
			Total year	2871	3.3	39.0	45.5	0.2	660	0.006	0.006–0.006	3.227	3.21–3.25	0.982
Leuciscus aspius	II	DNE/3	May	157	6.0	67.5		1	2398	0.006	0.005–0.009	3.051	2.98–3.13	0.994
			July	252	4.0	69.5		0.3	2580	0.007	0.006–0.009	3.032	2.98–3.08	0.994
			September	351	4.9	69.0		0.5	2731	0.003	0.003–0.004	3.222	3.17–3.28	0.992
			November	173	6.5	71.5		1.5	3351	0.002	0.002–0.003	3.315	3.23–3.40	0.990
			Total year	1003	4.0	71.5	120.0	0.3	3351	0.004	0.003–0.004	3.187	3.15–3.22	0.990
Leuciscus idus		3/3	May	721	5.0	49.0		0.7	1699	0.004	0.004–0.004	3.319	3.29–3.35	0.987
			July	942	3.0	48.0		0.2	1598	0.004	0.004–0.004	3.306	3.29–3.32	0.994
			September	966	4.0	47.0		0.6	1625	0.003	0.003–0.003	3.390	3.37–3.41	0.992
			November	403	6.5	47.0		2	1496	0.002	0.002–0.003	3.492	3.43–3.56	0.987
			Total year	3134	3.0	49.0	85.0	0.2	1699	0.003	0.003–0.004	3.364	3.35–3.38	0.987
Leuciscus leuciscus		3/3	May	77	3.5	19.5		0.3	74	0.003	0.002–0.003	3.439	3.35–3.52	0.986
			July	85	5.5	17.5		1	46	0.004	0.003–0.005	3.313	3.19–3.44	0.978
			September	90	4.8	20.0		0.7	75	0.003	0.003–0.004	3.349	3.28–3.42	0.993
			November	41	7.5	20.0		2	68	0.003	0.002–0.004	3.356	3.29–3.42	0.995
			Total year	297	3.5	20.0	40.0	0.3	75	0.003	0.003–0.004	3.348	3.30–3.40	0.996
Rutilus rutilus		DNE/CNE	May	779	3.5	29.5		0.3	311	0.004	0.004–0.004	3.347	3.32–3.37	0.988
			July	1194	3.2	28.5		0.2	303	0.004	0.004–0.004	3.345	3.32–3.37	0.987
			September	1343	3.5	43.5		0.3	1141	0.004	0.004–0.004	3.339	3.33–3.35	0.994
			November	573	3.8	36.0		0.4	627	0.003	0.003–0.003	3.448	3.41–3.49	0.987
			Total year	4135	3.2	43.5	50.2	0.2	1141	0.003	0.003–0.004	3.390	3.38–3.40	0.990
Scardinius erythrophthalmus		DNE/CNE	July	61	5.0	28.0		1	259	0.008	0.007–0.009	3.129	3.09–3.17	0.998
			September	42	7.0	17.0		3	55	0.007	0.004–0.011	3.194	2.99–3.41	0.970
			Total year	144	4.8	28.0	61.7	1	259	0.007	0.006–0.008	3.173	3.14–3.21	0.995

Table 1. Continued.

Species	Endangered status		Month	n	TL_{min}	TL_{max}	FishBase TL_{max}	W_{min}	W_{max}	Length–weight relation parameters				
	FFH	RL BB/D								a	95% CI of a	b	95% CI of b	r^2
Squalius cephalus		CNE/CNE	May	295	4.3	42.5		0.6	755	0.012	0.011–0.012	2.962	2.94–2.98	0.995
			July	351	5.5	28.5		1	274	0.004	0.005–0.006	3.246	3.22–3.28	0.992
			September	385	4.2	39.5		0.5	699	0.005	0.004–0.005	3.263	3.24–3.29	0.991
			November	293	4.2	43.0		0.4	1056	0.003	0.003–0.003	3.408	3.39–3.43	0.998
			Total year	1350	4.2	43.0	60.0	0.4	1056	0.005	0.005–0.005	3.240	3.22–3.26	0.990
Lota lota		2/2	May	54	3.0	33.0		0.2	282	0.006	0.004–0.014	2.993	2.80–3.19	0.967
			July	162	5.7	41.0		1	545	0.007	0.005–0.009	3.024	2.95–3.10	0.975
			September	171	8.0	41.5		3	367	0.017	0.013–0.022	2.711	2.63–2.80	0.969
			November	107	9.5	38.5		5	381	0.005	0.003–0.007	3.111	3.00–3.22	0.977
			Total year	498	3.0	41.5	152.0	0.2	545	0.010	0.008–0.012	2.882	2.83–2.94	0.965
Gymnocephalus cernua		DNE/CNE	May	74	6.2	16.0		2	52	0.008	0.006–0.011	3.111	2.99–3.23	0.980
			July	96	3.7	17.0		0.5	53	0.012	0.009–0.015	2.969	2.86–3.07	0.978
			September	194	6.0	18.0		2	87	0.004	0.003–0.004	3.462	3.38–3.54	0.980
			November	176	5.5	16.0		1.5	57	0.006	0.005–0.007	3.269	3.18–3.36	0.976
			Total year	562	3.7	18.0	25.0	0.5	87	0.006	0.005–0.007	3.272	3.22–3.32	0.974
Perca fluviatilis		DNE/CNE	May	626	3.3	40.5		0.3	868	0.006	0.005–0.007	3.234	3.20–3.27	0.985
			July	933	3.8	43.5		0.4	1230	0.005	0.005–0.005	3.280	3.27–3.29	0.995
			September	1279	5.0	43.5		1	1438	0.004	0.003–0.004	3.392	3.37–3.41	0.987
			November	564	5.0	40.5		1	970	0.005	0.004–0.005	3.327	3.30–3.35	0.993
			Total year	3438	3.3	43.5	60.0	0.3	1438	0.004	0.004–0.004	3.342	3.33–3.35	0.987
Sander lucioperca		V/CNE	July	50	4.5	71.5		0.5	3313	0.002	0.002–0.003	3.331	3.23–3.43	0.998
			September	59	7.5	76.5		2	4184	0.003	0.002–0.004	3.300	3.19–3.42	0.996
			November	52	9.0	76.0		4	4551	0.002	0.001–0.002	3.416	3.32–3.52	0.996
			Total year	198	4.5	76.5	100.0	0.5	4551	0.002	0.002–0.003	3.316	3.24–3.39	0.993

n = sample size, TL = total length [cm], W = weight [g], min = minimum, max = maximum, a = regression intercept, b = slope of regression line, CI = confidence interval, r^2 = coefficient of correlation. FFH = FFH Fauna-Flora-Habitat Directive (EU 1992): II = listed in the Annex II Animal and plant species of community interest whose conservation requires the designation of special areas of conservation; RL BB/D = RL-BB Red List of the Federal State of Brandenburg (Knuth et al. 1998); RL-D Red List of Germany (Bless et al. 1998): 2 = critically endangered, 3 = endangered, G = endangered status is assumed, V = declining, Pre-warning list, CNE = currently not considered endangered, DNE = definitely not endangered. Note: Total year can include additional data from other months with fewer individuals than 30 per species that were not separately shown in the table.

At the time of data collection, three of the 19 species were classified as critically endangered and six as endangered in the Red List of Fishes in Germany (Bless et al. 1998, Table 1). Furthermore, two species were classified as critically endangered and three species as endangered in the Red List of Fishes of the Federal State of Brandenburg (Knuth et al. 1998). Three of the 19 species are listed in Annex II of the Fauna-Flora-Habitat Directive (EU 1992, Table 1).

The linear regression analyses indicated that there were no significant differences in slopes between males and females in the seven species where this effect could be tested (Table 2).

The power regressions were significant for all species ($p < 0.001$). The r^2 was ≥ 0.99 for seven of the species and was greater than 0.96 for all other species except for *Cobitis taenia* with 0.93 (Table 1). The regression parameters a (intercept) and b (slope) differed between species. The parameters a and b ranged from 0.0005 ± 0.0001 (mean ± SE) (*Anguilla anguilla*, May) to 0.017 ± 0.003 (*Lota lota*, September) and from 2.711 ± 0.044 (*Lota lota*, September) to 3.926 ± 0.138 (*Cobitis taenia*, July), respectively. Both parameters varied also between the sampling months with comparably small standard errors in the estimates for a (Table 1). With *Rutilus rutilus*, for example, the parameter a ranged from 0.003 in November to 0.004 in the other sampling months. The parameter b ranged from 3.339 ± 0.005 in September to 3.448 ± 0.02 in November. The estimates of a for *Perca fluviatilis*, in contrast, varied between 0.004 in September to 0.006 in May. The b values were lowest in May (3.234 ± 0.017) and highest in September (3.392 ± 0.011). With *Esox lucius*, the estimates for a were higher and ranged from 0.005 in September to 0.008 in July. The b estimates were slightly lower than those of *Rutilus rutilus* and *Perca fluviatilis* and ranged from 2.931 ± 0.025 in July to 3.046 ± 0.034 in September (Table 1).

Discussion

Although various studies investigated the fish populations from the Elbe River, LWRs are only available for ten species (Hölker and Hammer 1994; Holubová et al. 2022). To the authors' best knowledge, this study provides the first references on LWRs for the *Romanogobio albipinnatus* worldwide, for 15 species in German waters and nine species from the Elbe River (Froese and Pauly 2022; Holubová et al. 2022). Finally, this study shows LWRs of seven fish species whose LWRs exist in fewer than five literature sources in Europe.

Due to the size selectivity of the fishing gear, the majority of samples did not include juveniles or very small individuals. According to Petrakis and Stergiou (1995), the respective LWR should only be used for the size range for which data were available when estimating the linear regression parameters. For this reason, the extrapolating of the relations to fish larvae (Pepin 1995), juveniles (Safran 1992), or immature stages (Bagenal and Tesch 1978) can lead to inaccurate results and is not recommended.

Our samples were always collected in the same four months in four consecutive years. For comparisons with, for example, other ecological regions or future studies, the calculated mean annual values can be considered

Table 2. Descriptive statistics and estimated length–weight-relation parameters by sex for seven freshwater fish species of the lowland Elbe River, Germany.

Species	Sex	n	TL_{min}	TL_{max}	W_{min}	W_{max}	Length–weight relation parameters					
							a	95% CI of a	b	95% CI of b	r^2
Gobio gobio	Male	40	9.5	16.5	6	37	0.009	0.005–0.016	2.972	2.77–3.17	0.964
	Female	37	9.5	17.0	7	45	0.005	0.003–0.010	3.183	2.94–3.43	0.964
	Both	77	9.5	17.0	6	45	0.007	0.004–0.010	3.094	2.94–3.25	0.963
Ballerus ballerus	Male	29	23.0	43.5	88	660	0.005	0.003–0.008	3.149	3.01–3.29	0.991
	Female	23	16.5	47.0	27	980	0.004	0.001–0.008	3.236	3.00–3.48	0.988
	Both	52	16.5	47.0	27	980	0.004	0.002–0.006	3.209	3.08–3.34	0.989
Leuciscus aspius	Male	45	12.5	64.5	13	2175	0.009	0.004–0.018	2.972	2.80–3.15	0.983
	Female	49	14.5	66.5	22	2639	0.002	0.001–0.003	3.402	3.26–3.55	0.991
	Both	94	12.5	66.5	13	2639	0.004	0.002–0.006	3.216	3.09–3.35	0.984
Leuciscus idus	Male	64	11.5	43.5	15	1089	0.005	0.003–0.007	3.258	3.15–3.37	0.991
	Female	62	12.5	48.0	15	1699	0.003	0.001–0.006	3.404	3.21–3.61	0.976
	Both	126	11.5	48.0	15	1699	0.002	0.001–0.004	3.450	3.31–3.59	0.976
Leuciscus leuciscus	Male	24	10.0	19.5	6	74	0.002	0.001–0.003	3.620	3.44–3.80	0.984
	Female	30	10.0	20.0	7	75	0.003	0.002–0.005	3.358	3.19–3.53	0.985
	Both	54	10.0	20.0	6	75	0.003	0.002–0.004	3.439	3.32–3.56	0.983
Squalius cephalus	Male	44	11.0	38.0	12	650	0.004	0.003–0.006	3.312	3.12–3.42	0.994
	Female	63	10.5	43.0	9	1056	0.003	0.003–0.004	3.383	3.33–3.44	0.997
	Both	107	10.5	43.0	9	1056	0.003	0.003–0.004	3.366	3.32–3.41	0.996
Lota lota	Male	26	11.0	38.5	9	381	0.007	0.003–0.017	3.000	2.73–3.27	0.959
	Female	37	11.0	37.0	9	404	0.008	0.002–0.028	2.946	2.59–3.31	0.917
	Both	63	11.0	38.5	9	404	0.008	0.004–0.016	2.967	2.74–3.20	0.933

n = sample size, TL = total length [cm], W = weight [g], min = minimum, max = maximum, a = regression intercept, b = slope of regression line, CI = confidence interval, r^2 = coefficient of correlation.

(Petrakis and Stergiou 1995; Gonçalves et al. 1997). The observed b values of the LWRs in our study were within the limits reported for all fish species (2–4 by Bagenal and Tesch 1978 and 2.5–3.5 by Froese 2006). Despite the different body shapes of the fish species, b is in the majority of fish species larger than 3.0 indicating positive allometric growth (increase in relative body thickness) (Froese 2006; Verreycken et al. 2011). In this study, two species (*Abramis brama* and *Esox lucius*) showed isometric growth ($b = 3$), one species (*Lota lota*) showed slightly negative allometric growth ($b < 3$), and the remaining species showed slightly positive to positive allometric growth ($b > 3$).

Additionally, we have also calculated month-specific LWRs that represent specific seasons of the year. LWRs are not constant throughout the year and can vary depending on factors such as food availability, gonad development, and spawning period (Le Cren 1951; Bagenal and Tesch 1978; Froese 2006; DeWeber et al. 2021). Parameter b is characteristic of the species (Mayrat 1970) and generally does not vary distinctly throughout the year (Le Cren 1951; Bagenal and Tesch 1978; Froese 2006). The small differences in b-values between sampling months within a species found in our study can be attributed to the following factors:

- differences in the number and size range of specimens examined,
- effect of the year or season and
- health and general fish condition (Le Cren 1951; Froese 2006).

The parameter a, however, can vary substantially in days, seasons, and/or habitats (Le Cren 1951; Bagenal and Tesch 1978; Froese 2006). The differences in the parameters between months and years found in our study highlight the importance of considering season and sampling year when calculating and applying LWRs.

Within a fish species, LWRs can significantly differ depending on sex, life stage (larvae, ages 0 and 1 and for sexually mature males and females), and stage of gonadal development (Le Cren 1951; Froese 2006; DeWeber et al. 2021). In the presently reported study, no significant differences between males and females were observed in the seven species that had been caught in sufficient numbers for comparisons (Table 2). This suggests a lack of pronounced sexual dimorphism concerning the LWR for these species, which is similar to the results of Morato et al. (2001) who found significant differences between males and females for only two of 15 coastal fish species of the Azores.

A limitation of the study is that the data and LWRs represent conditions from over 20 years ago which may no longer be representative of the Elbe River. Since conditions including productivity and temperature might have changed in the meantime, the data can be only used as examples for potentially typical LWRs for the studied species in the same ecoregion. These data nevertheless provide the first LWRs for many species of the study region, and future studies can investigate whether the LWRs have changed substantially over time.

Conclusions

The calculated LWRs allow us to dispense with weighing fish in the field during data collection and still get accurate weight estimates for fishes of the middle Elbe River. This allows less and shorter handling, less skin contact with objects, less damage to the mucosa, and minimizes stress, which is especially important for rare and protected fish species and leads to lower costs due to the time saved.

For the Elbe River, data regarding the abundances and biomass composition of catches as well as densities of the individual species in the shore zone and an open water area of groin fields, training walls, and mainstream exists (Fladung 2002a, 2002b). Thus, the additionally calculated LWRs will be useful for fisheries management and the protection of especially the endangered fish species in the Elbe River.

Acknowledgments

We thank Herbert Ebel and Peter Schoppe for their technical assistance and support and the fishermen for their cooperation in collecting samples. We also thank David Ritterbusch and Tyrell DeWeber for helpful discussions on earlier drafts of the manuscript and who kindly improved the English. The work was part of the project “Ökologische Zusammenhänge zwischen Fischgemeinschafts- und Lebensraumstrukturen der Elbe” supported by the Bundesministerium für Bildung, Forschung und Technologie (BMB+F, grant No. 0339578).

References

Bagenal TB, Tesch FW (1978) Age and growth. Pp. 101–136. In: Bagenal TB (Ed.) Methods for assessment of fish production in fresh waters. 3rd Edition. IBP Handbook No. 3. Blackwell Scientific Publications, Oxford, UK.

Baty F, Ritz C, Charles S, Brutsche M, Flandrois JP, Delignette-Muller ML (2015) A toolbox for nonlinear regression in R: The package nlstools. Journal of Statistical Software 66(5): 1–21. https://doi.org/10.18637/jss.v066.i05

Beyer JE (1991) On length–weight relationships. 2. Computing mean weights from length statistics. Fishbyte 9(2): 50–54.

Bless R, Lelek A, Waterstraat A (1998) Rote Liste der in Binnengewässern lebenden Rundmäuler und Fische (Cyclostomata & Pisces). Schriftenreihe für Landschaftspflege und Naturschutz 55: 53–59.

Byström P, Huss M, Persson L (2012) Ontogenetic constraints and diet shifts in Perch (*Perca fluviatilis*): Mechanisms and consequences for intra-cohort cannibalism. Freshwater Biology 57(4): 847–857. https://doi.org/10.1111/j.1365-2427.2012.02752.x

DeWeber JT, Rösch R, Baer J, Brinker A (2021) Long-term changes in body condition and gillnet selectivity in Lake Constance pelagic spawning whitefish (*Coregonus wartmanni*). Canadian Journal of Fisheries and Aquatic Sciences 78(7): 841–851. https://doi.org/10.1139/cjfas-2020-0231

Erzini K (1994) An empirical study of variability in length-at-age of marine fishes. Journal of Applied Ichthyology 10(1): 17–41. https://doi.org/10.1111/j.1439-0426.1994.tb00140.x

EU (1992) Council Directive 92/43/EEC of 21 May 1992 on the conservation of natural habitats and of wild fauna and flora. Official Journal of the European Union L 206: 22.7.1992, 7–50.

Evans DH, Claiborne JB (2005) The physiology of fishes. 3rd edn. CRC Press, 616 pp. https://doi.org/10.1201/9781420058093

Fladung E (2002a) Untersuchungen zum adulten Fischbestand im Hauptstrom (Fahrrinne) der Mittelelbe. Zeitschrift für Fischkunde. Supplementband 1: 121–131.

Fladung E (2002b) Der präadulte/adulte Fischbestand in Buhnenfeldern und Leitwerken der Mittelelbe. Zeitschrift für Fischkunde. Supplementband 1: 101–120.

Froese R (2006) Cube law, condition factor and weight–length relationships: History, meta-analysis and recommendations. Journal of Applied Ichthyology 22(2): 241–253. https://doi.org/10.1111/j.1439-0426.2006.00805.x

Froese R, Binohlan C (2000) Empirical relationships to estimate asymptotic length, length at first maturity and length at maximum yield per recruit in fishes, with a simple method to evaluate length frequency data. Journal of Fish Biology 56(4): 758–773. https://doi.org/10.1111/j.1095-8649.2000.tb00870.x

Froese R, Pauly D (2022) FishBase. [Version 10/2022] http://www.fishbase.org

Froese R, Tsikliras AC, Stergiou KI (2011) Editorial note on weight–length relations of fishes. Acta Ichthyologica et Piscatoria 41(4): 261–263. https://doi.org/10.3750/AIP2011.41.4.01

Froese R, Thorson JT, Reyes Jr RB (2014) A Bayesian approach for estimating length–weight relationships in fishes. Journal of Applied Ichthyology 30(1): 78–85. https://doi.org/10.1111/jai.12299

Gonçalves JMS, Bentes L, Lino PG, Ribeiro J, Canário AVM, Erzini K (1997) Weight–length relationships for selected fish species of the small-scale demersal fisheries of the south and south-west coast of Portugal. Fisheries Research 30(3): 253–256. https://doi.org/10.1016/S0165-7836(96)00569-3

Hartig F (2021) DHARMa: Residual diagnostics for hierarchical (multi-level/mixed) regression models. R package version 0.4.4. https://CRAN.R-project.org/package=DHARMa

Hölker F, Hammer C (1994) Growth and food of ruffe *Gymnocephalus cernuus* (L.) in the Elbe Estuary. Archiv für Fischerei- und Meeresforschung 42(1): 47–62.

Holubová K, Musilová Z, Horká P (2022) Regression analysis of the length–weight relationships for 17 common European fish in rivers in the Czech Republic. European Journal of Environmental Sciences 12(2): 90–92. https://doi.org/10.14712/23361964.2022.11

Knuth D, Rothe U, Zerning M (1998) Rote Liste und Artenliste der Rundmäuler und Fische des Landes Brandenburg (Cyclostomata u. Pisces). Naturschutz und Landschaftspflege Brandenburg, no. 7, Beilage, 19 pp.

Kolher N, Casey J, Turner P (1995) Length–weight relationships for 13 species of sharks from the western North Atlantic. Fish Bulletin 93(2): 412–418.

Kottelat M, Freyhof J (2007) Handbook of European freshwater fishes. Kottelat, Cornol, Switzerland and Freyhof, Berlin, Germany, 646 pp.

Koutrakis ET, Tsikliras AC (2003) Length–weight relationships of fishes from three northern Aegean estuarine systems (Greece). Journal of Applied Ichthyology 19(4): 258–260. https://doi.org/10.1046/j.1439-0426.2003.00456.x

Le Cren ED (1951) The length–weight relationship and seasonal cycle in gonad weight and condition in the perch (*Perca fluviatilis*). Journal of Animal Ecology 20(2): 201–219. https://doi.org/10.2307/1540

Martin-Smith KH (1996) Length/weight relationships of fishes in a diverse tropical freshwater community, Sabah, Malaysia. Journal of Fish Biology 49(4): 731–734. https://doi.org/10.1111/j.1095-8649.1996.tb00069.x

Mayrat A (1970) Allometric et taxinomie. Revue de Statistique Appliquee 18(4): 47–58.

Morato T, Afonso P, Lourinho P, Barreiros JP, Santos RS, Nash RDM (2001) Length–weight relationships for 21 coastal fish species of the Azores, North eastern Atlantic. Fisheries Research 50(3): 297–302. https://doi.org/10.1016/S0165-7836(00)00215-0

Ogle DH, Doll JC, Wheeler P, Dinno A (2021) FSA: Fisheries Stock Analysis. R package version 0.9.1. https://github.com/droglenc/FSA

Pauly D (1993) FishByte section editorial. Naga, ICLARM Quarterly 16, 26 pp.

Pepin P (1995) An analysis of the length–weight relationship of larval fish: Limitations of the general allometric model. Fish Bulletin 93(2): 419–426.

Petrakis G, Stergiou KI (1995) Weight–length relationships for 33 fish species in Greek waters. Fisheries Research 21(3–4): 465–469. https://doi.org/10.1016/0165-7836(94)00294-7

R Core Team (2021) R: A language and environment for statistical computing. R Foundation for Statistical Computing, Vienna, Austria. https://www.R-project.org/

Richter HC, Luckstadt C, Focken U, Becker K (2000) An improved procedure to assess fish condition on the basis of length–weight relationships. Archiv für Fischerei- und Meeresforschung 48(3): 255–264.

Ricker WE (1975) Computation and interpretation of biological statistics of fish populations. Bulletin of the Fisheries Research Board of Canada 191: 1–382.

Safran P (1992) Theoretical analysis of the weight–length relationship in fish juveniles. Marine Biology 112(4): 545–551. https://doi.org/10.1007/BF00346171

Simon M, Bekele V, Kulasová B, Maul C, Oppermann R, Řehák P (2005) Die Elbe und ihr Einzugsgebiet – Ein geographisch-hydrologischer und wasserwirtschaftlicher Überblick. Internationale Kommission zum Schutz der Elbe, Magdeburg, 258 pp.

Sinovčić G, Franičević M, Zorica B, Čikeš-Keč V (2004) Length–weight and length–length relationships for 10 pelagic fish species from the Adriatic Sea (Croatia). Journal of Applied Ichthyology 20(2): 156–158. https://doi.org/10.1046/j.1439-0426.2003.00519.x

Verreycken H, Van Thuyne G, Belpaire C (2011) Length–weight relationships of 40 freshwater fish species from two decades of monitoring in Flanders (Belgium). Journal of Applied Ichthyology 27(6): 1416–1421. https://doi.org/10.1111/j.1439-0426.2011.01815.x

Wootton RJ (1999) Ecology of teleost fishes. 2^{nd} edn. Fish and Fisheries Series No. 24, Springer Netherlands, 400 pp.

Acta Ichthyologica et Piscatoria 53, 2023, 137–145 | DOI 10.3897/aiep.53.103343

PENSOFT.

ACTA
ICHTHYOLOGICA
ET PISCATORIA

A new record of *Upeneus pori* (Actinopterygii: Syngnathiformes: Mullidae) from the South China Sea: Integrating morphology and DNA barcoding

Zhisen LUO[1], Murong YI[1], Sui GU[1], Hung-Du LIN[2], Yunrong YAN[1,3,4]

1 *College of Fisheries, Guangdong Ocean University, Zhanjiang, China*
2 *Affiliated School of National Tainan First Senior High School, Tainan, Taiwan*
3 *Southern Marine Science and Engineering Guangdong Laboratory (Zhanjiang), Zhanjiang, China*
4 *Guangdong Provincial Engineering and Technology Research Center of Far Sea Fisheries Management and Fishing of South China Sea, Guangdong Ocean University, Zhanjiang, China*

https://zoobank.org/5D4335AE-6435-4186-870C-630DA13704ED

Corresponding authors: Yunrong Yan (yryan_gdou@163.com); Murong Yi (murong_yi@outlook.com)

Academic editor: Jolanta Kiełpińska ♦ **Received** 11 March 2023 ♦ **Accepted** 29 August 2023 ♦ **Published** 2 October 2023

Citation: Luo Z, Yi M, Gu S, Lin H-D, Yan Y (2023) A new record of *Upeneus pori* (Actinopterygii: Syngnathiformes: Mullidae) from the South China Sea: Integrating morphology and DNA barcoding. Acta Ichthyologica et Piscatoria 53: 137–145. https://doi.org/10.3897/aiep.53.103343

Abstract

This study constitutes the first record of the Por's goatfish, *Upeneus pori* Ben-Tuvia et Golani, 1989, from the South China Sea. This fish had formerly only been reported in the western Indian Ocean. Six specimens of *U. pori* collected from the South China Sea were identified through comparisons of morphology and molecular analysis. *Upeneus pori* and *Upeneus tragula* Richardson, 1846 are very similar. The difference is that the former has seven spines in the first dorsal fin, lacks any spots or blotches on its body, and exhibits white or creamy white barbels. The latter has eight spines in the first dorsal fin, exhibits black spots on its body, and displays orange-colored barbels, along with different caudal fin patterns. Pairwise genetic distance computation demonstrated that *U. pori* exhibits a very low genetic distance from sequences of the other three recorded *U. pori* species found in the type locality of Israel, Red Sea, as documented in GenBank. These findings provide compelling evidence of the Por's goatfish's presence in the South China Sea.

Keywords

COI, morphometry, novel distribution, south coast of China, taxonomy

Introduction

The family Mullidae is composed of 100 species and six genera (Fricke et al. 2023) that are distributed in the Atlantic, Indian, and Pacific oceans and rarely found in brackish waters (Uiblein and Gouws 2014; Chen and Zhang 2015; Nelson et al. 2016). The mullids are otherwise known as goatfishes and have two independently moving hyoid barbels that contain chemical receptors used for detecting sand or holes in the reef to search for bottom-dwelling invertebrates. Until recently, the family Mullidae had been affiliated with the order Perciformes. Since 2022 it has been placed in Syngnathiformes (see Nash et al. 2022), which is accepted by (Fricke et al. 2023). A total of twenty-eight species of goatfishes, representing three genera (*Mulloidichthys*, *Parupeneus*, and *Upeneus*), have been recorded in China (Cheng et al. 1962; Shen 1993; Randall 2001). With the highly exhibited diversity of the goatfishes, the genus *Upeneus* Cuvier 1829 was revised by Lachner (1954), but only ten species were known at that time. Subsequently, Uiblein and Heemstra (2010) studied and verified the morphological characteristics of

26 species of *Upeneus* and summarized the taxonomy of this genus. They pointed out that 25 of the 26 species could be separated into four taxonomic groups (*japonicus* group, *tragula* group, *moluccensis* group, and *vittatus* group). Later, an increasing number of new species of *Upeneus* were described and new records of known species were reported worldwide using alpha taxonomy alone or in combination with barcoding approaches. To date, the number of valid species of the genus *Upeneus* has reached 47 species (Fricke et al. 2023) and there are seven taxonomic groups (*japonicus* group, *tragula* group, *moluccensis* group, *stenopsis* group, *margarethae* group, *suahelicus* group, *pori* group) (Uiblein and Maclaine 2021). The majority of these discoveries were concentrated in the Indian and Atlantic oceans (Yamashita et al. 2011; Nicolaidou et al. 2012; Uiblein and Lisher 2013; Bos 2014; Uiblein and White 2015; Uiblein et al. 2016, 2017, 2019, 2020; Deidun et al. 2018; Uiblein and Motomura 2021).

Since the discovery of *Upeneus quadrilineatus* Cheng et Wang, 1963, from the East China Sea, neither new species nor new records of *Upeneus* have been reported from this body of water. As recently as 2019, a new species *Upeneus heterospinus* Uiblein et Pavlov, 2019 was described, based on the material collected from the South China Sea (Uiblein et al. 2019). Thus, the following nine goatfishes of the genus *Upeneus* have been recorded in China: *Upeneus tragula* Richardson, 1846; *Upeneus vittatus* (Forsskål, 1775); *Upeneus subvittatus* (Temminck et Schlegel, 1843); *Upeneus sulphureus* Cuvier, 1829; *Upeneus moluccensis* (Bleeker, 1855); *Upeneus japonicus* (Houttuyn, 1782); *Upeneus luzonius* Jordan et Seale, 1907; *U. quadrilineatus*; and *U. heterospinus*. According to research related to the diversity and distribution of goatfishes in the western Pacific by Jiao and Chen (2000), the biodiversity of goatfish plummets from southern to northern waters in the China Sea. These authors also considered that the destruction of coral reefs has led to a sharp decline in fish production and some common species are difficult to find.

Materials and methods

Six specimens of fishes visually representing a species of the genus *Upeneus* were collected from the local fish markets in coastal cities near the northwestern South China Sea (Fig. 1). All specimens were caught by bottom trawling. Detailed collection information is given in Table 1. According to the key morphological characteristics provided by Ben-Tuvia and Golani (1989), these specimens were examined, identified, and deposited in the College of Fisheries, Guangdong Ocean University. We performed a morphometric examination on six samples according to the measurement and counting method by Uiblein and Heemstra (2010) and compared them with paratypes from the Red Sea described by Ben-Tuvia and Golani (1989). Standard length (SL) and other measurements were made

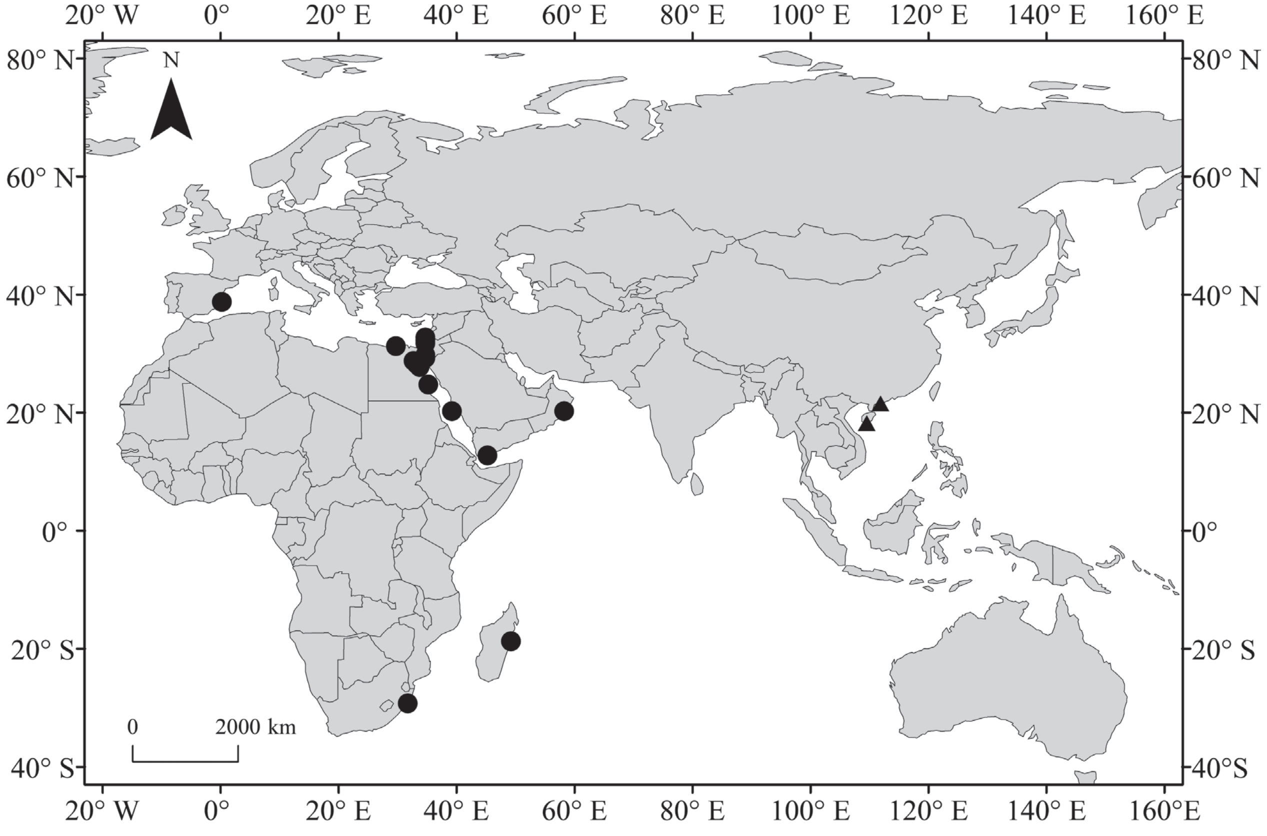

Figure 1. Distribution records for *Upeneus pori* in the world's oceans. The triangles indicate records added in this study and the circles denote historical records.

Table 1. Information on the *COI* sequences and collection in this study.

Species	Specimen No.	Sampling location	Coordinates	Accession No.	Source
U. pori	GOU103674	South China Sea, China	18.238°N, 109.509°E	GAF	
	GOU103676	South China Sea, China	18.238°N, 109.509°E	MW922385	This study
	GOU103678	South China Sea, China	18.238°N, 109.509°E	MW922386	This study
	GOU104100	South China Sea, China	21.572°N, 111.832°E	MW922387	This study
	GOU104101	South China Sea, China	21.572°N, 111.832°E	GAF	
	GOU104102	South China Sea, China	21.572°N, 111.832°E	MW922388	This study
	UpPo14A	Israel		KM538630	GenBank
	Upor	Egypt		LC572156	GenBank
	1059	Turkey		KY176690	GenBank
	P. 14829	Israel	31.799°N, 34.608°E	KF564319	GenBank
U. sulphureus	FSCS045-06	Guangdong, China	20.42°N, 109.84°E	EF607609	GenBank
	BW-A11206	Indonesia	8.80°S, 116.48°E	JN313348	GenBank
U. subvittatus	NS587	Nansha Island, China	5.317°N, 111.667°E	KY372338	GenBank
	NS586	Nansha Island, China	5.317°N, 111.667°E	KY372339	GenBank
U. quadrilineatus	BW-A6880	Jawa Timur, Indonesia	8.21667°S, 111.067°E	GU674207	GenBank
	BW-A6879	Indonesia	8.21667°S, 111.067°E	GU674208	GenBank
U. moluccensis	TR1879EK	Turkey	8.81°N, 78.14°E	KC501840	GenBank
	CIFE:FGB UM-01	India	8.81°N, 78.14°E	KJ920110	GenBank
U. japonicus	ASIZP0078749	Taiwan		KT718279	GenBank
	HMJ6	Shizuoka Japan	34.667°N, 138.333°E	JF952884	GenBank
U. tragula	GBMIN131725-17	Phu Quoc, Vietnam		KX887496	GenBank
	FSCS209-06	Guangdong, China	20.92°N, 110.54°E	EF607611	GenBank
Mullus argentinae	HRCB:53038	Sao Paulo, Brazil	26.352°S, 45.139°W	JQ365451	GenBank
Parupeneus multifasciatus	IRD BMF-162.2	Maluku, Indonesia	3.6876°S, 128.183°E	MN870495	GenBank

GAF = *COI* gene amplification failure.

with dial calipers from Shanghai Shenhan Measuring Tools Co., Ltd. with an accuracy of 0.1 mm.

Muscle tissues (50 mg) were stored in a 95% alcohol solution and in a –20°C freezer for later study. DNA was extracted by a Rapid Animal Genomic DNA Isolation Kit (Sangon Biotech, Inc., Shanghai, China). Using the universal primers FishF1 and FishR1, the *COI* gene was amplified (Ward et al. 2005). PCR was carried out in a 25 µL reaction mixture containing 12.5 µL of *Taq* PCR Master Mix (Sangon Biotech, Inc., Shanghai, China), 2 µL of $MgCl_2$, 5 µL of DNA template, 1 µL of forward, and reverse primer and 3.5 µL of ultrapure water. The thermal regime consisted of denaturation for three min at 95°C, followed by 33 cycles of 45 s at 92°C, 45 s at 50°C and one minute at 72°C, with post-extension at 72°C for ten min. Then, the temperature was maintained at 4°C. The PCR products were sequenced by Sangon Biotech Co., Ltd. (Shanghai) using an ABI PRISM 3730 DNA sequencer (Applied Biosystems, Foster City, CA, USA) with the BigDye Terminator kit (Applied Biosystems).

Sequence alignment and manual editing were performed using Sequencher 5.4.5 software. Four sequences were obtained and utilized to search for homologous sequences using BLAST on the NCBI website (Altschul et al. 1990) and then deposited in GenBank under accession numbers MW922385 to MW922388. The Maximum Likelihood (ML) method tree of 22 sequences was performed by the software PhyloSuite v.1.2.2 (Zhang et al. 2020), of which two sequences were downloaded from GenBank as out-group sequences: *Parupeneus multifasciatus* (Quoy et Gaimard, 1825), MN870495 and *Mullus argentinae* Hubbs et Marini, 1933, JQ365451. The HKY+G4+F model was selected for the best-fit model using the BIC criterion by ModelFinder (Kalyaanamoorthy et al. 2017). Maximum Likelihood phylogenies were inferred using IQ-TREE (Nguyen et al. 2015) with the HKY+G4+F model for 5000 ultrafast (Minh et al. 2013) bootstraps, as well as the Shimodaira–Hasegawa-like approximate likelihood-ratio test (SH-aLRT) (Guindon et al. 2010). The Kimura two-parameter model (K2P) model was used to calculate intra- and interspecific genetic distances of the genus *Upeneus*. Information on the *COI* sequences of *Upeneus* is provided in Table 1.

Results

The collected specimens represented a single species, *Upeneus pori*, which was confirmed using morphological methods as well as DNA barcoding.

Taxonomy

Family Mullidae Rafinesque, 1815

Genus *Upeneus* Cuvier, 1829

Upeneus pori Ben-Tuvia et Golani, 1989

(Figs. 2 and 3; Table 2)

Morphological characteristics. The morphometric measurements are shown in Table 2. Head medium, obtuse, and conical; body laterally compressed and elongated; maxilla slightly longer than the mandible; cordiform teeth present in both jaws, palatine, and vomer; single complete lateral-line on each body side; snout slightly inferior; body with rhomboidal ctenoid scales; two separate dorsal-fins; two barbels on the chin; upper lobe of the caudal fin larger than the lower lobe.

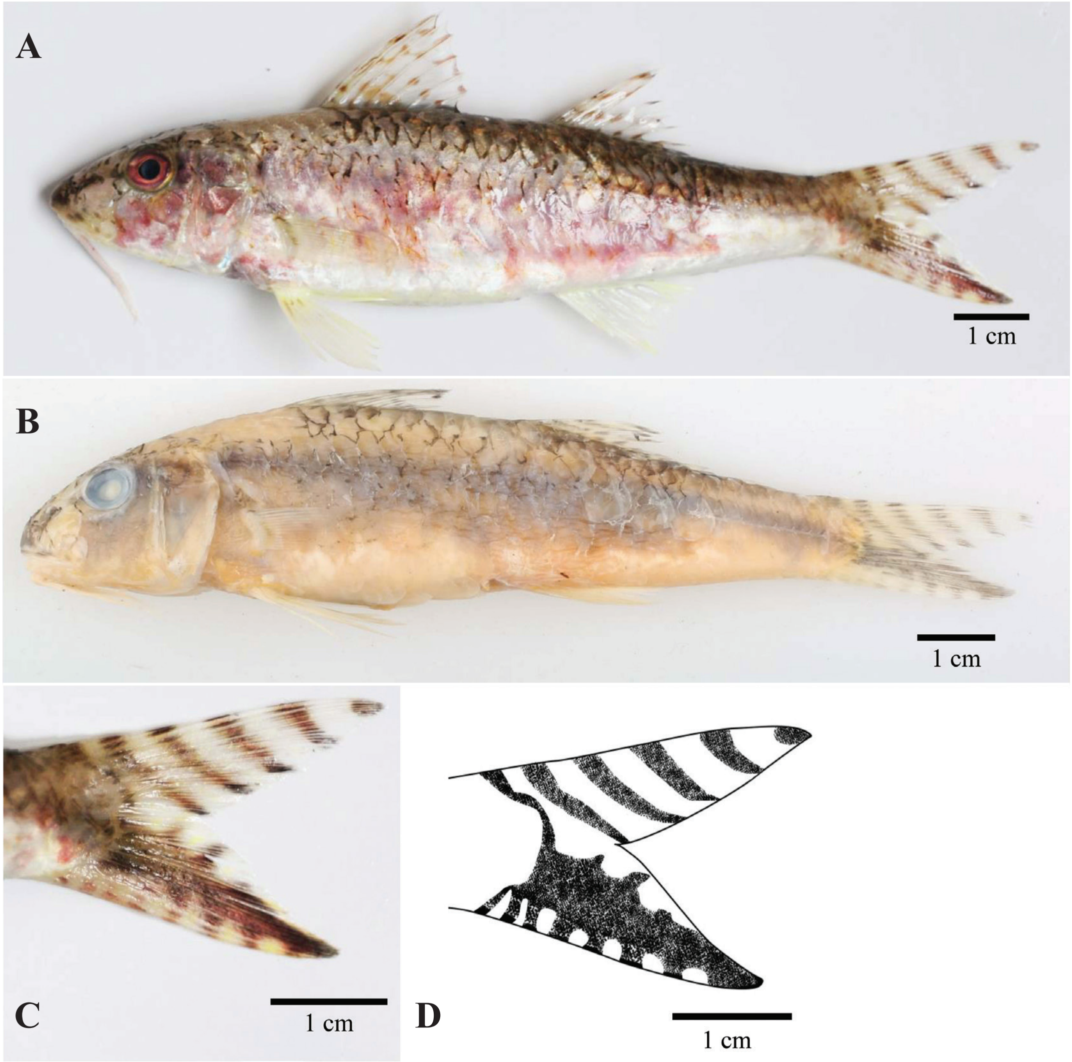

Figure 2. *Upeneus pori*, 106 mm SL, GOU104100, (**A**) fresh specimen; (**B**) preserved specimen; (**C**) caudal-fin characteristics; (**D**) drawing of caudal-fin patterns.

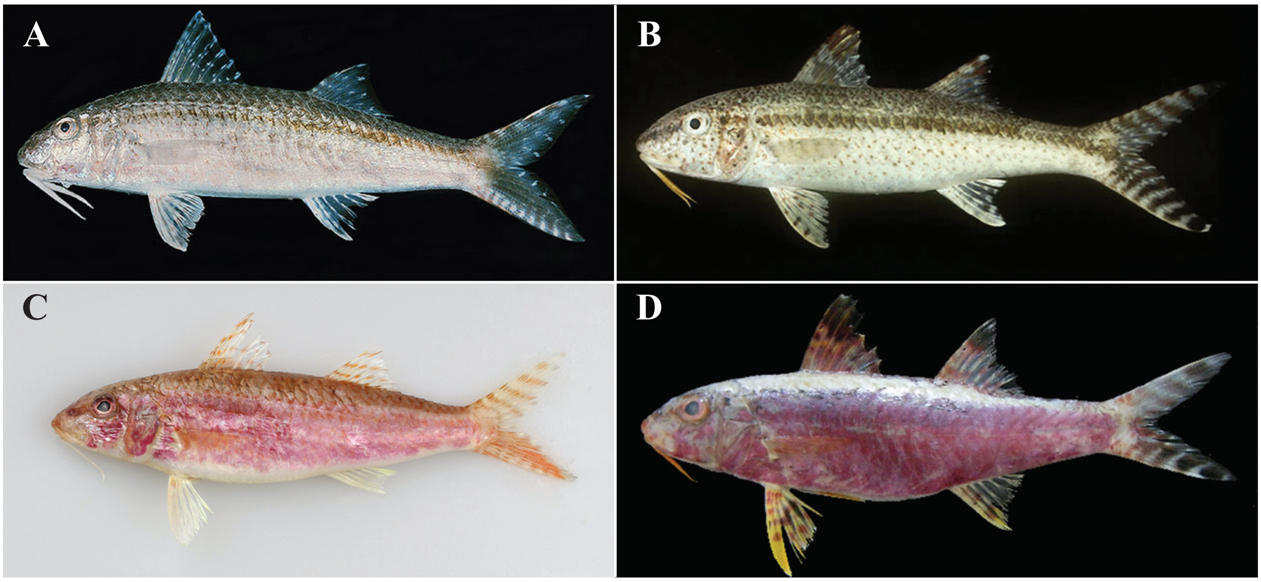

Figure 3. Comparison between *Upeneus pori* and *Upeneus tragula*. (**A**) *Upeneus pori*, fresh, 114 mm SL; (**B**) *Upeneus tragula*, fresh, 216 mm SL, (**C**) *Upeneus pori*, dead, 102 mm SL, GOU103678, this study; (**D**) *Upeneus tragula*, dead, 145.4 mm SL. Photos A and B by Randall JE (1997). Randall's tank photos. Collection of 10,000 large-format photos (slides) of dead fishes. Published in Froese and Pauly (2023). Photo D by Sahat Ratmuangkhwang; published in Froese and Pauly (2023).

Table 2. Presently reported (n = 6) morphometric measurements of *Upeneus pori* compared with the data of the paratypes in Ben-Tuvia and Golani (1989) (n = 22).

Character	*Upeneus pori*			
	Presently reported study		**Ben-Tuvia and Golani 1989**	
	Range	**Mean**	**Range**	**Mean**
SL [mm]	101.1–114.1	105	74–125	
	In % SL			
Body depth	24.4–26.4	25.2	21.8–25.9	23.9
Body width	14.3–17.2	15.8		
Head length	23.7–27.1	25.8	25.8–29.2	27.8
Snout length	7.4–10.0	8.3	9.7–12.1	10.9
Orbit diameter	5.4–6.7	6.3	6.4–8.5	7.2
Interorbital width	7.6–8.0	7.8	6.6–8.1	7.4
Upper jaw length	6.0–10.7	8.6		
Lower jaw length	5.4–9.1	7.6		
Predorsal length	29.8–35.2	32.6	32.0–38.2	35.6
Prepelvic length	27.7–29.3	28.8		
Preanal length	63.3–65.4	64.6		
Prepectoral length	25.9–29.9	27.5		
First dorsal-fin height	17.7–20.5	19.4	17.1–20.1	18.6
Second dorsal-fin height	13.5–16.8	15.1	13.0–16.9	15.1
Pectoral fin length	16.8–21.1	20.0	18.3–21.3	19.6
Pelvic fin length	13.8–18.2	17.4	16.5–20.5	18.3
Anal fin height	13.7–16.5	15.5	12.7–15.6	13.8
Caudal peduncle depth	9.9–10.9	10.2	9.4–11.1	10.0
Caudal peduncle length	21.0–25.2	23.1	21.9–27.8	25.6
Barbels length	16.7–18.1	17.2	15.3–20.1	17.1
Meristic counts				
Dorsal fin rays	VII, 9		VII, 9	
Anal fin rays	I-6–7		I-7	
Pectoral fin rays	14		14–15	
Lateral line scales	29–31		29–30	
Scales above lateral line	2			
Scales below lateral line	4–5			
Total developed gill rakers	3–5 + 13–14			
Total gill rakers	6–7 + 17–19		6–8 + 18–20	

SL = standard length.

Color. Mainly based on recently deceased specimens (Fig. 2A). Dorsally darkened, head and sides reddish-brown, belly whitish; mid-lateral body with faint brownish-red bar running from snout to base of caudal fin in fresh fish; barbels white or creamy white; first and second dorsal-fins with 3–4 sets of reddish-brown spots running horizontally; pectoral fins cream-colored to transparent; pelvic fins creamy-white and base of fins with several yellow marks; anal fin rays whitish with transparent membranes; upper lobe of caudal fin with 4–5 oblique reddish-brown stripes intersecting rays; middle part of lower lobe of caudal fin with wide reddish-brown band extending from base of caudal fin to tip of lower lobe; 3–4 red-brown stripes above wide band; 6–7 stripes with same color below wide band and all stripes approximately perpendicular to wide band; fluorescent yellow spots between stripes on both lobes of caudal fin, sometimes vague (Figs. 2C and 2D). The preserved specimens are dorsally dark-brown; all fins retain original spots, bars, or stripes; mid-lateral sides with faint dark grey bar (Fig. 2B).

Sequence analysis of the *COI* gene. The mean sequence of some mitochondrial cytochrome C oxidase (*COI*) genes, collected from fish specimens examined in the presently reported study, was 690 nucleotide sites. The base frequencies of A, C, T, and G of twenty *COI* sequences were 22.2%, 29.4%, 29.4%, and 19.0%, respectively and the A + T content (51.6%) was greater than the C + G content (48.4%). The intraspecific genetic distance ranged from 0% to 1.58% and the interspecific genetic distance ranged from 8.87% to 19.36% (Table 3). The interspecific genetic distance was much greater than the intraspecific genetic distance. According to the results of the maximum likelihood tree (Fig. 4), *Upeneus sulphureus*, *U. subvittatus*, *U. quadrilineatus*, *U. moluccensis*, *U. japonicus*, and *U. tragula* clustered and separated from *U. pori* with high bootstrap values and SH-aLRT values, respectively, indicating significant differentiation amongst them, of which the sequences in this study (GOU103676, GOU103678, GOU104100, and GOU104102) were clustered with the sequences (KM538630, LC572156, KY176690, and KF564319) distinguished as *U. pori* in the Red Sea area from GenBank with high SH-aLRT and ultrafast bootstrap values (97/99). The genetic distance (Table 4) shows that the *U. pori* collected in the South China Sea and the *U. pori* from the Red Sea belong to the species range.

Discussion

Upeneus pori was first reported in the Mediterranean by Kosswig (1950) as *U. tragula*. Then, Ben-Tuvia and Golani (1989) re-examined the specimens and suggested there was a new species of the genus *Upeneus* in the Red Sea and named the new one *Upeneus pori* in recognition of Professor Francis Dov Por's contribution to the field of the Lessepsian migration of organisms. Before this time, many scholars misidentified *U. pori* for other species of *Upeneus* (see Ben-Tuvia 1953, 1966; George and Athanassiou 1966, 1967). Although few resources of *U. pori* were investigated in the Chinese waters, we observed *U. pori* was often mingled with *U. tragula* for sale in the local fish markets. The reason for the above is that there is still a lack of systematic classification of *Upeneus* species in China. At the same time, some *Upeneus* species

Table 3. Interspecific (bottom half of matrix) and intraspecific (bold diagonal) sequence divergences of 7 species of *Upeneus*, corrected using the Kimura two-parameter (K2P) model.

	U. japonicus	*U. pori*	*U. tragula*	*U. sulphureus*	*U. subvittatus*	*U. quadrilineatus*	*U. moluccensis*
U. japonicus	**0.0039**						
U. pori	0.1328	**0.0000**					
U. tragula	0.1089	0.0950	**0.0000**				
U. sulphureus	0.1821	0.1751	0.1600	**0.0098**			
U. subvittatus	0.1936	0.1759	0.1686	0.1250	**0.0019**		
U. quadrilineatus	0.1645	0.1705	0.1555	0.1048	0.1072	**0.0000**	
U. moluccensis	0.1930	0.1675	0.1679	0.1285	0.0887	0.1012	**0.0158**

Table 4. Pairwise genetic distance calculated using the K2P model between the *COI* gene sequences of *Upeneus pori* from the South China Sea (this study) and the 12 sequences of different species of *Upeneus* from GenBank.

Group	Sequence	Group 1	2	3	4	5	6	7	8	9	10	11	12	13	14	15	16	17	18	19
1	GOU103676_*U. pori*_SCS																			
2	GOU103678_*U. pori*_SCS	0.0000																		
3	GOU104100_*U. pori*_SCS	0.0000	0.0000																	
4	GOU104102_*U. pori*_SCS	0.0000	0.0000	0.0000																
5	KM538630_*U. pori*_RS	0.0000	0.0000	0.0000	0.0000															
6	LC572156_*U. pori*_RS	0.0000	0.0000	0.0000	0.0000	0.0000														
7	KY176690_*U. pori*_RS	0.0000	0.0000	0.0000	0.0000	0.0000	0.0000													
8	KF564319_*U. pori*_RS	0.0000	0.0000	0.0000	0.0000	0.0000	0.0000	0.0000												
9	EF607609_*U. sulphureus*_SCS	0.1751	0.1751	0.1751	0.1751	0.1751	0.1751	0.1751	0.1751											
10	JN313348_*U. sulphureus*_IDOW	0.1751	0.1751	0.1751	0.1751	0.1751	0.1751	0.1751	0.1751	0.0098										
11	KY372338_*U. subvittatus*_SCS	0.1746	0.1746	0.1746	0.1746	0.1746	0.1746	0.1746	0.1746	0.1274	0.1250									
12	KY372339_*U. subvittatus*_SCS	0.1772	0.1772	0.1772	0.1772	0.1772	0.1772	0.1772	0.1772	0.1250	0.1226	0.0019								
13	GU674207_*U. quadrilineatus*_ IDOW	0.1705	0.1705	0.1705	0.1705	0.1705	0.1705	0.1705	0.1705	0.1037	0.1060	0.1084	0.1060							
14	GU674208_*U. quadrilineatus*_ IDOW	0.1705	0.1705	0.1705	0.1705	0.1705	0.1705	0.1705	0.1705	0.1037	0.1060	0.1084	0.1060	0.0000						
15	KC501840_*U. moluccensis*_ IDAW	0.1699	0.1699	0.1699	0.1699	0.1699	0.1699	0.1699	0.1699	0.1344	0.1222	0.0897	0.0920	0.1010	0.1010					
16	KT718279_*U. moluccensis*_SCS	0.1651	0.1651	0.1651	0.1651	0.1651	0.1651	0.1651	0.1651	0.1348	0.1226	0.0854	0.0876	0.1013	0.1013	0.0158				
17	KJ920110_*U. japonicus*_SCS	0.1303	0.1303	0.1303	0.1303	0.1303	0.1303	0.1303	0.1303	0.1742	0.1847	0.1922	0.1896	0.1620	0.1620	0.1927	0.1878			
18	JF952884_*U. japonicus*_JAW	0.1353	0.1353	0.1353	0.1353	0.1353	0.1353	0.1353	0.1353	0.1794	0.1900	0.1976	0.1949	0.1671	0.1671	0.1981	0.1932	0.0039		
19	KX887496_*U. tragula*_SCS	0.0951	0.0951	0.0951	0.0951	0.0951	0.0951	0.0951	0.0951	0.1625	0.1574	0.1699	0.1673	0.1555	0.1555	0.1677	0.1065	0.1682	0.1113	
20	EF607611_*U. tragula*_SCS	0.0951	0.0951	0.0951	0.0951	0.0951	0.0951	0.0951	0.0951	0.1625	0.1574	0.1699	0.1673	0.1555	0.1555	0.1677	0.1065	0.1682	0.1113	0.0000

SCS = South China Sea, RS = Red Sea, IDOW = Indonesian waters, IDAW = Indian waters, JAW = Japanese waters.

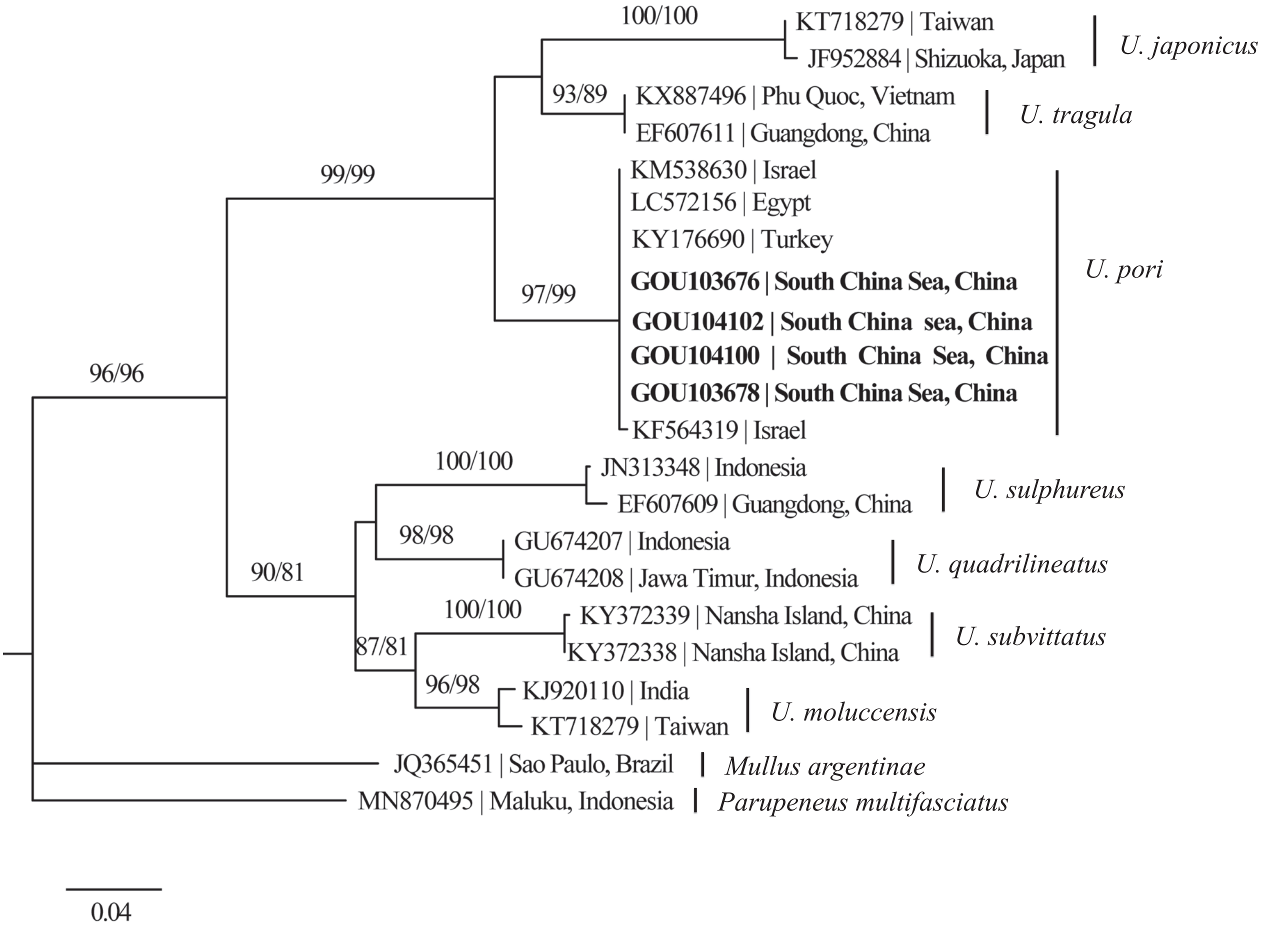

Figure 4. Maximum Likelihood phylogenetic tree of *Upeneus pori*, based on DNA sequences of the mitochondrial *COI* gene (bold fonts for sequences of this study, not bold for previous research). Numbers on the branches indicate the Shimodaira–Hasegawa-like approximate likelihood ratio test (SH-aLRT) and ultrafast bootstrap support (only values above 70% are displayed).

exhibit a similar body color after death (Figs. 3C and 3D), which can lead observers to believe it is the same fish. In addition, due to the lack of resources, it is highly likely to be ignored as another species and considered to be *U. tragula*. Here are different diagnoses between *U. pori* and *U. tragula* (Figs. 2A, 2C, and 2D; Figs. 3A and 3B; Table 5):

- barbels color: white or creamy-white vs. yellow barbels, but may be pale brown or orange in fresh fish;
- body pattern: without any spots or blotches vs. slightly darker above the lateral line, with irregular red, brown, or black spots and/or blotches;
- first dorsal-fin: seven spines, without blotch around tip, vs. eight spines, with a large blotch around tip;
- caudal-fin: different pattern shown in Uiblein and Heemstra (2010).

Table 5. Key features that distinguish *Upeneus pori* from *Upeneus tragula*.

Distinguishing key features	*Upeneus pori*	*Upeneus tragula*
Barbels color	Creamy-white	Yellow; pale brown/orange (fresh fish)
Body pattern	No spots or blotches	With irregular red, brown or black spots and/or blotches
First dorsal-fin	VII; no blotch around tip	VIII; with a blotch around tip

Uiblein and Heemstra (2010) established four taxonomic groups for separating morphologically similar species within the same group. They included 25 of the 26 species recorded in China, being separated in *japonicus* group, *tragula* group, *moluccensis* group, and *vittatus* group, which were distinguished by the differences in the number of spines in the first dorsal-fin, gill rakers, pectoral-fin rays, and stripes of the caudal-fin. *Upeneus pori* belonged to the *japonicus* group, as suggested by Uiblein and Heemstra (2010). New species and new records were gradually recorded, resulting in the taxonomic status of *Upeneus* being altered. The *vittatus* group was divided into the *stenopsis* group (Uiblein and Causse 2013) and the *suahelicus* group (Uiblein and Gouws 2015), causing *U. vittatus* to be ungrouped and the *vittatus* group to be cancelled. Uiblein et al. (2019) reported that *Upeneus margarethae* Uiblein et Heemstra, 2010; *Upeneus mouthami* Randall et Kulbicki, 2006; and *Upeneus randalli* Uiblein et Heemstra, 2011 differed from other *tragula* group species in the first dorsal-fin tip without dark pigmentation, total gill rakers 21–25 and 28–30 lateral-line scales so a new taxonomic group was proposed—the *margarethae* group. Uiblein and Maclaine (2021) proposed reclassifying *U. pori*, originally part of the *japonicus* group, into the newly established *pori* group. This reclassification is based on the limited distribution range exhibited by members of the *pori* group, as well as their shared coloration and morphological characteristics. These features distinguish them from other members of the *japonicus* group. As for Chinese records, they include the *margarethae* group (*U. heterospinus*), *japonicus* group (*U. japonicus*), *moluccensis* group (*U. moluccensis*, *U. quadrilineatus*, and *U. sulphureus*), *stenopsis* group (*U. subvittatus*), *tragula* group (*Upeneus sundaicus* (Bleeker, 1855), *U. luzonius*, and *U. tragula*), and ungrouped (*U. vittatus*). In this study, we have identified *U. pori*, a member of the *pori* group, which is recorded in China for the first time.

Conclusion

This study has a certain reference value for the taxonomy of the genus *Upeneus* in the coastal areas of China. For further research and an in-depth understanding of the taxonomy and phylogeny of *Upeneus* within China's regional distribution, it is necessary to collect sufficient samples in various Chinese waters and provide detailed morphological characteristics. Apart from morphology, molecular analysis enables us to collect more knowledge about the taxonomy and phylogeny of *Upeneus*, which also contributes to coastal ecosystem management measures and provides the basis for the protection of local species diversity.

The presently reported study confirms a new record of *Upeneus pori* from the South China Sea, based on morphological characteristics and DNA barcodes and this record expands the distributional range of *U. pori* in the world's oceans and enriches the species composition and biodiversity of the South China Sea. This study also emphasizes that it is essential to increase taxonomic studies to survey the South China Sea with its high species diversity to better protect species diversity and monitor marine fisheries in the South China Sea.

Acknowledgments

We gratefully acknowledge the funding support under the Guangdong Basic and Applied Basic Research Foundation, Grant/Award Number: [2019B1515120064]; Southern Marine Science and Engineering Guangdong Laboratory (Zhanjiang), Grant /Award Number: [ZJW-2019-08]; Science and Technology Plan Projects of Guangdong Province, China, Grant/Award Number: [2018B030320006].

References

Altschul SF, Gish W, Miller W, Myers EW, Lipman DJ (1990) Basic local alignment search tool. Journal of Molecular Biology 215(3): 403–410. https://doi.org/10.1016/S0022-2836(05)80360-2

Ben-Tuvia A (1953) Mediterranean fishes of Israel. Bulletin of the Sea Fisheries Research Station 8: 1–14.

Ben-Tuvia A (1966) Red Sea fishes recently found in the Mediterranean. Copeia 1966(2): 254–275. https://doi.org/10.2307/1441133

Ben-Tuvia A, Golani D (1989) A new species of goatfish (Mullidae) of the genus *Upeneus* from the Red Sea and the eastern Mediterranean. Israel Journal of Zoology 36: 103–112

Bos AR (2014) *Upeneus nigromarginatus*, a new species of goatfish (Perciformes: Mullidae) from the Philippines. Raffles Bulletin of Zoology 62: 750–758.

Chen D, Zhang M (2015) [Marine fishes of China.] China Ocean University Press, Qingdao, China, 2154 pp. [In Chinese]

Cheng Q, Wang C (1963) [Family Mullidae.] Pp. 341–345. In: Chu Y, Zhang C, Cheng Q (Eds) [Ichthyofauna of the East China Sea.] Science Press, Beijing, China. [In Chinese]

Cheng Q, Wang C, Tian M, Yang W, Sun B (1962) [Family Mullidae.] Pp. 548–563. In: Chu Y, Wang W, Zhang C, Zhang Y, Cheng Q, Wang C, Tian M, Yang W, Sun B, Zheng W, Yang D, Zheng B (Eds) [Fishes of the South China Sea.] Science Press, Beijing, China. [In Chinese]

Deidun A, Zava B, Insacco G, Foka M (2018) First record of the Por's goatfish *Upeneus pori* (Actinopterygii: Perciformes: Mullidae) from Italian waters (western Ionian Sea). Acta Ichthyologica et Piscatoria 48(1): 93–97. https://doi.org/10.3750/AIEP/02269

Fricke R, Eschmeyer WN, Van der Laan R (2023) Eschmeyer's catalog of fishes: Genera, species, references. California Academy of Sciences, San Francisco, CA, USA. [Accessed 15 August 2023] http://researcharchive.calacademy.org/research/ichthyology/catalog/fishcatmain.asp

Froese R, Pauly D (Eds) (2023) FishBase. [Version 06/2023] http://www.fishbase.org

George CJ, Athanassiou V (1966) Observations on *Upeneus asymmetricus* Lachner, 1954 in St. George Bay, Lebanon. Annali del Museo Civico di Storia Naturale di Genova 76: 68–74.

George CJ, Athanassiou V (1967) A two year study of the fishes appearing in the seine fishery of St. George Bay, Lebanon. Annali del Museo Civico di Storia Naturale di Genova 76: 37–294.

Guindon S, Dufayard JF, Lefort V, Anisimova M, Hordijk W, Gascuel O (2010) New algorithms and methods to estimate maximum-likelihood phylogenies: Assessing the performance of PhyML 3.0. Systematic Biology 59(3): 307–321. https://doi.org/10.1093/sysbio/syq010

Jiao Y, Chen DG (2000) [The diversity and distribution of goatfish (Mullidae) in Western Pacific.] Journal of Ocean University of China 30(1): 48–56. [In Chinese]

Kalyaanamoorthy S, Minh BQ, Wong TKF, von Haeseler A, Jermiin LS (2017) ModelFinder: Fast model selection for accurate phylogenetic estimates. Nature Methods 14(6): 587–589. https://doi.org/10.1038/nmeth.4285

Kosswig C (1950) Erythräische Fische im Mittelmeer und an der Grenze der Ägäis. Pp. 203–212. In: von Jordans A, Peus F (Eds.) Syllegomena Biologica. Festschrift zum 80. Geburtstage von Herrn Pastor Dr. Med. H.C. Otto Kleinschmidt, Lutherstadt Wittenberg am 13. Dezember 1950. Geest und Portig K.-G./A. Ziemsen Verlag: Leipzig und Wittenberg, Germany.

Lachner EA (1954) A revision of the goatfish genus *Upeneus* with descriptions of two new species. Proceedings of the United States National Museum 103(3330): 97–532. https://doi.org/10.5479/si.00963801.103-3330.497

Minh BQ, Nguyen MA, von Haeseler A (2013) Ultrafast approximation for phylogenetic bootstrap. Molecular Biology and Evolution 30(5): 1188–1195. https://doi.org/10.1093/molbev/mst024

Nash CM, Lungstrom LL, Hughes LC, Westneat MW (2022) Phylogenomics and body shape morphometrics reveal recent diversification in the goatfishes (Syngnatharia: Mullidae). Molecular Phylogenetics and Evolution 177: e107616. https://doi.org/10.1016/j.ympev.2022.107616

Nelson JS, Grande TC, Wilson VH (2016) Fishes of the world. 5th edn. John Wiley and Sons, Hoboken NJ, USA 386 pp. https://doi.org/10.1002/9781119174844

Nguyen LT, Schmidt HA, von Haeseler A, Minh BQ (2015) IQ-TREE: A fast and effective stochastic algorithm for estimating maximum-likelihood phylogenies. Molecular Biology and Evolution 32(1): 268–274. https://doi.org/10.1093/molbev/msu300

Nicolaidou A, Alongi G, Aydogan O, Catra M, Cavas L, Cevik C, Dosi A, Circosta V, Giakoumi S, Gimenez-Casalduero F, Filiz H, Izquierdo-Munoz A, Kalogirou S, Konstantinidis E, Kousteni V, Kout J, Legaki A, Megalofonou P, Ovalis P, Paolillo G, Paschos I, Perdikaris C, Poursanidis D, Ramos-Espla AA, Reizopoulou S, Sperone E, Taskin E, Tripepi S, Vazquez-Luis M (2012) New Mediterranean biodiversity records (June 2012). Mediterranean Marine Science 13(1): 162–174. https://doi.org/10.12681/mms.33

Randall JE (2001) FAO species identification guide for fishery purposes. The living marine resources of the Western Central Pacific, vol. 5. Bony fishes part 3 (Menidae to Pomacentridae). FAO, Rome, 3379 pp.

Shen SC (1993) [Fishes of Taiwan.] Department of Zoology, National Taiwan University, Taipei, 954 pp. [In Chinese]

Uiblein F, Causse R (2013) A new deep-water goatfish of the genus *Upeneus* (Mullidae) from Vanuatu, South Pacific. Zootaxa 3666(3): 337–344. https://doi.org/10.11646/zootaxa.3666.3.4

Uiblein F, Gledhill DC, Pavlov DA, Hoang TA, Shaheen S (2019) Three new goatfishes of the genus *Upeneus* (Mullidae) from the Indo-Pacific, with a redescription of colour patterns in *U. margarethae.* Zootaxa 4683(2): 151–196. https://doi.org/10.11646/zootaxa.4683.2.1

Uiblein F, Gledhill DC, Peristiwady T (2017) Two new goatfishes of the genus *Upeneus* (Mullidae) from Australia and Indonesia. Zootaxa 4318(2): 295–311. https://doi.org/10.11646/zootaxa.4318.2.4

Uiblein F, Gouws G (2014) A new goatfish species of the genus *Upeneus* (Mullidae) based on molecular and morphological screening and subsequent taxonomic analysis. Marine Biology Research 10(7): 655–681. https://doi.org/10.1080/17451000.2013.850515

Uiblein F, Gouws G (2015) Distinction and relatedness—Taxonomic and genetic studies reveal a new species group of goatfishes (*Upeneus*; Mullidae). Marine Biology Research 11(10): 1021–1042. https://doi.org/10.1080/17451000.2015.1064963

Uiblein F, Gouws G, Gledhill DC, Stone K (2016) Just off the beach: Intrageneric distinctiveness of the bandtail goatfish *Upeneus taeniopterus* (Mullidae) based on a comprehensive alpha-taxonomy and barcoding approach. Marine Biology Research 12(7): 675–694. https://doi.org/10.1080/17451000.2016.1190458

Uiblein F, Gouws G, Lisher M, Malauene BS (2020) *Upeneus floros*, a new goatfish from South Africa and Mozambique, with updated taxonomic accounts for *U. guttatus* and *U. pori* and a key to Western Indian Ocean *Upeneus* species (Mullidae). Zootaxa 4834(4): 523–555. https://doi.org/10.11646/zootaxa.4834.4.3

Uiblein F, Heemstra PC (2010) A taxonomic review of the western Indian Ocean goatfishes of the genus *Upeneus* (Family Mullidae), with descriptions of four new species. Smithiana Bulletin 11: 35–71.

Uiblein F, Lisher M (2013) A new goatfish of the genus *Upeneus* (Mullidae) from Angoche, northern Mozambique. Zootaxa 3717: 85–95. https://doi.org/10.11646/zootaxa.3717.1.7

Uiblein F, Maclaine J (2021) Description of *Upeneus madras* (Mullidae), a new goatfish species from SE India (NE Indian Ocean), with establishment of the pori-species group and a review of barbel colour in *Upeneus* species. Cybium 45(4): 283–296. https://doi.org/10.26028/cybium/2021-454-004

Uiblein F, Motomura H (2021) Three new goatfishes of the genus *Upeneus* from the eastern Indian Ocean and western Pacific, with an updated taxonomic account for *U. itoui* (Mullidae: *Japonicus*-species group). Zootaxa 4938(3): 298–324. https://doi.org/10.11646/zootaxa.4938.3.2

Uiblein F, White WT (2015) A new goatfish of the genus *Upeneus* (Mullidae) from Lombok, Indonesia and first verified record of *U. asymmetricus* for the Indian Ocean. Zootaxa 3980(1): 51–66. https://doi.org/10.11646/zootaxa.3980.1.3

Ward RD, Zemlak TS, Innes BH, Last PR, Hebert PD (2005) DNA barcoding Australia's fish species. Philosophical Transactions of the Royal Society of London. Series B, Biological Sciences 360(1462): 1847–1857. https://doi.org/10.1098/rstb.2005.1716

Yamashita M, Golani D, Motomura H (2011) A new species of *Upeneus* (Perciformes: Mullidae) from southern Japan. Zootaxa 3107(1): 47–58. https://doi.org/10.11646/zootaxa.3107.1.3

Zhang D, Gao F, Jakovlic I, Zou H, Zhang J, Li W, Wang G (2020) PhyloSuite: An integrated and scalable desktop platform for streamlined molecular sequence data management and evolutionary phylogenetics studies. Molecular Ecology Resources 20(1): 348–355. https://doi.org/10.1111/1755-0998.13096

Acta Ichthyologica et Piscatoria 53, 2023, 147–155 | DOI 10.3897/aiep.53.108918

PENSOFT.

ACTA ICHTHYOLOGICA ET PISCATORIA

Infection parameters of *Norileca indica* and a new record of *Ceratothoa carinata* (Crustacea: Isopoda: Cymothoidae) on *Selar crumenophthalmus* (Actinopterygii: Carangiformes: Carangidae) in the waters of the Sibuyan Sea, the Philippines

Sanny David P. LUMAYNO[1], Hannah Kathleen S. LABRADOR[1], Kyle Dominic E. BARNUEVO[1], Roxanne A. CABEBE-BARNUEVO[2], Rowena E. CADIZ[1], Ricardo P. BABARAN[2]

1 *Institute of Aquaculture, College of Fisheries and Ocean Sciences, University of the Philippines Visayas, Miagao, Iloilo, Philippines*

2 *Institute of Marine Fisheries and Oceanology, College of Fisheries and Ocean Sciences, University of the Philippines Visayas, Miagao, Iloilo, Philippines*

https://zoobank.org/F75E40AC-D8CC-4341-87C0-F041DAF953BD

Corresponding author: Sanny David P. Lumayno (splumayno@up.edu.ph)

Academic editor: Wojciech Piasecki ◆ **Received** 5 July 2023 ◆ **Accepted** 29 August 2023 ◆ **Published** 6 October 2023

Citation: Lumayno SDP, Labrador HKS, Barnuevo KDE, Cabebe-Barnuevo RA, Cadiz RE, Babaran RP (2023) Infection parameters of *Norileca indica* and a new record of *Ceratothoa carinata* (Crustacea: Isopoda: Cymothoidae) on *Selar crumenophthalmus* (Actinopterygii: Carangiformes: Carangidae) in the waters of the Sibuyan Sea, the Philippines. Acta Ichthyologica et Piscatoria 53: 147–155. https://doi.org/10.3897/aiep.53.108918

Abstract

Studies on cymothoid isopods as parasites affecting the marine fisheries and aquaculture industries are relatively scarce in the Philippines despite having detrimental impacts on their fish hosts. Parasitological examination on the bigeye scad, *Selar crumenophthalmus* (Bloch, 1793), a potential aquaculture species, in the waters of the Sibuyan Sea, Philippines was done on fish specimens collected on 21 April 2021. Out of the 88 specimens, a total of 13 big eye scads were infected with cymothoid isopod *Norileca indica* (Milne Edwards, 1840), found in the branchial cavities of the fish, resulting in a prevalence of 14.77%. A total of 20 individual isopods (13 females and seven males) were recovered, with a mean intensity of 1.53. Based on the morphological characteristics and as confirmed by the cytochrome oxidase subunit 1 (*CO1*) sequence, one host fish was also infected with *Ceratothoa carinata* (Bianconi, 1869). This appears to be the first record of *C. carinata* from the Philippines. To fully understand the implications of cymothoid parasites on the bigeye scad, further studies are recommended to account for the impacts of seasonality, reproductive stages of the host fish, and effects of abiotic factors such as water movement and depth.

Keywords

bigeye scad, carangid, *CO1*, cymothoid isopod, morphology, Panay Island, parasite infection

Introduction

The bigeye scad, *Selar crumenophthalmus* (Bloch, 1793), a potential aquaculture species, is one of the commercially important carangid fishes in the Philippines. According to the Philippine Statistics Authority (2023), the bigeye scad accounted for 6% (113 240 t) of the Philippines' overall marine fisheries production in 2022. Fishing gears such as purse seines, trawls, ring nets, drive-in nets, gill nets, hand lines, hoop nets, fish corrals, and bag nets, and even beach seines can be used to catch this species (Corpuz and Dalzell 1988). However, in the 1900s, unsustainable fishing methods caused the slow decrease of the majority of species around the world, including the bigeye scad populations (Dalzell and Peñaflor 1989; Dalzell et al. 1990). Overfishing and overexploitation have put further strain on the aquaculture industry to meet the continually expanding demand for fishery resources (Timi and Mackenzie 2015). Literature regarding the applications in aquaculture of the bigeye scad is very scarce and is only limited to rearing larvae and juveniles (Iwai et al. 1996; Welch et al. 2013; Elefante 2019). With the current advancement in aquaculture practices, the majority of systems now have access to hatchery-bred larvae, but this is not always the case. This leads some systems to rely on wild-caught fry or fish. High stocking density in the majority of aquaculture farms often leads to faster transmission of diseases and parasites from wild-caught stock that contaminates the culture system (Paperna 1987; Meyer 1991). The lack of appetite, slow growth, impaired reproduction, abnormalities in the body, a higher risk of bacterial or fungal infection in injuries caused by the parasite's attachment, and in severe cases, mortality, are only a few of the negative impacts brought on by these parasites (Meyer 1991; Smit et al. 2014).

Cymothoid isopods are parasitic in marine fishes and can infect the branchial cavity, buccal cavity, fins, and skin, or even penetrate the flesh of the host fish (Smit et al. 2014; Cruz-Lacierda and Nagasawa 2017; Aneesh et al. 2021a, 2021b). Two recorded bigeye scad parasites from the family Cymothoidae are *Norileca indica* (Milne Edwards, 1840) (see Ahmed and Khan 2012; Zubia et al. 2014; Cruz-Lacierda and Nagasawa 2017; Fafioye and Ayodele 2018) and *Ceratothoa carinata* (Bianconi, 1869) (see Martin et al. 2013; Hadfield et al. 2016). These parasites have been recorded in Australia, China, India, Indonesia, Mozambique, New Guinea, and Thailand (Martin et al. 2013; Hadfield et al. 2016; Anand Kumar et al. 2017; Seepana et al. 2021). In the Philippines, *N. indica* infecting bigeye scad was first recorded by Cruz-Lacierda and Nagasawa (2017) in the Panay Gulf and subsequently by Muji et al. (2021) in Batangas Bay. We are not aware of published reports of *C. carinata* collected within the country.

Due to the potential and economic significance of the bigeye scad in mariculture, it is essential to broaden the existing studies, particularly those on the effects of cymothoid infections in the Philippines. The study generally aimed to generate data on *N. indica* infections on the bigeye scad, caught in the Sibuyan Sea, Philippines. Specifically, the study assessed the prevalence and mean intensity of the *N. indica*. Incidentally, the study also documented the first record of *C. carinata* from the Philippines.

Materials and methods

Study area and sample collection. A total of 89 bigeye scad were purchased from commercial catches landed in two fish landing sites at northern Panay Island (Kalibo, Aklan and Tangalan, Aklan), Philippines in April 2021 (Fig. 1). Based on the reports of the fishers who operated the commercial fishing boats, these catches were fished using purse seines in the Sibuyan Sea. Fish samples were measured for total length (TL) to the nearest 1 mm, and

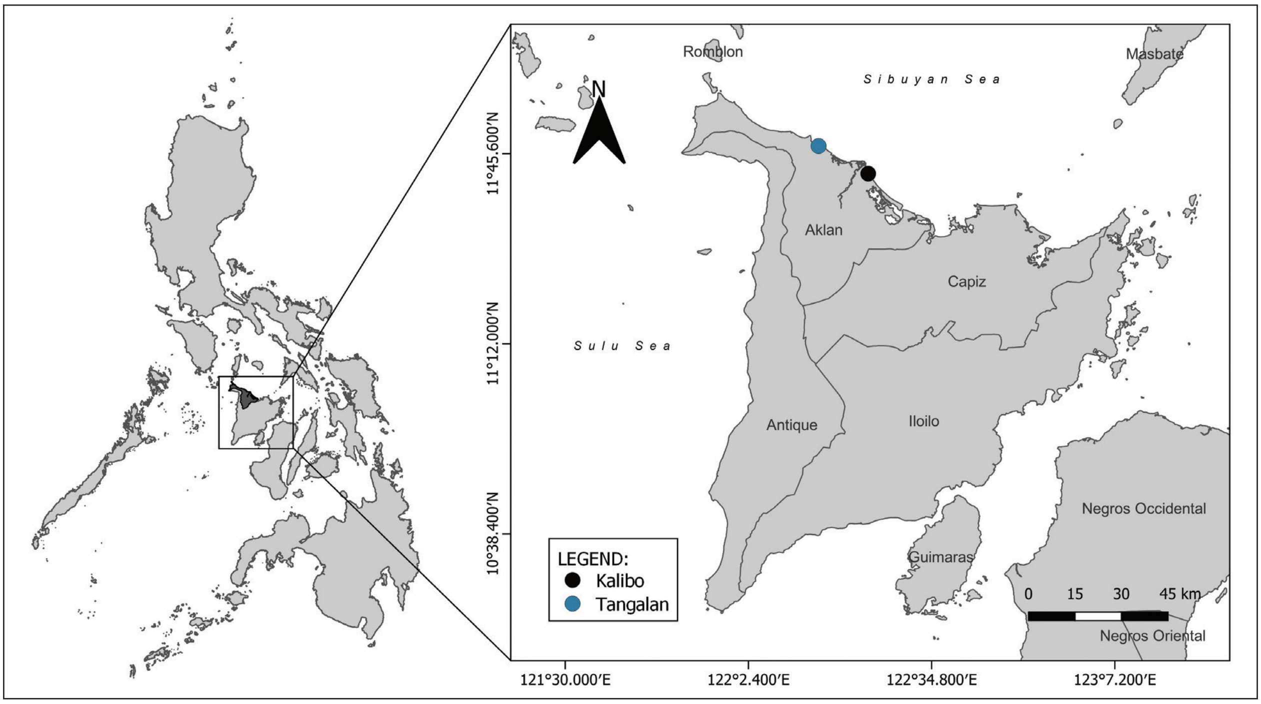

Figure 1. Map of commercial fish landing sites in northern Panay Island (Tangalan, Aklan and Kalibo, Aklan), Philippines. Fish samples were caught in the Sibuyan Sea, Philippines in April 2021.

body weight to the nearest 0.1 g. The fish samples were then examined externally, particularly in their branchial and buccal cavities for isopod parasites.

Each discovered isopod was extracted using fine forceps. Isopod samples were then measured for TL to the nearest 0.01 mm using a digital caliper, preserved in individual vials using absolute ethanol with a corresponding label, and kept in a –20°C freezer for further taxonomic and genetic identification. Morphological features included in the description were based on Martin et al. (2013), van der Wal et al. (2017), and Aneesh et al. (2022).

DNA barcoding. Genomic DNA was extracted from the appendages of females using the Wizard Genomic DNA Purification Kit (Promega) following the manufacturer's protocol. A targeted part of the mitochondrial cytochrome oxidase subunit 1 (*CO1*) gene of the specimen was amplified using the universal invertebrate primers 5′-GGTCAACAAATCATAAAGATATTGG-3′) and HC02198 (5′ TAAACTTCAGGGTGACCAAAAAATCA-3′) (Folmer et al. 1994). Pre-sequencing PCR was performed following the protocol of Aneesh et al. (2021c) with modifications. PCR reactions were performed with a total volume of 50 µL containing 25 µL of GoTaq G2 Colorless Master Mix (Promega), 2.5 µL of each 10 µM primer, 1 µL of 200 ng μL^{-1} DNA template, and 19 µL of nuclease-free water. The conditions were as follows: initial denaturation at 94°C for 5 min; followed by 35 cycles of 94°C denaturation for 30 s, annealing at 47°C for 50 s, and extension at 72°C for 2 min; and final extension of 72°C for 10 min. PCR was carried out in a T100 thermal cycler (Biorad Laboratories). The amplified 680 bp PCR products were sent to Macrogen (South Korea) for bidirectional sequencing.

The generated sequences were compared to available sequences in GenBank by BLAST (https://blast.ncbi.nlm.nih.gov/Blast.cgi). Sequences were aligned against published sequences of known cymothoid species retrieved from GenBank to determine their phylogenetic relations using the neighbor-joining method as implemented in MEGA 7 (Hall 2013). The resulting topology was assessed by bootstrapping with 1000 replications. The decapod *Penaeus merguiensis* De Man, 1888 was used as an outgroup. The sequences were also submitted to GenBank and were assigned the following accession numbers: OP808334, OP811246, and OP811247. Voucher specimens were deposited at the UPV Museum of Natural Sciences under accession numbers UPV MI 03831-03833.

Prevalence and mean intensity analyses. The prevalence and mean intensity of the isopod parasite were calculated based on Bush et al. (1997).

The prevalence is defined as the percentage of fish individuals infected with parasites of a given species related to the total number of fish examined, while the mean intensity specifies the total number of a certain parasite species per infected fish.

Results

Order Isopoda Latreille, 1817
Family Cymothoidae Leach, 1814
Genus *Norileca* Bruce, 1990

Norileca indica (Milne Edwards, 1840)

(Figs 2 and 3)

Livoneca indica.—Milne-Edwards 1840: 262.—Bleeker 1857: 21.—Schioedte and Meinert 1884: 362, pl. 15, figs 3–6.—Richardson 1910: 24.—Nierstrasz 1915: 99.—Nierstrasz 1931: 142.—Borcea 1933: 482.—Beumer et al. 1982: 33.

Lironeca indica.—Trilles 1976: 77, pl. 2, fig. 3.—Trilles 1979: 266.—Avdeev 1978: 281.—Rokicki 1982: 205, figs 1, 2.

Livoneca ornata.—Heller 1865: 145–146, pl.12, fig. 15.

Material examined. SC064 (ovigerous female): 20.75 mm TL, host *Selar crumenophthalmus*, Sibuyan Sea. SC064 (male): 12.26 mm TL, same data as preceding.

Additional material examined. Four ovigerous females with a size range of 14.72–25.44 mm TL and four males with a size range of 7.17–12.26 mm TL collected from the same host, *S. crumenophthalmus*, captured in the Sibuyan Sea. SC020 (female): 24.24 mm TL SC020 (male): 10.71 mm TL, SC030 (female): 23.34 mm TL, SC030 (male): 11.93 mm TL, SC050 (female): 25.44 mm TL, SC050 (male): 11.77 mm TL, SC086 (female): 14.72 mm TL, SC086 (male): 7.17 mm TL.

Morphological description of female. Body twisted; dorsal surface smooth and polished appearance; ventral area soft; narrowest body part at pereonite 1; widest

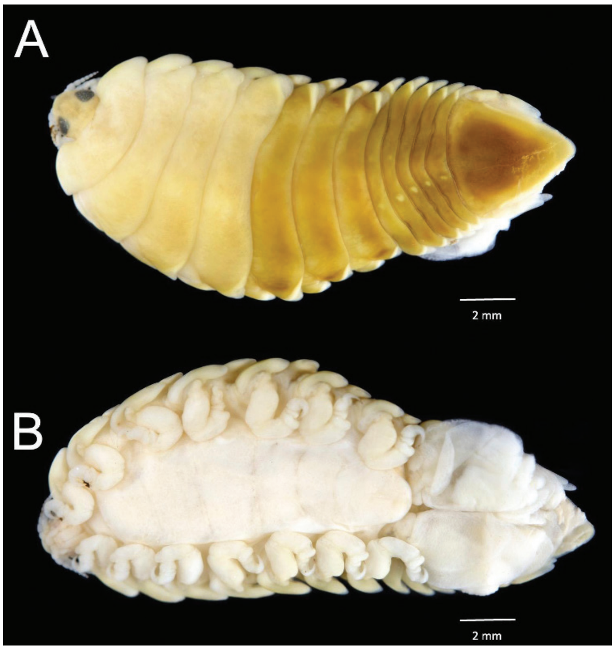

Figure 2. Ovigerous female (SC064) *Norileca indica* collected from the branchial cavity of *Selar crumenophthalmus* captured in the Sibuyan Sea, Philippines in April 2021 (**A** = dorsal view; **B** = ventral view).

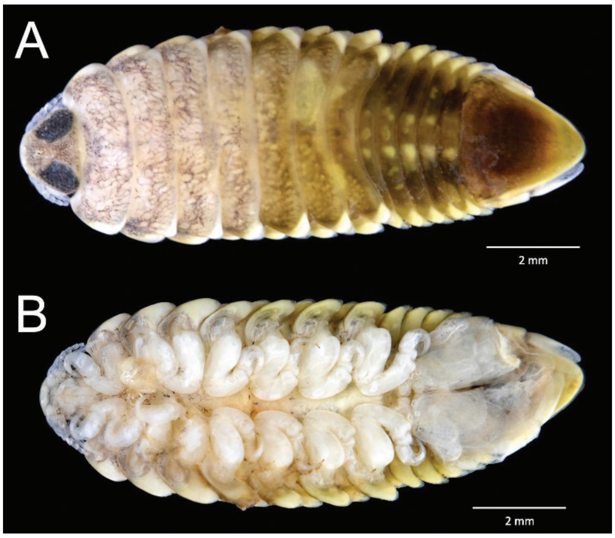

Figure 3. Male (SC064) *Norileca indica* collected from the branchial cavity of *Selar crumenophthalmus* captured in the Sibuyan Sea, Philippines in April 2021 (**A** = dorsal view; **B** = ventral view).

body part at pereonite 4. Cephalon: Triangular shape with rounded apex. Eyes: large and circular. Perionites: seven in total. Perionite 1: shortest in length. Perionites 6 and 7 narrower compared to perionites 1–5. Pleonites: narrow and positioned just behind perionite 7 overlapping with pleonite 2. Pleotelson: triangular and posteriorly pointed; dorsal surface smooth. Uropods: weak and short; visible on both sides of pleotelson in dorsal view; length not extending beyond pleotelson. Pereopods: seven pairs of soft-fleshed pereopods; pereopod 1 smallest; pereopods 2–7 gradually increasing in size. Color in preserved state: dorsal surface generally brown; anterior region light brown, transitioning to darker color towards posterior region; ventral area creamy white; pleotelson dark brown with light edges; uropods ranging from white to transparent; pereopods white.

Morphological description of male. Body size and shape: significantly smaller than females; body rather straight than twisted; dorsal surface smooth; ventral area predominantly covered with pereopods; narrowest body part at pereonite 1; widest body part at pereonite 5. Cephalon: triangular shape and rounded apex. Eyes: large and oval. Perionites: seven in total. Perionite 1 shortest. Perionites 1–4 with straight posterior margins. Perionites 5–7 with slightly concave posterior margins. Pleonites: narrow and positioned just behind perionite 7 overlapping with pleonite 1. Pleotelson: triangular and bluntly pointed; dorsal surface smooth. Uropods: weak; visible on both sides of pleotelson and nearly reaching apex of the pleotelson in dorsal view. Pereopods: seven pairs of soft-fleshed pereopods; pereopod 1 smallest; pereopods 2–4 approximately similar in size; pereopods 5–7 largest in size. Color in preserved state: dorsal surface pale brown with distinct black chromatophores; ventral area creamy white with brown coloration along edges; pleotelson dark brown with light brown edges; uropods ranging from white to transparent; pereopods white.

Order Isopoda Latreille, 1817
Family Cymothoidae Leach, 1814
Genus *Ceratothoa* Dana, 1852

Ceratothoa carinata (Bianconi, 1869)

(Fig. 4)

Cymothoa carinata.—Bianconi 1869: 210–211, pl. II, figs 2 (a–b).—Schioedte and Meinert 1883: 327–329, pl. XIII (Cym. XX) figs 1–2.—Trilles 1986: 623, tab. 1. Trilles 1994:—116–117.—Kensley 2001: 232.—Bruce 2007: 278.—Trilles 2008: 23.—Martin et al. 2013: 397–401, figs 1–3.—Nagasawa et al. 2014: 59–61, fig. 1.—Martin et al. 2015a: 266–267.

Cymothoa (*Ceratothoa*) *carinata*.—Hilgendorf 1879: 846.

Meinertia carinata.—Lanchester 1902: 378.—Stebbing 1910: 103–104.—Trilles 1972a: 1244–1245, 1256, pl. I, photos 5–7.—Trilles 1972b: 3–7, photos 1–4.—Avdeev 1979: 48, 50.

Codonophilus carinatus.—Nierstasz 1931: 132.

Ceratothoa curvicauda.—Nunomura 2006: 36–38, figs 12–13.

Ceratothoa sp. Saito 2009: 7–9, photos 1–2.

Material examined. SC005 (non-ovigerous female) extracted from the buccal cavity of the host fish: 20.30 mm TL, host *S. crumenophthalmus*, Sibuyan Sea.

Morphological description. Body shape rectangular, maintaining straight posture; longitudinal medial ridge along dorsal pereon surface present; widest part undetermined because of slight damaged of perionite 4 and 5; narrowest part observed at perionite 1. Cephalon: subtriangular in shape with rounded and broad apex. Eyes: circular, moderately small. Perionites: seven in total, becom-

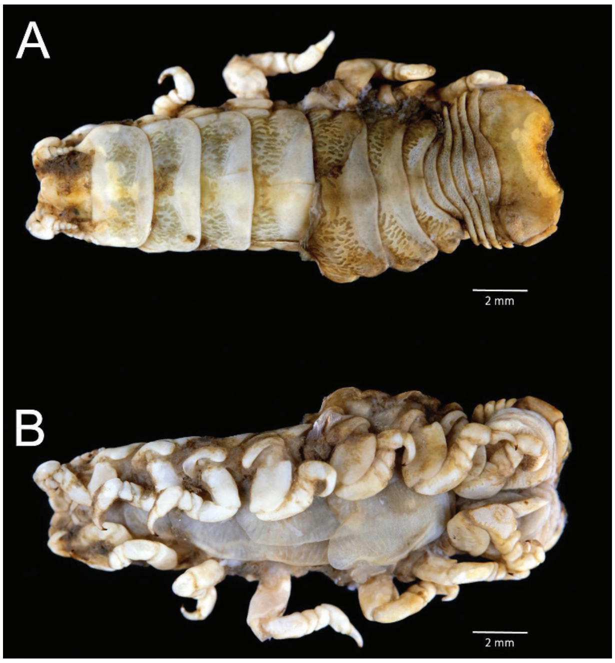

Figure 4. Non-ovigerous female (SC005) *Ceratothoa carinata* collected from the buccal cavity of *Selar crumenophthalmus* captured in the Sibuyan Sea, Philippines in April 2021 (**A** = dorsal view; **B** = ventral view).

ing narrower from perionites 5 to 7. Perionite 1: shortest; posterior margin straight; small conspicuous pointed structure extending to middle of eyes. Perionites 2–4: posterior margins straight. Perionites 5–6: posterior margins arched medially. Perionite 7: narrowest; posterior margin strongly curved medially. Pleonites: very narrow, positioned just behind perionite 7 extending to pleonite 1. Pleotelson: rather wide than long; dorsal surface with two sub-median depressions; posterior margins strongly concave. Uropods: weak; visible on both sides of pleotelson in dorsal view; similar in length to pleotelson. Pereopods: seven pairs of soft-fleshed pereopods. Pereopod 1: smallest. Pereopods 2–3: similar in size; slightly larger than previous. Pereopods 4–7: gradually increasing in size. Pereopods 5–7: largest. Color in preserved state: dorsal surface generally brown; anterior region white to brown, transitioning to darker color towards posterior region; ventral area light brown; pereopods white.

DNA barcoding. The morphological identification of the recovered parasites was confirmed by molecular analysis. Sequence analysis based on the mitochondrial *CO1* gene showed a high sequence similarity (more than 99%) of SC30 and SC064 to *N. indica*. The phylogenetic tree showing the relation of this study's specimens with other relevant cymothoid species is shown in Fig. 5. The resultant topology clearly indicates clustering of the presently reported specimens with *N. indica* KY849589.1 recovered from *S. crumenophthalmus* in the Andaman Islands, India (Praveenraj et al. 2019) and *N. indica* MF628260.1, MF628258.1, MF628259.1 from *S. crumenophthalmus* in Maputo Bay, Mozambique (van der Wal et al. 2017) supported by 99% bootstrap probability.

On the other hand, specimen SC005 showed greater than 98.00% sequence similarity with *C. carinata* confirming the morphological identification. To our knowledge, this is the first record of *C. carinata* in the Philippines. Phylogenetic analysis based on mitochondrial *CO1* genes also showed the clustering of the detected Isopoda with *C. carinata* LC724050.1, LC724049.1 recovered from *Decapterus maruadsi* (Temminck et Schlegel, 1843) in Sagami Bay, Kanagawa Japan (Fujita et al. 2023) and *C. carinata* MK652479.1 (Baillie et al. 2019) supported by 100% bootstrap probability (Fig. 5).

Prevalence and mean intensity of *Norileca indica*. In this study, 88 out of 89 bigeye scad specimens (as one fish contained *C. carinata*; specimen was not included in the analyses) of the bigeye scad collected during the month of April 2021 were examined, 13 individuals were found to have been infected with *N. indica*, leading to a prevalence of 14.77%. Of the 13 infected fish, 20 individual isopods (13 females and seven males) were extracted, resulting in a mean intensity of 1.53. All the female *N. indica* were extracted in the branchial cavities with their orientations mirroring the side of the branchial gill they attached to. Each male *N. indica* was seen along with the female isopod occupying the same gill holobranch on seven individuals of bigeye scad.

Discussion

In the presently reported study, we determined the presence of *N. indica* on the bigeye scad caught from the Sibuyan Sea in April 2021 for the first time. To date, there have only been two existing studies on the prevalence and mean intensity of *N. indica* on the bigeye scad from the Philippines. The mean intensity of *N. indica* infection in the bigeye scad

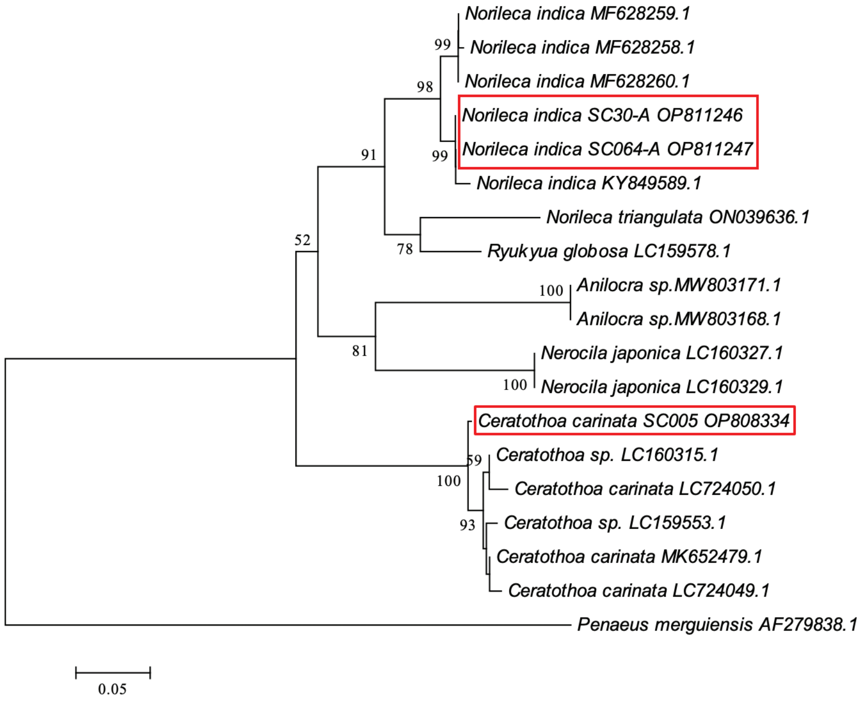

Figure 5. Neighbor-joining method used to estimate the phylogenetic relations among Cymothoidae based on mitochondrial *CO1* sequence. Bootstrap probabilities are indicated near the nodes. *Penaeus merguiensis* AF279838 was used as outgroup.

indicates the parasite load of an infected fish to be around one to two per host fish examined as also observed by Cruz-Lacierda and Nagasawa (2017) and Muji et al. (2021) in the Philippines. The presently reported study also recorded a prevalence of 14.8% which seems to be the lowest in comparison to the data recorded in the Panay Gulf (40.7%) and Batangas Bay (30%). When compared to the prevalence of *N. indica* in other southeast nations, the presently reported parameter is still quite low, especially when compared to India (Praveenraj et al. 2019; Purivirojkul and Songsuk 2020) and Thailand (Nagasawa and Petchsupa 2009) which recorded prevalence values of 21.46%–26.08% and 70%–100%, respectively. The low prevalence in this study might be due to the single sampling. Depending also on the month and year examined, parasite prevalence may vary (Cruz-Lacierda and Nagasawa 2017; Perdana et al. 2019; Jemi et al. 2020). Moreover, the prevalence of the parasite can also be attributed to the population and breeding season of the host fish (Jemi et al. 2020). Abiotic factors such as water movement and water depth may also contribute to the parasite prevalence variation (Rosa et al. 2021). To further understand the parasite–host relation in the Sibuyan Sea, monthly sampling and future studies on the bigeye scad population, reproductive biology, and analyses of associated abiotic variables are recommended.

Aside from *N. indica*, the presently reported study also collected a single specimen of another cymothoid parasite in the bigeye scad. The collected parasite was identified as *C. carinata* by its pleotelson which is rather wide than long with a concave posterior margin, subtriangular cephalon, and narrow pleonite. The identification was also confirmed by its *CO1* sequence. Similar to the report of Martin et al. (2013), no male parasites of this species were found. The hosts for this parasite have previously been identified as *S. crumenophthalmus* from Mozambique (Bianconi 1869; Hadfield et al. 2016) and Australia (Martin et al. 2013), *Decapterus macrosoma* Bleeker, 1851 from Japan (Nagasawa and Harada 2017) and India (Aneesh et al. 2022), *Decapterus maruadsi* from Japan (Nunomura 2006; Saito 2009; Nagasawa et al. 2014; Nagasawa and Harada 2016), *Decapterus maruadsi* (Temminck et Schlegel, 1844) from Japan (Nunomura 2006), *Pseudocaranx dentex* (Bloch et Schneider, 1801) from Japan (Nunomura 2006), and *Lutjanus adetii* (Castelnau, 1873) from New Caledonia (Trilles 1972a, 1972b; Martin et al. 2013). This study documents the first report of this cymothoid parasite from the Philippines.

Additionally, this study presents the first molecular characterization of cymothoid parasites infecting wild fish from the Philippine waters. DNA barcoding of *N. indica* and *C. carinata* using the sequence of the mitochondrial *CO1* gene generated a 680-bp amplicon which confirmed their morphological identification. Phylogenetic analysis of the sequences obtained in this study showed a close relation with *N. indica* isolates from India and Mozambique and *C. carinata* recovered in Japan. The use of DNA-based tools such as DNA barcoding in species identification is particularly helpful in the taxonomic studies of the family Cymothoidae as differentiating species under the family according to their morphological features appears to be challenging (Smit et al. 2014). Species identification based on the molecular structure offers multiple advantages over classical methods. However, to ensure the accuracy of the tool for future identifications, initial data on molecular characteristics submitted to public databases such as GenBank should be linked to a correctly identified specimen deposited in accessible repositories. Hence, this study utilized a combination of morphological and molecular identification methods to identify the cymothoid species recovered in *S. crumenophthalmus* from the Sibuyan Sea and to present a comprehensive initial data about the species in the region.

Conclusion

The presently reported study contributes to the limited data on parasites found in the bigeye scad from the Philippines, specifically *N. indica* and *C. carinata* as the first record of occurrence. Comprehensive studies are recommended to examine the physiological impacts of parasitism on bigeye scads at various life and reproductive stages, as well as in different seasons and fishing grounds throughout the country. Moreover, investigating mechanisms related to parasitism, host vulnerability, and immunity would be valuable, considering the potential of the bigeye scad as a species for aquaculture.

Acknowledgments

We gratefully acknowledge the research funding support of the Emerging Interdisciplinary Research (EIDR) Program from the Office of the Vice President for Academic Affairs (OVPAA), University of the Philippines (OVPAA-EIDR-C08-011-R) and the University of the Philippines Visayas Office of the Vice Chancellor for Research and Extension (SP20-13). We also thank the persons involved in the sample collection. We are also grateful to Christian C. Morales of the University of the Philippines Visayas Fisheries and Otolith Research Applications Laboratory of the College of Fisheries and Ocean Sciences for the map generation.

References

Ahmed F, Khan MA (2012) Ectoparasite, *Norileca indica* (Milne Edwards, 1840) (crustacean, Isopoda, Cymothoidae) from the mouth cavity and branchial chamber of *Rastrelliger kanagurta* (Cuv, 1817) from Karachi coast, Pakistan. International Journal of Biology and Biotechnology 9(1–2): 93–97.

Anand Kumar A, Rameshkumar G, Ravichandran S, Nagarajan R, Prabakaran K, Ramesh M (2017) Distribution of isopod parasites in commercially important marine fishes of the Miri coast, East Malaysia. Journal of Parasitic Diseases 41(1): 55–61. https://doi.org/10.1007/s12639-016-0749-6

Aneesh PT, Bruce NL, Kumar AB, Bincy MR, Sreenath TM (2021a) A taxonomic review of the buccal-attaching fish parasite genus *Lobothorax* Bleeker, 1857 (Crustacea: Isopoda: Cymothoidae) with description of a new species from southwestern India. Zoological Studies 60(13): 1–13. https://doi.org/10.6620/ZS.2021.60-13

Aneesh PT, Nashad M, Kumar AB, Bineesh KK, Hatha AAM (2021b) Review of the global distribution and hosts of the fish parasitic isopod genus *Renocila* Miers, 1880 (Crustacea: Cymothoidae) with the description of a new species from Andaman Islands, India. Journal of Natural History 55(43–44): 2761–2785. https://doi.org/10.1080/00222933.2021.2019341

Aneesh PT, Hadfield KA, Smit NJ, Kumar AB (2021c) Morphological description and molecular characterisation of a new species of *Anilocra* Leach, 1818 (Crustacea: Isopoda: Cymothoidae) from India. International Journal for Parasitology: Parasites and Wildlife 14: 321–328. https://doi.org/10.1016/j.ijppaw.2021.03.007

Aneesh PT, Helna AK, Kumar AB (2022) Redescription and further report of two buccal attaching fish parasitic cymothoids, *Ceratothoa carinata* (Bianconi, 1869) and *Cymothoa bychowskyi* Avdeev, 1979 (Crustacea: Isopoda) with a new record from the southern India Ocean. Journal of Natural History 56(17–20): 17–20, 1063–1089. https://doi.org/10.1080/00222933.2022.2099318

Avdeev VV (1978) Notes on the distribution of the marine Cymothoidae (Isopoda, Crustacea) in the Australian–New Zealand region. Folia Parasitologica 25(3): 281–283.

Avdeev VV (1979) Novye vidy roda *Cymothoa* (Isopoda, Cymothoidae) iz pribrežnyh rajonov severnoj i severno-zapadnoj Avstralii. New species of the genus *Cymothoa* (Isopoda, Cymothoidae) from the Indian Ocean. Parazitolgiâ 13(1): 50–55.

Baillie C, Welicky RL, Hadfield KA, Smit NJ, Mariani S, Beck RMD (2019) Hooked on you: Shape of attachment structures in cymothoid isopods reflects parasitic strategy. BMC Evolutionary Biology 19: e207 https://doi.org/10.1186/s12862-019-1533-x

Bellay S, De Oliveira EF, Almeida-Neto M, Mello MAR, Takemoto RM, Luque JL (2015) Ectoparasites and endoparasites of fish form networks with different structures. Parasitology 142(7): 901–909. https://doi.org/10.1017/S0031182015000128

Beumer JP, Ashburner LD, Burbury ME, Jette E, Latham DJ (1982) A checklist of the parasites of fishes from Australia and its adjacent Antarctic territories. Technical Communication No. 48. St Albans: Commonwealth Institute of Parasitology.

Bianconi G (1869) Specimina zoologica Mosambicana, Fasciculus XVII. Memorie dell'Acca- demia delle Scienze dell'Istituto di Bologna 9: 199–222.

Bleeker P. (1857) Recherches sur les Crustacés de L'Inde Archipelagique. II. Sur les Isopodes Cymothoadiens de L'Archipel Indien. Natuurkundige vereeniging in Nederlandsche-Indie, Batavia, Verhandelingen 2: 20–40. https://doi.org/10.5962/bhl.title.9908

Borcea I (1933) *Lironeca pontica* n. sp., parasites des Aloses et sardines de la Mer Noif. Bulletin du Muséum national d'histoire naturelle, 3e serie 5: 128–129.

Bruce NL (2007) Provisional list of the marine and freshwater isopods (Crustacea) of New Caledonia. Pp. 275–279. In: Payri CE, De Forges B (eds.) Compendium of marine species from New Caledonia. Documents scientifiques et techniques II7. Volume spécial. 2nd edn. IRD, Nouméa, France.

Bush AO, Lafferty KD, Lotz JM, Shostak AW (1997) Parasitology meets ecology on its own terms: Margolis et al. revisited. Journal of Parasitology 83(4): 575–583. https://doi.org/10.2307/3284227

Corpuz PV, Dalzell P (1988) A summary of the catch, fishing effort data and species composition collected by the DA/BFAR-ICLARM Small Pelagics Management Project. Department of Agriculture, Bureau of Fisheries and Aquatic Resources and International Center for Living Aquatic Resources Management, Manila, Philippines, 124 pp. https://hdl.handle.net/20.500.12348/3293

Cruz-Lacierda ER, Nagasawa K (2017) First record of *Norileca indica* (Isopoda, Cymothoidae) parasitic on *Selar crumenophthalmus* and *Decapterus kurroides* (Perciformes, Carangidae) in the Philippines. Comparative Parasitology 84(1): 60–63. https://doi.org/10.1654/1525-2647-84.1.60

Dalzell P, Peñaflor G (1989) The fisheries biology of the big-eye scad *Selar crumenophthalmus* (Bloch) in the Philippines. Asian Fisheries Science 3(1): 115–131. https://doi.org/10.33997/j.afs.1989.3.1.008

Dalzell P, Corpuz P, Arce F, Ganaden R (1990) Philippine small pelagic fisheries and their management. Aquaculture Research 21(1): 77–94. https://doi.org/10.1111/j.1365-2109.1990.tb00384.x

Elefante DJ (2019) Evaluation of larval culture methods for three marine finfish, *Monodactylus sebae*, *Lagodon rhomboides*, and *Selar crumenophthalmus*. Master's Thesis. University of Florida.

Fafioye O, Ayodele (2018) Length–weight relationship and condition factor of four fish species from Wasai Reservoir in Kano, Nigeria. Examines in Marine Biology and Oceanography 2(2): 227–230. https://doi.org/10.31031/EIMBO.2018.02.000543

Folmer O, Black M, Hoeh W, Lutz R, Vrijenhoek R (1994) DNA primers for amplification of mitochondrial cytochrome c oxidase subunit I from diverse metazoan invertebrates. Molecular Marine Biology and Biotechnology 3(5): 294–299.

Fujita H, Kawai K, Deville D, Umino T (2023) Quatrefoil light traps for free-swimming stages of cymothoid parasitic isopods and seasonal variation in their species compositions in the Seto Inland Sea, Japan. International Journal for Parasitology: Parasites and Wildlife 20: 12–19. https://doi.org/10.1016/j.ijppaw.2022.12.002

Hadfield KA, Bruce NL, Smit NJ (2016) Redescription of poorly known species of *Ceratothoa dana*, 1852 (Crustacea, Isopoda, Cymothoidae), based on original type material. ZooKeys 592: 39–91. https://doi.org/10.3897/zookeys.592.8098

Hall B (2013) Building phylogenetic trees from molecular data with MEGA. Molecular Biology and Evolution 30(5): 1229–1235. https://doi.org/10.1093/molbev/mst012

Heller C (1865) Crustaceen. Pp. 1–280. In: Reise der Österreichischen Fregatte Novara um die Erdre, in den Jahren 1857, 1858, 1859 unter den Befehlen des Commodore B. von Wüllerstorf-Urbair, Zoologischer Theil. Zweiter Band. III Abtheilung. Kaiserlich-Königlichen Hof- und Staatsdruckerei, Wien. https://doi.org/10.5962/bhl.title.1597

Hilgendorf F (1879) Die von Hrn. W. Peters in Moçambique gesammelten Crustaceen. Monatsbericht de Königlich Preussischen Akademie der Wissenschaften zu Berlin (Sitzung der Physikalisch-mathematischen Klasse) 1878: 782–851.

Iwai T Jr, Tamaru C, Yasukochi L, Alexander S, Yoshimura R, Mitsuyasu M (1996) Natural spawning of captive bigeye scad *Selar crumenophthalmus* in Hawaii. Journal of the World Aquaculture Society 27(3): 332–339. https://doi.org/10.1111/j.1749-7345.1996.tb00616.x

Jemi JN, Hatha AAM, Radhakrishnan CK (2020) Seasonal variation of the prevalence of cymothoid isopod *Norileca indica* (Crustacea, Isopoda), parasitizing on the host fish *Rastrelliger kanagurta* collected from the southwest coast of India. Journal of Parasitic Diseases 44(2): 314–318. https://doi.org/10.1007/s12639-020-01208-6

Kensley B (2001) Biogeography of the marine Isopoda of the Indian Ocean, with a checklist of species and records. Pp. 205–264. In: Kensley B, Brusca RC (eds.) Isopod systematics and evolution. Crustacean Issues 13. A.A. Balkema, Rotterdam/Brookfield.

Lanchester WF (1902) 3. On the Crustacea collected during the "Skeat expedition" to the Malay Peninsula. Part 2. Anomura, Cirripedia and Isopoda. Proceedings of the Zoological Society of London 1902: 363–381.

Martin MB, Bruce NL, Nowak BF (2013) Redescription of *Ceratothoa carinata* (Bianconi, 1869) and *Ceratothoa oxyrrhynchaena* Koelbel, 1878 (Crustacea: Isopoda: Cymothoidae), buccal-attaching fish parasites new to Australia. Zootaxa 3683(4): 395–410. https://doi.org/10.11646/zootaxa.3683.4.4

Meyer FP (1991) Aquaculture disease and health management. Journal of Animal Science 69(10): 4201–4208. https://doi.org/10.2527/1991.69104201x

Milne-Edwards H (1840) Histoire naturelle des crustacés: comprenent l'anatomie, la physiologie et la classification de ces animaux. Tome troisième. Roret, Paris. https://doi.org/10.5962/bhl.title.16170

Muji TFS, Sorreta JR, Ragaza JA (2021) Prevalence of Cymothoidae (Isopoda) infestation in bigeye scad (*Selar crumenophthalmus*) from Batangas, Philippines. IOP Conference Series. Earth and Environmental Science 934(1): 012081. https://doi.org/10.1088/1755-1315/934/1/012081

Nagasawa K, Harada S (2016) *Ceratothoa carinata* (Isopoda: Cymothoidae) from Japanese scad *Decapterus maruadsi* in coastal waters of the western North Pacific off central-western Japan. Biogeography 18: 67–70.

Nagasawa K, Harada S (2017) Shortfin scad, *Decapterus macrosoma*, a new host record for *Ceratothoa carinata* (Isopoda: Cymothoidae). Biogeography 19: 153–155. https://doi.org/10.11358/biogeo.19.153

Nagasawa K, Petchsupa N (2009) *Norileca indica* (Isopoda, Cymothoidae) parasitic on bigeye scad *Selar crumenophthalmus* in Thailand. Biogeography 11: 131–133.

Nagasawa K, Fukuda Y, Nishiyama M (2014) Further record of *Ceratothoa carinata* (Isopoda: Cymothoidae) parasitic on *Decapterus maruadsi* in Japanese waters. Biogeography 16: 59–61.

Nierstrasz HF (1915) VI.—Die Isopoden-Sammlung im Naturhistorischen Reichsmuseum zu Leiden — 1. Cymothoidae. Zoologische mededelingen 1: 71–108.

Nierstrasz HF (1931) Isopoda genuina. II. Flabellifera. Pp 123–233. In: Weber M, de Beaufort LF (eds.) Die Isopoden der Siboga-Expedition Siboga Expeditie (Uitkomsten op Zoölogisch, Botanisch, Oceanographisch en Geologisch Gebied verzameld in de Oost-Indische 1899–1900 aan boord HM Siboga onder commando van Luitenant ter Zee 1e kl. G.F. Tydeman). Brill, Leiden.

Nunomura N (2006) Marine isopod crustaceans in the Sagami Sea, central Japan. Memoirs of the National Science Museum 41: 1–42.

Paperna I (1987) Solving parasite-related problems in cultured marine fish. International Journal for Parasitology 17(2): 327–336. https://doi.org/10.1016/0020-7519(87)90107-X

Perdana A, Batubara A, Nur F, Aprilla R (2019) Population dynamics of sumbo fish *Selar crumenophthalmus* (Pisces: Carangidae) in Banda Aceh waters, Aceh, Indonesia. IOP Conference Series. Earth and Environmental Science 348: e012016. https://doi.org/10.1088/1755-1315/348/1/012016

Philippine Statistics Authority (2023) Selected Statistics on Agriculture and Fisheries 2018-2022. [Accessed 22 September 2023] https://psa.gov.ph/system/files/main-publication/1-%28ons-cleared%29-Publication%20on%20SSAF-signed_0.pdf?fbclid=IwAR0AocVhjFK9YVJLI8DFDeihIpq4PnzqUIXU45fAe-r7DXgO-uiPJNrborE

Praveenraj J, Saravanan K, Kumar PP, Kiruba-Sankar R, Roy SD (2019) Occurrence, prevalence and molecular characterization of *Norileca indica* (Milne Edwards, 1840) (Isopoda: Cymothoidae) on bigeyescad *Selar crumenophthalmus* (Bloch) from Andaman Islands India. Indian Journal of Geo-Marine Sciences 48(04): 452–456.

Purivirojkul W, Songsuk A (2020) New records of fish parasitic isopods (Crustacea: Isopoda) from the Gulf of Thailand. Animals 10(12): 2298. https://doi.org/10.3390/ani10122298

Richardson H (1910) Marine isopods collected in the Philippines by the U.S. Fisheries steamer Albatross in 1907–1908. Bureau of Fisheries Document no. 736. Department of Commerce and Labor, Bureau of Fisheries, Washington, DC. https://doi.org/10.5962/bhl.title.82673

Rokicki J (1982) *Lironeca indica* Edwards, 1840 (Crustacea, Isopoda) from *Selar crumenophthalmus* (Bloch). Wiadomości Parazytologiczne 28: 205–206.

Rosa FDAS, Baillie C, Medeiros TDN, Ready JS (2021) Habitat and host associations of the fish-burrowing parasite *Artystone minima* (Cymothoidae: Isopoda) in eastern Amazonia Biotropica 53(1): 307–316. https://doi.org/10.1111/btp.12876

Saito N (2009) [Note on a cymothoid isopod parasitic in the buccal cavity of the round scad, *Decapterus maruadsi* (Temminck et Schlegel, 1844).] Cancer 18: 7–9. [In Japanese]

Seepana R, Nigam NK, Musaliyarakam N, Chandrakasan S (2021) Occurrence of ectoparasitic isopod *Norileca indica* (H. Milne Edwards, 1840) on bigeye scad *Selar crumenophthalmus* (Bloch, 1793) from Great Nicobar Island, India. Journal of Parasitic Diseases 45(2): 306–312. https://doi.org/10.1007/s12639-020-01330-5

Schioedte JC, Meinert F (1883) Symbolæ ad monographium Cymothoarum crustaceorum familiæ. III. Saophridæ. IV. Ceratothoinæ. Naturhistorisk Tidsskrift, Kjøbenhavn 13: 281–378.

Smit NJ, Bruce NL, Hadfield KA (2014) Global diversity of fish parasitic isopod crustaceans of the family Cymothoidae. International Journal for Parasitology: Parasites and Wildlife 3(2): 188–297. https://doi.org/10.1016/j.ijppaw.2014.03.004

Stebbing TRR (1910) No. VI.—Isopoda from the Indian Ocean and British East Africa. Transactions of the Linnean Society of London. 2nd series Zoology 14: 83–122. [Reports of the Percy Sladen trust expedition to the Indian Ocean under the leadership of Mr J. Stanley Gardiner M.A. Volume 3.] https://doi.org/10.1111/j.1096-3642.1910.tb00525.x

Timi JT, Mackenzie K (2015) Parasites in fisheries and mariculture. Parasitology 142(1): 1–4. https://doi.org/10.1017/S0031182014001188

Trilles J-P (1972a) Les Cymothoidae (Isopoda, Flabellifera) du Muséum national d'Histoire naturelle de Paris. Étude critique accompagnée de précisions en particulier sur la répartition géographique et l'écologie des différentes espèces représentées. I. Les Ceratothoinae Schioedte et Meinert, 1883. Bulletin du Muséum national d'histoire naturelle, 3e Série Zoologie 70: 1231–1268.

Trilles J-P (1972b) Sur quatre isopodes cymothoïdes du Pacifique (Nouvelle Calédonie). Cahiers de l'Office de la Recherche Scientifique et Technique Outre-Mer, série Océanographique 10(1): 3–17.

Trilles J-P (1976) Les Cymothoidae (Isopoda, Flabellifera) des collections du Muséum national d'Histoire naturelle de Paris. IV. Les Lironecinae Schioedte et Meinert, 1884. Bulletin du Muséum national d'histoire naturelle, 3e serie, Zoologie 390: 773–800.

Trilles J-P (1979) Les Cymothoidae (Isopoda, Flabellifera; parasites de poissons) du Rijksmuseum van Natuurlijke Historie te Leiden II. Afrique, Amérique et régions Indo-Ouest-Pacifiques. Zoologische Mededelingen 54: 245–275.

Trilles J-P (1986) Les Cymothoidae (Crustacea, Isopoda, Flabellifera) d'Afrique. Bulletin du Muséum National d'Histoire Naturelle 8: 617–636. https://doi.org/10.5962/p.326714

Trilles JP (1994) Les Cymothoidae (Crustacea, Isopoda) du Monde. Prodrome pour une faune. Studia Marina 21–22: 1–288.

Trilles J-P (2008) Some marine isopods from the Senckenberg Research Instiure (Frankfurt am Main, Germany) (Crustacea, Isopoda: Cymothoidae, Aegidae, Corallanidae, Cirolanidae). Senckenbergiana Biologica 88: 21–28.

van der Wal S, Smit NJ, Hadfield KA (2017) Redescription and molecular characterisation of the fish parasitic isopod *Norileca indica* (Milne Edwards, 1840)(Crustacea: Isopoda: Cymothoidae) with a key to the genus. African Zoology 52(3): 163–175. https://doi.org/10.1080/15627020.2017.1382389

Welch A, Hoenig R, Stieglitz J, Daugherty Z, Sardenberg B, Miralao S, Farkas D, Benetti D (2013) Growth rates of larval and juvenile bigeye scad *Selar crumenophthalmus* in captivity. SpringerPlus 2(1): e634. https://doi.org/10.1186/2193-1801-2-634

Zubia M, Muhammad S, Omer M, Lakht-e-Zehra, So A (2014) Length–weight relationship, condition and relative condition factor of four mugilid species (Family Mugildae) from the Karachi coast of Pakistan. Journal of Coastal Development 17(1): 385.

Acta Ichthyologica et Piscatoria 53, 2023, 157–162 | DOI 10.3897/aiep.53.111525

PENSOFT.

ACTA
ICHTHYOLOGICA
ET PISCATORIA

First record of two fish species (Actinopterygii) in the Sukhyi Lyman, northwestern Black Sea, Ukraine

Serhii KHUTORNOI[1], Mikhail O. SON[1], Yuriy KVACH[1]

1 *Institute of Marine Biology, National Academy of Sciences of Ukraine, Odesa, Ukraine*

https://zoobank.org/CC623535-18FB-4F07-8B6C-97947217884F

Corresponding author: Yuriy Kvach (yuriy.kvach@gmail.com)

Academic editor: Jan Kotusz ♦ **Received** 27 August 2023 ♦ **Accepted** 22 September 2023 ♦ **Published** 12 October 2023

Citation: Khutornoi S, Son MO, Kvach Y (2023) First record of two fish species (Actinopterygii) in the Sukhyi Lyman, northwestern Black Sea, Ukraine. Acta Ichthyologica et Piscatoria 53: 157–162. https://doi.org/10.3897/aiep.53.111525

Abstract

Two new fish species were recorded while monitoring the fish fauna of Sukhyi Lyman (or Sukhyi Estuary), an estuary in the northwestern Black Sea (Ukraine) close to the marine port of Chornomorsk. A single pumpkinseed, *Lepomis gibbosus* (Linnaeus, 1758), was observed in May 1999, followed by numerous observations in May 2021, while a single peacock blenny, *Salaria pavo* (Risso, 1810), was photographed during snorkeling observations in September 2021. The estuary is a known hub for invasive alien species and other neobionts due to the presence of the marine port. The new population of pumpkinseed, a North American invasive species, in the estuary represents the next stage in the species' ongoing expansion along the Ukrainian Black Sea coast. Likewise, the appearance of the peacock blenny represents the latest stage in the "Mediterranization" of the Black Sea, a process that has been ongoing over the last several thousand years.

Keywords

Blenniidae, Centrarchidae, ichthyofauna, invasive alien species, *Lepomis gibbosus*, Mediterranean species, new records, range extension, *Salaria pavo*

Introduction

Alien species often represent a large fraction of the species in aquatic ecosystems, with fish overrepresented among such aquatic invaders (Strayer 2010). Such biological invasions have the potential to cause ecological changes negatively affecting both biodiversity and ecosystem state (Bax et al. 2003; Chan and Briski 2017). Many of these aquatic species have been introduced either accidentally, alongside commercial stocks, or in shipping ballast water (Panov et al. 2009).

Natural range extension is one of the main mechanisms controlling evolutionary diversification and maintenance of biodiversity (Parmesan and Yohe 2003). Historically, such processes were naturally controlled (e.g., by climatic or physical barriers); hence, long-distance expansion for many aquatic species usually took a very long time (Alexandrov et al. 2007; Polačik et al. 2008). In the modern period, however, human-mediated dispersal, e.g., by attachment to vessel bottoms or transport in ballast waters or tank sediments (Ricciardi 2006; Hänfling et al. 2011; Gruszka et al. 2013; Cupak et al. 2014; Ojaveer et al. 2002, 2017), has played an important role in the geographic spread of numerous aquatic invasive species (Lodge et al. 2016; Bullock et al. 2018).

In Ukraine, the list of non-indigenous fish fauna consists of 27 species (Kvach and Kutsokon 2017). Note that this does not include the so-called neolimnetic group or Mediterranean species, which are not considered non-indigenous to Ukraine as the border between their native and expanded ranges remains unclear (Kvach and Kutsokon 2017). The Sukhyi Lyman (or Sukhyi Estuary), an open water body situated in the northwestern Black Sea, was originally an estuary established by the interfluence of two rivers, the Dalnyk and Akkarzhanka (Starushenko and Bushuyev 2001). When the Port of Chornomorsk was built in 1957, the estuary was connected to the sea via a 14-m deep navigation canal. At present, the water body is classified as an anthropogenically transformed landform, with its lower part established as a sea bay with the middle and upper parts now oligohaline (Starushenko and Bushuyev 2001; Zaitsev et al. 2006). The salinity of the lower part ranges between 14‰ and 16‰, which is almost equal to that in the adjacent sea.

Recent studies have confirmed up to 58 fish species in the Sukhyi Lyman (Vinogradov and Khutornoy 2013), thanks in large part to the wide range of habitats in the estuary watershed. The presence of the seaport, however, acts as a potential hub for invasive species and, consequently, the waters of the Sukhyi Lyman have been regularly monitored for any change in the local fish fauna since the early 2000s. Here, we present new data on the discovery of two new fish species in the Sukhyi Lyman watershed.

Materials and methods

Fish fauna monitoring at Sukhyi Lyman has taken place regularly over the last two decades. At the same time, data is gathered on bottom-dwelling fauna via snorkeling observations. The snorkeling observations take place at a depth of 0.4 m at a site (46.332944ºN, 30.661555ºE) in the lower part of the estuary. The fish individuals are photographed under natural lighting using an Olympus digital camera. When possible, the fish were caught by a hand with a dipnet. In addition, the catches of both anglers and commercial fishers have been examined in the upper part of the estuary (46.392579ºN, 30.632233ºE) since 2019. A total of 15 fish individuals from the commercial catches were measured: the standard (SL, mm) and total (TL, mm) lengths were indicated. The standard deviation was calculated for mean parameters. Species are identified using the keys provided in Zander (1986) and Movchan (2011), with the taxonomic position, scientific name, and vernacular names provided by FishBase (Froese and Pauly 2023). The water salinity in the estuary was measured in the Hydrochemical Laboratory of the Institute of Marine Biology of the National Academy of Sciences (NAS) of Ukraine.

Results

In May 1999, a single pumpkinseed, *Lepomis gibbosus* (Linnaeus, 1758) (Centrarchiformes: Centrarchidae), was observed in the lower part of the estuary (46.332944ºN, 30.661555ºE) during snorkeling observations and caught by a dipnet. The individual was identified as a male (SL = 62 mm, TL = 75 mm). The salinity at the site was 17‰–18‰ (see Fig. 1). By May 2021, numerous observations were being recorded in angling and fisheries catches in the upper part of the estuary (46.392579ºN, 30.632233ºE), where the salinity was 2.2‰–3.0‰ (Fig. 2). The fish SL varied within 98–143 mm (129.6 ± 12.4 mm), while its

Figure 1. Map of the study area. Red circles are the sampling sites. The salinity parameters (*S*, ‰) are marked for the lower, central, and upper parts of the estuary.

TL within 119–170 mm (152.3 ± 13.6 mm). In September 2021, a single peacock blenny, *Salaria pavo* (Risso, 1810) (Blenniiformes: Blenniidae), was photographed in mussel beds on the rocky bottom of the lower part of the estuary (46.332944ºN, 30.661555ºE) during snorkeling observations. The fish was easily identifiable due to the presence of a high leather crest on the top of the head, which extended from the edge of the eyes to the origin of the dorsal fin (Fig. 3). The individual was identified as a mature male (by well-developed leather crest), but the exact size of the individual could not be identified on photographs.

Discussion

Our data confirm the presence of two new species, the pumpkinseed and peacock blenny, in the Sukhyi Lyman. The pumpkinseed is a North American freshwater centrarchid, currently classified as an invasive alien species of European Union Concern (European Commission 2019). Its presence in Ukrainian waters suggests either range extension through introduction as a "hitchhiker", either with commercially important fishes or through natural spread via coastal waters (Diripasko et al. 2008; Afanasyev et al. 2017; Kvach and Kutsokon 2017). The subsequent catching of multiple fish in the upper part of the estuary confirms the presence of an established population in the water body. Consequently, its original finding in the lower part of the Sukhyi Lyman was most likely an individual spreading from the upper part to the sea.

Nine blennid species (Actinopterygii: Blenniidae) have previously been confirmed in Ukrainian Black Sea waters (Movchan 2011). The peacock blenny, a Mediterranean marine species (Zander 1986), is rarely recorded in the northwestern Black Sea, having only previously been recorded near Cape Tarkhankut and Snake Island (Boltachev and Karpova 2017; Snigirov et al. 2012, 2020). Consequently, our discovery in the Sukhyi Lyman is just the third confirmed case of this species in the northwestern Black Sea. Our finding likely represents an example of the ongoing expansion of Atlanto–Mediterranean blennids into the northwestern Black Sea. The first examples of this expan-

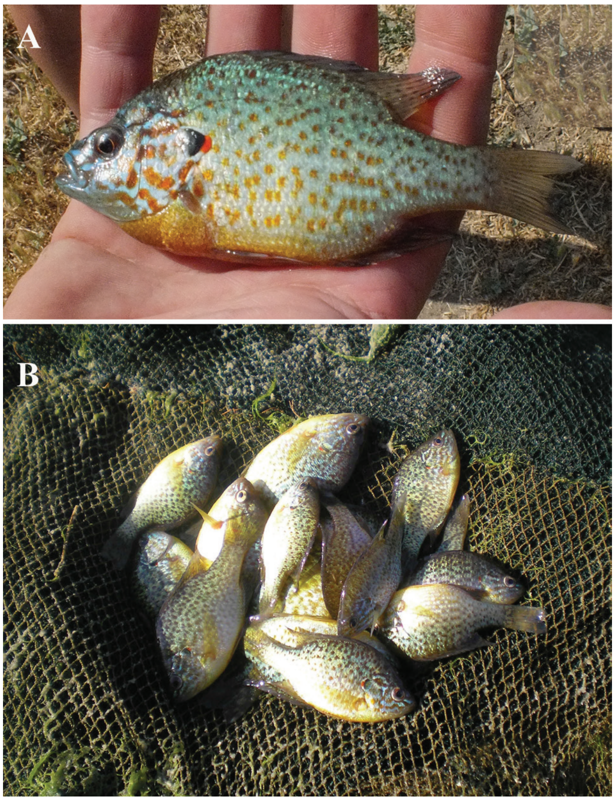

Figure 2. Pumpkinseed (*Lepomis gibbosus*) caught in the Sukhyi Lyman. (**A**) An individual caught while snorkeling (Photo: M. Son); (**B**) Individuals caught with a net by commercial fishers (Photo: Y. Kvach).

Figure 3. Male peacock blenny (*Salaria pavo*) observed by a scuba diver in the Sukhyi Lyman, with views from different angles (Photo: M. Son).

sion were recorded in 1998, when two new blenniid species were recorded in the Gulf of Odessa, i.e., the sphinx blenny, *Aidablennius sphynx* (Valenciennes, 1836), and Zvonimir's blenny, *Parablennius zvonimiri* (Kolombatovic, 1892) (see Khutornoy 1998). In 2019, Montagu's blenny, *Coryphoblennius galerita* (Linnaeus, 1758), was also recorded in the same region (Khutornoy and Kvach 2019).

The presence of the freshwater species, the pumpkinseed (*L. gibbosus*) in the mesohaline estuary is non-typical for this species, but this is not its first record in the brackish waters. Thus, the sporadic findings of this species are known from the Gulf of Odessa (the salinity of 16‰–17‰), gulfs of Yahorlyk and Tendra (up to 18‰) (Shcherbukha 1982; Tkachenko and Khutornoy 2001). The juveniles of this fish are characterized by relatively high tolerance to the natural marine water (Venâncio et al. 2019). The other fish species discovered, the peacock blenny (*S. pavo*), is a typical marine species inhabiting mainly intertidal rocky shores of the Mediterranean Sea and cannot be considered a typical estuarine fish (Steinitz 1954; Fishelson 1963). Nevertheless, this fish species is rather tolerant to the low salinity, which probably originates from its euryhaline ancestors (Plaut 1998).

As one of the largest seaports in the Black Sea, located within a large urban agglomeration, and the focus of both recreational fishing and commercial aquaculture, the Sukhyi Lyman is a high-risk area for biological pollution. Severe fragmentation of the estuary by dams and embayments, as well as its natural morphology, has resulted in the formation of many semi-isolated areas with different hydrological conditions. As a result, many alien species with diverse ecological preferences, including fully marine species, estuarine brackish water species, freshwater species and oligohaline Ponto–Caspian relicts, have become established and/or invasive (Zaitsev et al. 2006; Son 2007, 2008; Krasnovyd et al. 2012; Vinogradov and Khutornoy 2013; Son et al. 2013, 2020; Zhulidov et al. 2021). This diversity in habitat conditions also provides a diversity of invasive species pathways, with marine routes, whether by shipping or naturally through the channel connecting the estuary to the sea, being the most important. Passage through the channel is typical for the many mollusk, worm, and crustacean species now established (Zaitsev et al. 2006; Son et al. 2013; Zhulidov et al. 2021); however, fish stocking in the estuary's desalinated areas and incidental introduction of alien 'hitchhikers' alongside these stocked fish has also had an important impact (Kvach and Kutsokon 2017; Son et al. 2020). Finally, exotic and Ponto–Caspian mollusks have been introduced into small tributaries and the upper parts of the Sukhyi Lyman through natural dispersal, possibly with the additional help of migratory waterfowl (Son 2007, 2008). The most recent invasion registered since 2018–2020 is the now established population of the East Asian river prawn, *Macrobrachium nipponense* (De Haan, 1849) (see Bushuiev et al. 2023), while the Mediterranean Bucchich's goby, *Gobius bucchichi* Steindachner, 1870, is an example of the previous inadvertent introduction of a new component into the fish fauna of the estuary (Khutornoy unpublished[*]).

According to the standardized classification provided in the Convention on Biological Diversity[**] (Harrower et al. 2017), introduction pathways for non-native species include fishery in the wild (§ 1.3), contaminant on animals (excluding parasites and species transported by host and vector) (§ 3.4), ship/boat ballast water (§ 4.8), ship/boat hull fouling (§ 4.9), interconnected waterways/basins/seas (§ 5.1) and natural dispersal across borders of invasive alien species that have been introduced through pathways 1 to 5 (§ 6.1). Recent findings of non-native fishes in the northwestern Black Sea have been related to a number of these pathways, with the Chameleon goby, *Tridentiger trigonocephalus* (Gill, 1859), population near the Crimean coast, for example, being confirmed as the result of aquaria releases (Kvach and Kutsokon 2017), while two other species, the pumpkinseed and the Chinese sleeper, *Perccottus glenii* (Dybowski, 1877), were originally introduced due to human activity, but then spread naturally along river courses and eventually along the sea coast (Afanasyev et al. 2017; Kvach et al. 2021, 2022). Our finding of pumpkinseed in the Sukhyi Lyman, therefore, represents a continuation of the spread of this invasive alien species in waterbodies of southern Ukraine.

The second group of neobiota in the northwestern Black Sea are the Mediterranean and Atlanto–Mediterranid species, which have now spread into the northern Black Sea region (Kvach and Kutsokon 2017). This process, commonly termed Mediterranization, began in the early Pleistocene, either during the Earlier Würm or Main Würm interstadial seven to 12 thousand years ago (Slastenenko 1956; Flint 1957; Miller 1965; Zaitsev 1998). The previous findings of Bucchich's goby (*G. bucchichi*) and the chestnut goby, *Chromogobius quadrivittatus* (Steindachner, 1863), the latter near the coast north of Sukhyi Lyman (Vinogradov and Khutornoy 2013), were most likely a result of this process. Our discovery of a peacock blenny in the estuary represents further evidence of this ongoing process in the northwestern Black Sea. Note, however, that the presence of large ports in the region has no doubt supported the natural process of Mediterranization by transporting neobionts via ship/boat ballast water and/or hull fouling.

Acknowledgments

We thank Ruslana Migas (Institute of Marine Biology, National Academy of Sciences of Ukraine) for her help with map preparation. We also thank Dr Kevin Roche for his help in the English proofreading.

---

[*] Khutornoy SO (2021) Struktura pribereznih îhtîocenozîv pîvnîčno-zahîdnoï častini Čornogo morâ. [The structure of the offshore ichthyocenoses of the northwestern Black Sea.] PhD Thesis. Institute of Marine Biology of the NAS of Ukraine, Odesa. [In Ukrainian with English summary]

[**] https://www.cbd.int/

References

Afanasyev SA, Gupalo YA, Manturova OV (2017) Distribution and peculiarities of biology of the pumpkinseed *Lepomis gibbosus* (Perciformes: Centrarchidae) in the water bodies of Kyiv City. Hydrobiological Journal 53(3): 14–25. https://doi.org/10.1615/HydrobJ.v53.i3.20

Alexandrov B, Boltachev A, Kharchenko T, Lyashenko A, Son M, Tsarenko P, Zhukinsky V (2007) Trends of aquatic alien species invasions in Ukraine. Aquatic Invasions 2(3): 215–242. https://doi.org/10.3391/ai.2007.2.3.8

Bax N, Williamson A, Aguero M, Gonzalez E, Geeves W (2003) Marine invasive alien species: A threat to global biodiversity. Marine Policy 27(4): 313–323. https://doi.org/10.1016/S0308-597X(03)00041-1

Boltachev A, Karpova E (2017) Morskie ryby Krymskogo poluostrova. [Marine fishes of the Crimean Peninsula.] 2nd edn. Biznes-Inform, Simferopol, 367 pp. [In Russian]

Bullock JM, Bonte D, Pufal G, Carvalho CS, Chapman DS, Garcia C, Garcia D, Matthysen E, Delgado MM (2018) Human-mediated dispersal and the rewriting of spatial networks. Trends in Ecology and Evolution 33(12): 958–970. https://doi.org/10.1016/j.tree.2018.09.008

Bushuiev S, Snigirov S, Son M, Sokolov I, Kharlov G, Kvach Y (2023) Expansion of the alien East Asian river prawn *Macrobrachium nipponense* (De Haan, 1849) in southwestern Ukraine and assessment of its commercial usage prospects. Aquatic Invasions 18(2): 231–246. https://doi.org/10.3391/ai.2023.18.2.104092

Chan FT, Briski E (2017) An overview of recent research in marine biological invasions. Marine Biology 164(6): 121. https://doi.org/10.1007/s00227-017-3155-4

Cupak J, Hałupka M, Gruszka P (2014) Porastanie kadłubów małych statków jako sposób rozprzestrzeniania się makrozoobentosu. Ship hull fouling as a means of makrozoobenthos dispersal. Inżynieria Ekologiczna 37: 72–79. [In Polish]

Diripasko OA, Demchenko NA, Kulik PV, Zabroda TA (2008) Rasširenie areala solnečnogo okunâ, *Lepomis gibbosus* (Centrarchidae, Perciformes), na vostok Ukrainy. [An expansion of the pumpkinseed, *Lepomis gibbosus* (Centrarchidae, Perciformes), area of distribution into the east of Ukraine.] Vestnik Zoologii 42(3): 269–273. [In Russian with English summary]

European Commission (2019) Commission implementing regulation (EU) 2019/1262 of 25 July 2019 amending Implementing Regulation (EU) 2016/1141 to update the list of invasive alien species of Union concern. Official Journal of the European Union, L 199: 1–4.

Fishelson L (1963) Observations on littoral fishes of Israel I. Behaviour of *Blennius pavo* Risso (Teleostei, Blenniida). Israel Journal of Zoology 12(1–4): 67–80.

Flint RF (1957) Glacial and Pleistocene geology. John Wiley and Sons, New York, 553 pp.

Froese R, Pauly D (Eds) (2023) FishBase. [Version 06/2023] https://www.fishbase.org

Gruszka P, Rokicka-Praxmajer J, Cupak J, Radziejewska T, Wolska M (2013) Unintended "biological cargo" of ships entering the River Odra estuary: Assemblages of organisms in ballast tanks. Scientific Journals of Maritime University of Szczecin 33(105): 22–29.

Hänfling B, Edwards F, Gherardi F (2011) Invasive nonindigenous Crustacea: Dispersal, establishment, impact and control. BioControl 56(4): 573–595. https://doi.org/10.1007/s10526-011-9380-8

Harrower CA, Scalera R, Pagad S, Schönrogge K, Roy HE (2017) Guidance for interpretation of CBD categories on introduction pathways. Technical note prepared by IUCN for the European Commission. https://www.cbd.int/doc/c/9d85/3bc5/d640f059d03acd717602cd76/sbstta-22-inf-09-en.pdf

Khutornoy SA (1998) Ryby pribrežnyh akvatorij g. Odessy. [Fishes of the coastal waters of the City of Odesa.] Naučnye Trudy Zoologičeskogo muzeâ Odesskogo gosudarstvennogo universiteta 3: 42–45. [In Russian]

Khutornoy S, Kvach Y (2019) First record of the Montague's blenny (*Coryphoblennius galerita* (L., 1758) (Actinopterygii: Blenniidae) in the mesohaline waters of the North-Western Black Sea, Ukraine. BioInvasions Records 8(4): 917–923. https://doi.org/10.3391/bir.2019.8.4.20

Krasnovyd V, Kvach Y, Drobiniak O (2012) The parasite fauna of the gobiid fish (Actinopterygii: Gobiidae) in the Sukhyi Lyman, Black Sea. Vestnik Zoologii 46(6): 483–490.

Kvach Y, Kutsokon Y (2017) The non-indigenous fishes in the fauna of Ukraine: A potentia ad actum. BioInvasions Records 6(3): 269–279. https://doi.org/10.3391/bir.2017.6.3.13

Kvach Y, Karavanskyi Y, Tkachenko P, Zamorov V (2021) First record of the invasive Chinese sleeper, *Perccottus glenii* Dybowski, 1877 (Gobiiformes: Odontobutidae) in the Black Sea. BioInvasions Records 10(2): 411–418. https://doi.org/10.3391/bir.2021.10.2.19

Kvach Y, Kutsokon Y, Demchenko V, Yuryshynets V, Kudryashov S, Abramiuk I (2022) Post-invasion spread of Chinese sleeper (*Perccottus glenii*) in the Lower Danube drainage (Budjak region of Ukraine). BioInvasions Records 11(2): 547–559. https://doi.org/10.3391/bir.2022.11.2.27

Lodge DM, Simonin PW, Burgiel SW, Keller RP, Bossenbroek JM, Jerde CL, Kramer AM, Rutherford ES, Barnes MA, Wittmann ME, Chadderton WL, Apriesnig JL, Beletsky D, Cooke RM, Drake JM, Egan SP, Finnoff DC, Gantz CA, Grey EK, Hoff MH, Howeth JG, Jensen RA, Larson ER, Mandrak NE, Mason DM, Martinez FA, Newcomb TJ, Rothlisberger JD, Tucke AJ, Warziniack TW, Zhang H (2016) Risk analysis and bioeconomics of invasive species to inform policy and management. Annual Review of Environment and Resources 41(1): 453–488. https://doi.org/10.1146/annurev-environ-110615-085532

Miller PJ (1965) *Relictogobius kryzhanovskii* and the penetration of Mediterranean gobies into the Black Sea. Nature 208(5009): 474–475. https://doi.org/10.1038/208474a0

Movchan YV (2011) Ribi Ukraïni. [Fishes of Ukraine.] Zoloti Vorota, Kyiv, 444 pp. [In Ukrainian]

Ojaveer H, Leppäkoski E, Olenin S, Ricciardi A (2002) Ecological impacts of Ponto–Caspian invaders in the Baltic Sea. European inland waters and the Great Lakes: an inter-ecosystem comparison. Pp. 412–425. In: Leppäkoski E, Golasch S (Eds.) Invasive aquatic species of Europe: distribution, impacts and management. Kluwer Scientific Publishers, Dorthrecht. https://doi.org/10.1007/978-94-015-9956-6_41

Ojaveer H, Olenin S, Narscius A, Florin AB, Ezhova E, Gollasch S, Jensen KR, Lehtiniemi M, Minchin D, Normant-Saremba M, Strake S (2017) Dynamics of biological invasions and pathways over time: A case study of a temperate coastal sea. Biological Invasions 19(3): 799–813. https://doi.org/10.1007/s10530-016-1316-x

Panov VE, Alexandrov B, Arbačiauskas K, Binimelis R, Copp GH, Grabowski M, Lucy F, Leuven RSEW, Nehring S, Paunović M, Semenchenko V, Son MO (2009) Assessing the risks of aquatic species invasions via European inland waterways: From concepts to environmental indicators. Integrated Environmental Assessment and Management 5(1): 110–126. https://doi.org/10.1897/IEAM_2008-034.1

Parmesan C, Yohe G (2003) A globally coherent fingerprint of climate change impacts across natural systems. Nature 421(6918): 37–42. https://doi.org/10.1038/nature01286

Plaut I (1998) Comparison of salinity tolerance and osmoregulation in two closely related species of blennies from different habitats. Fish Physiology and Biochemistry 19(2): 181–188. https://doi.org/10.1023/A:1007798712727

Polačik M, Janáč M, Trichkova T, Vassilev M, Keckeis H, Jurajda P (2008) The distribution and abundance of the *Neogobius* fishes in their native range (Bulgaria) with notes on the non-native range in the Danube River. River Systems 18(1–2): 193–208. https://doi.org/10.1127/lr/18/2008/193

Ricciardi A (2006) Patterns of invasion in the Laurentian Great Lakes in relation to changes in vector activity. Diversity and Distributions 12(4): 425–433. https://doi.org/10.1111/j.1366-9516.2006.00262.x

Shcherbukha AY (1982) Fauna Ukraïni. [Fauna of Ukraine.] Volume 8, Issue 4. Naukova Dumka, Kyiv, 384 pp. [In Ukrainian]

Slastenenko E (1956) Karadeniz havzasi baliklari. [The fishes of the Black Sea basin.] EBK Yayini, Istanbul, 711 pp. [In Turkish with English summary]

Snigirov S, Goncharov O, Sylantyev S (2012) The fish community in Zmiinyi Island waters: Structure and determinants. Marine Biodiversity 42(2): 225–239. https://doi.org/10.1007/s12526-012-0109-4

Snigirov SM, Zamorov VV, Karavanskyi YV, Pitsyk VZ, Kurakin OP, Abakumov OM, Liumkis PV, Snigirov PM, Morozov YV, Kvach YV, Kutsokon YK (2020) Taksonomîčna ta ekologo-faunîstična harakteristika sučasnoï îhtîofauni Odeskoï zatoki, Dnîstrovskogo peredgirlovogo uzmor'â î priberežnih vod o. Zmîïnij. [Taxonomic and eco-faunistic features of the nowadays fish fauna of the Gulf of Odesa, the Dniester mouth forefront near-shores and coastal waters of the Snake (Zmiinyi) Island.] Odesa National University Herald Biology 25(2): 113–139. https://doi.org/10.18524/2077-1746.2020.2(47).218060 [In Ukrainian with English summary]

Son MO (2007) Native range of the zebra mussel and quagga mussel and new data on their invasions within the Ponto–Caspian region. Aquatic Invasions 2(3): 174–184. https://doi.org/10.3391/ai.2007.2.3.4

Son MO (2008) Rapid expansion of the New Zealand mud snail *Potamopyrgus antipodarum* (Gray, 1843) in the Azov–Black Sea region. Aquatic Invasions 3(3): 335–340. https://doi.org/10.3391/ai.2008.3.3.9

Son MO, Novitsky RA, Dyadichko VG (2013) Recent state and mechanisms of invasions of exotic decapods in Ukrainian rivers. Vestnik Zoologii 47(1): e45–e50.

Son MO, Morhun H, Novitskyi RO, Sidorovskyi S, Kulyk M, Utevsky S (2020) Occurrence of two exotic decapods, *Macrobrachium nipponense* (de Haan, 1849) and *Procambarus virginalis* Lyko, 2017, in Ukrainian waters. Knowledge and Management of Aquatic Ecosystems 421(421): 40. https://doi.org/10.1051/kmae/2020032

Starushenko LI, Bushuyev SG (2001) Pričernomorskie limany Odeŝiny i ih rybohozâjstvennoe značenie. [Black Sea estuaries and lagoons of the Odessa region and their fisheries importance.] Astroprint, Odesa, 151 pp. [In Russian]

Steinitz H (1954) The distribution and evolution of the fishes of Palestine. Istanbul Üniversitesi Fen Fakültesi Hidrobiyoloji (B) 1(4): 225–227.

Strayer DL (2010) Alien species in fresh waters: Ecological effects, interactions with other stressors, and prospects for the future. Freshwater Biology 55(s1): 152–174. https://doi.org/10.1111/j.1365-2427.2009.02380.x

Tkachenko PV, Khutornoy SA (2001) Sovremennyj sostav i tendencii izmeneniâ ihtiofauny pribrežnyh učastkov severo-zapadnoj časti Černogo morâ. [Modern composition and trends of changes in the fish fauna of the costal sites of the northwestern Black Sea.] Pp. 363–369. In: Ivanov IA (Ed.) Ekologičeskaâ bezopaskost' pribrežnoj i šel'fovoj zon i kompleksnoe ispol'zovanie resursov šel'fa. [Ecological safety of the coastal and shelf zones and complex usage of shelf sources.] Issue 2. Ekosi-Gidrofizika, Sevastopol. [In Russian]

Venâncio C, Castro BB, Ribeiro R, Antunes SC, Lopes I (2019) Sensitivity to salinization and acclimation potential of amphibian (*Pelophylax perezi*) and fish (*Lepomis gibbosus*) models. Ecotoxicology and Environmental Safety 172: 348–355. https://doi.org/10.1016/j.ecoenv.2019.01.099

Vinogradov AK, Khutornoy SA (2013) Ihtiofauna Odesskogo regiona severo-zapadnoj časti Černogo morâ (biologičeskie, ekologičeskie, ekologo-morfologičeskie osobennosti). [The fish fauna of Odessa region of the northwestern Black Sea (biological, ecological, eco-morphological features).] Astroprint, Odessa, 224 pp. [In Russian]

Zaitsev YP (1998) Samoe sinee v Mire. [The bluest in the World.] UN Publications, New York, 142 pp. [In Russian]

Zaitsev YP, Aleksandrov BG, Minicheva GG (2006) Severo-zapadnaâ čast Černogo morâ: biologiâ i ekologiâ. [Northwestern Black Sea: biology and ecology.] Naukova Dumka, Kyiv, 703 pp. [In Russian]

Zander CD (1986) Blenniidae. Pp. 1096–1112. In: Whitehead PJP, Bauchot M-L, Hureau J-C, Nielsen J, Tortonese E (Eds) Fishes of the North-eastern Atlantic and the Mediterranean, Volume 3. UNESCO, Paris.

Zhulidov AV, Kozhara AV, Son MO, Morhun H, van der Velde G, Leuven RSEW, Gurtovaya TY, Zhulidov DA, Kalko EA, Kuklina YA, Kosmenko LS, Santiago-Fandino VJR, Nalepa TF (2021) Additional records of the bivalves *Mytilopsis leucophaeata* (Conrad, 1831) (Dreissenidae) and *Arcuatula senhousia* (Benson, 1842) (Mytilidae) in the Ponto–Caspian region. BioInvasions Records 10(1): 119–135. https://doi.org/10.3391/bir.2021.10.1.14

Acta Ichthyologica et Piscatoria 53, 2023, 163–172 | DOI 10.3897/aiep.53.105367

PENSOFT.

ACTA
ICHTHYOLOGICA
ET PISCATORIA

Graded levels of dietary pink oyster mushroom, *Pleurotus djamor* meal, affect growth, feed efficiency, lipase activity, and fiber content in final whole body of fingerlings of the Nile tilapia, *Oreochromis niloticus* (Actinopterygii: Cichliformes: Cichlidae)

Mario Eduardo SOSA[1], Silvia CAPPELLO-GARCÍA[1], Rafael MARTÍNEZ-GARCÍA[1], Susana CAMARILLO-COOP[1], Rocío GUERRERO-ZARATE[1], Otilio MÉNDEZ-MARÍN[1], Carlos Alfonso ÁLVAREZ-GONZALÉZ[1*], Uriel RODRÍGUEZ-ESTRADA[1,2*]

1 *Juarez Autonomous University of Tabasco (UJAT), Academic Division of Biological Sciences (DACBiol), Laboratory of Physiology of Aquatic Resources (LAFIRA), Villahermosa, Tabasco, Mexico*

2 *National Council of Humanities, Science and Technology (CONAHCYT), Mexico scientist program (IxM), México City, Mexico*

https://zoobank.org/50043678-A74B-4DB8-BCE0-8F1202903B25

Corresponding authors: Uriel Rodríguez-Estrada (rodriguez_estrada_uriel@yahoo.com), Carlos A. Álvarez-Gonzaléz (alvarez_alfonso@hotmail.com)

Academic editor: Kasi Marimuthu ♦ **Received** 27 April 2023 ♦ **Accepted** 1 September 2023 ♦ **Published** 23 October 2023

Citation: Sosa ME, Cappello-García S, Martínez-García R, Camarillo-Coop S, Guerrero-Zarate R, Méndez-Marín O, Álvarez-Gonzaléz CA, Rodríguez-Estrada U (2023) Graded levels of dietary pink oyster mushroom, *Pleurotus djamor* meal, affect growth, feed efficiency, lipase activity, and fiber content in final whole body of fingerlings of the Nile tilapia, *Oreochromis niloticus* (Actinopterygii: Cichliformes: Cichlidae). Acta Ichthyologica et Piscatoria 53: 163–172. https://doi.org/10.3897/aiep.53.105367

Abstract

The presently reported study was aimed to determine the effects of graded levels of dietary pink oyster mushroom (*Pleurotus djamor*) meal (POMM), in growth, feed efficiency, protein utilization, digestive enzymes activities, and whole-body proximate composition of Nile tilapia, *Oreochromis niloticus* (Linnaeus, 1758), fingerlings (0.3 ± 0.01 g). The experimental design included a control diet (POMM0) formulated with soybean meal, as the main protein source, and four diets designed with increasing levels of POMM: 25% (POMM25); 50% (POMM50); 75% (POMM75); and 100% (POMM100). Experimental diets were administered to 420 fish, randomly distributed in 15, 100-L tanks. The feeding experiment lasted 45 days. Diets and the final whole body were submitted to a proximate composition analysis. Growth, feed efficiency, protein utilization, and digestive enzyme activities were assessed. Compared to POMM0 and POMM25, weight gain (WG), and specific growth rate (SGR), significantly ($P < 0.05$) decreased in fish that were fed POMM50, POMM75, and POMM100%. Feed conversion ratio (FCR), protein efficiency ratio (PER), and survival rate (SR) were not significantly affected by experimental diets. Daily feed intake (DFI), and daily protein intake (DPI), decreased as POMM increased in diets. Compared to POMM0 experimental group, condition factor (K), showed a significantly higher value in fish that were fed POMM50, and POMM100 experimental diets. Crude fiber of the final whole body of POMM100 resulted in significantly higher ($P < 0.05$) compared to that shown in fish fed the rest of the experimental diets. Acid and alkaline proteases, trypsin, chymotrypsin, leucine aminopeptidase, and amylase of Nile tilapia fingerlings, were not significantly affected by experimental diets. Compared to fish fed POMM0 and POMM25 diets, experimental fish fed POMM50, POMM75, and POMM100 showed a reduction in lipase activity. In conclusion, a POMM level higher than 25% affects growth and lipase activity. While a POMM level higher than 50% affects fiber content in a whole body of the final fish.

---

[*] Both authors contributed equally to this study.

Keywords

carcass, digestive physiology, fiber, growth, mushroom meal, tilapia

Introduction

The expansion of the aquaculture industry is evidently accompanied by an urgent need for aquafeed production (Gambelli et al. 2019; Botta et al. 2020; Chu et al. 2020). This condition leads to the necessity of a steady supply of protein. Traditionally, fishmeal (FM) and soybean meal (SBM) have been the primary protein source ingredient in fish feeds (Wang et al. 2020). However, their over-exploitation has led to a shortage of these commodities (Galkanda-Arachchige and Davis 2019; Ye et al. 2019; Li et al. 2023; Nunes et al. 2022; Soltan et al. 2023). Therefore, several studies have been conducted to investigate alternative and unconventional protein meals for aquaculture diets. One of these, are mushrooms (Chelladurai and Venmathi-Maran 2019).

Edible mushrooms are a rich source of caloric value, essential fatty acids, amino acids, protein levels, vitamins, and minerals. To date, there are several studies focusing on the research of products derived from mushrooms as dietary inclusion in feeds for farmed aquatic organisms (Safari and Sarkheil 2018; Chelladurai and Venmathi Maran 2019; Dawood et al. 2020a). The majority of the studies using mushrooms have been mainly focused on the effects on aquatic organism immunity, hematological profiles, disease resistance, and growth (Katya et al. 2016; Chelladurai and Venmathi Maran 2019; Dawood et al. 2020a).

Pleurotus spp. is an edible mushroom that belongs to the order Agaricales and the family Pleurotaceae (see Justo et al. 2011). Pink oyster mushroom (POM), *P. djamor*, is mainly produced for research and food purposes for human nutrition in Brazil and Mexico (Chintati et al. 2022). Previous studies have shown that this species contains 31.48–35.50 g 100 g^{-1} of protein, while crude fiber content, ranges from 8.00 to 14.60 g 100 g^{-1}. (Jegadeesh et al. 2020). Although *P. djamor* has been widely studied as an additive supplemented at low inclusion levels (Nattoh et al. 2016; Zhang et al. 2016; Hu et al. 2017; Jiao et al. 2017; Maity et al. 2019; Pereira de Oliveira and Naozuka 2019; Vasconez-Velez 2019), only a few studies have focused on the use of *P. djamor* as a dietary supplement in fish feed formulations. Cruz-García et al. (2022) studied the effects of mushroom (*Pleurotus djamor* var. *roseus*) meal as a feed supplement on the hematological responses and growth of the Nile tilapia, *Oreochromis niloticus* (Linnaeus, 1758), fingerlings when fed diets formulated with 0%, 15%, 20%, and 25% of *P. djamor*. Therefore, the presently reported research aims to study the effects (growth, feed efficiency, protein utilization, whole body proximate composition, and digestive enzyme activities) of increasing levels (0%, 25%, 50%, 75%, and 100%) of *P. djamor* meal, in diets for Nile tilapia fingerlings (used as model fish species).

Material and methods

Experimental Nile tilapia fingerlings. Masculinized, Nile tilapia (*Oreochromis niloticus*) fingerlings (genetically improved farmed tilapia = GIFT strain; Ponzoni et al. 2011) (0.3 ± 0.01 g) were obtained from the brood stock in the Tropical Aquaculture Laboratory of the Academic Division of Biological Sciences (DACBiol), Juarez Autonomous University of Tabasco (UJAT). Before the feeding experiment, the health status of Nile tilapia fingerlings was checked by visual observation, according to indications proposed by Johansen et al. (2006). 420 fish were randomly distributed in 15 (100 L) plastic tanks.

POM (CH-240). POM, strain CH-240, belonging to the herbarium of the DACBiol-UJAT, was reared in an edible mushroom greenhouse (28°C, using coconut paste as substrate), the harvest of the mushroom was carried out when there was a complete extension of the pileus. All farming processes were carried out in an innocuous environment, to avoid contaminating *P. djamor* culture. Collected mushrooms were dried in an oven, pulverized with a hammer mill, and analyzed for proximate composition (AOAC 2019).

Experimental diets. Iso-nitrogenous and iso-lipidic diets were designed, including a control diet formulated with SBM (as the main protein source) and four diets formulated with increasing levels of POMM. In each diet, the protein level was adjusted by reducing SBM levels. Experimental diets were assigned as follows: 25% (POMM25), 50% (POMM50), 75% (POMM75), and 100% (POMM100) (Table 1). Diet formulation followed the method proposed by Álvarez-González et al. (2001). Experimental diets were designed with the assistance of MIXITWIN V. 5.0 (Agricultural Software Consultants, San Diego, CA, USA) software. Diets were manufactured according to previously standardized methods at DACBiol-UJAT. Experimental diets were submitted to a proximate composition analysis AOAC (2019).

Feeding test and rearing system. Experimental diets were administered in triplicate during a 45-day period, at satiation level. Each experimental tank was randomly assigned to each diet and the feeder (person in charge of

Table 1. Dietary ingredients and proximate composition of experimental diets for fingerlings of Nile tilapia (*Oreochromis niloticus*), formulated with increasing levels of POMM (pink oyster mushroom meal).

Ingredient [%]	**Treatment (substitution level)**				
	POMM0	**POMM25**	**POMM50**	**POMM75**	**POMM100**
Soybean meal 44%[c]	21	15	11	5	0
Pink oyster mushroom meal[b]	0	11	22	33	44
Sorghum meal 9%[c]	26	21	12	7	1
Pork meal 50%[a]	25	25	26	26	26
Fish meal 65%[a]	14	14	15	15	15
Sardine Oil[a]	6	6	6	6	6
Soybean Oil[d]	3	3	3	3	3
Grenetine[e]	2	2	2	2	2
Previt[f]	1.5	1.5	1.5	1.5	1.5
Premin[f]	1	1	1	1	1
Vitamin C[g]	0.5	0.5	0.5	0.5	0.5
Proximate composition (dry matter)					
Crude Protein [%]	33.13	32.42	32.76	31.98	32.03
Crude lipid [%]	13.77	13.85	13.99	14.08	14.23
Ash [%]	11.94	12.26	12.88	13.20	13.78
Crude fiber [%]	2.39	3.63	4.91	6.15	7.40
Nitrogen-free extract [%]	38.78	37.84	35.46	34.59	32.56
Energy [kJ kg^{-1}]	19.93	19.63	19.36	19.06	18.78

Numbers following POMM denote percentage of diet substitution with pink oyster mushroom meal.

[a] Marine and Agricultural Protein (Proteínas marinas y agropecuarias S.A. de C.V., Guadalajara, Jalisco.

[b] Edible mushroom greenhouse, Academic Division of Biological Science (DACBiol), Juarez Autonomous University of Tabasco (UJAT), Villahermosa, Tabasco.

[c] GALMEX Comercializadora de Insumos Agrícolas S.A. de C.V., Villahermosa, Tabasco (19800-20100 IU g^{-1}).

[d] Pronat Ultra, Mérida, Yucatán.

[e] D'gari, Productos alimenticios y dietéticos relámpago, S.A. de C.V., Tlalpan, D.F.

[f] Consorcio Súper S.A. de C.V., Guadalajara, Jalisco.

[g] DSM® C-EC (Roche) active agent 35%.

feeding daily), was rotated to obtain a blinded feed delivery. The feeding test was conducted in a recirculating aquaculture system (RAS) (2 L min^{-1}) maintaining a constant aeration. To decrease the effects of the natural high temperature *per se* existing in Villahermosa city (tropical weather), the RAS was designed and built under a controlled air conditioner environment, hence decreasing significant oscillation of temperature during all feeding experiments. Fish were fed three times per day (09:00, 13:00, and 17:00 h). Unconsumed feed and feces were siphoned 30 min after each feeding. RAS water was replaced (50%) every week. Water quality was monitored daily: Dissolved oxygen (DO) (5.19 ± 0.3 mg L^{-1}) and temperature (28 ± 0.1°C) were measured with a YSI 55 oximeter, with an accuracy of 0.1°C and 0.01 mg L^{-1}, respectively. While pH (7.2 ± 0.1) was assessed with a potentiometer (Hanna Instruments, HI 98311, Rhode Island, USA). These parameters were measured in both experimental tanks and in the 4 m^3 main reservoir of RAS.

Growth, feed efficiency, protein utilization, and survival. All fish per tank were sampled (benzocaine 20% w/v. SIGMA–Aldrich, USA), for weight and total length every 15 days. Animals used for organ sampling were carried out following the guidelines of the Mexican Norm NOM-062-ZOO-1999 (NOM 2001) for the management of animals in a laboratory for experimental use. At the end of the feeding test, in addition to weight sampling, growth performance (weight gain, W_G [%]; specific growth rate, SGR [% day^{-1}]; condition factor, *K*), feed utilization parameters (feed conversion ratio, FCR; daily feed intake, DFI [g day^{-1}]; daily protein intake, DPI [g day^{-1}]; protein efficiency ratio, PER, and survival rate SR [%]) were calculated as follows:

$$W_G = 100\ W_{FF} \times W_{IF}{}^{-1}$$

$$\mathrm{SGR} = 100\ [\ln W_{FF} - \ln W_{IF}] \times t^{-1}$$

$$K = 100[W_{FF} \times L_{FF}{}^{3}]$$

$$\mathrm{FCR} = W_{FC} \times W_G{}^{-1}$$

$$\mathrm{DFI} = (W_{CD} \times t^{-1}) \times N_F$$

$$\mathrm{DPI} = (W_{PCD} \times t^{-1}) \times N_F$$

$$\mathrm{PER} = W_G \times W_{PI}{}^{-1}$$

$$\mathrm{SR} = 100(N_{IF} - N_{FF}) \times N_{FF-1}$$

where W_{FF} is the final mean weight of fish [g], W_{IF} is the initial mean weight [g], *t* is the time of rearing [day], L_{FF} is the final mean length of fish [cm], W_{FC} is the weight of the total feed consumed [g], W_{CD} is the weight of feed consumed per day [g], N_F is the number of fish, W_{PCD} is the weight of protein consumed per day [g], W_{PI} is protein intake [g], N_{IF} is initial number of fish. N_{FF} is the final number of fish.

Proximate composition analysis. POMM, experimental diets and final whole body were submitted to proximate composition analysis (AOAC 2019) at the Chemistry Laboratory of Norwest Biological Research Center (CIBNOR), La Paz, BCS, Mexico. Before sending to laboratory analysis, and to preserve biochemical profiles intact, whole body samples were lyophilized. Nitrogen free extract (NFE) [g kg^{-1}] and gross energy (E_G) [kJ kg^{-1}], were manually calculated as follows:

$$\text{NFE} = 100 - (\text{CP} + \text{CL} + \text{CF} + A)$$

$$E_G = [100\ (\text{CP} \times 23.6) + (\text{CL} \times 39.5) + (\text{NFE} \times 17.2)]$$

where CP is crude protein content [%], CL is crude lipid content [%], CF is crude fiber content [%], and A is the ash content [%], NFE is the nitrogen free extract [%]. The numerical values in the gross energy formula represent respective energy conversion factors.

Digestive enzyme activity sampling and analysis. Upon completion of the feeding test, three fish (per experimental tank), 9 fish (per experimental group), and 45 fish (per all tested groups), were starved for 24 h and then the final sampling was carried out. Fish were anesthetized with 20% w/v benzocaine (SIGMA-Aldrich, USA). Fish were slaughtered under freezing conditions to avoid organisms suffering. Then, fish were dissected to extract the stomach and intestine for digestive enzyme activity analysis. The stomach samples were homogenized in a buffer solution of glycine-HCl 0.1 M, pH 2 and the intestines were homogenized in the solution of Tris-HCl 100 mM + $CaCl_2$ 10 mM pH 9. Both samples were centrifuged at 16 000 *g* for 30 min to extract the supernatant or enzymatic extract by separating in 400 µL aliquots and freezing at –20°C until their further use. The soluble protein concentration was evaluated using a bovine serum albumin calibration curve (600 mg mL^{-1}).

Alkaline protease activity was determined according to (Walter 1984), using Hammerstein-grade casein 0.5% in buffer (100 mmol L^{-1} Tris-HCl; 10 mmol L^{-1} $CaCl_2$, pH 9); one unit of activity was defined as 1-µg of tyrosine released per min at absorbance 280 nm (abs$_{280}$) The acid protease activity was determined using Anson (1938) technique, and hemoglobin (1%) in a buffer solution of glycine-HCl 0.1 M, pH 2. The released peptide levels were determined through a quartz cell (700 µL) at 280 nm in the spectrophotometer. Trypsin activity determination used the Erlanger et al. (1961) technique with the substrate BAPNA (N-α-benzoyl-DL-arginine p-nitroanilide) with dimethyl sulfoxide (DMSO). Sample reading was conducted with a spectrophotometer at 410 nm. Chymotrypsin activity was determined following the method proposed by Del Mar et al. (1979). Absorbance was measured at 405 nm. Leucine aminopeptidase activity was evaluated following the methodology proposed by Maraux et al. (1973). Absorbance was measured at 410 nm. The α-amylase activity was determined by the method of Robyt and Whelan (1968), using soluble starch (2%) in a buffer (100 mmol L^{-1} citrate-phosphate; 50 mol L^{-1} NaCl, pH 7.5). Lipase activity was measured as previously described by Versaw et al. (1989) but using ß-naphthyl acetate 100 mmol L^{-1} as substrate; one unit of activity was defined as 1 µg de naphthol released per min at 540 nm.

The enzymatic activity of the extracts was determined with the following equations:

1. Units per mL = [Δabs × final reaction volume (mL) CEM^{-1} × time (min) × extract volume (mL)], and
2. Units × mg of protein^{-1} = Units per mL mg of soluble protein^{-1}. Δabs is determined by the length of the wave of each technique and the CEM is the molar extinction coefficient for the reaction product (mL × µg^{-1} × cm^{-1}). All enzyme activities were expressed per mg of protein. Protein concentration was determined according to Bradford (1976), using a standard curve with bovine serum albumin (BSA). All assays were performed in triplicate.

Statistical analysis. Data was statistically analyzed by one-way ANOVA, previously verified the assumptions of normality (Kolmogorov–Smirnov test) and homoscedasticity (Levine test). Where significant differences were assessed, applying a Tukey test. Analyses were performed with the statistical software Statistica TM v.8.0 (StatSoft, Tulsa, OK, USA) using a significance value of $P < 0.05$. The results were presented as mean ± standard deviation, SD.

Results

Proximate composition of POMM. The proximate composition of POMM is shown in Table 2. Crude protein and crude fiber showed similar values. As expected, crude lipid recorded a remarkably lower value (0.50%). While the nitrogen-free extract recorded the highest content (45.96%), compared to other nutrients.

Table 2. Proximate composition of POMM (pink oyster mushroom meal) in diets for fingerlings of Nile tilapia (*Oreochromis niloticus*).

Component	Value
Moisture [%]	4.61
Crude protein [%]	21.37
Crude lipid [%]	0.50
Crude fiber [%]	20.05
Ash [%]	7.51
Nitrogen-free extract [%]	45.96
Gross energy [kJ kg^{-1}]	13.15

Proximate composition of experimental diets. Experimental diets did not show relevant differences regarding crude protein, crude lipid, ash, and energy. However, crude fiber and ash increased as the POMM level increased in experimental diets. While nitrogen-free extract decreased as POMM level increased in diets (Table 1).

Growth performance, feed utilization, and survival. All experimental diets were well accepted by the fish during the feeding test. Experimental diets did not affect feed conversion rate (FCR), protein efficiency ratio (PER), and survival rate (SR). In contrast, fish that were fed the POMM25 diet did not show significant ($P > 0.05$) differences in weight gain (WG), and specific growth rate (SGR), compared to those shown in experimental group POMM0. While POMM50, POMM75, and POMM100 experimental groups, showed significantly ($P < 0.05$) lower WG and SGR compared to those shown in POMM0 experimental group. Although K did not show significant ($P > 0.05$) differences among POMM0, POMM25, and POMM75 experimental groups, there was a significantly higher ($P < 0.05$) K value in POMM50 and POMM100 experimental groups, compared to that recorded in POMM0 experimental group. DFI and DPI significantly ($P < 0.05$) decreased as levels of POMM increased in experimental diets (Table 3).

Whole body proximate composition. There were no significant ($P > 0.05$) differences, among experimental groups, in terms of moisture, crude protein, and crude lipid contents. In contrast, crude fiber resulted significantly ($P < 0.05$) higher in the POMM100 experimental group compared to that shown in the rest of the experimental groups (Table 4).

Digestive enzyme activities. Acid protease, alkaline protease, trypsin, chymotrypsin, leucine aminopeptidase, and amylase activities were not significantly ($P > 0.05$) affected by consumed experimental diets. However, lipase activity resulted significantly ($P < 0.05$) lower in POMM50, POMM75, and POMM100 experimental groups compared to that observed in POMM0 and POMM25%. There was no significant ($P > 0.05$) difference in lipase activity between POMM0 and POMM25% (Table 5).

Discussion

The presently reported study was designed to determine the effects on growth, feed efficiency, protein utilization, survival, final whole body proximate composition, and digestive enzyme activities of Nile tilapia fingerlings, which were fed diets formulated with increasing levels of a locally available and unconventional protein meal, POMM. Levels of protein and lipid content of POM in this study are similar to those previously reported in Cruz-Solorio et al. (2014) and Salmones (2017). Mushroom species are characterized by their high fiber content.

Table 3. Growth, feed performance, protein utilization and survival of fingerlings of Nile tilapia (*Oreochromis niloticus*) fed formulated diets with increasing levels of POMM (pink oyster mushroom meal) for 45 days.

Parameter	Treatment (substitution level)				
	POMM0	POMM25	POMM50	POMM75	POMM100
Initial weight [g]	0.30 ± 0.05	0.31 ± 0.02	0.29 ± 0.06	0.30 ± 0.03	0.31 ± 0.02
Final weight [g]	1.98 ± 0.10^{a}	1.71 ± 0.19^{ab}	1.34 ± 0.11^{bc}	1.30 ± 0.10^{c}	1.20 ± 0.12^{c}
WG [%]	659.2 ± 97.7^{a}	553.1 ± 23.4^{ab}	462.4 ± 35.9^{bc}	433.7 ± 80.4^{c}	388.1 ± 22.9^{c}
SGR [% day^{-1}]	4.49 ± 0.28^{a}	4.16 ± 0.08^{ab}	3.83 ± 0.15^{bc}	3.70 ± 0.32^{c}	3.52 ± 0.11^{c}
K	1.64 ± 0.04^{b}	1.66 ± 0.03^{ab}	1.72 ± 0.02^{a}	1.69 ± 0.02^{ab}	1.71 ± 0.03^{a}
FCR^{Q}	2.54 ± 0.35	2.34 ± 0.10	2.84 ± 0.24	2.95 ± 0.51	3.22 ± 0.21
DFI [g day^{-1}]	0.110 ± 0.00^{a}	0.086 ± 0.00^{b}	0.086 ± 0.00^{b}	0.083 ± 0.00^{c}	0.082 ± 0.00^{d}
DPI [g day^{-1}]	0.037 ± 0.01^{a}	0.029 ± 0.01^{b}	0.028 ± 0.00^{c}	0.027 ± 0.00^{d}	0.026 ± 0.01^{e}
PER	1.20 ± 0.18	1.32 ± 0.06	1.09 ± 0.09	1.08 ± 0.20	0.97 ± 0.06
SR [g]	100 ± 0.00	100 ± 0.00	100 ± 0.00	100 ± 0.00	100 ± 0.00

Numbers following POMM denote percentage of diet substitution with pink oyster mushroom meal. Values in each row superscript with different lower-case letters indicate significant differences between groups ($P < 0.05$). WG = weight gain; SGR = specific growth rate; K = condition factor; FCR = feed conversion ratio; DFI = daily food intake; DPI = daily protein intake; PER = protein efficiency ratio; SR = survival rate.

Table 4. Whole body proximate composition of fingerlings of Nile tilapia (*Oreochromis niloticus*), fed formulated diets with increasing levels of POMM (pink oyster mushroom meal), for 45 days.

Proximate composition [%]	Treatment (substitution level)				
	POMM0	POMM25	POMM50	POMM75	POMM100
Moisture	6.54 ± 1.53	5.76 ± 1.74	6.19 ± 1.54	7.82 ± 0.69	5.21 ± 1.03
Crude protein	57.35 ± 2.80	56.66 ± 1.30	55.13 ± 1.40	53.13 ± 0.80	52.77 ± 1.20
Crude lipid	22.97 ± 1.14	24.50 ± 1.45	23.68 ± 2.08	26.64 ± 2.78	26.49 ± 1.50
Crude Fiber	0.14 ± 0.00^{b}	0.00 ± 0.00^{bc}	0.00 ± 0.00^{bc}	0.16 ± 0.02^{b}	0.24 ± 0.03^{a}

Numbers following POMM denote percentage of diet substitution with pink oyster mushroom meal.
Values in each row superscript with different lower-case letters indicate significant differences between groups ($P < 0.05$).

Table 5. Digestive enzyme activities of fingerlings of Nile tilapia (*Oreochromis niloticus*), fed formulated diets with increasing levels of POMM (pink oyster mushroom meal), for 45 days.

Enzyme activity [U mg protein^{-1}]	**Treatment (substitution level)**				
	POMM0	**POMM25**	**POMM50**	**POMM75**	**POMM100**
Acid protease	4.72 ± 3.52	5.68 ± 1.58	6.57 ± 1.62	6.07 ± 0.78	6.30 ± 1.36
Alkaline protease	9.93 ± 3.28	8.36 ± 3.30	9.17 ± 3.10	10.20 ± 1.48	10.29 ± 0.84
Trypsin	$6.47 \times 10^{-3} \pm 2.15 \times 10^{-3}$	$7.83 \times 10^{-3} \pm 1.78 \times 10^{-3}$	$5.99 \times 10^{-3} \pm 2.71 \times 10^{-3}$	$5.94 \times 10^{-3} \pm 1.13 \times 10^{-3}$	$7.15 \times 10^{-3} \pm 6.02 \times 10^{-4}$
Chymotrypsin	$2.35 \times 10^{-2} \pm 4.87 \times 10^{-4}$	$2.41 \times 10^{-2} \pm 1.47 \times 10^{-3}$	$2.22 \times 10^{-2} \pm 2.98 \times 10^{-3}$	$2.25 \times 10^{-2} \pm 2.92 \times 10^{-3}$	$2.19 \times 10^{-2} \pm 2.55 \times 10^{-3}$
Leucine aminopeptidase	$8.66 \times 10^{-4} \pm 2.96 \times 10^{-4}$	$1.11 \times 10^{-3} \pm 1.38 \times 10^{-4}$	$1.13 \times 10^{-3} \pm 3.37 \times 10^{-4}$	$8.96 \times 10^{-4} \pm 2.09 \times 10^{-4}$	$1.15 \times 10^{-3} \pm 4.34 \times 10^{-4}$
Lipase	130.09 ± 13.24^{a}	130.47 ± 12.31^{a}	96.05 ± 17.56^{b}	84.51 ± 7.27^{b}	90.29 ± 23.09^{b}
Amylase	141.63 ± 41.78	176.20 ± 7.69	168.51 ± 22.36	154.45 ± 27.63	147.14 ± 20.44

Numbers following POMM denote percentage of diet substitution with pink oyster mushroom meal. Values in each row with different superscript letters indicate significant differences between groups ($P < 0.05$).

In this research, 20.05% of fiber was recorded in POMM. In contrast, lower crude fiber levels (8.60%–9.29%) in two strains of *Pleurotus* spp. were recorded by Cruz-Solorio et al. (2014).

The presently reported study showed that a maximum of 25% of POMM can be supplemented in Nile tilapia fingerlings without affecting the WG and SGR of fish. POM has nutritional, nutraceutical, and biodegradable features (Dulay et al. 2017). Limited inclusion of POMM may be attributed to the presence of certain biochemical components naturally occurring in POMM that at high levels could produce certain growth depressing effects (Salmones 2017). The nutritional quality of *Pleurotus* has been widely studied and it has been robustly demonstrated. Previous studies have detected 16 components (2-pentanone, 3-pentanone, methyl butyrate, and 2-methyl-3 pentanone, 3-octanol, 3-octanone, among the main ones) influencing *P. djamor* flavor, hence palatability (Zhang et al. 2022a; Andrew 2023), affecting fish acceptance to feeds. This fact could explain why the DFI of Nile tilapia fingerlings during a 45-day period decreased as higher levels of POMM were supplemented in experimental diets. Previous studies have demonstrated that high-fiber content diets decrease feed intake in species such as rainbow trout (Hilton et al. 1983). Other elements that are predominant in POM are bioactive components with anti-carcinogenic, immune stimulants, antibiotic, anti-inflammatory, immune stimulant, and antioxidant properties (Salmones 2017). These components confer certain benefits (when present at certain levels) to fish physiology, growth performance, feed efficiency, and nutrient utilization, as evidenced in Dawood et al. (2020a), who found that Nile tilapia fingerlings fed 2% and 4% supplementation levels of dietary white bottom mushroom powder, improved growth performance, digestibility, and feed intake. Dawood et al. (2020b) suggested that these benefits may be due to the content of non-digestible polysaccharides (acting as prebiotics), that can modulate the intestinal microbiota to secrete digestive enzymes in the fish's gastrointestinal tract Moumita and Das (2022). In contrast, in the presently reported study, growth performance and feed utilization decreased as the POMM level increased in the experimental diet in Nile tilapia fingerlings. This can be explained by two factors. Firstly, the amount of POMM supplemented in experimental diets was remarkably higher (from 11% to 44% of the total content of each diet) (Table 2), so bioactive components (such as antimicrobial, antioxidant, immune stimulant) naturally existing in *P. djamor*, were considerably higher. This abundant presence of bioactive components may cause a depressed growth rather than stimulating it. Secondly, a gradual increase of POMM in experimental diets, inevitably added higher fiber amounts to the feed. POMM showed 20% of crude fiber while in experimental diets this nutrient consequently increased as POMM level increased. Results revealed that the POMM25 experimental diet had 3.63% of crude fiber. This diet did not compromise the growth of Nile tilapia fingerlings, while diets with a higher inclusion level of POMM showed a higher fiber content (4.91%, 6.15%, and 7.14%; POMM50, POMM75, and POMM100 diets, respectively) and a significantly lower growth of experimental fish. Hilton et al. (1983), reported a reduction in the growth of rainbow trout when fed high-fiber diet. At certain levels, dietary fiber apparently influences the movement of nutrients along the gastrointestinal tract and significantly increases nutrient absorption (Lin et al. 2020). Fiber is the non-nutritive portion of feed ingredients. This nutrient is indigestible for carnivorous fish, while others such as channel catfish, have intestinal microflora capable of digesting small portions of dietary fiber (McLean 2023). Some herbivorous fish, such as grass carp, *Ctenopharyngodon idella* (Valenciennes, 1844), derive nutrients from fiber but some such as blue tilapia, *Oreochromis aureus* (Steindachner, 1864), do not (Turchini et al. 2018). High fiber content often results in growth depression (Zhang et al. 2022b), as seen in the presently reported study.

In aquaculture, condition factor (*K*) is a numerical value given to aquatic organisms that reflects this condition. A low *K* value could be determined by several factors such as stress, disease, starvation, and deficient nutrient composition in diets among the main ones. A high *K* value indicates a healthy fish and an optimal nutrient balance in diet (Kim and Cho 2019). The presently reported study recorded a slight or significant increased *K* value in fish fed diets supplemented with increasing levels of POMM, compared to fish fed POMM0 diet. This result suggests that experimental diets cover the necessary nutritional requirements for Nile tilapia fingerlings and even higher inclusion levels of POMM did not compromise the condition of the fish.

The results of SR indicated that increased levels of POMM did not affect Nile tilapia fingerlings' health for a 45-day period. A previous study testing dietary white button mushroom supplemented at 0, 0.5, 1, 2, and 4% in Nile tilapia, demonstrated that the survival of experimental fish was not significantly affected by any experimental diet (Dawood et al. 2020a).

In our presently reported study, the final whole-body proximate composition (moisture, crude protein, and crude lipid) was not affected in experimental fish after a 45-day feeding period. However, experimental fish that were fed the POMM100 diet, recorded a significantly higher crude fiber, compared to that shown in the remaining experimental groups. These higher values are attained due to the high level of fiber content (7.4%) in the POMM100 experimental diet. During all the history of fish nutrition science, fiber has been considered as an energy depletion agent, with undesirable effects when fish consume diets with high contents of fiber (Adorian et al. 2016). This statement correlates with presently reported research where high levels of crude fiber in experimental diets, mainly produced two effects: a decreased growth in experimental Nile tilapia fingerlings and an accumulation of this nutrient in final whole body proximate composition. Fiber accumulation in whole body composition is explained because this nutrient is poorly digested by the majority of fish species, including Nile tilapia (Hilton et al. 1983).

The presently reported study analyzed digestive enzyme activities of Nile tilapia fingerlings that were fed with diets formulated with increasing levels of POMM. Acid proteases, alkaline proteases, trypsin, and chymotrypsin did not show significant differences among experimental groups. These enzymes have been proposed as indicators of the nutritional status of fish. The activity of these enzymes indicates the digestive system functionality and ability of nutrient assimilation in the intestine (Wang et al. 2022). This enzymatic unaffected status can be correlated with the presence of sufficient protein in experimental diets, whereas a low value shall be correlated with starvation or feed deficiency (Xavier et al. 2023). Additionally, the activities of enzymes digesting proteins in fish revealed the effects of diets on the physiological status of experimental fish (Guerrero-Zarate et al. 2019). In our study, the activity of leucine aminopeptidase of experimental Nile tilapia fingerlings showed no significant differences among experimental groups. This enzyme is considered an indicator of nutritional quality, since greater digestion, at a parietal level from luminal digestion by endoproteases, hydrolyzes peptides to release amino acids and to promote their absorption (Wang et al. 2022). This enzyme is a proteolytic enzyme that hydrolyses the peptide bond adjacent to a free amino group. Hence, it can be inferred that leucine aminopeptidase can hydrolyze ingested proteins of mushroom meal (Solovyev et al. 2023).

In presently reported research, lipase activity showed a significant decrease in experimental groups fed POMM50, POMM75, and POMM100 diets, which is correlated with a lower growth performance. There are several factors impacting lipid enzyme secretions including feeding habits, feed preferences, formulation of diets, and ANFs (Thongprajukaew and Rodjaroen 2020). In the presently reported study, fiber could have reduced the activity of lipase in experimental fish (Mirghaed et al. 2018). This can be explained by the interference of fiber in not only the hydrolysis of lipids but also in the absorption of fatty acids (Dawood et al. 2020b).

In this research, α-amylase activities did not show significant differences among experimental groups. α-amylase activity is modified according to the ingredients of diet formulation (Mohtashemipour et al. 2023). In this regard, α-amylase is positively correlated with dietary carbohydrate level (Qu et al. 2022). The ability to secrete more α-amylase for dietary polysaccharides hydrolysis seems to be more efficient in herbivorous and omnivorous species (e.g., Nile tilapia) than in carnivorous fish such as rainbow trout, *Oncorhynchus mykiss* (Walbaum, 1792), where this digestive enzyme is not efficiently expressed (Bjørgen et al. 2020). It is well demonstrated that omnivore species like the Nile tilapia has a better starch digestion rather than opportunistic carnivore species (Ferreira et al. 2022). This fact can explain that even at high nitrogen-free extract in all experimental diets in this study, no differences in α-amylase activity among experimental groups were shown.

Conclusions

Diets formulated with increasing levels of POMM did not compromise feed efficiency, protein utilization, survival, and digestive enzyme activities (except that of lipase), of Nile tilapia fingerlings. In contrast, levels above 25% affected growth, DFI, and DPI. While an accumulation of fiber in the final whole body of fish that were fed diets formulated with 100% of POMM, was promoted. This may be attained due to two factors: firstly, the interference of fiber in the hydrolysis of lipids and in the absorption of fatty acids, and, secondly, fiber is poorly digested, therefore it is accumulated in the final whole body of Nile tilapia fingerlings. Further studies are suggested to assess the metabolic pathways through which fiber naturally occurring in POMM interferes with the lipid metabolism of Nile tilapia.

Acknowledgments

The authors would like to acknowledge the financial support granted to this study by the Investigadores e Investigadoras por Mexico program of the Consejo Nacional de Humanidades, Ciencias y Tecnología (CONAHCYT) of Mexico.

References

Adorian TJ, Rodrigues-Goulart F, Mombach PI, de Menezes-Lobato N, Dalcin M, Molinari M, Lazzari R, Picolli da Silva L (2016) Effect of a different dietary concentrates on the metabolism and indirect immune response in silver catfish. Animal Feed Science and Technology 215: 124–132. https://doi.org/10.1016/j.anifeedsci.2016.03.001

Álvarez-González CA, Civera-Cerecedo R, Ortiz-Galindo JL, Dumas S, Moreno-Legorreta M, Grayeb-Del Alamo T (2001) Effect of dietary protein level on growth and body composition of juvenile spotted sand bass, *Paralabrax maculatofasciatus*, fed practical diets. Aquaculture 194(1–2): 151–159. https://doi.org/10.1016/S0044-8486(00)00512-3

Andrew SM (2023) Production and nutritional value of *Pleurotus floridanus* grown on rice straw supplemented with *Leucanea leucocephala* foliage. Environmental and Sustainability Indicators 17: e100223. https://doi.org/10.1016/j.indic.2022.100223

Anson ML (1938) The estimation of pepsin, trypsin, papain and cathepsin with hemoglobin. Journal of General Physiology 22(1): 79–89. https://doi.org/10.1085/jgp.22.1.79

AOAC (2019) Official methods of analysis. 16th edn. Association of Official Analytical Chemists, Washington DC, USA, 1018 pp.

Bjørgen H, Li Y, Kortner T, Krogdahl Å, Koppang EO (2020) Anatomy, immunology, digestive physiology and microbiota of the salmonid intestine: Knows and unknows under the impact of an expanding industrialized production. Fish and Shellfish Immunology 107(A): 172–186. https://doi.org/10.1016/j.fsi.2020.09.032

Botta R, Asche F, Borsum JS, Camp EV (2020) A review of global oyster aquaculture production and consumption. Marine Policy 117: 103952. https://doi.org/10.1016/j.marpol.2020.103952

Bradford MM (1976) A rapid and sensitive method for the quantization of microgram quantities of protein utilizing the principle of protein-dye binding. Analytical Biochemistry 72(1–2): 248–254. https://doi.org/10.1016/0003-2697(76)90527-3

Chelladurai G, Venmathi Maran BA (2019) Dietary supplementation of mushroom extract enhances growth and antioxidant levels of *Babylonia spirata* (Mollusca: Gastropoda). Aquaculture Reports 15: e100218. https://doi.org/10.1016/j.aqrep.2019.100218

Chintati G, Osorio da Rosa L, Poleto L, Santo Branco C, Camassola M, Fontana RC, Dillon AJP (2022) Effect of different substrates on *Pleurotus* spp. Cultivation in Brazil—Ergothioneine and lovastatin. Journal of Food Composition and Analysis 107: e104367. https://doi.org/10.1016/j.jfca.2021.104367

Chu YI, Wang CM, Park JC, Lader PF (2020) Review of cage containment tank design for offshore fish farming. Aquaculture 519: e734928. https://doi.org/10.1016/j.aquaculture.2020.734928

Cruz-García LF, Ponce-Palafox JT, Hernández-Hernández LH, Tello-Salgado I, Hernández-Ocampo H, Benítez-Mandujano MA (2022) Effects of mushroom (*Pleurotus djamor* var. *roseus*) meal as feed supplement on the hematological responses and growth performance of Nile tilapia (*Oreochromis niloticus*) fingerlings. Latin American Journal of Aquatic Research 50(1): 13–21. https://doi.org/10.3856/vol50-issue1-fulltext-2700

Cruz-Solorio A, Garín-Aguilar ME, Leal-Lara H, Ramírez-Sotelo MG, Valencia del Toro G (2014) Proximate composition of *Pleurotus* fruit body flour and protein concentrate. Journal of Chemical, Biological and Physical Sciences 4(5): 52–60.

Dawood MAO, Eweedah NM, El-Sharawy ME, Awad SS, Doan HV, Paray BA (2020a) Dietary white bottom mushroom improved the growth, immunity, antioxidative status and resistance against heat stress in Nile tilapia (Oreo*chromis niloticus*). Aquaculture 523: e735229. https://doi.org/10.1016/j.aquaculture.2020.735229

Dawood MAO, Eweedah NM, Khalafalla MM, Khalid A, El Asely A, Fadl SE, Amin AA, Paray BA, Ahmed HA (2020b) *Saccharomyces cereviciae* increases the acceptability of Nile tilapia (*Oreochromis niloticus*) to the palm seed meal. Aquaculture Reports 17: e100314. https://doi.org/10.1016/j.aqrep.2020.100314

Del Mar EG, Largman C, Brodrick JW, Geokas MC (1979) A sensitive new substrate for chymotrypsin. Analytical Biochemistry 99(2): 316–320. https://doi.org/10.1016/S0003-2697(79)80013-5

Dulay RMR, Miranda LA, Malasaga JS, Kalaw SP, Reyes RG, Hou CT (2017) Antioxidant and antibacterial activities of acetonitrile and hexane extracts of *Lentinus tigrinus* and *Pleurotus djamor*. Biocatalysis and Agricultural Biotechnology 9: 141–144. https://doi.org/10.1016/j.bcab.2016.12.003

Erlanger B, Kokowsky N, Cohen W (1961) The preparation and properties of two new chromogenic substrates of trypsin. Archives of Biochemistry and Biophysics 95(2): 271–278. https://doi.org/10.1016/0003-9861(61)90145-X

Ferreira A, Cahú T, Xu J, Blennow A, Bezerra R (2022) A highly stable raw starch digestion α-amylase from Nile tilapia (*Oreochromis niloticus*) viscera. Food Chemistry 354: e129513. https://doi.org/10.1016/j.foodchem.2021.129513

Galkanda-Arachchige H, Davis DA (2019) Evaluation of differently processed soybean meal products as ingredients in practical diets for Pacific white shrimp *Litopenaeus vannamei*. Aquaculture Nutrition 26(2): 287–295. https://doi.org/10.1111/anu.12989

Gambelli D, Vairo D, Solfanello F, Zanoli R (2019) Economic of organic aquaculture: A systematic review. Marine Policy 108: e103542. https://doi.org/10.1016/j.marpol.2019.103542

Gatlin DM III (2010) Principles of fish nutrition. Southern Regional Aquaculture Center (SRAC). Publication No. 5003.

Guerrero-Zarate R, Álvarez-González CA, Jesús-Contreras R, Peña-Marín ES, Martínez-García R, Galaviz MA, López LM, Llera-Herrera R (2019) Evaluation of carbohydrate/lipid ratios on growth and metabolic response in tropical gar (*Atractosteus tropicus*) juvenile. Aquaculture Research 50(7): 1812–1823. https://doi.org/10.1111/are.14060

Hilton JW, Atkinson JL, Slinger SJ (1983) Effect of increased dietary fiber on the growth of rainbow trout (*Salmo gairdneri*). Canadian Journal of Fisheries and Aquatic Sciences 40(1): 81–85. https://doi.org/10.1139/f83-012

Hu Y, Tian G, Zhao L, Wang H, Ng TB (2017) A protease-resistance α-galactosidae from *Pleurotus djamor* with broad pH stability and good hydrolytic activity toward raffinose family oligosaccharides. International Journal of Biological Macromolecules 94(A): 122–130. https://doi.org/10.1016/j.ijbiomac.2016.10.005

Jegadeesh R, Lakshmanan H, Jang K-Y, Oh M, Oh YL, Im J-H (2020) Nutritional composition and antioxidant activity of pink oyster mushroom (*Pleurotus djamor* var. roseus) grown on a paddy straw substrate. Journal of Mushrooms 18(3): 189–200. https://doi.org/10.2174/1871525718666200303123557

Jiao F, Wang X, Song X, Jing H, Li S, Ren Z, Gao Z, Zhang J, Jia L (2017) Processing optimization and anti-oxidative activity of enzymatic extractable polysaccharides from *Pleurotus djamor.*

International Journal of Biological Macromolecules 98: 469–478. https://doi.org/10.1016/j.ijbiomac.2017.01.126

Johansen R, Needham JR, Colquhoun DJ, Poppe TT, Smith AJ (2006) Guidelines for health and welfare monitoring of fish use in research. Laboratory Animals 40(4): 323–340. https://doi.org/10.1258/002367706778476451

Justo A, Vizzini A, Minnis AM, Menolli N Jr, Capelari M, Rodríguez O, Malysheva E, Contu M, Ghignone S, Hibbett DS (2011) Phylogeny of the Plutaceae (Agaricales, Basidiomycota): Taxonomy and character evolution. Fungal Biology 115(1): 1–20. https://doi.org/10.1016/j.funbio.2010.09.012

Katya K, Yun Y-H, Yun H, Lee J-Y, Bai SC (2016) Effects of dietary fermented by-product of mushroom, *Pleurotus ostreatus*, as an additive on growth, serological characteristics and nonspecific immune response in juvenile Amur catfish, *Silurus asotus*. Aquaculture Research 47(5): 1622–1630. https://doi.org/10.1111/are.12623

Kim HS, Cho HS (2019) Dietary inclusion effect of feed ingredients showing high feeding attractiveness to rockfish (*Sebastes schlegeli* Hilgendorf 1880) on the growth performance, feed utilization, condition factor and whole body composition of fish (II). Comparative Biochemistry and Physiology, Part A: Molecular and Integrative Physiology 231: 66–73. https://doi.org/10.1016/j.cbpa.2019.01.011

Li H, Xue R, Sun J, Ji H (2023) Improving flesh quality of grass cat (*Ctenopharyngodon idellus*) by completely replacing dietary soybean meal with yellow mealworm (*Tenebrio molitor*). Animal Nutrition 12: 375–387. https://doi.org/10.1016/j.aninu.2022.12.004

Lin S-M, Zhou X-M, Zhou Y-L, Kuang W-M, Chen Y-J, Luo L, Dai F-Y (2020) Intestinal morphology, immunity and microbiota response to dietary fibers in largemouth bass, *Micropterus salmoide* [sic]. Fish and Shellfish Immunology 103: 135–142. https://doi.org/10.1016/j.fsi.2020.04.070

Maity GN, Maity P, Choudhury I, Bhattacharyya N, Acharya K, Dalai S, Mondal S (2019) Structural studies of a water insoluble β-glucan from *Pleurotus djamor* and its cytotoxic effect against PA1, ovarian carcinoma cells. Carbohydrate Polymers 222: 114990. https://doi.org/10.1016/j.carbpol.2019.114990

Maraux S, Louvard D, Barath J (1973) The aminopeptidase from hog-intestinal brush border. Biochimica et Biophysica Acta—Enzymology 321(1): 282–295. https://doi.org/10.1016/0005-2744(73)90083-1

McLean E (2023) 4.23—Feed ingredients for sustainable aquaculture. Pp. 392–423. In: Ferranti P. (Ed.) Sustainable food science—A comprehensive approach. Elsevier. https://doi.org/10.1016/B978-0-12-823960-5.00085-8

Mirghaed AT, Yarahmadi P, Hosseinifar SH, Tahmasebi D, Gheisvandi N, Ghaedi A (2018) The effects of singular or combined administration of fermented fiber and probiotic mucosal immune parameters, digestive enzyme activity, gut microbiota and growth performance of Caspian white fish (*Rutilus frisii kutum*) fingerlings. Fish and Shellfish Immunology 77: 194–199. https://doi.org/10.1016/j.fsi.2018.02.007

Mohtashemipour H, Mohammadian T, Mesbah M, Rezaie A, Mozanzadeh MT (2023) Acidifier supplementation in low-fish meal diets improved growth performance and health indices in Asian seabass (*Lates calcarifer*). Aquaculture Reports 29: 101502. https://doi.org/10.1016/j.aqrep.2023.101502

Moumita S, Das B (2022) Assessment of the prebiotic potential and bioactive components of common edible mushrooms in India and formulation of symbiotic microcapsules. LWT—Food Science and Technology 156: e113050. https://doi.org/10.1016/j.lwt.2021.113050

Nattoh G, Musieba F, Gatebe E, Mathara J (2016) Towards profiling differential distribution of bioactive molecules across four phenologies in *Pleurotus djamor* R22. Asian Pacific Journal of Tropical Disease 6(6): 472–480. https://doi.org/10.1016/S2222-1808(16)61071-X

NOM (2001) Norma Oficial Mexicana NOM-062-ZOO-1999, Especificaciones técnicas para la producción, cuidado y uso de los animales de laboratorio. Diario Oficial (Primera Sección), miércoles 2 de agosto de 2001. Gobierno de México. Pp. 107–165.

Nunes AJP, Dalen LL, Leonardi G, Burri L (2022) Developing sustainable, cost-effective and high-performance shrimp feed formulations containing low fish meal levels. Aquaculture Reports 27: e101422. https://doi.org/10.1016/j.aqrep.2022.101422

Pereira de Oliveira A, Naozuka J (2019) Preliminary results on the feasibility of producing selenium-enriched pink (*Pleurotus djamor*) and white (*Pleurotus ostreatus*) oyster mushrooms: Bioaccumulation bio-accessibility, and Se-proteins distribution. Microchemical Journal 145: 1143–1150. https://doi.org/10.1016/j.microc.2018.12.046

Ponzoni RW, Nguyen NH, Khaw HL, Hamzah A, Bakar KRA, Yee HY (2011) Genetic improvement of Nile tilapia (*Oreochromis niloticus*) with special reference to the work conducted by the WorldFish Center with the GIFT strain. Reviews in Aquaculture 3(1): 27–41. https://doi.org/10.1111/j.1753-5131.2010.01041.x

Qu H, Ke W, Wen Z, Guo B, Lu X, Zhao Y, Yang Y (2022) Effects of dietary carbohydrate on growth, feed utilization, hepatic glucose and lipid metabolism in endangered Yangtze sturgeon (*Acipenser dadryanus*). Aquaculture Reports 26: 101334. https://doi.org/10.1016/j.aqrep.2022.101334

Robyt JF, Whelan W (1968) Starch and its derivatives. Chapman and Hall, London.

Safari O, Sarkheil M (2018) Dietary administration of eryngii mushroom (*Pleurotus eryngii*) powder on haemato-immunological responses, bactericidal activity of skin mucus and growth performance of koi carp fingerlings (*Cyprinus carpio* koi). Fish and Shellfish Immunology 80: 505–513. https://doi.org/10.1016/j.fsi.2018.06.046

Salmones D (2017) *Pleurotus djamor*, un hongo con potencial aplicación biotecnológica para el neotrópico. Revista Mexicana de Micología 46: 73–85. https://doi.org/10.33885/sf.2017.46.1177

Solovyev M, Kashinskaya E, Gisbert E (2023) A meta-analysis for assessing the contributions of trypsin and chymotrypsin as the two major endoproteases in protein hydrolysis in fish intestine. Comparative Biochemistry and Physiology, Part A: Molecular and Integrative Physiology 278: e111372. https://doi.org/10.1016/j.cbpa.2023.111372

Soltan NM, Soaudy MR, Abdella MM, Hassaan MS (2023) Partial dietary fishmeal replacement with a mixture of plant protein sources supplemented with exogenous enzymes modify growth performance, digestibility, intestinal morphology, haemato-biochemical and immune responses for Nile tilapia, *Oreochromis niloticus*. Animal Feed Science and Technology 299: e115642. https://doi.org/10.1016/j.anifeedsci.2023.115642

Thongprajukaew K, Rodjaroen S (2020) The optimal period for changing the feeding regime of mono-sex male Nile tilapia (*Oreochromis niloticus*). Aquaculture Reports 17: e100392. https://doi.org/10.1016/j.aqrep.2020.100392

Turchini GM, Trushenski JT, Glencross BD (2018) Thoughts for the future of aquaculture nutrition: Realigning perspective to reflect contemporary issues related to judicious use of marine resources in aquafeeds. North American Journal of Aquaculture 81(1): 13–39. https://doi.org/10.1002/naaq.10067

Vasconez-Velez ME, Rodrigues da Luz JM, Soares da Silva MC, Soares-Cardoso W, de Souza-López L, Vieira NA, Kasuya MCM (2019) Production of bioactive compounds by the mycelial growth of *Pleurotus djamor* in whey powder enriched with selenium. LWT—Food Science and Technology 114: e108376. https://doi.org/10.1016/j.lwt.2019.108376

Versaw WK, Cuppett SL, Winters DD, Williams LE (1989) An improved colorimetric assay for bacterial lipase in nonfat dry milk. Journal of Food Science 54(6): 1557–1558. https://doi.org/10.1111/j.1365-2621.1989.tb05159.x

Walter H (1984) Proteinases: Methods with hemoglobin, casein and azocoll as substrates. Pp. 270–277. In: Bergmeyern HJ (Ed.) Methods of enzymatic analysis. Verlag Chemie, Weinham, Germany.

Wang J, Zhang H, Yang Q, Tan B, Dong X, Chi S, Liu H, Zhang S (2020) Effects of replacing soybean meal with cottonseed meal on growth, feed utilization and non-specific immune enzyme for juvenile white shrimp, *Litopenaeus vannamei*. Aquaculture Reports 16: e100255. https://doi.org/10.1016/j.aqrep.2019.100255

Wang J, Lan K, Wu G, Wang Y, Zhou C, Lin H, Ma Z (2022) Effects of dietary carbohydrate level on growth, feed utilization, energy retention, body composition, and digestive and metabolic enzyme activities of juvenile cobia, *Rachycentron canadum*. Aquaculture Reports 25: e101211. https://doi.org/10.1016/j.aqrep.2022.101211

Xavier B, Mergarajan S, Balla V, Sadu N, Ranjan R, Babu PPS, Ghosh S, Gopalakrishnan A (2023) Impact of starvation and re-feeding on growth and metabolic responses of Indian pompano (*Trachintus mookalee*) juveniles. Aquaculture 572: e739514. https://doi.org/10.1016/j.aquaculture.2023.739514

Ye H, Xu M, Liu Q, Sun Z, Zou C, Chen L, Su N, Ye C (2019) Effects of replacing Fish meal with soybean meal on growth performance, feed utilization and physiological status of juvenile obscure puffer, *Takifugu obscurus*. Comparative Biochemistry and Physiology, Part C: Toxicology and Pharmacology : 216: 75–81. https://doi.org/10.1016/j.cbpc.2018.11.006

Zhang J, Liu M, Yang Y, Lin L, Xu N, Zhao H, Jia L (2016) Purification, characterization and hepatoprotective activities of mycelia zinc polysaccharides by *Pleurotus djamor*. Carbohydrate Polymers 136: 588–597. https://doi.org/10.1016/j.carbpol.2015.09.075

Zhang W, Han Y, Shi K, Wang J, Yang C, Xu X (2022a) Effect of different sulfur-containing compounds on the structure, sensory properties and antioxidant activities of Maillard reaction products obtained from *Pleurotus citrinopileatus* hydrolysates. LWT—Food Science and Technology 171: e114144. https://doi.org/10.1016/j.lwt.2022.114144

Zhang Y, Liang X, Zhan W, Han M, Liu F, Xie Q, Guo D, Chen L, Lou B (2022b) Effects of dietary protein levels on growth performance, muscle composition and fiber recruitment of juvenile small yellow croaker (*Larimichthys polyactis*). Aquaculture Reports 27: e101335. https://doi.org/10.1016/j.aqrep.2022.101335

Acta Ichthyologica et Piscatoria 53, 2023, 173–189 | DOI 10.3897/aiep.53.105910

PENSOFT.

ACTA
ICHTHYOLOGICA
ET PISCATORIA

New developments in the analysis of catch time series as the basis for fish stock assessments: The CMSY++ method

Rainer FROESE[1], Henning WINKER[2], Gianpaolo CORO[3], Maria-Lourdes "Deng" PALOMARES[4], Athanassios C. TSIKLIRAS[5], Donna DIMARCHOPOULOU[6,7], Konstantinos TOULOUMIS[8], Nazli DEMIREL[9], Gabriel M. S. VIANNA[10], Giuseppe SCARCELLA[11], Rebecca SCHIJNS[4], Cui LIANG[12,13], Daniel PAULY[4]

1 *Helmholtz Centre for Ocean Research, GEOMAR, Kiel, Germany*
2 *Joint Research Centre, European Commission, Ispra, Italy*
3 *Institute of Information Science and Technologies, National Research Council of, Pisa, Italy*
4 *Sea Around Us, Institute for the Oceans and Fisheries, University of British Columbia, Vancouver, BC Canada*
5 *Laboratory of Ichthyology, School of Biology, Aristotle University of Thessaloniki, Thessaloniki, Greece*
6 *Biology Department, Dalhousie University, Halifax, Nova Scotia, Canada*
7 *Biology Department, Woods Hole Oceanographic Institution, Woods Hole, MA, USA*
8 *Hellenic Agricultural Organisation—Dimitra, Fisheries Research Institute, Nea Peramos, Kavala, Greece*
9 *Institute of Marine Sciences and Management, Istanbul University, Istanbul, Turkiye*
10 *Sea Around Us—Indian Ocean, School of Biological Sciences, University of Western Australia, Crawley, WA, Australia*
11 *National Research Council (CNR) - Institute for Marine Biological Resources and Biotechnologies (IRBIM), Ancona, Italy*
12 *CAS Key Laboratory of Marine Ecology and Environmental Sciences, Institute of Oceanology, Chinese Academy of Sciences, Qingdao, China*
13 *Laboratory for Marine Ecology and Environmental Science, Qingdao National Laboratory for Marine Science and Technology, Qingdao, China*

https://zoobank.org/3A7322C1-230A-49DE-A10C-1A0B6DFEB382

Corresponding author: Rainer Froese (rfroese@geomar.de)

Academic editor: Wojciech Piasecki ♦ **Received** 4 May 2023 ♦ **Accepted** 17 September 2023 ♦ **Published** 30 October 2023

Citation: Froese R, Winker H, Coro G, Palomares MLD, Tsikliras AC, Dimarchopoulou D, Touloumis K, Demirel N, Vianna GMS, Scarcella G, Schijns R, Liang C, Pauly D (2023) New developments in the analysis of catch time series as the basis for fish stock assessments: The CMSY++ method. Acta Ichthyologica et Piscatoria 53: 173–189. https://doi.org/10.3897/aiep.53.105910

Abstract

Following an introduction to the nature of fisheries catches and their information content, a new development of CMSY, a data-limited stock assessment method for fishes and invertebrates, is presented. This new version, CMSY++, overcomes several of the deficiencies of CMSY, which itself improved upon the "Catch-MSY" method published by S. Martell and R. Froese in 2013. The catch-only application of CMSY++ uses a Bayesian implementation of a modified Schaefer model, which also allows the fitting of abundance indices should such information be available. In the absence of historical catch time series and abundance indices, CMSY++ depends strongly on the provision of appropriate and informative priors for plausible ranges of initial and final stock depletion. An Artificial Neural Network (ANN) now assists in selecting objective priors for relative stock size based on patterns in 400 catch time series used for training. Regarding the cross-validation of the ANN predictions, of the 400 real stocks used in the training of ANN, 94% of final relative biomass (B/k) Bayesian (BSM) estimates were within the approximate 95% confidence limits of the respective CMSY++ estimate. Also, the equilibrium catch-biomass relations of the modified Schaefer model are compared with those of alternative surplus-production and age-structured models, suggesting that the latter two can be strongly biased towards underestimating the biomass required to sustain catches at low abundance. Numerous independent applications demonstrate how CMSY++ can incorporate, in addition to the required catch time series, both abundance data and a wide variety of ancillary information. We stress, however, the caveats and pitfalls of naively using the built-in prior options, which should instead be evaluated case-by-case and ideally be replaced by independent prior knowledge.

Keywords

data limited stock assessments, Elasmobranchii, finfish, global fisheries, informative priors, shellfish, stock status, Teleostei

Introduction

National and international organizations, notably the Food and Agricultural Organization of the United Nations (FAO), have been tasked with evaluating the global status of fisheries, including countries or regions without age-structured stock assessments. Thus, their staff resorted to developing graphical typologies of annual catch time series, allowing inference on the status of the underlying stocks (e.g., Caddy and Gulland 1983). One of these typologies (see fig. 7 in Csirke 1984) was quite influential and was reprinted in a major textbook (fig. 11 in Hilborn and Walters 1992) and in a review (Kleisner et al. 2013). Additionally, based on these typologies, other FAO staff created stock-status plots (Grainger and Garcia 1996), now a regularly updated part of the bi-annual *State of Fisheries and Aquaculture* (SOFIA) (Fig. 1). The detailed methodology for creating FAO's recent stock status plots and for selecting the stocks they represent could be more transparent (Ye 2011); notably, it is unclear how much they depend on the catch trend typologies mentioned above versus "formal" stock assessment outputs, particularly in the Global South, where these assessments are less frequent. However, as shown in Kleisner et al. (2013), their basic trends can be straightforwardly reproduced by the simplified method detailed in Froese and Kesner-Reyes (2002) and Pauly et al. (2008).

Although helpful to get a "big picture" overview of fisheries, the empirical catch-only methods behind the stock status plots (Csirke 1984; Grainger and Garcia 1996; Froese and Kesner-Reyes 2002; Froese et al. 2012) are not sufficient for stock-specific status classification and were never meant to assess single stocks for fisheries management. However, especially the approach of Froese and Kesner-Reyes (2002), which scales catches relative to their maximum and evaluates them relative to their occurrence before or after the maximum, has formed the basis of subsequent approaches (Froese et al. 2012; Kleisner et al. 2013) and was used to derive preliminary priors of stock status in the Catch-MSY method of Martell and Froese (2013) and the CMSY method of Froese et al. (2017).

The purpose of this study was to present recent developments and advances in these methods, such as considering the inverse correlation between productivity and carrying capacity for an examined stock, the application of an Artificial Neural Network (ANN) to predict preliminary stock status from time series of catches, and the use of scatterplot catch and biomass data of hundreds of stocks to derive empirical uncertainty ranges for relative biomass priors predicted from relative catch.

The origins of CMSY++. CMSY++ and its predecessors are based on the first derivative of the logistic curve of population growth (Verhulst 1838), with numbers of individuals replaced by the sum of their body weights (Schaefer 1954, 1957)

$$B_{t+1} = \left\{B_t + r\left(1 - B_t/k\right) - C_t e^{\varepsilon_t}\right\} e^{\eta_t} \qquad [1]$$

where B_t is the biomass and C_t is the catch in tonnes in year *t*, *r* (year^{-1}) is the intrinsic rate of population growth, and *k* is the carrying capacity of the environment for this population in tonnes, ε_t represents the normally distributed observation error of catches and η_t the process error, respectively, and are implemented as lognormal error terms. Display of these lognormal error terms is omitted in subsequent equations. Thus, if a reasonable estimate of start biomass and *k* is available to quantify the unexploited and initial stock size, and if a reasonable estimate of *r* can be inferred from life-history traits (as done in FishBase; Froese and Pauly 2023), a time series of biomass, based on the time series of catches, can be projected, with maximum sustainable fishing mortality F_{MSY} = *r*/2 and minimum biomass that can produce maximum sustainable yield (MSY) as B_{MSY} = *k*/2. This approach, known as "stochastic reduction analysis" (Kimura and Tagart 1982; Walters et al. 2006), was applied, e.g., by Martell (unpublished[*]) to a well-studied stock of lingcod (*Ophiodon elongatus* Girard, 1854) in British Columbia, and by Christensen (2006) to marine mammals globally.

While examining in depth the method that formed the basis of his Bachelor's thesis (Martell unpublished), Steven Martell found that in a wide-ranging plot of *k* vs. *r*, only a small cluster of *k* and *r* pairs were "viable", i.e., did not lead to a population crash nor suggested that a heavily fished population remained close to carrying capacity, and resulted in a final relative biomass within the expected range based on independent information.

Thus, was born the "Catch-MSY" method of Martell and Froese (2013), where in Monte-Carlo fashion, thousands of potential biomass trajectories were filtered according to the above criteria, and "viable" *r*–*k* pairs then formed a triangle in log space (see fig. 1c in Martell and

---

[*] Martell S (1997) Reproductive outputs and demographics of lingcod (*Ophiodon elongatus*) in Howe Sound. BSc Thesis, University of British Columbia, Vancouver, BC, Canada.

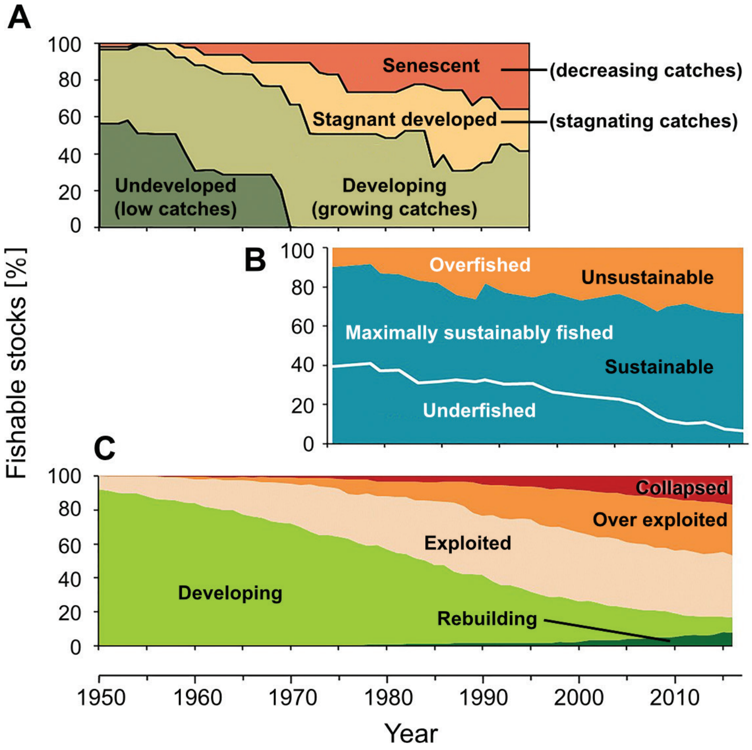

Figure 1. Common versions of "catch-only" assessments, which may be verified against real stock assessments: **A**: The key graph in Grainger and Garcia (1996), for which the status of the world's marine exploited stocks was inferred from the slope of polynomials fitted to catch time series, as subsequently done for years by FAO; **B**: Reproduction of fig. 19 in SOFIA (FAO 2020), which summarizes the status of global stocks based on an opaque mix of methods ranging from real stock assessments to subjective interpretation of catch trends in data-poor fisheries (see Ye 2011); **C**: Stock status plots based on the simplification of the catch-only method in **A** by Froese and Kesner-Reyes (2002), as implemented by Pauly et al. (2008) to work with the catch "reconstructed" globally by the Sea Around Us. Note that **C** considers stock rebuilding, but that, as a whole, **A**, **B**, and **C** convey the same message.

Froese 2013). Reasonable estimates of MSY (with confidence limits) could be derived from the geometric mean of viable *r* and *k* values inserted in the equation MSY = *r* · *k*/4 where an under-estimation of *r* was compensated for by an over-estimation of *k* or vice versa (Schiller 2014).

However, as Martell and Froese (2013) explicitly pointed out, the geometric means of viable *r* and *k* values diverged systematically from independent estimates based on full assessments, with *r* being typically underestimated and *k* being overestimated. Despite the explicit warning to use only MSY and not the reference points $F_{\text{MSY}} = r/2$ and $B_{\text{MSY}} = k/2$ for management purposes, subsequent independent tests of the Catch-MSY method (Rosenberg et al. 2014; Chong et al. 2019; Dowling et al. 2019; Zhou et al. 2018; Free et al. 2020; Pons et al. 2020) often gave low scores to the method because they ignored that warning and reproduced the known biases in *r* and *k*.

From Catch-MSY to CMSY. Froese et al. (2017) addressed several shortcomings of the Catch-MSY method, mainly by devising an empirical method that identified the most probable *r*–*k* pair not at the center, but near the tip of the triangle of viable pairs. Basically, the 75th percentile of viable *r* values was used as the best *r* estimate and a central value of viable *k* values within the confidence limits of *r* was used as the best *k* estimate. This enhanced method, called CMSY, could produce reasonable predictions of relative biomass (B_t/B_{MSY}) and exploitation rate (F_t/F_{MSY}). CMSY also included a number of additional improvements, such as a narrower range of potential *k* values based on maximum catch and the prior *r*-range (derived from FishBase; Froese and Pauly 2023), and default ranges (i.e., if not supplied by the user) for priors for relative biomass derived from the empirical rules used by Froese and Kesner-Reyes (2002) and Froese et al. (2012) for the construction of stock-status plots. Also, a Bayesian state-space surplus production model (BSM) was added to provide a second set of results based on abundance indices (catch per unit of effort, stock size index, acoustic or trawl survey trends, etc.) if such information was available.

Moreover, CMSY was formulated to account for the generally observed reduction of recruitment at low population sizes (Ricker 1954; Beverton and Holt 1957; Barrowman and Myers 2000; Froese et al. 2017) replacing Equation 1 by

$$B_{t+1} = B_t + (4B_t/k)r(1 - B_t/k)B_t - C_t \mid B_t/k < 0.25 \qquad [2]$$

where ($4B_t/k$) creates a linear decline of *r* if biomass falls below *k*/4, to account for reduced recruitment and thus productivity at low population size. Half of B_{MSY}, which is *k*/4 in the Schaefer model context, is usually chosen as the proxy demarcation of the biomass below which recruitment may be impaired (e.g., ICES 2021, p. 3). This empirical feature makes it unnecessary to require additional parameters for a stock-recruitment relation (as in, e.g., Schnute and Richards 2002), which are typically not known in data-limited stocks. This feature was subsequently adopted in other surplus production modelling software, such as JABBA (Winker et al. 2018) and sraplus (Ovando et al. 2021). It accounts for the "weak" Allee effect (Allee 1938; Walters and Kitchell 2001) or the beginning of depensation, as defined by Perälä et al. (2022), but not for the "strong" Allee effect of Hutchings (2015), which describes an even more drastic decline of recruitment and thus resilience and productivity at very low population size. More importantly, by reducing r, it reduces the reference point for maximum sustainable fishing mortality $F_{\text{MSY}} = r/2$, a major advance over models that consider F_{MSY} as a constant reference point even when the rate of recruitment, which is a major component of productivity and thus of r and F_{MSY}, is known to be impaired. Fig. 2 shows a schematic plot of Equation 2, indicating areas of recruitment overfishing ($B/k < 0.25$), growth overfishing ($B/k < 0.5$) and sustainable fishing ($B/k > 0.5$) (Froese and Proelss 2012). While the equilibrium curve of Equation 2 suggests that, theoretically, a stock can be maintained indefinitely at any B/k level, stocks below $B/k = 0.5$ are likely to fail to fulfill their natural roles as prey and/or predator (Pauly and Froese 2021; Scotti et al. 2022) and the resulting changes in the ecosystem are likely to make such fisheries unsustainable.

A recent study by Bouch et al. (2021) showed that if CMSY was applied with default prior settings and compared against data-rich assessments, 14 of 17 final biomass estimates (82%) differed less than 50% from official biomass estimates, while a data-moderate method (SPiCT) only had 6 (35%) estimates in that range (fig. 4 in Bouch et al. 2021). On the other hand, Ovando et al. (2022) criticized default priors in catch-only methods and highlighted the importance of setting reasonably accurate priors of r–k for providing an accurate estimate of stock status. Sharma et al. (2021) found that CMSY results for the final year improved substantially with the quality of the prior information. Pons et al. (2020) reported that CMSY reduced the bias in estimates of F/F_{MSY} by more than 50% compared to Catch-MSY based on a simulation study. Zhou et al. (2018) also found that CMSY is more accurate than the original Catch-MSY method and that it performed well in estimating the final relative stock size of 13 Australian stocks in comparison with the official age-structured assessment estimates. As a further confirmation of usefulness, CMSY was fitted with results that were deemed reasonable to a multitude of species and stocks globally (Cheung et al. 2022), in Europe (Froese et al. 2018a), Eastern Mediterranean (Demirel et al. 2020; Saygu et al. 2023), Canada (Schijns 2020; Schijns et al. 2021), China and surroundings (Zhang et al. 2018; Liang et al. 2020; Roa-Ureta 2020; Wang et al. 2020a, 2020b; Kang et al. 2022), Africa (Musinguzi et al. 2020; Palomares et al. 2020a), Mexico (Ferrer et al. 2022), and other countries and regions (Cruz et al. 2020; Palomares et al. 2019, 2020b, 2021) (Fig. 3). Interestingly, CMSY has recently been extended to a bio-economic stock assessment using price data in addition to the time series of catch (Lancker et al. 2023).

However, there remained a stumbling block also identified by Bouch et al. (2021): the use of rigid constraints, either entered by the user or generated by the software as internal heuristics, that the biomass trajectory was forced to accommodate. Setting appropriate initial biomass priors at the start of the time series (B_{start}/k) is a general challenge in cases where the catch series is short and does not include historical catches that would reflect the initial lightly exploited stock biomass (i.e., $B_{\text{start}}/k = 0.9$–1.0). Noting this, the ICES benchmark workshop on SPiCT assessments (ICES 2021: WKMSYSPiCT), for example,

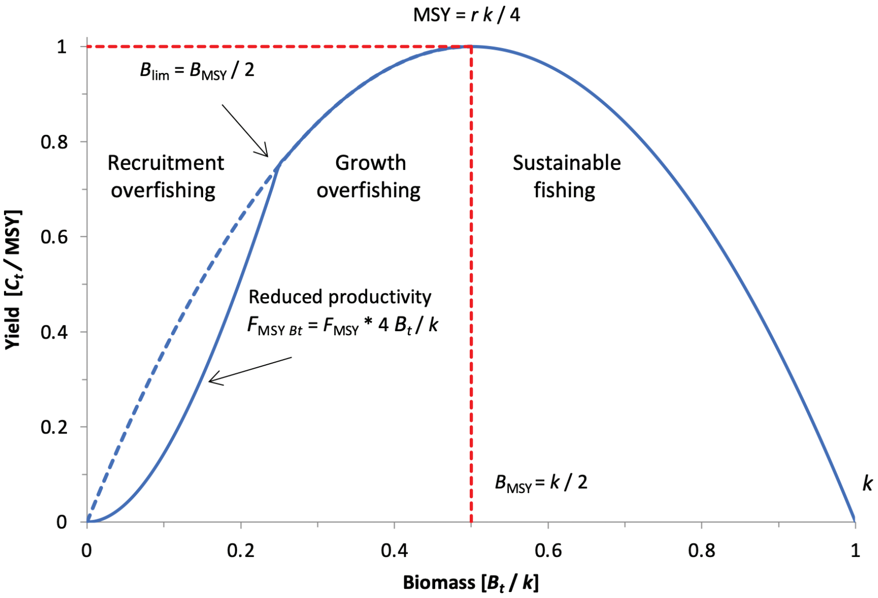

Figure 2. Schematic representation of the surplus production model used by CMSY, with indication of impaired recruitment due to small stock size, where F_{MSY} is reduced linearly with decline in biomass.

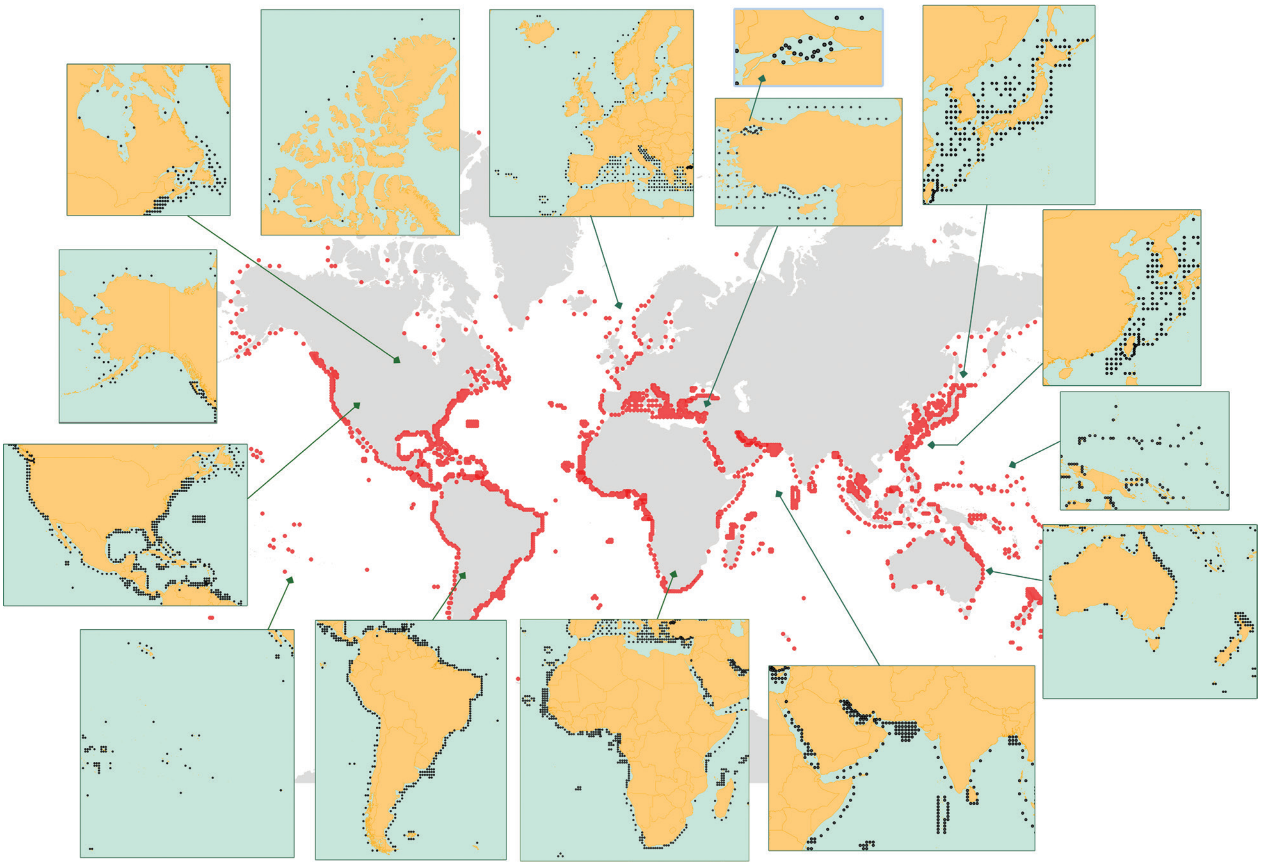

Figure 3. Maps showing the locations of the centroids of the over 2000 stock assessments performed with CMSY (~20%) and CMSY ++ (~80%) in all parts of the world. Generally, the assessments in wealthier countries (USA, Canada, Australia, New Zealand, EU-member states) were complemented with CPUE or other ancillary data, and well-informed priors for the terminal B/k values; such information was often lacking for many countries in low latitudes, but the results still matched what was known of their fisheries. Based on original Sea Around Us data, and previous analyses in Froese et al. (2018a); Zhang et al. (2018); Demirel et al. (2020); Cruz et al. (2020); Schijns (2020); Liang et al. (2020); Roa-Ureta (2020); Wang et al. (2020a,b); Musinguzi et al. (2020); and Palomares et al. (2019, 2020a, 2020b).

recommended that priority should be on reconstructing catch time series, but where this is not possible and initial catches are already close to the observed maximum, the B_{start}/k prior should be set to 0.5 or lower.

The remaining constraints, i.e., the biomass priors in the Bayesian context, were:

- The fraction expressing the biomass depletion (from carrying-capacity) assumed to have already occurred at the start of the time series (B_{start}/k);
- The fraction expressing the biomass depletion assumed to have occurred at some intermediate year of the time series (B_{int}/k); and
- The fraction expressing the biomass at the end of the catch time series (B_{end}/k).

From CMSY to CMSY++. Following the publication of the CMSY method (Froese et al. 2017), the code implementing it underwent a series of improvements, also in response to feedback from its users. Notably an option to consider the degree of technological creep, i.e., an increase in catch per unit of effort (CPUE) not caused by increase in biomass, was introduced based on Palomares and Pauly (2019).

In a workshop held in November 2019 in Thessaloniki, Greece, it became evident that the Bayesian model (BSM) requiring time series of catch and abundance as main input could also be run without abundance data, making it a “catch-only” Bayesian method that could replace the Monte-Carlo approach used in the original CMSY. In other words, CMSY++ and BSM are nested within a single JAGS model and use the same parameterization and catch input, the only difference being that CMSY++ has no input of abundance data. This enables a consistent and continuous transition to fitting abundance indices to as little as two observations should such information become available. In cases where the abundance index is informative about the trend of the abundance trajectory, the user has the option to relax or disable the terminal and intermediate depletion priors. This is particularly relevant for estimating the short-term response to management interventions such as catch quota reductions (Wetzel and Punt 2015).

Also, in Catch-MSY and CMSY, a prior for carrying capacity was derived from the reasoning that a lower limit of k should be larger than the highest observed catch, that an upper limit of k should be 10–100 times higher than the lower limit, and that higher productivity r would suggest a narrower prior range of k. Building on the good correlation between maximum catch and MSY observed in hundreds of stocks (Fig. 4), CMSY++ instead derives a heuristic prior for MSY from maximum catch and then obtains a prior for k from $k_{prior} = 4\ MSY_{prior}/r_{prior}$. Note that this method only works if catches in the time series have exceeded MSY (see Fig. 4 for examples where that requirement was violated).

Another important improvement was the replacement of the rigid uniform r–k prior space with a multivariate lognormal (MVLN) prior that accounts for the negative correlation between k and r within a population, and where lower probabilities are assigned to peripheral r–k pairs further away from the core of the ellipsoid r–k distribution (Fig. 5b). The MVLN prior for r–k is a function of the means and the covariance matrix of $\log(r_{prior})$ and $\log(k_{prior})$; see details below.

The challenge of deriving more rigid biomass priors was also addressed in another major development. An Artificial Neural Network (ANN) now provides the option to predict default relative biomass priors (B/k) from catch relative to prior MSY, based on traits of catch patterns derived from hundreds of test stocks (but see discussion below, stressing that ANN is just a "convenience-add-on", meant to assist users in selecting the best available prior information).

Other improvements include:

- The rigid, uniform prior B/k ranges of CMSY were replaced with beta-distributions which have the desirable property for biomass depletion priors of being bounded by 0 and 1 (Winker et al. 2018) with increasing skewness as either end of the spectrum is approached; this resembles the uneven distribution of relative biomass around the equilibrium curve in Fig. 6.
- To correct a remaining bias of r–k pairs towards high k and low r, the lower right focus of the ellipse containing "viable" r–k pairs was used as "best" estimate, with confidence intervals derived from pairs where r was larger than the 25th percentile of "viable" r.

In summary, the purpose of this study is to present the history and latest developments of the catch-only CMSY++ method, and to compare its predictions with those of a regular surplus production model, which has time series of abundance information as additional input, everything else being equal.

Materials and methods

Description of the stocks used for preliminary testing and training. A data set with times series of catch and abundance for 400 different stocks was assembled to train the Artificial Neural Network and to understand the correlation between the MSY prior derived from maximum catch and MSY estimated by BSM from catch and abundance (Fig. 4). The stocks stem from 11 large marine ecosystems covering 87 marine ecoregions worldwide, including 10 Arctic stocks, 101 North Pacific stocks, 181 North Atlantic stocks, 14 South Pacific and South Atlantic stocks, 36 tropical stocks, 5 stocks from South Africa, 26 stocks from Australia, and 27 wide-ranging stocks. About three quarters of the species are demersal and one quarter is pelagic. There are 321 teleost, 22 elasmobranch, and 57 invertebrate stocks. Invertebrates are mainly represented by crustaceans (shrimps and lobsters) and mollusks (bivalves and cephalopods). Resilience categories range from very low to medium. Recent biomass was severely depleted in 106 (27%) of the stocks. Twenty-five stocks (6%) had recent biomass close to the unexploited level. The longest time series started in 1876 (with the actual years analyzed starting in 1940) and the shortest in 2005. For use in training, some of the time series were shortened to exclude recent periods where e.g., declining catch was not caused by low or declining biomass and thus the assumed relation between catch and biomass was broken (see also discussion of caveats below). Catch and abundance data were derived from official stock assessment reports such as summarized in ICES Stock Assessment Graphs (https://standardgraphsicesdk/stockListaspx) for the Northeast Atlantic and in NOAA Stock SMART (https://wwwstnmfsnoaagov/stocksmart?app=browse-by-stock) for North America. More details on the stocks and the sources are available in the files Train_Catch_9.csv, Train_ID_9.csv and Out_Train_ID_9.csv, which are available from https://oceanrep.geomar.de/53324/.

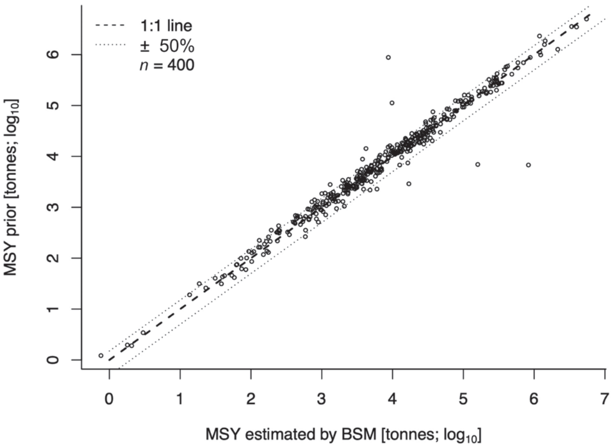

Figure 4. Plot of MSY prior derived from maximum catch over MSY estimated with BSM for the 400 stocks used for training ANN. The outliers are stocks where catches never exceeded MSY, for which neither CMSY nor the method to drive MSY priors should be used. The dashed 1:1 line indicates identical values whereas the dotted lines indicate deviations of ±50%. Note that CMSY++ estimates of MSY would fall vertically between the MSY priors and the 1:1 line.

Simulated data. Simulated catch and CPUE data (24 stocks) were created so that the simulated parameter values and stock status estimates were "true" known quantities for performance evaluation. For convenience, k was set to 1000 and r was set at 0.06, 0.25, 0.5, and 1.0 to represent species

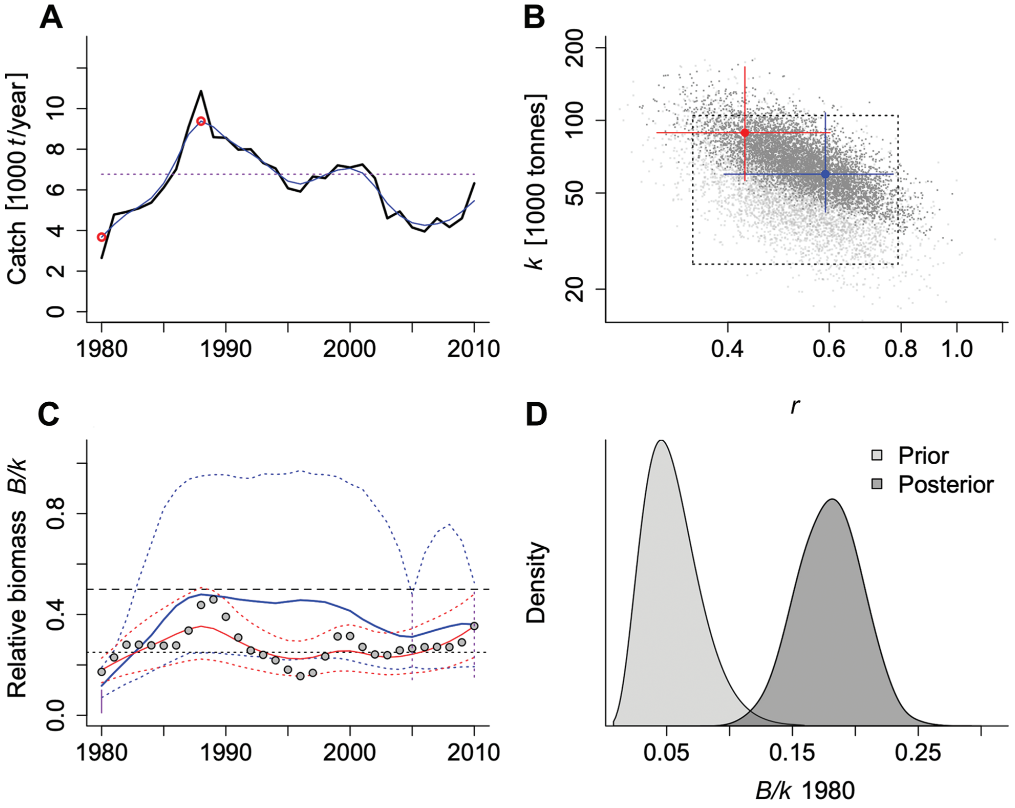

Figure 5. Examples of graphical output of CMSY++, here for European plaice (*Pleuronectes platessa*) in the eastern English Channel. Panel (**A**) shows the time series of catch from 1980 to 2011, with the thin blue curve representing smoothed catch and the red circles the smoothed minimum and maximum values. Panel (**B**) shows as dotted box the prior range for *r* and *k*. The dots in light grey indicate potential *r*–*k* pairs and the dark grey dots indicate pairs determined as viable by the catch-only CMSY++ analysis. The blue cross indicates the best CMSY++ estimate for *r*–*k*, with approximate 95% confidence limits. The red cross indicates the corresponding estimate derived from catch and CPUE by BSM. Panel (**C**) shows the time series of relative biomass *B*/*k* as estimated by CMSY++ (blue curve) and BSM (red curve) with dotted 95% confidence limits. The grey points indicate the available CPUE data. The horizontal lines indicate B_{MSY} at 0.5 *k* and B_{lim} at 0.25 *k*. The vertical purple line in the lower left corner indicates the *B*/*k* prior set by the user to 0.01–0.1. The dotted vertical lines in 2005 and 2011 are the prior *B*/*k* ranges set by the Neural Network. Panel (**D**) compares the density of the light-grey *B*/*k* prior set by the user for 1980 with the corresponding dark-grey posterior density estimated by BSM.

with very low, low, medium, and high resilience, respectively. For a simulated time series horizon of 50 years, biomass patterns of continuously high, continuously low, high to low, low to high, low–high–low, and high–low–high were created. The desired patterns were produced by inserting high or low catches into Equation 2 and calculating the biomass in subsequent years. The simulated data and the CMSY++ results are available from https://oceanrep.geomar.de/53324/ [files SimSpecCPUE_4_NA.csv, SimCatchCPUE_4.csv, Out_July082021_SimSpecCPUE_4_NA.csv, CMSY++16_Sim_8.R].

Derivation of $\mathrm{MSY}_{\mathrm{prior}}$ and multivariate-lognormal *r*–*k* distribution. Similar to other well-established surplus productions models such as SPiCT (Pedersen and Berg 2017) or JABBA (Winker et al. 2018), CMSY++ assumes lognormal prior distributions for *r*, *k*, and MSY, thus avoiding negative values in ranges of uncertainty for these parameters. Building on the good empirical relation between maximum catch and plausible MSY ranges observed among the 400 stocks used for testing (Fig. 4), a prior for MSY was attained as follows: if the time series of catch was more or less flat or ascending such that the maximum catch occurred in its last 5 years, then the mean of the three highest catches was taken as prior for MSY. This was done because a flat or ascending time series without recent decline was deemed unlikely to have exceeded MSY by much, if at all. In contrast, if catches were declining after a peak, that peak was likely overshooting MSY. Therefore, under such conditions, ¾ of the mean of the 5 highest catches in the time series was taken as prior for MSY. The mean of three or five catches was chosen to reduce the misleading impact of single, extraordinary high catches. Note that this procedure assumes that MSY is equal to or smaller than the highest catch values, i.e., this approach and CMSY in general are not suitable for lightly exploited stocks where catch never approached MSY (see fig. 3 in Martell and Froese 2013), or where such catches were not included in the time series.

Log(r_{prior}) is derived from life-history traits and log($\text{MSY}_{\text{prior}}$) is derived from maximum catch, i.e., these methods of derivation are uncorrelated, there is no circularity in the derivation, and the priors can thus be drawn from lognormal distributions without violating statistical assumptions about independence. These priors then provide the solution for $k_{\text{prior}} = 4\ \text{MSY}_{\text{prior}}/r_{\text{prior}}$. Note that if no variability were assumed for $\text{MSY}_{\text{prior}}$, this would result in a fixed log(k)–log(r) correlation of –1 (equation 5 in Froese et al. 2017). In reality, correlations vary between zero and –1, e.g., between –0.44 and –0.98 in the BSM results for the 400 training stocks (see Out_Train_ID_9.csv available from https://oceanrep.geomar.de/53324/).

The Schaefer model can be expressed as a function of r and MSY, without k (Equation 3); however, this arrangement does not change the dynamics of the model and the new term for surplus production seems less intuitive than the original one (Equation 1).

$$B_{t+1} = B_t + r \cdot B_t - \frac{(rB_t)^2}{4\text{MSY}} - C_t \qquad [3]$$

To retain the original form of the CMSY base model (Equation 2) with parameters r and k, the within-stock correlation between r and k was accounted for in a MVLN distribution implemented by: (1) drawing a large sample (n = 10 000) of independent random deviates of log($\tilde{r}$) and log($\widetilde{MSY}$) from their prior distributions; (2) computing the corresponding log($\tilde{k}$) = log(4) + log($\widetilde{MSY}$) – log($\tilde{r}$) and (3) computing the means and the covariance of log($\tilde{r}$) and log($\tilde{k}$), which are (4) then passed on as covariance matrix for the r–k ~ MVLN prior in the CMSY++ and BSM model formulations (see bsm() function in CMSY++16R code, which is available from https://oceanrep.geomar.de/53324/). The biomass dynamic in Equation 3 was implemented as a Bayesian state-space model that accounted for random variability in population dynamics (process error) and catch (observation error) (see Equation 1). This way, biomass over time was modelled as a sequence of random variables. This avoided the model to be completely driven by priors, which occurs when random variables are linked through a deterministic function (Borel's paradox: Schweder and Hjort 1996).

Application of an Artificial Neural Network in prediction of *B*/*k* priors. A feed-forward Artificial Neural Network (ANN) (Fritsch et al. 2019) was chosen for classifying stock status as being above or below the MSY level to accommodate Equation 4. ANN input consists of characteristics of the catch time series such as overall shape, difference between minimum and maximum catch, and slope in the first and final years. The network was trained with time series of 400 stocks (see detailed description above), which were selected to reflect the interplay of their catch and abundance data as described by Equation 2, so that the ANN could detect and learn typical patterns that allowed for the prediction of relative biomass (B/k) priors from relative catch (C/MSY). The time series of B/k were estimated with BSM from catch and abundance data and were treated as "true" for the purpose of the training. Specifically, ANN was set to predict whether B was above or below B_{MSY} for the start year, an intermediate year, and the final year of the time series. ANN was designed to have one classification output neuron that simulated a variable A_t with a binary probability distribution with values of either 1 (B/k above 0.5) or –1 (B/k below 0.5) The equilibrium B/k prior for reference year t, with catch value C_t, was then derived as

$$(B/k)_{t\ \text{prior}} = \frac{1 + A_t\sqrt{1 - C_t/\text{MSY}_{\text{prior}}}}{2} \qquad [4]$$

Note that Equation 4 only gives real number solutions if $C_t < = \text{MSY}_{\text{prior.}}$ Therefore, its application was restricted to cases where $C_t < 0.99\ \text{MSY}_{\text{prior}}$. The optimal ANN topology was found using the growing strategy (Bishop 1995), while performing 20-fold cross-validations with 95% to 5% random separation into training and test data sets and was made up of one hidden layer with 71 neurons. As an alternative model, we also tested a Long Short Memory "end-to-end" model (Hochreiter and Schmidhuber 1997) that accepted the entire catch time series as input but did not produce better predictions. During the cross-validation process, the ANN accuracy was assessed based on the calculation of correct classifications of relative biomass (B/k) being above or below the MSY threshold for the start, intermediate and end years. Using more classes or continuous output ended in lower accuracy and more frequent over-fitting, i.e., in a lower generalization capacity. Moreover, using ANNs instead of other models was justified by the importance of processing the time series data as a whole, i.e., by automatically modelling inter-sample correlation, which is a primary driver of time series classification accuracy (Coro et al. 2021). After selecting and training the optimal model, we used simulated stocks to assess the ANN prediction accuracy of biomass being above or below B_{MSY} for the start, intermediate, and end year of the time series, while using the "true" values to calculate the percentage of the correct predictions. Also, the "true" B/k value in the last year was compared with the respective CMSY++ estimate, with approximate 95% confidence limits.

How uncertainty of *B*/*k* priors was established. Equation 4 describes how a point estimate of relative equilibrium biomass (B/k) was derived from catch relative to MSY. Catch and biomass are rarely in equilibrium in real world stocks and the width and shape of uncertainty vary with the position of the equilibrium point estimate in B_t/k–C_t/MSY space (see distribution of points around the equilibrium curve in Fig. 6). As a pragmatic solution, ranges of uncertainty were derived as follows: (1) the 5th and 95th percentile of B_t/k values and the median of C_t/MSY values were determined for all points where

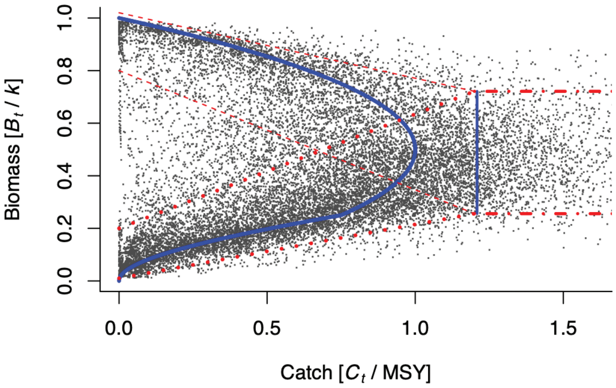

Figure 6. Scatterplot of relative biomass (B_t/k) over relative catch (C_t/MSY), both estimated with BSM, with 18 341 points for 400 stocks. The blue curve is the equilibrium biomass prediction from Equation 2. The vertical blue line indicates the range that contains 90% of the (B_t/k) points for catches above MSY. The red dashed lines indicate approximate 95% confidence ranges for prior B_t/k.

catch exceeded MSY (C_t/MSY > 1); (2) B_t/k values that bracketed most of the variability for the case of close to zero catches (C_t/MSY = 0) were chosen for high and low biomass; (3) the B_t/k values in (2) were treated as intercepts of linear regression lines that connected them to the 5th and 95th B_t/k percentiles determined in (1); and (4) for catches larger than 1.21 MSY (the median of catches above MSY), a fixed range of uncertainty in B_t/k was used. The resulting equations for prior B_t/k ranges as a function of C_t/MSY and their being above or below B_{MSY} are shown in Table 1.

Table 1. Equations to estimate ranges of uncertainty of default B_t/k priors derived from reported catch relative to the prior for MSY.

Prior B_t/k	Uncertainty range	B_t above or below B_{MSY} or catch above MSY
Upper range	$1.02 - 0.247 * C_t/\text{MSY}_{\text{prior}}$	Above B_{MSY}
Lower range	$-0.8 - 0.45 * C_t/\text{MSY}_{\text{prior}}$	Above B_{MSY}
Upper range	$-0.2 + 0.431 * C_t/\text{MSY}_{\text{prior}}$	Below B_{MSY}
Lower range	$0.01 + 0.203 * C_t/\text{MSY}_{\text{prior}}$	Below B_{MSY}
Upper range	$0.721\ k$	Catch above MSY
Lower range	$0.256\ k$	Catch above MSY

For example, for a catch of 0.5·MSY and a biomass below 0.5 · k, the dashed red lines in Fig. 6 propose a prior B/k range of 0.11–0.42; for catches at or above MSY, the parallel red lines propose a prior B/k range of 0.26–0.72. Remember that the pattern-based ANN B/k priors thus derived are only a "convenience-add-on" meant to assist CMSY++ users in evaluating and objectively selecting the best possible prior ranges for the analysis (see also discussion of biomass priors below).

Derivation of equilibrium curves. The equilibrium curve for the interplay between relative biomass (B/k) and relative catch (C/MSY) for the modified Schaefer model shown in Figs. 5 and 7 was derived from

$$\frac{C}{\text{MSY}} = \left(4\frac{B}{k} - \left(2\frac{B}{k}\right)^2\right)\cdot \text{RC} \qquad [5]$$

where RC stands for recruitment correction with RC = 4 B/k if $B/k < 0.25$ and RC = 1 otherwise (same as in Equation 2)

The equilibrium curve for the Fox (1970) model shown in Fig. 7 was derived from

$$\frac{C}{\text{MSY}} = e\frac{B}{k}\left(1-\log\left(e\cdot\frac{B}{k}\right)\right) \qquad [6]$$

where e stands for Euler's number 2.718.

For comparative purposes, equilibrium yield curves were extracted from 14 Stock Synthesis models, which had been used for quota advice for tunas, billfishes, hakes, monkfish, snapper, herring, and sardine by national or Regional Fisheries Management Organizations including NOAA, ICES, ICCAT, and IOTC. All Stock Synthesis models had been fitted assuming a Beverton–Holt stock-recruitment function. In Stock Synthesis, the equilibrium curves are computed internally based on the age-structured equilibrium dynamics (cf. Winker et al. 2020) and can be extracted using the R package "*r4ss*" (Taylor et al. 2021). The median of the 14 equilibrium curves with approximate 95% confidence limits (2.5th and 97.5th percentiles) are illustrated in Fig. 7, where the spawning stock biomass ratio SSB/SSB_0 corresponds to B/k and $\text{SSB}_{\text{MSY}}/\text{SSB}_0$ corresponds to B_{MSY}/k where yield (surplus production) is at its maximum (MSY).

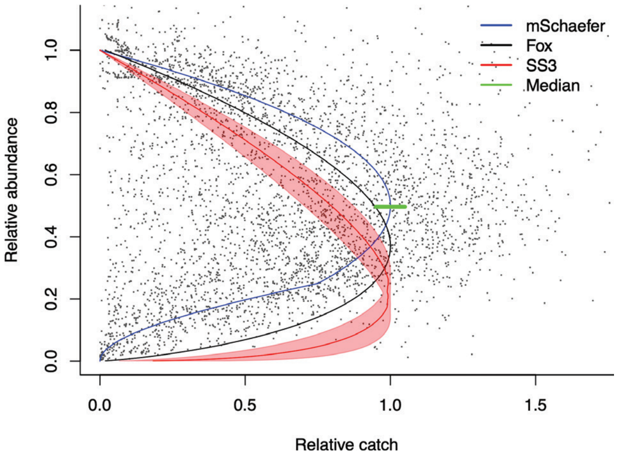

Figure 7. Scatterplot of 4805 observations of abundance relative to maximum abundance for 94 stocks where maximum abundance was deemed close to unexploited (B/k) and catch relative to a prior for MSY derived from maximum catch, i.e., no modelling was involved in generating the data. The upper blue curve represents the modified Schaefer model (mSchaefer) used by CMSY++. The middle black curve represents the Fox model. The lower red curve with approximate 95% confidence limits represents 14 stocks assessed with the Stock Synthesis model (SS3). The short green bold line indicates the median of relative population size = 0.497 for available points from 0.95 to 1.05 relative catch levels.

All data and code used in this study are available from https://oceanrep.geomar.de/53324/ and https://github.com/SISTA16/cmsyPlusPlus.

Results

Cross-validation of the ANN predictions. The task of ANN was to predict from properties of the time series of catches whether relative biomass (*B*/*k*) was above or below the MSY threshold (B_{MSY}/k) in a given year. The percentages of correct classifications are presented in Table 2 and are 99%–100% for stocks that were included in the training, as expected. For stocks that were excluded from the training, cross-validation accuracy ranged from 68% accuracy for the first year in the time series to 91% for the intermediate and final year (Table 2). Of the 400 real stocks used in the training of ANN, 377 (94%) BSM estimates of final *B*/*k* were within the approximate 95% confidence limits of the respective CMSY++ estimate. Of the 23 mismatches, 13 were cases where BSM estimated relative biomass of less than 0.1 *B*/*k*, and the approximate lower confidence limit of the CMSY++ estimate was also below 0.1 *B*/*k*, albeit above the BSM estimate, i.e., both methods predicted the stock as severely depleted. Detailed results are available in the file Out_Train_ID_9.csv that can be retrieved from https://oceanrep.geomar.de/53324/.

Table 2. Percentages of correct ANN predictions of biomass being above or below the MSY-level for subsets of a training set with altogether 400 stocks, where *n* indicates the number of stocks with $C_t < 0.99$ MSY for the selected year. Cross-validation accuracy is the mean of 20 runs of 5% newly randomly selected stocks that were excluded from the training, with indication of minimum and maximum values, and training set accuracy applies to classification of stocks that were included in the training data set.

Relative biomass	*n*	Cross-validation accuracy [%]	Min [%]	Max [%]	Training set accuracy [%]
Start *B*/*k*	290	67.5	42.9	92.9	99.0
Intermediate *B*/*k*	348	90.6	76.5	100.0	98.9
End *B*/*k*	291	91.0	80.0	100.0	99.7

Performance of ANN and CMSY++ against simulated data. The results of applying CMSY++ with *B*/*k* priors predicted by ANN to simulated stocks are given in Table 3. ANN made correct predictions of biomass being above or below B_{MSY} in 10 of 21 applicable cases of start biomass (48%), 16 of 24 cases of intermediate biomass (67%), and 12 of 23 applicable cases of end biomass (52%). The "true" value of *B*/*k* was contained in the approximate 95% confidence limits of the CMSY++ estimate in 12 of 24 cases (50%). Of the 12 cases where the ANN predictions for end biomass were correct, 10 CMSY++ predictions (83%) contained the true value in their approximate 95% confidence limits. Of the 11 applicable cases where ANN predictions for relative end biomass were wrong, 9 CMSY++ predictions (82%) were also wrong. Note that ANN was on purpose not trained on the artificial, often unrealistic and sometimes extreme catch patterns of the simulated stocks, which were designed to test the limits of the method; see Discussion below.

Discussion

ANN and CMSY++ performance against real and simulated stocks. CMSY++ performed well (68%–91% correct ANN predictions in cross-validation, see Table 2; 94% correspondence of CMSY++ predictions for final biomass with BSM results) against 400 real world stocks, which had been selected because their interplay between catch and biomass largely followed Equation 2. We believe that it is more appropriate and informative to compare data-limited results (here from CMSY++ with catch data) against results obtained with the same accepted model, but with substantially more data (here from BSM with time series of catch and abundance), rather than against very different models with very different data requirements and assumptions. Exploring in depth the differences in results obtained from surplus production models (such as BSM) versus data-rich age-structured models is beyond the scope of this study; but see the discussion around Fig. 7 below for the existence of and possible reasons for some of those differences.

Not surprisingly, ANN predictions for biomass being above or below B_{MSY} were less satisfactory for simulated stocks (only 48%–67% correct predictions, Table 3), because several of the simulated stocks had catch and abundance patterns which purposely were not present in the real-world data on which ANN had been trained. For example, 50 years ago many stocks were still underexploited (confirm Fig. 1) and ANN thus correlated low catches in that period with large stock size. Instead, half of the stocks in the simulation were set to start with low catches and low biomass, thus causing about half of the wrong ANN classifications (5 A/B of 11 wrong classifications for the start year in Table 3). Similarly, the simulations used high catches in the first year to bring down high biomass and to force the desired depletion patterns, whereas in the real world, high catches at or above MSY and high biomass rarely occur together (see Figs. 5 and 7). Other rarely found patterns in the real world pertain to the simulations that included very lightly exploited stocks where catch never exceeded MSY or biomass never fell below B_{MSY} and thus were never fully exploited (the High–High scenarios in Table 3). While ANN and CMSY++ underestimated final biomass in all four High–High scenarios, the "true" *B*/*k* values from the simulations were still contained within the confidence limits of the predictions. In other words, with the training applied to ANN, the results that will be obtained from simulation exercises fully depend on the resemblance of the simulated scenarios to real world stocks. Instead, the simulations were used to explore the behavior of CMSY++ in extreme scenarios to better understand its limitations.

Table 3. Results of ANN and CMSY++ predictions for 24 simulated stocks with very low to high resilience and six different biomass patterns. The ANN predictions of biomass being above (A) or below (B) B_{MSY} for the start, intermediate, and end year of the time series are compared with the "true" values and indicated as e.g., B/A, where the first letter is the ANN prediction, and the second letter is the "true" status. Also, the "true" *B*/*k* value in the last year is given and compared with the respective CMSY++ estimate, with approximate 95% confidence limits in parentheses. Wrong predictions by ANN or CMSY++ are marked in bold.

Resilience	Biomass pattern	ANN prediction			True *B*/*k*	CMSY++ estimated *B*/*k*
		Start	Intm	End		
High	High–High	**B/A**	**B/A**	**B/A**	0.71	0.63 (0.46–0.76)
	High–Low	**B/A**	B/B	B/B	0.27	0.41 (0.25–0.60)
	High–Low–High	A/A	B/B	**B/A**	0.66	0.53 (0.30–0.69)
	Low–High	B/B	B/B	A/A	0.75	**0.59 (0.41–0.74)**
	Low–High–Low	**A/B**	B/B	B/B	0.17	**0.40 (0.21–0.59)**
	Low–Low	B/B	B/B	B/B	0.31	0.44 (0.27–0.64)
Medium	High–High	**B/A**	**B/A**	A/A	0.70	0.65 (0.47–0.79)
	High–Low	**B/A**	B/B	B/B	0.16	0.31 (0.15–0.47)
	High–Low–High	**B/A**$^{\mathrm{F}}$	B/B	**B/A**	0.72	**0.41 (0.22–0.62)**
	Low–High	B/B	**B/A**	**B/A**	0.80	**0.40 (0.25–0.57)**
	Low–High–Low	**A/B**	B/B	B/B	0.24	0.36 (0.22–0.53)
	Low–Low	B/B	B/B	**A/B**	0.30	**0.58 (0.41–0.75)**
Low	High–High	A/A	**B/A**	A/A	0.68	0.63 (0.45–0.80)
	High–Low	**B/A**$^{\mathrm{F}}$	B/B	B/B	0.24	0.37 (0.23–0.51)
	High–Low–High	**B/A**	B/B	**B/A**	0.65	**0.32 (0.17–0.46)**
	Low–High	B/B	**B/A**	A/A	0.71	0.57 (0.41–0.75)
	Low–High–Low	**A/B**	**B/A**	**A/B**	0.32	**0.54 (0.34–0.73)**
	Low–Low	B/B	B/B	**A/B**	0.23	**0.55 (0.38–0.72)**
Very low	High–High	A/A	**B/A**	A/A	0.72	0.59 (0.41–0.76)
	High–Low	**B/A**	B/B	**A/B**	0.31	**0.50 (0.35–0.66)**
	High–Low–High	**B/A**$^{\mathrm{F}}$	B/B	**B/A**	0.57	**0.13 (0.06–0.24)**
	Low–High	**A/B**	**B/A**	A/A$^{\mathrm{F}}$	0.68	**0.47 (0.30–0.65)**
	Low–High–Low	**A/B**	B/B	B/B	0.32	0.36 (0.20–0.56)
	Low–Low	B/B	B/B	**A/B**	0.26	**0.58 (0.41–076)**

Intm = intermediate. The superscript $^{\mathrm{F}}$ indicates cases where catch exceeded the prior for MSY and a fixed *B*/*k* range of 0.26–0.72 was applied.

In addition, priors are as important as data in a Bayesian context, especially in data-limited applications, and it should not come as a surprise that wrong input (here: wrong prior information about the likely *B*/*k* range) led to wrong results. In contrast, the simulations suggest that if the final *B*/*k* prior range is broadly set correctly, then there is a high probability that CMSY++ will give reasonable predictions of stock status (see fig. 4 in Bouch et al. 2021 and results by Sharma et al. 2021 for independent confirmation). The main reason for the introduction of ANN was to make the derivation of the default *B*/*k* prior ranges more objective, with unknown rules developed and applied by the neural network. However, it is important to stress again that these default *B*/*k* priors are just a convenient add-on to CMSY++, and that the ANN predictions are to be replaced by evidence-based prior knowledge of stock status wherever possible (Table 4).

Addressing some common misconceptions. In medicine, asking a patient (or others who know that person) specific questions about their medical history, a process called *anamnesis*, is an essential part of formulating a diagnosis and developing a plan for recovery and well-being. The similarities to the process of stock assessment and management are obvious. Yet, one of the most common criticisms of CMSY is its strong dependence on such *anamnesis* or "anecdotal" knowledge about past and present fishing pressure or stock status. Some have even suggested the dependence of CMSY on *B*/*k* priors is so strong that the analysis might as well be skipped, and the priors be used directly for stock status classification. This would be analogous to using the *anamnesis* directly and forego its subsequent verification in the full diagnostic examination, surely not a serious proposal in a medical context.

Table 4. Proposed relative biomass ranges according to estimated depletion, to be used as priors in CMSY++ analyses. Select the depletion level where one or more text descriptions are true.

Depletion level	*B*/*k* range	Alternative descriptions of stock status or fishery
Very strong	0.01–0.2	Strongly overfished; severely depleted; collapsed; closed; abandoned; unprofitable; minimal catch; truncated size/age structure; strongly reduced recruitment; only sporadic recruitment; low abundance in much of previous area
Strong	0.01–0.4	Overfished; depleted; outside safe biological limits; reduced recruitment; reduced catch; increased cost of fishing; increased effort; reduced profits; reduction of mean size in the catch and in surveys; disappearance of fish from areas where they used to be
Medium	0.2–0.6	Fully exploited; high catch; high fishing effort; high cost of fishing but still reasonable profits; first signs of decline in average size and reduced abundance in some areas; occasional low recruitments
Low	0.4–0.8	Pretty good catch; good catch per effort; high profits; many large fish; healthy size/age structure; high abundance throughout area; regular recruitment; healthy fishery
Very low	0.75–1.0	Underdeveloped fishery; low market demand; only occasional catches; only bycatch; not vulnerable to common gears

Figure 5 shows an example of a misleading prior being strongly corrected by the data, here for European plaice (*Pleuronectes platessa* Linnaeus, 1758) in the eastern English Channel. Because abundance of that stock was very low in 1980 (Fig. 5a; ICES 2020), the user had set the *B*/*k* prior for that year to 0.01–0.1, with a central value around 0.05 (lower left corner of Fig. 5c). However, the *B*/*k* posteriors of both CMSY++ and BSM overlap only marginally with that prior and instead estimate a central value close to 0.2, i.e., about 4 times higher than suggested (Figs. 5c–5d). In other words, the prior user perception of stock status was not compatible with the available data, and the change from uniform to beta-distribution of the *B*/*k* prior allowed for the substantial correction of the prior knowledge.

Another misunderstanding of the Bayesian approach is the use of very wide, uninformative priors with the explicit purpose of reducing their influence on the results, e.g., by providing a uniform *B/k* prior range for final biomass of 0.1–0.9 *k*. Such prior informs the analysis that, with equal probability, the stock may be nearly collapsed or nearly unexploited. We are not aware of a single stock where such statement would be true. In other words, the objectivity that an uninformative prior is supposed to bring to the analysis is in reality the feeding of knowingly erroneous input to the model. Instead, in recognition of the importance of a realistic prior for a realistic analysis, real effort must be invested to determine the best possible prior information. We stress again that the built-in *B*/*k* prior predictions by ANN are a not-required add-on of CMSY++, to be replaced by independent *B*/*k* prior knowledge whenever possible (Table 4). To that end, stock assessments whose results will be used by managers should be done case-by-case, and not in a batch mode, so that due attention is paid to selecting the appropriate priors.

Setting appropriate initial biomass priors at the start of the time series (B_{start}/k) is not specific to CMSY++, but a general challenge for parameterizing surplus production models in cases where the catch series is fairly short and does not include historical catches that would reflect the initial lightly exploited stock biomass (i.e., B_{start}/k = 0.9–1.0).

There may also be concerns that deriving priors from the time series of catch data violates the requirement of Bayesian prior beliefs to be established before the data are considered. We agree with this principle and Table 4 gives examples on how independent beliefs about stock status can be translated into numerical prior ranges. Only for cases where such information is not available should the priors proposed by CMSY++ be used, which are based on ANN having looked at patterns in the catch data and comparing them with catch patterns of 400 stocks for which the biomass was known.

The CMSY user guide (available from https://oceanrep.geomar.de/id/eprint/52147/) provides a table with suggested *B/k* ranges according to the perception or "narrative" about the depletion of the stock. This approach is expanded upon in Table 4, giving examples of typical terms used to describe depletion levels. It is hard to imagine a fisher, fish processor or fisheries manager being unable to correctly assign an important stock to one of these broad categories. Also, with the exception of stocks that are nearly unexploited or collapsed, the proposed *B/k* ranges in Table 4 span 40% of the possible range and include, respectively, total collapse to near sustainability (0.01–0.4 *k*), outside of safe biological limits to securely sustainable level (0.2–0.6 *k*), and below B_{MSY} to near *k* (0.4–0.8 *k*). In other words, these ranges do not preempt the CMSY++ analysis or unduly predetermine the results. It makes a big difference for managers whether a stock is likely to be recruitment-impaired (0.2 *k*) or safely above the MSY threshold (0.6 *k*). If a stock seems to fall between two of these categories, intermediate prior *B*/*k* ranges can of course be used. If length frequency data are available, these can be used to obtain independent and objective *B/k* priors (Froese et al. 2018b, 2019; Musinguzi et al. 2020).

Caveats to using CMSY++. We have argued above that in the absence of abundance data, the catch-only implementation of CMSY++ performs reasonably well in classifying the stock status and thus in assisting the prioritization of management interventions (cf. Sharma et al. 2021). However, CMSY++ does strongly depend on accurate catch data and if, for example, a reduction in catch is enforced by management, a catch-only approach has clear limitations in monitoring its effectiveness to meet the rebuilding objectives (Wetzel and Punt 2015). This is because validating that the model can correctly predict the stock's response will ultimately require more observations (Kell et al. 2021). If, for example, a fishery is completely closed by law, the zero-catch signal does not allow any inferences about stock size development. Ideally, rebuilding of stocks should be aligned with data collection programs designed to monitor the progress and provide a feedback control to stakeholders and to BSM, which is included in the CMSY++ package and automatically activated if abundance data are provided. This enables a seamless transition from the CMSY catch-only approach to regular surplus-production modelling (BSM).

As indicated above, catch patterns can be used to make empirical predictions about relative stock sizes at selected points (e.g., start, end, intermediate) in the time series. In CMSY, that was done by a list of empirical if-then rules; in CMSY++, this is now done by an Artificial Neural Network (ANN). However, in both cases empirical predictions of relative biomass from catch patterns will only work if the interplay between catch and biomass is mainly driven by Equation 2. That will be the case if a more or less constant fishing effort is applied or if management follows a harvest control rule and sets catch limits based on relative stock size. It will, however, not work if strong changes in catch occur for other reasons, such as drastic variation in demand, or a species being newly protected from fishing, or declining carrying capacity because of warming waters, or increasing carrying capacity because the stock is released from predation mortality because a main predator has collapsed or disappeared. The presence of such circumstances has to be considered by the local experts, and the default biomass priors may then have to be corrected accordingly. To help with a better understanding of cases where CMSY++ works well with its default settings and cases where expert knowledge is required to get meaningful results, a number of selected stock assessments is presented and discussed in the Suppl. material 1.

More generally, especially in depleted stocks, a minor overestimation in stock size, such as estimating final B/k as 0.2 instead of 0.1, will lead to a substantial underestimation of fishing mortality. In addition, especially in large species where several age classes contribute to the catch, the contribution of early year classes may already be substantial although they are not yet fully selected by the gear. This reduces their specific F and the overall estimate of fishing mortality if compared with official assessments, which typically base their estimate of F only on fully selected age classes (see examples in the Suppl. material 1). Therefore, management based on surplus production models such as CMSY++ or BSM should focus on predicted biomass and not on predicted fishing mortality, which may be underestimated for fully selected age classes.

Comparing the modified Schaefer model to other models. In the course of searching for relative biomass priors for CMSY++, we realized that the equilibrium biomass predicted by the modified Schaefer model provided a very reasonable fit for the widely scattered catch and biomass data of the 400 stock assessments that we examined (Figs. 6 and 7). In contrast, problematic implementations of surplus-production models, such as those of Fox (1970) and Pella and Tomlinson (1969) became apparent (Fig. 7). As Pauly and Froese (2021) pointed out, these models are based on unjustified departures from the ecological foundation of the original model proposed by Graham (1935), operationalized by Schaefer (1957), and modified to account for reduced recruitment at low stock sizes by Froese et al. (2017) (equation 2, fig. 2).

The critique of Pauly and Froese (2021) centered on the low estimates of the minimum biomass required to produce MSY, fixed at 37% of carrying capacity in the Fox model, with some assessments using target values as low as 30% in Pella and Tomlinson (1969) or age-structured models (MRAG 2016). Recall that MSY is instead generated at 50% of carrying capacity in the original Schaefer model, based on the widely corroborated logistic curve of population growth (Verhulst 1838).

An apparently overlooked objective comparison of different models is how well their predictions fit observed catch and abundance data across many stocks. To avoid any confounding model assumption effects, a model-independent approach was used to generate points of the ratios Catch/MSY and B/k in Fig. 7, which is a novel feature that allows an objective comparison of the assumptions and prediction of the various models and should be explored in more depth in subsequent studies. Instead of using one of the above-mentioned assessment models to predict relative catch and relative biomass, MSY values were derived based on the maximum catch as described for MSY prior generation above and B/k observations were approximated as observed CPUE relative to the highest CPUE apparently close to representing carrying capacity. A subset of 94 of the 400 real stocks analyzed in this study met these requirements. While one could argue about the appropriateness of the methods to standardize the biomass and catch values shown in Fig. 7, the point here is that they did not favor one model over the other.

Similar to Fig. 6, Fig. 7 shows that the equilibrium yield curve of the modified Schaefer model traces the highest density of points reasonably well, whereas the Fox model traces only the lowest biomass values for a given catch. Equilibrium yield curves, which were extracted from age-structured assessments using Stock Synthesis (SS3; Methot and Wetzel 2013) with an integrated Beverton and Holt stock-recruitment function fell completely outside of the range of points at low stock sizes (i.e., $B/k < 0.25$). In other words, the Fox and SS3 models systematically overestimated the average productivity (i.e., the equilibrium yield curve) at low stock sizes, which can have severe implications for rebuilding of stocks (cf. Hutchings 2015; Perälä et al. 2022). Mangel et al. (2013) also criticize data-rich models for their strong dependence on typically unknown inputs such as the steepness parameter of the Beverton and Holt stock recruitment relation (Mace and Doonan 1988) or the rate of natural mortality, the arbitrary settings of which may then pre-determine key outputs, such as the biomass required to produce MSY.

The model comparison presented in Fig. 7 is preliminary and qualitative and should be repeated with a larger number of stocks, considering that some of the low catches at lower stock sizes may have been mandated by harvest control rules. However, Fig. 7 clearly points at a potentially large and highly risk prone bias associated with models that predict maximum sustainable catches at low stock sizes and overestimate the population growth potential at dangerously low stock levels.

Summary. CMSY++ has developed into a versatile integrative method that can incorporate, in addition to the required catch time series, abundance data and a wide variety of ancillary information (e.g., Froese et al. 2018b) in a rigorous Bayesian context that tends to reduce the dependency on prior information while remaining robust and thus usable in data-limited situations such as common in many parts of the world.

The majority of the independent tests of CMSY used the default priors and thus did not really test the CMSY method *per se*. With CMSY++, such tests would reproduce the 9%–32% failure rate of the Artificial Neural Network, with even higher percentages if applied to stocks whose catches were reduced for reasons external to the dynamics of the fish population in question, such as changes in market demand or environmentally-mediated productivity. Similarly, any failure rate can be produced with simulated stocks that deviate substantially from the 400 stocks used in training ANN. Instead, in order to be more realistic, tests should assume that local experts are able to provide priors that are not wider than about 40% of the maximum possible range and that include the "true" value.

CMSY++, either applied as a data-poor (catch-only) or preferentially as a data-moderate (catch and CPUE) method, allows the assessment of stocks for which at least catch data are known. That is especially important for data-poor areas that have been generally excluded from Ecosystem Based Fisheries Management (EBFM) programs (Link 2010) because of ignorance regarding stock status (Townsend et al. 2019). In addition to the large number of data-deficient areas, stocks that have low commercial interest have generally been overlooked in assessments and the conservation status of marine megafauna is unknown in many areas, such as the Mediterranean and the Black Sea (Stergiou and Tsikliras 2006). CMSY++ and related methods (e.g., Winker et al. 2018; Froese et al. 2018b, 2020) can provide assessments for these important ecosystem components. Such standardized and comparable stock assessments applied on a global scale (Fig. 3) will contribute to a much-needed better understanding of the world's fisheries and ecosystems (Pauly et al. 2018).

Acknowledgments

Rainer Froese acknowledges support by the German Federal Nature Conservation Agency (BfN); Maria-Lourdes D Palomares and Daniel Pauly acknowledge support from the *Sea Around Us*, itself funded by a number of philanthropic foundations, notably the Minderoo Foundation, which underwrote the work leading to the update of the reconstructed catches to 2018 and the majority of the CMSY++ assessments in the global map shown as Fig. 3. We also thank Nicolas Bailly and Elizabeth Bato David for their assistance in creating this map. Athanassios C Tsikliras was partly supported by the European Union's Horizon 2020 Research and Innovation Program (H2020-BG-10-2020-2), grant number No 101000302—EcoScope (Ecocentric management for sustainable fisheries and healthy marine ecosystems). The article reflects only the authors' view and the Commission is not responsible for any use that may be made of the information it contains.

Data availability

All data, scripts, and supplementary material are available from https://oceanrep.geomar.de/53324/ and https://github.com/SISTA16/cmsyPlusPlus.

References

Allee WC (1938) The social life of animals. WW Norton, New York, NY, USA.

Barrowman NJ, Myers RA (2000) Still more spawner-recruitment curves: The hockey stick and its generalizations. Canadian Journal of Fisheries and Aquatic Sciences 57(4): 665–676. https://doi.org/10.1139/f99-282

Beverton RJH, Holt SJ (1957) On the dynamics of exploited fish populations. Fisheries Investigation Series, II; 19. Her Majesty's Stationary Office, London, UK.

Bishop CM (1995) Neural Networks for Pattern Recognition. Clarendon Press, Oxford, UK. https://doi.org/10.1201/9781420050646.ptb6

Bouch P, Minto C, Reid DG (2021) Comparative performance of data-poor CMSY and data-moderate SPiCT stock assessment methods when applied to data-rich, real-world stocks. ICES Journal of Marine Science 78(1): 264–276. https://doi.org/10.1093/icesjms/fsaa220

Caddy JF, Gulland JA (1983) Historical patterns of fish stocks. Marine Policy 7(4): 267–278. https://doi.org/10.1016/0308-597X(83)90040-4

Cheung WWL, Palacios-Abrantes J, Frölicher TL, Palomares ML, Clarke T, Lam VWY, Oyinlola MA, Pauly D, Reygondeau G, Sumaila RU, Teh CLL, Wabnitz CCC (2022) Rebuilding fish biomass for the world's marine ecoregions under climate change. Global Change Biology 28(21): 6254–6267. https://doi.org/10.1111/gcb.16368

Chong L, Mildenberger TK, Rudd MB, Taylor MH, Cope JM, Branch TA, Wolff M, Stabler M (2019) Performance evaluation of data-limited, length-based stock assessment methods. ICES Journal of Marine Science 77(1): 97–108. https://doi.org/10.1093/icesjms/fsz212

Christensen LB (2006) Marine mammal populations: Reconstructing historical abundances at the global scale. Fisheries Centre Research Reports, Vol. 14, No. 9. University of British Columbia, Vancouver, BC, Canada, 161 pp. https://doi.org/10.14288/1.0074757

Coro G, Massoli FV, Origlia A, Cutugno F (2021) Psycho-acoustics inspired automatic speech recognition. Computers and Electrical Engineering 93: 107238. https://doi.org/10.1016/j.compeleceng.2021.107238

Cruz R, Santana JV, Barreto CG, Borda CA, Torres MT, Gaeta JC, Da Silva JL, Saraiva SZ, Salazar IS, Cintra IH (2020) Towards the rebuilding of spiny lobster stocks in Brazil: A review. Crustaceana 93(8): 957–983. https://doi.org/10.1163/15685403-bja10073

Csirke J [Chair] (1984) Report of the working group on fisheries management, implications and interactions. Pp. 18–29. In: Sharp GD, Csirke J (Eds.) Proceedings of the expert consultation to examine changes in abundance and species composition of neritic fish resources, San José, Costa Rica, April 1983. FAO Fisheries Report No. 291, Vol. 1.

Demirel N, Zengin M, Ulman A (2020) First large-scale eastern Mediterranean and Black Sea stock assessment reveals a dramatic decline. Frontiers in Marine Science 7: 103. https://doi.org/10.3389/fmars.2020.00103

Dowling NA, Smith AD, Smith DC, Parma AM, Dichmont CM, Sainsbury K, Wilson JR, Dougherty DT, Cope JM (2019) Generic solutions for data-limited fishery assessments are not so simple. Fish and Fisheries 20(1): 174–188. https://doi.org/10.1111/faf.12329

FAO (2020) The state of world fisheries and aquaculture, SOFIA, 2018: Sustainability in Action Food and Agriculture Organization, Rome, 244 pp.

Ferrer EM, Giron-Nava A, Aburto-Oropeza O (2022) Overfishing increases the carbon footprint of seafood production from small-scale fisheries. Frontiers in Marine Science 9: e768784. https://doi.org/10.3389/fmars.2022.768784

Fox Jr WW (1970) An exponential yield model for optimizing exploited fish populations. Transactions of the American Fisheries Society 99(1): 80–88. https://doi.org/10.1577/1548-8659(1970)99<80:AESMFO>2.0.CO;2

Free CM, Jensen OP, Anderson SC, Gutierrez NL, Kleisner KM, Longo C, Minto C, Osio GC, Walsh JC (2020) Blood from a stone: Performance of catch-only methods in estimating stock biomass status. Fisheries Research 223: 105452. https://doi.org/10.1016/j.fishres.2019.105452

Fritsch S, Guenther F, Guenther MF (2019) 'neuralnet' R Package Training of Neural Networks. https://cranr-project.org/web/packages/neuralnet/neuralnet.pdf

Froese R, Kesner-Reyes K (2002) Impact of fishing on the abundance of marine species ICES CM 2002/L:12, Copenhagen, 12 pp.

Froese R, Pauly D (Eds) (2023) FishBase. [Version 06/2023] http://www.fishbase.org

Froese R, Proelss A (2012) Evaluation and legal assessment of certified seafood. Marine Policy 36(6): 1284–1289. https://doi.org/10.1016/j.marpol.2012.03.017

Froese R, Zeller D, Kleisner K, Pauly D (2012) What catch data can tell us about the status of global fisheries. Marine Biology 159(6): 1283–1292. https://doi.org/10.1007/s00227-012-1909-6

Froese R, Demirel N, Gianpaolo C, Kleisner KM, Winker H (2017) Estimating fisheries reference points from catch and resilience. Fish and Fisheries 18(3): 506–526. https://doi.org/10.1111/faf.12190

Froese R, Winker H, Coro G, Demirel N, Tsikliras AC, Dimarchopoulou D, Scarcella G, Quaas M, Matz-Lück N (2018a) Status and rebuilding of European fisheries. Marine Policy 93: 159–170. https://doi.org/10.1016/j.marpol.2018.04.018

Froese R, Winker H, Coro G, Demirel N, Tsikliras AC, Dimarchopoulou D, Scarcella G, Probst WN, Dureuil M, Pauly D (2018b) A new approach for estimating stock status from length frequency data. ICES Journal of Marine Science 75(6): 2004–2015. https://doi.org/10.1093/icesjms/fsy078

Froese R, Winker H, Coro G, Demirel N, Tsikliras AC, Dimarchopoulou D, Scarcella G, Probst WN, Dureuil M, Pauly D (2019) On the pile-up effect and priors for Linf and M/K: Response to a comment by Hordyk et al. on "A new approach for estimating stock status from length frequency data". ICES Journal of Marine Science 76(2): 461–465. https://doi.org/10.1093/icesjms/fsy199

Froese R, Winker H, Coro G, Demirel N, Tsikliras AC, Dimarchopoulou D, Scarcella G, Palomares MLD, Dureuil M, Pauly D (2020) Estimating stock status from relative abundance and resilience. ICES Journal of Marine Science 77(2): 527–538. https://doi.org/10.1093/icesjms/fsz230

Graham M (1935) Modern theory of exploiting a fishery and application to North Sea trawling. ICES Journal of Marine Science 10(3): 264–274. https://doi.org/10.1093/icesjms/10.3.264

Grainger RJR, Garcia SM (1996) Chronicle of marine fisheries landings (1950–1994): Trend analysis and fisheries potential. FAO Fisheries Technical Paper, Rome, 51 pp.

Hilborn R, Walters CJ (1992) Quantitative fisheries stock assessment: Choice, dynamics and uncertainty. Chapman and Hall, New York, NY, USA, 570 pp. https://doi.org/10.1007/978-1-4615-3598-0

Hochreiter S, Schmidhuber J (1997) Long short-term memory. Neural Computation 9(8): 1735–1780. https://doi.org/10.1162/neco.1997.9.8.1735

Hutchings JA (2015) Thresholds for impaired species recovery. Proceedings of the Royal Society B: Biological Sciences 282(1809): e20150654. https://doi.org/10.1098/rspb.2015.0654

ICES (2020) Plaice (*Pleuronectes platessa*) in Division 7d (eastern English Channel) In Report of the ICES Advisory Committee, 2020 ICES Advice 2020, ple277d. https://doi.org/10.17895/ices.advice.5873

ICES (2021) Benchmark workshop on the development of MSY advice for category 3 stocks using Surplus Production Model in Continuous Time; SPiCT (WKMSYSPiCT). ICES Scientific Reports 3, 1–317. https://doi.org/10.17895/ices.pub.7919

Kang B, Wang L, Liu M (2022) Species traits determined different responses to "zero-growth" policy in China's marine fisheries. Scientific Reports 12(1): 20410. https://doi.org/10.1038/s41598-022-24897-w

Kell LT, Sharma R, Kitakado T, Winker H, Mosqueira I, Cardinale M, Fu D (2021) Validation of stock assessment methods: Is it me or my model talking? ICES Journal of Marine Science 78(6): 2244–2255. https://doi.org/10.1093/icesjms/fsab104

Kimura DK, Tagart JV (1982) Stock reduction analysis, another solution to the catch equations. Canadian Journal of Fisheries and Aquatic Sciences 39(11): 1467–1472. https://doi.org/10.1139/f82-198

Kleisner K, Zeller D, Froese R, Pauly D (2013) Using global catch data for inferences on the world's marine fisheries. Fish and Fisheries 14(3): 293–311. https://doi.org/10.1111/j.1467-2979.2012.00469.x

Lancker K, Voss R, Zimmermann F, Quaas MF (2023) Using the best of two worlds: A bio-economic stock assessment (BESA) method using catch and price data. Fish and Fisheries 24(5): 744–758. https://doi.org/10.1111/faf.12759

Liang C, Xian W, Pauly D (2020) Assessments of 15 exploited fish stocks in Chinese, South Korean and Japanese waters using the CMSY and BSM methods. Frontiers in Marine Science 7: 623. https://doi.org/10.3389/fmars.2020.00623

Link JS (2010) Ecosystem-based fisheries management: Confronting tradeoffs. Cambridge University Press, Cambridge, UK. https://doi.org/10.1017/CBO9780511667091

Mace PM, Doonan IJ (1988) A generalised bioeconomic simulation model for fish population dynamics New Zealand Fishery Assessment Research Document 88/4 Fisheries Research Centre, MAFFish, POB 297, Wellington, NZ.

Mangel M, MacCall AD, Brodziak J, Dick EJ, Forrest RE, Pourzand R, Ralston S (2013) A perspective on steepness, reference points, and stock assessment. Canadian Journal of Fisheries and Aquatic Sciences 70(6): 1–1. https://doi.org/10.1139/cjfas-2012-0372

Martell S, Froese R (2013) A simple method for estimating MSY from catch and resilience. Fish and Fisheries 14(4): 504–514. https://doi.org/10.1111/j.1467-2979.2012.00485.x

Methot Jr RD, Wetzel CR (2013) Stock synthesis: A biological and statistical framework for fish stock assessment and fishery management. Fisheries Research 142: 86–99. https://doi.org/10.1016/j.fishres.2012.10.012

MRAG (2016) Full assessment: New Zealand Orange Roughy fisheries Volume 2: Stakeholder comments; surveillance levels natural resources assessment and management. MRAG Americas Inc.

Musinguzi L, Bassa S, Natugonza V, Van Steenberge M, Okello W, Sboeks J, Froese R (2020) Assessment of exploited fish species in the Lake Edward system. Journal of Applied Ichthyology 37(2): 216–226. https://doi.org/10.1111/jai.14161

Ovando D, Hilborn R, Monnahan C, Rudd M, Sharma R, Thorson JT, Rousseau Y, Ye Y (2021) Improving estimates of the state of global fisheries depends on better data. Fish and Fisheries 22(6): 1–15. https://doi.org/10.1111/faf.12593

Ovando D, Free CM, Jensen OP, Hilborn R (2022) A history and evaluation of catch-only stock assessment models. Fish and Fisheries 23(3): 616–630. https://doi.org/10.1111/faf.12637

Palomares MLD, Khalfallah M, Woroniak J, Pauly D (Eds) (2020a) Assessments of marine fisheries resources in West Africa with emphasis on small pelagics. Fisheries Centre Research Reports, Vol. 28, No. 4. University of British Columbia, Vancouver, BC, Canada, 108 pp. https://dx.doi.org/10.14288/1.0394987

Palomares MLD, Pauly D (2019) On the creeping increase of vessels' fishing power Special issue on "Managing local and global fisheries in the Anthropocene". Ecology and Society 24(3): 31. https://doi.org/10.5751/ES-11136-240331

Palomares MLD, Derrick B, Nöel S-L, Tsui G, Woroniak J, Froese R, Pauly D (2019) A global assessment of the status of exploited marine fish and invertebrate populations. A report prepared by the Sea Around Us for OCEANA, 97 pp.

Palomares MLD, Froese R, Derrick B, Meeuwig JJ, Nöel S-L, Tsui G, Pauly D (2020b) Fishery biomass trends of exploited fish populations in marine ecoregions, climatic zones and ocean basins. Estuarine, Coastal and Shelf Science 243: 106896. https://doi.org/10.1016/j.ecss.2020.106896

Palomares MLD, Baxter S, Bailly N, Chu E, Derrick B, Frias-Donaghey M, Nöel SL, Page E, Schijns R, Woroniak J, Abucay L, David E, de Leo S, Nevado MK, Ortiz S, Parducho VA, Yap PS, Ansell M, Hood L, Vianna G, White R, Zeller D, Pauly D (2021) Estimating the biomass of commercially exploited fisheries stocks left in the ocean. Fisheries Centre Research Reports, Vol. 29, No. 3. University of British Columbia, Vancouver, BC, Canada, 74 pp. https://dx.doi.org/10.14288/1.0404487

Pauly D, Froese R (2021) MSY needs no epitaph—but it was abused. ICES Journal of Marine Science 78(6): 2204–2210. https://doi.org/10.1093/icesjms/fsaa224

Pauly D, Alder J, Booth S, Cheung WWL, Christensen V, Close C, Zeller D (2008) Fisheries in large marine ecosystems: descriptions and diagnoses The UNEP large marine ecosystem report: A perspective on changing conditions in LMEs of the World's Regional Seas. UNEP Regional Seas Reports and Studies (182): 23–40.

Pauly D, Cheung WWL, Sumaila UR (2018) What are global fisheries studies. Pp. 33–37. In: Pauly D, Ruiz-Leotaud V (Eds) Marine and freshwater miscellanea. Fisheries Centre Research Reports, Vol. 26, No. 2. University of British Columbia, Vancouver, BC, Canada, 83 pp. https://dx.doi.org/10.14288/1.0372513

Pedersen MW, Berg CW (2017) A stochastic surplus production model in continuous time. Fish and Fisheries 18(2): 226–243. https://doi.org/10.1111/faf.12174

Pella JJ, Tomlinson PK (1969) A generalized stock production model. Inter-American Tropical Tuna Commission; Bulletin 13: 419–496.

Perälä T, Hutchings JA, Kuparinen A (2022) Allee effects and the Allee-effect zone in northwest Atlantic cod. Biology Letters 18(2): 20210439. https://doi.org/10.1098/rsbl.2021.0439

Pons M, Cope JM, Kell LT (2020) Comparing performance of catch-based and length-based stock assessment methods in data-limited fisheries. Canadian Journal of Fisheries and Aquatic Sciences 77(6): 1026–1037. https://doi.org/10.1139/cjfas-2019-0276

Ricker WE (1954) Stock and recruitment. Journal of the Fisheries Research Board of Canada 11(5): 559–623. https://doi.org/10.1139/f54-039

Roa-Ureta RH (2020) Stock assessment of octopus in four regions of the Philippines and nationally. Scientific Report No. 3. Sustainable Fisheries Partnership Foundation, Honolulu, and Bureau of Fisheries and Aquatic Resources, Philippines, 36 pp.

Rosenberg AA, Fogarty MJ, Cooper AB, Dickey-Collas M, Fulton EA, Gutiérrez NL, Yimin Y (2014) Developing new approaches to global stock status assessment and fishery production potential of the seas. Fisheries and aquaculture circular No. 1086. FAO, Rome, 175.

Saygu İ, Akoglu E, Gül G, Bedikoğlu D, Demirel N (2023) Fisheries impact on the Sea of Marmara ecosystem structure and functioning during the last three decades. Frontiers in Marine Science 9: 1076399. https://doi.org/10.3389/fmars.2022.1076399

Schaefer MB (1954) Some aspects of the dynamics of populations important to the management of the commercial marine fisheries. Inter-American Tropical Tuna Commission; Bulletin 1: 27–56.

Schaefer MB (1957) A study of the dynamics of the fishery for yellowfin tuna in the eastern tropical Pacific Ocean. Inter-American Tropical Tuna Commission; Bulletin 2(6): 243–285.

Schijns R (2020) What has Canada caught, and how much is left? Reconstructing and assessing fisheries in three oceans. MSc Thesis, University of British Columbia, Vancouver, BC, Canada, 128 pp. https://dx.doi.org/10.14288/1.0394806

Schijns R, Froese R, Hutchings J, Pauly D (2021) Five centuries of cod catches in eastern Canada. ICES Journal of Marine Science 78(8): 2675–2683. https://doi.org/10.1093/icesjms/fsab153

Schiller LL (2014) Tuna be, or not tuna be: using catch data to observe the ecological impact of commercial tuna fisheries in the Pacific Ocean at varying spatial scales. MSc thesis, University of British Columbia, BC, Canada, Vancouver, 155 pp. https://dx.doi.org/10.14288/1.0166022

Schnute JT, Richards LJ (2002) Surplus production models. Pp. 104–126. In: Hart PJB, Reynolds JD (Eds) Handbook of fish biology and fisheries Vol. 2. Blackwell Publishing, Malden, MA, USA.

Schweder T, Hjort NL (1996) Bayesian synthesis or likelihood synthesis—What does Borel's paradox say? Memorandum 13/1996, Department of Economics, Oslo University, Oslo, Norway.

Scotti M, Opitz S, MacNeil L, Kreutle A, Pusch C, Froese R (2022) Ecosystem-based fisheries management increases catch and carbon sequestration through recovery of exploited stocks: The western Baltic Sea case study. Frontiers in Marine Science 9: 879998. https://doi.org/10.3389/fmars.2022.879998

Sharma R, Winker H, Levontin P, Kell L, Ovando D, Palomares MLD, Pinto C, Ye Y (2021) Assessing the potential of catch-only models to inform on the state of global fisheries and the UN's SDGs. Sustainability 13(11): e6101. https://doi.org/10.3390/su13116101

Stergiou KI, Tsikliras AC (2006) Underrepresentation of regional ecological research output by bibliometric indices. Ethics in Science and Environmental Politics 2006: 15–17. https://doi.org/10.3354/esep006015

Taylor IG, Doering KL, Johnson KF, Wetzel CR, Stewart IJ (2021) Beyond visualizing catch-at-age models: Lessons learned from the r4ss package about software to support stock assessments. Fisheries Research 239: e105924. https://doi.org/10.1016/j.fishres.2021.105924

Townsend H, Harvey CJ, deReynier Y, Davis D, Zador SG, Gaichas S, Weijerman M, Hazen EL, Kaplan IC (2019) Progress on implementing ecosystem-based fisheries management in the United States through the use of ecosystem models and analysis. Frontiers in Marine Science 6: 641. https://doi.org/10.3389/fmars.2019.00641

Verhulst P-F (1838) Notice sur la loi que la population suit dans son accroissement. Correspondance mathématique et physique 10: 113–121.

Walters CJ, Kitchell JF (2001) Cultivation/depensation effects on juvenile survival and recruitment: Implications for the theory of fishing. Canadian Journal of Fisheries and Aquatic Sciences 58(1): 39–50. https://doi.org/10.1139/f00-160

Walters CJ, Martell SJD, Korman J (2006) A stochastic approach to stock reduction analysis. Canadian Journal of Fisheries and Aquatic Sciences 63(1): 212–223. https://doi.org/10.1139/f05-213

Wang Y, Wang Y, Liang C, Zhang H, Xian W (2020a) Assessment of 12 fish species in the Northwest Pacific using the CMSY and BSM methods. Frontiers in Marine Science 7: 616. https://doi.org/10.3389/fmars.2020.00616

Wang Y, Liang C, Wang Y, Xian W, Palomares ML (2020b) Stock status assessments for 12 exploited fishery species in the Tsushima warm current region, southwest Japan and east China, using the CMSY and BSM methods. Frontiers in Marine Science 7: e640. https://doi.org/10.3389/fmars.2020.00640

Wetzel CR, Punt AE (2015) Evaluating the performance of data-moderate and catch-only assessment methods for US west coast groundfish. Fisheries Research 171: 170–187. https://doi.org/10.1016/j.fishres.2015.06.005

Winker H, Carvalho F, Kapur M (2018) JABBA: Just Another Bayesian Biomass Assessment. Fisheries Research 204: 275–288. https://doi.org/10.1016/j.fishres.2018.03.010

Winker H, Carvalho F, Thorson JT, Kell LT, Parker D, Kapur M, Sharma R, Booth AJ, Kerwath SE (2020) JABBA-Select: Incorporating life history and fisheries' selectivity into surplus production models. Fisheries Research 222: 105355. https://doi.org/10.1016/j.fishres.2019.105355

Ye Y (2011) Assessment methodology. Pp. 327–334. In: Review of the state of world marine fishery resources. FAO Fisheries and Aquaculture Technical Paper No. 569, FAO, Rome.

Zhang K, Zhang J, Xu Y, Sun M, Chen Z, Yuan M (2018) Application of a catch-based method for stock assessment of three important fisheries in the East China Sea. Acta Oceanologica Sinica 37(2): 102–109. https://doi.org/10.1007/s13131-018-1173-9

Zhou S, Punt AE, Smith ADM, Ye Y, Haddon M, Dichmont CM, Smith DC (2018) An optimized catch-only assessment method for data poor fisheries. ICES Journal of Marine Science 75(3): 964–976. https://doi.org/10.1093/icesjms/fsx226

Supplementary material 1

Some comments on the suitability of stocks for analysis with CMSY++

Authors: Rainer Froese, Henning Winker, Gianpaolo Coro, Maria-Lourdes "Deng" Palomares, Athanassios C. Tsikliras, Donna Dimarchopoulou, Konstantinos Touloumis, Nazli Demirel, Gabriel M. S. Vianna, Giuseppe Scarcella, Rebecca Schijns, Cui Liang, Daniel Pauly

Data type: pdf

Link: https://doi.org/10.3897/aiep.53.105910.suppl1

Acta Ichthyologica et Piscatoria 53, 2023, 191–199 | DOI 10.3897/aiep.53.113745

PENSOFT.

ACTA
ICHTHYOLOGICA
ET PISCATORIA

The invasive mollusk *Rapana venosa* (Mollusca: Neogastropoda: Muricidae) in the mid-southern Black Sea: Distribution, growth, and stock structure

Murat DAĞTEKİN[1]

1 *Central Fisheries Research Institute, 61250 Yomra, Trabzon, Turkiye*

https://zoobank.org/DEF071B9-DBC7-4958-B26C-875C319A6566

Corresponding author: Murat Dağtekin (muratdagtekin998@gmail.com)

Academic editor: Adnan Tokaç ♦ **Received** 30 June 2023 ♦ **Accepted** 6 October 2023 ♦ **Published** 31 October 2023

Citation: Dağtekin M (2023) The invasive mollusk *Rapana venosa* (Mollusca: Neogastropoda: Muricidae) in the mid-southern Black Sea: Distribution, growth, and stock structure. Acta Ichthyologica et Piscatoria 53: 191–199. https://doi.org/10.3897/aiep.53.113745

Abstract

The rapa whelk, *Rapana venosa* (Valenciennes, 1846), known also as the veined rapa whelk or the Asian rapa whelk, settled in the Black Sea in 1940 and within the past 30 years has become an important economic contribution to local fishers along the coastline. This study examines the annual change in biomass, population structure, and interaction of the species with the ecosystem of rapa whelk in the mid-southern Black Sea. The samples were collected monthly in 2011 and 2012 by hydraulic dredge at different sites. Stock biomass was estimated at five different subregions and along four depth contours. In 2012 the biomass of rapa whelk increased significantly in in all subregions compared with the previous year sampling. Food availability is the main factor for species distribution, and in parallel, striped Venus clams, *Chamelea gallina* (Linnaeus, 1758), the main food source for rapa whelks, was significantly concentrated in the study area. The von Bertalanffy growth parameters (VBGP) were expressed as $L_t = 121.78(1 - e^{-0.246(t + 0.33)})$. As a fisheries management point, our results highlight the overpopulation of rapa whelk in the region.

Keywords

alien species, biomass, Black Sea, *Rapana venosa*, spatial distribution, VBGP

Introduction

One of the biggest challenges to biodiversity and community structure is the encroachment of non-indigenous species into ecosystems (Mack et al. 2000; Bailey et al. 2020). One of such species is *Rapana venosa* (Valenciennes, 1846), a large predatory marine gastropod, known as the rapa whelk, the veined rapa whelk, or the Asian rapa whelk, and it represents one of four major successful invasions of estuarine ecosystems worldwide that have been documented so far (Harding and Mann 2005; Slynko et al. 2020). The other three were the zebra mussel, *Dreissena polymorpha* (Pallas, 1771); European green crab, *Carcinus maenas*, (Linnaeus, 1758); and sea walnut, *Mnemiopsis leidyi* Agassiz, 1865. The rapa whelk is indigenous to the western Pacific's coastal and estuarine waters. This species is distributed in various parts of the world, including the Sea of Japan, Yellow Sea, Bay of Bohai, East China Sea, northern Adriatic Sea, Black Sea, Aegean Sea, Sea of Marmara, Gulf of Quiberon, and North Atlantic (Mann et al. 2004). It is an invasive alien species transported to the Black Sea via ballast water from the Pacific Ocean during the 1940s (Mann et al. 2004). Since 1969, it has created a dynamic stock (Bilecik 1975), with high adaptation capability in the Black Sea. Following its introduction, the rapa whelk spread rapidly throughout the Black Sea between the 1970s and 1980s (Bilecik 1990), due to its extremely high tolerance to environmental changes, such as low salinity, water pollution, and low oxygen (Munari and Mistri 2011). Sağlam et al.

(2009) reported that the reproductive period of *R. venosa* along the coast of Türkiye occurs between June and August. As far as reproductive success is concerned, each female produces an average of 575 capsules per breeding season (Sağlam and Düzgüneş 2007). Rapa whelk shows the imposex characteristics (Smith 1971), which has also been proven for Black Sea populations (Micu et al. 2009). Imposex individuals are formed as a result of the toxic effects of antifouling agents on organisms. This could be briefly explained as superimposition of male sexual organs (penis and vas deferens) on female gastropods (An et al. 2013). Fast growing was reported up to 40–45 mm in length in the first 2–3 years, with 8–9 years of longevity (Sampson et al. 2014). However, growth is slower in some regions such as the eastern Black Sea region due to nutritional and environmental factors (Dağtekin et al. 2023).

Rapa whelks caused serious destruction to the benthic life of the Black Sea (Zolotarev 1996; Sağlam et al. 2008; Sağlam and Düzgüneş 2014; Sampson et al. 2014; Dağtekin et al. 2016). Extensive damage, caused by those predatory gastropods, was observed on mussel beds (Bilecik 1990). The rapa whelk is a major predator of many bivalve species such as mussels, *Mytilus galloprovincialis* Lamarck, 1819; striped Venus clams, *Chamelea gallina* (Linnaeus, 1758); and oysters, *Ostrea edulis* Linnaeus, 1758, throughout the world's oceans (Savini et al. 2002). Since the 1950s, the depletion of large stocks of commercial bivalves (especially *M. galloprovincialis*) and the associated communities was reported in the Black Sea (Zolotarev 1996; Uyan and Aral 2003; Salomidi et al. 2012). In Ukrainian waters, the destruction of oyster banks (*O. edulis* and *Magallana gigas* (Thunberg, 1793)) around Kerch Strait and Karkinitsky Bay was also reported (Bondarev 2014).

Despite its negative environmental effects, *R. venosa* is a commercially important whelk in the Turkish Black Sea. Since the early 1980s, it has been intensively fished by beam trawls and divers in the southeastern Black Sea. Landings have decreased in recent years after showing a great increase (Fig. 1). In Bulgaria, *R. venosa* became a target of the fishing industry in the 1990s. Data show that catches vary between 3000–5000 tonnes. The rapa whelk, which is an important species for Romanian fisheries, constitutes more than half of the total catch. Similarly, the rapa whelk is an important target species in Ukrainian fisheries. However, until recent years, Ukraine ranked only fourth in rapa whelk fisheries in the Black Sea. This was mostly because, rapa whelk just began to spread throughout the northwestern portion of the Sea, from 2000 (GFCM 2023). The rapa whelk is not consumed domestically as human food, but the vast majority of products in Türkiye are exported to international seafood markets (Dağtekin et al. 2016). Other countries in the Black Sea region also export some of the catch for domestic consumption (GFCM 2023). In recent years, while about half of the world's stocks have been estimated, problems have been experienced in analyzing a significant portion of them. The main reason for this is the problems in obtaining reliable data. In addition to catch data, survey data are needed (Ovando et al. 2021). This study aimed to contribute to the creation of stock assessment and management plans by producing solutions for the above-mentioned lack of data on a regional basis. Another factor is the destruction of the benthic habitats and discards rates of the fishing gear used to catch this species (Erik and Dağtekin 2022). Because when the fishing effort increases, the negative impact on the benthic habitat may also increase.

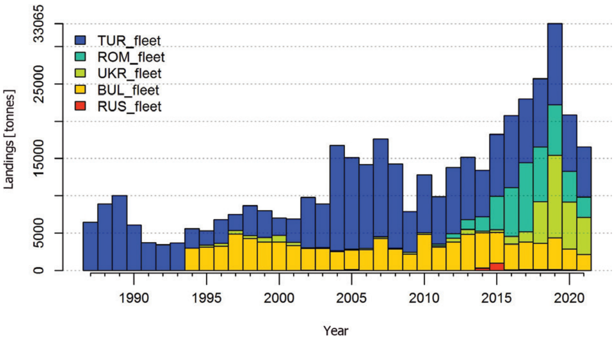

Figure 1. Amount of *Rapana venosa* landing in the Black Sea basin (GFCM 2023).

The presently reported study was intended to determine the growth characteristics, distribution pattern, and stock structure of *R. venosa* in the mid-southern Black Sea. Despite its commercial importance, information on the life history, distribution, and status of rapa whelk is scarce in the Black Sea. Therefore, growth parameters, length–weight relations, mortality, and exploitation rates were estimated to contribute to its population status. The difference in its distribution and estimated biomass was considered within the area colonized by the striped Venus clam (*C. gallina*) beds is an essential commercial bivalve species in Turkish fisheries. Exploitation rate and stock distribution results were considered for better management actions in the fishing areas.

Materials and methods

Sampling. The presently reported study was carried out in the western Black Sea, especially in the important region where the sandy substrate is dense and baby clam beds can be found. This study was carried out considering the reproduction season of *Rapana venosa*, because during the reproduction period, this species migrates toward the coasts (Sağlam et al. 2009). The hydraulic dredge was used in this study and was based on the design of dredges used in Türkiye (300 cm long, 180 cm wide). The cutting blade was 80 cm wide and extended 20 cm below the dredge. During all tows in each experiment, tow speeds (2 knots), tow duration (Each operation took 2 min), the ratio of warp length to water depth, and water pressure at the water pump on deck (3 bars) were similar in commercial operations. The samples were stored without sieving and transferred to the laboratory in a cooler for further analysis. For each sample, the total length

(TL) was measured using a Vernier caliper to the nearest 0.1 cm, and the total wet weight (TW) was weighed using an electronic scale to the nearest 0.01 g. The study region covered the mid-southern coast of the Turkish Black Sea between Sinop and Cide. It was divided into five sub-regions (Cide, İndebolu, Türkeli, Ayancık, and Sarıkum) and four depth contours (0–5 m, 5–10 m, 10–15 m, 15–20 m). The coastal length between these areas is approximately 90 nautical miles (Fig. 2).

Estimation of growth parameters and mortality rates. The estimation of length–weight relations (LWRs) was calculated according to the Ricker (1975) equation as

$$W = aL^b$$

This formula can be expressed in the linearized form as

$$\log W = \log a + b \log L$$

where W is the total body weight in grams, L is the total body length in cm, b is the slope, and a is the intercept. The growth parameters of von Bertalanffy were estimated according to Beverton and Holt (1959) as

$$L_t = L_\infty(1 - e^{-K(t - t_0)})$$

where L_t is the length at time t, L_∞ is the theoretical asymptotic length, K is the growth coefficient and t_0 is the theoretical age at length zero. The values of L_∞ and K were calculated in the ELEFAN in the TropFishR version 1.6.3 (Mildenberger et al. 2017). The value of t_0 was calculated using the following empirical equation of Pauly (1980)

$$\mathrm{Log}\ (-t_0) = -0.3922 - 0.2752 \log (L_\infty) - 1.038 \log (K)$$

Natural mortality (M) was calculated using Then's growth formula empirical equation (Then et al. 2015)

$$M = 4.118K^{0.73} L_\infty^{-0.33}$$

where M is natural mortality, L_∞ and K parameters of von Bertalanffy equation.

Total mortality (Z) was estimated utilizing a catch curve. Fishing mortality (F) was determined as

$$Z = F + M$$

while exploitation rate (E) was calculated as suggested by Pauly et al. (1984)

$$E = F \times Z^{-1}$$

Estimation of stock size. The swept area method was used to estimate rapa whelk stock size in the whole study region and separately for individual sub-regions. In this study, data were collected annually from the same 174 stations, selected to best represent the continental shelf of the western region of Türkiye (Table 1).

The swept area formula proposed by Sparre and Venema (1992) was used to determine the area covered by the hydraulic dredge in one hour to calculate the swept area's size.

$$A_S = D \times L_{HR} \times X_2$$

where: A_S is the swept area [km^2], X_2 is a fraction expressing the width of the swept area, D = towing distance, and L_{HR} is the length of the head rope. The towing distance (D) was estimated in units of km^2 (1 nautical mile = 1.852 km), by

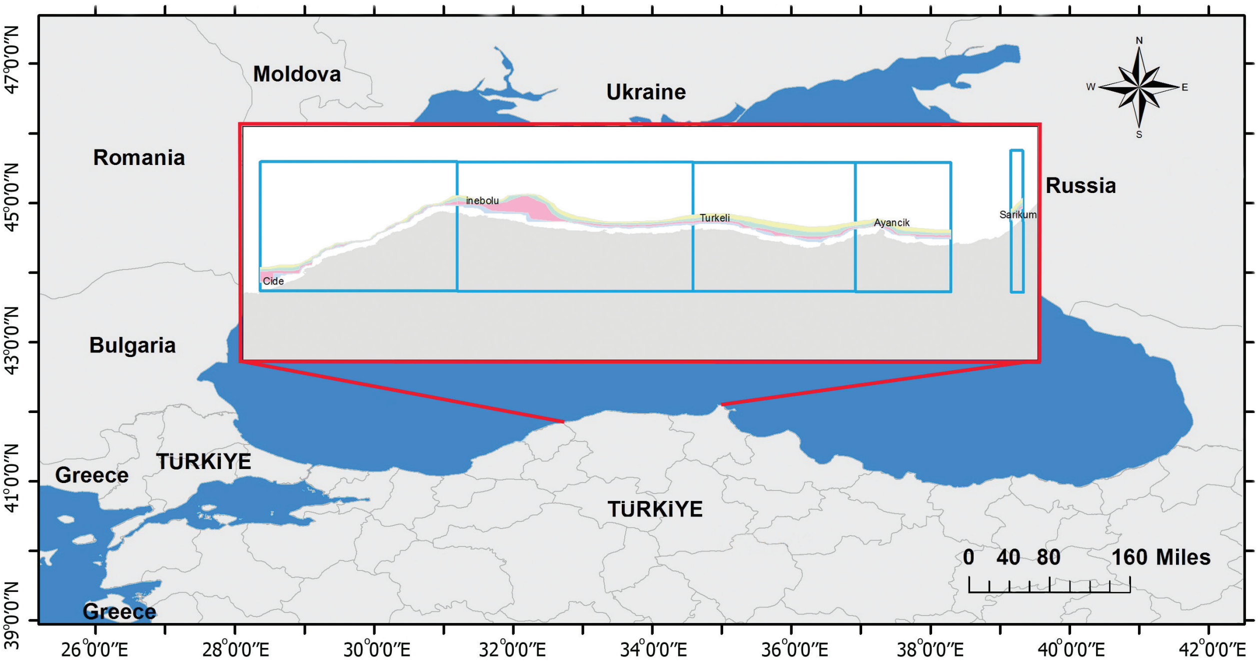

Figure 2. Study region and sub-region in the mid-southern part of the Black Sea.

$$D = 60\sqrt{(\mathrm{Lat1}-\mathrm{Lat2})^2 + (\mathrm{Lon1}-\mathrm{Lon2})^2 \times \cos^2 0.5(\mathrm{Lat1}+\mathrm{Lat2})}$$

Lat1 is the latitude at the start of the haul (degrees) and Lat2 is the latitude at the end of the haul (degrees). Similarly, Lon1 is the longitude at the start of the haul (degrees) and Lon2 is the longitude at the end of the haul (degrees).

The catch per unit area (C_A) [kg · km^{-2}] was determined as

$$C_A = \overline{\frac{C_W}{A_S}}$$

where C_W is the weight of rapa whelk collected in one sampling and A_S is the area swept in one haul [km^2].

The mean biomass per unit area ($\overline{B}$) [kg · km^{-2}], was estimated as follows.

$$\overline{B} = \frac{\overline{C_W / A_S}}{X_1}$$

where X_1 is the coefficient of catch. The hydraulic dredge coefficient of fishing has been accepted as “1”. This reflects the dredge efficiency and is considered to have collected all samples during towing.

The total biomass (B_T) [kg · km^{-2}] was estimated as

$$B_\mathrm{T} = \frac{\overline{C_W / A_S}}{X_1} \times A_\mathrm{T}$$

where A_T is km^2 total size of area under investigation.

Analysis of Variance (ANOVA) was used to test differences for estimated stock sizes among sub-regions, depths, and years. ArcGIS software package was used for rapa whelk distribution biomass. Data were analyzed in R (R Core Team 2020).

Table 1. Area covered by the beds of *Rapana venosa* in the mid-southern part of the Black Sea, according to sub-areas and number of hauls.

Sub-area	Depth [m]	Number of hauls	Area [km^2]
Cide	15–20	13	13.75
	10–15	13	13.09
	5–10	12	17.29
	0–5	11	8.94
Inebolu	15–20	15	24.24
	10–15	12	25.42
	5–10	9	56.65
	0–5	5	21.5
Türkeli	15–20	12	35.44
	10–15	13	28.26
	5–10	10	16.15
	0–5	11	12.97
Ayancık	15–20	6	15.44
	10–15	6	10.96
	5–10	8	7.22
	0–5	6	6.62
Sarıkum	15–20	3	2.25
	10–15	3	1.91
	5–10	3	1.16
	0–5	3	0.82

Results

Growth and mortality. The mean TL of rapa whelk, *Rapana venosa*, in 2011 was 47.43 ± 0.36 mm and the mean TW was 24.20 ± 0.66 g (Figs. 3, 4). In 2012, the mean TL was 59.82 ± 0.52 mm, and the mean TW was 48.18 ± 1.22 g. The LWR of the *R. venosa* was found to be $\mathrm{TW} = 0.004\mathrm{TL}^{2.82}$ in 2011 and $\mathrm{TW} = 0.0001\mathrm{TL}^{3.08}$ in 2012.

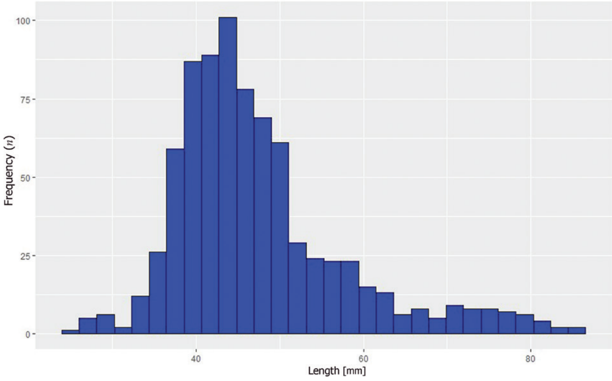

Figure 3. Length frequency of *Rapana venosa* from the mid-southern part of the Black Sea in 2011.

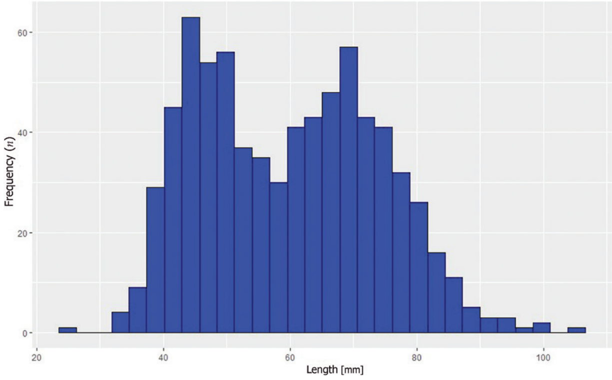

Figure 4. Length frequency of *Rapana venosa* from the mid-southern part of the Black Sea in 2012.

The results of growth parameter analysis showed that rapa whelk can reach an asymptotic length (L_∞) of 121.78 mm, with a mean K of 0.246 per year and the age of t_0 at −0.33 years. L_t can be estimated by obtaining the parameter values of K, L_∞, and t_0 (Fig. 5). The growth curves for this species followed the relation of $L_t = 121.78\,(1 - e^{-0.246(t\,+\,0.33)})$. Total mortality ($Z$) was estimated at 1.151 in the sampling region (Fig. 6). Natural mortality (M) and fishing mortality (F) rates were calculated as 0.304 yr^{-1} and 0.847 yr^{-1}, respectively. The exploitation rate (E) of the population was calculated as 0.735 yr^{-1}.

Stock distribution and structure. Results showed that *R. venosa* biomass increased threefold from 2011 to 2012 and reached 1062.41 tonnes during the sampling period. In 2011, the highest stock size was estimated in Inebolu, while the lowest was in Sarıkum. In 2012, it was determined that the biomass was higher in the Cide region (Table 2).

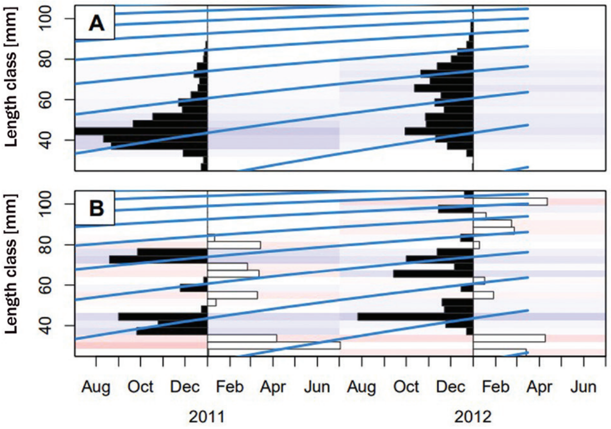

Figure 5. Uploaded raw (**A**) and restructured (**B**) length-frequency data of *Rapana venosa* from the mid-southern part of the Black Sea with overlaid von Bertalanffy growth (VBG) curves fitted by ELEFAN with a genetic algorithm. Ideally, the growth curves overlay with length bins with a high count or high positive value (blue shading) for raw (**A**) and restructured (**B**) data, respectively.

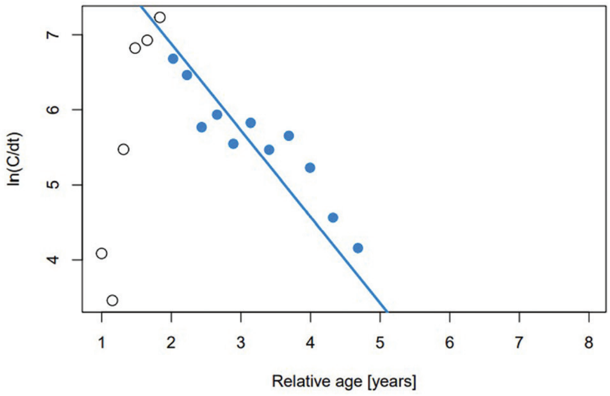

Figure 6. The logarithm of catch per length interval of *Rapana venosa* from the mid-southern part of the Black Sea against relative age. Blue points correspond to points used in the regression analysis (blue line) of the catch curve for the estimation of total mortality (Z), which corresponds to the slope of the displayed regression line. C is the number of specimens caught within a length class, dt is time needed by rapa whelk to grow through a length class].

Table 2. Estimated biomass of *Rapana venosa* from the mid-southern part of the Black Sea.

Year	Sub-area	Biomass [tonnes]	Confidence interval [tonnes]
2011	Cide	76.24	±73.55
2011	Inebolu	134.24	±203.02
2011	Türkeli	98.58	±58.67
2011	Ayancık	37.66	±37.16
2011	Sarıkum	17.18	±22.99
Total		363.92	±395.39
2012	Cide	330.62	±31.83
2012	Inebolu	140.89	±65.79
2012	Türkeli	268.89	±230.46
2012	Ayancık	301.64	±332.23
2012	Sarıkum	20.36	±37.73
Total		1062.41	±984.51

Estimated biomass values showed significant differences between the years. However, no significant differences were found among sub-regions and depths for overall results (Table 3; Fig. 7), while in 2012, significant differences were found due to the low stock size in the Sarıkum sub-region. The stock size was increased five times in the Cide, while threefold was estimated in Türkeli, and ten times in Ayancık from 2011 to 2012. Inebolu and Sarıkum showed no difference between years (Figs. 8, 9).

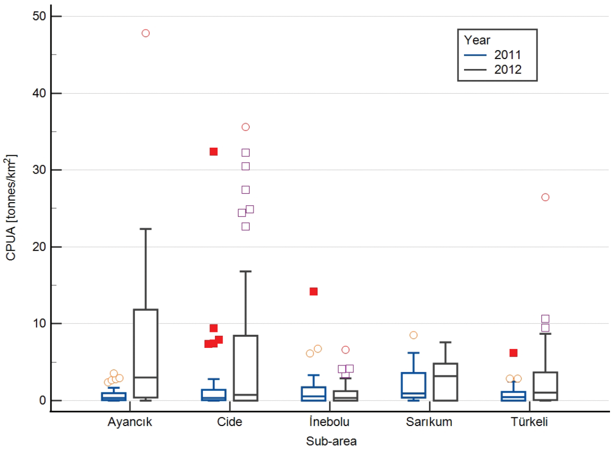

Figure 7. Box plots of estimated stock size of *Rapana venosa* with 95% CI according to sub-region, and years in the mid-southern part of the Black Sea. Horizontal lines in the boxes represent the mean values, and whiskers represent the standard deviations. Error bars represent 95% confidence intervals.

Discussion

LWR changes depending on many factors such as access to food, nutritional habits, season, gonad development, and reproduction time (Erkoyuncu 1995). According to Erik et al. (2017), *Rapana venosa* has different growth characteristics on the east, central, and west Turkish Black Sea coasts. It is stated that the main reason for the difference in LWR is the physical aspects such as a substrate. The LWR in 2011 was similar to those reported in previous studies in the Black Sea (Table 4).

Table 3. ANOVA table for differences in estimated stock biomass of *Rapana venosa* from the mid-southern part of the Black Sea among sub-regions, depth, and years.

Factor	Df	SS	MS	*F*	*P*
			All		
Sub-region	4	10743.98	2685.99	2.09	0.11
Depth	3	3039.35	1013.12	0.79	0.51
Year	1	12201.05	12201.05	10.84	**0.00**
			2011		
Sub-region	4	2197.34	549.34	1.61	0.22
Depth	3	254.05	84.68	0.19	0.90
			2012		
Sub-region	4	16775.73	4193.93	3.37	**0.04**
Depth	3	4646.76	1548.92	0.80	0.51

Bold prints denotes significance level ($P < 0.05$). Df = degrees of freedom, SS = sum of squares, MS = mean square, F = F-value.

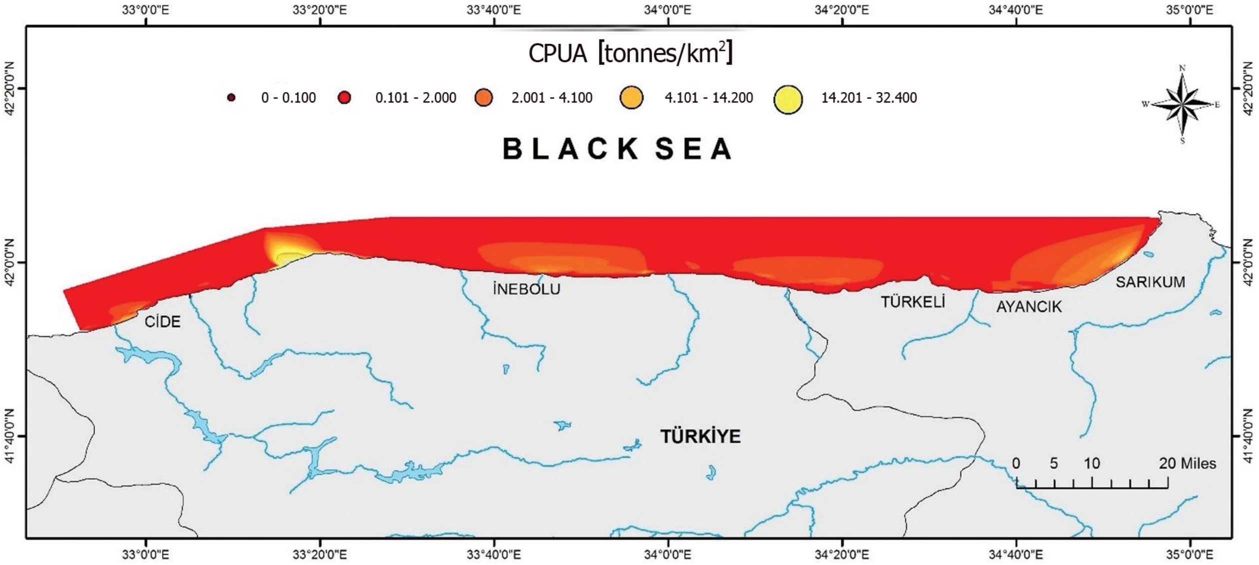

Figure 8. The catch per unit area [kg · km^{-2}] distribution of *Rapana venosa* from the mid-southern part of the Black Sea in 2011.

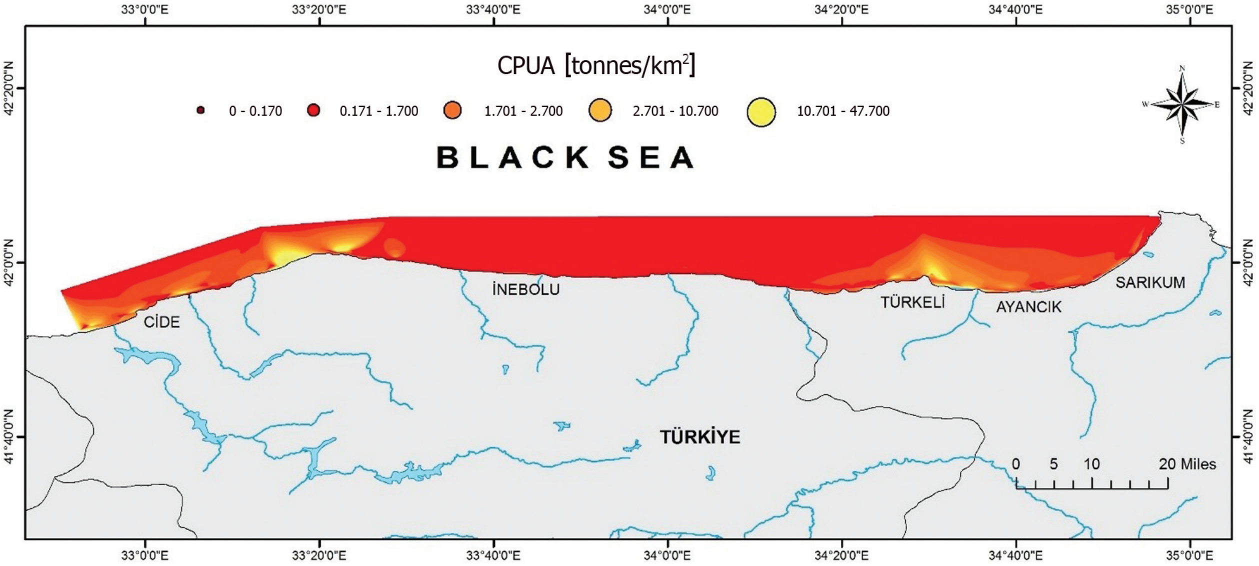

Figure 9. The catch per unit area [kg · km^{-2}] distribution of *Rapana venosa* from the mid-southern part of the Black Sea in 2012.

The *b* value of *R. venosa* in 2012 was 3.08. These findings are similar to the values found by Şahin et al. (2009) in the eastern Black Sea. Rapa whelk has been evaluated as not a slow-growing species. It is well known that food availability and environmental conditions such as temperature, pH, salinity, and water geography are crucial to species growth (Jennings et al. 2001). In this study, the fishing mortality rate was found to be significantly higher than the natural mortality rate, which indicated that the mortality of *R. venosa* was mainly caused by fishing activities. Additionally, lower *M* to higher *F* can be evaluated as the occurrence of overfishing, in which younger individuals were caught more than old ones (Sparre and Venema 1992). The exploitation rate of 0.735 also clearly indicated that the exploitation for rapa whelk was higher than the optimum exploitation level as it was suggested $E = 0.5$ for the optimum exploitation of resource (Gulland 1983). Therefore, fisheries management should consider precautionary approaches to ensure the sustainability of the *R. venosa* stock in the region. It is thought that high fecundity will be effective in maintaining the current level of stocks despite the high fishing pressure (Harding 2003). Since it is an important source of income for fishermen today, there is no expectation of stakeholders to completely remove it from the ecosystem (Dağtekin et al. 2023).

Considering sub-regions, the *R. venosa* population in Cide, Türkeli, and Ayancık increased significantly in one year, related to the increase in *C. gallina* in abundance. Inebolu sub-region was an important distribution area of *R. venosa*, and estimated stock sizes are the highest. Additionally, the amount of *C. gallina*, its main prey, was high (62 000 tonnes) in this area (Dağtekin et al. 2016). Food availability is the main factor for species distribution and affects population

Table 4. Comparison of length–weight relations of *Rapana venosa* from various studies carried out in the Black Sea.

Region	*a*	*b*	R^2	Year	Reference
East Black Sea	0.0004	2.798		1991	Düzgüneş et al. 1992
Bulgaria	0.0005	2.813			Prodanov et al. 1995
East Black Sea	0.0001	3.146			Sağlam, unpublished
Romania	0.0002	2.568			Micu et al. 2008
East Black Sea	0.0006	2.712		2007	Saglam et al. 2008
East Black Sea	0.00009	3.145			Şahin et al. 2009
Trabzon (EBS)	0.0004	2.826	0.89	2007	Sağlam et al. 2015
Terme (EBS)	0.0006	2.735	0.84	2007	Sağlam et al. 2015
Samsun (EBS)	0.0011	2.556	0.85	2007	Sağlam et al. 2015
Yakakent (EBS)	0.0076	2.728	0.91	2015	Bayraklı et al. 2016
Türkiye	0.0002	2.876	0.98	2016	Erik et al. 2017
Türkiye	0.0002	2.9868		2017	GFCM 2023
Türkiye	0.0001	3.085		2018	GFCM 2023
Türkiye	0.0001	3.104		2019	GFCM 2023
Türkiye	0.0002	2.949		2020	GFCM 2023
Türkiye	0.0002	2.981		2021	GFCM 2023
Türkiye	0.0002	2.921		2022	GFCM 2023
Ukraine	0.334	2.725		2017	GFCM 2023
Ukraine	0.4304	2.533		2018	GFCM 2023
Ukraine	0.2328	2.893		2019	GFCM 2023
Ukraine	0.469	2.568		2020	GFCM 2023
Ukraine	0.309	2.756		2021	GFCM 2023
Bulgaria	0.16	2.99		2017	GFCM 2023
Bulgaria	0.1642	2.99		2018	GFCM 2023
Bulgaria	0.0005	2.726		2021	GFCM 2023
Bulgaria	0.00024	2.915		2022	GFCM 2023
West Black Sea	0.0004	2.824	0.89	2011	Presently reported study
West Black Sea	0.0001	3.089	0.94	2012	Presently reported study

EBS = East Black Sea.

* Sağlam H (2003) Doğu Karadeniz'deki deniz salyangozunun *Rapana thomasiana* Crosse, 1861 Biyoekolojisi. Doktora tezi Trabzon, Türkiye. 101 pp. [In Turkish]

growth. Düzgüneş et al. (1992) reported that *R. venosa* biomass is between 18 and 160 tonnes · km^{-2} in the eastern Black Sea. Sağlam et al. (2015) found Trabzon and Samsun (The eastern Black Sea) respectively 2.25 and 4.17 tonnes · km^{-2}. Comparing our results with previous studies showed that the stock sizes are lower than those calculated for the Samsun shelf area (eastern part of the Black Sea), where *R. venosa* fishing is the most concentrated. The fact that *R. venosa* fishing is not common (only scuba diving) in our sampling area, but the higher abundance of two important prey items (*Chamelea gallina* and *Anadara inaequivalvis* (Bruguière, 1789)) is thought to be the factors responsible for the increase in the estimated stock size of *R. venosa* in 2012 (Dağtekin et al. 2016). Depending on the season, the regions and depths utilized by *R. venosa* vary; while it shows a dense distribution at depths down to 15 m in the summer months, it migrates down to the depth range of 40–45 m in winter (Sağlam et al. 2009). Based on the number of empty bivalve shells collected during the research, it can be said that *R. venosa* exerts severe predator pressure on *C. gallina*. It is known that fishing mortality owing to hydraulic dredges and sudden changes in environmental parameters impact the natural mortality of bivalve species (López-Rocha et al. 2018). Therefore, it is recommended to develop a policy against the population growth of rapa whelk in a certain sub-region, such as Inebolu.

Conclusions

In conclusion, many studies on the *Rapana venosa* stocks have settled along the Black Sea coastline and become an important economic contribution for fishers over the past 30 years. Some researchers have suggested that this species should be removed entirely owing to its substantial harmful effects (Čuhčin 1984; STECF 2017). Zengin and Knudsen (2006) showed that the rapa whelks exert pressure on *Mytilus galloprovincialis*, *Chamelea gallina*, and *Anadara* spp. Several studies emphasize that due to *R. venosa* having destroyed the mussel beds, their population may not be able to increase (Dalgıç and Karayücel 2007). Today, mussel beds are considered seriously threatened by all Black Sea countries and there has also been an increase in *R. venosa* caught in the Black Sea recently (STECF 2017). On the other hand, many undesirable species continue to enter the Black Sea due to both climate change and biological pollution. The Pacific oyster, *Magallana gigas* (Thunberg, 1793), which is widely distributed in the Black Sea nowadays, is the best example of this situation (Aydın and Gül 2021). Therefore, it would be good to make evaluations by bringing all these components together. The kind of changes that will occur in the functioning of *R. venosa* in the ecosystem with these species should be investigated. It is important that studies on *R. venosa* are carried out continuously. Habitat-based assessments are needed in fisheries management. Dağtekin et al. 2022 found that the mean length was low in the Eastern Black Sea region. While there is predator pressure in this region, there have been decreases in the Samsun shelf region due to excessive fishing pressure.

Additionally, the rapa whelk has become a component of the Black Sea ecosystem. Therefore, there is a need for clear outcomes to be discussed and actions to be implemented to monitor the fisheries of this species. This includes creating and monitoring management scenarios or taking the necessary measures to eliminate this species from the ecosystem owing to the damage it causes to the habitat.

Acknowledgments

This study was supported by the General Directorate of Agricultural Research and Policies (GDAR), Ankara, Türkiye (Project no:TAGEM/HAYSÜD/2011/09/02/05). This study was carried out within the Central Fisheries Research Institute.

References

An LH, Zhang Y, Song SS, Liu Y, Li ZC, Chen H, Zheng BH (2013) Imposex effects on the veined rapa whelk (*Rapana venosa*) in Bohai Bay, China. Ecotoxicology 22: 538–547. https://doi.org/10.1007/s10646-013-1046-0

Aydın M, Gül M (2021) Presence of the Pacific oyster (*Crassostrea gigas* Thunberg, 1793) in the Black Sea. Journal of Anatolian Environmental and Animal Sciences 6(1): 14–17. https://doi.org/10.35229/jaes.800160

Bailey SA, Brown L, Campbell ML, Canning-Clode J, Carlton JT, Castro N, Zhan A (2020) Trends in the detection of aquatic non-indigenous species across global marine, estuarine and freshwater ecosystems: A 50-year perspective. Diversity and Distributions 26(12): 1780–1797. https://doi.org/10.1111/ddi.13167

Bayraklı B, Özdemir S, Özdemir ZB (2016) Yakakent Bölgesindeki (Güney Karadeniz) deniz salyangozlarının (*Rapana venosa* Valenciennes, 1846) boy-ağırlık ilişkileri, kondisyon indeksleri ve et verimleri. [Length–weight relationships, condition factor index and meat yield of rapa whelks (*Rapana venosa* Valenciennes, 1846) in the Yakakent Regions (southern Black Sea).] Alınteri Zirai Bilimler Dergisi 31(2): 65–71. [In Turkish]

Beverton RJH, Holt SJ (1959) Chapter 10. A review of the lifespans and mortality rates of fish in nature, and their relationship to growth and other physiological characteristics. Pp. 142–180. Wolstenholme GEW, O'Conner M (Eds.) Ciba Foundation Colloquia on Ageing; Volume 5; The lifespan of animals. J. and A. Churchill, London, UK. https://doi.org/10.1002/9780470715253.ch10

Bilecik N (1975) La répartition de *Rapana thomasiana thomasiana* Crosse sur le littoral turc de la Mer Noire s'étandant d'Igneada jusqu'à Calti Burnu. Rapports et procès-verbaux des réunions de Commission International pour l'Exploration de la Mer Méditerranee 23: 169–171.

Bilecik N (1990) Deniz Salyangozu *Rapana venosa* (V)'nın Türkiye'nin Karadeniz sahillerindeki dağılımı ve Karadeniz balıkçılığındaki etkisi. TOKB Su Ürünleri Araştırma Enstitüsü Yayını, Bodrum. [In Turkish]

Bondarev IP (2014) Dynamics of *Rapana venosa* (Valenciennes, 1846) (Gastropoda: Muricidae) population in the Black Sea. International Journal of Material Science 4(3): 42–56.

Čuhčin VD (1984) Èkologiâ brûhonogih mollûskov Černogo Morâ. [Ecology of the gastropod mollusks of the Black Sea.] Naukova Dumka, Kiev, USSR, 175 pp. [In Russian]

Dağtekin M, Erbay M, Dalgıç G, Akpınar Özcan İ, Aydın M, Özdemir S, Karayücel S (2016) Batı Karadeniz'de (Sinop-Cide) dağılım gösteren beyaz kum midyesi (*Chamelea gallina* (L., 1758)) stoklarının tahmini üzerine bir ön çalışma. TAGEM/HAYSÜD/2011/09/02/05, Trabzon, Türkiye, 97 pp. [In Turkish]

Dağtekin M, Ceyhan V, Dağtekin BB (2023) Stakeholders' perspectives on the management measures in *Rapana venosa* fisheries in the Black Sea Turkish coast. Thalassas. https://doi.org/10.1007/s41208-023-00601-1

Dalgıç G, Karayücel S (2007) Investigations stock of the striped Venus (*Chamelea gallina* L., 1758) in Ordu's coastal zone of the eastern Black Sea. Journal of Fisheries International 2(1): 12–16.

Düzgüneş E, Ünsal S, Feyzioglu M (1992) Doğu Karadeniz'deki deniz salyangozu *Rapana thomasiana* Gross, 1861 stoklarının tahmini. Proje no: DEBAG 143/6. KTU Sürmene Deniz Bilimleri Fakültesi, Trabzon, Türkiye, 43 pp. [In Turkish]

Erik G, Dağtekin M (2022) Effect of fishery closure on discard composition of rapa whelk, *Rapana venosa* (Valenciennes, 1846) beam trawl fisheries in Black Sea. Turkish Journal of Fisheries and Aquatic Sciences 22(5). https://doi.org/10.4194/TRJFAS19046

Erik G, Dağtekin M, Çankaya A, Kutlu S, Genç Y, Özaydın E, Balçık Mısır G, Özkaya E (2017) Karadeniz'de deniz salyangozu (*Rapana venosa*, Valenciennes, 1846) balıkçılığının izlenmesi. Su Ürünleri Grup Değerlendirme Toplantısı, 13–17 Şubat 2017, Antalya, Türkiye, 76 pp. [In Turkish]

Erkoyuncu İ (1995) Balıkçılık biyolojisi ve populasyon dinamiği No: 95. Ondokuz Mayıs Üniversitesi Yayınları, Samsun, Türkiye. [In Turkish]

GFCM (2023) General Fisheries Commission for the Mediterranean—GFCM. Validated stock assessment forms (SAFs). https://www.fao.org/gfcm/data/safs/fr/

Gulland JA (1983) Fish stock assessment: A manual of basic methods. FAO/Wiley Series on Food and Agriculture, Rome, 241 pp.

Harding JM (2003) Predation by blue crabs, *Callinectes sapidus*, on rapa whelks, *Rapana venosa*: Possible natural controls for an invasive species? Journal of Experimental Marine Biology and Ecology 297(2): 161–177. https://doi.org/10.1016/j.jembe.2003.07.005

Harding JM, Mann R (2005) Veined rapa whelk (*Rapana venosa*) range extensions in the Virginia waters of Chesapeake bay, USA, Journal of Shellfish Research 24(2): 381–385. https://doi.org/10.2983/0730-8000(2005)24[381:VRWRVR]2.0.CO;2

Jennings S, Kaiser MJ, Reynold JD (2001) Marine fisheries ecology. Blackwell Science, Oxford.

López-Rocha JA, Melo FJFR, Gastélum-Nava E, Larios-Castro E, Romo-Piñera A (2018) Morphometric relationship, growth parameters, and natural mortality as estimated primary inputs for fishery management in new fishing areas for bivalve molluscs (Bivalvia: Veneridae). Journal of Shellfish Research 37(3): 591–600. https://doi.org/10.2983/035.037.0312

Mack RN, Simberloff D, Lonsdale WM, Evans H, Clout M, Bazzaz FA (2000) Biotic invasions: Causes, epidemiology, global consequences, and control. Ecological Applications 10(3): 689–710. https://doi.org/10.1890/1051-0761(2000)010[0689:BICEGC]2.0.CO;2

Mann R, Occhipinti A, Harding JM (Eds) (2004) Alien species alert: *Rapana venosa* (veined whelk). ICES Cooperative Research Report No. 264, 14 pp. https://doi.org/10.17895/ices.pub.5471

Micu S, Comanescu G, Kelemen B (2009) The imposex status in *Rapana venosa* population from Agigea littoral. Analele Științifice ale Universității „Al. I. Cuza" Iași, s. Biologie animală 55: 133–137.

Mildenberger TK, Taylor MH, Wolff M (2017) TropFishR: An R package for fisheries analysis with length-frequency data. Methods in Ecology and Evolution 8(11): 1520–1527. https://doi.org/10.1111/2041-210X.12791

Munari C, Mistri M (2011) Short-term hypoxia modulates *Rapana venosa* (Muricidae) prey preference in Adriatic lagoons. Journal of Experimental Marine Biology and Ecology 407(2): 166–170. https://doi.org/10.1016/j.jembe.2011.06.003

Ovando D, Hilborn R, Monnahan C, Rudd M, Sharma R, Thorson JT, Ye Y (2021) Improving estimates of the state of global fisheries depends on better data. Fish and Fisheries 22(6): 1377–1391. https://doi.org/10.1111/faf.12593

Pauly D (1980) On the interrelationship with the natural mortality, growth parameter and environmental temperature in 175 fish stocks. ICES Journal of Marine Science 39(2): 175–192. https://doi.org/10.1093/icesjms/39.2.175

Pauly D, Ingles J, Neal R (1984) Application to shrimp stocks of objective methods for the estimation of growth, mortality and recruitment-related parameters from length-frequency data (ELEFAN I and II). Fishing News Books Ltd.

Prodanov K, Konsulova T, Todorova V (1995) Growth rate of *Rapana thomasiana* along the Bulgarian Black Sea Coast. In Rapport Du Xxxıve Congres De La Commission Internationale Pour L'exploratıon Scientifique De La Mer Mediterranee, 27–31 March 1995, Malta, Volume 34, 40 pp., Congress of CIESM.

R Core Team (2020) R: A language and environment for statistical computing. R Foundation for Statistical Computing, Vienna, Austria. https://www.R-project.org/

Ricker WE (1975) Computation and interpretation of biological statistics of fish populations. Bulletin of the Fisheries Research Board of Canada 191: 1–382.

Sağlam H, Düzgüneş E (2007) Deposition of egg capsule and larval development of *Rapana venosa* (Gastropoda: Muricidae) from the south-eastern Black Sea. Journal of the Marine Biological Association of the United Kingdom 87(4): 953–957. https://doi.org/10.1017/S0025315407056330

Sağlam H, Düzgüneş E (2014) Rapa whelk (*Rapana venosa* Valenciennes, 1846) fisheries in the Black Sea. Pp. 305–339. In: Duzgunes E, Ozturk B, Zengin M (Eds) Turkish fisheries in the Black Sea. Turkish Marine Research Foundation (TUDAV) No. 40. Istanbul, Türkiye.

Sağlam H, Kutlu S, Bascinar S, Dagtekin M, Selen H, Sahin A (2008) Deniz salyangozu avcılığında direce alternatif farklı tuzak modellerinin geliştirilmesi. Proje No: TAGEM/HAYSÜD/2005/09/02/02. Su Ürünleri Merkez Araştırma Enstitüsü, Trabzon, Türkiye, 94 pp. [In Turkish]

Sağlam H, Düzgüneş E, Öğüt H (2009) Reproductive ecology of the invasive whelk *Rapana venosa* Valenciennes, 1846, in the south-eastern Black Sea (Gastropoda: Muricidae). ICES Journal of Marine Science 66(9): 1865–1867. https://doi.org/10.1093/icesjms/fsp184

Sağlam H, Kutlu S, Dagtekin M, Bascinar S, Sahin A, Selen H, Duzgunes E (2015) Population biology of *Rapana venosa* (Valenciennes, 1846) (Gastropoda: Neogastropoda) in the south-eastern Black Sea of Türkiye. Cahiers de Biologie Marine 56(4): 363–368.

Şahin C, Emiral H, Okumuş İ, Gözler AM, Kalayci F, Hacimurtezaoglu N (2009) The benthic exotic species of the Black Sea: Blood cockle (*Anadara inaequivalvis*, Bruguiere, 1789: Bivalve) and rapa whelk (*Rapana thomasiana*, Crosse, 1861: Mollusc). Journal of Animal and Veterinary Advances 8(2): 240–245.

Salomidi M, Katsanevakis S, Borja Á, Braeckman U, Damalas D, Galparsoro I, Mifsud R, Mirto S, Pascual M, Pipitone C, Rabaut M, Todorova V, Vassilopoulou V, Vega Fernandez T (2012) Assessment of goods and services, vulnerability, and conservation status of European seabed biotopes: A stepping stone toward ecosystem-based marine spatial management. Mediterranean Marine Science 13(1): 49–88. https://doi.org/10.12681/mms.23

Sampson D, Damalas D, Chato Osio G (2014) Scientific, Technical and Economic Committee for Fisheries (STECF): Black Sea assessments (STECF-14-14). Publications Office of the European Union, Luxembourg, EUR 26896 EN, JRC 92436, 421 pp.

Savini D, Harding JM, Mann R (2002) Rapa whelk *Rapana venosa* (Valenciennes, 1846) predation rates on hard clams *Mercenaria mercenaria* (Linnaeus, 1758). Journal of Shellfish Research 21: 777–779.

Slynko E, Slynko YV, Rabushko VI (2020) Adaptive strategy of *Rapana venosa* (Gastropoda, Muricidae) in the invasive population of the Black Sea. Biosystems Diversity 28(1): 48–52. https://doi.org/10.15421/012008

Smith BS (1971) Sexuality in the American mud snail, *Nassarius obsoletus* Say. Journal of Molluscan Studies 39(5): 377–381. https://doi.org/10.1093/oxfordjournals.mollus.a065117

Sparre P, Venema SC (1992) Introduction to Tropical Fish Stock Assessment. Part 1. Manual No: 306/1. FAO Fisheries Technical Paper, Rome.

STECF (2017) Scientific, Technical and Economic Committee for Fisheries (STECF)—Stock assessments in the Black Sea (STECF-17-14). Publications Office of the European Union, Luxembourg. 496 pp.

Then AY, Hoenig JM, Hall NG, Hewitt DA (2015) Evaluating the predictive performance of empirical estimators of natural mortality rate using information on over 200 fish species. ICES Journal of Marine Science 72(1): 82–92. https://doi.org/10.1093/icesjms/fsu136

Uyan O, Aral O (2003) The larval development stages of the Japanese snail, *Rapana thomasiana*, Gross 1861, in the egg capsule. Turkish Journal of Zoology 27: 331–337.

Zengin M, Knudsen S (2006) Multidisciplinary modelling of Black Sea fisheries: A case study from Samsun Türkiye. Black Sea Ecosystem 2005 and Beyond, 1st Biannual Scientific Conference, BSERP/BSC, 8–10 May 2006 İstanbul, Türkiye.

Zolotarev V (1996) The Black Sea ecosystem changes related to introduction of new mollusc species. Marine Ecology 17(1–3): 227–236. https://doi.org/10.1111/j.1439-0485.1996.tb00504.x

Acta Ichthyologica et Piscatoria 53, 2023, 201–207 | DOI 10.3897/aiep.53.110519

PENSOFT.

ACTA ICHTHYOLOGICA ET PISCATORIA

Length–weight relations of 44 fish species (Actinopterygii) inhabiting an unprotected tropical coastal biological corridor of Yucatan, Mexico

María Eugenia VEGA-CENDEJAS[1], Mirella HERNÁNDEZ DE SANTILLANA[1], Sonia PALACIOS-SÁNCHEZ[1]

1 *Centro de Investigación y de Estudios Avanzados del Instituto Politécnico Nacional, Unidad Mérida, Mérida (CINVESTAV), Yucatán, Mexico*

https://zoobank.org/A865B16B-3505-4CEF-8E7F-A863D292A3B3

Corresponding author: María Eugenia Vega-Cendejas (maruvega@cinvestav.mx)

Academic editor: Rodolfo Reyes ♦ **Received** 3 August 2023 ♦ **Accepted** 23 October 2023 ♦ **Published** 24 November 2023

Citation: Vega-Cendejas ME, Hernández de Santillana M, Palacios-Sánchez S (2023) Length–weight relations of 44 fish species (Actinopterygii) inhabiting an unprotected tropical coastal biological corridor of Yucatan, Mexico. Acta Ichthyologica et Piscatoria 53: 201–207. https://doi.org/10.3897/aiep.53.110519

Abstract

Length–weight relations (LWRs) were estimated for 44 fish species, representing 23 families, collected from an unprotected coastal biological corridor of the Yucatan Peninsula. The following species were studied (in alphabetical order): *Acanthostracion quadricornis* (Linnaeus, 1758); *Albula vulpes* (Linnaeus, 1758); *Anchoa hepsetus* (Linnaeus, 1758); *Anchoa lamprotaenia* Hildebrand, 1943, *Anchoa lyolepis* (Evermann et Marsh, 1900), *Anchoa mitchilli* (Valenciennes, 1848); *Archosargus rhomboidalis* (Linnaeus, 1758); *Ariopsis felis* (Linnaeus, 1766); *Bagre marinus* (Mitchill, 1815); *Bairdiella chrysoura* (Lacepède, 1802); *Caranx latus* Agassiz, 1831; *Chaetodipterus faber* (Broussonet, 1782); *Chriodorus atherinoides* Goode et Bean, 1882; *Cynoscion arenarius* Ginsburg, 1930; *Elops saurus* Linnaeus, 1766; *Eucinostomus argenteus* Baird et Girard, 1855; *Eucinostomus gula* (Quoy et Gaimard, 1824); *Eucinostomus harengulus* Goode et Bean, 1879; *Harengula jaguana* Poey, 1865; *Hyporhamphus unifasciatus* (Ranzani, 1841); *Lagodon rhomboides* (Linnaeus, 1766); *Lutjanus griseus* (Linnaeus, 1758); *Menticirrhus americanus* (Linnaeus, 1758); *Menticirrhus littoralis* (Holbrook, 1847); *Menticirrhus saxatilis* (Bloch et Schneider, 1801); *Mugil curema* Valenciennes, 1836; *Mugil trichodon* Poey, 1875; *Oligoplites saurus* (Bloch et Schneider, 1801); *Opisthonema oglinum* (Lesueur, 1818); *Opsanus beta* (Goode et Bean, 1880); *Orthopristis chrysoptera* (Linnaeus, 1766); *Prionotus tribulus* Cuvier, 1829; *Rypticus maculatus* Holbrook, 1855; *Selene vomer* (Linnaeus, 1758); *Sphoeroides spengleri* (Bloch, 1785); *Sphoeroides testudineus* (Linnaeus, 1758); *Strongylura notata* (Poey, 1860); *Strongylura timucu* (Walbaum, 1792); *Symphurus plagiusa* (Linnaeus, 1766); *Synodus foetens* (Linnaeus, 1766); *Trachinotus carolinus* (Linnaeus, 1766); *Trachinotus falcatus* (Linnaeus, 1758); *Trachinotus goodei* Jordan et Evermann, 1896; *Urobatis jamaicensis* (Cuvier, 1816). A new maximum standard length (SL) was recorded for *Anchoa lamprotaenia*. Positive allometric growth was reported in ten species, negative allometric growth in sixteen species, and isometric growth in eighteen species.

Keywords

Length–weight relations, nursery habitats, wetlands, Yucatan Peninsula

Introduction

Length–weight relations (LWRs) of fishes are a key element for the study of their biology, taxonomy, physiology, ecology (Vega-Cendejas et al. 2017), and fish population dynamics (Kohler et al. 1995). They are useful to calculate the expected weight from the known length of fish and vice versa (Xie et al. 2015; Kuriakose 2017), to estimate the isometric or allometric growth (Teixeira-de Mello et al. 2006), as an indicator of fatness and the relative well-being of the fish population, the standing stock biomass and comparing the ontogeny of fish populations from different regions (Petrakis and Stergiou 1995). This relation has also been used for species-specific life history comparisons between regions (Wotton 1990), and evaluations of parasite effects (Teixeira-de Mello and Eguren 2008).

The presently reported study was an effort to determine LWRs for 44 fish species from Yucatan, southern Gulf of Mexico. The fish were collected from a chain of unprotected littoral habitats which we will later refer to as the Yucatan Coastal Biological Corridor (YCBC). A biological corridor is a delimited geographic space that promotes connectivity between landscapes, ecosystems, and natural or modified habitats and ensures the maintenance of biological diversity and ecological processes. It also allows genetic exchange between fragmented populations and the integration of these areas into land use planning plans. Studying these areas provides valuable information to propose new locations that require protection, as well as to identify high-priority network linkages between existing marine protected areas (Pendoley et al. 2014) and to define essential habitats for target species (Turk-Boyer et al. 2014).

Biological corridors emerge as a mechanism that attempts to give greater variability to the conservation of species found in wild areas, allowing the movement of biota from one protected area to another or between fragments of ecosystems (Moran et al. 2019). The YCBC unites ecologically protected natural areas through regions with various productive activities and different land uses. Its importance lies in the fact that this system is unique in the association of the species with the habitat and its ecological process, in the way in which the populations that inhabit the coast using their natural resources. This area has been recognized for having great biodiversity, characterized by the heterogeneity of its habitats with the presence of wetlands, coastal lagoons, and petenes on its coastline. However, the YCBC, which stretches 128 km, has been modified by various anthropogenic activities such as the construction of docks and ports, as well as by artisanal and industrial fishing, aquaculture, and ecotourism (Herrera-Silveira and Morales-Ojeda 2009). Studies in this area have indicated that diversity and abundance of fishery resources increase inside protected areas. However, the surrounding unprotected areas require strategies to allow the free flow of species from one protected area to the other (Palacios-Sánchez et al. 2019).

Material and methods

The YCBC, as part of the Mesoamerican Corridor is located in the tropical region of the southeastern Gulf of Mexico (21°02′48.66″–21°21′28.20″W, 89°07′8.04″–90°16′45.84″N), which includes 350 km of costal zone habitats (Euán-Avila et al. 2014) and connects two important reserves in the Yucatan Peninsula—Celestun in the West and Ria Lagartos in the East (Palacios-Sánchez et al. 2019) (Fig. 1).

Sampling of the fish specimens was carried out monthly for three years (October 2001 through April 2004) in 24 localities of the YCBC. Fish samples were collected during the first six hours of light of the day using a benthic trawling net (15 m long × 1.5 m, 2.54 cm mesh) in all the habitats (wetlands, coastal lagoons, coastline). At each station, to carry out sampling, we walked perpendicular

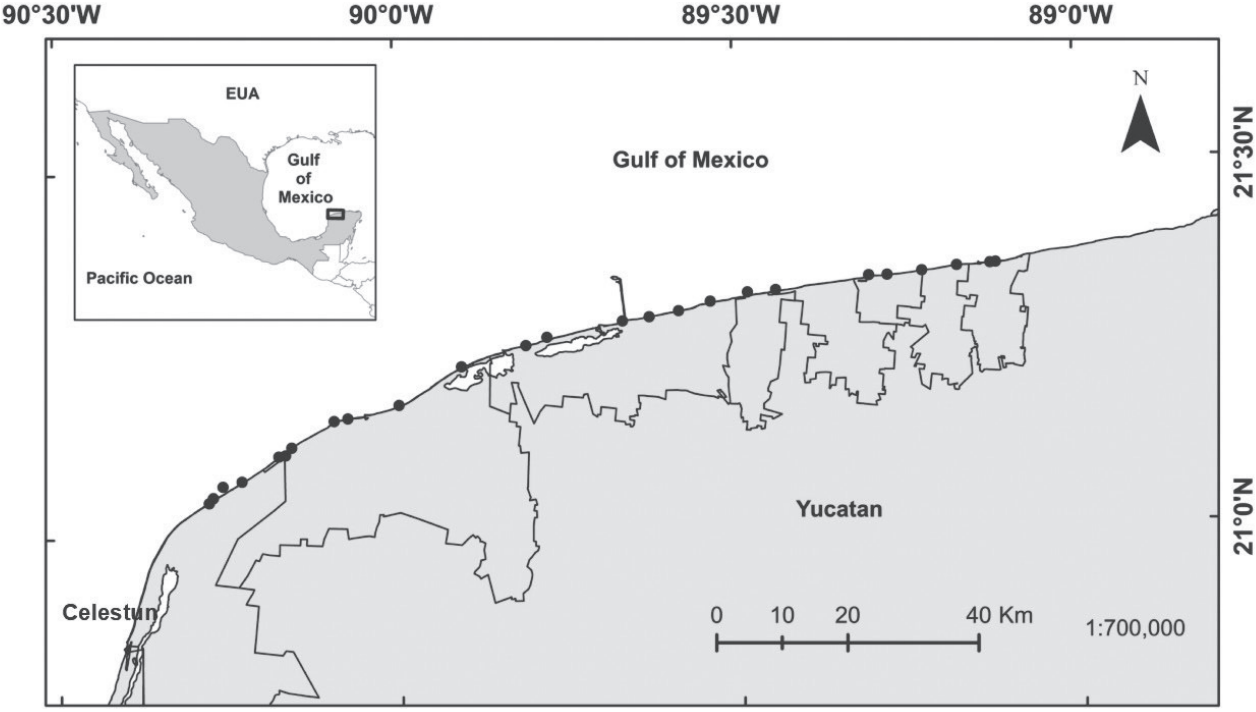

Figure 1. Sampling stations in the study area in the unprotected Yucatan Coastal Biological Corridor, southern Gulf of Mexico.

to the coast, measuring the distance from the shore to record the sampled area. The trawl net was dragged manually, making two replicates per station, separated by 10 m. Collected fishes were euthanized in ice slurry, preserved (70% ethanol), and transported to the laboratory where they were identified using specialized references (Allen 1985; Carpenter 2002a, 2002b; McEachran and Fechhelm 1998, 2005, among others), measured for standard length (SL) (to the nearest 0.1 cm), and weighed (to the nearest 0.01 g). A representative sample of each species was deposited and cataloged in the Ichthyology Collection of the Centro de Investigación y de Estudios Avanzados del Instituto Politécnico Nacional, Mérida, Mexico (CINV-NEC), reference number YUC-PEC.084.0999.

We calculated the LWRs using the allometric formula

$$W = aL^b$$

where W is the weight of the fish [g], L is the standard length [cm], a is the intercept, and b is the allometric coefficient/slope. The values of a and b were calculated with Statgraphics software (Centurion XV, Version 15.1.02, Copyright 1982–2006 StatPoint, Inc.) with a linear least squares regression using a logarithmic scale. Based on the value of the slope (b), the growth of a fish species was considered negative allometric ($b < 3$), positive allometric ($b > 3$), or isometric ($b = 3$) (Froese et al. 2011). Outliers were removed using logarithmic plots, and limits for a and b were estimated by a student's t-test with a 95% confidence (Froese 2006). In some cases, when the number of specimens was too small or the size range was too narrow to estimate the LWRs parameters a and b, we assumed an isometric relation ($b = 3$) (Froese 2006; Hay et al. 2020) and the value of the intercept a will be obtained with the following formula:

$$a = \frac{\sum_{i=1}^{n} \frac{W}{L^3}}{n}$$

where W refers to the weight [g], L to the standard length [cm], and n to the number of specimens.

Results

The descriptive statistics and the estimated LWRs parameters for 44 species which represents 23 families are summarized in Table 1, including *Urobatis jamaicensis* (Cuvier, 1816) [Urotrygonidae]; *Albula vulpes* (Linnaeus, 1758) [Albulidae]; *Elops saurus* Linnaeus, 1766 [Elopidae]; *Anchoa hepsetus* (Linnaeus, 1758), *Anchoa lamprotaenia* Hildebrand, 1943, *Anchoa lyolepis* (Evermann et Marsh, 1900), *Anchoa mitchilli* (Valenciennes, 1848) [Engraulidae]; *Harengula jaguana* Poey, 1865, *Opisthonema oglinum* (Lesueur, 1818) [Dorosomatidae]; *Ariopsis felis* (Linnaeus, 1766), *Bagre marinus* (Mitchill, 1815) [Ariidae]; *Synodus foetens* (Linnaeus, 1766) [Synodontidae]; *Opsanus beta* (Goode et Bean, 1880) [Batrachoididae]; *Mugil curema* Valenciennes, 1836, *Mugil trichodon* Poey, 1875 [Mugilidae]; *Strongylura notata* (Poey, 1860), *Strongylura timucu* (Walbaum, 1792) [Belonidae]; *Chriodorus atherinoides* Goode et Bean, 1882, *Hyporhamphus unifasciatus* (Ranzani, 1841) [Hemiramphidae]; *Caranx latus* Agassiz, 1831, *Oligoplites saurus* (Bloch et Schneider, 1801), *Selene vomer* (Linnaeus, 1758), *Trachinotus carolinus* (Linnaeus, 1766), *Trachinotus falcatus* (Linnaeus, 1758), *Trachinotus goodei* Jordan et Evermann, 1896 [Carangidae]; *Symphurus plagiusa* (Linnaeus, 1766) [Cynoglossidae]; *Eucinostomus argenteus* Baird et Girard, 1855, *Eucinostomus gula* (Quoy et Gaimard, 1824), *Eucinostomus harengulus* Goode et Bean, 1879 [Gerreidae]; *Rypticus maculatus* Holbrook, 1855 [Grammistidae]; *Orthopristis chrysoptera* (Linnaeus, 1766) [Haemulidae]; *Lutjanus griseus* (Linnaeus, 1758) [Lutjanidae]; *Prionotus tribulus* Cuvier, 1829 [Triglidae]; *Chaetodipterus faber* (Broussonet, 1782) [Ephippidae]; *Bairdiella chrysoura* (Lacepède, 1802), *Cynoscion arenarius* Ginsburg, 1930, *Menticirrhus littoralis* (Holbrook, 1847), *Menticirrhus americanus* (Linnaeus, 1758), *Menticirrhus saxatilis* (Bloch et Schneider, 1801) [Sciaenidae]; *Archosargus rhomboidalis* (Linnaeus, 1758), *Lagodon rhomboides* (Linnaeus, 1766) [Sparidae]; *Acanthostracion quadricornis* (Linnaeus, 1758) [Ostraciidae]; *Sphoeroides spengleri* (Bloch, 1785), *Sphoeroides testudineus* (Linnaeus, 1758) [Tetraodontidae].

All LWRs estimates were statistically significant ($P < 0.05$). New maximum lengths are reported for one species *Anchoa lamprotaenia* (12.2 cm SL). The scaled herring, *Harengula jaguana*, was the most abundant fish species (3769 specimens), followed by the broad-striped anchovy, *Anchoa hepsetus* (3559 specimens). However, even though the sampling continued for three years, a lower number of specimens was obtained (10–12 specimens) for some of the species (*Urobatis jamaicensis*, *Bagre marinus*, *Mugil curema*, *Strongylura timucu*, *Selene vomer*, *Rypticus maculatus*, *Prionotus tribulus*, *Chaetodipterus faber*), due to their low abundance and occurrence in these coastal ecosystems. Estimates of a and b for the LWRs, the coefficient of determination R^2, and 95% confidence limits for b are given in Table 1. A negative allometric growth was recorded in 16 species, a positive allometric growth in 10 species, and isometric growth in 18 species.

Discussion

The coefficient of determination (R^2) ranged from 0.861 (*Anchoa hepsetus*) to 0.996 (*Albula vulpes*, *Archosargus rhomboidalis*). This low value is related to the high dispersion of the length data. It is important also to mention that the length range of specimens is not the only magnitude that influences the value of R^2. Other factors such as the size of the sample, the length of the specimens, the gonad maturity, and diet are of importance. The exact relation between length and weight differs among species according to their inherited body shape, and within a species according to the condition (robustness) of individual fish. The condition fac-

Table 1. Length–weight relations for 44 species of the unprotected Yucatan Coastal Biological Corridor, Mexico.

Species	*n*	SL [cm]	Weight [g]	*a*	CI 95% *a*	*b*	CI 95% *b*	Growth type	R^2	Reference data	
										L_m [cm]	L_max [cm]
Urotrygonidae											
Urobatis jamaicensis	10	12.5–29.9	22.0–239.9	0.010	0.009–0.0011	3.000	—	I	—	$20.0_{\mathrm{TL,\,1}}$	76.0_{TL}
Albulidae											
Albula vulpes	13	3.2–13.1	0.3–32.8	0.008	0.006–0.010	3.229	3.085–3.373	+A	0.996	21.0_{FL}	104.0_{TL}
Elopidae											
Elops saurus	20	12.7–31.5	24.1–196.5	0.007	0.006–0.008	3.000	—	I	—	32.5_{SL}	100.0_{TL}
Engraulidae											
Anchoa hepsetus	3559	3.4–6.7	0.4–2.4	0.019	0.018–0.020	2.508	2.475–2.542	–A	0.861	$4.3_{\mathrm{TL,\,2}}$	15.3_{TL}
Anchoa lamprotaenia	360	**2.9–12.2**	0.12–34.5	0.005	0.005–0.006	3.315	3.278–3.352	+A	0.989	$5.0_{\mathrm{SL,\,3}}$	12.0_{TL}
Anchoa lyolepis	39	3.9–6.3	0.5–2.2	0.009	0.008–0.009	3.000	—	I	—	$8.2_{\mathrm{SL,\,28}}$	12.0_{TL}
Anchoa mitchilli	1232	2.3–6.1	0.1–2.4	0.009	0.009–0.010	2.999	2.944–3.055	–A	0.905	$4.0_{\mathrm{SL,\,4}}$	10.0_{TL}
Dorosomatidae											
Harengula jaguana	3769	2.1–12.8	0.1–36.3	0.008	0.007–0.008	3.381	3.366–3.397	+A	0.979	$8.0_{\mathrm{SL,\,5}}$	21.2_{TL}
Opisthonema oglinum	92	3.8–17.1	0.8–86.2	0.011	0.009–0.012	3.122	3.020–3.224	+A	0.976	11.5_{FL}	38.0_{TL}
Ariidae											
Ariopsis felis	1388	4.0–26.3	0.9–240.7	0.016	0.015–0.017	2.948	2.924–2.972	–A	0.977	$15.0_{\mathrm{SL,\,6}}$	70.0_{TL}
Bagre marinus	12	7.2–15.3	5.0–50.2	0.015	0.014–0.016	3.000	—	I	—	$32.8_{\mathrm{FL,\,8}}$	$100_{\mathrm{TL,\,7}}$
Synodontidae											
Synodus foetens	52	3.9–41.4	0.4–166.0	0.016	0.011–0.022	2.751	2.620–2.882	–A	0.974	19.0_{SL}	53.8_{TL}
Batrachoididae											
Opsanus beta	23	4.5–10.4	1.9–24.8	0.012	0.007–0.019	3.301	3.032–3.571	+A	0.972	7.6_{SL}	$32.4_{\mathrm{SL,\,9}}$
Mugilidae											
Mugil curema	10	2.0–23.9	0.1–153.4	0.016	0.014–0.018	3.000	—	I	—	$16.4_{\mathrm{TL,\,10}}$	91.0_{TL}
Mugil trichodon	20	2.1–15.3	0.1–64.6	0.013	0.009–0.018	3.180	3.034–3.326	+A	0.991	16.0_{FL}	46.0_{TL}
Belonidae											
Strongylura notata	104	24.0–46.0	23.7–124.8	0.009	0.005–0.015	2.524	2.364–2.683	–A	0.909	22.6_{TL}	61.0_{TL}
Strongylura timucu	10	7.2–36.5	0.3–72.0	0.0012	0.001–0.0014	3.000	—	I	—	—	61.0_{TL}
Hemiramphidae											
Chriodorus atherinoides	36	3.8–17.8	0.2–40.2	0.008	0.005–0.011	3.312	2.971–3.652	+A	0.933	—	26.0_{TL}
Hyporhamphus unifasciatus	173	5.0–25.5	0.4–86.7	0.003	0.003–0.0033	3.000	—	I	—	$18.5_{\mathrm{FL,\,28}}$	30.0_{TL}
Carangidae											
Caranx latus	14	7.0–14.9	7.5–82.0	0.021	0.020–0.022	3.000	—	I	—	37.0_{FL}	101.0_{FL}
Oligoplites saurus	28	2.2–23.8	0.1–145.3	0.010	0.010–0.011	3.000	—	I	—	$19.8_{\mathrm{SL,\,11}}$	$42.5_{\mathrm{SL,\,13}}$
Selene vomer	11	2.3–9.2	0.4–23.4	0.049	0.031–0.079	2.700	2.374–3.025	–A	0.982	$24.1_{\mathrm{TL,\,29}}$	48.3_{TL}
Trachinotus carolinus	123	1.5–9.5	0.5–20.7	0.026	0.025–0.027	3.000	—	I	—	$25.0_{\mathrm{FL,\,12}}$	64.0_{TL}
Trachinotus falcatus	491	2.0–14.5	0.4–104.1	0.045	0.042–0.049	2.850	2.800–2.900	–A	0.963	48.6_{FL}	122.0_{TL}
Trachinotus goodei	34	2.8–16.9	0.8–119.4	0.029	0.021–0.041	2.927	2.778–3.078	–A	0.983	$26.0_{\mathrm{TL,\,12}}$	50.0_{TL}
Cynoglossidae											
Symphurus plagiusa	14	7.5–14.4	3.6–28.7	0.009	0.008–0.009	3.000	—	I	—	10.1_{TL}	21.0_{TL}
Gerreidae											
Eucinostomus argenteus	347	2.0–14.5	0.2–45.1	0.022	0.020–0.024	3.006	2.954–3.058	I	0.975	$12.0_{\mathrm{TL,\,14}}$	21.2_{TL}
Eucinostomus gula	388	2.6–9.1	0.4–20.7	0.016	0.015–0.018	3.219	3.161–3.277	+A	0.970	$9.0_{\mathrm{FL,\,14}}$	25.5_{TL}
Eucinostomus harengulus	19	5.5–8.2	3.0–12.5	0.021	0.019–0.022	3.000	—	I	—	12.0_{SL}	15.0_{SL}
Grammistidae											
Rypticus maculatus	10	6.4–8.9	5.2–13.6	0.019	0.018–0.020	3.000	—	I	—	$8.9_{\mathrm{TL,\,16}}$	$24.0_{\mathrm{TL,\,15}}$
Haemulidae											
Orthopristis chrysoptera	15	4.2–20.5	1.5–158.7	0.022	0.021–0.023	2.844	2.601–3.086	–A	0.992	20.0_{SL}	46.0_{FL}
Lutjanidae											
Lutjanus griseus	42	4.8–18.5	2.9–128.4	0.034	0.025–0.045	2.891	2.766–3.015	–A	0.984	$18.0_{\mathrm{SL,\,17}}$	89.0_{TL}
Triglidae											
Prionotus tribulus	10	2.6–14.3	0.6–61.6	0.026	0.024–0.028	3.000	—	I	—	$8.4_{\mathrm{TL,\,18}}$	35.0_{TL}
Ephippidae											
Chaetodipterus faber	10	2.8–7.4	1.5–23.8	0.064	0.060–0.068	3.000	—	I	—	$9.9_{\mathrm{TL,\,19}}$	91.0_{TL}
Sciaenidae											
Bairdiella chrysoura	114	3.3–17.7	0.7–111.2	0.021	0.018–0.024	2.966	2.909–3.022	–A	0.990	$9.1_{\mathrm{SL,\,20}}$	30.0_{TL}
Cynoscion arenarius	64	2.6–20.9	0.3–109.3	0.018	0.015–0.021	2.914	2.853–2.976	–A	0.994	$14.0_{\mathrm{SL,\,21}}$	63.5_{TL}
Menticirrhus littoralis	69	2.6–15.7	0.2–63.2	0.014	0.012–0.017	2.943	2.856–3.031	–A	0.984	$19.8_{\mathrm{TL,\,23}}$	$60.0_{\mathrm{SL,\,22}}$
Menticirrhus americanus	104	2.4–14.8	0.2–57.3	0.010	0.009–0.012	3.149	3.093–3.206	+A	0.992	$15.0_{\mathrm{TL,\,24}}$	$60.0_{\mathrm{TL,\,25}}$
Menticirrhus saxatilis	57	2.5–19.0	0.4–102.2	0.014	0.012–0.017	2.997	2.908–3.086	–A	0.986	25.6_{TL}	46.0_{TL}

Table continues on next page.

Table 1. Continued.

Species	n	SL [cm]	Weight [g]	a	CI 95% a	b	CI 95% b	Growth type	R^2	Reference data	
										L_m [cm]	L_{max} [cm]
Sparidae											
Archosargus rhomboidalis	139	2.7–21.0	0.5–327.0	0.023	0.021–0.024	3.148	3.116–3.179	+A	0.996	8.0_{SL}	33.0_{TL}
Lagodon rhomboides	230	4.7–13.0	2.6–62.4	0.041	0.032–0.052	2.846	2.740–2.953	–A	0.929	$8.0_{SL, 26}$	40.0_{TL}
Ostraciidae											
Acanthostracion quadricornis	16	12.9–21.7	79.9–283.6	0.033	0.031–0.035	3.000	—	I	—	19.8_{TL}	55.0_{TL}
Tetraodontidae											
Sphoeroides spengleri	19	3.8–6.3	1.7–6.9	0.029	0.028–0.030	3.000	—	I	—	$18.8_{SL, 28}$	30.0_{TL}
Sphoeroides testudineus	110	2.3–20.0	3.8–378.7	0.055	0.039–0.077	2.880	2.753–3.008	–A	0.925	$10.0_{TL, 27}$	38.8_{TL}

n = number of individuals, SL = standard length, TL = total length, a = intercept (equation parameter), b = slope (allometry coefficient), 95% CI = 95% confidence limits (for both equation parameters), R^2 = coefficient of determination, L_m = size at first maturity, L_{max} = maximum length. Species in bold denote new maximum length. I = isometric growth, –A = negative allometric growth, +A = positive allometric growth. Isometric growth is assumed in the species with low number of specimens and/or narrow range sizes (no value for 95% CI b) (Froese 2006; Hay et al. 2020). Length values without references subscripts comprise information from FishBase. Subscript references: 1 = Yáñez-Arancibia and Amezcua (1979), 2 = Munroe et al. (2015a), 3 = Munroe et al. (2015b), 4 = Vega-Cendejas et al. (2017), 5 = Munroe et al. (2019), 6 = Betancur (2015), 7 = Chao et al. (2015), 8 = Caballero-Chávez (2013), 9 = Collette et al. (2019), 10 = Yago-Bruno et al. (2020), 11 = Duque-Nivia et al. (1995), 12 = Alvarez-Lajonchere and Ibarra Castro (2012), 13 = Ospina-Arango et al. (2008), 14 = Mexicano-Címtora (1999), 15 = Anderson et al. (2015), 16 = Bullock and Smith (1991), 17 = Allen (1985), 18 = Hoff (1992), 19 = Soeth et al. (2018), 20 = Grammer et al. (2009), 21 = Nemeth et al. (2006), 22 = Chao et al. (2020a), 23 = Aloisio and Nelson (2004), 24 = Chao et al. (2020b), 25 = McEachran and Fechhelm (2005), 26 = Russell et al. (2014), 27 = Shao et al. (2014), 28 = Bouchon-Navaro et al. (2006); 29 = Becerra et al. (2013).

tor sometimes reflects food availability and growth within the weeks before sampling. But the condition is variable and dynamic. Individual fish within the same sample vary considerably, and the average condition of each population varies seasonally and yearly (Kuriakose 2017).

The exponent b presented a mean value of 2.997 (DE: 0.18) with values ranging from 2.508 estimated for *Anchoa hepsetus* to 3.381 for *Harengula jaguana*. The lower values may have resulted from the fact that the majority of the specimens analyzed were juveniles (<4.3 cm) due to their type of habitat (wetlands, petenes, swamps), while in the case of *H. jaguana* it is attributed to its maturity stage. The LWRs parameters of *Rypticus maculatus* (Grammistidae) and *Anchoa lamprotaenia* (Engraulidae) are herein published for the first time in both the scientific literature and databases, such as FishBase (Froese and Pauly 2023) (Table 1). A new maximum length was recorded for *A. lamprotaenia* (12.2 cm SL). Overall, LWRs were highly significant for all species ($P < 0.001$). Changes in b reflect mostly the species morphology and environmental factors such as temperature, salinity, food (quantity, quality, and size), sex, health, and developmental stage (Sparre 1992). In the case of *Sphoeroides testudineus* a (0.055) and b (2.880) were very similar to those previously reported in a hyperhaline coastal lagoon located near this unprotected coastal region (Vega-Cendejas et al. 2017). The number of explanatory variables considered in the model also conditions the value of this coefficient. Carlander (1977) demonstrated that values of $b < 2.5$ or > 3.5 are often derived from samples with narrow size ranges. The mean condition of specimens as well as the difference in condition between small and large specimens vary between season localities and years, resulting in different weight relations. The influence of extreme values of b on mean b decreases with the number of estimates (Froese 2006).

For species with low numbers or low size ranges (Carlander 1997) (*Urobatis jamaicensis*, *Elops saurus*, *Anchoa lyolepis*, *Bagre marinus*, *Mugil curema*, *Strongylura timucu*, *Chriodorus atherinoide*s, *Hyporhamphus unifasciatus*, *Caranx latus*, *Oligoplites saurus*, *Trachinotus carolinus*, *Symphurus plagiusa*, *Eucinostomus harengulus*, *Rypticus maculatus*, *Prionotus tribulus*, *Chaetodipterus faber*, *Acanthostracion quadricornis*, *Sphoeroides spengleri*), LWRs were calculated assuming $b = 3.0$, being the value of the slope considered by the formula of Hay et al. (2020).

Conclusions

The results provided in this study can be very useful for the management of coastal ecosystems, including wetlands, which are required to maintain their diversity due to the increase in human activity in this unprotected coastal region (tourism, fisheries, habitat degradation). Additionally, this information is very useful for the development of trophic models using ECOPATH, which are of significant value in making predictions about the conservation status of this critical habitat for fishery and ecologically important species that use the ecosystem in the juvenile stage.

Acknowledgments

We are very grateful to the Comisión Nacional de Biodiversidad, México (CONABIO) for financial support for the research project (CONABIO-027) and to Alex Acosta, Walter Canto, Daniel Arceo, Víctor Castillo, Oscar Reyes, Orlando Cervantes, and M. Angel Villalobos for field assistance and support in sample processing.

References

Allen GR (1985) Snappers of the world: An annotated and illustrated catalogue of lutjanid species known to date. FAO Fisheries Synopsis. FAO, Rome, 6, 207 pp.

Aloisio SB, Nelson FF (2004) Reproductive biology of *Menticirrhus littoralis* in southern Brazil (Actinopterygii: Perciformes: Sciaenidae). Neotropical Ichthyology 2(1): 31–36. https://doi.org/10.1590/S1679-62252004000100005

Alvarez-Lajonchere L, Ibarra-Castro L (2012) Relationships of maximum length, length at first sexual maturity, and growth performance index in nature with absolute growth rates of intensive cultivation of some tropical marine fish. Journal of the World Aquaculture Society 43(5): 607–620. https://doi.org/10.1111/j.1749-7345.2012.00591.x

Anderson W, Carpenter KE, Gilmore G, Milagrosa Bustamante G, Polanco Fernandez A, Robertson R (2015) *Rypticus maculatus*. The IUCN Red List of threatened species 2015. e.T16759353A16781863. https://doi.org/10.2305/IUCN.UK.2015-2.RLTS.T16759353A16781863.en

Becerra da Silva C, Araújo M, Vieira C (2013) Sustainability of capture of fish bycatch in the prawn trawling in northeastern Brazil. Neotropical Ichthyology 11(1): 133–142. https://doi.org/10.1590/S1679-62252013000100016

Betancur R (2015) *Ariopsis felis*. The IUCN Red List of threatened species 2015: e.T190456A1952682. https://doi.org/10.2305/IUCN.UK.2015-2.RLTS.T190456A1952682.en

Bouchon-Navaro Y, Bouchon C, Kopp D, Louis M (2006) Weight–length relationships for 50 fish species collected in seagrass beds of the Lesser Antilles. Journal of Applied Ichthyology 22(4): 322–324. https://doi.org/10.1111/j.1439-0426.2006.00715.x

Bullock H, Smith GB (1991) Sea basses (Pisces: Serranidae). Memoirs of the Hourglass Cruises. Marine Research Laboratory, Florida Department of Natural Resources, St. Petersburg, Florida, 205 pp.

Caballero-Chávez V (2013) Madurez y reproducción de bagre bandera *Bagre marinus* en el sudeste de Campeche. Ciencia Pesquera 21(2): 13–19.

Carlander KD (1977) Handbook of freshwater fishery biology. Vol. 2. Life history data on centrarchid fishes of the United States and Canada. Iowa State University Press, Ames, IA, USA.

Carpenter KE (Ed.) (2002a) The living marine resources of the Western Central Atlantic. Volume 2: Bony fishes part 1 (Acipenseridae to Grammatidae). FAO Species Identification Guide for Fishery Purposes and American Society of Ichthyologists and Herpetologists Special Publication No. 5. FAO, Rome, 601–1374.

Carpenter KE (Ed.) (2002b) The living marine resources of the Western Central Atlantic: volume 3 -Bony fishes part 2 -(Opistognathidae to Molidae), sea turtles and marine mammals. FAO Species Identification Guide for Fishery Purposes and American Society of Ichthyologists and Herpetologists Special Publication No. 5. FAO, Rome, 1375–2127.

Chao L, Vega-Cendejas M, Tolan J, Jelks H, Espinosa-Perez H (2015) *Bagre marinus*. The IUCN Red List of threatened species 2015: e.T196806A2476570. https://doi.org/10.2305/IUCN.UK.2015-2.RLTS.T196806A2476570.en

Chao L, Espinosa-Perez H, Aguilera Socorro O, Haimovici M (2020a) *Menticirrhus littoralis*. The IUCN Red List of threatened species 2020: e.T46105545A82677213. https://doi.org/10.2305/IUCN.UK.2020-2.RLTS.T46105545A82677213.en

Chao L, Espinosa-Perez H, Aguilera Socorro O, Haimovici M (2020b) *Menticirrhus americanus*. The IUCN Red List of threatened species 2020: e.T195075A82668543. https://doi.org/10.2305/IUCN.UK.2020-2.RLTS.T195075A82668543.en

Collette BB, Aiken KA, Polanco Fernandez A, Vega-Cendejas M (2019) *Opsanus beta*. The IUCN Red List of threatened species 2019. e.T190257A86399458. https://doi.org/10.2305/IUCN.UK.2019-2.RLTS.T190257A86399458.en

Duque-Nivia G, Acero AP, Santos-Martinez A (1995) Aspectos reproductivos de *Oligoplites saurus* y *O. palometa* (Pisces: Carangidae) en la Ciénega Grande de Santa Marta, Caribe Colombiano. Caribbean Journal of Science 31(3–4): 317–326.

Euán-Avila J, García de Fuentes A, Liceaga Correa MA, Munguia Gil A (Eds.) (2014) La costa del Estado de Yucatán, un espacio de reflexión sobre la sociedad-naturaleza, en el contexto del ordenamiento territorial. Tomo II. Plaza y Valdés.

Froese R (2006) Cube law, condition factor and weight–length relationships: History, meta- analysis and recommendations. Journal of Applied Ichthyology 22(4): 241–253. https://doi.org/10.1111/j.1439-0426.2006.00805.x

Froese R, Pauly D (Eds.) (2022) FishBase. [Version 04/2022] http://www.fishbase.org

Froese R, Tsikliras AC, Stergiou KI (2011) Editorial note on weight–length relations of fishes. Acta Ichthyologica et Piscatoria 41(4): 261–263. https://doi.org/10.3750/AIP2011.41.4.01

Grammer GL, Brown-Peterson NJ, Peterson MS, Comyns BH (2009) Life history of silver perch *Bairdiella chrysoura* (Lacepède, 1803) in north-central Gulf of Mexico estuaries. Gulf of Mexico Science 27(1): 62–73. https://doi.org/10.18785/goms.2701.07

Hay A, Xian W, Bailly N, Liang C, Pauly D (2020) The why and how of determining length–weight relationships of fish from preserved museum specimens. Journal of Applied Ichthyology 36(3): 373–379. https://doi.org/10.1111/jai.14014

Herrera-Silveira JA, Morales-Ojeda SM (2009) Evaluation of the health status of a coastal ecosystem in southeast Mexico: Assessment of water quality, phytoplankton and submerged aquatic vegetation. Marine Pollution Bulletin 59(1–3): 72–86. https://doi.org/10.1016/j.marpolbul.2008.11.017

Hoff JG (1992) Comparative biology and population dynamics of searobins (genus *Prionotus*) with emphasis on populations in the northwestern Gulf of Mexico. Dissertations, Theses, and Masters Projects. Paper 1539616697. https://doi:10.25773/v5-c67f-dt79

Kohler N, Casey J, Turner P (1995) Length–weight relationships for 13 species of sharks from the western North Atlantic. Fish Bulletin 93: 412–418.

Kuriakose S (2017) Estimation of length weight relationship in fishes. Summer School on Advanced Methods for Fish Stock Assessment and Fisheries Management. Lecture Note Series No. 2/2017. CMFRI; Kochi, Kochi, 215–220.

McEachran JD, Fechhelm JD (1998) Fishes of the Gulf of Mexico, Volumen 1: Myxiniformes to Gasterosteiformes. University of Texas Press, Austin, TX, USA.

McEachran JD, Fechhelm JD (2005) Fishes of the Gulf of Mexico, Volume 2: Scorpaeniformes to Tetraodontiformes. University of Texas Press, Austin, TX, USA. https://doi.org/10.7560/706347

Mexicano-Cíntora G (1999) Crecimiento y reproducción de la mojarra, *Eucinostomus gula* de Celestún, Yucatán, México. Proceedings of the Gulf and Caribbean Fisheries Institute 45: 524–536.

Moran M, Monroe A, Stallcup L (2019) A proposal for practical and effective biological corridors to connect protected areas in northwest Costa Rica. Nature Conservation 36: 113–137. https://doi.org/10.3897/natureconservation.36.27430

Munroe T, Aiken KA, Brown J, Grijalba Bendeck L (2015a) *Anchoa hepsetus*. The IUCN Red List of threatened species 2015: e.T16406327A16510237. https://doi.org/10.2305/IUCN.UK.2015-4.RLTS.T16406327A16510237.en

Munroe T, Aiken KA, Brown J, Grijalba Bendeck L (2015b) *Anchoa lamprotaenia*. The IUCN Red List of threatened species 2015: e.T16406525A16509907. https://doi.org/10.2305/IUCN.UK.2015-4.RLTS.T16406525A16509907.en

Munroe TA, Aiken KA, Brown J, Grijalba Bendeck L, Vega-Cendejas M (2019) *Harengula jaguana*. The IUCN Red List of threatened species 2019: e.T190478A86377366. https://doi.org/10.2305/IUCN.UK.2019-2.RLTS.T190478A86377366.en

Nemeth DJ, Jackson JB, Knapp AR, Purtlebaugh CH (2006) Age and growth of sand seatrout (*Cynoscion arenarius*) in the estuarine waters of the eastern Gulf of Mexico. Gulf of Mexico Science 24(1): 45–60. https://doi.org/10.18785/goms.2401.07

Ospina-Arango JF, Pardo-Rodríguez FI, Álvarez-León R (2008) Madurez gonadal de la ictiofauna presente en la Bahía de Cartagena, Caribe Colombiano. Boletín Científico Centro de Museo de Historia Natural 12: 117–140.

Palacios-Sánchez SE, Vega-Cendejas ME, Hernández-de-Santillana M, Aguilar-Medrano R (2019) Anthropogenic impacts in the nearshore fish community of the Yucatan Coastal Corridor. A comparison of protected and unprotected areas. Journal for Nature Conservation 51: 125721. https://doi.org/10.1016/j.jnc.2019.125721

Pendoley KL, Schofield G, Whittock PA, Ierodiaconou D, Hays GC (2014) Protected species use of a coastal marine migratory corridor connecting marine protected areas. Marine Biology 161(6): 1455–1466. https://doi.org/10.1007/s00227-014-2433-7

Petrakis G, Stergiou KI (1995) Weight–length relationships for 33 fish species in Greek waters. Fisheries Research 21(3–4): 465–469. https://doi.org/10.1016/0165-7836(94)00294-7

Russell B, Carpenter KE, MacDonald T, Vega-Cendejas M (2014) *Lagodon rhomboides*. The IUCN Red List of threatened species 2014. e.T170250A1301642. https://doi.org/10.2305/IUCN.UK.2014-3.RLTS.T170250A1301642.en

Shao K, Matsuura K, Leis JL, Hardy G, Larson H, Liu M (2014) *Sphoeroides testudineus*. The IUCN Red List of threatened species 2014: e.T193813A2281154. https://doi.org/10.2305/IUCN.UK.2014-3.RLTS.T193813A2281154.en

Soeth M, Fávaro LF, Spach HL, Daros FA, Woltrich AE, Correia AT (2018) Age, growth, and reproductive biology of the Atlantic spadefish *Chaetodipterus faber* in southern Brazil. Ichthyological Research 66(1): 140–154. https://doi.org/10.1007/s10228-018-0663-2

Sparre P (1992) Introduction to tropical fish stock assessment. Part I. Manual. FAO Fishery Technical Paper. 306/1. Rev. I, FAO, Rome.

Teixeira-de Mello F, Eguren G (2008) Prevalence and intensity of black-spot disease in fish community from Cañada del Dragón stream (Montevideo, Uruguay). Limnetica 27: 251–258. https://doi.org/10.23818/limn.27.20

Teixeira-de Mello F, Iglesias C, Borthagaray A, Mazzeo N, Vilches J, Larrea D, Ballabio R (2006) Ontogenetic allometric coefficient changes. Implication of diet shift and morphometric attributes in *Hoplias malabaricus* (Bloch) (Characiformes, Erythrinidae). Journal of Fish Biology 69(6): 1770–1778. https://doi.org/10.1111/j.1095-8649.2006.01245.x

Turk-Boyer P, Morzaria-Luna H, Martinez-Tovar I, Downton-Hoffmann C, Munguia-Vega A (2014) Ecosystem-based fisheries management of a biological corridor along the northern Sonora coastline (NE Gulf of California). Pp. 125–154. In: Amezcua F, Bellgraph B (Eds.) Fisheries management of Mexican and Central American Estuaries. Estuaries of the World. Springer, Dordrecht, Netherlands. https://doi.org/10.1007/978-94-017-8917-2_9

Vega-Cendejas ME, Peralta-Meixuero MA, Hernández de SM (2017) Length–weight relationships of fishes that inhabit a hyperhaline coastal lagoon: Ria Lagartos, Yucatan, Mexico. Acta Ichthyologica et Piscatoria 47(4): 411–415. https://doi.org/10.3750/AIEP/02239

Wotton RJ (1990) Ecology of teleost fishes. Chapman and Hall, London, UK. https://doi.org/10.1007/978-94-009-0829-1

Xie JY, Kang ZJ, Yang J, Yang DD (2015) Length–weight relationships for 15 fish species from the Hunan Hupingshan National Nature Reserve in central China. Journal of Applied Ichthyology 31(1): 221–222. https://doi.org/10.1111/jai.12465

Yago-Bruno SN, Mariana Barros A, Jailza F, Jackellynne FF, Ladilson Rodrigues S, Marina BF (2020) Length at first sexual maturity of economically important fishes in the Brazilian Northeast Coast. Ocean and Coastal Research 68: e20311. https://doi.org/10.1590/s2675-28242020068311

Yáñez-Arancibia A, Amezcua LF (1979) Ecología de *Urolophus jamaicensis* (Cuvier) en Laguna de Terminos un sistema estuarino del sur del Golfo de México (Pisces: Urolophidae). Anales del Centro de Ciencias del Mar y Limnologia. Universidad Nacional Autónoma de México 6(2): 123–13.

Acta Ichthyologica et Piscatoria 53, 2023, 209–216 | DOI 10.3897/aiep.53.109943

PENSOFT.

ACTA ICHTHYOLOGICA ET PISCATORIA

Redescription and extended distribution of a poorly known Australian anchovy, *Stolephorus advenus* (Actinopterygii: Clupeiformes: Engraulidae)

Harutaka HATA[1], Hiroyuki MOTOMURA[2]

1 *National Museum of Natural History, Smithsonian Institution, Washington, DC, USA*
2 *Kagoshima University Museum, Kagoshima, Japan*

https://zoobank.org/E37473DF-52DC-4D34-8DAC-694A1D4CEF09

Corresponding author: Harutaka HATA (k2795502@kadai.jp)

Academic editor: Jan Kotusz ♦ **Received** 23 July 2023 ♦ **Accepted** 31 October 2023 ♦ **Published** 24 November 2023

Citation: Hata H, Motomura H (2023) Redescription and extended distribution of a poorly known Australian anchovy, *Stolephorus advenus* (Actinopterygii: Clupeiformes: Engraulidae). Acta Ichthyologica et Piscatoria 53: 209–216. https://doi.org/10.3897/aiep.53.109943

Abstract

The false Indian anchovy, *Stolephorus advenus* Wongratana, 1987 (Engraulidae), previously known only from the type specimen from the Northern Territory, Australia, is redescribed herewith and its validity confirmed, on the basis of the holotype and nine additional specimens from the northern coast of Australia. Although the significance of differences between *S. advenus* and some congeners with a similarly short maxilla has been unclear, the diagnostic reliability of some characters, including melanophores absent on the dorsal- and anal-fin bases, pectoral fin and occipital region, fewer pseudobranchial filaments, and greater number of prepelvic scutes, is confirmed. An extended distribution of the species around the northern coast of Australia is also reported.

Keywords

Clupeomorpha, ichthyofauna, *Stolephorus balinensis*, *Stolephorus indicus*, taxonomy

Introduction

Stolephorus Lacepède, 1803, an Indo–Pacific genus of marine and/or brackish water anchovies (Engraulidae), comprises 45 valid species (Whitehead et al. 1988; Wongratana et al. 1999; Kimura et al. 2009; Hata and Motomura 2018a, 2018b, 2018c, 2018d, 2021a, 2021b, 2021c, 2022a, 2022b, 2023; Hata et al. 2019, 2020a, 2020b, 2021, 2022a, 2022b, 2023; Gangan et al. 2020). Although the genus was previously considered congeneric with the morphologically similar genus *Encrasicholina* Fowler, 1938 (e.g., Whitehead 1967, 1972; Wongratana 1983), the two genera were separated by Nelson (1983) and Whitehead et al. (1988), with Lavoué et al. (2017) later proposing that *Stolephorus* represented the earliest generic offshoot within Engraulinae. *Stolephorus advenus* Wongratana, 1987 (false Indian anchovy) has been known to date only from the holotype, collected from Cobourg Peninsula, Australia, and was, in all respects, very poorly known.

During an examination of Australian species of *Stolephorus*, nine additional specimens of *S. advenus*, collected from several localities along the northern coast of Australia, were identified. The specimens, with additional morphological and biological information confirming the validity of the species, are described in detail herein.

Methods

Counts and measurements follow Hata and Motomura (2017), and are presented as percentage of standard length or head length. All measurements were made with digital calipers to the nearest 0.1 mm. "Pelvic scute" refers to the scute associated with the pelvic-fin insertion, whereas "prepelvic", "postpelvic", and "predorsal scutes" refer to the scutes anterior to the pelvic scute, posterior to the pelvic scute, and just anterior to the dorsal-fin origin, respectively. Abbreviations are as follows—SL is the standard length; UGR, LGR, and TGR are the rakers on upper limb, lower limb, and total gill rakers, respectively, with associated numbers indicating the specific gill arch; and SMX-MX is the distance between posterior margins of supramaxilla and maxilla. Institutional abbreviations follow Sabaj (2020).

Comparative material examined. *Stolephorus balinensis* (Bleeker, 1849), 119 specimens, 43.4–148.4 mm SL: listed in Hata and Motomura (2023) and 15 additional specimens: BBM-ICH 1963-1348-38, 3 specimens, 84.1–99.3 mm SL, Muar, Johor Strait, Malaysia; BPBM 19216, 2 of 5 specimens, 98.4–102.0 mm SL, Ambon, Indonesia; BPBM 26469, 2 specimens, 86.0–94.2 mm SL, Cebu Island, Philippines; BPBM 29883, 2 specimens, 124.8–125.3 mm SL, Montong, west coast of Lombok, Indonesia; CAS 230421, 1 of 4 specimens, 91.7 mm SL, southwest of Babelthuap Island, Palau (07°23′17″N, 134°30′40″E), 2–6 feet (approx. 0.6–1.8 m) depth; CAS 235774, 99.9 mm SL, 1 of 3 specimens, mouth of Mae Nam Prasae River, Rayong (12°41′45″N, 101°42′11″E); CAS-SU 29219, 4 specimens, 84.1–89.9 mm SL, Palau.

Stolephorus belaerius Hata, Lavoué et Motomura, 2021, 27 specimens, 63.4–127.1 mm SL: listed in Hata et al. (2021) and 2 additional specimens: CAS 58503, 97.3 mm SL, Mombasa, Kenya; LACM 31618-18, 76.3 mm SL, 1 of 5 specimens, Hasini Creek, Manda Island, Kenya.

Stolephorus commersonnii Lacepède, 1803, 16 specimens, 62.1–112.3 mm SL: listed in Hata et al. (2021).

Stolephorus horizon Hata et Motomura, 2023, 34 specimens, 62.3–108.1 mm SL; *Stolephorus indicus* (van Hasselt, 1823), 41 specimens, 53.3–133.6 mm SL; *Stolephorus meteorum* Hata, Lavoué, Bogorodsky, Alpermann, et Motomura 2023, 20 specimens, 49.2–115.0 mm SL; *Stolephorus scitulus* (Fowler, 1911), 46 specimens, 47.6–102.7 mm SL: listed in Hata and Motomura (2023).

Results

Family Engraulidae
Stolephorus Lacepède, 1803

Stolephorus advenus Wongratana, 1987

English name: false Indian anchovy
(Fig. 1; Tables 1, 2)

Stolephorus advenus Wongratana, 1987—Wongratana (1987a): 106, fig. 2 (type locality: north of Saulte Point, Cobourg Peninsula, Northern Territory, Australia).—Wongratana (1987b: 7 (Cobourg Peninsula, Northern Territory, Australia).—Whitehead et al. (1988): 403, unnumbered figs. (north of Saulte Point, Cobourg Peninsula, Northern Territory, Australia).—Wongratana et al. (1999): 1726, unnumbered figs. (north of Saulte Point, Cobourg Peninsula, Northern Territory, Australia).—Paxton et al. (2006): 314 (north of Saulte Point, Cobourg Peninsula, Northern Territory, Australia).—Hata et al. (2021): 332 (north of Saulte Point, Cobourg Peninsula, Northern Territory, Australia).

Material examined. 10 specimens, 49.1–79.6 mm SL, all specimens collected from Australia.

Holotype. NTM S. 10031-153, 72.2 mm SL, holotype of *Stolephorus advenus*, north of Saulte Point, Cobourg Peninsula, Northern Territory, 18 Oct. 1981, H. Larson leg.

Non-type specimens. CSIRO A 2911, 53.3 mm SL, Gulf of Carpentaria, approx. 13 km east of Sydney Island,

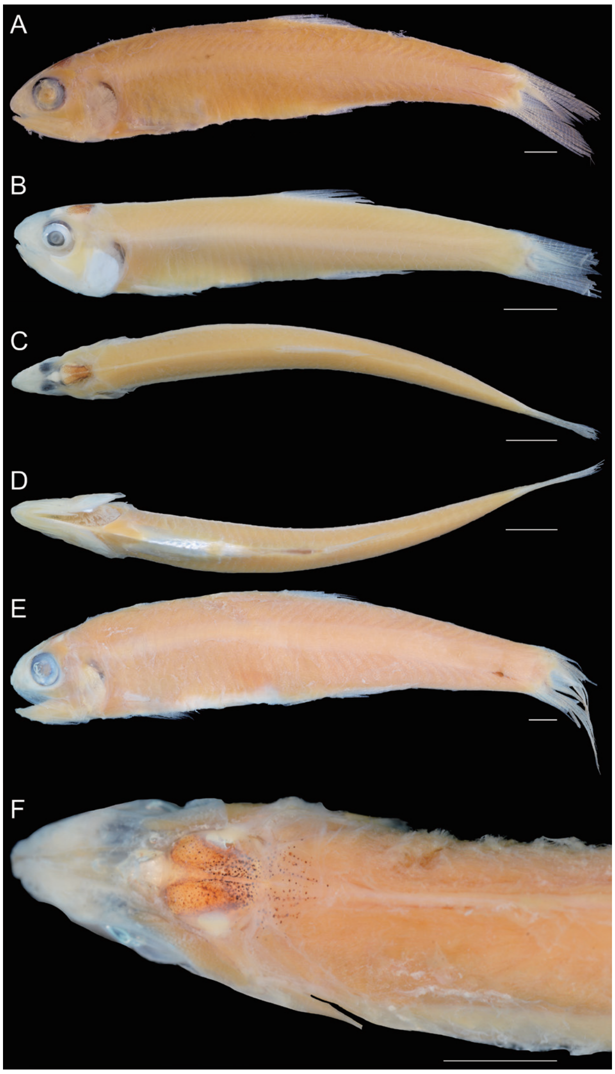

Figure 1. Specimens of *Stolephorus advenus* [**A**: holotype, NTM S. 10031-153, 72.2 mm SL, Cobourg Peinsula, Northern Territory, Australia (photograph taken by S. Tashiro); **B**: lateral, **C**: dorsal, and **D**: ventral views of non-type specimen, NTM S. 13803-003, 49.1 mm SL, Clarence Strait, Northern Territory, Australia (melanophores absent on occipital region); **E**: lateral view of whole body and **F**: dorsal view of head of non-type specimen, CSIRO CA 2688, 79.6 mm SL, Gulf of Carpentaria, Northern Territory (melanophores scattered on occipital region); scale bars indicate 0.5 mm].

Queensland (16°42′36″S, 139°34′48″E), 16.5 m depth; CSIRO A 2916, 56.3 mm SL, CSIRO A 2917, 52.3 mm SL, Gulf of Carpentaria, approx. 14 km east of Sydney Island, Queensland (16°40′12″S, 139°36′30″E), 14.6 m depth; CSIRO B 288, 3 specimens, 53.8–56.3 mm SL, Gulf of Carpentaria, approx. 9 km east of Sydney Island, Queensland (16°43′00″S, 139°33′00″E), 16.5 m depth; CSIRO CA 2555, 74.2 mm SL, approx. 20 km east of Tasman Point, Groote Eylandt, Northern Territory (14°20′S, 136°10′E), 18 m depth; CSIRO CA 2688, 79.6mm SL, north of Groote Eylandt, Gulf of Carpentaria, Northern Territory; NTM S. 13803-003, 49.1 mm SL, Howard Channel, Clarence Strait, Northern Territory (12°05′S, 131°02′E).

Diagnosis. A species of *Stolephorus* with the following combination of characters: maxilla short, 13.7%–14.5% of SL, its posterior tip not reaching anterior margin of preopercle; posterior margin of preopercle convex, rounded; no predorsal scutes; prepelvic scutes 6 or 7 (modally 7); pelvic scute without spine; dorsal fin with three unbranched and 12–15 (14) branched rays; anal fin with three unbranched and 15–17 (16) branched rays, its origin just below base of ninth to eleventh dorsal-fin ray; 1UGR 17–19 (18), 1LGR 24–27 (25), 1TGR 42–45 (42), 2UGR 10–13 (11), 2LGR 20–23 (22), 2TGR 30–35 (33), 3UGR 8–11 (9), 3LGR 11–13 (12), 3TGR 20–22 (21), 4UGR 6–9 (7), 4LGT 9–10 (9), 4TGR 15–18 (17); gill rakers 3 or 4 (4) on posterior face of third gill arch; transverse scales 8; pseudobranchial filaments 15–18 (16); total vertebrae 41 or 42 (42); pelvic fin short, 7.6%–8.0% of SL, tip of depressed pelvic fin not reaching posteriorly to vertical through dorsal-fin origin; head short, 21.6%–22.9% of SL; body rather deep, 17.4%–20.9% of SL; pectoral fin rather long, 13.5%–14.2% of SL; pairs of dark patches on parietal area (sometimes also on occipital area); no dark lines on dorsum; no black spots on suborbital area and tip of lower jaw; no melanophores on bases of dorsal and anal fins, and pectoral fin.

Description. Counts and measurements, expressed as percentages of SL, given in Tables 1 and 2. Body laterally compressed, elongate, deepest at dorsal fin origin. Dorsal profile of head and body gently elevated from snout tip to dorsal-fin origin, thereafter gradually lowering to uppermost point of caudal-fin base. Ventral profile of head and body gently lowering from lower-jaw tip to below pectoral fin, thereafter nearly straight (parallel to body axis) to anal-fin origin, gradually elevated along anal-fin base, thereafter nearly straight (parallel to body axis) to lowermost point of caudal-fin base. Abdomen rounded, covered with six or seven spine-like prepelvic scutes anterior to pelvic fin insertion. Pelvic scute without spine. Postpelvic and predorsal scutes absent. Anus just anterior to anal-fin origin. Snout round, projecting, length less than eye diameter. Eye large, round, covered with adipose eyelid, positioned laterally on head dorsal to horizontal through pectoral-fin insertion, visible in dorsal view. Pupil round. Orbit elliptical. Nostrils close to each other, anterior to or-

Table 1. Meristics of examined specimens of *Stolephorus advenus*.

Count	Holotype	Non-types	Modal value
	NTM S. 10031-153	*n* = 9	
Dorsal-fin rays (unbranched)	3	3	3
Dorsal-fin rays (branched)	15	15–17	14
Anal-fin rays (unbranched)	3	3	3
Anal-fin rays (branched)	16	15–17	16
Pectoral-fin rays (unbranched)	1	1	1
Pectoral-fin rays (branched)	16	11–15	12
Pelvic-fin rays (unbranched)	Broken	1	1
Pelvic-fin rays (branched)	Broken	6	6
Caudal-fin rays	19	19	19
Gill rakers on 1st gill arch (upper)	19	17–18	18
Gill rakers on 1st gill arch (lower)	25	24–27	25
Gill rakers on 1st gill arch (total)	44	42–45	42
Gill rakers on 2nd gill arch (upper)	13	10–12	11
Gill rakers on 2nd gill arch (lower)	20	20–23	22
Gill rakers on 2nd gill arch (total)	33	30–35	33
Gill rakers on 3rd gill arch (upper)	11	8–9	9
Gill rakers on 3rd gill arch (lower)	11	11–13	12
Gill rakers on 3rd gill arch (total)	22	20–22	21
Gill rakers on 4th gill arch (upper)	9	6–7	7
Gill rakers on 4th gill arch (lower)	9	9–10	9
Gill rakers on 4th gill arch (total)	18	15–17	17
Gill rakers on posterior face of 3rd gill arch	4	3–4	4
Prepelvic scutes	7	6–7	7
Scale rows in longitudinal series	38	36–38	38
Transverse scales	8	8	8
Pseudobranchial filaments	Broken	15–18	16
Total vertebrae	42	41–42	42
Pectoral-fin rays with melanophores	0	0	0

Table 2. Morphometrics of examined specimens of *Stolephorus advenus*.

Character	Holotype	Non-types	Mean values
	NTM S. 10031-153	*n* = 9	
	Absolute values [mm]		
Standard length (SL)	72.2	49.1–79.6	
	Relative values (% SL)		
Head length	22.6	21.6–22.9	22.2
Body depth	19.7	17.4–20.9	19.4
Pre-dorsal fin length	53.7	52.1–53.8	53.2
Snout tip to pectoral fin insertion	23.5	21.9–26.0	23.5
Snout tip to pelvic fin insertion	43.0	40.4–43.9	42.4
Snout tip to anal fin origin	62.5	61.0–64.7	62.6
Dorsal fin base length	14.8	13.3–14.3	13.9
Anal fin base length	15.1	14.7–16.3	15.4
Caudal peduncle length	24.8	21.2–23.4	22.7
Caudal peduncle depth	9.1	8.0–8.9	8.6
D–P1	—	34.2–38.9	36.4
D–P2	Broken	21.1–24.4	22.8
D–A	—	18.6–21.1	20.1
P1–P2	Broken	18.0–21.5	19.8
P2–A	Broken	19.8–21.1	20.3
Pectoral fin length	14.1	13.5–14.2	13.8
Pelvic fin length	Broken	7.6–8.0	7.7
Maxilla length	14.3	13.7–14.5	14.2
Mandibular length	14.9	13.5–4.9	14.3
Supramaxilla end to maxilla end	—	1.3–1.9	1.7
1st unbranched dorsal-fin ray length	1.3	1.0–1.7	1.4
2nd unbranched dorsal-fin ray length	6.8	5.7–7.1	6.5
3rd dorsal-fin ray length	Broken	13.4–13.5	13.4
1st unbranched anal-fin ray length	Broken	0.7–1.3	1.0
2nd unbranched anal-fin ray length	4.9	4.0	4.5
3rd anal-fin ray length	Broken	Broken	
Orbit diameter	11.4	7.1–8.4	8.3
Eye diameter	6.9	5.5–6.8	6.4
Snout length	3.3	3.6–4.4	3.8
Interorbital width	—	4.6–5.0	4.9
Postorbital length	9.9	10.5–13.3	11.0

Abbreviations: D–P1 (distance from dorsal-fin origin to pectoral-fin insertion); D–P2 (distance from dorsal-fin origin to pelvic-fin insertion); D–A (distance between origins of dorsal and anal fins); P1–P2 (distance between insertions of pectoral and pelvic fins); P2–A (distance between pelvic-fin insertion and anal-fin origin).

bit. Mouth large, inferior, ventral to body axis, extending backward beyond posterior margin of eye. Maxilla short, its posterior tip slightly short of anterior margin of preopercle. Lower jaw slender. Single row of conical teeth on each jaw and palatines. Several conical teeth on vomer. Small fine teeth patch on pterygoids. No teeth on upper edge of hyoid. Several rows of conical teeth on upper edges of basihyal. Posterior margins of preopercle, subopercle and opercle rounded, smooth. Gill membrane without serrations. Interorbital space flat. Interorbital width less than eye diameter. Pseudobranchial filaments present, length of longest filament less than eye diameter. Gill rakers long, slender, rough, visible from side of head when mouth opened. Isthmus muscle long, reaching anteriorly posterior margin of gill membranes. Urohyal hidden by isthmus muscle (not visible without dissection). Gill membrane on each side joined distally, most of isthmus muscle exposed (not covered by gill membrane). Head scales absent. Fins scaleless, except for broad triangular sheath of scales on caudal fin. Dorsal-fin origin posterior to vertical through base of last pelvic-fin ray, slightly posterior to middle of body. Dorsal and anal fins with three anteriormost rays closely spaced and unbranched. First dorsal- and anal-fin rays minute. Dorsal profile of dorsal fin elevated from dorsal-fin origin to third fin ray tip, thereafter lowering to last dorsal-fin ray tip. Anal-fin origin just below base of ninth to eleventh dorsal-fin ray. Posterior tip of depressed anal fin not reaching caudal-fin base. Uppermost pectoral-fin ray unbranched, inserted below midline of body. Posterior tip of pectoral fin not reaching vertical through pelvic-fin insertion. Dorsal, ventral, and posterior contours of pectoral fin nearly straight. Pelvic fin shorter than pectoral fin; pelvic-fin insertion anterior to vertical through dorsal-fin origin. Posterior tip of depressed pelvic fin not reaching vertical through dorsal-fin origin. Caudal fin forked, tips of both lobes pointed.

Coloration of preserved specimens. Body uniformly pale ivory or pale brown. Indistinct light brown longitudinal band narrower than eye running from opercle to caudal-fin base. Paired dark patches on parietal regions, but no melanophores on occipital area (a few melanophores in some specimens). No dark lines on dorsum.

No melanophores on dorsal, pectoral, pelvic, and anal fins, and lateral surface of head. Melanophores scattered along caudal-fin rays. Fins pale, semi-transparent. Melanophores scattered on gill rakers, gill arch, gill filaments, inner side of hyoid, and pseudobranchial.

Distribution. *Stolephorus advenus* has been recorded along the northern coast of Australia from Clarence Strait, Northern Territory to southern Gulf of Carpentaria (around Sydney Island, Queensland) (Wongratana 1987a; Whitehead et al. 1988; Wongratana et al. 1999, this study; Fig. 2).

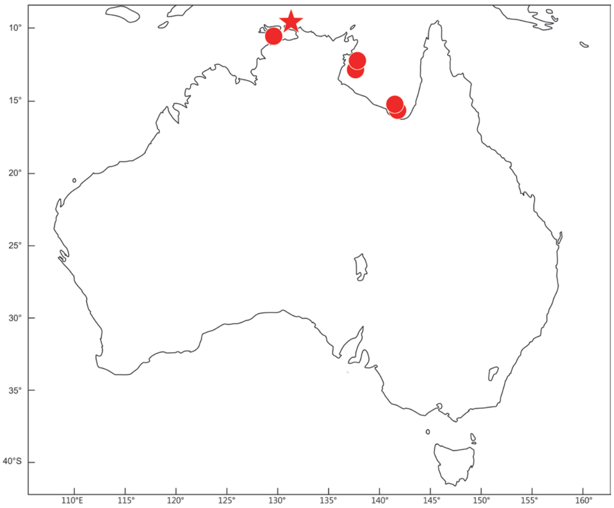

Figure 2. Distributional records of *Stolephorus advenus* based on specimens examined in this study (red star: type locality; red dot: non-type specimens).

Discussion

Stolephorus advenus was described by Wongratana (1987a) based on a single specimen (holotype), collected from Cobourg Peninsula, Australia (Fig. 1A). Although the original description stated that the holotype had five prepelvic scutes and 24 1LGR, re-examination of the specimen confirmed the presence of seven prepelvic scutes and 25 1LGR. The pelvic fin was also missing from the holotype, but Wongratana (1987a) speculated that when depressed, the pelvic fin of *S. advenus* would not have reached the vertical through the dorsal-fin origin. The additional specimens examined in the presently reported study confirm the validity of that speculation. Although Wongratana (1987a) and Wongratana et al. (1999) stated that *S. advenus* lacked melanophores on the occipital region, some of the additional specimens actually have melanophores scattered on that region (Fig. 1F). Furthermore, following their revisional studies of *Stolephorus*, Whitehead et al. (1988) and Wongratana et al. (1999) indicated that *S. advenus* could be distinguished from all congeners, except *Stolephorus indicus*, by the short maxilla (posteriorly not reaching the preopercle posterior margin) and 1LGR fewer than 30. However, since those studies, numerous new or cryptic species of *Stolephorus* have been described, with Whitehead's et al. (1988) "*Stolephorus indicus*" actually representing at least seven species, *Stolephorus balinensis*, *Stolephorus belaerius*, *Stolephorus commersonnii*, *Stolephorus horizon*, *Stolephorus indicus*, *Stolephorus meteorum*, and *Stolephorus scitulus*. Accordingly, *S. advenus* can be presently distinguished from all other congeners, except the latter seven species previously regarded as "*S. indicus*", by having a shorter maxilla (see above), 1LGR fewer than 30, the pelvic fin not reaching posteriorly the vertical through the dorsal-fin origin, and no dark lines on the dorsum. In addition, *S. advenus* differs from all seven species previously included in "*S. indicus*" as follows: maxilla not reaching posteriorly anterior margin of preopercle, 13.7%–14.5% of SL [vs. just reaching or slightly beyond anterior margin; longer than 15% of SL (14.3%–17.5% in *S. balinensis*)]; no melanophores scattered along bases of dorsal and anal fins, or on entire pectoral fin [vs. melanophores present along bases of dorsal and anal fins, and on upper part of pectoral fin (no melanophores on pectoral fin of *S. horizon*)]; ventral scutes 6 or 7 [vs. 5 or fewer (rarely 6 in *S. balinensis* and *S. meteorum*)], and pseudobranchial filaments 15–18 (vs. 19 or more). Furthermore, the shorter head of *S. advenus* (21.6%–22.9% of SL) separates it from *S. horizon* (22.6%–25.2%), *S. indicus* (23.0%–26.7%), and *S. meteorum* (23.7%–26.0%). The body depth of *S. advenus* (17.4%–20.9% of SL) is greater than that of *S. commersonnii* (14.2%–17.8%) and *S. scitulus* (14.6%–16.9%), the pectoral fin is longer (13.5%–14.2% of SL in *S. advenus*) than in *S. balinensis* (11.3%–13.9%), and the pelvic fin is shorter (7.6%–8.0% of SL in *S. advenus*) than in *S. belaerius* (7.9%–10.3%) (Whitehead et al. 1988; Wongratana et al. 1999; Kimura et al. 2009; Hata and Motomura 2018a, 2018b, 2018c, 2018d, 2021a, 2021b, 2021c, 2022a, 2022b, 2023; Hata et al. 2019, 2020a, 2020b, 2021, 2022a, 2022b, 2023; Gangan et al. 2020; this study; Fig. 3).

Although the known distribution of the species was limited to the type locality (Cobourg Peninsula, Northern Territory, Australia), both Whitehead et al. (1988) and Wongratana et al. (1999) suggested that *S. advenus* may be distributed (hence question marks on their distribution maps) along the northern coast of Western Australia and the Gulf of Carpentaria. Such a distribution is partially confirmed in the presently reported study (Fig. 2), since there are still no specimens recorded in Western Australia. The biology or habitat of *S. advenus* is also still totally unknown. Whitehead et al. (1988) and Wongratana et al. (1999) presumed that the species is coastal pelagic, and schooling. The collection of some of the specimens described here in coastal waters 14.6–18 m depth is indeed suggestive that the species is coastal. Based on the standard length of the holotype, Whitehead et al. (1988) and Wongratana et al. (1999) also suggested a maximum standard length of 7.2 cm, which is slightly shorter than the largest specimen (CSIRO CA 2688, 79.6 mm SL) measured in the present study.

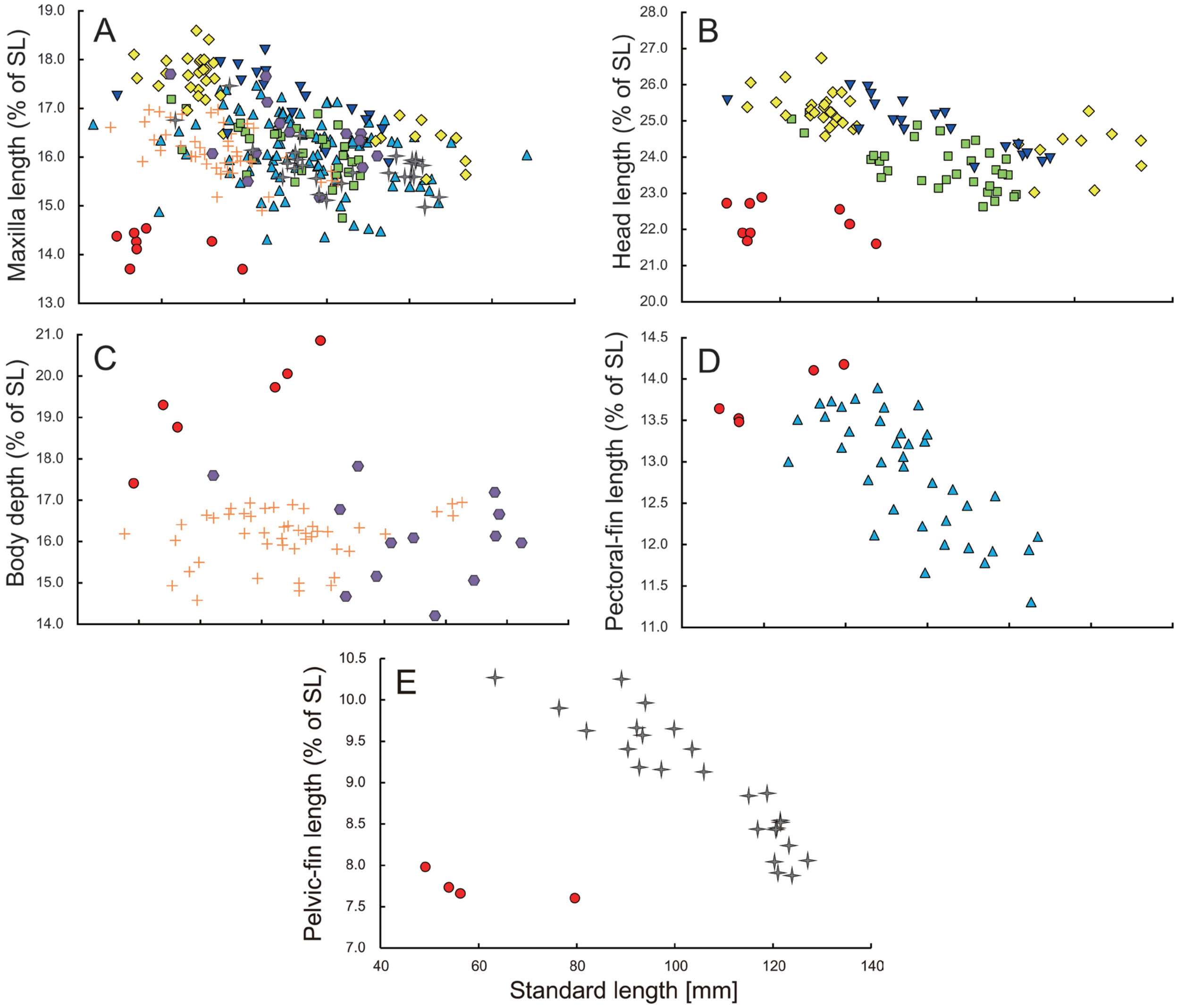

Figure 3. Maxilla length (**A**), head length (**B**), body depth (**C**), pectoral-fin length (**D**), and pelvic-fin length (**E**) (all as % of standard length; SL) relative to SL in *Stolephorus advenus* (red circles), *S. balinensis* (blue triangles), *S. belaerius* (gray stars), *S. commersonnii* (purple hexagons), *S. horizon* (green squares), *S. indicus* (yellow diamonds), *S. meteorum* (dark blue inverted triangles), and *S. scitulus* (orange crosses).

Acknowledgments

We are especially grateful to N. Bailly (BC), A. Suzumoto and L. O'Hara (BPBM), D. Catania and M. Hoang (CAS), A. Graham and J. Pogonoski (CSIRO), M. Nakae (NSMT), and B. Russell, M. Hammer, and G. Dally (NTM) for opportunities to examine specimens of *Stolephorus*. We also thank S. Tashiro (formerly KAUM), T. Clardy (LACM), and T. Munroe, K. Murphy, D. Pitassy, L. Willis, and A. Reft (USNM) for their curatorial assistance, and G. Hardy (Ngunguru, New Zealand), for checking an early version of the manuscript. This study was supported in part by the Sasakawa Scientific Research Grant from the Japan Science Society (28-745); a Grant-in-Aid from the Japan Society for the Promotion of Science for JSPS Fellows (DC2: 29-6652); JSPS KAKENHI Grant Numbers 19K23691; and JSPS Overseas Research Fellowships (202160519).

References

Bleeker P (1849) Bijdrage tot de kennis der ichthyologische fauna van het eiland Bali, met beschrijving van eentige nieuwe species. Verhandelingen van het Bataviaasch Genootschap van Kunsten en Wetenschappen 22(7): 1–11.

Fowler HW (1911) Notes on clupeoid fishes. Proceedings of the Academy of Natural Sciences of Philadelphia 63: 204–221.

Gangan SS, Pavan-Kumar A, Jahageerdar S, Jaiswar AK (2020) A new species of *Stolephorus* (Clupeiformes: Engraulidae) from the Bay of Bengal. Zootaxa 4743(4): 561–574. https://doi.org/10.11646/zootaxa.4743.4.6

Hata H, Motomura H (2017) A new species of anchovy, *Encrasicholina auster* (Clupeiformes: Engraulidae) from Fiji, southwestern Pacific.

New Zealand Journal of Zoology 44(2): 122–128. https://doi.org/10.1080/03014223.2016.1268177

Hata H, Motomura H (2018a) *Stolephorus continentalis*, a new anchovy from the northwestern South China Sea, and redescription of *Stolephorus chinensis* (Günther 1880) (Clupeiformes: Engraulidae). Ichthyological Research 65(3): 374–382. https://doi.org/10.1007/s10228-018-0621-z

Hata H, Motomura H (2018b) *Stolephorus insignus*, a new anchovy from the western Pacific, and redescription of *Stolephorus apiensis* (Jordan and Seale 1906) (Clupeiformes: Engraulidae). Ichthyological Research 66(2): 280–288. https://doi.org/10.1007/s10228-018-00675-5

Hata H, Motomura H (2018c) Additional specimens of the poorly known anchovy *Stolephorus multibranchus* (Clupeiformes: Engraulidae) from Kosrae, Caroline Islands. Biogeography 20: 78–84. https://doi.org/10.11358/biogeo.20.78

Hata H, Motomura H (2018d) Redescription and distributional range extension of the poorly known anchovy *Stolephorus nelsoni* (Clupeiformes: Engraulidae). Acta Ichthyologica et Piscatoria 48(4): 381–386. https://doi.org/10.3750/AIEP/02501

Hata H, Motomura H (2021a) Two new species of *Stolephorus* (Teleostei: Clupeiformes: Engraulidae) from the western Pacific. Raffles Bulletin of Zoology 69: 109–117. https://doi.org/10.26107/RBZ-2021-0009

Hata H, Motomura H (2021b) *Stolephorus grandis*, a new anchovy (Teleostei: Clupeiformes: Engraulidae) from New Guinea and Australia. Zootaxa 5004(3): 481–489. https://doi.org/10.11646/zootaxa.5004.3.5

Hata H, Motomura H (2021c) A new species of the anchovy genus *Stolephorus* Lacepède 1803 from North Sumatra, Indonesia, and redescriptions of *Stolephorus pacificus* Baldwin 1984 and *Stolephorus teguhi* Kimura, Hori and Shibukawa 2009 (Teleostei: Clupeiformes: Engraulidae). Zoological Studies 60: 65. https://doi.org/10.6620/ZS.2021.60-65

Hata H, Motomura H (2022a) Description of *Stolephorus hindustanensis*, a new anchovy from the western coast of India and redescription of *Stolephorus ronquilloi* Wongratana, 1983 (Teleostei: Clupeiformes: Engraulidae). Taxonomy 2: 124–135. https://doi.org/10.3390/taxonomy2010010

Hata H, Motomura H (2022b) *Stolephorus lotus*, a new anchovy (Teleostei: Clupeiformes: Engraulidae) from the Northern Territory, Australia. Zoological Studies 61: 87. https://doi.org/10.6620/ZS.2022.61-87

Hata H, Motomura H (2023) Description of *Stolephorus horizon* n. sp. from Fiji and Tonga, and redescription of *Stolephorus scitulus* (Fowler, 1911) (Teleostei: Clupeiformes: Engraulidae). Taxonomy 3(3): 356–380. https://doi.org/10.3390/taxonomy3030021

Hata H, Lavoué S, Motomura H (2019) Taxonomic status of seven nominal species of the anchovy genus *Stolephorus* described by Delsman (1931), Hardenberg (1933), and Dutt and Babu Rao (1959), with redescriptions of *Stolephorus tri* (Bleeker 1852) and *Stolephorus waitei* Jordan and Seale 1926 (Clupeiformes: Engraulidae). Ichthyological Research 67(1): 7–38. https://doi.org/10.1007/s10228-019-00697-7

Hata H, Lavoué S, Motomura H (2020a) *Stolephorus babarani*, a new species of anchovy (Teleostei: Clupeiformes: Engraulidae) from Panay Island, central Philippines. Zootaxa 4178(4): 509–520. https://doi.org/10.11646/zootaxa.4718.4.5

Hata H, Lavoué S, Motomura H (2020b) *Stolephorus acinaces*, a new anchovy from the northern Borneo, and redescription of *Stolephorus andhraensis* (Babu Rao 1966) (Clupeiformes: Engraulidae). Marine Biodiversity 50(6): 102. https://doi.org/10.1007/s12526-020-01115-2

Hata H, Lavoué S, Motomura H (2021) Taxonomic status of nominal species of the anchovy genus *Stolephorus* previously regarded as synonyms of *Stolephorus commersonnii* Lacepède 1803 and *Stolephorus indicus* (van Hasselt 1823), and descriptions of three new species (Clupeiformes: Engraulidae). Ichthyological Research 68(3): 327–372. https://doi.org/10.1007/s10228-020-00792-0

Hata H, Lavoué S, Motomura H (2022a) Description of three new species previously identified as *Stolephorus bengalensis* (Dutt and Babu Rao, 1959) or *Stolephorus insularis* Hardenberg, 1933, and a redescription of *S. bengalensis* (Chordata, Osteichthyes, Clupeiformes, Engraulidae). ZooKeys 1121: 145–173. https://doi.org/10.3897/zookeys.1121.84171

Hata H, Lavoué S, Motomura H (2022b) A new species of *Stolephorus* from the eastern Indian Ocean and redescription of *Stolephorus dubiosus* Wongratana, 1983, with comments on the evolution of prepelvic scute numbers within *Stolephorus* (Clupeiformes: Engraulidae). Zoological Studies 61: 58. https://doi.org/10.6620/ZS.2022.61-58

Hata H, Lavoué S, Bogorodsky SV, Alpermann TJ, Motomura H (2023) *Stolephorus meteorum*, a new anchovy (Teleostei: Clupeiformes: Engraulidae: Engraulinae) from the Red Sea. Ichthyology and Herpetology 111(2): 191–203. https://doi.org/10.1643/i2022064

Kimura S, Hori K, Shibukawa K (2009) A new anchovy, *Stolephorus teguhi* (Clupeiformes: Engraulidae), from North Sulawesi, Indonesia. Ichthyological Research 56(3): 292–295. https://doi.org/10.1007/s10228-009-0103-4

Lavoué S, Bertrand JAM, Wang H-Y, Chen W-J, Ho H-C, Motomura H, Hata H, Sado T, Miya M (2017) Molecular systematics of the anchovy genus *Encrasicholina* in the northwestern Pacific. PLoS One 12(7): e081329. https://doi.org/10.1371/journal.pone.0181329

Nelson GJ (1983) *Anchoa argentivittata*, with notes on other eastern Pacific anchovies and the Indo–Pacific genus *Encrasicholina.* Copeia 1983(1): 48–54. https://doi.org/10.2307/1444697

Paxton JR, Gates JE, Bray DJ, Hoese DF (2006) Engraulidae. Anchovies. Pp. 310–317. In: Hoese DF, Bray DJ, Paxton JR, Allen GR (Eds.) Zoological Catalogue of Australia. Vol. 35. Fishes. Parts 1–3. CSIRO Publishing, Collingwood, Vic, Australia.

Sabaj MH (2020) Codes for natural history collections in Ichthyology and Herpetology. Copeia 108(3): 593–669. https://doi.org/10.1643/ASIHCODONS2020

van Hasselt JC (1823) Uittrekesel uit een' brief van Dr. J. C. van Hasselt, aan den Heer C. J. Temminck. Algemeene Konst- en Letter-bode voor het Jaar I Deel 21: 329–331.

Whitehead PJP (1967) The clupeoid fishes of Malaya. Journal of the Marine Biological Association of India 9(2): 223–280. https://doi.org/10.5962/p.119073

Whitehead PJP (1972) A synopsis of the clupeoid fishes of India. Journal of the Marine Biological Association of India 14(1): 160–256.

Whitehead PJP, Nelson GJ, Wongratana T (1988) FAO species catalogue. Vol. 7. Clupeoid fishes of the world (suborder Clupeoidei). An annotated and illustrated catalogue of the herrings, sardines, pilchards, sprats, shads, anchovies and wolf-herrings. Part 2 - Engraulidae. FAO Fisheries Synopsis No. 125 7 (2): i–viii + 305–579.

Wongratana T (1983) Diagnoses of 24 new species and proposal of a new name for a species of Indo–Pacific clupeoid fishes. Japanese Journal of Ichthyology 29(4): 385–407.

Wongratana T (1987a) Four new species of clupeoid fishes (Clupeidae and Engraulidae) from Australian waters. Proceedings of the Biological Society of Washington 100(1): 104–111.

Wongratana T (1987b) Two new species of anchovies of the genus *Stolephorus* (Engraulidae), with a key to species of *Engraulis*, *Encrasicholina*, and *Stolephorus.* American Museum Novitates 2876: 1–8.

Wongratana T, Munroe TA, Nizinski MS (1999) Order Clupeiformes. Engraulidae. Anchovies. Pp. 1698–1753. In: Carpenter KE, Niem VH (Eds.) FAO Species Identification Guide for Fishery Purposes. The Living Marine Resources of the Western Central Pacific, Vol. 3. Batoid Fishes, Chimaeras and Bony Fishes Pt. 1 (Elopidae to Linophrynidae). FAO, Rome.

Acta Ichthyologica et Piscatoria 53, 2023, 217–226 | DOI 10.3897/aiep.53.108838

PENSOFT.

ACTA
ICHTHYOLOGICA
ET PISCATORIA

Two new records of moray eels representing genera *Gymnothorax* and *Strophidon* (Actinopterygii: Anguilliformes: Muraenidae) from the Philippines

Roxanne A. CABEBE-BARNUEVO[1,2*], El Andro A. OBAR[1], Dianne Frances A. PENUELA[1], Hiroyuki MOTOMURA[3], Ricardo P. BABARAN[1], Maria Celia D. MALAY[1**]

1 *University of the Philippines Visayas, Miagao, Iloilo, Philippines*
2 *Department of Science and Technology, Science Education Institute, Bicutan, Taguig City, Philippines*
3 *Kagoshima University Museum, Kagoshima, Japan*

https://zoobank.org/2E55CF5D-1C86-4BC8-8AA4-E61D2F8F0E6B

Corresponding author: Maria Celia D. Malay (mdmalay@up.edu.ph)

Academic editor: Ronald Fricke ♦ **Received** 30 June 2023 ♦ **Accepted** 29 September 2023 ♦ **Published** 24 November 2023

Citation: Cabebe-Barnuevo RA, Obar EAA, Penuela DFA, Motomura H, Babaran RP, Malay MCD (2023) Two new records of moray eels representing genera *Gymnothorax* and *Strophidon* (Actinopterygii: Anguilliformes: Muraenidae) from the Philippines. Acta Ichthyologica et Piscatoria 53: 217–226. https://doi.org/10.3897/aiep.53.108838

Abstract

In this study, we report the collection of moray eel species *Gymnothorax nudivomer* (Günther, 1867) and *Strophidon dorsalis* (Seale, 1917) from the Western Visayas region, Philippines. Both represent new records for the country. A single specimen of *G. nudivomer* measuring 619 mm total length (TL) was collected from Iloilo Fish Port Complex, Iloilo and a specimen of *S. dorsalis* measuring 777 mm TL was collected from the fish market of Batan, Aklan. Detailed morphological descriptions and mitochondrial cytochrome oxidase I (*COI*) barcode sequences are provided. A comprehensive list of geographic records for both species, as well as a list of all species representing the genera *Gymnothorax* and *Strophidon* reported in the Philippines is also provided in this report.

Keywords

new country records, moray eel, morphology, Panay Island, taxonomy

Introduction

The family Muraenidae is considered one of the more diverse eel groups, having 228 valid species belonging to 16 genera (Fricke et al. 2023). Muraenids, commonly known as moray eels, are distinct from other eels by having 1 or 2 lateral-line pores before the gill opening, posterior nostril high on the head and usually positioned before or above the eye, small and rounded gill openings, and lack of pectoral and pelvic fins (Böhlke et al. 1999).

Moray eels are widely distributed in tropical and subtropical seas. The majority of species are found in coral reefs, shallow-water rocky areas, and moderately deep habitats down to 500 m, while a few species inhabit brackish coastal waters, rivers, or anchialine caves (e.g., Chen et al. 1994; Böhlke et al. 1999; Tsukamoto et al. 2014; Quindo and Bucol 2019; Böhlke and Smith 2002; Huang et al. 2023a). In the Philippines, 83 species representing 10 genera have been reported (Jordan and Seale 1907; Herre 1923; Herre 1953; Allen and Erdmann 2012; Smith 2012; Kottelat 2013;

---

[*] Current affiliation: Kagoshima University Museum, Kagoshima, Japan.

[**] Current affiliation: Marine Science Institute, University of the Philippines Diliman, Quezon City, Philippines.

Motomura et al. 2017; Huang et al. 2021; Smith and Böhlke 2022; Huang et al. 2023a, 2023b; Fricke et al. 2023). Recent studies described new muraenid species from Palawan (Huang et al. 2020), Cagayan (Huang et al. 2021), Negros Oriental (Huang et al. 2021), Cebu (Huang et al. 2023b), and Bohol (Huang et al. 2023a). Taking into account the abundance of reef and shallow-water habitats in the Philippine archipelago, many more new species and new records are expected to be found through ichthyological surveys.

Two new Philippine records of moray eels and their partial cytochrome oxidase I (*COI*) DNA sequences are reported in this study. One of the new records, *Gymnothorax nudivomer* (Günther, 1867), belongs to a large genus (143 valid species; Fricke et al. 2023) known for having variable body color patterns and teeth structure, anus near mid-length of the body, and dorsal fin originating before or above gill opening (Smith et al. 2019). The second new record, *Strophidon dorsalis* (Seale, 1917), belongs to a small genus (only five valid species; Huang et al. 2020; Fricke et al. 2023) characterized by having an extremely long, uniformly brown or variegated body, infraorbital pores 3–5, branchial pores 1–8, and a total vertebrae count of 155–213 (Huang et al. 2020). To our knowledge, 36 species of *Gymnothorax* and two species of *Strophidon* have been reported from the Philippines prior to this study (i.e., Jordan and Seale 1907; Herre 1923; Herre 1953; Smith and Böhlke 1997; Böhlke 2000; Allen and Erdmann 2012; Motomura et al. 2017; Smith et al. 2019; Huang et al. 2020, 2021; Smith and Böhlke 2022). Therefore, this study updates the inventory of marine eel species in the country and contributes to the establishment of a *COI* gene-sequence library for Philippine marine fishes.

Materials and methods

Fish specimens were bought directly from the Iloilo Fish Port Complex (IFPC), Iloilo Province, and the fish market in Batan, Aklan Province (Figs. 1, 2). The type of fishing gear was noted if available. Curatorial protocols followed Motomura and Ishikawa (2013). Measurements were taken using digital calipers to the nearest 1 mm following the method of Böhlke and Randall (2000) and expressed as percentages in total length (TL) and head length (HL). Meristic characters were determined following the diagram of Böhlke and Randall (2000) and Huang et al. (2020). All specimens are deposited at the Museum of Natural Sciences, University of the Philippines Visayas, Miag-ao (UPVMI).

The fish muscle tissue samples were collected from the nape area on the right side of the body and preserved in absolute ethanol. DNA extractions were carried out according to the instructions of the GF-1 Nucleic Acid Extraction Kit (Vivantis Technologies Sdn. Bhd, Malaysia). The combination of the forward and reverse primers below designed by Ward et al. (2005) was used to amplify the mitochondrial cytochrome c oxidase subunit I (*COI*) gene:

FishF1-5′TCAACCAACCACAAAGACATTGGCAC3′
FishR1-5′TAGACTTCTGGG TGGCCAAAGAATCA3′

The 25 µL PCR reaction was composed of 18.4 µL nuclease-free water, 2.25 µL 10× buffer, 1.25 µL $MgCl_2$ (25 mM), 0.5 µL dNTP mix (10 mM), 0.25 µL of each primer, 0.1 µL Taq DNA polymerase (Vivantis Technologies Sdn. Bhd, Malaysia), and 2 µL DNA template. The PCR thermocycling conditions used are as follows: initial step at 95°C for 2 min, 35 cycles of 94°C for 30 s (denaturation), 54°C for 30 s (annealing), and 72°C for 1 min (extension), with a final extension at 72°C for 10 min. The PCR products were visualized using 1% agarose gel with gel red. Purification of PCR products was carried out using GF-1 PCR Clean-up Kit. The genomic DNA was quantified using a MultiSkanTM Skyhigh Microplate Spectrophotometer (Thermo Fisher Scientific). The PCR products were sent to Macrogen Inc. (South Korea) for sequencing. The forward and reverse sequences were checked, trimmed, and realigned using Unipro UGENE software (Okonechnikov et al. 2012).

Results and Discussion

Family Muraenidae Rafinesque, 1810
Genus *Gymnothorax* Bloch, 1795

Gymnothorax nudivomer (Günther, 1867)

English common name: yellowmouth moray
(Fig. 3; Table 1)

Material examined. UPVMI-03157, 619 mm TL, Iloilo Fish Port Complex (IFPC), Iloilo City, Panay Island, Philippines, 8 June 2022, R. Cabebe-Barnuevo and R.P. Babaran leg.

Morphological diagnosis and description. Body elongated, large; tapering towards caudal area. Head large; eyes moderate in size, and situated slightly closer to snout (19% of HL) than rear of lower jaw (22% of HL, see Table 1). Mouth large; snout short and blunt; anterior nostril short, tubular, and located at snout tip; posterior nostril large, elliptic, and located above and before anterior margin of eye; upper and lower jaws subequal; teeth not visible when mouth closed; teeth on both jaws uniserial, sharply pointed; anterior teeth large and triangular; posterior teeth short and serrated. Dorsal-fin base very long; its origin anterior to gill opening. Anal-fin base shorter; its origin just behind anus. Caudal fin confluent with dorsal and anal fins. Pectoral and pelvic fins absent. Gill opening moderately large and elongated; located on middle side of body. Anus moderate in size, circular, and positioned anterior to midpoint of body. Supraorbital pores 3: first pore located on snout tip, small and circular; second pore located above anterior nostril, largest in size, circular; third located above first infraorbital pore, equal in size with first pore, circular. Infraorbital pores 4, along upper jaw; first pore located below base of anterior nostril; second pore between anterior nostril and anterior margin of eye; third pore before anterior margin of eye; fourth pore located beyond posterior margin of eye. Preoperculo-mandibular pores 6, along lower jaw;

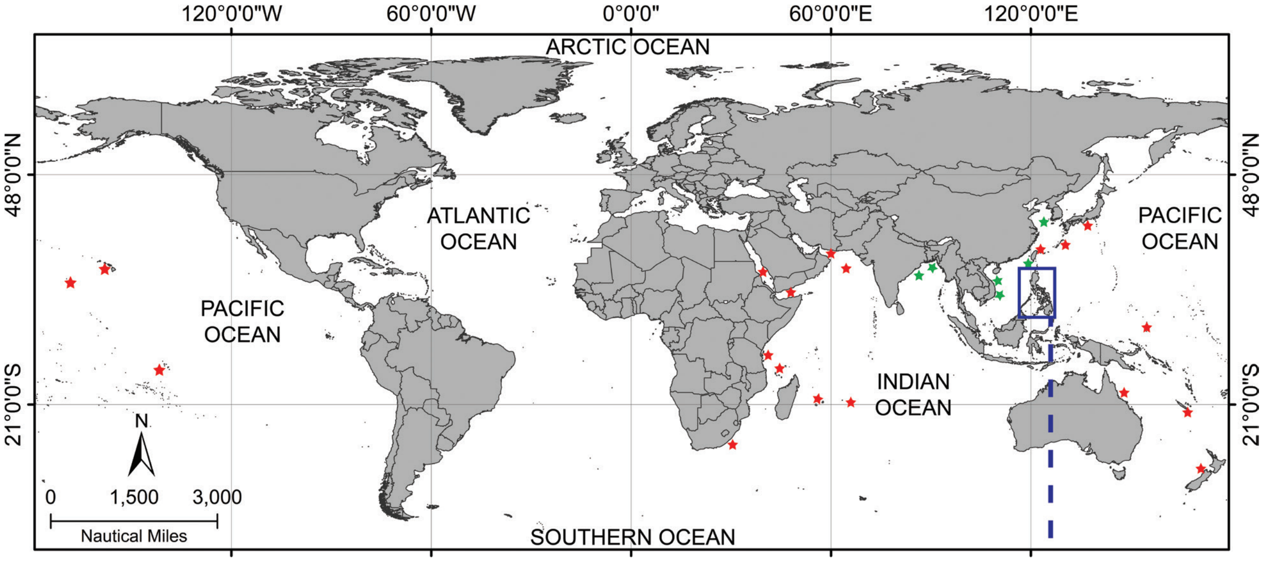

Figure 1. Global geographic distribution of *Gymnothorax nudivomer* (red star) and *Strophidon dorsalis* (green star).

all pores positioned anterior to rictus. Branchial pore 1, located along posterodorsal head anterior to gill opening, posterior to dorsal-fin origin. Teeth pointed and uniserial; intermaxillary teeth 7; median intermaxillary teeth 1; vomerine teeth absent.

Fresh coloration. Body yellow to light brown, becoming darker on caudal area; covered entirely with white spots of varying sizes; white spots on head and anterior body area very small, becoming large towards caudal area; white spots on dorsal and anal fins similar in body spots; white spots on caudal area composed of both rounded and irregular in shape; posterior margin of caudal fin white; eyes with vertical black bar; inner mouth bright yellow; gill opening black.

Color of preserved specimen. Body light brown, becoming darker on caudal area; white spots still visible; posterior margin of caudal fin white; inner mouth white; gill opening black.

Distribution. Widely distributed across the Indo–Pacific Ocean. Specific reports are summarized in Table 2.

DNA Barcode. A *COI* sequence fragment measuring 605 basepairs (bp) was submitted to GenBank under accession number OR214978.

Remarks. *Gymnothorax nudivomer* was originally described as *Muraena nudivomer* from the Zanzibar Archipelago by Günther (Playfair and Günther 1867). It was then widely reported as *G. nudivomer* distributed across the Indo–Pacific Ocean at depths of 2–271 m (Mundy 2005; Fricke et al. 2009). This species can reach up to 1800 mm in length (Böhlke and Randall 2000). In Böhlke et al. (1999), *G. nudivomer* was listed as one of the moray eels occurring within the western central Pacific but it was not stated if the species was collected specifically within Philippine waters. Furthermore, according to the list of reef fishes by Allen and Erdmann (2012) from the East Indies (which includes the countries of Myanmar, Thailand, Indonesia, Singapore, Malaysia, Brunei, Papua New Guinea, Solomon Islands, and the Philippines), *G. nudivomer* was not known to exist in the country. Finally, Herre (1953) provided a list of approximately 2145 Philippine species, however, this species was not among them. Hence, the presently reported study treats the specimen collected from Iloilo as the first report (new country record) from Philippine waters. Table 2 and Figs. 1, 2 provide the geographic distribution of the species while Table 3 includes other species within the genus *Gymnothorax* reported in the country. Reports that

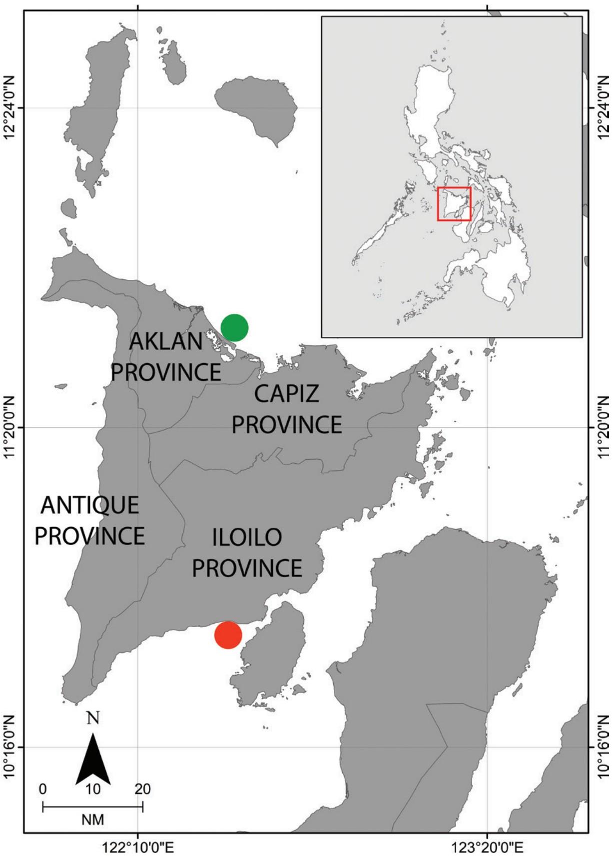

Figure 2. Geographic distribution of *Gymnothorax nudivomer* (red dot) and *Strophidon dorsalis* (green dot) in Western Visayas, Philippines (the inset to Fig. 1)

did not clearly specify that the data collection occurred within the Philippines have been excluded from the list.

This fish is commonly known as the yellowmouth moray and can be easily identified by its tapering body form, white spots scattered throughout the body, and yellow coloration inside the mouth. *Gymnothorax elegans* and *G. nudivomer* are closely related species (Smith et al. 2019), but can easily be distinguished based on their color patterns. *Gymnothorax elegans* Bliss, 1883 has larger and distinct patterns of white markings throughout the body that forms into bars towards the caudal fin (i.e., fig. 13, Smith et al. 2019), in contrast to *G. nudivomer*, which has relatively smaller, rounded spots on the body, that becomes a larger and elongated circle towards the caudal fin (i.e., Fig. 3, this publication; fig. 24, Smith et al. 2019).

Family Muraenidae Rafinesque, 1810
Genus *Strophidon* McClelland, 1844

Strophidon dorsalis (Seale, 1917)

English common name: three-pore moray

(Fig. 4; Table 1)

Material examined. UPVMI-03151, 777 mm TL, off Batan, Aklan Province, Panay Island, Philippines, bottom set gillnet, 31 May 2021, Sunshine Sucgang leg.

Morphological diagnosis and description. Body elongated and cylindrical, becoming compressed behind anus towards tail area. Head moderately long with wrin-

Table 1. Morphological counts and measurements of *Gymnothorax nudivomer* and *Strophidon dorsalis* expressed in absolute and relative values.

Character	*G. nudivomer* UPVMI-03157	*S. dorsalis* UPVMI-03151
Counts		
Supraorbital pores	3	3
Infraorbital pores	4	4
Preoperculo-mandibular pores	6	6
Branchial pores	1	2
Vomerine teeth	Absent	4
Intermaxillary teeth	7	6
Median Intermaxillary teeth	1	3
Inner maxillary teeth	—	5
Inner dentary teeth	—	4
Measurements. Absolute values [mm]		
Total length (TL)	619	777
Head length (HL)	78	95
Measurements. Relative values [%TL]		
Head length	14	12
Body depth at gill opening	10	4
Body depth at anus	8	4
Pre-dorsal length	10	8
Pre-anal length	43	43
Measurements. Relative values [%HL]		
Length of upper jaw	45	32
Length of lower jaw	45	30
Snout length	19	11
Eye diameter	8	6
Interorbital width	15	7
Distance between eye and snout	19	11
Distance between eye and rear of lower jaw	22	18

Note: All measurements were rounded off to the nearest 1 mm.

Figure 3. *Gymnothorax nudivomer*, UPVMI-03157, 619 mm TL, Iloilo Fish Port Complex (IFPC), Iloilo City, Philippines.

Table 2. Published reports on the occurrence of *Gymnothorax nudivomer* and *Strophidon dorsalis* along with their synonyms, organized chronologically by year of publication.

Species	Status	Location	Reference
Gymnothorax nudivomer			
Muraena nudivomer	Original name	Zanzibar	Playfair and Günther 1867
Lycodontis nudivomer	Junior synonym	Red Sea	Dor 1984
		Mozambique (Inhaca)	Smith 1962
Gymnothorax xanthostomus	Junior synonym	Hawaiian Islands	Snyder 1904
Gymnothorax insignis	Junior synonym	Mauritius	Seale 1917
Gymnothorax nudivomer	Valid name	Red Sea	Goren and Dor 1994; Randall and Golani 1995; Fowler and Steinitz 1956; Castle and McCosker 1986; Khalaf and Disi 1997; Golani and Fricke 2018; Smith et al. 2019
		North Pacific Ocean (Hawaii; Johnston Islands)	Randall et al. 1981; Uchida and Uchiyama 1986; Castle and McCosker 1986; Chave and Mundy 1994; Böhlke and Randall 2000; Mundy 2005; Randall 2007
		Taiwan (Nanfangao, Hualien and Taitung counties)	Chen at al. 1994; Ramos-Castro et al. 2020
		Indian Ocean (Mauritius and East Africa from Zanzibar to Transkei, Mascarene Islands, Mayotte)	Quéro and Saldanha 1995; Fricke 1999; Laboute and Grandperrin 2000; Böhlke and Randall 2000; Fricke et al. 2009; Fricke et al. 2011; Allaria 2016; Eudeline 2022; Smith and Böhlke 2022
		Gulf of Oman	Randall 1995; Böhlke and Randall 2000
		New Caledonia	Böhlke and Randall 2000
		South Pacific Ocean (Marquesas Islands)	Böhlke and Randall 2000
		Australia (From Cape York to the southeastern border of Queensland)	Böhlke and McCosker 2001;
		Japan (Kochi Prefecture, Okinawa Islands, Osumi Islands (Iwo-jima Island and Yakushima Island), Amami-oshima Island)	Nakabo 2002; Motomura et al. 2013; Jeong and Motomura 2021; Motomura and Harazaki 2017; Nakae et al. 2018; Motomura et al. 2019
		Marianas Islands	Myers and Donaldson 2003
		Arabian Sea (Coast of Oman, Gulf of Aden, Eastern Coast of Somali)	Manilo and Bogorodsky 2003
		Tonga Island	Randall et al. 2004
		Yemen (Socotra Archipelago)	Zajonz et al. 2019
		Philippines (Iloilo Province)	**Presently reported study**
Strophidon dorsalis			
Gymnothorax dorsalis	Original name	Hongkong	Seale 1917
		Malaysia	Böhlke 1997
		Taiwan	Böhlke 1997; Loh et al. 2011
		South China Sea	Randall and Lim 2000
		Thailand (Prachuap Khiri Khan)	Yoshida et al. 2013
		Indian waters (Bengal Bay, West coast of India)	Ray et al. 2015; Kumar et al. 2020
		Pakistan	Psomadakis et al. 2015
Strophidon dorsalis	Valid name	Taiwan (Pingtung County, Kaohsiung City)	Ho et al. 2015; Huang et al. 2020
		Vietnam (Nha Trang, Da Nang, Thua Thien-Hue Province)	Loh et al. 2015; Huang et al. 2020
		India (West Bengal Coast, Odisha)	Mohapatra et al. 2016; 2021
		Korea (Jindo Island)	Kang et al. 2020
		Philippines (Aklan Province)	**Presently reported study**

kled skin. Eyes moderate in size, and situated closer to snout (11% of HL) than rear of lower jaw (18% of HL, see Table 1). Mouth large; snout short and blunt; anterior nostril located at snout tip, short and tubular; posterior nostril located above anterior margin of eye, large and circular; upper jaw slightly more pronounced relative to lower jaw; teeth on both jaws sharply pointed. Dorsal-fin base very long; origin anterior to gill opening. Anal-fin base shorter; origin just behind anus. Caudal fin slightly damaged but still visibly connected with dorsal and anal fins. Pectoral and pelvic fins absent. Gill opening moderately large and elongated; located on lower portion of body. Anus moderate in size, circular, and positioned anterior to midpoint of body. Supraorbital pores 3: first pore located on snout tip, small and circular; second pore located above anterior nostril; third located above first infraorbital pore, largest in size and somewhat elongated circular pore. Infraorbital pores 4, located along upper jaw; first pore located below base of anterior nostril; second pore between anterior nostril and anterior margin of eye; third pore below ventral margin of eye; fourth pore located beyond posterior margin of eye. Preoperculo-mandibular pores 6, located

Table 3. List of species under the genera *Gymnothorax* and *Strophidon* reported in Philippine waters.

Species	Reference
Genus *Gymnothorax*	
G. angusticauda (Weber et de Beaufort, 1916)	Smith et al. 2018
G. annulatus Smith et Böhlke, 1997	Smith and Böhlke 1997; Allen and Erdmann 2012; Smith 2012
G. castlei Böhlke et Randall, 1999	Allen and Erdmann 2012
G. chilospilus Bleeker, 1864	Herre 1923, 1953; Smith 2012
G. chlamydatus Snyder, 1908	Allen and Erdmann 2012
G. enigmaticus McCosker et Randall, 1982	McCosker and Randall 1982
G. favagineus Bloch et Schneider, 1801	Herre 1923, 1953; Allen and Erdmann 2012
G. fimbriatus (Bennett, 1832)	Motomura et al. 2017
G. flavimarginatus (Rüppell, 1830)	Herre 1923, 1953
G. fuscomaculatus (Schultz, 1953)	Allen and Erdmann 2012; Smith and Böhlke 2022
G. herrei Beebe et Tee-Van, 1933	Allen and Erdmann 2012; Smith 2012; Smith and Böhlke 2022
G. isingteena (Richardson, 1845)	Balisco et al. 2023
G. kidako (Temminck et Schlegel, 1846)	Herre 1923, 1953
G. margaritophorus Bleeker, 1864	Herre 1953
G. meleagris (Shaw, 1795)	Herre 1923, 1953
G. microstictus Böhlke, 2000	Allen and Erdmann 2012; Böhlke 2000
G. minor (Temminck et Schlegel, 1846)	Wagey et al. 2015
G. monochrous (Bleeker, 1856)	Allen and Erdmann 2012
G. monostigma (Regan, 1909)	Allen and Erdmann 2012; Smith and Böhlke 2022
G. nudivomer (Günther, 1867)	**Presently reported study**
G. phasmatodes (Smith, 1962)	Allen and Erdmann 2012; Smith and Böhlke 2022
G. philippinus Jordan et Seale, 1907	Jordan and Seale 1907; Herre 1923; Allen and Erdmann 2012; Smith 2012
G. pictus (Ahl, 1789)	Herre 1923, 1953; Smith and Böhlke 2022
G. pindae Smith, 1962	Böhlke 2000
G. polyuranodon (Bleeker, 1854)	Herre 1923, 1953; Smith and Böhlke 2022
G. prionodon Ogilby, 1895	Wagey et al. 2015
G. pseudoherrei Böhlke, 2000	Allen and Erdmann 2012; Smith 2012; Böhlke 2000; Smith and Böhlke 2022
G. pseudokidako Huang, Loh et Liao, 2021	Huang et al. 2021
G. pseudothyrsoideus (Bleeker, 1853)	Herre 1953; Allen and Erdmann 2012; Motomura et al. 2017; Smith and Böhlke 2022
G. punctatofasciatus Bleeker, 1863	Herre 1923, 1953; Allen and Erdmann 2012
G. richardsonii (Bleeker, 1852)	Herre 1923, 1953; Smith and Böhlke 2022
G. robinsi Böhlke, 1997	Allen and Erdmann 2012; Smith and Böhlke 2022
G. rueppelliae (McClelland, 1844)	Herre 1953
G. thyrsoideus (Richardson, 1845)	Herre 1923, 1953
G. tile (Hamilton, 1822)	Herre 1923, 1953; Allen and Erdmann 2012
G. undulatus (Lacepède, 1803)	Herre 1923, 1953
G. *zonipectis* Seale, 1906	Herre 1923, 1953; Smith 2012
Genus *Strophidon*	
S. dorsalis (Seale, 1917)	**Presently reported study**
S. sathete (Hamilton, 1822)	Motomura et al. 2017; Smith and Böhlke 2022
S. tetraporus Huang, Mohapatra, Thu, Chen et Liao, 2020	Huang et al. 2020

along lower jaw; all pores positioned anterior to rictus. Branchial pores 2, located along postero-dorsal head anterior to gill opening. Teeth on both jaws pointed; intermaxillary teeth 6; median intermaxillary teeth 3; inner maxillary teeth 5; vomerine teeth 4; inner dentary teeth 4.

Fresh coloration. Body brown becoming dark towards caudal area; margins of dorsal and anal fins dark brown; caudal fins dark brown to black.

Color of preserved specimen. Body uniformly dark brown; fins dark brown to black.

Distribution. Tropical to subtropical Indo–West Pacific Ocean. Specific reports are summarized in Table 2.

DNA Barcode. A 568 bp *COI* sequence fragment was submitted to GenBank under accession number OR214977.

Remarks. *Strophidon dorsalis* was originally placed in the genus *Gymnothorax* by Seale (1917) based on collections from Hong Kong. However, Loh et al. (2015) suggested that *Gymnothorax dorsalis* belongs to the genus *Strophidon* based on molecular data and similarities in some morphological features. Following the work of Loh et al. (2015), *S. dorsalis* was reported from Taiwan (Ho et al. 2015; Huang et al. 2020), Vietnam (Loh et al. 2015; Huang et al. 2020), India (Mohapatra et al. 2016, 2021), and Korea (Kang et al. 2020). Based on the report of Böhlke (1997), this species can be found in depths down to 110 m. The largest recorded specimen, measuring 1262 mm TL, collected from Vietnam was reported by Huang et al. (2020). Randall and Lim (2000) included *Gymnothorax dorsalis* on their list of fishes from the South China Sea which covers Taiwan, the Philippines, and Borneo. However, it was not specified whether the specimen was collected in Philippine waters. As a result, this study confirms the presence of the species in the Philippine waters. Table 2 provides a list of all published geographic

Figure 4. *Strophidon dorsalis*, UPVMI-03151, 777 mm TL, off Batan, Aklan, Philippines.

records of the species while Table 3 includes other species within the genus *Strophidon* reported in the country.

This species can be distinguished from its congeners based on the following combination of characters: body uniformly brown, anus located anterior to the midpoint of the body, 3–4 infraorbital pores, 2–7 inner maxillary teeth, 3–5 inner dentary teeth, 62–73 pre-anal vertebrae, and 155–174 total vertebrae (Böhlke and Smith 2002; Huang et al. 2020). *Strophidon dorsalis* and *S. sathete* (Hamilton, 1822) are considered sister species (Loh et al. 2015). Based on the summarized morphological comparisons of the species under the genus *Strophidon* given by Huang et al. (2020), they have overlapping meristic counts which include infraorbital pores (both 3–4), supraorbital (both 3), preoperculo-mandibular (5–7 vs. 6–7), branchial pores (2–6 vs. 2–7), and pre-anal vertebrae (62–73 vs. 73–82). Moreover, these two species have unpatterned body coloration, short snouts, and an anus located before body midlength. However, *S. dorsalis* can further be distinguished from *S. sathete* based on the number of teeth on the inner maxillary (2–7 vs. 10–15), teeth on the inner dentary (3–5 vs. 6–11), and total vertebrae (155–174 vs. 187–213). The specimen used in the study was initially identified as *S. dorsalis* based on the number of infraorbital pores (4) and fewer teeth on the lower jaw, and this was supported by the generated *COI* sequence.

Conclusions and recommendations

The presently reported study provides two new country records of moray eels, *Gymnothorax nudivomer* and *Strophidon dorsalis*, from Philippine waters. Additionally, a list of geographic records for both species is provided, along with the list of all species under the two genera *Gymnothorax* and *Strophidon* documented in the country. The morphological descriptions and mitochondrial cytochrome oxidase I (*COI*) barcode sequences provided will aid in the more accurate identification of these species. Moreover, the findings expand our understanding of the distribution of these species and contribute to ongoing efforts to establish a comprehensive genetic library for marine fish species in the Philippines.

Due to a lack of studies, there are still many unreported marine fish species from the Philippines. Some of the recently reported species are presumed to have been overlooked because they share local names with similar-looking species. One of the best examples is the local name for all species of *Strophidon* found in Western Visayas, which is “*nipa-nipa*”. Therefore, we recommend assigning specific local names (standard names) to these newly-reported species to increase public awareness of their occurrence within the country, and help the scientific community distinguish between species. However, assigning Philippine local names requires additional research, including an updated compilation of all moray eels found in the country and their respective local names.

Acknowledgments

We gratefully acknowledge funding support from the UP System Emerging Inter-Disciplinary Research Program (OVPAA-EIDR-C08-011-R), the Leverage Fund from the Office of the Vice Chancellor for Research and Extension (OVCRE), University of the Philippines Visayas (2020-13-SP), and the Comission on Higher Education (CHED). We thank the Department of Agriculture, Bureau of Fisheries and Aquatic Resources (DA-BFAR), Provincial Government Unit, and the Office of Provincial Agriculture (PAO) from Aklan Province especially Ms. Grace-an Villareal Perlas (Aklan PAO staff), Sunshine Sucgang (field enumerator of the project), and BFAR staff at Iloilo Fish Port Complex (IFPC) for their administrative support, generous assistance and contributions throughout project. We are also grateful to the Philippine Genome Center-Visayas Satellite Facility (PGC-VSF), the National Institute of Molecular Biology and Biotechnology (UPV-NIMBB), and the UPV Museum of Natural Sciences (UPV-MNS). Our gratitude and appreciation to E. Delloro Jr., K.D. Barnuevo, M.V. Aranjuez, N. Ylaron, D. Mediodia, L. Mooc, C. Garinggan, J. Ariñez, A.G. Deallo, N. Cartago, J. Velo, S. Garcia, and C. Javier, for their generous help throughout the project. This study was supported in part by JSPS KAKENHI Grant Numbers 20H03311 and 21H03651; the JSPS Core-to-Core CREPSUM JPJSCCB20200009; and the "Establishment of Global Research and Education Network in the Amami Islands" project of the Kagoshima University adopted by the Ministry of Education, Culture, Sports, Science and Technology, Japan. We thank the two anonymous reviewers for their comments that helped improve the quality of our study.

References

Allaria M (2016) Poissons de Mayotte. Guide Océan Indien, 388 pp.

Allen GR, Erdmann MV (2012) Reef fishes of the East Indies. Volumes I–III. Tropical Reef Research, Perth, Australia. https://doi.org/10.1896/054.064.0104

Balisco RAT, Ticzon VS, Samaniego BR, Huang WC, Gonzales BJ, Liao TY (2023) Marine fishes of Palawan, Philippines: Species diversity, new records, and conservation status. Regional Studies in Marine Science 60: 102825. https://doi.org/10.1016/j.rsma.2023.102825

Böhlke EB (1997) Notes on the identity of elongate unpatterned Indo–Pacific morays, with description of a new species (Muraenidae, Subfamily Muraeninae). Proceedings of the Academy of Natural Sciences of Philadelphia 147: 89–109. http://www.jstor.org/stable/40650

Böhlke EB (2000) Notes on the identity of small, brown, unpatterned Indo–Pacific moray eels, with descriptions of three new species (Anguilliformes: Muraenidae). Pacific Science 54(4): 395–416.

Böhlke EB, McCosker JE (2001) The moray eels of Australia and New Zealand, with the description of two new species (Anguilliformes: Muraenidae). Records of the Australian Museum 53(1): 71–102. https://doi.org/10.3853/j.0067-1975.53.2001.1325

Böhlke EB, Randall JE (2000) A review of the moray eels (Anguilliformes: Muraenidae) of the Hawaiian Islands, with descriptions of two new species. Proceedings of the Academy of Natural Sciences of Philadelphia 150: 203–278.

Böhlke EB, Smith DG (2002) Type catalogue of Indo–Pacific Muraenidae. Proceedings of the Academy of Natural Sciences of Philadelphia 152(1): 89–172. https://doi.org/10.1635/0097-3157(2002)152[0089:TCOIPM]2.0.CO;2

Castle PHJ, McCosker JE (1986) Family No. 41: Muraenidae. Pp. 165–176, Pls. 7–8. In: Smith MM, Heemstra PC (Eds.) Smiths' sea fishes, Springer Berlin, Heidelberg. https://doi.org/10.1007/978-3-642-82858-4

Chave EH, Mundy BC (1994) Deep-sea benthic fish of the Hawaiian Archipelago, Cross Seamount, and Johnston Atoll. Pacific Science 48(4): 367–409.

Chen HM, Shao KT, Chen CT (1994) A review of the muraenid eels (Family Muraenidae) from Taiwan with descriptions of twelve new records. Zoological Studies 33(1): 44–64.

Dor M (1984) Checklist of the fishes of the Red Sea. CLOFRES. Israel Academy of Sciences and Humanities, Jerusalem.

Eudeline R (2022) Illustrated checklist of Anguilliformes (Pisces, Teleostei) of the lagoon of Mayotte (Western Indian Ocean) with 14 new records. Marine and Fishery Sciences 35(1): 123–161. https://doi.org/10.47193/mafis.3512022010103

Fowler HW, Steinitz H (1956) Fishes from Cyprus, Iran, Iraq, Israel and Oman. Bulletin of the Research Council of Israel 5B(3–4): 260–292.

Fricke R (1999) Fishes of the Mascarene Islands (Réunion, Mauritius, Rodriguez): an annotated checklist with descriptions of new species. Koeltz Scientific Books, Koenigstein, Germany, 759 pp.

Fricke R, Mulochau T, Durville P, Chabanet P, Tessier E, Letourneur Y (2009) Annotated checklist of the fish species (Pisces) of La Réunion, including a Red List of threatened and declining species. Stuttgarter Beiträge zur Naturkunde A. Neue Serie 2: 1–168.

Fricke R, Kulbicki M, Wantiez L (2011) Checklist of the fishes of New Caledonia, and their distribution in the Southwest Pacific Ocean (Pisces). Stuttgarter Beiträge zur Naturkunde A. Neue Serie 4: 341–463.

Fricke R, Eschmeyer WN, Van der Laan R (Eds.) (2023) Eschmeyer's catalog of fishes: genera, species, references. California Academy of Sciences, San Francisco, CA, USA. [Electronic version accessed 19 October 2023] http://researcharchive.calacademy.org/research/ichthyology/catalog/fishcatmain.asp

Golani D, Fricke R (2018) Checklist of the Red Sea fishes with delineation of the Gulf of Suez, Gulf of Aqaba, endemism and Lessepsian migrants. Zootaxa 4509(1): 1–215. https://doi.org/10.11646/zootaxa.4509.1.1

Goren M, Dor M (1994) An updated checklist of the fishes of the Red Sea. CLOFRES II. The Israel Academy of Sciences and Humanities, Jerusalem, 120 pp.

Herre AW (1923) A review of the eels of the Philippine Archipelago. Philippine Journal of Science (23): 123–236.

Herre AW (1953) Check list of Philippine fishes. US Fish and Wildlife Service. Research Report No. 20, 977 pp.

Ho HC, Smith DG, McCosker JE, Hibino Y, Loh KH, Tighe KA, Shao KT (2015) Annotated checklist of eels (orders Anguilliformes and Saccopharyngiformes) from Taiwan. Zootaxa 4060(1): 140–189. https://doi.org/10.11646/zootaxa.4060.1.16

Huang WC, Mohapatra A, Thu PT, Chen HM, Liao TY (2020) A review of the genus *Strophidon* (Anguilliformes: Muraenidae), with description of a new species. Journal of Fish Biology 97(5): 1462–1480. https://doi.org/10.1111/jfb.14514

Huang WC, Smith DG, Loh KH, Liao TY (2021) Two new moray eels of genera *Diaphenchelys* and *Gymnothorax* (Anguilliformes: Muraenidae) from Taiwan and the Philippines. Zoological Studies 60: e24. https://doi.org/10.6620/ZS.2021.60-24

Huang WC, Liao TY, Tan HH (2023a) *Uropterygius cyamommatus*, a new moray eel (Anguilliformes: Muraenidae) from anchialine caves in Christmas Island, Australia, and Panglao Island, the Philippines. Raffles Bulletin of Zoology 71: 268–278. https://doi.org/10.26107/RBZ-2023-0021

Huang WC, Balisco RA, Evacitas FC, Liao TY (2023b) Description of a new moray eel (Anguilliformes: Muraenidae) from the Philippines, with a preliminary assessment of genetic and morphological variations of the *Uropterygius concolor* species complex. Journal of Fish Biology 103(3): 1–10. https://doi.org/10.1111/jfb.15472

Jeong B, Motomura H (2021) An annotated checklist of marine and freshwater fishes of five islands of Mishima in the Osumi Islands, Kagoshima, southern Japan, with 109 new records. Bulletin of the Kagoshima University Museum 16: 1–116.

Jordan DS, Seale A (1907) Fishes of the islands of Luzon and Panay. Bulletin of the Bureau of Fisheries 26(1): 1–48.

Kang CB, Kim MJ, Kim JK, Song CB (2020) New record of a moray eel, *Strophidon dorsalis* (Muraenidae, Anguilliformes) from Korea. Korean Journal of Ichthyology 32(3): 191–196. https://doi.org/10.35399/ISK.32.3.9

Khalaf MA, Disi AM (1997) Fishes of the Gulf of Aqaba. Publications of the Marine Science Station Aqaba 8: 1–252.

Kottelat M (2013) The fishes of the inland waters of southeast Asia: A catalogue and core bibliography of the fishes known to occur in freshwaters, mangroves and estuaries. Raffles Bulletin of Zoology (Suppl. 27): 1–663.

Kumar R, Dineshbabu AP, Jaiswar AK, Shenoy L, Kumar AP, Rahangdale S, Vase VK, Damodar D, Bharadiya S, Gohel J (2020) New geographical record for muraenid eels (Anguilliformes: Muraenidae) along the northeast Arabian Sea, Western Indian Ocean. Thalassas 36(2): 365–370. https://doi.org/10.1007/s41208-020-00215-x

Laboute P, Grandperrin R (2000) Poissons de Nouvelle-Calédonie. Éditions Catherine Ledru, Nouméa, 520 pp.

Loh KH, Shao KT, Chen HM (2011) Length–weight relationships for 39 species of moray eel from the waters around Taiwan. Journal of Applied Ichthyology 27(3): 945–948. https://doi.org/10.1111/j.1439-0426.2010.01601.x

Loh KH, Shao KT, Ho HC, Lim PE, Chen HM (2015) A new species of moray eel (Anguilliformes: Muraenidae) from Taiwan, with comments on related elongate unpatterned species. Zootaxa 4060(1): 30–40. https://doi.org/10.11646/zootaxa.4060.1.5

Manilo LG, Bogorodsky SV (2003) Taxonomic composition, diversity and distribution of coastal fishes of the Arabian Sea. Journal of Ichthyology 43(1): 75–149.

McClelland J (1844) Apodal fishes of Bengal. Calcutta Journal of Natural History 5(18): 151–226.

McCosker JE, Randall JE (1982) Synonymies of Indian Ocean eels, with the description of *Gymnothorax enigmaticus*, a moray previously known as *G. ruppeli*. Proceedings of the California Academy of Sciences 43(2): 17–24.

Mohapatra A, Ray D, Smith DG, Mishra SS (2016) A new species of elongate unpatterned moray eel of the genus *Gymnothorax* (Muraenidae: Muraeninae) from the Bay of Bengal. Zootaxa 4150(5): 591–598. https://doi.org/10.11646/zootaxa.4150.5.6

Mohapatra A, Tudub PC, Mohantya SR, Mishra SS (2021) First report of three eel species (Order: Anguilliformes) from Andhra Pradesh coast, India. Indian Journal of Geo-Marine Sciences 50(05): 419–422. https://doi.org/10.56042/ijms.v50i05.66239

Motomura H, Harazaki S (2017) Annotated checklist of marine and freshwater fishes of Yaku-shima island in the Osumi Islands, Kagoshima, southern Japan, with 129 new records. Bulletin of the Kagoshima University Museum 9: 1–183.

Motomura H, Ishikawa S (2013) Fish collection building and procedures manual: English edition. The Kagoshima University Museum, Kagoshima and the Research Institute for Humanity and Nature, Kyoto, 70 pp.

Motomura H, Dewa S, Furuta K, Matsuura K (Eds.) (2013) Fishes of Iwo-jima and Take-shima islands, Mishima, Kagoshima, Japan. Kagoshima University Museum, Kagoshima and National Museum of Nature and Science, Tsukuba, 390 pp.

Motomura H, Alama UB, Muto N, Babaran RP, Ishikawa S (Eds.) (2017) Commercial and bycatch market fishes of Panay Island, Republic of the Philippines. Kagoshima University Museum, Kagoshima, University of the Philippines Visayas, Iloilo, and Research Institute for Humanity and Nature, Kyoto.

Motomura H, Hagiwara K, Senou H, Nakae M (Eds.) (2019) Identification guide to fishes of the Amami Islands in the Ryukyu Archipelago, Japan. Minaminippon Shimbun Kaihatsu Center, Kagoshima, 436 pp.

Mundy BC (2005) Checklist of the fishes of the Hawaiian Archipelago. Bishop Museum Bulletins in Zoology No. 6, 704 pp.

Myers RF, Donaldson TJ (2003) The fishes of the Mariana Islands. Micronesica 35–36: 598–652.

Nakabo T (2002) Fishes of Japan with Pictorial Keys to the Species. Third Edition (English Version). Tokai University Press, 866 pp.

Nakae M, Motomura H, Hagiwara K, Senou H, Koeda K, Yoshida T, Tashiro S, Jeong B, Hata H, Fukui Y, Fujiwara K, Yamakawa T, Aizawa M, Shinohara G, Matsuura K (2018) An annotated checklist of fishes of Amami-oshima Island, the Ryukyu Islands, Japan. Memoirs of the National Museum of Nature and Science, Tokyo 52: 205–361.

Okonechnikov K, Golosova O, Fursov M (2012) Unipro UGENE: A unified bioinformatics toolkit. Bioinformatics 28(8): 1166–1167. https://doi.org/10.1093/bioinformatics/bts091

Playfair RL, Günther A (1867) The fishes of Zanzibar, with a list of the fishes of the whole east coast of Africa. John van Voorst, London, 220 pp.

Psomadakis PN, Osmany HB, Moazzam M (2015) Field identification guide to the living marine resources of Pakistan. FAO species identification guide for fishery purposes. FAO, Rome, 486 pp.

Quéro JC, Saldanha L (1995) Poissons anguilliformes de l'Ile de la Réunion (Océan Indien): Description d'une nouvelle espèce. Cybium 19(1): 61–88. https://doi.org/10.26028/cybium/1995-191-004

Quindo JPV, Bucol AA (2019) Recent record of the tiger freshwater moray *Gymnothorax polyuranodon*, and an updated location list for the Philippines. Southeast Asia Vertebrate Records 2019: 48–49.

Ramos-Castro M, Chen HM, Mao BS (2020) Descriptions of neurocranium morphology in 34 species of moray eels (Muraenidae) found in Taiwan. Zootaxa 4810(1): 81–109. https://doi.org/10.11646/zootaxa.4810.1.4

Randall JE (1995) Coastal fishes of Oman. University of Hawaii Press, Honolulu, HI, USA, 439 pp.

Randall JE (2007) Reef and shore fishes of the Hawaiian Islands. University of Hawai'i, Sea Grant College Program, Honolulu, HI, USA, 560 pp.

Randall JE, Golani D (1995) Review of the moray eels (Anguilliformes: Muraenidae) of the Red Sea. Bulletin of Marine Science 56(3): 849–880.

Randall JE, Lim KKP (Eds.) (2000) A checklist of the fishes of the South China Sea. Raffles Bulletin of Zoology Supplement No. 8: 569–667.

Randall JE, Aida K, Oshima Y, Hori K, Hashimoto Y (1981) Occurrence of a crinotoxin and hemagglutinin in the skin mucus of the moray eel *Lycodontis nudivomer*. Marine Biology 62(2): 179–184. https://doi.org/10.1007/BF00388181

Randall JE, Williams JT, Smith DG, Kulbicki M, Mou Tham G, Mou TG, Labrosse P, Kronen M, Clua E, Mann BS (2004) Checklist of the shore and epipelagic fishes of Tonga. Atoll Research Bulletin (502): 1–35. https://doi.org/10.5479/si.00775630.502.1

Ray D, Mohapatra A, Smith DG (2015) A new species of short brown unpatterned moray eel of the genus *Gymnothorax* (Anguilliformes: Muraenidae) from the Bay of Bengal. Zootaxa 4027(1): 140. https://doi.org/10.11646/zootaxa.4027.1.8

Seale A (1917) New species of apodal fishes. Bulletin of the Museum of Comparative Zoology 61(4): 79–94.

Smith JLB (1962) The moray eels of the western Indian Ocean and the Red Sea. Ichthyological Bulletin No. 23: 421–444.

Smith DG (2012) A checklist of the moray eels of the world (Teleostei: Anguilliformes: Muraenidae). Zootaxa 3474(1): 1–64. https://doi.org/10.11646/zootaxa.3474.1.1

Smith DG, Böhlke EB (1997) A Review of the Indo–Pacific banded morays of the *Gymnothorax reticularis* group, with descriptions of three new species (Pisces, Anguilliformes, Muraenidae). Proceedings of the Academy of Natural Sciences of Philadelphia 148: 177–188.

Smith DG, Böhlke EB (2022) Family Muraenidae, Moray eels. Pp. 37–79. In: Heemstra PC, Heemstra E, Ebert DA, Holleman W, Randall JE (Eds.) Coastal fishes of the western Indian Ocean. Volume 2. South African Institute for Aquatic Biodiversity, Makhanda, South Africa, 614 pp.

Smith DG, Hibino Y, Ho HC (2018) Two new elongate unpatterned moray eels from Taiwan and Vietnam, with notes on two congeners (Anguilliformes: Muraenidae). Zootaxa 4454(1): 33–42. https://doi.org/10.11646/zootaxa.4454.1.5

Smith DG, Bogorodsky SV, Mal AO, Alpermann TJ (2019) Review of the moray eels (Anguilliformes: Muraenidae) of the Red Sea, with description of a new species. Zootaxa 4704 (1): 1–87. https://doi.org/10.11646/zootaxa.4704.1.1

Snyder JO (1904) A catalogue of the shore fishes collected by the steamer Albatross about the Hawaiian Islands in 1902. Bulletin of the United States Fish Commission 22(1): 513–538.

Tsukamoto K, Watanabe S, Kuroki M, Aoyama J, Miller MJ (2014) Freshwater habitat use by a moray eel species, *Gymnothorax polyuranodon*, in Fiji shown by otolith microchemistry. Environmental Biology of Fishes 97(12): 1377–1385. https://doi.org/10.1007/s10641-014-0228-9

Uchida RN, Uchiyama JH (1986) Fishery atlas of the Northwestern Hawaiian Islands. NOAA Technical Report No. 38: 136–142.

Wagey BT, Bucol AA, Katuuk V (2015) The moray eel fishery in the seagrass beds of Siquijor Island, central Philippines, with remarks on two new Philippine records of the genus *Gymnothorax.* IAMURE International Journal of Ecology and Conservation 13(1): 1–13. https://doi.org/10.7718/ijec.v13i1.853

Ward RD, Zemlak TS, Innes BH, Last PR, Hebert PDN (2005) DNA barcoding Australia's fish species. Philosophical Transactions of the Royal Society of London. Series B, Biological Sciences 360(1462): 1847–1857. https://doi.org/10.1098/rstb.2005.1716

Yoshida T, Motomura H, Musikasinthorn P, Matsuura K (2013) Fishes of northern Gulf of Thailand. National Museum of Nature and Science, Tsukuba, Research Institute for Humanity and Nature, Kyoto, and Kagoshima University Museum, Kagoshima, 239 pp.

Zajonz U, Lavergne E, Bogorodsky SV, Saeed FN, Aideed MS, Krupp F (2019) Coastal fish diversity of the Socotra Archipelago, Yemen. Zootaxa 4636(1): 1–108. https://doi.org/10.11646/zootaxa.4636.1.1

Acta Ichthyologica et Piscatoria 53, 2023, 227–242 | DOI 10.3897/aiep.53.112183

PENSOFT.

ACTA
ICHTHYOLOGICA
ET PISCATORIA

Comparative phylogeography of two codistributed species of the genus *Herichthys* (Actinopterygii: Cichliformes: Cichlidae) in northeastern Mexico

Fabian PÉREZ-MIRANDA[1,2], Omar MEJÍA[1], Benjamín LÓPEZ[3], Eduardo SOTO-GALERA[1], Amairany BERNAL-PORTILLO[1], Wilfredo A. MATAMOROS[2,4]

1 *Departamento de Zoología, Escuela Nacional de Ciencias Biológicas, Instituto Politécnico Nacional, Ciudad de México, Mexico*
2 *Instituto de Ciencias Biológicas, Universidad de Ciencias y Artes de Chiapas, Tuxtla Gutiérrez, Chiapas, Mexico*
3 *Universidad Michoacana de San Nicolás Hidalgo, Michoacán de Ocampo, Mexico*
4 *Field Museum of Natural History, Chicago, IL, USA*

https://zoobank.org/1302CFAD-D245-496B-AFB1-B6E48E90A786

Corresponding author: Fabian Pérez-Miranda (monodactilo@hotmail.com)

Academic editor: Predrag Simonović ♦ **Received** 4 September 2023 ♦ **Accepted** 3 November 2023 ♦ **Published** 7 December 2023

Citation: Pérez-Miranda F, Mejía O, López B, Soto-Galera E, Bernal-Portillo A, Matamoros WA (2023) Comparative phylogeography of two codistributed species of the genus *Herichthys* (Actinopterygii: Cichliformes: Cichlidae) in northeastern Mexico. Acta Ichthyologica et Piscatoria 53: 227–242. https://doi.org/10.3897/aiep.53.112183

Abstract

Phylogeographic patterns of freshwater fishes in coastal regions are highly susceptible to eustatic sea level changes associated with Pleistocene glaciations. In this context, the Plain Coastal Gulf in northeastern Mexico represents an ideal study area due to its low elevation. Herein, we compare the phylogeographic structures of two cichlid species of the genus *Herichthys* Baird et Girard, 1854 widely distributed in the Pánuco–Tamesí system in northeastern Mexico using two mitochondrial markers. The species studied were: *Herichthys carpintis* (Jordan et Snyder, 1899) and *Herichthys pantostictus* (Taylor et Miller, 1983). We estimate their genetic diversity, gene flow, and demographic history and perform biogeographic reconstructions using a Bayesian computation approach and environmental niche modeling. The biogeographic reconstruction suggests a different history for each species. Environmental niche modeling indicates that both species experienced a demographic expansion during the Pleistocene but responded differently to Pleistocene climatic changes. In summary, their current sympatric distribution could be the outcome of contemporary and not historical processes reflecting a pseudo-incongruent pattern.

Keywords

Bayesian computation, gene flow, niche modeling, paleohydrography

Introduction

Evolutionary biogeography seeks to reconcile dispersal and vicariance paradigms through five stages that reconstruct a geobiotic scenario that attempts to explain biotic component evolution based on geological data (Morrone 2007). One stage involves dating the vicariant events using molecular clocks and phylogeographic studies. Phylogeography deals with how genetic lineages are arranged through geographic space (Avise 2009). Therefore, comparative phylogeography studies are relevant since they enable us to interpret how different cenocrons (biotic elements) have been integrated into a horobiota (a snapshot of a biota in a particular time) (Morrone 2020). In a comparative phylogeographic study, three different scenarios could arise. First, in a concerted response, the codistributed species respond similarly to geological and climatic events leading to a congruent pattern. Second, in an independent response, the codistributed species show independent responses to simultaneous regional processes. Third, in a multiple response, the species could show similar spatial congruence but different temporal frames leading to a pseudo-congruent pattern or different responses both in space and time leading to a pseudo-incongruent pattern (Bagley and Johnson 2014). The cooling and heating periods experienced by the planet during the Pleistocene led to speciation and extinction events and changes in the distributional patterns of species worldwide (Hewitt 1996, 2000, 2004). However, Pleistocene glaciations also affect populations, leaving genetic signatures that are traceable through phylogeographic studies (Hewitt 2003; Lister et al. 2005; Comte and Grenouillet 2015).

These phenomena are more evident in freshwater ecosystems due to climate changes and geological factors, such as volcanism and orogenesis, playing a fundamental role in drainages rearrangement, leading to isolation, reconnection, and formation of new rivers and lakes (Bermingham and Martin 1998; Waters and Wallis 2000; Rincon-Sandoval et al. 2019). Their effects are particularly apparent in species distributed toward the coastal shoreline (Abreu et al. 2020; Pio and Carvalho 2021) due to the Pleistocene's eustatic sea level changes leading to the exposition and covering of the continental shelf, promoting both population connection and isolation (Hewitt 2004; Lambeck and Chappell 2001).

Due to Mexico's complex geologic and paleohydrographic history, its freshwater fishes are ideal for phylogeographic studies (Marshall and Liebherr 2000; Morrone 2004; Domínguez-Domínguez and Pérez-Ponce de León 2009), their study has already led to several published papers in selected taxonomical groups, including atherinopsids (Bloom et al. 2009; García-Martínez et al. 2020), characids (Strecker et al. 2004; Ornelas-García et al. 2008; Hausdorf et al. 2011; Coghill et al. 2014), cyprinids (García-Andrade et al. 2021), and poecilids (Mateos et al. 2002; Chen and Borowsky 2004; Mateos 2005; Gutiérrez-Rodríguez et al. 2007; Bagley et al. 2013).

Cichlids are one of the most diverse clades of freshwater fishes in Mexico. However, despite their species abundance, phylogeographic studies with them are scarce (e.g., Barluenga and Meyer 2010; Bagley et al. 2017; McMahan et al. 2017). The genus *Herichthys* Baird and Girard, 1854 represents an excellent model for evolutionary and biogeographic studies since it includes species of wide and restricted geographic distributions that have been extensively studied in recent years, from systematics to molecular clocks and biogeography among others (Pérez-Miranda et al. 2018, Pérez-Miranda et al. 2020).

In this study, we compared the phylogeographic structures of two cichlid species of the genus *Herichthys* that have a wide geographic distribution in the Pánuco–Tamesí system: *Herichthys carpintis* (Jordan et Snyder, 1899) and *Herichthys pantostictus* (Taylor et Miller, 1983). The latter species was included in the past in the genus *Nosferatu* (see De la Maza-Benignos et al. 2015), however, as pointed out by Říčan et al. (2016), the shape of the teeth that are the diagnostic character of the genus is a plesiomorphic state for the *Theraps–Parannetroplus* clade and it is also present in some species of the genus *Herichthys* turning the genus *Nosferatu* in a paraphyletic and not natural group. Therefore, all species previously placed in the genus *Nosferatu* by De la Maza-Benignos et al. (2015) should now be included in the genus *Herichthys* (see Fricke et al. 2023; Froese and Pauly 2023; WoRMS Editorial Board 2023). The Pánuco–Tamesí system drains part of the Gulf Coastal Plain in northeastern Mexico covering a surface of near 157 752 km^2 and comprises 11 sub-basins (FAO 2022). This vast region is characterized by altitudes ranging from 0 to 600 m above sea level and was prone to the effects of marine transgressions and regressions during the Pleistocene glaciation periods (Álvarez 1961; Bagley et al. 2013). While both species have a sympatric distribution throughout most of their geographic range, their current geographic distribution patterns are likely the result of different evolutionary and biogeographic histories (Pérez-Miranda et al. 2020). While *H. carpintis*' sister species, *Herichthys tepehua* De la Maza-Benignos, Ornelas-García, Lozano-Vilano, García-Ramírez et Doadrio, 2014 is distributed towards the coastline, *H. pantostictus*' sister group, comprising *Herichthys bartoni* (Bean, 1982) and *Herichthys labridens* (Pellegrin, 1903), is distributed inland (Pérez-Miranda et al. 2018).

Therefore, we expected these species to show a pseudo-incongruent pattern due to different past distributions and recent community assemblies with a scarce or null shared history between them. We test our prediction by evaluating the effect of Pleistocene glaciations on the colonization and connectivity of *H. carpintis* and *H. pantostictus* populations by determining the numbers and ages of their genetic populations, the gene flow among them, and their demographic history and colonization processes using two mitochondrial markers, COI, and D-loop.

Material and methods

Sampling and genetic analysis. The specimens of *Herichthys carpintis* and *Herichthys pantostictus* used were collected between 2000 and 2016 and covered the known geographic distribution of both species (Suppl. material 1). Tissue samples were obtained from 96 *H. carpintis* individuals and 60 *H. pantostictus* individuals. DNA extraction was performed according to the protocol of Aljanabi and Martinez (1997) for amplifying mitochondrial markers cytochrome oxidase subunit 1 (COI) and D-loop. For the mitochondrial COI marker, we complemented our *H. carpintis* data set with an additional 104 previously generated sequences available in two Barcode of Life Data (BOLD) projects (FFPTR and HBGM).

Polymerase chain reactions (PCRs) had a final volume of 25 µL. For the COI marker, we used the primers reported by Ward et al. (2005) with the conditions reported by León-Romero et al. (2012) to amplify a fragment of 589 bp for the D-loop marker, we designed FPM-F

(5′-CTTTGGGAGTTAGGGGTGA-3′) and FPM-R (5′-CACTGAAGATGTTAAGACGG-3′) primers to amplified a 687 bp fragment in a reaction mix comprising 1× PCR buffer, 3 mM $MgCl_2$, 200 µM dNTPs, 0.15 µM of each primer, 40 ng of DNA template, and 1 U of GoTaq (Invitrogen) using the following conditions: initial preheating at 95°C for 5 min, followed by 35 cycles of denaturing at 96°C for 1 min, annealing at 60°C for 1.5 min, and extension at 72°C for 1 min, with a final 5 min extension at 72°C. PCR products were purified, and both strands were sequenced at the Laboratorio Nacional de Genómica para la Biodiversidad campus (Irapuato, México).

Sequences were aligned with Clustal X versión 2.0 (Larkin et al. 2007) and edited in Seaview (Gouy et al. 2010). The final numbers of available sequences were 195 for COI and 73 for D-loop in *H. carpintis* and 41 for COI and 54 for D-loop in *H. pantostictus*.

Population genetics. We are aware of the potential caveats of dealing with sample size and their effect on genetic diversity and other population genetics estimators. For the aforementioned, we evaluate if the number of analyzed individuals was enough using the function HACSim s implemented in the R library HACSim to build an accumulation curve and to estimate the R-value that represents the estimated fraction of species haplotype diversity captured from sampling (Phillips et al. 2020).

After that, we assessed the number of genetic clusters (*k*) (hereinafter referred to as populations) using the “optimise.baps” option in the *fastbaps* library (Tonkin-Hill et al. 2019) of the R statistical software version 4.0.4 (RStudio Team 2020). Each population’s diversity parameters, such as haplotypic (*h*) and nucleotidic (π) diversity, were estimated using Arlequin v.3.5.2 (Excoffier and Lischer 2010).

A time-calibrated phylogenetic tree was estimated for each species and molecular marker in BEAST v 1.7.5 (Drummond et al. 2205), to date the trees, we used secondary calibration points previously estimated for *H. carpintis* and *H. pantostictus* (see Pérez-Miranda et al. 2020) which used different calibration points including fossil record and vicariant events (but see also Říčan et al. 2013); for *H. carpintis*, we used the split with her sister species *H. tepehua* (outgroup in the phylogeny) occurred 2.5 Ma, meanwhile, for *H. pantostictus* we used its divergence time against her sister clade (*H. bartoni* + *H. labridens*) (outgroup in the phylogeny) occurred 6.5 Ma. Four independent runs of 10 million generations, sampling every 10 000 generations, were performed assuming a GTR substitution model, a strict molecular clock, and a Yule speciation model; convergence among chains was assumed if the ESS values were higher than 200, then, the trees were summarized using LogCombiner v.1.7.4 (Drummond and Rambaut 2007), and a consensus tree was constructed after a 25% burn-in using TreeAnotator v2.6.6 (Drummond and Rambaut 2007).

To evaluate gene flow levels among populations, we used the Bayesian approach implemented in migrate v.4.4.2 (Beerli 1998; Beerli and Felsenstein 2001) using a static heating scheme with four temperature chains (1, 1.5, 3, and 1 000 000), with each analysis comprising 10 000 000 genealogies sampled every 1000 generations after a 10% burn-in. We used the full matrix model as a null hypothesis for each species and molecular marker and postulated several gene flow models following Miller et al. (2005). Since *H. pantostictus* is mainly distributed inland, its colonization process should be from inland towards the coastline. In contrast, since *H. carpintis* is mainly distributed along the coastal shoreline, its colonization process should be from the coastline towards the inland.

Ten gene flow models were evaluated for *H. pantostictus* (five per molecular marker), and 11 models were evaluated for *H. carpintis* (six for COI and five for D-loop; see Suppl. material 2 for complete details). We compared gene flow models using a Bayes Factor test with the Bezier approach’s marginal likelihood (Beerli et al. 2019) using the BF function in R’s *mtraceR* library (Pacioni et al. 2015).

Effective population size changes were inferred using Tajima’s *D* and Fu’s F_s tests in Arlequín v.3.5.2 (Excoffier and Lischer 2010). In addition, effective population size changes through time were inferred from Bayesian skyline plots (BSPs) created using BEAST v1.7.5 (Drummond et al. 2005) with a lumping approach since coalescent-based tests are extremely sensitive to sample size (Heller et al. 2013). The BSPs plots were created using four Markov chains of 10 000 000 generations, sampled every 1000 generations, and a strict molecular clock with the same calibration points mentioned above. The chains’ results were combined using LogCombiner v1.7.4 after a 25% burn-in (Drummond and Rambaut 2007), and the BSPs were plotted in Tracer v1.5 (Rambaut et al. 2018).

Biogeographic scenarios and niche modeling. We tested two biogeographic scenarios for the colonization routes of each species using the approximate Bayesian computation (ABC) approach implemented in the DIYABC software (Cornuet et al. 2010). Scenario one assumed a coastal-to-inland colonization process. Scenario two assumed an inland-to-coastal colonization process. The scenarios were compared using reference tables simulating 1×10^6 datasets based on haplotype numbers and the Tajima and Fu test values. First, considering the reference tables’ first 10 000 scenarios, we used a principal component analysis to evaluate whether the generated dataset’s distribution approached that of the observed dataset. Then, a normalized Euclidean distance between the simulated and the observed datasets was calculated to determine the most plausible scenario. Finally, considering the 1% of generated datasets closest to the observed datasets, a direct and logistic regression was used to estimate the posterior probability and the type I and type II errors for each scenario with a 95% highest posterior distribution (HPD). Therefore, the most probable scenario was chosen based on the highest posterior probability and the absence of overlap in the HDP intervals (Cornuet et al. 2010).

Finally, we used an environmental niche model (ENM) approach to evaluate the possible effects of Pleistocene glaciations on both species' demographic history. The suitability areas for each species were determined using the maximum entropy algorithm implemented in Maxent v.3.2.19 (Phillips et al. 2006) applied to the Mejía et al. (2022) collecting dataset. First, the *spThin* R library (Aiello-Lammens et al. 2015) was used to reduce spatial autocorrelation by pruning collection records that are <1 kilometer, leaving a total of 205 collection records for *H. carpintis* and a total of 124 collection records for *H. pantostictus*. Then, the geographic space *M* for each species was defined with the Pfafstetter HydroBasin levels 6 and 7 (Lehner and Grill 2013) in QGIS v.3.16.5 (QGIS Development Team 2009). The 19 WorldClim bioclimatic variables (Hijmans et al. 2005) were downloaded for the current period. The paleoclimatic projections used the MPI-ESM-P general circulation model in three temporal frames: the last interglacial period (LIG; 120 ka), the last glacial maximum (LGM; 21 ka), and the mid-Holocene (6 ka). Additionally, three topographic variables (aspect, topographic position index, and slope) were calculated based on a digital elevation model from Hydrosheds (Lehner et al. 2008) using the terrain function of the *raster* R library (Hijmans and Van Etten 2012). The number of variables in the ENM was reduced using the variance inflation factor (VIF) with the *vifcor* and *vifstep* functions in the *usdm* R library (Naimi et al. 2014).

The ENMs were constructed using the *dismo* (Hijmans et al. 2020), *ENMeval* (Muscarella et al. 2014), *rmaxent* (Baumgartner et al. 2017), and *kuenm* (Cobos et al. 2019) R libraries. We used 30% of the collection records for model construction and the remaining 70% for model training with several combinations of feature classes (linear, quadratic, product, and threshold) and regularization multipliers (1, 2, 5, 10, 15, and 20; Warren and Seifert 2011). Finally, the best ENM models were selected using the Akaike information criteria (Akaike 1974) and partial receiver operating characteristic (ROC) curve values over 1000 bootstraps (Peterson and Nyari 2008).

Results

Population genetics. The new sequences of *Herichthys carpintis* and *Herichthys pantostictus*, generated for this study, were deposited in GenBank under the accession numbers OP738881–OP738896; OP738385–OP738395, and OP751419–OP751525 (Suppl. material 3). The R values recovered from the HACSim curves were higher than 0.9 for both species and molecular markers (Suppl. material 4) and suggest that the number of individuals analyzed was enough to recover the genetic diversity of both species.

The *fastbaps* analysis recovered three genetic clusters (populations) for each molecular marker. In *H. pantostictus*, based on the COI marker, population one (Guayalejo) comprised five individuals and had a geographic centroid near the coastal shoreline at the northern limit of its distribution. Population two (Pánuco) comprised 20 individuals with a geographic centroid located near the center of its geographic distribution. Population three (Tanconchín) comprised 16 individuals with a geographic centroid in the south of its distribution (Fig. 1). Based on the D-loop marker, population four (Tamesí) comprised 23 individuals and had a geographic centroid toward the north of its distribution. Population five (Valles) comprised 19 individuals and had a geographic centroid at the center of its distribution. Population 6 (Naranjos) comprised 12 individuals and had a geographic centroid toward the South of its distribution (Fig. 1).

In *H. carpintis*, based on the COI marker, population one (Ozuluama) comprised 90 individuals and had a geographic centroid in the south of its distribution. Population two (Adjuntas) comprised 15 individuals and had a geographic centroid in the center of its distribution. Population three (Mante) comprised 90 individuals and had a geographic centroid in the north of its distribution. For the D-Loop marker, population four (Jaumave) comprised 50 individuals and had a geographic centroid in the north of its distribution. Population five (Tempoal) comprised 12 individuals and had a geographic centroid in the center of its distribution. Population six (Gallinas) comprised 11 individuals and had a geographic centroid in the center of its distribution toward the inland (Fig. 1).

The *h* values in *H. pantostictus* populations ranged from 0.542 in Tanconchín to 0.900 in Guayalejo for the COI marker and from 0.544 in Valles to 0.573 in Tamesí for the D-loop. In *H. carpintis* populations, *h* values were low for the COI marker, ranging from 0.391 in Mante to 0.664 in Ozuluama, but high for the D-loop marker, ranging from 0.818 in Gallinas to 1.000 in Tempoal. The π values were low in the majority of populations, ranging from 0.001 for the COI marker in the *H. carpintis* Adjuntas and Mante populations to 0.026 for the D-loop marker in the *H. carpintis* Jaumave population (Table 1).

The molecular clock analysis inferred similar root ages for both markers in *H. pantostictus* (6.9 Ma, HPD 5.3–8.4 Ma). Population ages inferred based on the COI marker were 0.69 Ma (HPD 0.2–1.1 Ma) for Guayalejo, 1.91 Ma (0.8–3.0 Ma) for Pánuco, and 2.68 Ma (HPD 1.1–4.6 Ma) for Tanconchín. Population ages inferred from the D-loop marker were 2.55 Ma (HPD 1.2–3.8 Ma) for Naranjos, 2.15 Ma (HPD 1.0–3.3 Ma) for Valles, and 2.53 Ma (HPD 1.2–3.8 Ma) for Tamesí (Fig. 2). However, they provided opposing ancient population geographic locations. The youngest population was located toward the coastline for the COI marker (Guayalejo) but inland for the D-loop marker (Valles). In *H. carpintis*, the inferred root ages were 1.9 Ma (HPD 1.5–2.3 Ma) with the COI marker and 2.3 Ma (HPD 1.6–2.9 Ma) with the D-loop marker. Population ages inferred based on the COI were 1.47 Ma (HPD 0.9–1.9 Ma) for Ozuluama, 0.82 Ma (HPD 0.3 1–3 Ma) for Adjuntas, and 1.24 Ma (0.7–1.7 Ma) for Mante. Population ages inferred based on the D-loop marker were 1.9 Ma (HPD 1.5–2.3 Ma) for

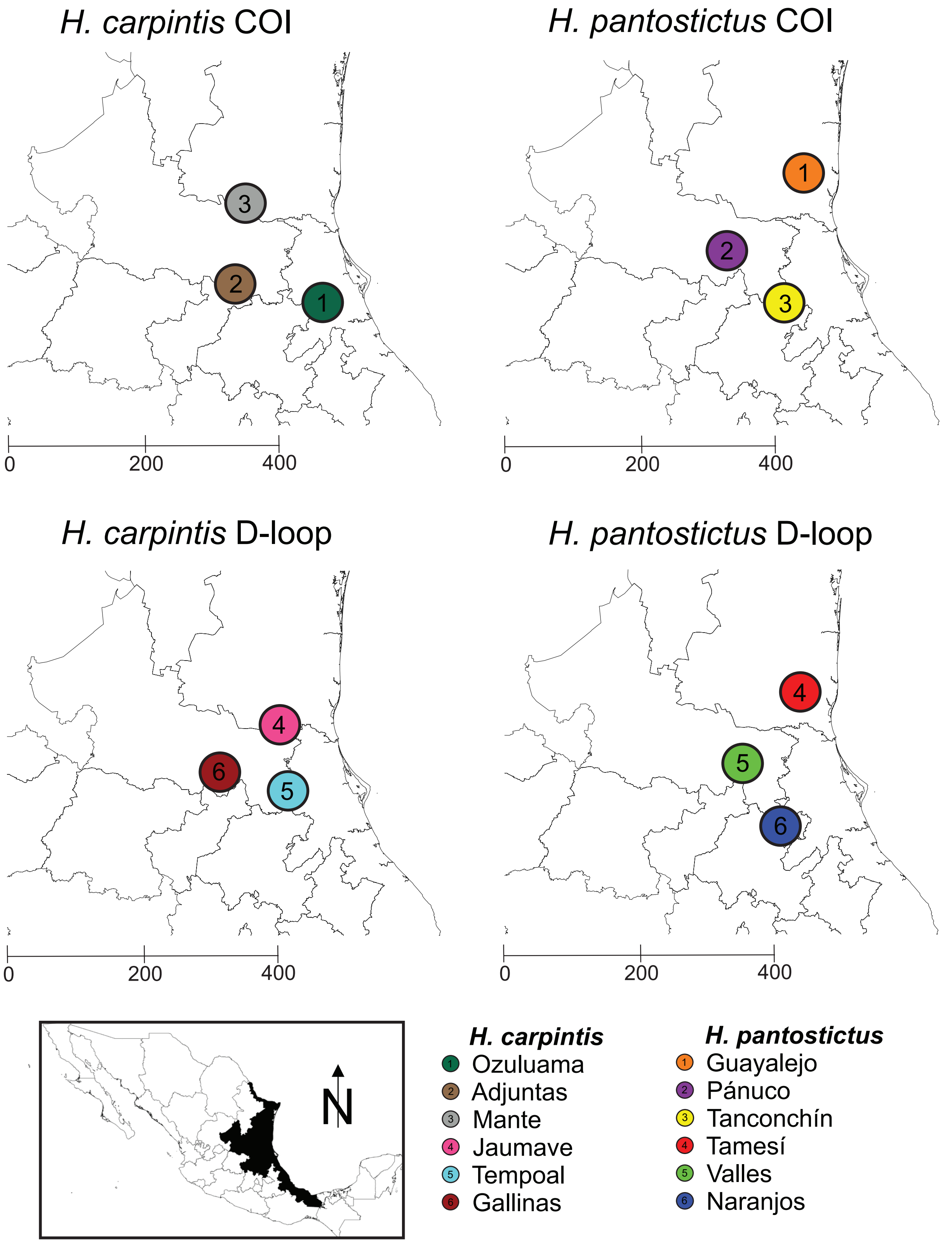

Figure 1. Geographic distribution of genetics populations of *Herichthys carpintis* and *Herichthys pantostictus* recovered by fastbaps. Each circle represents the geographic centroid of the localities that contribute to the formation of the genetic group

Jaumave, 1.2 Ma (HPD 0.8–1.6 Ma) for Tempoal, and 0.7 Ma (0.3–1.0 Ma) for Gallinas (Fig. 2). Therefore, the youngest *H. carpintis* population was toward the inland with both markers: Adjuntas with the COI marker and Gallinas with the D-loop marker (Fig. 2).

The migrate analysis, which estimated gene flow, suggested that the most probable model for *H. pantostictus* based on the COI marker was colonization from inland towards the coastline (maximum likelihood [ML] = −1101.44, $P = 0.964$; Suppl. material 5), with Tanconchín

Table 1. Summary of the genetic diversity statistics recovered in *Herichthys pantostictus* and *Herichthys carpintis* for the mitochondrial molecular markers COI and D-loop.

Species	Marker	*k*	*n*	*h*	π	*D*	F_s
H. pantostictus	COI	Guayalejo	5	0.900	0.003	–1.094	-3.578^{P2}
		Pánuco	20	0.447	0.002	-1.719^{P1}	-34.080^{P2}
		Tanconchín	16	0.542	0.003	-2.003^{P1}	-27.681^{P2}
	D–loop	Tamesí	23	0.573	0.003	-2.006^{P1}	-27.762^{P2}
		Valles	19	0.544	0.003	-1.894^{P1}	-28.311^{P2}
		Naranjos	12	0.848	0.007	0.483	-11.383^{P2}
H. carpintis	COI	Ozuluama	90	0.664	0.004	1.209	1.530
		Adjuntas	15	0.562	0.001	0.139	-10.727^{P2}
		Mante	90	0.391	0.001	–0.886	-14.130^{P2}
	D–loop	Jaumave	50	0.995	0.026	–1.099	-24.227^{P2}
		Tempoal	12	1.000	0.018	0.487	-4.241^{P1}
		Gallinas	11	0.818	0.007	–0.712	-2.855^{P1}

$^{P1} = P < 0.05$, $^{P2} = P < 0.001$; *k* = number of genetic clusters recovered by *fastbaps*, *n* = number of individuals examined, *h* = haplotypic diversity, π = nucleotidic diversity, *D* = Tajima *D* test values, *Fs* = Fu test values.

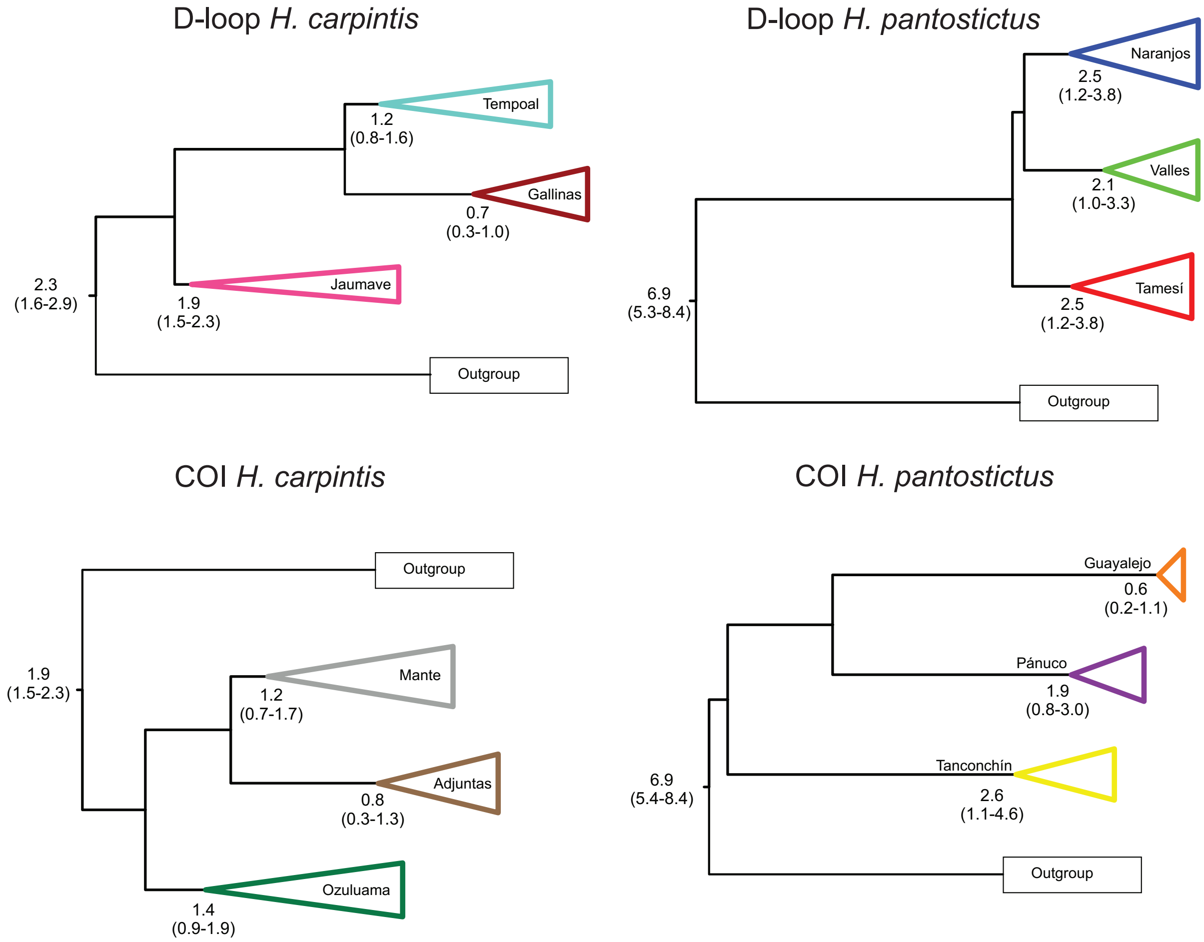

Figure 2. Molecular dated phylogeny of the genetic clusters recovered in *Herichthys carpintis* and *Herichthys pantostictus* for the mitochondrial markers COI and D-loop. The median divergence time (Ma) and the HPD intervals (Ma) are shown below the nodes. The colors represent the genetic clusters depicted in Fig. 1

giving rise to Pánuco (*M* = 138; 95% HPD: 0–420), followed by Pánuco giving rise to Guayalejo (*M* = 138; 95% HPD: 0–937; Fig. 3). However, for the D-loop marker, the colonization process occurred from the distribution's center to the North and then to the South (ML = −1040.74, *P* = 0.668; Suppl. material 5), with Valles giving rise to Tamesí (*M* = 322; 95% HPD: 83–357), followed by Tamesí giving rise to Naranjos (*M* = 415; 95% HPD: 0–483; Fig. 3).

The gene flow estimation for *H. carpintis* suggests that the colonization process occurred from the coastline toward the inland for the COI marker (ML = −3099.68, *P* = 1.000), with Ozuluama giving rise to Mante (*M* = 82;

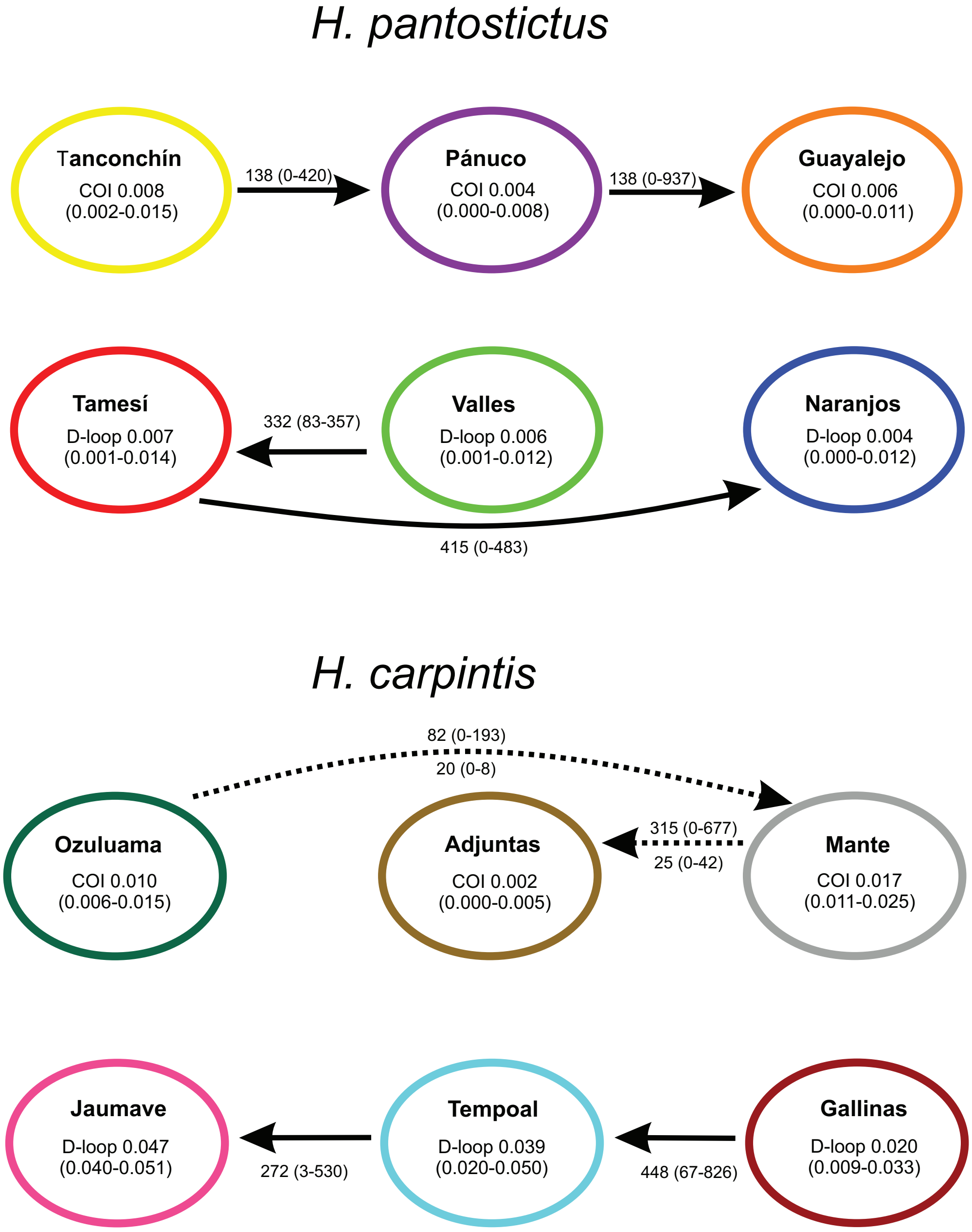

Figure 3. Gene flow among populations of *Herichthys carpintis* and *Herichthys pantostictus* according to the most probable model recovered in Bayes Factor analysis (see Suppl. materials 2, 4 for complete details). Theta values and 95% HPD intervals are shown within each genetic cluster. The values on the arrows show the number of migrants from one population to another with the minimum and maximum values maximum in parentheses; solid arrows indicate a single gene flow event, dashed arrows indicated recurrent gene flow (values below), after the initial migrant event (values above).

95% HPD: 0–193), followed by Mante giving rise to Adjuntas (*M* = 315; 95% HPD: 0–677; Fig. 3). Finally, for the D-loop, the colonization process occurred from inland to the coastline (ML = −4002.55, *P* = 1.000), with Gallinas giving rise to Tempoal (*M* = 448; 95% HPD: 67–286), followed by Tempoal giving rise to Jaumave (*M* = 275; 95% HPD: 3–530; Fig. 3).

The Tajima’s D and Fu’s F tests used to evaluate effective population size changes suggest a demographic expansion of the *H. pantostictus* populations, except the Tajima tests for both COI and D-loop markers in the Naranjos and Guayalejo populations (Table 1). Both markers’ BSPs provided similar results (Fig. 4). For the COI marker, a slight demographic decrease occurred at ~1 Ma, followed by a sudden expansion at ~250 kya. Similarly, for the D-loop marker, a demographic expansion occurred at ~250 kya (Fig. 4). However, in *H. carpintis*, the Tajima test was non-significant in all populations with both markers. In contrast, the Fu test suggested an expansion in all populations with both markers, except for Ozuluama with the COI marker (Table 1). Finally, both markers’ BSPs suggested a demographic expansion starting at 100 kya for the COI marker and 1 Ma for the D-loop marker (Fig. 4).

Biogeographic scenarios and niche modeling. The ABC analysis inferred opposing biogeographic histories for *H. pantostictus* with each molecular marker. For the COI marker, the most probable scenario suggests colonization from the coastline to inland populations (scenario one; logistic posterior probability = 0.596; 95% HPD: 0.587–0.604). In contrast, scenario two was the most plausible for the D-loop marker, suggesting an inland to coastline colonization (P = 0.804; 95% HPD = 0.797–0.813; Table 2; Suppl. material 6). However, for *H. carpintis*, scenario one was inferred as the most probable scenario for both molecular markers, suggesting colonization from the coastline to inland (Table 2; Suppl. material 6).

Finally, in the ENM, eight bioclimatic (BIO2, BIO3, BIO5, BIO9, BIO13, BIO14, BIO15, and BIO18) and three topographic variables were retained after the VIF test. The potential geographic distribution models for *H. pantostictus* and *H. carpintis* showed good performance (area under the ROC curve [AUC] >0.8; AUC [partial ROC curve] >1.1; Table 3) without over-adjustment (AUC difference = 0.143–0.190 for *H. pantostictus* and 0.159–0.178 for *H. carpintis*; Table 3). For both species, most of the observed variance was explained by the warmest month's maximum

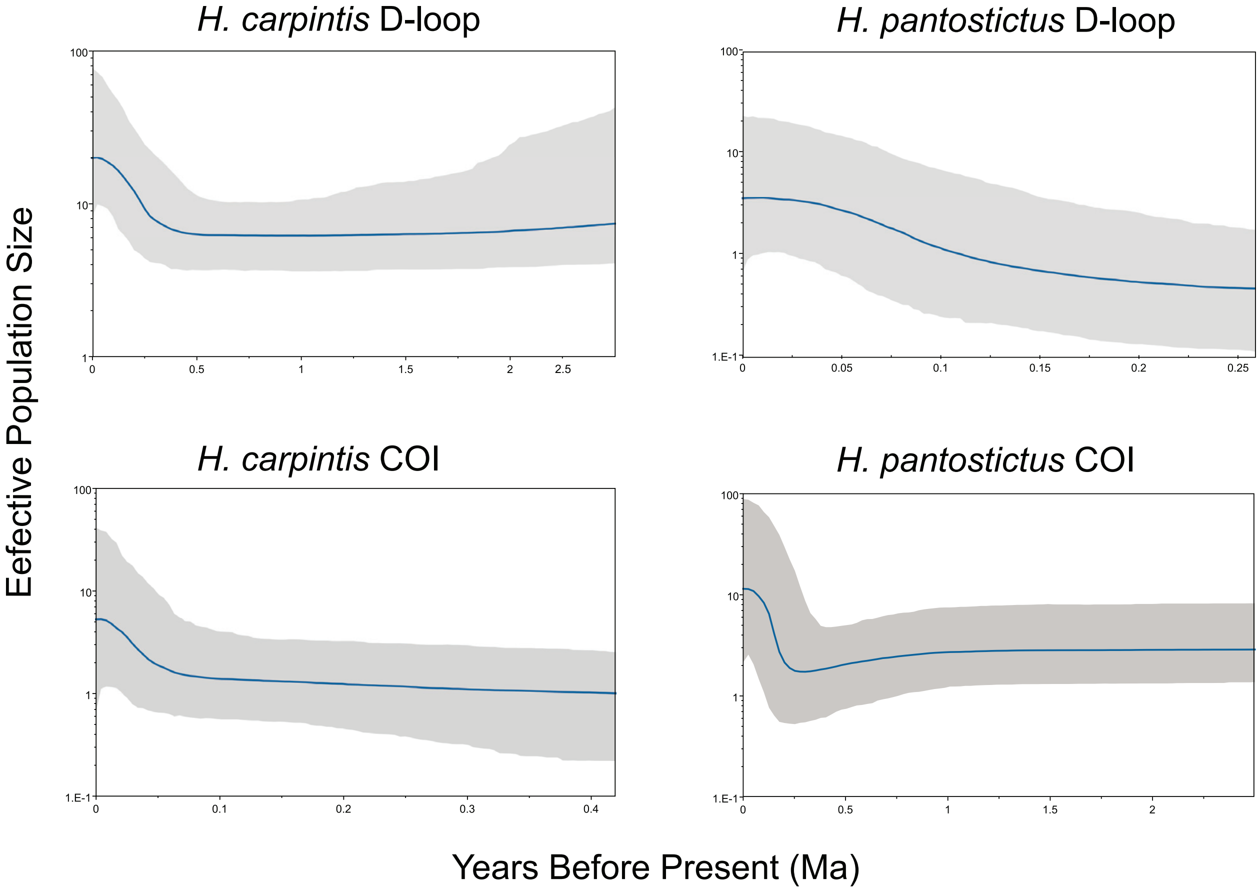

Figure 4. Bayesian skyline plots (BSP) of *Herichthys carpintis* and *Herichthys pantostictus* recovered from the analysis of the lumping populations of each of the molecular markers analyzed in this study.

Table 2. Scenarios used in the Approximate Bayesian computation (ABC) for the biogeographic history of *Herichthys pantostictus* and *Herichthys carpintis* for the two molecular markers used in this study. The posterior probability for the direct and the logistic regression as well as probability of type I and type II errors are indicated for each one of the postulated scenarios. Selected scenarios are set in bold typeface.

Species	Marker	Set	Scenario	Posterior probability				Type I error		Type II error	
				Direct	95% HPD	Logistic	95% HPD	Direct	Logistic	Direct	Logistic
H. pantostictus	COI	**Coast–Inland**	**1**	**0.504**	**0.066, 0.942**	**0.596**	**0.587, 0.604**	**0.457**	**0.463**	**0.512**	**0.542**
		Inland–Coast	2	0.496	0.058, 0.934	0.404	0.396, 0.413	0.524	0.514	0.645	0.487
	D-loop	Coast–Inland	1	0.376	0.000, 0.801	0.195	0.187, 0.203	0.588	0.642	0.745	0.789
		Inland–Coast	**2**	**0.624**	**0.199, 1.000**	**0.805**	**0.797, 0.813**	**0.489**	**0.514**	**0.564**	**0.561**
H. carpintis	COI	**Coast–Inland**	**1**	**0.81**	**0.466, 1.000**	**0.997**	**0.997, 0.998**	**0.401**	**0.402**	**0.654**	**0.641**
		Inland–Coast	2	0.19	0.000, 0.534	0.003	0.002, 0.003	0.506	0.48	0.895	0.985
	D-loop	**Coast–Inland**	**1**	**0.522**	**0.084, 0.960**	**0.699**	**0.713, 0.764**	**0.284**	**0.236**	**0.689**	**0.657**
		Inland–Coast	2	0.478	0.040, 0.916	0.301	0.237, 0.287	0.311	0.343	0.716	0.764

Table 3. Best Maxent model selected for *Herichthys pantostictus* and *Herichthys carpintis* for each one of the four periods considered in this study. LIG (Last interglacial 120 ky), LGM (Last Glacial Maximum (21 ky), mid Holocene (6 ky), Current. Best fit MaxEnt model select for each of species for the four periods considered.

Period	Parameter						
	AUC	Diff. AUC	AICc	pROC	*w*	Area [km^2]	Area [%]
H. pantostictus							
LIG	0.898	0.172	2912.548	1.458	0.750	148262.6	90.0
LGM	0.873	0.190	2954.457	1.267	0.895	129617	80.0
Mid Holocene	0.876	0.143	2941.143	1.555	0.889	109585	68.0
Current	0.885	0.174	2942.630	1.294	0.817	154917	96.0
H. carpintis							
LIG	0.912	0.161	4079.705	1.246	1.000	119371.4	81.4
LGM	0.871	0.167	4129.669	1.395	0.968	118783	81.0
Mid Holocene	0.878	0.159	4118.810	1.294	0.998	113358	77.3
Current	0.859	0.178	4138.734	1.142	0.970	117648	80.3

ROC = receiver operating characteristic, AUC = area under the curve, Diff. AUC = mean difference in the AUC values between the training data and the test data, AICc = Akaike information criterion, pROC = partial ROC values, *w* = Akaike weight, Area = total suitability area available for the taxon in km^2 and expressed in km^2 or as a percentage of the total geographic extent (*M*).

temperature (BIO5 = 14.441% for *H. pantostictus* and 15.506% for *H. carpintis*), the warmest quarter's precipitation (BIO18 = 44.390% for *H. pantostictus* and 20.216% for *H. carpintis*), and altitude (13.361% for *H. pantostictus* and 50.890% for *H. carpintis*).

The geographic extension of suitable climatic areas decreased by 22% from the LIG to the mid-Holocene for *H. pantostictus* (Table 3; Fig. 5 A–C). However, while a similar pattern was inferred for *H. carpintis*, it had a smaller decrease (Table 3; Fig. 5 E–G). Finally, an increase in suitable areas was inferred for both species from the mid-Holocene (6 kya) to the present, which was small (3%) for *H. carpintis* and larger (28%) for *H. pantostictus*.

Discussion

Population structure and diversity. The number of genetic populations recovered in a phylogeographic study depends on several factors, such as the choice of molecular marker; the size of the fragment; sample size; evolutionary processes such as selection, mutation, and genetic drift; and the species' intrinsic attributes related to habitat and life history traits (Gavrilets 2003; Sofia et al. 2006; Matsumoto and Hilsdorf 2009). In cichlids, we must expect that species distributed in lakes will show a near panmictic with a low population structure, and species distributed in rivers, such as the species analyzed in this study, will show a highly structured population. This pattern does not always occur. For example, there are riverine species without genetic structure, such as the South American *Gymnogeophagus setequedas* Reis, Malabarba et Pavanelli, 1992 (see Souza-Shibatta et al. 2018) and other Neotropical cichlids found in rivers in South Mexico (Elías et al. 2020). However, like this study's results, structured populations in riverine environments have been recovered in species distributed in Mexico, such as *Trichromis salvini* (Günther, 1862) (see Elías et al. 2020) and other South American species (Abreu et al. 2020; Pio and Carvalho 2021).

One possible explanation for the presence of genetic structure in this study could be associated with the Pleistocene glacial periods with more arid environments, leading to water body desiccation and a lack of connectivity and gene flow (Strecker et al. 2004; Gutiérrez-Rodríguez et al. 2007). Then, during the interglacial period, wetter conditions increase water levels, habitat connectivity, and gene flow (Elías et al. 2020). Another possible explanation could be that both species analyzed in this study had populations distributed toward the coastline. In other South American tropical fish species, it has been postulated that high sea level fluctuation due to Pleistocene climatic changes led to sea level transgression and regression. Therefore, when the sea level rose, the mouth of the rivers was displaced inland, promoting population isolation. In contrast, when the sea level dropped, the influence of the freshwater could extend into the continental shelf, promoting connections between previously isolated populations and gene flow (Abreu et al. 2020, Pio and Carvalho 2021).

The potential effect of sea level fluctuations and Pleistocene climatic changes could be masked by ENM caveats. Most ENM algorithms identify suitability areas through correlations with species occurrence data, ignoring factors such as habitat saturation, response to environmental changes, and biotic interactions (Cordellier and Pfenninger 2009; Wiens et al. 2009). Moreover, they cannot deal with aquatic organisms since climatic variables are optimized for terrestrial organisms, leading to suitability area overestimations (Domisch et al. 2011; Elith et al. 2011). Nevertheless, a potential Pleistocene climatic change effect was effectively detected in *Herichthys pantostictus* through the 12% reduction in its suitability area from LGM to mid-Holocene compared to the 4% reduction for *Herichthys carpintis* in the same period (Table 3). Indeed, a close inspection of Fig. 5 showed that

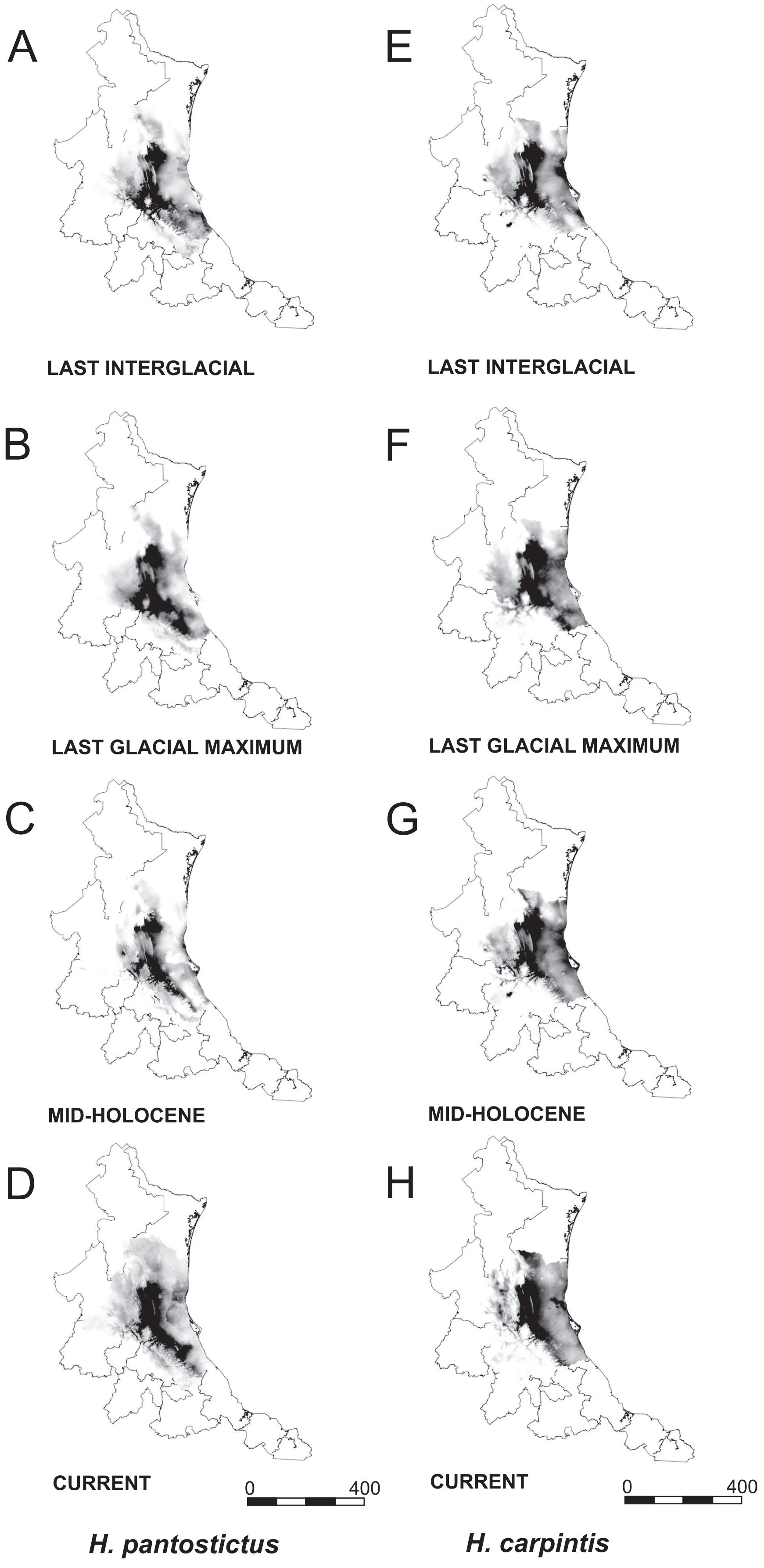

Figure 5. Potential geographic distribution of *Herichthys carpintis* and *Herichthys pantostictus* identified using an ecological niche modelling under current bioclimatic conditions (1950–2000), as well as projections to three paleoclimatic periods (LIG, 120kya; LGM; 21kya; Mid Holocene, 6 kya). Darker areas represent the pixels of major suitability conditions for the presence of the taxon.

most of *H. pantostictus*' lost areas were located toward the coastline. Therefore, despite sympatry across most of their geographic distribution, both species showed different responses to environmental variables, as has been previously proposed based on the inequivalence in their environmental niches (see table S3 in Mejía et al. 2022).

Low genetic diversity levels have been associated with the absence (Olivieri et al. 2008; Craul et al. 2009; McMahan et al. 2017) or the presence of genetic structure (Agbebi et al. 2016). In this study, *h* values ranged from medium (0.390) to high (1.000) with low π values (0.001–0.026), suggesting a sudden population expansion (Duftner et al. 2006; Barluenga and Meyer 2010; Ferreira et al. 2015; Azevedo et al. 2017) that could cause the absence of population genetic structure. However, this apparent absence of genetic structure can be counteracted by the cichlids' life history traits, such as territoriality, parental care, and philopatric behavior, which restrict the displacement of individuals and allow new genetic variants to arise (Budaev et al. 1999; Sofia et al. 2008; Pereira et al. 2009; Sefc 2011). Therefore, the genetic structures of *H. carpintis* and *H. pantostictus* we inferred in this study could be the result of populations that experienced a demographic expansion and life-history-related traits.

Demographic history and ENMs. The BSPs for both markers and species (Fig. 4) suggest a population expansion, consistent with other neotropical cichlids (Barluenga and Meyer 2010; Bagley et al. 2017; McMahan et al. 2017). The demographic expansion found in this study could be attributable to the Pleistocene's heating and cooling periods, as has been proposed for other neotropical fishes (Bagley et al. 2013; McMahan et al. 2017, Beltrán-López et al. 2018). Nevertheless, our study results do not correspond with the results found in the ENM, where a reduction in the available suitability areas was inferred for both species since the LIG (Table 3). In *H. carpintis*, the results suggest a slight reduction (4%) in the suitability area from LIG to mid-Holocene (Table 3) but a drastic reduction (22%) for *H. pantostictus* that must have impacted its demographic history. However, this pattern was not present in the BSP (Fig. 4).

These results could be attributable to different factors. For *H. carpintis*, the ENM showed that since the LIG, the most suitable areas for this species were toward the coastline and have existed up to the present (Fig. 5). Therefore, sea level invasions and regressions during glacial periods had a negligible effect on this species' effective population but did affect its spatial expansion. The gene flow analysis and DIYABC scenarios suggest a coast-to-inland colonization process for *H. carpintis*, consistent with that proposed for other cichlids in Middle America (Bagley et al. 2013; McMahan et al. 2017).

For *H. pantostictus*, the ENM suggested that the most suitable areas were inland since the LGM. Therefore, we expect that eustatic sea level changes must have impacted this species' population size over time. Dry conditions and low precipitation characterized the LGM in Central Mexico, with the evaporation of some water bodies (Caballero et al. 2010) explaining the drastic reduction in this species' available suitable areas from the LGM to mid-Holocene and the apparent slight reduction in its effective population size inferred in the BSP with the COI marker (Fig. 4). Another possible scenario is that the ancestral *H. pantostictus* population was on the coastline and the increase in sea level forced the species to move to inland, as suggested by the DIYABC results with the COI marker (Table 2). Therefore, we could suggest that, contrary to expectations, glacial periods did not significantly affect the demographic history of these cichlid species in Northeast Mexico, as has been previously documented in other codistributed species (Rocamontes-Morales et al. 2021).

Conclusions

This study's results suggest that both species (*Herichthys carpintis* and *Herichthys pantostictus*) arose and developed in different geographic areas: *H. carpintis* in lacustrine environments and low-flow rivers in coastal regions and *H. pantostictus* in clear water inland rivers with medium to high flows. The current sympatry of both species is more compatible with a pseudo-incongruence pattern resulting from dispersal events during the Pleistocene, supported by the DIYABC results for *H. carpintis* with both markers and *H. pantostictus* with the D-loop marker, than an independent response to paleoclimatic events, supported by the ENMs and the DIYABC results for *H. pantostictus* with the COI marker. However, further analysis with other molecular markers is required to disentangle both species' biogeographic histories and to fully understand the complex history of this region of northeastern Mexico.

Acknowledgments

Fabian Pérez-Miranda acknowledges CONACyT for a postdoctoral fellowship, and we also thank Gerardo Zúñiga for his comments.

References

Abreu JMS, Waltz BT, Albert JS, Piorski NM (2020) Genetic differentiation through dispersal and isolation in two freshwater fish species from coastal basins of northeastern Brazil. Neotropical Ichthyology 18(3): e190114. https://doi.org/10.1590/1982-0224-2019-0114

Agbebi OT, Echefu CJ, Adeosun IO, Ajibade AH, Adegbite EA, Adebambo AO, Ilori MB, Durosaro SO, Ajibike AB (2016) Mitochondrial diversity and time divergence of commonly cultured cichlids in Nigeria. British Biotechnology Journal 13(2): 1–7. https://doi.org/10.9734/BBJ/2016/25470

Aiello-Lammens ME, Boria RA, Radosavljevic A, Vilela B, Anderson RP (2015) spThin: An R package for spatial thinning of species occurrence records for use in ecological niche models. Ecography 38(5): 541–545. https://doi.org/10.1111/ecog.01132

Akaike H (1974) A new look at the statistical model identification. IEEE Transactions on Automatic Control 19(6): 716–723. https://doi.org/10.1109/TAC.1974.1100705

Aljanabi SM, Martinez I (1997) Universal and rapid salt-extraction of high quality genomic DNA for PCR-based techniques. Nucleic Acids Research 25(22): 4692–4693. https://doi.org/10.1093/nar/25.22.4692

Álvarez M Jr (1961) Provincias fisiográficas de la República Mexicana. Boletín de la Sociedad Geológica Mexicana 24(2): 5–20. https://doi.org/10.18268/BSGM1961v24n2a1

Avise JC (2009) Phylogeography: Retrospect and prospect. Journal of Biogeography 36(1): 3–15. https://doi.org/10.1111/j.1365-2699.2008.02032.x

Azevedo RS, Bitencourt A, Silva DA, Amorim A, Mazzoni R, Carvalho EF, Amaral CRL (2017) Genetic diversity of *Geophagus brasiliensis* from the South American Atlantic Rainforest. Forensic Science International. Genetics Supplement Series 6: e433–e434. https://doi.org/10.1016/j.fsigss.2017.09.149

Bagley JC, Johnson JB (2014) Testing for shared biogeographic history in the lower Central American freshwater fish assemblage using comparative phylogeography: Concerted, independent, or multiple evolutionary responses? Ecology and Evolution 4(9): 1686–1705. https://doi.org/10.1002/ece3.1058

Bagley JC, Sandel M, Travis J, Lozano-Vilano MDL, Johnson JB (2013) Paleoclimatic modeling and phylogeography of least killifish, *Heterandria formosa*: Insights into Pleistocene expansion-contraction dynamics and evolutionary history of North American Coastal Plain freshwater biota. BMC Evolutionary Biology 13(1): 223. https://doi.org/10.1186/1471-2148-13-223

Bagley JC, Matamoros WA, McMahan CD, Tobler M, Chakrabarty P, Johnson JB (2017) Phylogeography and species delimitation in convict cichlids (Cichlidae: *Amatitlania*): implications for taxonomy and Plio–Pleistocene evolutionary history in Central America. Biological Journal of the Linnean Society. Linnean Society of London 120(1): 155–170. https://doi.org/10.1111/bij.12845

Barluenga M, Meyer A (2010) Phylogeography, colonization and population history of the Midas cichlid species complex (*Amphilophus* spp.) in the Nicaraguan crater lakes. BMC Evolutionary Biology 10(1): 326. https://doi.org/10.1186/1471-2148-10-326

Baumgartner J, Wilson P, Esperon-Rodriguez M (2017) Rmaxent: tools for working with Maxent in R. R package version 0.4.1.9000. https://rdrr.io/github/johnbaums/rmaxent/f/README.md

Beerli P (1998) Estimation of migration rates and population sizes in geographically structured populations. Pp. 39–54. In: Carvalho G (Ed.) NATO Advanced Science Institutes Series, Series A. Life Sciences 306: 39–54.

Beerli P, Felsenstein J (2001) Maximum likelihood estimation of a migration matrix and effective population sizes in n subpopulations by using a coalescent approach. Proceedings of the National Academy of Sciences of the United States of America 98(8): 4563–4568. https://doi.org/10.1073/pnas.081068098

Beerli P, Mashayekhi S, Sadeghi M, Khodaei M, Shaw K (2019) Population genetic inference with MIGRATE. Current Protocols in Bioinformatics 68(1): e87. https://doi.org/10.1002/cpbi.87

Beltrán-López RG, Domínguez-Domínguez O, Pérez-Rodríguez R, Piller K, Doadrio I (2018) Evolving in the highlands: the case of the Neotropical Lerma live-bearing *Poeciliopsis infans* (Woolman, 1894) (Cyprinodontiformes: Poeciliidae) in Central Mexico. BMC Evolutionary Biology 18(1): 56. https://doi.org/10.1186/s12862-018-1172-7

Bermingham E, Martin AP (1998) Comparative mtDNA phylogeography of neotropical freshwater fishes: Testing shared history to infer the evolutionary landscape of lower Central America. Molecular Ecology 7(4): 499–517. https://doi.org/10.1046/j.1365-294x.1998.00358.x

Bloom DD, Piller KR, Lyons J, Mercado-Silva N, Medina-Nava M (2009) Systematics and biogeography of the silverside tribe Menidiini (Teleostomi: Atherinopsidae) based on the mitochondrial ND2 gene. Copeia 2009(2): 408–417. https://doi.org/10.1643/CI-07-151

Budaev SV, Zworykin DD, Mochek AD (1999) Individual differences in parental care and behaviour profile in the convict cichlid: A correlation study. Animal Behaviour 58(1): 195–202. https://doi.org/10.1006/anbe.1999.1124

Caballero M, Lozano-García S, Vázquez-Selem L, Ortega B (2010) Evidencias de cambio climático y ambiental en registros glaciales y en cuencas lacustres del centro de México durante el último máximo glacial. Boletín de la Sociedad Geológica Mexicana 62(3): 359–377. https://doi.org/10.18268/BSGM2010v62n3a4

Chen KC, Borowsky RL (2004) Comparative phylogeography of *Xiphophorus variatus* and *Heterandria jonesi* (Poeciliidae) using RAPD data. Ichthyological Exploration of Freshwaters 15(1): 25–40.

Cobos ME, Peterson AT, Barve N, Osorio-Olvera L (2019) kuenm: An R package for detailed development of ecological niche models using Maxent. PeerJ 7: e6281. https://doi.org/10.7717/peerj.6281

Coghill LM, Hulsey CD, Chaves-Campos J, de Leon FJG, Johnson SG (2014) Next generation phylogeography of cave and surface *Astyanax mexicanus*. Molecular Phylogenetics and Evolution 79: 368–374. https://doi.org/10.1016/j.ympev.2014.06.029

Comte L, Grenouillet G (2015) Distribution shifts of freshwater fish under a variable climate: Comparing climatic, bioclimatic and biotic velocities. Diversity and Distributions 21(9): 1014–1026. https://doi.org/10.1111/ddi.12346

Cordellier M, Pfenninger M (2009) Inferring the past to predict the future: Climate modelling predictions and phylogeography for the freshwater gastropod *Radix balthica* (Pulmonata, Basommatophora). Molecular Ecology 18(3): 534–544. https://doi.org/10.1111/j.1365-294X.2008.04042.x

Cornuet JM, Ravigné V, Estoup A (2010) Inference on population history and model checking using DNA sequence and microsatellite data with the software DIYABC (v1. 0). BMC Bioinformatics 11(1): 401. https://doi.org/10.1186/1471-2105-11-401

Craul M, Chikhi L, Sousa V, Olivieri GL, Rabesandratana A, Zimmermann E, Radespiel U (2009) Influence of forest fragmentation on an endangered large-bodied lemur in northwestern Madagascar. Biological Conservation 142(12): 2862–2871. https://doi.org/10.1016/j.biocon.2009.05.026

De la Maza-Benignos M, Ornelas-García CP, Lozano-Vilano MDL, García-Ramírez ME, Doadrio I (2015). Phylogeographic analysis of genus *Herichthys* (Perciformes: Cichlidae), with descriptions of *Nosferatu* new genus and *H. tepehua* n. sp. Hydrobiologia 748: 201–231. https://doi.org/10.1007/s10750-014-1891-8

Domínguez-Domínguez O, Pérez-Ponce de León G (2009) ¿La mesa central de México es una provincia biogeográfica? Análisis descriptivo basado en componentes bióticos dulceacuícolas. Revista Mexicana de Biodiversidad 80(3): 835–852. https://doi.org/10.22201/ib.20078706e.2009.003.178

Domisch S, Jaehnig SC, Haase P (2011) Climate-change winners and losers: Stream macroinvertebrates of a submontane region in Central Europe. Freshwater Biology 56(10): 2009–2020. https://doi.org/10.1111/j.1365-2427.2011.02631.x

Drummond AJ, Rambaut A (2007) BEAST: Bayesian evolutionary analysis by sampling trees. BMC Evolutionary Biology 7(1): 214. https://doi.org/10.1186/1471-2148-7-214

Drummond AJ, Rambaut A, Shapiro BETH, Pybus OG (2005) Bayesian coalescent inference of past population dynamics from molecular sequences. Molecular Biology and Evolution 22(5): 1185–1192. https://doi.org/10.1093/molbev/msi103

Duftner N, Sefc KM, Koblmueller S, Nevado B, Verheyen E, Phiri H, Sturmbauer C (2006) Distinct population structure in a phenotypically homogeneous rock-dwelling cichlid fish from Lake Tanganyika. Molecular Ecology 15(9): 2381–2395. https://doi.org/10.1111/j.1365-294X.2006.02949.x

Elías DJ, McMahan CD, Matamoros WA, Gómez-González AE, Piller KR, Chakrabarty P (2020) Scale (s) matter: Deconstructing an area of endemism for Middle American freshwater fishes. Journal of Biogeography 47(11): 2483–2501. https://doi.org/10.1111/jbi.13941

Elith J, Phillips SJ, Hastie T, Dudík M, Chee YE, Yates CJ (2011) A statistical explanation of MaxEnt for ecologists. Diversity and Distributions 17(1): 43–57. https://doi.org/10.1111/j.1472-4642.2010.00725.x

Excoffier L, Lischer HE (2010) Arlequin suite ver 3.5: A new series of programs to perform population genetics analyses under Linux and Windows. Molecular Ecology Resources 10(3): 564–567. https://doi.org/10.1111/j.1755-0998.2010.02847.x

FAO (2022) Hydrological basins of the world. https://data.apps.fao.org/catalog/dataset/f2615a41-6383-4aa4-aa21-743330eb03ae

Ferreira DG, Galindo BA, Frantine-Silva W, Almeida FS, Sofia SH (2015) Genetic structure of a Neotropical sedentary fish revealed by AFLP, microsatellite and mtDNA markers: A case study. Conservation Genetics 16(1): 151–166. https://doi.org/10.1007/s10592-014-0648-2

Fricke. R, Eschmeyer WN, van der Laan R (Eds.) (2023) Eschmeyer's catalog of fishes: genera, species, references. California Academy of Sciences, San Francisco, CA, USA. [Electronic version accessed 13 November 2023] http://researcharchive.calacademy.org/research/ichthyology/catalog/fishcatmain.asp

Froese R, Pauly D (Eds.) (2023) FishBase. [Version 10/2023] http://www.fishbase.org

García-Andrade AB, Beltrán-Lopéz RG, Pérez-Rodríguez R, Domínguez-Domínguez O, Mejía-Mojica H, Doadrio I (2021) Evolutionary history of the Aztec shiner *Aztecula sallaei* (Günther, 1868) (Teleostei: Cyprinidae): An endemic and monotypic species of Mexico. Journal of Zoological Systematics and Evolutionary Research 59(8): 2103–2118. https://doi.org/10.1111/jzs.12555

García-Martínez RM, Barriga-Sosa I, López B, Mejía O (2020) Colonization routes and demographic history of *Chirostoma humboldtianum* in the central Mexican plateau. Journal of Fish Biology 97(4): 1039–1050. https://doi.org/10.1111/jfb.14462

Gavrilets S (2003) Perspective: models of speciation: what have we learned in 40 years? Evolution; International Journal of Organic Evolution 57(10): 2197–2215. https://doi.org/10.1111/j.0014-3820.2003.tb00233.x

Gouy M, Guindon S, Gascuel O (2010) SeaView version 4: A multiplatform graphical user interface for sequence alignment and phylogenetic tree building. Molecular Biology and Evolution 27(2): 221–224. https://doi.org/10.1093/molbev/msp259

Gutiérrez-Rodríguez C, Morris MR, Dubois NS, de Queiroz K (2007) Genetic variation and phylogeography of the swordtail fish *Xiphophorus cortezi* (Cyprinodontiformes, Poeciliidae). Molecular Phylogenetics and Evolution 43(1): 111–123. https://doi.org/10.1016/j.ympev.2006.10.022

Hausdorf B, Wilkens H, Strecker U (2011) Population genetic patterns revealed by microsatellite data challenge the mitochondrial DNA based taxonomy of *Astyanax* in Mexico (Characidae, Teleostei). Molecular Phylogenetics and Evolution 60(1): 89–97. https://doi.org/10.1016/j.ympev.2011.03.009

Heller R, Chikhi L, Siegismund HR (2013) The confounding effect of population structure on Bayesian skyline plot inferences of demographic history. PLoS One 8(5): e62992. https://doi.org/10.1371/journal.pone.0062992

Hewitt GM (1996) Some genetic consequences of ice ages, and their role in divergence and speciation. Biological Journal of the Linnean Society. Linnean Society of London 58(3): 247–276. https://doi.org/10.1006/bijl.1996.0035

Hewitt GM (2000) The genetic legacy of the Quaternary ice ages. Nature 405(6789): 907–913. https://doi.org/10.1038/35016000

Hewitt GM (2003) Ice ages: their impact on species distributions and evolution. Pp. 339–361. In: Rothschild LJ, Lister AM (Eds.) Evolution on planet Earth, 1st edn. Academic Press, New York, NY, USA. https://doi.org/10.1016/B978-012598655-7/50045-8

Hewitt GM (2004) Genetic consequences of climatic oscillations in the Quaternary. Philosophical Transactions of the Royal Society of London. Series B, Biological Sciences 359(1442): 183–195. https://doi.org/10.1098/rstb.2003.1388

Hijmans RJ, Van Etten J (2012) raster: Geographic analysis and modeling with raster data. R package version 2.0-12. http://CRAN.R-project.org/package=raster

Hijmans RJ, Cameron SE, Parra JL, Jones PG, Jarvis A (2005) Very high resolution interpolated climate surfaces for global land areas. International Journal of Climatology 25(15): 1965–1978. https://doi.org/10.1002/joc.1276

Hijmans RJ, Phillips S, Leathwick J, Elith J (2020) dismo: Species Distribution Modeling. R package version 1.3-3. http://cran.r-project.org/web/packages/dismo/index.html

Lambeck K, Chappell J (2001) Sea level change through the last glacial cycle. Science 292(5517): 679–686. https://doi.org/10.1126/science.1059549

Larkin MA, Blackshields G, Brown NP, Chenna R, McGettigan PA, McWilliam H, Valentin F, Wallace IM, Wilm A, Lopez R, Thompson JD, Gibson TJ, Higgins DG (2007) Clustal W and Clustal X version 2.0. Bioinformatics (Oxford, England) 23(21): 2947–2948. https://doi.org/10.1093/bioinformatics/btm404

Lehner B, Grill G (2013) Global River hydrography and network routing: Baseline data and new approaches to study the world's large river systems. Hydrological Processes 27(15): 2171–2186. https://doi.org/10.1002/hyp.9740

Lehner B, Verdin K, Jarvis A (2008) New global hydrography derived from spaceborne elevation data. Eos 89(10): 93–94. https://doi.org/10.1029/2008EO100001

León-Romero Y, Mejía O, Soto-Galera E (2012) DNA barcoding reveals taxonomic conflicts in the *Herichthys bartoni* species group (Pisces: Cichlidae). Molecular Ecology Resources 12(6): 1021–1026. https://doi.org/10.1111/1755-0998.12018

Lister AM, Sher AV, van Essen H, Wei G (2005) The pattern and process of mammoth evolution in Eurasia. Quaternary International 126: 49–64. https://doi.org/10.1016/j.quaint.2004.04.014

Marshall CJ, Liebherr JK (2000) Cladistic biogeography of the Mexican transition zone. Journal of Biogeography 27(1): 203–216. https://doi.org/10.1046/j.1365-2699.2000.00388.x

Mateos M (2005) Comparative phylogeography of livebearing fishes in the genera *Poeciliopsis* and *Poecilia* (Poeciliidae: Cyprinodontiformes) in central Mexico. Journal of Biogeography 32(5): 775–780. https://doi.org/10.1111/j.1365-2699.2005.01236.x

Mateos M, Sanjur OI, Vrijenhoek RC (2002) Historical biogeography of the livebearing fish genus *Poeciliopsis* (Poeciliidae: Cyprinodontiformes). Evolution; International Journal of Organic Evolution 56(5): 972–984. https://doi.org/10.1111/j.0014-3820.2002.tb01409.x

Matsumoto CK, Hilsdorf AWS (2009) Microsatellite variation and population genetic structure of a neotropical endangered Bryconinae species *Brycon insignis* Steindachner, 1877: Implications for its conservation and sustainable management. Neotropical Ichthyology 7(3): 395–402. https://doi.org/10.1590/S1679-62252009000300006

McMahan CD, Ginger L, Cage M, David KT, Chakrabarty P, Johnston M, Matamoros WA (2017) Pleistocene to Holocene expansion of the black-belt cichlid in Central America, *Vieja maculicauda* (Teleostei: Cichlidae). PLoS One 12(5): e0178439. https://doi.org/10.1371/journal.pone.0178439

Mejía O, Martínez-Méndez N, Pérez-Miranda F, Matamoros WA (2022) Climatic niche evolution of a widely distributed Neotropical freshwater fish clade. Biological Journal of the Linnean Society. Linnean Society of London 135(4): 839–855. https://doi.org/10.1093/biolinnean/blab153

Miller RR, Minckley WL, Norris SM (2005) Freshwater fishes of Mexico. University of Chicago Press, Chicago, IL, USA, 490 pp.

Morrone JJ (2004) Panbiogeografía, componentes bióticos y zonas de transición. Revista Brasileira de Entomologia 48(2): 149–162. https://doi.org/10.1590/S0085-56262004000200001

Morrone JJ (2007) Hacia una biogeografía evolutiva. Revista Chilena de Historia Natural 80(4): 509–520. https://doi.org/10.4067/S0716-078X2007000400011

Morrone JJ (2020) Biotic assembly in evolutionary biogeography: A case for integrative pluralism. Frontiers of Biogeography 12(4): e48819. https://doi.org/10.21425/F5FBG48819

Muscarella R, Galante PJ, Soley-Guardia M, Boria RA, Kass JM, Uriarte M, Anderson RP (2014) ENM eval: An R package for conducting spatially independent evaluations and estimating optimal model complexity for Maxent ecological niche models. Methods in Ecology and Evolution 5(11): 1198–1205. https://doi.org/10.1111/2041-210X.12261

Naimi B, Hamm NA, Groen TA, Skidmore AK, Toxopeus AG (2014) Where is positional uncertainty a problem for species distribution modelling? Ecography 37(2): 191–203. https://doi.org/10.1111/j.1600-0587.2013.00205.x

Olivieri GL, Sousa V, Chikhi L, Radespiel U (2008) From genetic diversity and structure to conservation: Genetic signature of recent population declines in three mouse lemur species (*Microcebus* spp.). Biological Conservation 141(5): 1257–1271. https://doi.org/10.1016/j.biocon.2008.02.025

Ornelas-García CP, Domínguez-Domínguez O, Doadrio I (2008) Evolutionary history of the fish genus *Astyanax* Baird & Girard (1854) (Actinopterygii, Characidae) in Mesoamerica reveals multiple morphological homoplasies. BMC Evolutionary Biology 8(1): 340. https://doi.org/10.1186/1471-2148-8-340

Pacioni C, Hunt H, Allentoft ME, Vaughan TG, Wayne AF, Baynes A, Haouchar D, Dorthc J, Bunce M (2015) Genetic diversity loss in a biodiversity hotspot: Ancient DNA quantifies genetic decline and former connectivity in a critically endangered marsupial. Molecular Ecology 24(23): 5813–5828. https://doi.org/10.1111/mec.13430

Pereira LHG, Foresti F, Oliveira C (2009) Genetic structure of the migratory catfish *Pseudoplatystoma corruscans* (Siluriformes: Pimelodidae) suggests homing behaviour. Ecology Freshwater Fish 18(2): 215–225. https://doi.org/10.1111/j.1600-0633.2008.00338.x

Pérez-Miranda F, Mejía O, Soto-Galera E, Espinosa-Pérez H, Piálek L, Říčan O (2018) Phylogeny and species diversity of the genus *Herichthys* (Teleostei: Cichlidae). Journal of Zoological Systematics and Evolutionary Research 56(2): 223–247. https://doi.org/10.1111/jzs.12197

Pérez-Miranda F, Mejia O, López B, Říčan O (2020) Molecular clocks, biogeography and species diversity in *Herichthys* with evaluation of the role of Punta del Morro as a vicariant brake along the Mexican Transition Zone in the context of local and global time frame of cichlid diversification. PeerJ 8: e8818. https://doi.org/10.7717/peerj.8818

Peterson AT, Nyari AS (2008) Ecological niche conservatism and Pleistocene refugia in the thrush-like mourner, *Schiffornis* sp., in the neotropics. Evolution 62(1): 173–183. https://doi.org/10.1111/j.1558-5646.2007.00258.x

Phillips SJ, Anderson RP, Schapire RE (2006) Maximum entropy modeling of species geographic distributions. Ecological Modelling 190(3–4): 231–259. https://doi.org/10.1016/j.ecolmodel.2005.03.026

Phillips JD, Gillis DJ, Hanner RH (2020) HACSim: An R package to estimate intraspecific sample sizes for genetic diversity assessment using haplotype accumulation curves. PeerJ. Computer Science 6: e243. https://doi.org/10.7717/peerj-cs.243

Pio NL, Carvalho TP (2021) Evidence on the paleodrainage connectivity during Pleistocene: Phylogeography of a hypoptopomatine endemic to southeastern Brazilian coastal drainages. Neotropical Ichthyology 19(2): e200128. https://doi.org/10.1590/1982-0224-2020-0128

QGIS Development Team (2009) QGIS Geographic Information System. Open Source Geospatial Foundation. http://qgis.org

Rambaut A, Drummond AJ, Xie D, Baele G, Suchard MA (2018) Posterior summarization in Bayesian phylogenetics using Tracer 1.7. Systematic Biology 67(5): 901–904. https://doi.org/10.1093/sysbio/syy032

Říčan O, Piálek L, Zardoya R, Doadrio I, Zrzavý J (2013) Biogeography of the Mesoamerican Cichlidae (Teleostei: Heroini): colonization through the GAARlandia land bridge and early diversification. Journal of Biogeography 40(3): 579–593. https://doi.org/10.1111/jbi.12023

Říčan O, Piálek L, Dragová K, Novák J (2016) Diversity and evolution of the Middle American cichlid fishes (Teleostei: Cichlidae) with revised classification. Vertebrate Zoology 66: 1–102. https://doi.org/10.3897/vz.66.e31534

Rincon-Sandoval M, Betancur-R R, Maldonado-Ocampo JA (2019) Comparative phylogeography of trans-Andean freshwater fishes based on genome-wide nuclear and mitochondrial markers. Molecular Ecology 28(5): 1096–1115. https://doi.org/10.1111/mec.15036

Rocamontes-Morales JA, Gutiérrez-Rodríguez C, Rios-Cardenas O, Hernandez-Romero PC (2021) Genetic and morphological differentiation in the green swordtail fish, *Xiphophorus hellerii*: The influence of geographic and environmental factors. Hydrobiologia 848(19): 4599–4622. https://doi.org/10.1007/s10750-021-04664-0

RStudio Team (2020) RStudio: integrated development for R. Rstudio Team, PBC, Boston, MA. https://www.rstudio.com/

Sefc KM (2011) Mating and parental care in Lake Tanganyika's cichlids. International Journal of Evolutionary Biology 2011: 1–20. https://doi.org/10.4061/2011/470875

Sofia SH, Silva CR, Galindo BA, Almeida FS, Sodre LM, Martinez CB (2006) Population genetic structure of *Astyanax scabripinnis* (Teleostei, Characidae) from an urban stream. Hydrobiologia 553(1): 245–254. https://doi.org/10.1007/s10750-005-1106-4

Sofia SH, Galindo BA, Paula FM, Sodré LM, Martinez CB (2008) Genetic diversity of *Hypostomus ancistroides* (Teleostei, Loricariidae) from an urban stream. Genetics and Molecular Biology 31(1 suppl): 317–323. https://doi.org/10.1590/S1415-47572008000200027

Souza-Shibatta L, Kotelok-Diniz T, Ferreira DG, Shibatta OA, Sofia SH, De Assumpcao L, Suelen F, Pini R, Makrakis S, Makrakis MC (2018) Genetic diversity of the endangered neotropical cichlid fish (*Gymnogeophagus setequedas*) in Brazil. Frontiers in Genetics 9: 13. https://doi.org/10.3389/fgene.2018.00013

Strecker U, Faúndez VH, Wilkens H (2004) Phylogeography of surface and cave *Astyanax* (Teleostei) from Central and North America based on cytochrome b sequence data. Molecular Phylogenetics and Evolution 33(2): 469–481. https://doi.org/10.1016/j.ympev.2004.07.001

Tonkin-Hill G, Lees JA, Bentley SD, Frost SD, Corander J (2019) Fast hierarchical Bayesian analysis of population structure. Nucleic Acids Research 47(11): 5539–5549. https://doi.org/10.1093/nar/gkz361

Ward RD, Zemlak TS, Innes BH, Last PR, Hebert PD (2005) DNA barcoding Australia's fish species. Philosophical Transactions of the Royal Society of London. Series B, Biological Sciences 360(1462): 1847–1857. https://doi.org/10.1098/rstb.2005.1716

Warren DL, Seifert SN (2011) Ecological niche modeling in Maxent: The importance of model complexity and the performance of model selection criteria. Ecological Applications 21(2): 335–342. https://doi.org/10.1890/10-1171.1

Waters JM, Wallis GP (2000) Across the southern Alps by river capture? Freshwater fish phylogeography in South Island, New Zealand. Molecular Ecology 9(10): 1577–1582. https://doi.org/10.1046/j.1365-294x.2000.01035.x

Wiens JA, Stralberg D, Jongsomjit D, Howell CA, Snyder MA (2009) Niches, models, and climate change: Assessing the assumptions and uncertainties. Proceedings of the National Academy of Sciences of the United States of America 106(Suppl. 2): 19729–19736. https://doi.org/10.1073/pnas.0901639106

WoRMS Editorial Board (2023). World Register of Marine Species. https://www.marinespecies.org [Accessed 13 November 2023] https://doi.org/10.14284/170

Supplementary material 1

List of specimens

Authors: Fabian Pérez-Miranda, Omar Mejía, Benjamín López, Eduardo Soto-Galera, Amairany Bernal-Portillo, Wilfredo A. Matamoros

Data type: xlsx

Explanation note: List of the specimens analysed in this study for the two mitochondrial markers. The specimens are deposited in the Colección Nacional de Peces Dulceacuícolas de la Escuela Nacional de Ciencias Biológicas.

Link: https://doi.org/10.3897/aiep.53.112183.suppl1

Supplementary material 2

Gene flow models used in this study

Authors: Fabian Pérez-Miranda, Omar Mejía, Benjamín López, Eduardo Soto-Galera, Amairany Bernal-Portillo, Wilfredo A. Matamoros

Data type: xlsx

Explanation note: Gene flow models used in this study for the analysis of mitchondrial markers COI and D-loop in *Herichthys pantostictus* and *Hericthys carpintis*. The selected models according with Bayes Factor (BF) are highlighted in bold. See Suppl. material 3: table S3 for further details.

Link: https://doi.org/10.3897/aiep.53.112183.suppl2

Supplementary material 3

GenBank numbers

Authors: Fabian Pérez-Miranda, Omar Mejía, Benjamín López, Eduardo Soto-Galera, Amairany Bernal-Portillo, Wilfredo A. Matamoros

Data type: xlsx

Explanation note: List of accession numbers in GenBank for the unique haplotypes generated in this study.

Link: https://doi.org/10.3897/aiep.53.112183.suppl3

Supplementary material 4

Accumulation curves

Authors: Fabian Pérez-Miranda, Omar Mejía, Benjamín López, Eduardo Soto-Galera, Amairany Bernal-Portillo, Wilfredo A. Matamoros

Data type: pdf

Explanation note: Haplotype accumulation curves to estimate the fraction of haplotype diversity captured from sample size used in this study. A) Haplotype accumulation curve for the COI marker in *H. pantostictus*. B) Haplotype accumulation curve for the D loop marker in *H. pantostictus*. C) Haplotype accumulation curve for the COI marker in *H. carpintis*. D) Haplotype accumulation curve for the D loop marker in *H. carpintis*. The R value represent the fraction of haplotype diversity recovered by sample size.

Link: https://doi.org/10.3897/aiep.53.112183.suppl4

Supplementary material 5

Bayes factor comparison among gene flow models

Authors: Fabian Pérez-Miranda, Omar Mejía, Benjamín López, Eduardo Soto-Galera, Amairany Bernal-Portillo, Wilfredo A. Matamoros

Data type: xlsx

Explanation note: Model comparison of the different gene flow models analysed in the populations of *Herichthys pantostictus* and *Herichthys carpintis* for the mitochondrial markers COI and D-loop. The models were compared through a Bayes Factor (BF) using the Bezier marginal likelihood obtained in Migrate. See Suppl. material 2: table S2 for complete details of models. lML (Bezier likelihood), LBF (Likelihood Bayes Factor), mod. rank (model ranking), mod.prob (model probability).

Link: https://doi.org/10.3897/aiep.53.112183.suppl5

Supplementary material 6

Competing scenarios

Authors: Fabian Pérez-Miranda, Omar Mejía, Benjamín López, Eduardo Soto-Galera, Amairany Bernal-Portillo, Wilfredo A. Matamoros

Data type: pdf

Explanation note: Schematic representation of the different competing scenarios considering to test the colonization routes of *H. carpintis* and *H. pantostictus* by Approximate Bayesian Computation (ABC) of the mitochondrial DNA markers COI and D-loop. In the first scenario a costal to inland colonization process was inferred, on the other hand, in the second scenario, a inland to coast colonization process was assumed.

Link: https://doi.org/10.3897/aiep.53.112183.suppl6

Acta Ichthyologica et Piscatoria 53, 2023, 243–251 | DOI 10.3897/aiep.53.114798

PENSOFT.

ACTA
ICHTHYOLOGICA
ET PISCATORIA

New records of two cusk eels of the genus *Neobythites* from Taiwan, with a northward range extension of *N. australiensis* Nielsen, 2002 (Actinopterygii: Ophidiiformes: Ophidiidae)

Yo SU[1], Hsiu-Chin LIN[1,2], Hsuan-Ching HO[3,4,5,6]

1 *Department of Marine Biotechnology and Resources, National Sun Yat-sen University, Kaohsiung, Taiwan*
2 *Doctoral Degree Program in Marine Biotechnology, National Sun Yat-sen University, Kaohsiung, Taiwan*
3 *Department and Graduate Institute of Aquaculture, National Kaohsiung University of Science Technology, Kaohsiung, Taiwan*
4 *National Museum of Marine Biology and Aquarium, Pingtung, Taiwan*
5 *Institute of Marine Biology, National Dong Hwa University, Pingtung, Taiwan*
6 *Australian Museum, Sydney, Australia*

https://zoobank.org/F0F9EE40-EFCA-4E57-BBC3-E87A9E1E8C60

Corresponding author: Hsaun-Ching Ho (ogcoho@gmail.com)

Academic editor: Ronald Fricke ◆ **Received** 27 October 2023 ◆ **Accepted** 31 October 2023 ◆ **Published** 7 December 2023

Citation: Su Y, Lin H-C, Ho H-C (2023) New records of two cusk eels of the genus *Neobythites* from Taiwan, with a northward range extension of *N. australiensis* Nielsen, 2002 (Actinopterygii: Ophidiiformes: Ophidiidae). Acta Ichthyologica et Piscatoria 53: 243–251. https://doi.org/10.3897/aiep.53.114798

Abstract

Two species of cusk eels, *Neobythites australiensis* Nielsen, 2002 and *Neobythites japonicus* Uiblein et Nielsen, 2023 were collected from southwestern and northeastern Taiwan, respectively. They represent the first record of both species from Taiwan. The former specimen represents the first record from the Northern Hemisphere, and the latter specimen represents the second record of *N. japonicus*. As a result, eight species of *Neobythites* are recognized in Taiwan. We provide a detailed description of the two specimens, comparison with other available specimens, discussion of intraspecific variations, and a dichotomous key to species of *Neobythites* in Taiwan.

Keywords

biodiversity, cusk eel, ichthyology, new record, Ophidiidae

Introduction

The cusk eel genus *Neobythites* Goode et Bean, 1885 is the most diverse group in the family Ophidiidae, with 60 species currently recognized as valid (Nielsen 2002; Nielsen et al. 2009; Ohashi et al. 2012; Uiblein and Nielsen 2018, 2021, 2023). Species of this genus are characterized by having a tapering caudal portion; operculum with one strong spine; pelvic-fin rays 2; medial basibranchial tooth patch 2; preopercle with 0 to 3 spines; snout length equal or longer than the width of eye window (Nielsen 2002).

Six *Neobythites* species have been documented from Taiwan (Yeh et al. 2005, 2006; Ohashi 2019), viz. *Neobythites bimaculatus* Nielsen, 1997, *Neobythites fasciatus* Smith et Radcliffe, 1913, *Neobythites longipes* Smith et Radcliffe, 1913, *Neobythites sivicola* (Jordan et Snyder, 1901), *Neobythites stigmosus* Machida, 1984, and *Neobythites unimaculatus* Smith et Radcliffe, 1913.

Neobythites australiensis Nielsen, 2002 was described based on specimens collected from western Australia. Subsequently, Okamoto et al. (2011) reported a single specimen collected from the Okinawa Island, representing the second record, and also the first record in the Northern Hemisphere. Uiblein and Nielsen (2023) reviewed the ocellus-bearing *Neobythites* from the western Pacific Ocean, described five new species, and recognized the specimen of *N. australiensis* reported by Okamoto et al. (2011) as a new species, *Neobythites japonicus* Uiblein et Nielsen, 2023.

Recently, two unusual specimens of *Neobythites* were collected from Taiwan. Both were initially identified as *N. australiensis* with several morphological differences noticed and the authors of the present publication submitted a report to document the new finding. However, with the five new species published by Uiblein and Nielsen (2023) during the reviewing process of the first version of this paper, we reviewed our study and re-identified them as *N. australiensis* and *N. japonicus*, respectively, based on their diagnostic characters newly proposed. As a result, the former specimen represents the first record of *N. australiensis* from the western Pacific Ocean and the latter represents the second specimen of *N. japonicus* other than the holotype. Here we provide detailed descriptions of these two specimens, compare them with those available specimens, and discuss the intraspecific variations. A dichotomous key to all *Neobythites* species in Taiwan is provided as well.

Materials and methods

Specimens were fixed with 10% formaldehyde and subsequently transferred to 70% ethanol for permanent preservation. Terminology and methodology follow Nielsen (2002) and Ohashi et al. (2012). Vertebral counts follow Nielsen et al. (1999). Description and measurement of otoliths follow Lin and Chang (2012) and Uiblein and Nielsen (2023). Paired-fin characters were presented as left/right when available. Only developed rakers are included in gill-raker counts. The term “ocellus” on the dorsal fin was defined as a dark blotch surrounded by a white ring (Nielsen 2002; Uiblein and Nielsen 2005, 2023). The counts of medial fins and vertebrae were determined by X-radiograph. Measurements were taken using 150 mm digital calipers or 300 mm calipers for lengths longer than 150 mm and rounding to the nearest 0.1 mm. Standard length (SL) and head length (HL) were used throughout except otherwise indicated. Specimens are deposited at the Pisces Collection, National Museum of Marine Biology and Aquarium, Pingtung, Taiwan (NMMB-P).

Comparative material. *Neobythites bimaculatus*: NMMB-P33881 (4 specimens, 106.9–117.0 mm SL), off Dong-sha Island (Pratas Island), 13 February 2019, collected by H.-C. Ho. *Neobythites longipes*: NMMB-P35534 (1, 183.6), off Dong-gang fishing port, 12 March 2023, collected by H.-C. Ho. *Neobythites sivicola*: NMMB-P 34995 (3, 126.5–157.8), off Diao-yu Islands, Yilan, northeastern Taiwan, 1 May 2020, collected by H.-C. Ho. *Neobythites stigmosus*: NMMB-P25803 (1, 152.4), off Ke-Tzu-Liao (ca. 22°42′53″N, 120°13′12″E), Kaohsiung, southwestern Taiwan, 29 March 2017, collected by H.-C. Ho. NMMB-P34112 (1, 159.7), off Dong-gang fishing port, 1 April 2019, collected by H.-C. Ho. *Neobythites unimaculatus*: NMMB-P24561 (1, 131.7), off Dong-gang fishing port, 11 February 2015, collected by H.-C. Ho.

Results

Family Ophidiidae
Genus *Neobythites* Goode et Bean, 1885

Neobythites australiensis Nielsen, 2002

English name: Australian cusk eel
Chinese name: 澳大利亞新鼬鳚
(Figs 1–2; Tables 1–3)

Neobythites australiensis Nielsen, 2002.—Nielsen (2002): 20 (Original description. Type locality: Southwest of Rowley Shoals, 18°04′35.99″S, 118°22′00″E, western Australia, depth 327–328 m).—Hoese et al. (2006): 562 (listed).—Uiblein and Nielsen (2005): 365 (in part).—Uiblein and Nielsen (2023): 187 (in part).

Specimen examined. NMMB-P37710, 1 specimen, 152.7 mm SL, off Dong-gang fishing port (ca. 22°22′22″N, 120°27′34″E), Pingtung, southwestern Taiwan, northern South China Sea, 12 March 2023, collected by H.-C. Ho.

Description of NMMB-P37710. Meristic and morphometric characters are provided in Tables 1–2. Dorsal-fin rays 92, originating over 5th vertebra. Pectoral-fin rays 27/29. Pelvic-fin rays 2/2. Anal-fin rays 73, originating below 21st dorsal-fin ray and 15th vertebra. Caudal-fin rays 4 (upper lobe) + 4 (lower lobe). Preopercular spines 2. Gill rakers on outer face of first gill arch 2 + 1 + 6 = 9. Pseudobranchial filaments 7. Precaudal vertebrae 13; caudal vertebrae 39 (not including ural centra); total vertebrae 52 (not including ural centra). Pyloric caeca 15.

Body compressed and elongated, depth at dorsal-fin origin 5.3 in SL, at anal-fin origin 5.4 in SL. Head length 4.5 in SL. Eye window small, horizontal width 5.1 in HL; snout rounded, its length 3.9 in HL, extending before premaxilla; interorbital space narrow, width 4.5 in HL; postorbital length 1.6 in HL.

Mouth large, upper-jaw length 1.8 in HL; posterior end of maxilla truncated, exceeding beyond vertical through posterior margin of eye window. Two nostrils, anterior nostril forming short tube and situated at about midline of snout; posterior nostril larger than anterior one, situated right in front of eye and lower than horizontal through anterior nostril. Symphysis of premaxillae forming notch, edentate. Premaxilla, dentary, vomer, and palatine with villiform teeth. Vomerine tooth patch triangular, slightly concave at both sides anteriorly. Palatine tooth patch rather broad, gradually thinner anteriorly. Opercle with one strong spine, its end not exceeding beyond flap of opercle.

Gill rakers rod-shaped, somewhat laterally compressed, covered with small teeth on tips and inner surfaces; rakers on outer row of first arch longest; inner surface of first arch and both inner and outer surfaces of second to fourth arches short; fifth ceratobranchail with bump-like rakers on outer face and single, long and slender tooth patch on inner face. Oval tooth patch present on upper ends of second and third epibranchials. Triangular tooth patch on second and third pharyngobranchials. Oval, somewhat rectangular tooth patch on fourth pharyngobranchial. Two basibranchials: anterior one elongated and posterior one oval.

Small cycloid scales present on head, body, and dorsal-and anal-fin bases, all embedded under skin. Lateral line single, situated at upper one-fifth of body; originating from upper part of gill opening and indistinct on posterior portion of body.

Pectoral fin short, its length 1.5 in HL, its tip slightly pointed, not reaching vertical through anus. Pelvic-fin length 1.2 in HL, rather short, its tip not reaching anus. Caudal fin rounded, slightly pointed.

Osteology (Fig. 1C). First neural spine short, length about half of second neural spine; bases of first-two neural spines not thickened; parapophysis developed on seventh to 13th vertebra; pleural ribs present on third to 12th vertebra, and with epipleural on anterior five pleural ribs; epineurals absent. Anal-fin pterygiophores anterior to first haemal spine 5.

Otolith. Sagittal otolith (Fig. 2) oblong, length 25.1% HL, length/depth ratio 1.84. Both dorsal and ventral margins smoothly curved, with small lobes forming crenation on antero-dorsal and both antero- and postero-ventral margins; distal surface slightly concave; proximal surface slightly convex. Sulcus groove mesial, shallow, horizontal, and archaesulcoid; its length 21.2% HL; both colliculums present, with ostial colliculum elongated and caudal colliculum oval; both crista superior and crista inferior

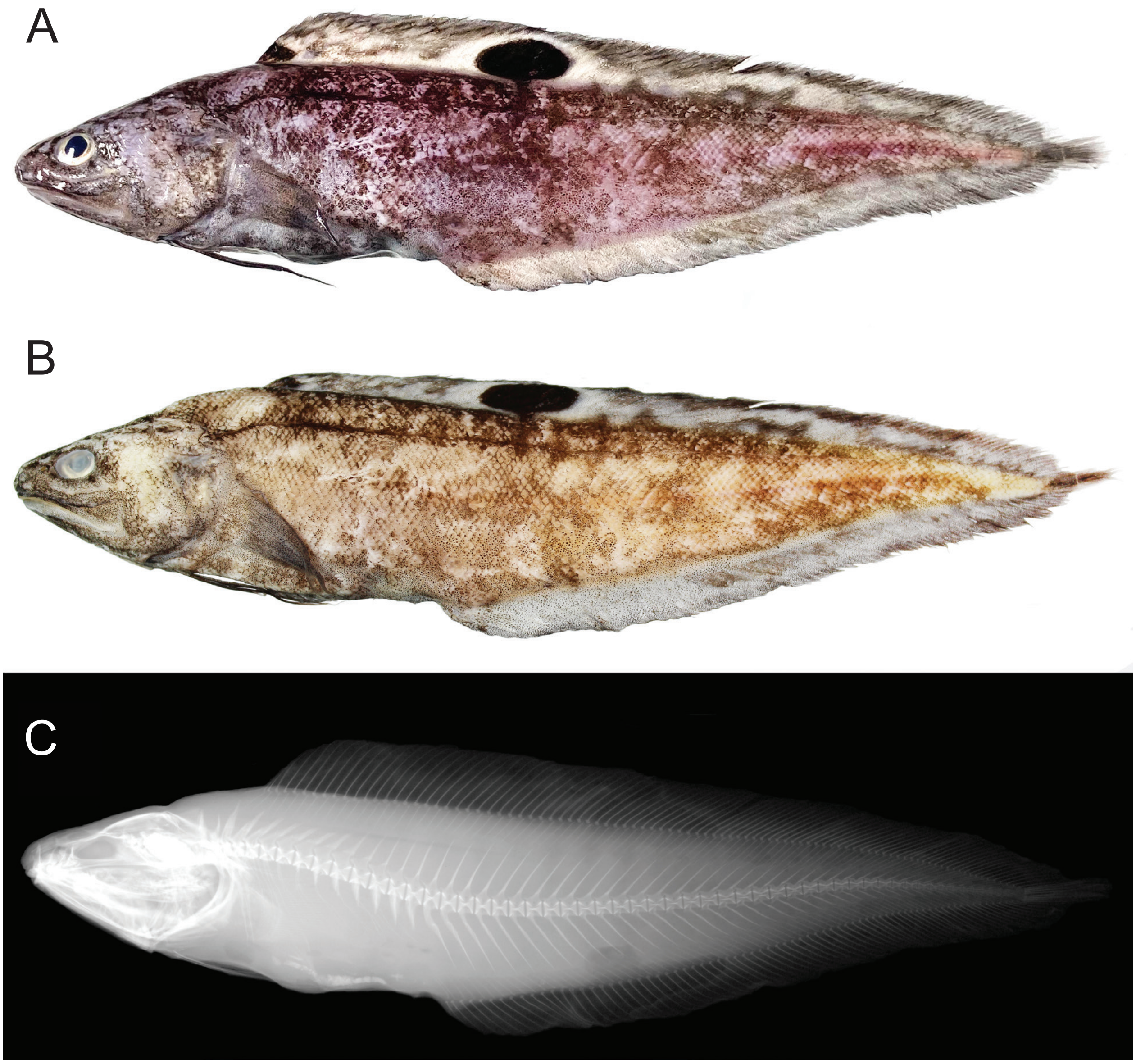

Figure 1. *Neobythites australiensis* Nielsen, 2002, NMMB-P37710, 152.7 mm SL. **A.** Fresh condition. **B.** Preserved condition. **C.** X-radiograph.

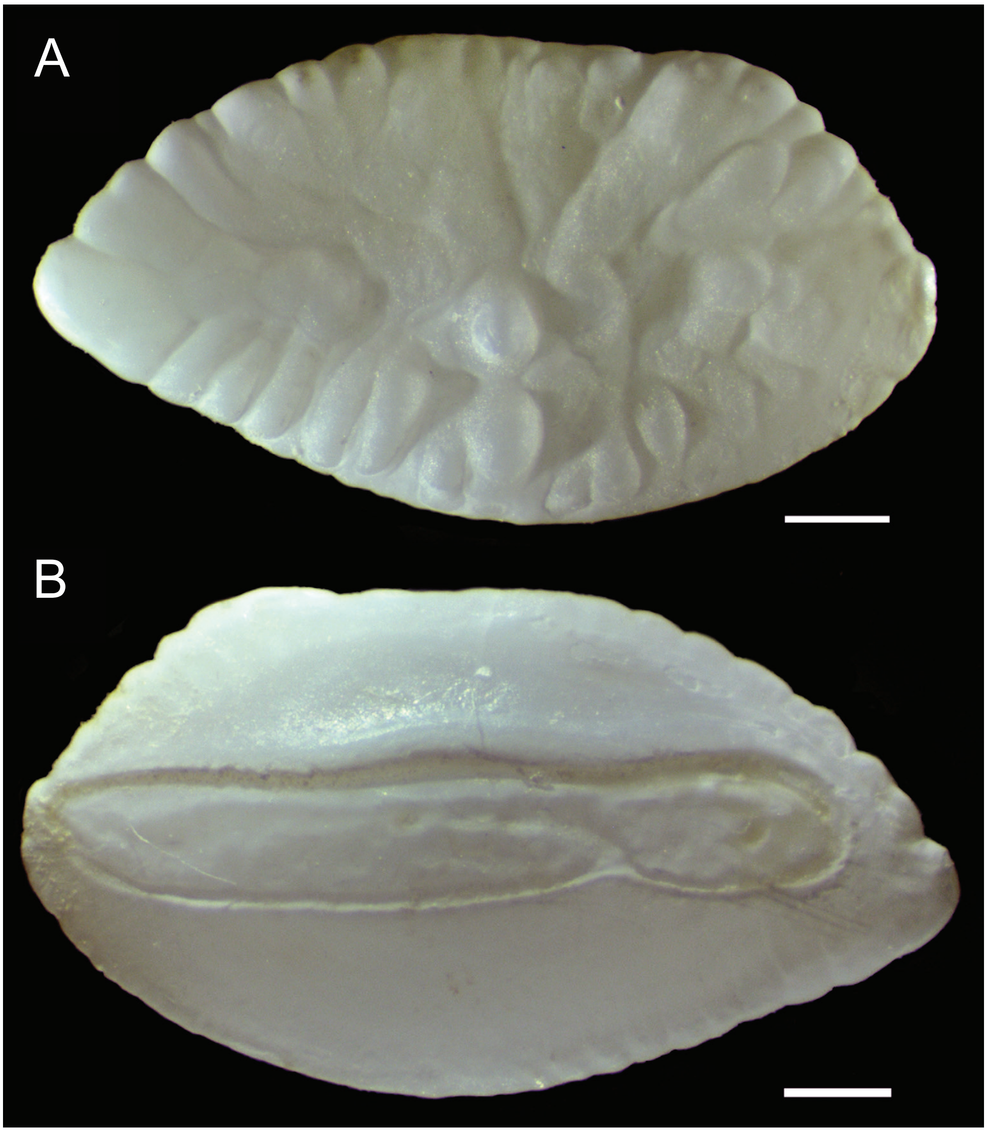

Figure 2. Right sagittal otolith of *Neobythites australiensis* Nielsen, 2002, 8.5 mm otolith length, taken from NMMB-P37710, 152.7 mm SL. **A**. Distal view. **B**. Proximal view. Scale bar = 1 mm.

Table 1. Meristic data of *Neobythites australiensis* Nielsen, 2002 and *N. japonicus* Uiblein et Nielsen, 2023. Data of other specimens were retrieved from Nielsen (2002) and Uiblein and Nielsen (2023). Paired-fin characters are presented as left/right.

	N. australiensis		***N. japonicus***	
Character	**This study**	**Nielsen 2002**	**This study**	**Uiblein and Nielsen 2023**
	NMMB-P37710	**Type specimens**	**NMMB-P37712**	**Holotype**
Dorsal-fin rays	92	88–92	91	91
Pectoral-fin rays	27/29	26–27	27/27	26
Anal-fin rays	73	73–77	75	75
Caudal-fin rays	4 + 4 = 8	8	4 + 4 = 8	8
Preopercular spines	2	2	2	2
Gill rakers	2 + 1 + 6 = 9	9–10	3 + 1 + 8 = 12	11
Pseudobranchial filaments	7	8–11	4	6
Vertebrae	13 + 39 = 52	13 + 40–41 = 53–54	13 + 40 = 53	13 + 39 = 52
Pyloric caeca	15	—	—	—
Dorsal-fin origin over vertebra	5th	5th–6th	5th	5th
Anal-fin origin under dorsal-fin ray	21st	21st–23rd	21st	21st
Anal-fin origin under vertebra	15th	16th–17th	15th	15th

poorly developed; rostrum absent; excisura absent; dorsal depression very shallow; ventral depression absent.

Coloration. When fresh (Fig. 1A), body somewhat purplish, with brown reticulate patterns on head and body. Dorsal fin dusky, with pale vermicular patterns. Anal fin dusky, without any ocellus, its anterior potion rather pale. Pectoral, pelvic, and caudal fins dusky. When preserved (Fig 1B), body color similar fresh but slightly paler. Sin-

Table 2. Morphometric data of *Neobythites australiensis* Nielsen, 2002 and *N. japonicus* Uiblein et Nielsen, 2023. Data of other specimens were retrieved from Nielsen (2002) and Uiblein and Nielsen (2023).

Character	*N. australiensis*		*N. japonicus*	
	This study	Nielsen 2002	This study	Uiblein and Nielsen 2023
	NMMB-P37710	Type specimens	NMMB-P37712	Holotype
Absolute values [mm]				
SL	152.7	180–245	158.9	167
Relative values (% SL)				
HL	22.0	23.5–24.5	22.6	23.0
Snout length	5.7	—	5.4	—
Horizontal eye window	4.3	4.2–4.7	4.3	4.1
Postorbital length	13.5	14.0–15.5	13.9	14.0
Interorbital width	4.9	—	5.5	—
Upper-jaw length	12.1	12.0–13.5	11.9	11.0
Pectoral-fin length	14.5	—	14.7	—
Pelvic-fin length	17.8	14.0–19.0	17.5	16.0
Predorsal length	24.2	24.5–27.5	24.6	25.0
Prepectoral length	22.4	—	22.7	—
Prepelvic length	16.3	—	17.0	—
Preanal length	41.7	43.0–49.5	43.0	44.0
Body depth at dorsal-fin origin	19.0	—	19.8	—
Body depth at anal-fin origin	18.6	17.5–19.5	19.4	18.0
Pelvic-fin–anal-fin length	26.4	24.5–29.0	27.3	27.0
Snout to ocelli	45.1	44.5–49.0	49.4	46.0
Longest gill filament on anterior gill arch	1.7	1.6–1.8	1.7	1.6
Relative values (% HL)				
Longest gill filament on anterior gill arch	7.7	6.7–7.4	7.6	7.1

HL = head length, SL = standard length.

gle ocellus on dorsal fin, covering 19th–35th dorsal-fin rays, with central blotch covering 21st–30th dorsal-fin rays; anterior dorsal fin with single black blotch, covering 1st–4th dorsal-fin rays. Oral cavity, including underside of tongue, lower gill arches, and rakers pale or scattered with sparse melanophores; pyloric caeca pale. Mouth roof behind vomer, inner face of opercle, and upper gill arches dusky. Peritoneum black.

Distribution. Originally described from northwestern Australia. Although Uiblein and Nielsen (2023) described the previous record from the Pacific Ocean (Okamoto et al. 2011) as *N. japonicus*, the presently reported specimen from Taiwan confirmed the occurrence of this species and suggested a wide distribution in the west Pacific and east Indian Ocean. Inhabits depths down to 350 m (Nielsen 2002).

Remarks. The presently reported specimen was identified as *Neobythites australiensis* in having one ocellus on the dorsal fin, situated posterior to a vertical through the anus; a black blotch on anterior dorsal fin; no ocellus on the anal fin; two preopercular spines; short pelvic fins, their tips not reaching anus (Nielsen 2002).

However, there are a number of differences compared to the previous record (Tables 1–2). The Taiwanese specimen has slightly fewer pseudobranchial filaments (7, vs. 8–11); fewer caudal vertebrae (39, vs. 40–41); shorter head length (22.0% SL, vs. 23.5–24.5% SL); shorter postorbital length (13.5% SL, vs. 14.0–15.5% SL); shorter predorsal length (24.2% SL, vs. 24.5–27.5% SL); shorter preanal length (41.7% SL, vs. 43.0–49.5% SL); and longer anterior gill filaments (7.7% SL, vs. 6.7–7.4% SL). These minor differences are considered as intraspecific variations. The condition of 29 pectoral-fin rays on right side of our specimen is higher than other known specimens (26–27).

Among species recorded in Taiwan, *N. australiensis* most resembles *N. unimaculatus* in having one ocellus on the dorsal fin (vs. none or more than one in other species), however, *N. australiensis* is readily distinguishable from *N. unimaculatus* in having a blotch situated at the anterior most dorsal-fin rays (vs. blotch absent; Nielsen 2002; this study); dorsal-fin rays 88–92 (vs. 99–106); anal-fin rays 73–75 (vs. 83–92); total vertebrae 52–54 (vs. 57–62).

Neobythites japonicus Uiblein et Nielsen, 2023

English name: Japanese cusk eel
New Chinese name: 日本新鼬鳚
(Figs 3–4; Tables 1–3)

Neobythites japonicus Uiblein et Nielsen, 2023.—: Uiblein and Nielsen (2023): 188 (Original description. Type locality: West of Okinawa Island, Japan, depth ca. 100 m. Holotype: KAUM–I. 37071).

Neobythites australiensis (non Nielsen).—Okamoto et al. (2011): 69 (misidentification).

Specimen examined. NMMB-P37712, 1 specimen, 158.9 mm SL, off Daxi fishing port (ca. 24°53′37″N, 121°55′26″E), 30 Jan 2023, collected by J.-F. Huang.

Description of NMMB-P37712. Meristic and morphometric characters are provided in Tables 1–2. Dorsal-fin rays 92, originate over 5th vertebra. Pectoral-fin rays 27/27. Pelvic-fin rays 2/2. Anal-fin rays 75, originate below 21st dorsal-fin ray and 15th vertebra. Caudal-fin rays 4 (upper lobe) + 4 (lower lobe). Preopercular spines 2. Gill rakers on outer face of first gill arch 3 + 1 + 8 = 12. Pseudobranchial filaments 4. Precaudal vertebrae 13; caudal vertebrae 40 (not including ural centra); total vertebrae 53 (not including ural centra).

Body compressed and elongated, depth at dorsal-fin origin 5.0 in SL, at anal-fin origin 5.2 in SL. Head length 4.4 in SL. Eye window small, horizontal width 5.3in HL; snout rounded, its length 4.1 in HL, extending before premaxilla; interorbital space narrow, width 4.1 in HL; postorbital length 1.6 in HL. Mouth large, upper-jaw length 1.9 in HL; posterior end of maxilla truncated, exceeding beyond vertical through posterior margin of eye window. Two nostrils, anterior nostril forming short tube and situated at about midline of snout; posterior nostril oval, larger than anterior one situated in front of eye and lower than horizontal through ventral margin of eye window. Symphysis of premaxillae forming notch, edentate. Premaxilla, dentary, vomer, and palatine with villiform teeth. Vomerine tooth patch triangular, slightly concave at both sides anteriorly. Palatine tooth patch rather broad, slightly widened at middle portion. Opercle with one strong spine, its end not exceeding beyond flap of opercle.

Gill rakers rod-shaped, somewhat laterally compressed, covered with small teeth on tips and inner surfaces; rakers on outer row of first arch longest; inner surface of first arch and both inner and outer surfaces of second to fourth arches short; fifth ceratobranchail with bump-like rakers on outer face and single, long and slender tooth patch on inner face. Oval tooth patch present on upper ends of second and third epibranchials. Triangular tooth patch on second and third pharyngobranchials. Oval, somewhat rectangular tooth patch on fourth pharyngobranchial. Two basibranchials: anterior one slender and elongated, with anterior portion wider than rest; posterior one oval.

Small cycloid scales present on head, body, and dorsal-and anal-fin bases, all embedded under skin. Lateral line single, situated at upper one-fifth of body; originating from upper part of gill opening and indistinct on posterior portion of body.

Pectoral fin short, its length 1.5 in HL, its tip slightly pointed, not reaching vertical through anus. Pelvic-fin length 1.3 in HL, rather short, its tip not reaching anus. Caudal fin rounded, slightly pointed.

Osteology (Fig. 3C). First neural spine short, length about half of second neural spine; bases of first-two neural spines not thickened; parapophysis developed on eighth to 13th vertebra; pleural ribs present on third to 12th vertebra, and with epipleural on anterior seven pleural ribs epineurals absent. Anal-fin pterygiophores anterior to first haemal spine 4.

Otolith. Sagittal otolith (Fig. 4) oblong, length 24.1% HL, length/depth ratio 1.82. Both dorsal and ventral margins smoothly curved, with small lobes forming crenation on antero-dorsal and both antero- and postero-ventral margins; distal surface slightly concave; proximal surface slightly convex. Sulcus groove mesial, shallow, horizontal, and archaesulcoid; its length 19.1% HL; both colliculums present, with ostial colliculum elongated and caudal colliculum oval; both crista superior and crista inferior poorly developed; rostrum absent; excisura absent; dorsal depression very shallow; ventral depression absent.

Coloration. When fresh (Fig. 3A), body pale, and somewhat purplish, with brown reticulate patterns on

Table 3. Morphometric data of sagittal otoliths of *Neobythites australiensis* Nielsen, 2002 and *N. japonicus* Uiblein et Nielsen, 2023. Data of other specimens were retrieved from Uiblein and Nielsen (2023).

Character	*N. australiensis*		*N. japonicus*	
	This study	**Uiblein and Nielsen 2023**	**This study**	**Uiblein and Nielsen 2023**
	NMMB-P37710	**Type specimens**	**NMMB-P37712**	**Holotype**
		Absolute values [mm]		
SL	152.7	180–245	158.9	167
HL	33.6	—	35.9	—
		Relative values (% SL)		
Otolith length	5.5	5.8–5.9	5.4	5.3
Otolith height	3.0	2.7–2.9	3.0	2.6
Sulcus length	4.7	4.7–4.8	4.3	4.2
Ostium length	3.1	3.1–3.3	3.0	2.9
Ostium height	0.76	0.63–0.64	0.84	0.65
		Relative values (% HL)		
Otolith length	25.1	—	24.1	—
Otolith height	13.7	—	13.3	—
Sulcus length	21.2	—	19.1	—
Ostium length	14.3	—	13.2	—
Ostium height	3.5	—	3.7	—
		Relative values (% sulcus length)		
Ostium length	67.4	66.0–70.0	69.1	69.0
Ostium height	16.2	13.0–14.0	19.6	15.0
		Relative values (% ostium length)		
Ostium height	24.1	19.0–20.0	28.3	23.0

HL = head length, SL = standard length.

head and body, some of which forming blotches. Dorsal fin dusky, with irregular-sized pale blotches. Anal fin dusky, without any ocellus, its anterior potion rather pale. Both margins of dorsal and anal fins whitish. Pectoral, pelvic, and caudal fins dusky. When preserved (Fig. 3B), body color similar fresh but slightly paler. Two ocelli present on dorsal fin, anterior one covering 1st–11th dorsal-fin rays, with central blotch covering 4th–9th dorsal-fin rays; posterior one covering 21st–35th dorsal-fin rays, with central blotch covering 23rd–33rd dorsal-fin rays. Oral cavity, including underside of tongue, lower gill arches, and rakers pale or scattered with sparse melanophores. Mouth roof behind vomer, upper gill arches, and inner face of opercle dusky. Peritoneum black.

Distribution. Originally described from the Okinawa Island, Japan (Okamoto et al. 2011; Uiblein and Nielsen 2023). The presently reported specimen represents the second specimen other than the holotype and the southernmost record of this species. Inhabits depths down to ca. 100 m (Okamoto et al. 2011).

Remarks. The presently reported specimen was identified as *N. australiensis* before Uiblein and Nielsen (2023) described *N. japonicus*. It was soon re-identified as *N. japonicus* in having two ocelli on the dorsal fin, the first situated at anterior-most dorsal-fin rays and the second situated posterior to a vertical through the anus; no ocellus on the anal fin; two preopercular spines; short pelvic fins, their tips not reaching anus (Uiblein and Nielsen 2023).

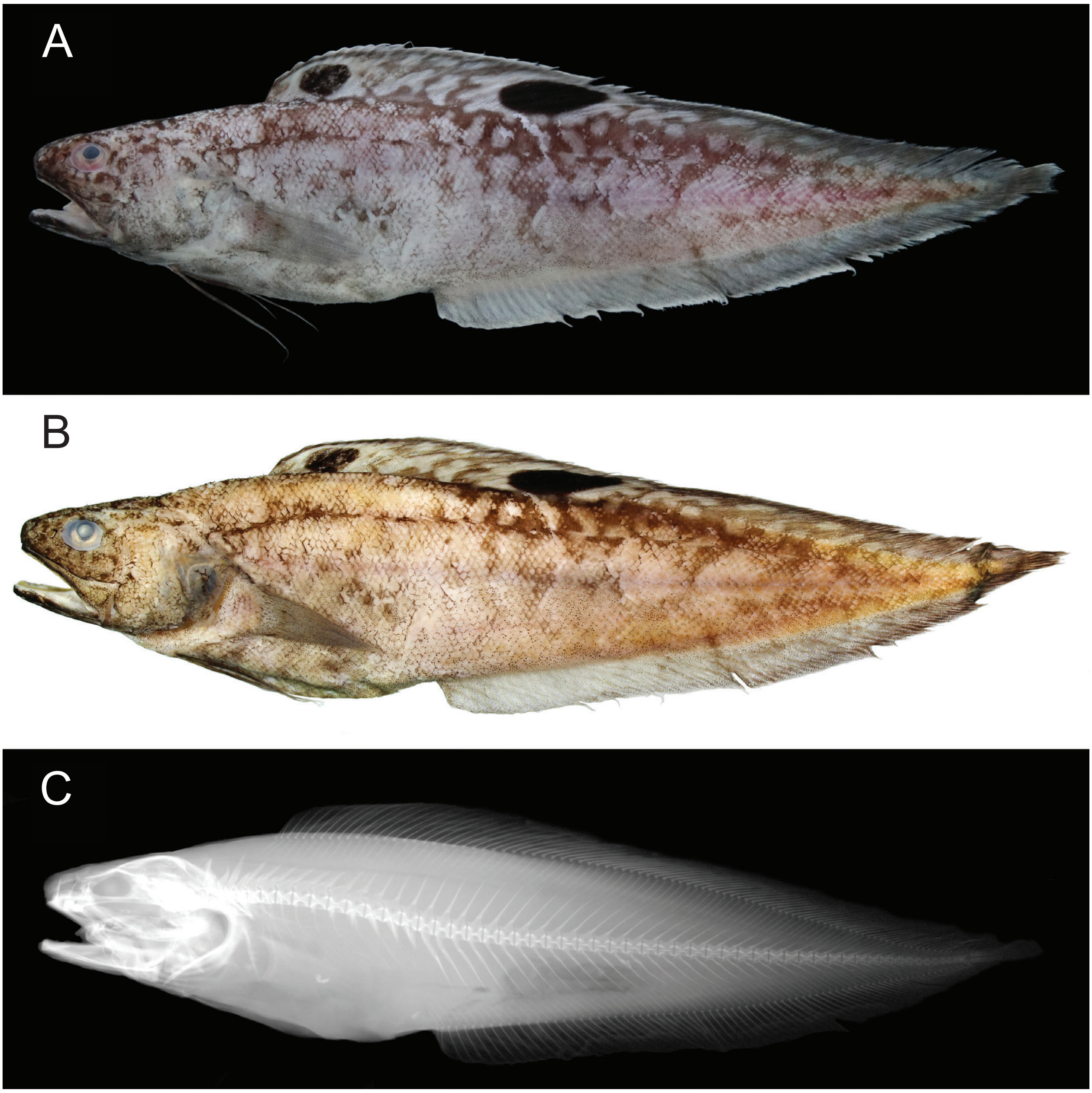

Figure 3. *Neobythites japonicus* Uiblein et Nielsen, 2023, NMMB-P37712, 158.9 mm SL. **A.** Fresh condition, photo by J.-F. Huang. **B.** Preserved condition. **C.** X-radiograph.

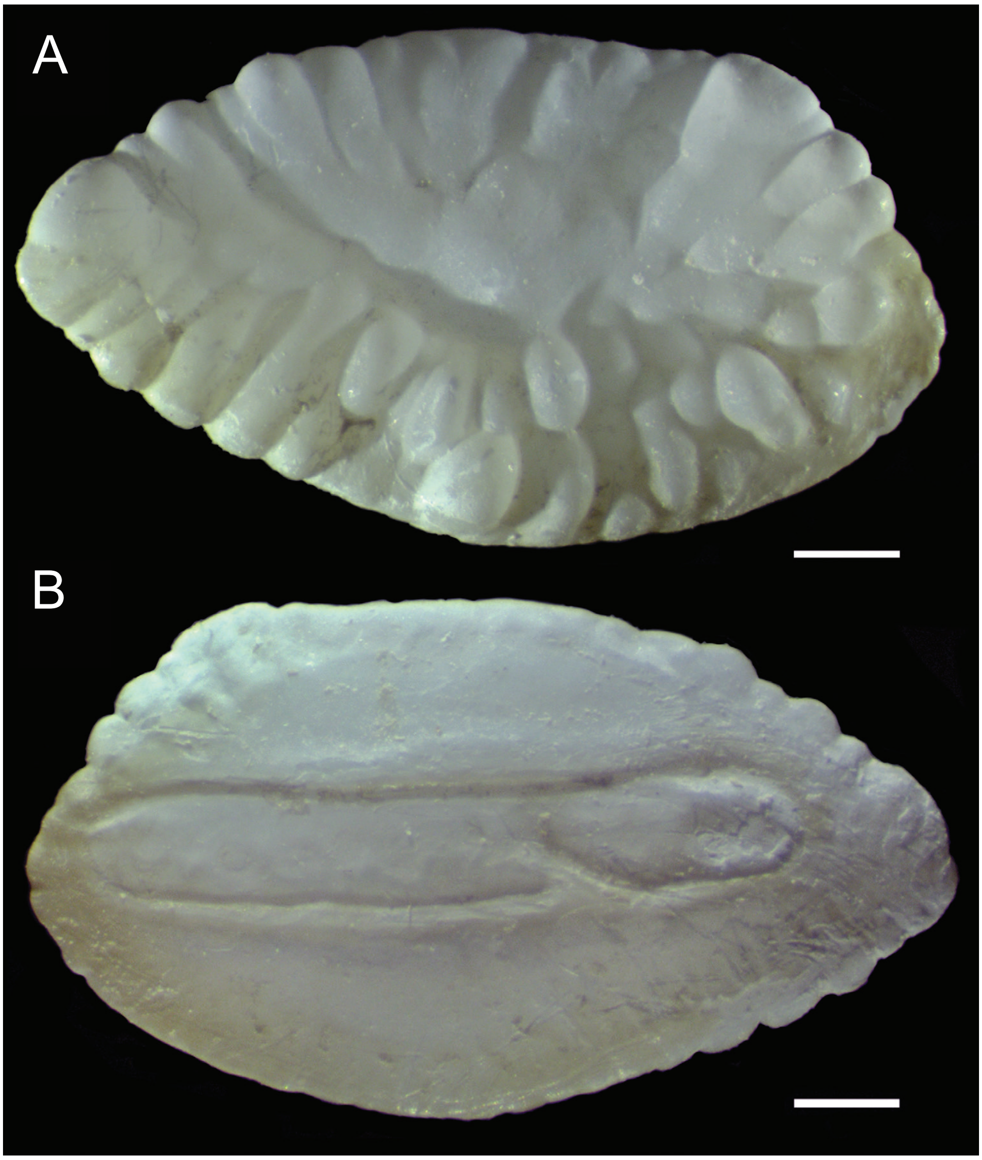

Figure 4. Right sagittal otolith of *Neobythites japonicus* Uiblein et Nielsen, 2023, 8.7 mm otolith length, taken from NMMB-P37712, 158.9 mm SL. **A**. Distal view. **B**. Proximal view. Scale bar = 1 mm.

However, there are still a number of minor differences comparing to the holotype (Tables 1–2). The Taiwanese specimens have fewer pseudobranchial filaments (4, vs. 6); more caudal vertebrae (40, vs. 39); shorter preanal length (43.0% SL, vs. 44.5% SL); and longer anterior gill filaments (7.6% HL, vs. 7.0% HL). These differences are considered as intraspecific variations.

Among species recorded in Taiwan, *N. japonicus* mostly resembles *N. bimaculatus* in having two ocelli (sometimes three) on the dorsal fin (vs. one or more than two in other species). However, *N. japonicus* is readily distinguishable from *N. bimaculatus* in having the anterior ocelli situated at the anteriormost dorsal-fin rays and the posterior ocelli situated at the middle portion of the dorsal fin (vs. both ocelli at the middle portion of the dorsal fin, sometimes a third ocellus present (Nielsen 1997, 2002; this study); dorsal-fin rays 91 (vs. 99–106); anal-fin rays 75 (vs. 83–92); total vertebrae 53 (vs. 57–62).

Key to species *Neobythites* from Taiwan

1A Dorsal fin without ocelli or blotches .... *N. sivicola*
1B Dorsal fin with ocelli or blotches 2
2A Pelvic fin long, their ends reaching anus.. *N. longipes*
2B Pelvic fin short, their ends not reaching anus.. 3
3A Anal fin with ocelli or blotches 4
3B Anal fin without ocelli or blotches 5

4A Four ocelli on dorsal fin .... *N. fasciatus*
4C Three ocelli on dorsal fin .... *N. stigmosus*
5A One ocellus on dorsal fin.. 6
5B Two ocelli on dorsal fin.. 7
6A Dorsal-fin rays 99–106; anal-fin rays 83–92; anterior dorsal fin without black blotches............. *N. unimaculatus*
6B Dorsal-fin rays 88–92; anal-fin rays 73–75; anterior dorsal fin with a small black blotch.............*N. australiensis*
7A Dorsal-fin rays 99–106; anal-fin rays 83–92; dorsal fin with two ocelli behind central ocellus...... *N. bimaculatus*
7B Dorsal-fin rays 91; anal-fin rays 75; dorsal fin without ocelli behind central ocellus .... *N. japonicus*

Acknowledgments

We thank J.-F. Huang for providing specimen of *N. japonicus* and its fresh photo; P.-N. Lee (NMMBA) for curatorial assistance; M.-H. Chiang (NMMBA) for assistance in X-radiograph. This study was supported by National Museum of Marine Biology and Aquarium and National Kaohsiung University of Science Technology.

References

Hoese DF, Paxton JR, Gates JE, Bray DJ (2006) Ophidiidae. Pp. 556–566. In: Hoese DF, Bray DJ, Paxton JR, Allen GR (Eds.) Zoological Catalogue of Australia. CSIRO Publishing, Collingwood. Zoological Catalogue of Australia. Volume 35. Fishes, pt.1, 556.

Lin C-H, Chang C-W (2012) Otolith atlas of Taiwan fishes. National Museum of Marine Biology and Aquarium, Pingtung, Taiwan, 416 pp. [In Chinese and English]

Nielsen JG (1997) Deepwater ophidiiform fishes from off New Caledonia with six new species. Pp. 51–82. In: Séret B (Ed.) Résultats des Campagnes MUSORSTOM, Vol. 17. Mémoires du Muséum National d'Histoire Naturelle, Paris (N.S.) (Série A) Zoologie 174.

Nielsen JG (2002) Revision of the Indo–Pacific species of *Neobythites* (Teleostei, Ophidiidae), with 15 new species. Galathea Report 19: 5–104.

Nielsen JG, Cohen DM, Markle DF, Robins CR (1999) Ophidiiform fishes of the world (Order Ophidiiformes). An annotated and illustrated catalogue of pearlfishes, cusk-eels, brotulas and other ophidiiform fishes known to date. FAO, Rome, 178 pp.

Nielsen JG, Uiblein F, Mincarone MM (2009) Ocellus-bearing *Neobythites* species (Teleostei: Ophidiidae) from the west Atlantic with description of a new species. Zootaxa 2228(1): 57–68. https://doi.org/10.11646/zootaxa.2228.1.4

Ohashi S (2019) Family Ophidiidae. Pp. 381–392. In: Koeda K, Ho H-C (Eds.) Fishes of southern Taiwan. National Marine Museum of Biology and Aquarium, Checheng, Taiwan. [In Chinese and English]

Ohashi S, Nielsen JG, Yabe M (2012) A new species of the ophidiid genus *Neobythites* (Teleostei: Ophidiiformes) from Tosa Bay, Kochi Prefecture, Japan. Bulletin of the National Museum of Natural Science. Ser. A. (Suppl. 6): 27–32.

Okamoto M, Nielsen JG, Motomura H (2011) First record of the cusk-eel, *Neobythites australiensis* Nielsen (Ophidiiformes: Ophidiidae), from the Northern Hemisphere. Biogeography. International Journal of Biogeography, Phylogeny, Taxonomy, Ecology, Biodiversity, Evolution, and Conservation Biology 13: 69–71.

Uiblein F, Nielsen JG (2005) Ocellus variation and possible functions in the genus *Neobythites* (Teleostei: Ophidiidae). Ichthyological Research 52(4): 364–372. https://doi.org/10.1007/s10228-005-0298-y

Uiblein F, Nielsen JG (2018) Review of the steatiticus-species group of the cuskeel genus *Neobythites* (Ophidiidae) from the Indo–Pacific, with description of two new species. Zootaxa 4387(1): 157–173. https://doi.org/10.11646/zootaxa.4387.1.7

Uiblein F, Nielsen JG (2021) New record of the cuskeel genus *Neobythites* (Pisces, Ophidiidae) from the Solomon Sea with description of a new species and notes on colour patterns. Cybium 45(2): 83–88. https://doi.org/10.26028/cybium/2021-452-001

Uiblein F, Nielsen JG (2023) Five new ocellus-bearing species of the cusk-eel genus *Neobythites* (Ophidiidae, Ophidiiformes) from the west Pacific, with establishment of three new species groups. Zootaxa 5336(2): 179–205. https://doi.org/10.11646/zootaxa.5336.2.2

Yeh HM, Lee MY, Shao KT (2005) Fifteen Taiwanese new records of ophidiid fishes (Pisces: Ophidiidae) collected from the deep waters by the RV '*Ocean Researcher I*'. Taiwan Shuichanxue Hui Kan 32(3): 279–299. https://doi.org/10.29822/JFST.200509.0008

Yeh HM, Lee MY, Shao KT (2006) *Neobythites longipes* Smith and Radcliffe, 1913, a Taiwanese new record of ophidiid fish (Pisces: Ophidiidae). Taiwan Shuichanxue Hui Kan 33(4): 357–364. https://doi.org/10.29822/JFST.200612.0006

Acta Ichthyologica et Piscatoria 53, 2023, 253–261 | DOI 10.3897/aiep.53.113220

PENSOFT.

ACTA
ICHTHYOLOGICA
ET PISCATORIA

TNF-A, IL-6, HSP-70, fish growth hormone, and growth performance of sea trout, *Salmo trutta* (Actinopterygii: Salmoniformes: Salmonidae) after long-term dietary administration of β-glucan and BGN-2

Olga REVINA[1,2], Vjačeslavs REVINS[1], Dina CĪRULE[1], Anda VALDOVSKA[2]

1 *Institute of Food Safety, Animal Health and Environment BIOR, Rīga, Latvia*
2 *Latvia University of Life Sciences and Technologies, Jelgava, Latvia*

https://zoobank.org/EC9722BB-24CD-4FA6-9022-849F780D8669

Corresponding author: Olga Revina (dr.revina@gmail.com)

Academic editor: P. Simonović ♦ **Received** 24 September 2023 ♦ **Accepted** 15 November 2023 ♦ **Published** 14 December 2023

Citation: Revina O, Revins V, Cīrule D, Valdovska A (2023) TNF-A, IL-6, HSP-70, fish growth hormone, and growth performance of sea trout, *Salmo trutta* (Actinopterygii: Salmoniformes: Salmonidae) after long-term dietary administration of β-glucan and BGN-2. Acta Ichthyologica et Piscatoria 53: 253–261. https://doi.org/10.3897/aiep.53.113220

Abstract

The presently reported study intended to examine the effect of the oral administration of an immunomodulator β-glucan and β-glucan-containing product (BGN-2) on the levels of tumor necrosis factor-alpha (TNF-α), interleukin-6 (IL-6), fish heat shock protein 70 (HSP-70), and fish growth hormone (GH) as well as growth performance of cultured sea trout juveniles. The sea trout is a migratory sea-run brown trout, *Salmo trutta* Linnaeus, 1758. The fish (total of 15 000) were divided into four experimental and one control group including control (consisting of basal diet) (D1); basal diet + 1 g kg^{-1} β-glucan (D2); basal diet + 3 g kg^{-1} β-glucan (D3); basal diet + 6 g kg^{-1} BGN-2 (D4); basal diet + 14 g kg^{-1} BGN-2 (D5). The fish fed D4 and D5 diets showed significantly higher IL-6, HSP-70, and GH expression levels than other treatments ($P < 0.05$). Sea trout fed D4 and D5 diets showed significant improvements in growth performance compared to the fish fed the control diet. In conclusion, our results suggest that dietary supplementation with the product BGN-2 provides great immunostimulation and could be used as an effective measure to improve growth performance in juvenile sea trout.

Keywords

glucan, immunostimulants, sea trout

Introduction

The decline of wild salmonid populations is a direct result of extensive human influence and the consequences of climate change on their natural environment (Fraser 2008). The sea trout is a historically significant fish species for Latvia. The sea trout is a migratory sea-run brown trout, *Salmo trutta* Linnaeus, 1758. Latvia has a long tradition of artificial rearing salmonid fishes, dating back more than 130 years. The principal species have been "Baltic" Atlantic salmon, *Salmo salar* Linnaeus, 1758) and sea trout (brown trout), *Salmo trutta* (Purvina et al. 2019). Currently, Latvia is actively involved in the artificial reproduction and conservation of the natural sea trout population. During the juvenile stage, sea trout exhibit slow growth. According to the *Restocking plan of fish resources, 2017–2020 (Latvia)* (Kučinskis and Dūklavs 2016) state fish hatcheries can release sea trout when the mean weight of the group reaches 15 g, with the smallest fish in the group weighing at least 13 g. It is of utmost importance for Latvian state fish hatcheries to rear high-weight and healthy sea trout on time.

Therefore, there is a pressing need for well-structured breeding and rearing initiatives that emphasize nutritional approaches. This includes the study of feeding behaviors and the development of initial diets that are crafted from ecologically sustainable components (Fraser 2008; Hoffmann et al. 2021). One of the most persuasive immunity boosters in aquaculture is β-glucan (Ringø et al. 2011; Vetvicka et al. 2013). In order to increase disease resistance (thereby reducing the use of antibiotics), improve growth performance and weight gain, and support fish health immunostimulants have been used as dietary additives in cultured fish (Vallejos-Vidal et al. 2016).

Immunological studies prove that the immune system of fish is comparable to those of mammals, characterized by different types of leukocytes, complement factors, immunoglobulins (Ig), toll-like receptors (TLRs), major histocompatibility complex (MHC), T-cell receptors (TCR), and cytokines (Sakamoto and McCormick 2006; Yada 2007; Firdaus-Nawi and Zamri-Saad 2016). β-glucan stands out as an effective immunostimulant due to its remarkable ability to bind to various receptors on immune cells, primarily leukocytes. β-glucan is detected by complement receptor C3 and TLRs. This binding triggers a cascade of immune responses, including heightened bactericidal activity, increased cytokine production, and enhanced cellular survival capacity. Upon encountering these immune cell surface receptors, β-glucan prompts the release of cytokines (e.g., tumor necrosis factor-alpha (TNF-α); interleukins, interferons, lymphokines, and chemokines) (Brown et al. 2003; Hadiuzzaman et al. 2022). This process has been observed to activate immunocompetent cells in fish, such as monocytes, macrophages, and neutrophils, which subsequently engage in pathogen elimination through mechanisms like phagocytosis, oxidative burst, and cytotoxic killing activities. Additionally, β-glucan contributes to the generation of immunological memory and specific antibodies by activating T and B lymphocytes (Hadiuzzaman et al. 2022).

Researchers have demonstrated that β-glucan can modulate essential biochemical markers, such as serum hemoglobin, serum protein, and total hemocyte count, as well as crucial immunological parameters like lysozyme activity, phagocytic activity, oxidative burst activity, and phenoloxidase activity. This leads to a more robust immune profile, making it highly valuable in the treatment of fish and aquatic organisms. Fish supplemented with β-glucan have shown reduced sensitivity in genes associated with acute inflammatory reactions (Falco et al. 2012; Miest et al. 2016; Hadiuzzaman et al. 2022).

TNF-α and interleukin-6 (IL-6) are among the most significant cytokines produced by macrophages and monocytes and are listed as a humoral immune component (Calder 2007). TNF-α is a multifunctional cytokine involved in systemic inflammation and has pro-inflammatory and anti-inflammatory properties (Costa et al. 2011; Zou and Secombes 2016; Eggestøl et al. 2020). It also plays a major role in the regulation of immune responses, hematopoiesis, multiple homeostatic, and controlling infection (Atzeni and Sarzi-Puttini 2013; Hong et al. 2013).

Heat shock proteins (HSPs) are a family of highly conserved stress proteins that are produced by cells in response to stressful conditions and are indicators of cellular stress and animal health status (Cara et al. 2005). HSP expression is influenced by a variety of biological stressors, such as infectious pathogens, and abiotic factors, such as sudden changes in water temperature and environmental pollutants (Iwama et al. 1998). HSPs are classified by their molecular weight (kilodalton): HSP40, HSP70, etc. (Li and Srivastava 2003; Kumar et al. 2015).

Fish growth hormone (GH) has a role in feeding, growth-promoting, immune function, and osmoregulation in teleost fish (Lal and Singh 2005; Sakamoto and McCormick 2006). Smith (1956) was the first to describe the positive effects of GH treatment on salinity tolerance, and increased capacity of brown trout (*Salmo trutta*). Later it became known that this consequence was due to the ability of GH to raise the size and number of gill chloride cells, Na(+)/K(+)/2Cl(–) cotransporter (NKCC) and Na(+)/K(+)-ATPase (NKA), branchial ion transporters necessitated in salt secretion (Tipsmark et al. 2002; McCormick et al. 2009). For anadromous salmonids, GH plays an essential role in parr–smolt transformation and adaptation for seawater entry (Sakamoto and McCormick 2006). Smoltification includes many metabolic and behavioral changes, as well as the development of hypoosmoregulatory ability (Stefansson et al. 1991).

The presently reported study intended to investigate the immunomodulatory effects of two *Saccharomyces cerevisiae*-derived (yeast) β-glucan products on juvenile sea trout. These products included a commercially available purified β-glucan product (Angel Yeast Co., Ltd., China), as well as a biological product known as BGN-2 (JP Biotechnology, Ltd., Latvia), using a patented technological method. BGN-2 comprises derivatives of the yeast *S. cerevisiae* obtained during the ethanol production process from grain (Revina et al. 2019, 2020).

In the presently reported study, the hypothesis suggests that the prolonged administration of various oral doses of β-glucan products exerts an influence on the expression of TNF-α, IL-6, HSP-70, and GH, potentially enhancing both the health and growth performance of sea trout.

Materials and methods

Experimental fish and culture condition. The research was developed at the state fish farm Pelci of the Institute of Food Safety, Animal Health and Environment BIOR, Latvia (56°55′16.3″N, 021°58′28.6″E) (Pelci) using riverine water.

At the farming trial, 15 000 sea trout juveniles (2.3 ± 0.30 g, mean weight ± SE) were randomly placed into five 1.8 m^3 tanks (n = 3000 in each tank), with a volume of 1.2 m^3, in a flow-through rearing system. The quality of water was regularly monitored. The fish were acclimated for 2 weeks.

All of the sea trout used in the trial were planned to be released in natural watercourses in April of the same year, according to the *Restocking plan of fish resources 2017–2020, Latvia* (Kučinskis and Dūklavs 2016). This study was carried out in strict accordance with the recommendations of the national regulations on ethics and research in Latvia (Rozenkopfs and Rudze 2003). All efforts were made to minimize animal suffering according to the guidelines of Latvian law and EU directive No. 2010/63/EU (Anonymous 2010).

Fish diet and preparation of feed. A basal diet was formulated according to the nutrition requirement of sea trout (National Research Council 1999; Kamalam et al. 2020). The basal diet was the commercial dry diet for fish Aller Futura EX (Aller Aqua, Ltd., Poland) (appropriated size according to Aller Aqua manufacturer recommendations). The specific composition of the formulation is considered proprietary information held by Aller Aqua. However, based on the information provided on the label, the feed appears to contain a mixture of ingredients, including fish meal, fish oil, functional ingredients, grain products, krill meal, single-cell proteins, vegetable proteins, vitamins, and minerals. To prepare experimental diets, β-glucan powder (Angel Yeast Co, Ltd., China; extracted from *S. cerevisiae*) and BGN-2 powder (JP Biotechnology, Ltd., Latvia) were added to the basal diet. The experimental diets were top-coated with rapeseed (*Brassica napus*) oil, mixed with supplements and air-dried (Revina et al. 2019, 2020).

Five experimental diets were designed as follows: control (consisting of basal diet) (D1), basal diet + 1 g kg^{-1} β-glucan (D2), basal diet + 3 g kg^{-1} β-glucan (D3), basal diet + 6 g kg^{-1} BGN-2 (D4), and basal diet + 14 g kg^{-1} BGN-2 (D5). The dosage of Angel yeast product was 1 g kg^{-1} and 3 g kg^{-1}; the dosage of JP Biotechnology product (BGN-2) was 6 g kg^{-1} and 14 g kg^{-1}, equivalent to the final concentration of pure β-glucan in the final feed in a ratio of 1 g kg^{-1} and 3 g kg^{-1} (according to JP Biotechnology data).

The feed was delivered by an automatic fish feeder following a feeding regime of 4 times/hour, with 4 s feeding/time, at approximately 2% of body weight per day.

Enzyme-linked immunosorbent assay. Tumor necrosis factor-α (TNF-α) (CSB-E13254Fh), fish growth hormone (GH) (CSB-E12121Fh), fish heat shock protein-70 (HSP-70) (CSB-E16327Fh), and interleukin-6 (IL-6) (CSB-E13258Fh) levels were determined in samples of the muscle tissue homogenates via enzyme-linked immunosorbent assay (ELISA), using commercially available kits for fish from CUSABIO (Wuhan, China, http://www.cusabio.com). Samples were taken five times, from September to January. Each month, three pooled samples (n = 5 fish in one pooled sample) from each experimental group were collected.

Collection, storage, and analysis of samples were carried out according to CUSABIO manufacturer's instructions (see above). Supernatants were stored at –80°C for further analyses. Concentrations were measured at 450 nm on a Thermo Labsystems Multiskan Ascent 354 Microplate Reader (Thermo Labsystems Inc., USA).

Evaluation of growth performance. The weight and length of 50 randomly selected fish from each group were measured individually every 30 days, throughout the treatment period (Hopkins 1992; Aviva and Watson 2013).

Growth performance indices including weight gain (W_G) [g], coefficient of variation (CV) [%], size heterogeneity of the weight (SH), specific growth rate (SGR) [$\%\text{day}^{-1}$], and Fulton's condition factor (K) were calculated using the following formulae inspired by Hopkins (1992), Afrooz et al. (2014) and Gora et al. (2019):

$$W_G = W_F - W_I$$

$$\text{CV} = (\text{SD}_{\text{IW}} \times W_{\text{IW}}^{-1}) \times 100$$

$$\text{SH} = \text{CV}_F \times \text{CV}_I^{-1}$$

$$\text{SGR} = (\text{Ln } W_F - \text{Ln } W_I) \times t^{-1} \times 100$$

$$K = (W \times 10^5) \times L^{-3}$$

where W_F is the mean final weight of fish [g], W_I is the mean initial weight [g], SD_{IW} is the standard deviation of individual weight, W_{IW} is the mean individual weight [g], CV_F is the final coefficient of variation, CV_I is the initial coefficient of variation, t is the time of rearing [day], W is the weight, and L is the mean total length.

Statistical analysis. The results were analyzed statistically by the R (version 3.6.2) environment with RStudio software (Wickham et al. 2023). The results were presented as mean ± SEM. The normality and homogeneity of the data were checked with the tests of Shapiro–Wilk's and Bartlett, respectively when the data passed the tests, they were compared by one-way analysis of variance (ANOVA), followed by Duncan's test ($P < 0.05$). Otherwise, was done data logarithmic transformation (Aviva and Watson 2013; Wickham et al. 2023).

Results

Mean TNF-α, IL-6, GH, and HSP-70 concentrations are presented in Table 1. All the examined parameters were lower in the control group (D1). However, the mean TNF-α did not exhibit statistically significant differences ($P < 0.05$) among the diet groups throughout the study period. In turn, the TNF-α concentration in the D2 group was significantly higher in September and October in comparison to the control group (Fig. 1). In September, it reached its maximum level within the D2 group.

Table 1. Expression of TNF-α, IL-6, GH, and HSP-70 in juveniles of sea trout, *Salmo trutta*, subjected to long-term dietary administration of β-glucan and BGN-2 in experimental groups (treatments).

Group	Parameter			
	TNF-α [(pg/mL)/10]	IL-6 [pg/mL]	GH [pg/mL]	HSP-70 [pg/mL]
D1	740.67 ± 44.37^{a}	172.83 ± 0.91^{b}	3371.42 ± 16.88^{c}	239.01 ± 1.17^{c}
D2	959.83 ± 70.68^{a}	176.36 ± 1.16^{ab}	3436.01 ± 36.50^{bc}	267.84 ± 5.82^{ab}
D3	872.75 ± 42.28^{a}	178.28 ± 0.89^{ab}	3479.20 ± 14.72^{abc}	263.96 ± 4.63^{abc}
D4	870.69 ± 35.00^{a}	179.07 ± 0.77^{a}	3674.71 ± 60.07^{ab}	291.62 ± 6.06^{a}
D5	871.43 ± 33.59^{a}	180.81 ± 0.71^{a}	3722.67 ± 62.40^{a}	257.82 ± 2.53^{bc}

Values are mean ± SEM. Values in a row with different superscripts are significantly different ($P < 0.05$). Abbreviations: TNF-α = tumor necrosis factor-alpha, IL-6 = interleukin-6, GH = fish growth hormone, HSP-70, fish heat shock protein, BGN-2 = β-glucan containing product; Diets: D1 = control (consisting of basal diet), D2 = basal diet + 1 g kg^{-1} β-glucan, D3 = basal diet + 3 g kg^{-1} β-glucan, D4 = basal diet + 6 g kg^{-1} BGN-2, D5 = basal diet + 14 g kg^{-1} BGN-2.

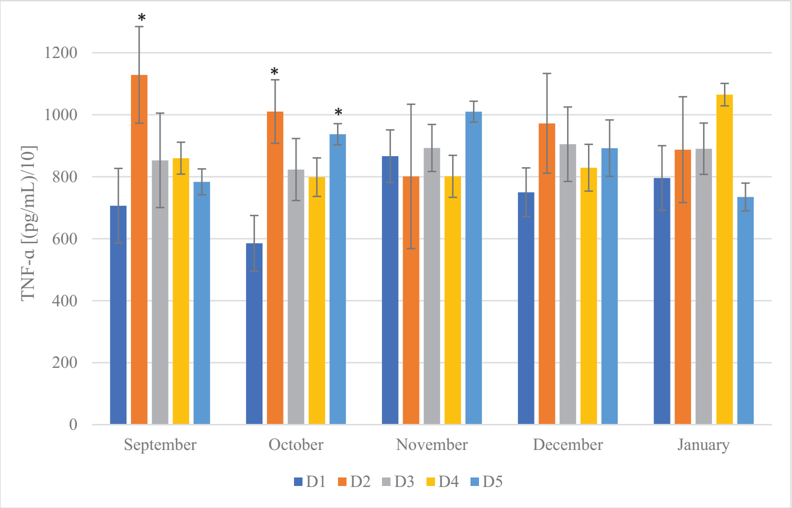

*, statistically significant values ($P < 0.05$) compared to control

Figure 1. Concentrations of TNF-α (tumor necrosis factor-alpha) in juveniles of sea trout, *Salmo trutta*, subjected to dietary administration of β-glucan and BGN-2 (β-glucan containing product) in consecutive months of the experiment.

Our findings indicate that the mean IL-6 concentration was significantly higher in the D4 and D5 groups compared to D1, with no significant difference observed when compared to D2 and D3. The lowest mean IL-6 levels were observed in D1 (Table 1). Notably, IL-6 reached its maximum level in D5 (Fig. 2). Additionally, the IL-6 levels in D5 significantly increased in November.

A significantly higher GH concentration was observed in D5 (Fig. 3), followed by D4, D3, D2, and D1 groups, indicating a positive correlation with the diet group. Also, in the D4 group, GH is higher, compared to the control group (D1).

TNF-α, IL-6, and GH levels did not vary significantly in the D2 and D3 groups during the whole trial of this study compared to the control.

In September, there was no significant difference in HSP-70 between the trial groups and the control. From October to the end of the study, the concentration of HSP-70 in the D4 group was the highest, it was significantly higher than the control group. Also, a high concentration was observed in the D2 group (Fig. 4).

Growth performance, mean final weight, weight gain, coefficient of variation, size heterogeneity, specific growth rate, and Fulton's condition factor are presented in Table 2.

Initially, there were no statistically significant differences in the initial mean weight among the diet groups. However, at the end of the study, it was observed that the final mean weight in groups D4 and D5 was significantly higher compared to the control group (D1). Consequently, the weight gain of fish from groups D4 and D5 was higher.

The same was observed for the specific growth rates (SGR) where fish from D4 and D5 displayed an increased SGR compared to other diet groups. The final mean length in D4 and D5 was significantly higher compared to D1 and D2.

Fulton's condition factor (K) was significantly affected by dietary treatment. The lowest K was recorded in D4 and D5, while the highest value was observed in D1 and D2. The results obtained at the end of the study showed that fish fed the D2 and D3 did not show a statistically significant difference ($P < 0.05$) from fish fed the control diet. The results showed that the growth performance of sea trout in the control group was at the lowest level and showed a significant difference ($P < 0.05$) with the D4 and D5 diet groups.

Results of other aspects of these experiments have been reported in previous papers (Revina et al. 2019, 2020).

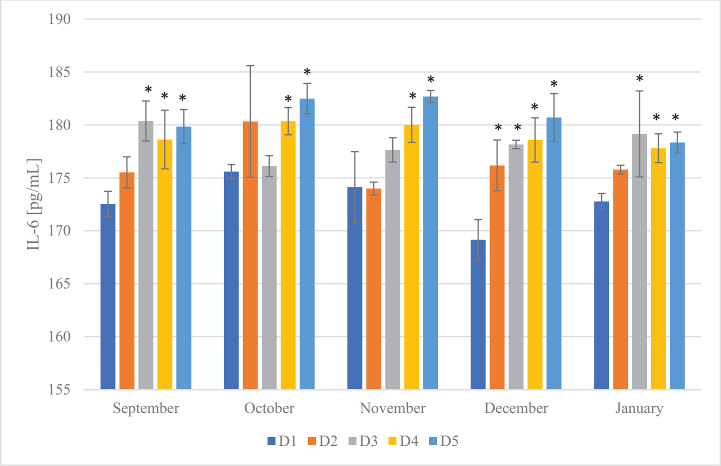

*, statistically significant values ($P < 0.05$) compared to control

Figure 2. Concentrations of IL-6 (interleukin-6) in juveniles of sea trout, *Salmo trutta*, subjected to dietary administration of β-glucan and BGN-2 (β-glucan containing product) in consecutive months of the experiment.

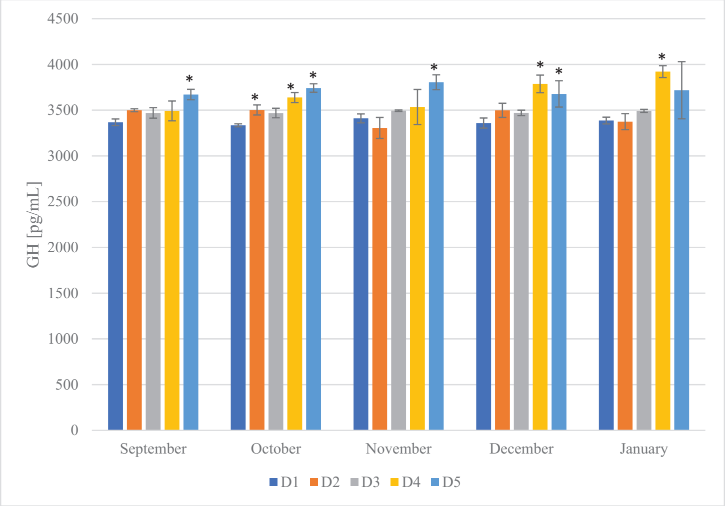

*, statistically significant values ($P < 0.05$) compared to control

Figure 3. Concentrations of GH (fish growth hormone) in juveniles of sea trout, *Salmo trutta*, subjected to dietary administration of β-glucan and BGN-2 (β-glucan containing product) in consecutive months of the experiment.

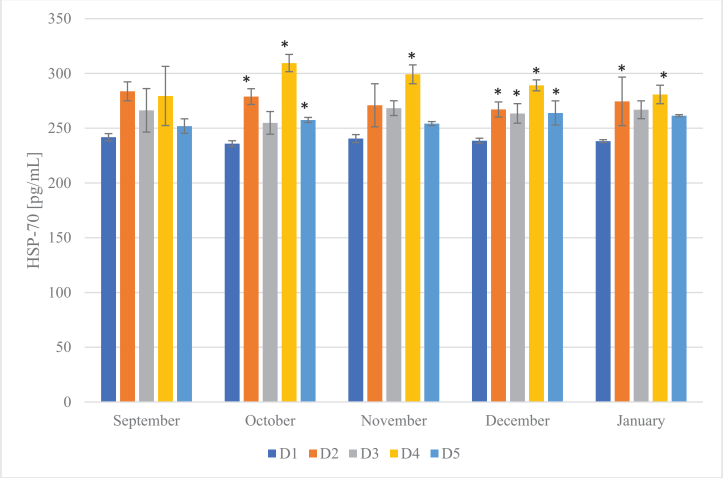

*, statistically significant values ($P < 0.05$) compared to control

Figure 4. Concentrations of HSP-70 (fish heat shock protein) in juveniles of sea trout, *Salmo trutta*, subjected to dietary administration of β-glucan and BGN-2 (β-glucan containing product) in consecutive months of the experiment.

Table 2. Growth performance of juveniles of sea trout, *Salmo trutta*, subjected to long-term dietary administration of β-glucan and BGN-2 in experimental groups (treatments) by the end of trial.

Group	Parameter							
	W_I	W_F	L_F	W_G	CV	SH	SGR	K
D1	2.50 ± 0.21^{a}	11.84 ± 0.78^{c}	9.33 ± 0.24^{a}	9.34	28.76	0.90	0.73	1.60 ± 0.11^{a}
D2	2.59 ± 0.17^{a}	13.31 ± 0.84^{bc}	9.50 ± 0.24^{a}	10.72	27.50	1.10	0.77	1.58 ± 0.10^{a}
D3	2.67 ± 0.21^{a}	16.18 ± 0.77^{abc}	11.12 ± 0.32^{ab}	13.51	20.79	0.69	0.85	1.18 ± 0.12^{ab}
D4	2.67 ± 0.17^{a}	16.76 ± 0.64^{ab}	11.91 ± 0.28^{b}	14.09	16.55	0.66	0.86	0.99 ± 0.04^{b}
D5	2.76 ± 0.16^{a}	19.88 ± 0.74^{a}	12.81 ± 0.26^{b}	17.12	16.15	0.73	0.93	0.94 ± 0.04^{b}

Values (of W_I, W_F, L_F, and K) are mean ± SE; mean values with different superscript letters in a row are significantly different ($P < 0.05$), according to Duncan's multiple range tests. Abbreviations: W_I = initial mean weight [g], W_F = final mean weight [g], L_F = final mean length [cm], W_G = weight gain [g], CV = coefficient of variation [%], SH = size heterogeneity (weight), SGR = specific growth rate [% day^{-1}], K = condition factor, BGN-2 = β-glucan containing product; Diets: D1 = control (consisting of basal diet), D2 = basal diet + 1 g kg^{-1} β-glucan, D3 = basal diet + 3 g kg^{-1} β-glucan, D4 = basal diet + 6 g kg^{-1} BGN-2, D5 = basal diet + 14 g kg^{-1} BGN-2.

Discussion

The use of natural immunostimulants offers important advantages for aquaculture. These substances enhance the immune response and strengthen disease resistance, contributing to improved health and overall well-being in aquatic organisms. Furthermore, these products are environmentally friendly, biodegradable, and safe for humans (Vetvicka et al. 2013; Rodrigues et al. 2020). Also, β-glucan is widely acknowledged as a beneficial growth promoter for fish (Ji et al. 2017).

In teleost fishes, such as Atlantic salmon, *Salmo salar* and rainbow trout, *Oncorhynchus mykiss* (Walbaum, 1792), the administration of β-glucans enhances the regenerative capacity of immunosuppressed cells, thereby bolstering their ability to combat infectious diseases (Petit and Wiegertjes 2016). Research investigations have revealed that the immunomodulating effects of β-glucan can be characterized as follows: (1) Prebiotic effects of β-glucan involve an indirect form of immunomodulation, encompassing the fermentation of β-glucan by native bacteria, resulting in alterations in microbial composition and a shift in the production of short-chain fatty acid (SCFA) metabolites within the gastrointestinal tract (GIT) of fish. (2) In addition, β-glucan contributes to the direct immunomodulation of the host through receptor-mediated recognition mechanisms occurring within the GIT of fish (Petit et al. 2022). This, in turn, leads to improved digestion and increased nutrient absorption efficiency from their diets (Dawood et al. 2020).

While the exact mechanism by which β-glucan influences the fish's immune system remains uncertain, there is substantial evidence indicating its ability to boost phagocytic activity and increase the expression of cytokines in different types of immune cells, including macrophages, dendritic cells, and neutrophils (Di Domenico et al. 2017).

The results of our studies are consistent with other authors (Kim et al. 2009, Vetvicka et al. 2013), who have demonstrated that the impact of β-glucan on cytokine expression is rapid and does not necessitate long-term administration. The effect becomes evident within the initial months of application. The level of IL-6 remained significantly higher in the D4 and D5 groups compared to the control group throughout the study. This can be attributed to β-glucan's engagement with β-glucan receptors, leading to the enhancement of various immune functions, including the release of cytokines such as IL-6 (Rodrigues et al. 2020).

The inclusion of β-glucan at a dose of 1 g kg^{-1} (D2) in the diet leads to a significant rise in TNF-α levels during the months of September and October. In subsequent months, the expression of TNF-α in all groups remains without significant statistical difference. Similar results were obtained by other researchers (Sealey et al. 2008; Rodríguez et al. 2009), who proved that β-glucan had no impact on the expression of TNF-α. TNF-α is mainly produced by activated macrophages, natural killer (NK) cells, and lymphocytes (Atzeni and Sarzi-Puttini 2013), it is expressed in most examined teleost tissue (Eggestøl et al. 2020). Our hypothesis suggests that β-glucan supplements improve the functional capabilities of macrophages, leading to a slight increase in TNF-α levels, but not reaching statistical significance. It is possible, that if fish were infected with pathogens, the release of TNF-α might be higher. In addition, some studies have confirmed a significant increase in TNF-α during prolonged stress (Dawood et al. 2020). Since our fish were maintained under optimal conditions, this factor is excluded. Regrettably, there is currently a dearth of information regarding these potential effects of β-glucan in fish.

GH plays a crucial role in regulating various physiological functions of fish such as development, growth, osmoregulation, immune systems, reproduction function, etc. (Lal and Singh 2005; Abdolahnejad et al. 2015). In the presently reported study, it was found that the inclusion of the BGN-2 product in the diet had a significantly positive impact on GH expression in groups D4 and D5. This positive GH expression can help explain the increase in growth parameters of sea trout observed in the presently reported and previous studies, especially during the winter months (Revina et al. 2020). However, in contrast, our study did not show any significant beneficial effect of pure β-glucan on GH expression in groups D2 and D3. Our results are consistent with other authors, who suggested that pure β-glucan does not have a significant impact on GH.

More authors demonstrated that dietary β-glucan has played a major role in regulating stress- and immune-related factors through expressing HSP-70 (Ji et al. 2017; Salah et al. 2017). HSP-70 is typically expressed in the cells of fish that have experienced environmental stressors (Dawood et al. 2020). In the initial month of the study, no significant effect was observed when adding β-glucan additives to the sea trout diet (Fig. 4). However, a notable effect was observed with the BGN-2 product at a dose of 6 g kg^{-1} (D4). Additionally, a substantial impact was seen in D2.

This study highlights the beneficial outcomes resulting from the oral administration of the BGN- 2 product at doses of 6 g kg^{-1} and 14 g kg^{-1} on the growth performance of sea trout. These findings align with previous research (Hoang et al. 2018), which also demonstrated the growth-enhancing effects of β-glucan in various aquaculture species. Fish from D1, D2, D3, and D4 groups exhibited excellent condition. According to several studies, Fulton's condition factor for salmonids is considered excellent when it falls within the range of 0.95 to 1.44 (Mahmoudi et al. 2014; Wali et al. 2019).

This study adds to the growing body of evidence supporting the efficacy of β-glucan, specifically the BGN-2 product, in promoting the growth of sea trout. The results suggest that the administration of β-glucan products at the specified doses can positively influence the growth parameters of sea trout, contributing to the development of more efficient and sustainable aquaculture practices.

In summary, all of our research (Revina et al. 2019, 2020) strongly recommends incorporating the BGN-2 product at a dosage of 6 g kg^{-1} into the sea trout diet. This approach enhances the immunomodulatory response, and overall health, and represents an effective strategy for increasing sea trout production. Our study affirms that the utilization of BGN-2 products has a positive impact on the welfare, innate immune system, and growth performance of sea trout.

Acknowledgments

The presently reported study was supported financially by the research project "Strengthening the Scientific Capacity of LLU" No. Z-27 – The application of β-glucan to ensure sea trout health. The authors would like to express their gratitude to the Institute of Food Safety, Animal Health, and Environment "BIOR" for the support in carrying out this study. This manuscript is supported by the Institute of Food Safety, Animal Health, and Environment BIOR.

References

Abdolahnejad Z, Pourkazemi M, Khoshkholgh MR, Yarmohammadi M (2015) Expression of growth hormone gene during early development of Siberian sturgeon (*Acipenser baerii*). Molecular Biology Research Communications 4: 181–188. https://doi.org/10.22099/mbrc.2015.3166

Afrooz E, Gholamreza E, Seyed ARH (2014) Length–weight relationship and Fultons condition factor of *Carasobarbus luteus* (Heckel, 1843) in Hoor Al-azim wetland. Journal of Ecology and the Natural Environment 6(7): 238–243. https://doi.org/10.5897/JENE2014.0449

Anonymous (2010) Directive 2010/63/EU of the European Parliament and of the Council of 22 September 2010 on the protection of animals used for scientific purposes. The European Parliament and the Council of the European Union. Official Journal of the European Union L 276/33.

Atzeni F, Sarzi-Puttini P (2013) Tumor Necrosis Factor. Pp. 229–231. In: Brenner's Encyclopedia of Genetics. 2nd edn. Elsevier Inc. https://doi.org/10.1016/B978-0-12-374984-0.01594-1

Aviva P, Watson P (2013) Statistics for veterinary and animal science. 3rd edn. British Medical Journal Publishing Group, Wiley-Blackwell, 408 pp.

Brown GD, Herre J, Williams DL, Willment JA, Marshall ASJ, Gordon S (2003) Dectin-1 mediates the biological effects of β-glucans. Journal of Experimental Medicine 197(9): 1119–1124. https://doi.org/10.1084/jem.20021890

Calder PC (2007) Immunological parameters: What do they mean? Journal of Nutrition 137(3): 773S–780S. https://doi.org/10.1093/jn/137.3.773S

Cara JB, Aluru N, Moyano FJ, Vijayan MM (2005) Food-deprivation induces HSP70 and HSP90 protein expression in larval gilthead sea bream and rainbow trout. Comparative Biochemistry and Physiology Part B: Biochemistry and Molecular Biology 142(4): 426–431. https://doi.org/10.1016/j.cbpb.2005.09.005

Costa MM, Maehr T, Diaz-Rosales P, Secombes CJ, Wang T (2011) Bioactivity studies of rainbow trout (*Oncorhynchus mykiss*) interleukin-6: Effects on macrophage growth and antimicrobial peptide gene expression. Molecular Immunology 48(15–16): 1903–1916. https://doi.org/10.1016/j.molimm.2011.05.027

Dawood MAO, Metwally AES, El-Sharawy ME, Atta AM, Elbialy ZI, Abdel-Latif HMR, Paray BA (2020) The role of β-glucan in the growth, intestinal morphometry, and immune-related gene and heat shock protein expressions of Nile tilapia (*Oreochromis niloticus*) under different stocking densities. Aquaculture 523: e735205. https://doi.org/10.1016/j.aquaculture.2020.735205

Domenico DJ, Canova R, Soveral FL, Nied CO, Costa MM, Frandoloso R, Kreutz LC (2017) Immunomodulatory effects of dietary β-glucan in silver catfish (*Rhamdia quelen*). Pesquisa Veterinaria Brasileira 37(1): 73–78. https://doi.org/10.1590/s0100-736x2017000100012

Eggestøl HØ, Lunde HS, Haugland GT (2020) The proinflammatory cytokines TNF-α and IL-6 in lumpfish (*Cyclopterus lumpus* L.)—Identification, molecular characterization, phylogeny and gene expression analyses. Developmental and Comparative Immunology 105: 103608. https://doi.org/10.1016/j.dci.2020.103608

Rozenkopfs O, Rudze L (2003) National regulations on ethics and research in Latvia. European Commission, Directorate-General for Research and Society. Office for Official Publications of the European Communities, Luxembourg.

Falco A, Frost P, Miest J, Pionnier N, Irnazarow I, Hoole D (2012) Reduced inflammatory response to *Aeromonas salmonicida* infection in common carp (*Cyprinus carpio* L.) fed with β-glucan supplements. Fish and Shellfish Immunology 32(6): 1051–1057. https://doi.org/10.1016/j.fsi.2012.02.028

Firdaus-Nawi M, Zamri-Saad M (2016) Major components of fish immunity: A review. Pertanika Journal of Tropical Agricultural Science 39: 393–420.

Fraser DJ (2008) How well can captive breeding programs conserve biodiversity? A review of salmonids. Evolutionary Applications 1(4): 535–586. https://doi.org/10.1111/j.1752-4571.2008.00036.x

Gora AH, Ambasankar K, Sandeep KP, Rehman S, Agarwal D, Ahmad I, Ramachandran K (2019) Effect of dietary supplementation of crude microalgal extracts on growth performance, survival and disease resistance of *Lates calcarifer* (Bloch, 1790) larvae. Indian Journal of Fisheries 66(1): 64–72. https://doi.org/10.21077/ijf.2019.66.1.79076-09

Hadiuzzaman M, Moniruzzaman M, Shahjahan M, Bai SC, Min T, Hossain Z (2022) β-glucan: Mode of action and its uses in fish immunomodulation. Frontiers in Marine Science 9: e905986. https://doi.org/10.3389/fmars.2022.905986

Hoang DH, Lam HS, Nguyen CV (2018) Efficiency of dietary β-glucan supplementation on growth, body composition, feed, and nutrient utilization in juveniles of pompano fish (*Trachinotus ovatus*, Linnaeus, 1758). Israeli Journal of Aquaculture—Bamidgeh 70. https://doi.org/10.46989/001c.20924

Hoffmann L, Rawski M, Pruszyńska-Oszmałek E, Kołodziejski P, Mazurkiewicz J (2021) Environmentally sustainable feeding system for sea trout (*Salmo trutta* m. *trutta*): Live food and insect meal-based diets in larval rearing. Aquaculture Reports 21: 100795. https://doi.org/10.1016/j.aqrep.2021.100795

Hong S, Li R, Xu Q, Secombes CJ, Wang T (2013) Two types of TNF-α exist in teleost fish: Phylogeny, expression, and bioactivity analysis of Type-II TNF-α3 in rainbow trout *Oncorhynchus mykiss.* Journal of Immunology 191(12): 5959–5972. https://doi.org/10.4049/jimmunol.1301584

Hopkins K (1992) Reporting fish growth: A review of the basics. Journal of the World Aquaculture Society 23(3): 173–179. https://doi.org/10.1111/j.1749-7345.1992.tb00766.x

Iwama GK, Thomas PT, Forsyth RB, Vijayan MM (1998) Heat shock protein expression in fish. Reviews in Fish Biology and Fisheries 8(1): 35–56. https://doi.org/10.1023/A:1008812500650

Ji L, Sun G, Li J, Wang Y, Du Y, Li X, Liu Y (2017) Effect of dietary β-glucan on growth, survival and regulation of immune processes in rainbow trout (*Oncorhynchus mykiss*) infected by *Aeromonas salmonicida*. Fish and Shellfish Immunology 64: 56–67. https://doi.org/10.1016/j.fsi.2017.03.015

Kamalam BS, Rajesh M, Kaushik S (2020) Nutrition and feeding of rainbow trout (*Oncorhynchus mykiss*). Pp. 299–332. In: Ninawe AS, Dhanze JR, Dhanze R, Indulkar ST (Eds.) Fish nutrition and its relevance to human health. CRC Press, London, UK. https://doi.org/10.1201/9781003107583

Kim YS, Ke F, Zhang QY (2009) Effect of β-glucan on activity of antioxidant enzymes and Mx gene expression in virus infected grass carp. Fish and Shellfish Immunology 27: 336–340. https://doi.org/10.1016/j.fsi.2009.06.006

Kučinskis M, Dūklavs J (2016) Par Zivju resursu mākslīgās atražošanas plānu 2017.–2020. gadam. Ministru kabineta rīkojums Nr. 684. [Restocking plan of fish resources 2017–2020. Order of the Cabinet of Ministers No. 684.] Latvijas Vēstnesis Nr. 227. https://www.vestnesis.lv/op/2016/227.12

Kumar A, Ashraf S, Goud TS, Grewal A, Singh SV, Yadav BR, Upadhyay RC (2015) Expression profiling of major heat shock protein genes during different seasons in cattle (*Bos indicus*) and buffalo (*Bubalus bubalis*) under tropical climatic condition. Journal of Thermal Biology 51: 55–64. https://doi.org/10.1016/j.jtherbio.2015.03.006

Lal B, Singh AK (2005) Immunological and physiological validation of enzyme-linked immunosorbent assay for growth hormone of the Asian catfish, *Clarias batrachus*. Fish Physiology and Biochemistry 31(2–3): 289–293. https://doi.org/10.1007/s10695-006-0038-x

Li Z, Srivastava P (2003) Heat-shock proteins. Current Protocols in Immunology 58: Appendix 1, Appendix 1T. https://doi.org/10.1002/0471142735.ima01ts58

Mahmoudi R, Soltani M, Abbas M, Sohrab RG, Abolghasem K (2014) Morphometric relationship between length–weight, length–length and condition factor in farmed rainbow trout (*Oncorhynchus mykiss)*. Bulletin of Environment. Pharmacology and Life Sciences 3(4): 215–220.

McCormick SD, Regish AM, Christensen AK (2009) Distinct freshwater and seawater isoforms of Na+/K +-ATPase in gill chloride cells of Atlantic salmon. Journal of Experimental Biology 212(24): 3994–4001. https://doi.org/10.1242/jeb.037275

Miest JJ, Arndt C, Adamek M, Steinhagen D, Reusch TBH (2016) Dietary β-glucan (MacroGard®) enhances survival of first feeding turbot (*Scophthalmus maximus*) larvae by altering immunity, metabolism and microbiota. Fish and Shellfish Immunology 48: 94–104. https://doi.org/10.1016/j.fsi.2015.11.013

National Research Council (1999) Nutrient requirements of fish. National Academies Press, Washington, DC, USA, 128 pp. https://doi.org/10.17226/2115

Petit J, Wiegertjes GF (2016) Long-lived effects of administering β-glucans: Indications for trained immunity in fish. Developmental and Comparative Immunology 64: 93–102. https://doi.org/10.1016/j.dci.2016.03.003

Petit J, de Bruijn I, Goldman MRG, van den Brink E, Pellikaan WF, Forlenza M, Wiegertjes GF (2022) β-glucan-induced immuno-modulation: A role for the intestinal microbiota and short-chain fatty acids in common carp. Frontiers in Immunology 12: 761820. https://doi.org/10.3389/fimmu.2021.761820

Purvina S, Medne R, Bajinskis J, Kondratyeva N (2019) Success of long term salmonid restocking in Latvia. Environmental and Experimental Biology 17: 31–32.

Revina O, Revins V, Cirule D, Valdovska A (2019) The effect of dietary β-glucans supplements on the haematological parameters of the sea trout. Research For Rural Development 247–251. https://doi.org/10.22616/rrd.25.2019.037

Revina O, Avsejenko J, Revins V, Sargautis D, Cīrule D, Valdovska A (2020) Effect of dietary supplementation with β-glucan on growth performance and skin-mucus microbiota of sea trout (*Salmo trutta*). Fisheries and Aquatic Life 28(3): 155–165. https://doi.org/10.2478/aopf-2020-0019

Ringø E, Olsen RE, Vecino JLG, Wadsworth S (2011) Use of immunostimulants and nucleotides in aquaculture: A review. Journal of Marine Science: Research and Development 02(1): 1–22. https://doi.org/10.4172/2155-9910.1000104

Rodrigues MV, Zanuzzo FS, Koch JFA, Oliveira CAF, Sima P, Vetvicka V (2020) Development of fish immunity and the role of β-glucan in immune responses. Molecules 25(22): e5378. https://doi.org/10.3390/molecules25225378

Rodríguez I, Chamorro R, Novoa B, Figueras A (2009) β-glucan administration enhances disease resistance and some innate immune responses in zebrafish (*Danio rerio*). Fish and Shellfish Immunology 27(2): 369–373. https://doi.org/10.1016/j.fsi.2009.02.007

Rozenkopfs O, Rudze L (2003) National regulations on ethics and research in Latvia. European Commission, Directorate-General for Research and Society. Office for Official Publications of the European Communities, Luxembourg.

Sakamoto T, McCormick SD (2006) Prolactin and growth hormone in fish osmoregulation. General and Comparative Endocrinology 147(1): 24–30. https://doi.org/10.1016/j.ygcen.2005.10.008

Salah AS, Nahas AFE, Mahmoud S (2017) Modulatory effect of different doses of β-1,3/1,6-glucan on the expression of antioxidant, inflammatory, stress and immune-related genes of *Oreochromis niloticus* challenged with *Streptococcus iniae.* Fish and Shellfish Immunology 70: 204–213. https://doi.org/10.1016/j.fsi.2017.09.008

Sealey WM, Barrows FT, Hang A, Johansen KA, Overturf K, LaPatra SE, Hardy RW (2008) Evaluation of the ability of barley genotypes containing different amounts of β-glucan to alter growth and disease resistance of rainbow trout *Oncorhynchus mykiss.* Animal Feed Science and Technology 141(1–2): 115–128. https://doi.org/10.1016/j.anifeedsci.2007.05.022

Smith WDC (1956) The role of the endocrine organs in the salinity tolerance of trout. Memoirs of the Society for Endocrinology 5: 83–101.

Stefansson SO, Bjömsson BT, Hansen T, Haux C, Taranger GL, Saunders RL (1991) Growth, parr–smolt transformation, and changes in growth hormone of Atlantic salmon (*Salmo salar*) reared under different photoperiods. Canadian Journal of Fisheries and Aquatic Sciences 48(11): 2100–2108. https://doi.org/10.1139/f91-249

Tipsmark CK, Madsen SS, Seidelin M, Christensen AS, Cutler CP, Cramb G (2002) Dynamics of Na+,K+,2Cl- cotransporter and Na+,K+-ATPase expression in the branchial epithelium of brown trout (*Salmo trutta*) and Atlantic salmon (*Salmo salar*). Journal of Experimental Zoology 293(2): 106–118. https://doi.org/10.1002/jez.10118

Vallejos-Vidal E, Reyes-López F, Teles M, MacKenzie S (2016) The response of fish to immunostimulant diets. Fish and Shellfish Immunology 56: 34–69. https://doi.org/10.1016/j.fsi.2016.06.028

Vetvicka V, Vannucci L, Sima P (2013) The effects of β-glucan on fish immunity. North American Journal of Medical Sciences 5(10): e580. https://doi.org/10.4103/1947-2714.120792

Wali A, Tasaduq SH, Balkhi MH, Bhat BA, Bhat FA, Qadri S, Mohamad I (2019) Morphometry and length–weight relationship of rainbow trout *Oncorhynchus mykiss* Walbaum, 1792 (*Salmoniformes: Salmonidae*) from Kashmir. Journal of Entomology and Zoology Studies 7: 1653–1656.

Wickham H, Çetinkaya-Rundel M, Grolemund G (2023) R for data science: Import, tidy, transform, visualize, and model data. 2nd edn. O'Reilly Media, Sebastopol, CA, USA, 576 pp.

Yada T (2007) Growth hormone and fish immune system. General and Comparative Endocrinology 152(2–3): 353–358. https://doi.org/10.1016/j.ygcen.2007.01.045

Zou J, Secombes C (2016) The function of fish cytokines. Biology 5(2): e23. https://doi.org/10.3390/biology5020023

Acta Ichthyologica et Piscatoria 53, 2023, 263–270 | DOI 10.3897/aiep.53.112253

PENSOFT.

ACTA
ICHTHYOLOGICA
ET PISCATORIA

A checklist of dead fishes (Actinopterygii and Elasmobranchii) associated with the algal bloom event of the summer of 2022 on the Yucatan coasts, southern Gulf of Mexico

Rosalía AGUILAR-MEDRANO[1], María Eugenia VEGA-CENDEJAS[2], Ariel A. CHI ESPÍNOLA[2]

1 *Departamento de Ecología Marina, Centro de Investigación Científica y de Educación Superior de Ensenada, Ensenada, B.C. Mexico*
2 *Laboratorio de Taxonomía y Ecología de Peces, Centro de Investigación y de Estudios Avanzados del IPN, Mérida, Yuc., Mexico*

https://zoobank.org/291D8F7A-104F-49FF-A032-790FC1C5CBE1

Corresponding author: Rosalía Aguilar-Medrano (rosalia@cicese.mx)

Academic editor: Adnan Tokaç ♦ **Received** 6 September 2023 ♦ **Accepted** 22 November 2023 ♦ **Published** 29 December 2023

Citation: Aguilar-Merdano R, Vega-Cendejas ME, Chi Espínola AA (2023) A checklist of dead fishes (Actinopterygii and Elasmobranchii) associated with the algal bloom event of the summer of 2022 on the Yucatan coasts, southern Gulf of Mexico. Acta Ichthyologica et Piscatoria 53: 263–270. https://doi.org/10.3897/aiep.53.112253

Abstract

Harmful algal blooms (HABs) are natural phenomena that occur when colonies of microalgae grow out of control and produce toxic or harmful effects on the surrounding fauna. In August 2022, an HAB, dominated by the diatom, *Cylindrotheca closterium* (Ehrenberg) Reimann et J.C. Lewin, 1964, occurred on the Yucatan coast, southern Gulf of Mexico. In the presently reported study, two photo transects were established along the coastline, one at the onset of the bloom, at Telchac port, and the other at the final phase of the event, at Chixchulub port. The affected fish species were documented photographically and a taxonomic list, with their abundance, density, and biomass is presented, as well as a summary of the affected ecosystems according to the affinity of these species. A total of 54 species were recorded; 48 in Telchac and 21 in Chicxulub, with 15 species occurring at both sites. The affected species have a greater affinity to reef systems, beaches, and estuaries, in that order, between 3 m and 113 m depth. In the International Union for the Conservation of Nature (IUCN) nomenclature, the majority of the species are in the “least concern” category, however, species were also recorded in the “near threatened”, “vulnerable”, and “endangered” categories. Therefore, it is extremely important to monitor these events and report the affected species, since the increase in the frequency of these phenomena due to local and global factors can have significant repercussions on species endemic to the coastal zone.

Keywords

Cylindrotheca closterium, dead fishes, harmful algal bloom, red tide, Yucatan Peninsula

Introduction

Harmful algal blooms (HABs), colloquially known as red tides, are a natural phenomenon that occurs when colonies of microalgae (in the sea or in freshwater) grow out of control and produce toxic or harmful effects on the surrounding fauna (Hallegraeff et al. 1995). There are toxic and non-toxic HABs; in the toxic ones the algae produce toxins that affect or kill organisms, while the non-toxic ones can also cause the death of organisms, but this is because of the low concentration of oxygen in the environment due to their high density (Sidabutar et al. 2021). Although HABs are a natural phenomenon, they are magnified by changes in the concentration of nutrients (eutrophication) and in the temperature of the ecosystem, which is why these phenomena are expected to become more frequent and intense due to global warming and the increase in contamination (Anderson 1989; Smayda 1990; Hallegraeff 1993; Hallegraeff 2023).

When HABs appear on the coasts, they cause not only ecological impacts but also strong economic impacts on the local community, directly affecting fishing, as well as the restaurant and tourist industry. On 3 August 2022, fishermen noticed occurrence of live octopuses on the shore, and on 4 August dead and intoxicated fish started to deposit on the beach due to the HAB effects, dominated by *Cylindrotheca closterium* (Ehrenberg) Reimann et J.C. Lewin, 1964, a non-toxic diatom species (Herrera-Silveira et al. 2022). The stranding of dead and intoxicated fishes began at San Felipe port on the east of the Yucatan coast and gradually moved to the west until reaching the coasts of Chelem, Yucatan. On the night of 4 August, the communities at the coast began cleaning and burying the dead fish; the stranding of dead and moribund fish lasted approximately one week. HABs dominated by *C. closterium* have been documented in the area because of increased concentrations of nutrients such as nitrite, nitrate, phosphate, and urea (Poot-Delgado and Okolodkov 2020). During this phenomenon, the stranding of great diversity and abundance of fishes was documented photographically in order to present a taxonomic list of the affected species, as well as their abundance, density, and biomass, in addition to determining the affected ecosystems according to the affinity of these species.

Materials and methods

The shore was monitored based on two photo transects, the first, at the early site of the stranding, on 5 August, covering 1 km of the shore (Telchac) and the second one at the final phase of the event, on 12 August, covering 10 m (Chixchulub) (Fig. 1A). On shore, we randomly established a starting point and walked east–west, taking photographs of the organisms already deposited on the beach by using a PVC square frame of 1 m^2 and a camera held at an approximate height of 1 m (Fig. 1B). No specimens were collected.

The stranded organisms were identified up to the species level based on photographs. The identification was facilitated by the relatively fresh coloration of the specimens. Once we had a list of species, using FishBase (Froese and Pauly 2023) and Robertson and Van Tasell (2023), we collected information (1) on the size and weight of the species to make an approximation of the biomass; and (2) in order to determine the main habitat associated with the affected species, the depth range and the habitats (Fig. 1C) where the species have been recorded such as reef, estuary, and beach, among others, were recorded and used as a binary variable indicating the presence as (1) if the species have been recorded in that habitat or absence (0) if the species have not been reported in that habitat. Finally, the conservation status of the recorded species, according to the categories of the Red List of the International Union for the Conservation of Nature (IUCN), was recorded.

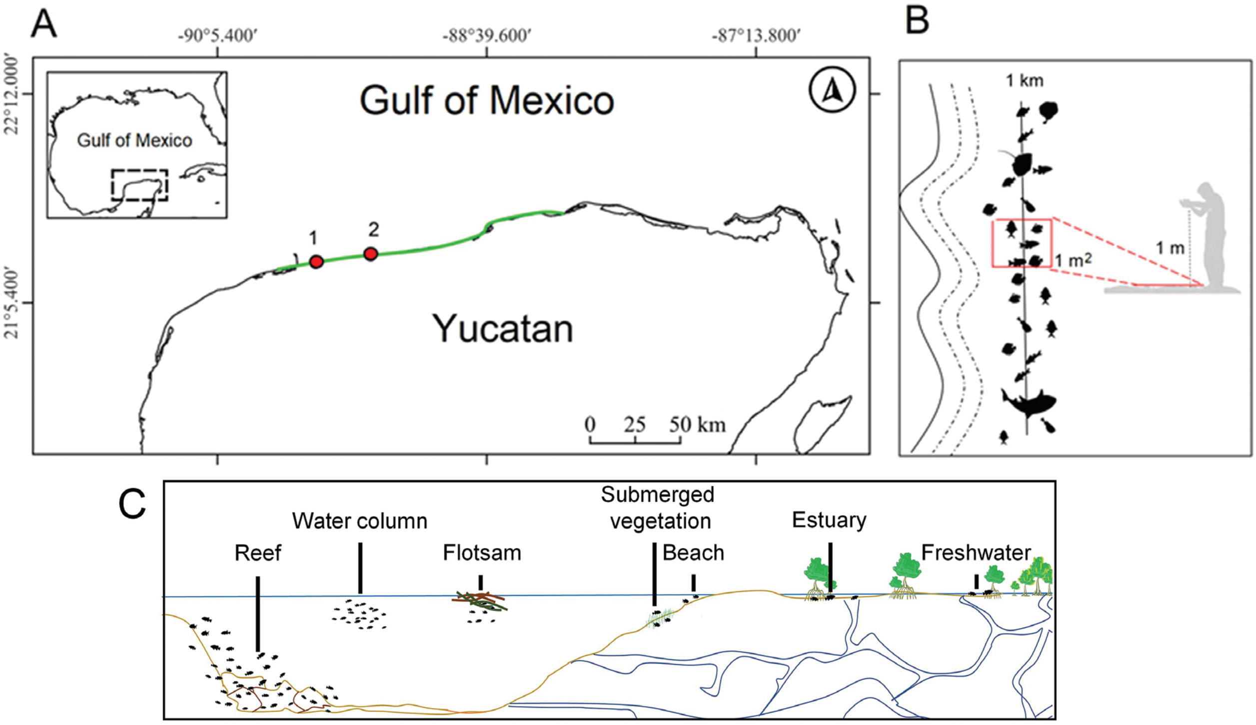

Figure 1. Diagrams showing the study area on the Yucatan coast, Mexico. (**A**) map of the study area (Sampling sites: 1 = Chicxulub, 2 = Telchac port). The green line marks the stretch of the shore affected by the harmful algal bloom in summer 2022. (**B**) Diagrammatic representation of a photo transect on the coastline. (**C**) Diagrammatic representation of the habitats where the affected species have been recorded.

Species richness was determined as the number of species recorded on both photo transects, abundance as the total number of individuals recorded per species, density as the number of organisms per species per 1 m^2, and biomass as the weight [g] per species per 1 m^2.

Results

Because the photo transect in Telchac was established at the beginning of the HAB, the beach cleaning campaigns had not started and a greater number of species could be observed, while in Chicxulub the photo transect was smaller and recorded less extensive diversity because the cleaning campaigns were already ongoing, however, it was possible to list species not recorded in Telchac.

Richness. A total of 54 species were recorded (Table 1), 48 in Telchac and 21 in Chicxulub. Six species not recorded in Telchac were recorded in Chicxulub: *Abudefduf saxatilis*, *Caranx hippos*, *Chilomycterus schoepfii*, *Gymnothorax saxicola*, *Ogcocephalus parvus*, and *Sphoeroides testudineus*. Of the total, five species were elasmobranchs and 49 actinopterygians. The families with the highest number of affected species were Haemulidae, Sciaenidae, and Serranidae with three species each.

Abundance. Telchac presented the mean abundance” of 6.4 individuals per species (range 1–36 ind./spec.) and Chicxulub 16.95 individuals per species (range 1–245 ind./spec.), the overall mean value was 12.4 ind./spec. (range 1–281 ind./spec.) (Table 2). Among the ten most abundant species, both localities share *Opsanus beta*, *Sphoeroides spengleri*, and *Haemulon plumieri*. In both locations, *Opsanus beta* presented the highest values of abundance and thus was the most abundant species with a total of 281 individuals recorded, followed by *Acanthostracion quadricornis* with 61 individuals, *Hypoplectrus puella* with 27, *Harengula jaguana* 26, and *Eques lanceolatus* 25 (Fig. 2).

Density. In Telchac a mean density of 0.2142 ind. · m^{-2} (range 0.03–1.2 ind. · m^{-2}) was recorded, while in Chicxulub 0.4241 ind. · m^{-2} (range 0.025–6.13 ind. · m^{-2}), the overall mean value was 0.25 ind. · m^{-2} (range 0.025–3.66 ind. · m^{-2}) (Table 2). In both locations, *O. beta* presented the highest values of density. Among the ten species with the highest density, both sites share *Opsanus beta*, *Sphoeroides spengleri*, and *Haemulon plumieri*. The species with the highest density were *Opsanus beta* 3.66 ind. · m^{-2}, *Hypoplectrus puella* 0.90 ind. · m^{-2}, *Harengula jaguana* 0.87 ind. · m^{-2}, *Eques lanceolatus* 0.83 ind. · m^{-2}, and *Acanthostracion quadricornis* 0.79 ind. · m^{-2} (Fig. 2).

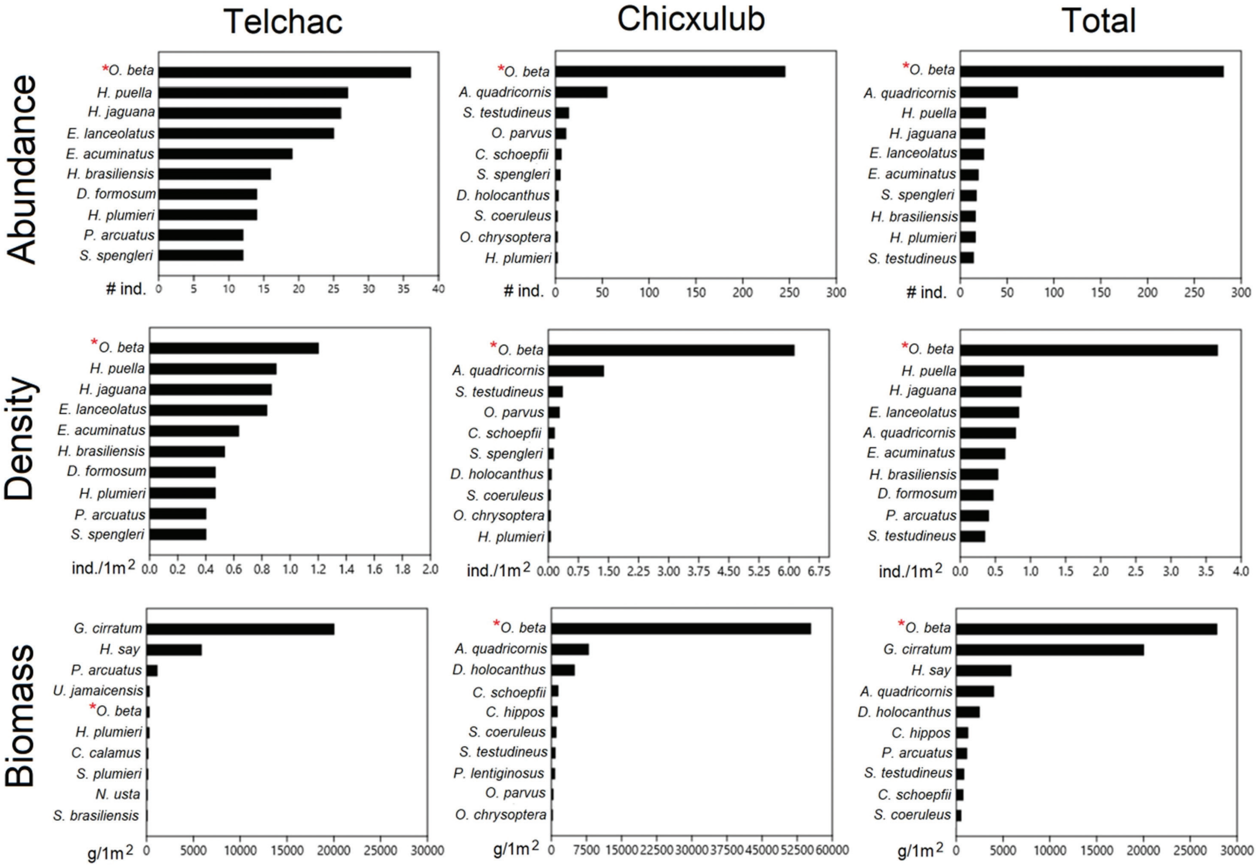

Figure 2. Community descriptors. Abundance, density, and biomass of fish species affected by the harmful algal bloom off the coast of Yucatan, Mexico in summer 2022.

Table 1. Fish species affected by the harmful algal bloom off the coast of Yucatan, Mexico in summer 2022.

Species	Family
Abudefduf saxatilis (Linnaeus, 1758)	Pomacentridae
Achirus lineatus (Linnaeus, 1758)	Achiridae
Opsanus beta (Goode et Bean, 1880)	Batrachoididae
Sanopus reticulatus Collette, 1983	Batrachoididae
Strongylura marina (Walbaum, 1792)	Belonidae
Strongylura notata (Poey, 1860)	Belonidae
Oligoplites saurus (Bloch et Schneider, 1801)	Carangidae
Caranx hippos (Linnaeus, 1766)	Carangidae
Chaetodon ocellatus Bloch, 1787	Chaetodontidae
Harengula jaguana Poey, 1865	Clupeidae
Dactylopterus volitans (Linnaeus, 1758)	Dactylopteridae
Hypanus say (Lesueur, 1817)	**Dasyatidae**
Chilomycterus schoepfii (Walbaum, 1792)	Diodontidae
Diodon holocanthus Linnaeus, 1758	Diodontidae
Anchoa hepsetus (Linnaeus, 1758)	Engraulidae
Eucinostomus gula (Quoy et Gaimard, 1824)	Gerreidae
Eugerres plumieri (Cuvier in Cuvier et Valenciennes, 1830)	Gerreidae
Ginglymostoma cirratum (Bonnaterre, 1788)	**Ginglymostomatidae**
Haemulon aurolineatum Cuvier in Cuvier et Valenciennes, 1830	Haemulidae
Haemulon plumieri (Lacepede, 1801)	Haemulidae
Orthopristis chrysoptera (Linnaeus, 1766)	Haemulidae
Chriodorus atherinoides Goode et Bean, 1882	Hemiramphidae
Hemiramphus brasiliensis (Linnaeus, 1758)	Hemiramphidae
Neoniphon marianus (Cuvier in Cuvier et Valenciennes, 1829)	Holocentridae
Lachnolaimus maximus (Walbaum, 1792)	Labridae
Lutjanus campechanus (Poey, 1860)	Lutjanidae
Ocyurus chrysurus (Bloch, 1791)	Lutjanidae
Gymnothorax saxicola Jordan et Davis, 1891	Muraenidae
Narcine bancroftii (Griffith et Smith, 1834)	**Narcinidae**
Ogcocephalus parvus Longley et Hildebrand, 1940	Ogcocephalidae
Ogcocephalus cubifrons (Richardson, 1836)	Ogcocephalidae
Lepophidium jeannae Fowler, 1941	Ophidiidae
Acanthostracion quadricornis (Linnaeus, 1758)	Ostraciidae
Pomacanthus arcuatus (Linnaeus, 1758)	Pomacanthidae
Holacanthus ciliaris (Linnaeus, 1758)	Pomacanthidae
Pseudobatos lentiginosus Garman, 1880	**Rhinobatidae**
Scarus coeruleus (Bloch, 1786)	Scaridae
Nicholsina usta (Valenciennes in Cuvier et Valenciennes, 1840)	Scaridae
Pareques acuminatus (Bloch et Schneider, 1801)	Sciaenidae
Pareques umbrosus (Jordan et Eigenmann, 1889)	Sciaenidae
Eques lanceolatus (Linnaeus, 1758)	Sciaenidae
Scorpaena brasiliensis Cuvier in Cuvier et Valenciennes, 1829	Scorpaenidae
Scorpaena plumieri Bloch, 1789	Scorpaenidae
Diplectrum formosum (Linnaeus, 1766)	Serranidae
Hypoplectrus puella (Cuvier in Cuvier et Valenciennes, 1828)	Serranidae
Serranus subligarius (Cope, 1870)	Serranidae
Calamus calamus (Valenciennes, 1830)	Sparidae
Lagodon rhomboides (Linnaeus, 1766)	Sparidae
Synodus foetens (Linnaeus, 1766)	Synodontidae
Sphoeroides spengleri (Bloch, 1785)	Tetraodontidae
Sphoeroides testudineus (Linnaeus, 1758)	Tetraodontidae
Prionotus alatus Goode et Bean, 1883	Triglidae
Prionotus longispinosus Teague, 1951	Triglidae
Urobatis jamaicensis (Cuvier, 1816)	**Urotrygonidae**

Family names set in bold font represent Elasmobranchii. All other families represent Actinopterygii.

Biomass. In Telchac the mean biomass was 593.69 g · m^{-2} and the total biomass (range 0.39–20 000 g · m^{-2}) and in Chicxulub it was 3750.46 g · m^{-2} (range 35.4–55 370 g · m^{-2}), the overall mean value was 1249.51 g · m^{-2} (range 0.39–27 820.6 g · m^{-2}) (Table 2). Among the ten species with the highest density, both sites only share *Opsanus beta*. The species with the highest biomass in Telchac were *Ginglymostoma cirratum* reaching 20 000 g · m^{-2}, *Hypanus say* 5847 g · m^{-2}, and *Pomacanthus arcuatus* 1110 g · m^{-2}, while in Chicxulub—*Opsanus beta* with 55 370 g · m^{-2}, *Acanthostracion quadricornis* 7920 g · m^{-2}, and *Diodon holocanthus* 4867.20 g · m^{-2}. In total, the species with the highest biomass were *Opsanus beta* (27 820 g · m^{-2}), *Ginglymostoma cirratum* (20 000 g · m^{-2}), and *Hypanus say* (5847 g · m^{-2}) (Fig. 2).

Table 2. Ecological variables associated with the fish species affected by the harmful algal bloom, Yucatan, Mexico, in summer 2022.

Species	*N*	ML [cm]	Weight [g]	Depth [m]		Habitat							IUCN category				
				Min	Max	Re	Fs	Es	Sv	Be	Wc	Fw	DD	LC	NT	V	E
Abudefduf saxatilis	1	23.0	90.6	0	41	1	1	0	0	0	1	0	0	1	0	0	0
Achirus lineatus	1	23.0	101.4	1	110	1	0	1	0	1	0	1	0	1	0	0	0
Opsanus beta	281	38.0	226.0	0	5	1	0	0	1	1	0	0	0	1	0	0	0
Sanopus reticulatus	3	42.0	226.0	0	10	1	0	0	0	0	1	0	0	0	0	0	1
Strongylura marina	1	73.0	370.0	0	5	0	0	0	0	0	1	1	0	1	0	0	0
Strongylura notata	1	45.0	71.8	0	5	1	0	0	0	0	1	0	0	1	0	0	0
Oligoplites saurus	2	35.0	118.1	0	30	0	1	0	0	1	1	1	0	1	0	0	0
Caranx hippos	1	124.0	21019.4	0	350	1	0	0	0	1	1	0	0	1	0	0	0
Chaetodon ocellatus	1	20.0	285.0	0	91	1	0	0	1	0	0	0	0	1	0	0	0
Harengula jaguana	26	27.5	45.1	0	10	0	0	0	0	0	1	0	0	1	0	0	0
Dactylopterus volitans	2	45.0	92.3	1	150	1	0	1	1	1	0	0	0	1	0	0	0
Hypanus say	9	78.0	19490.0	0	20	0	0	1	0	1	0	1	0	1	0	0	0
Chilomycterus schoepfii	9	33.0	550.0	0	77	1	0	1	1	0	0	0	0	1	0	0	0
Diodon holocanthus	4	60.0	942.0	0	104	1	0	1	0	1	0	0	0	1	0	0	0
Anchoa hepsetus	1	8.0	11.8	0	70	0	0	0	0	0	1	0	0	1	0	0	0
Eucinostomus gula	5	22.7	35.4	0	71	1	0	0	1	1	0	0	0	1	0	0	0
Eugerres plumieri	3	40.0	347.0	0	30	1	0	1	0	1	0	1	0	1	0	0	0
Ginglymostoma cirratum	1	300.0	60000.0	0	130	1	0	0	0	1	0	0	1	0	0	0	0
Haemulon aurolineatum	2	25.0	799.2	1	103	1	0	0	0	0	0	0	0	1	0	0	0
Haemulon plumieri	16	53.0	101.7	1	74	1	0	0	0	1	0	0	0	1	0	0	0
Orthopristis chrysoptera	3	46.0	108.0	5	20	1	0	1	0	1	0	0	0	1	0	0	0
Chriodorus atherinoides	3	20.6	73.6	0	5	0	0	1	0	0	1	1	0	1	0	0	0
Hemiramphus brasiliensis	16	41.0	73.1	0	5	1	0	1	0	0	0	1	0	1	0	0	0
Neoniphon marianus	3	22.0	336.0	15	151	1	0	0	0	0	0	0	0	1	0	0	0
Lachnolaimus maximus	5	91.0	119.0	0	91	1	0	0	1	1	0	0	0	0	0	1	0
Lutjanus campechanus	1	100.0	619.0	10	190	0	0	0	0	0	0	0	0	0	0	0	0
Ocyurus chrysurus	1	86.3	1005.0	0	180	1	0	0	0	1	1	0	1	0	0	0	0
Gymnothorax saxicola	1	62.0	129.2	2	213	0	0	0	0	1	0	0	0	1	0	0	0
Narcine bancroftii	4	65.0	85.0	0	189	0	0	0	0	0	0	0	0	0	0	0	0
Ogcocephalus parvus	11	10.0	34.0	29	360	1	0	1	0	1	0	0	0	1	0	0	0
Ogcocephalus cubifrons	7	38.0	34.0	0	70	0	0	0	0	0	0	0	0	0	0	0	0
Lepophidium jeannae	1	30.5	308.0	26	280	0	0	1	0	1	0	0	0	1	0	0	0
Acanthostracion quadricornis	61	55.0	215.0	2	90	1	0	0	1	1	0	0	0	1	0	0	0
Pomacanthus arcuatus	12	60.0	2775.0	1	101	1	0	0	1	0	0	0	0	1	0	0	0
Holacanthus ciliaris	2	45.0	1487.0	1	125	1	0	0	0	0	0	0	0	1	0	0	0
Pseudobatos lentiginosus	4	76.0	696.6	0	30	0	0	1	0	1	0	0	0	0	1	0	0
Scarus coeruleus	3	120.0	488.0	2	25	1	0	0	0	1	0	0	0	1	0	0	0
Nicholsina usta	8	30.0	303.0	1	73	1	0	1	1	1	0	0	0	1	0	0	0
Pareques acuminatus	19	25.0	91.0	3	113	0	0	0	0	0	0	0	0	1	0	0	0
Pareques umbrosus	4	20.0	91.0	4	110	1	0	1	0	1	0	0	0	1	0	0	0
Eques lanceolatus	25	30.0	36.5	2	230	1	0	1	0	1	0	0	0	1	0	0	0
Scorpaena brasiliensis	4	35.0	552.0	1	204	1	0	1	0	1	0	0	0	1	0	0	0
Scorpaena plumieri	7	45.0	552.0	1	80	1	0	0	0	1	0	0	0	1	0	0	0
Diplectrum formosum	14	30.0	48.3	1	132	1	0	0	1	1	0	0	0	1	0	0	0
Hypoplectrus puella	27	16.7	42.8	3	90	1	0	1	1	0	0	0	0	1	0	0	0
Serranus subligarius	1	10.0	393.0	3	80	1	0	1	0	1	0	0	0	1	0	0	0
Calamus calamus	10	56.0	433.0	1	75	1	0	0	1	1	0	0	0	1	0	0	0
Lagodon rhomboides	1	40.0	114.2	1	20	1	0	1	1	1	0	1	0	1	0	0	0
Synodus foetens	4	43.0	97.0	1	200	0	0	1	0	1	0	0	0	1	0	0	0
Sphoeroides spengleri	17	16.0	25.0	2	74	1	0	1	1	1	0	0	0	1	0	0	0
Sphoeroides testudineus	14	30.0	57.3	1	20	1	0	1	0	1	0	1	0	1	0	0	0
Prionotus alatus	1	20.0	75.4	35	611	0	0	1	0	1	0	0	0	1	0	0	0
Prionotus longispinosus	1	35.0	75.4	9	219	0	0	1	0	1	0	0	0	1	0	0	0
Urobatis jamaicensis	5	70.0	5003.0	1	160	1	0	1	0	1	0	0	0	1	0	0	0
Total	670					38	2	25	14	35	10	9	2	46	1	1	1
Mean	12.41	48.80	2250.0	3.09	113												
Min	1.0	8.0	11.8	0	5												
Max	281.0	300.0	60000.0	35.0	611												

N = number of specimens, Min = minimum, Max = maximum, Re = reef, Fs = flotsam, Es = estuary, Sv = submerged vegetation, Be = beach, Wc = water column, Fw = freshwater, DD = "data deficient", LC = "least concern", NT = "near threatened", V = "vulnerable", E = "endangered".

Habitat. The species affected by the HAB presented a range of sizes between 8 and 300 cm, the majority, 42 species, with sizes between 8 and 62 cm and an overall mean value of 47.69 cm (Table 2). They were associated with seven general habitats, reefs, beaches, estuaries, submerged vegetation, water column, freshwater, and flotsam. A total of 28.6% of the affected species had an affinity for reefs, 26.3% for beaches, and 18.8% for estuaries, adding up to 74% of the affected species, another small percentage was divided between submerged vegetation, water column, freshwater, and flotsam (Fig. 3A). These species occur not deeper than 611 m, although, the majority had a minimum depth range between 0 and 5 m and a maximum between 5 m and 150 m, so the mean range was between 3 and 113 m of depth (Fig. 3B). The majority of the species (46 species) are in the category "least concern", *Ginglymostoma cirratum* and *Ocyurus chrysurus* in the category "data deficient", *Pseudobatos lentiginosus* "near threatened" *Lachnolaimus maximus* "vulnerable", *Sanopus reticulatus* "endangered" (Fig. 3C). A total of four individuals of *Pseudobatos lentiginosus*, five individuals of *Lachnolaimus maximus*, and three individuals of *Sanopus reticulatus* were recorded.

Discussion

Different authors recorded between 14 and 94 fish species on the Yucatan coast (Córdova-Tapia and Zambrano 2016; Palacios-Sánchez et al. 2019; Aguilar-Medrano et al. 2020), 159 in the Campeche Bank (Aguilar-Medrano and Vega-Cendejas 2019), and 183 on reefs (Núñez-Lara et al. 2015). According to the presently reported results, the species affected were most commonly associated with reefs, beaches, and estuaries in a depth range of 3 m to 110 m. We recorded in only two days of sampling, 54 species of bony and cartilaginous fishes, so it can be assumed that a greater number of species were affected during the whole duration of the HAB.

In total, 680 organisms were recorded, 281 representing *Opsanus beta*. This type of phenomenon occurs mainly in the coastal zone and *Opsanus beta* is a coastal species, distributed between 0 m and 5 m of depth, which is why it was highly affected, recording the highest abundance, density, and biomass. However, since this species is in the category of "least concern" and it is distributed from the east coast of Florida to Belize, we can assume that the HAB did not cause significant damage to its populations. However, a

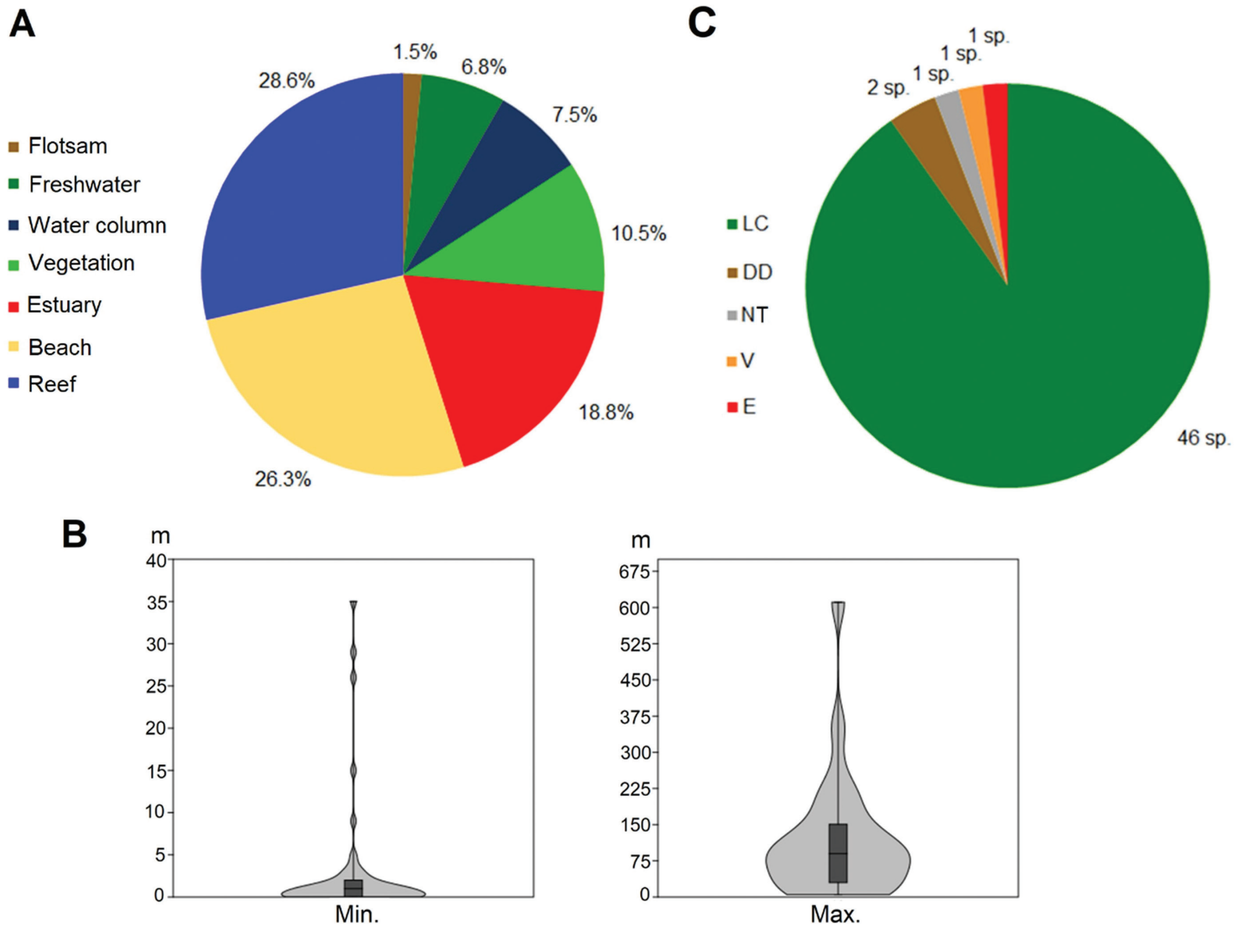

Figure 3. Ecological affinity, depth, and conservation status of species affected by the harmful algal bloom off the coast of Yucatan, Mexico in summer 2022; (**A**) percentage of species with affinity to the recorded habitats; (**B**) distribution in the water column, minimum and maximum depth; (**C**) number of species in the Red List categories. Abbreviations: Min = minimum, Max = maximum, LC = "least concern", DD = "data deficient", NT = "near threatened", V = "vulnerable", E = "endangered".

species with similar habits is *Sanopus reticulatus*, which is microendemic to the west coast of the Yucatan Peninsula and is in the "endangered" category. Although only three individuals of this species were recorded, these were recorded at the beginning of the HAB, so we can assume that more organisms were affected during the course of the HAB, and thus this could have affected their populations.

Among the species with the highest abundance and density were *Acanthostracion quadricornis*, *Hypoplectrus puella*, *Eques lanceolatus*, and *Harengula jaguana*. These species have a wide distribution in the Gulf of Mexico and the Caribbean; they are coastal inhabitants of beaches, reefs, and submerged vegetation, except for *Harengula jaguana* which is found in coastal schools in the water column, all of these species are in the conservation category "least concern". *Lachnolaimus maximus* is also widely distributed in the Gulf of Mexico and the Caribbean, it is a coastal inhabitant of beaches, reefs, and submerged vegetation; however, it is in the "vulnerable" category. Only five individuals of this species were recorded, four at the beginning of the HAB and one at the end, so we assume a low impact of the HAB on the species population.

Four cartilaginous species stand out among the species with the highest biomass, *Ginglymostoma cirratum*, which reaches 60 kg and 300 cm of total length (TL), of which only one individual was recorded, *Hypanus say* with 19.5 kg and 78 cm of TL, of which nine individuals were recorded, *Urobatis jamaicensis* with 5 kg and 76 cm TL of which six individuals were recorded, and *Pseudobatos lentiginosus* with 700 g and 76 cm of TL of which four individuals were recorded. The species *Hypanus say* and *Urobatis jamaicensis* are in the conservation category "least concern", *Ginglymostoma cirratum* in "data deficient" and *Pseudobatos lentiginosus* "near threatened." The latter species is distributed in South and North Carolina, the coast of Florida, and the whole Gulf of Mexico; however, it is an uncommon species (Lieske and Myers 1994), with a very low reproductive resilience rate, where the population doubles in a minimum time of more than 14 years (Froese et al. 2017), therefore, three individuals recorded at the beginning of the HAB and one at the end, indicate its possible effect on a greater number of individuals throughout the time duration of the HAB.

On the coast of Yucatan, tourism, urbanization, sewage discharges, livestock, agriculture, shrimp farming, and atmospheric deposition have been implicated as the most important continental sources of nutrient inputs into the coastal ecosystem (Aranda-Cirerol et al. 2011; Padilla 2015; Castillo-Pavón and Méndez-Ramírez 2017; Aguilar-Medrano et al. 2020; Poot-Delgado and Okolodkov 2020), swine being the greatest single nutrient input (Drucker et al. 2003; Aranda-Cirerol et al. 2011). The increase in the nutrients along with the non-existent or inefficient wastewater treatment plants, are the main causes of water quality problems in the area (Castillo-Pavón and Méndez-Ramírez 2017; Aguilar-Maldonado et al. 2018). As is known, nutrients can stimulate or enhance the impact of HABs (Anderson et al. 2008; Glibert et al. 2010; Aranda-Cirerol et al. 2011) thus, if nothing is done to stop the input of nutrients into the Yucatan coast, we can expect an increase of the HABs in the area. Although the majority of the species recorded are in the IUCN red list category "least concern", the increase in the frequency of these events due to local and global factors can cause damage to endemic species in coastal areas such as *Sanopus reticulatus*, which is in the category "endangered" and is microendemic to the Yucatan coastal area.

Acknowledgments

All the authors are recipients of the National System of Researchers grant (CONAHCYT-SNI).

References

Aguilar-Maldonado JA, Santamaría-Del-Ángel E, González-Silvera A, Cervantes-Rosas OD, Sebastiá-Frasquet MT (2018) Mapping satellite inherent optical properties index in coastal waters of the Yucatán Peninsula (Mexico). Sustainability 10(6): 1894. https://doi.org/10.3390/su10061894

Aguilar-Medrano R, Vega-Cendejas ME (2019) Implications of the environmental heterogeneity on the distribution of the fish functional diversity of the Campeche Bank, Gulf of Mexico. Marine Biodiversity 49(4): 1913–1929. https://doi.org/10.1007/s12526-019-00954-y

Aguilar-Medrano R, Hernandez de Santillana M, Vega-Cendejas ME (2020) Using fish assemblages to understand environmental connectivity and usage. A contribution to the conservation of the Yucatan Wetland. Estuarine, Coastal and Shelf Science 239: e106766. https://doi.org/10.1016/j.ecss.2020.106766

Anderson DM (1989) Toxic algal blooms and red tides: A global perspective. Pp. 11–16. In: Okaichi T, Anderson DM, Nemoto T (Eds.) Red tides: Biology, environmental science and toxicology. Elsevier Science, New York.

Anderson DM, Burkholder JM, Cochlan WP, Glibert PM, Gobler CJ, Heil CA, Kudela RM, Parsons ML, Rensel JAJ, Townsend DW, Trainer VL, Vargo GA (2008) Harmful algal blooms and eutrophication: Examining linkages from selected coastal regions of the United States. Harmful Algae 8(1): 39–53. https://doi.org/10.1016/j.hal.2008.08.017

Aranda-Cirerol N, Comín F, Herrera-Silveira J (2011) Nitrogen and phosphorus budgets for the Yucatán littoral: An approach for groundwater management. Environmental Monitoring and Assessment 172(1–4): 493–505. https://doi.org/10.1007/s10661-010-1349-z

Castillo-Pavón O, Méndez-Ramírez JJ (2017) The tourist developments and their environmental effects in the Mayan Riviera, 1980–2015. Quivera 19: 101–118.

Córdova-Tapia F, Zambrano L (2016) Fish functional groups in a tropical wetland of the Yucatan Peninsula, Mexico. Neotropical Ichthyology 14(2): e150162. https://doi.org/10.1590/1982-0224-20150162

Drucker AD, Escalante Semerena R, Gómez-González V, Magaña-Rueda S (2003) La industria porcina en Yucatán: Un análisis de la generación de aguas residuales. Instituto de Investigaciones Económicas. Universidad Nacional Autónoma de México 34(135): 105–124. https://doi.org/10.22201/iiec.20078951e.2003.135.7505

Froese R, Demirel N, Coro G, Kleisner KM, Winker H (2017) Estimating fisheries reference points from catch and resilience. Fish and Fisheries 18(3): 506–526. https://doi.org/10.1111/faf.12190

Froese R, Pauly D (Eds.) (2023) FishBase. [Version 06/2023] http://www.fishbase.org

Glibert PM, Allen JI, Bouwman AF, Brown CW, Flynn KF, Lewitus AJ, Madden CJ (2010) Modeling of HABs and eutrophication: Status, advances, challenges. Journal of Marine Systems 83(3–4): 262–275. https://doi.org/10.1016/j.jmarsys.2010.05.004

Hallegraeff GM (1993) A review of harmful algal blooms and their apparent global increase. Phycologia 32(2): 79–99. https://doi.org/10.2216/i0031-8884-32-2-79.1

Hallegraeff GM (2023) Harmful algal blooms: a global overview. Pp. 25–49. In: Hallegraeff GM, Anderson DM, Cembella AD (Eds.) Manual on harmful marine microalgae. UNESCO, France.

Hallegraeff GM, Anderson DM, Cembella AD (1995) Manual of Harmful Marine Microalgae. Intergovernmental Oceanographic Commission, UNESCO, France, 565 pp.

Herrera-Silveira J, Aguilar-Trujillo A, Merino-Virgilio F, Medina-Euán D (2022) Marea Roja en Yucatán. Boletín Extraordinario SIMAR-CONABIO.

Lieske E, Myers R (1994) Collins pocket guide. Coral reef fishes. Indo-Pacific and Caribbean including the Red Sea. Harper Collins Publishers, 400 pp.

Núñez-Lara E, Arias-González JE, Legendre P (2015) Spatial patterns of Yucatan reef fish communities: Testing models using a multi-scale survey design. Journal of Experimental Marine Biology and Ecology 324(2): 157–169. https://doi.org/10.1016/j.jembe.2005.04.011

Padilla NS (2015) The environmental effects of Tourism in Cancun, Mexico. International Journal of Environmental Science and Technology 6: 282–294.

Palacios-Sánchez SE, Vega-Cendejas ME, Hernández-de-Santillana JM, Aguilar-Medrano R (2019) Anthropogenic impacts in the nearshore fish community of the Yucatan Coastal Corridor. A comparison of protected and unprotected areas. Journal for Nature Conservation 51: 125721. https://doi.org/10.1016/j.jnc.2019.125721

Poot-Delgado CA, Okolodkov YB (2020) Bloom of *Cylindrotheca closterium* originating from shrimp farming discharges in the SE Gulf of Mexico. Harmful Algae News No 66: 10.

Robertson DR, Van Tassell J (Eds.) (2023) Shorefishes of the Greater Caribbean: online information system. Version 3.0 Smithsonian Tropical Research Institute, Balboa, Panamá.

Sidabutar T, Srimariana ES, Cappenberg H, Wouthuyzen S (2021) An overview of harmful algal blooms and eutrophication in Jakarta Bay, Indonesia. IOP Conference Series: Earth and Environmental Science 869: e012039. https://doi.org/10.1088/1755-1315/869/1/012039

Smayda TJ (1990) Novel and nuisance phytoplankton blooms in the sea: Evidence for a global epidemic. Pp. 29–40. In: Granéli E, Sundström B, Edler L, Anderson DM (Eds.) Toxic marine phytoplankton. Elsevier Science, New York, NY, USA.